Fall 2010

Structural and Mechanistic Aspects of Copper Catalyzed Atom Transfer Radical Addition Reactions in the Presence of Reducing Agents

William Eckenhoff

STRUCTURAL AND MECHANISTIC ASPECTS OF COPPER CATALYZED ATOM TRANSFER RADICAL ADDITION REACTIONS IN THE PRESENCE OF REDUCING AGENTS

A Dissertation

Submitted to the Bayer School of Natural and Environmental Sciences

Duquesne University

In partial fulfillment of the requirements for

the degree of Doctor of Philosophy

By

William T. Eckenhoff

December 2010

STRUCTURAL AND MECHANISTIC ASPECTS OF COPPER CATALYZED ATOM TRANSFER RADICAL ADDITION REACTIONS IN THE PRESENCE OF REDUCING AGENTS

By

William T. Eckenhoff

Approved November 11, 2010

Dr. Tomislav Pintauer Assistant Professor of Chemistry and Biochemistry Committee Chair	Dr. Partha Basu Professor of Chemistry and Biochemistry Committee Member
Dr. Fraser F. Fleming Professor of Chemistry and Biochemistry Committee Member	Dr. Krzysztof Matyjaszewski J.C. Warner Professor of Natural Sciences Carnegie Mellon University External Reviewer
David W. Seybert Dean, Bayer School of Natural and Environmental Sciences Professor of Chemistry and Biochemistry	Dr. Ralph Wheeler Chair, Department of Chemistry and Biochemistry Professor of Chemistry and Biochemistry

ABSTRACT

STRUCTURAL AND MECHANISTIC ASPECTS OF COPPER CATALYZED ATOM TRANSFER RADICAL ADDITION REACTIONS IN THE PRESENCE OF REDUCING AGENTS

By

William T. Eckenhoff

December 2010

Dissertation supervised by Tomislav Pintauer

The focus of this dissertation was to improve the atom transfer radical addition (ATRA) by decreasing the amount of copper catalyst needed to achieve good yields of the monoadduct. This is a fundamental organic reaction in which an alkyl halide is added to the carbon-carbon double bond of an alkene via a free radical mechanism. Before 2006, these reactions required between 5 and 30 mol% of a copper catalyst relative to alkene in order to achieve good yields of the desired monoadduct due to the accumulation of copper(II) as a result of unavoidable radical termination reactions. The solution to this problem was found for the mechanistically similar atom transfer radical polymerization (ATRP) where the addition of a reducing agent, such as free radical initiators, magnesium, zinc, tin-2-ethylhexanoate, or ascorbic acid, served to continuously

regenerate copper(I) *in situ*, allowing for the significant decrease in the amount of copper catalyst.

We utilized tris(2-pyridylmethyl)amine (TPMA) as a complexing ligand, due to its high activity in ATRA and also high stability. 2,2'-azobis(isobutyronitrile) (AIBN), which decomposes into free radicals at a constant rate at 60°C, was used as a reducing agent and were able to show that polychlorinated and polybrominated methanes could be efficiently added across a variety of alkenes. Catalyst loadings as low as 0.0005 mol% (relative to alkene) were required for alkenes that do not readily undergo free radical polymerization such as α-olefins. However, significantly higher concentrations of copper catalyst were required for highly active alkenes such as styrene and methyl acrylate (0.2 mol%). Nonetheless, the turn over numbers (TONs) utilizing AIBN were the highest so far reported for any metal mediated ATRA. In order to achieve better control of monoadduct formation in these highly active systems, we utilized low temperature free radical initiator 2,2'-azobis(4-methoxy-2,4-dimethyl-valeronitrile) (V-70). The results of this study were truly remarkable, providing good control over ATRA of methyl acrylate, methyl methacrylate, vinyl acetate and styrene with very low catalyst loadings (0.2 to 0.01 mol%).

Encouraged by these results, we sought more highly active complexes for use in ATRA with reducing agents. Previous studies have established that the equilibrium constant for atom transfer generally correlates with the redox potentials of the corresponding copper complexes. According to this relationship, Me_6TREN (tris(2-(dimethyl)aminoethyl)amine) ligand was expected to be even more active than TPMA. However, Me_6TREN was found to be slightly less effective than TPMA as a complexing

ligand in copper mediated ATRA systems, which was attributed to disproportionation of the unstable copper(I) complex with Me_6TREN ligand.

To better understand the correlation between the structure of the copper complex and its activity in ATRA, copper complexes with the TPMA ligand were isolated and characterized with a variety of anions and auxiliary ligands. We observed that copper(I) TPMA complexes contained coordinated halide anions, which was surprising taking into account the tetradentate nature of the TPMA ligand. This raised questions as to how coordinatively saturated complexes such as these could have such a high activity in ATRA, which is widely accepted to proceed via inner sphere electron transfer (ISET). In ISET, the alkyl halide must be within bonding distance to copper in order for bond homolysis of the alkyl halide to occur. We investigated this mechanism by examining the effect of the anion and coordinating ligands, such as halides, acetonitrile, 4,4'-dipyridyl, and triphenylphosphine. It was determined that ATRA with copper TPMA complexes most likely operates by partial ligand dissociation in order to allow ISET to proceed.

This work provided a significant contribution to decreasing catalyst loadings in ATRA, which could increase its usefulness in the synthesis of small molecules, including natural products and pharmaceutical drugs.

ACKNOWLEDGEMENT

First and foremost, I would like to thank my advisor, Dr. Tomislav Pintauer, without whom, none of this work would have been possible. Throughout the past several years, Tom has pushed me to be better nearly everyday and I am very grateful for that. The challenges presented to the group caused us all to experience highs and lows, which catalyzed the formation of some wonderful friendships that will persist for years to come. I know Tom will do great things and I look forward to following his career.

I would also like to thank my committee members from Duquesne University, Dr. Partha Basu and Dr. Fraser Fleming, who have served on every defense of mine in graduate school, barring rotation II. Their attentiveness to detail and questioning has pushed me to become a far better and more knowledgeable scientist.

I am very grateful to Dr. Krzysztof Matyjaszewski for agreeing to be my outside reader as well as providing valuable insights throughout my PhD career. The data and discoveries from his laboratories at Carnegie Mellon University were instrumental in my understanding of the Atom Transfer Radical Addition and provided the impetus for my dissertation projects.

Financial support from the Department of Chemistry and Biochemistry at Duquesne University as well as from the National Science Foundation was much appreciated.

While working in the lab, I was surrounded by a great group of fellow graduate students and undergraduates. I would like to thank in particular, Dr. Marielle Balili and Carolynne Ricardo, who have been worked with me from the first day and are truly special people. I will always remember fun times in the lab and trips to ACS meetings

with them. I had a great deal of fun working with Raj Kaur, from whom I expect great things, and I sincerely wish her the very best. I would also like to thank graduate students April Hill, Anita Dasu, and Merton Pajibo for being wonderful group members. I also had the opportunity to work with some incredibly talented undergraduates: Matthew Taylor, Ashley Biernesser, Sean Noonan, and Tom Ribelli. Working alongside of them has been a lot of fun and I have absolute confidence that these students will be highly successful in whatever they decide to pursue.

There are several people at Duquesne who made my Ph.D. experience much easier who I owe a great deal of gratitude. Sandy Russell and Amy Stroyne have been so helpful in so many ways, whether it be simply encouragement, paperwork or sending out samples. The instrumentation staff, Dan Bodnar, Dave Hardesty, and Lance Crosby, also were crucial for maintaining research progress as well as being great people to talk to and learn from. I cannot begin to count the number of instances where one of them fixed an instrument I needed or make modifications in our lab. I would like to thank Heather Costello for her always-helpful manor in basically everything concerning graduate students on the administrative end.

Last, but certainly not least, I must thank my family for their unwavering support though this time. My extraordinary wife, Dana, has stuck with me for the highs and lows that come with graduate school and put up with many Saturday trips to Duquesne to mount crystals. My parents, who understand this process from personal experience, have been very helpful and supportive throughout. They have even been known to bring a projector and screen to thanksgiving to hear my practice research talks, which is certainly above and beyond what I expected.

TABLE OF CONTENTS

LIST OF TABLES

Page

LIST OF FIGURES

Page

LIST OF SCHEMES

Page

LIST OF ABBREVIATIONS

AIBN	2,2'-azobis(isobutyronitrile)
ATRA	atom transfer radical addition
ATRC	atom transfer radical cyclization
ATRP	atom transfer radical polymerization
bpy	2,2'-bipyridine
BzBr	benzyl bromide
BzCl	benzyl chloride
CBr_4	carbon tetrabromide
CCl_4	carbon tetrachloride
$CHBr_3$	bromoform
$CHCl_3$	chloroform
CH_3CN	acetonitrile
dipy	4,4'-dipyridyl
DMCBCy	1,4,8,11-tetraazacyclotetradecane
DMF	dimethylformamide
EtBriB	ethyl-2-bromoisobutyrate
EXAFS	extended X-ray absorption fine structure
HMTETA	1,1,4,7,10,10-hexamethyltriethylenetetramine
ICAR	initiators for continuous activator regeneration
ISET	inner sphere electron transfer
MBriB	methyl-2-bromoisobutyrate
MBrP	methyl-2-bromopropionate

Me_4CYLAM	1,4,8,11-tetraaza-1,4,8,11-tetramethylcyclotetradecane
MeOH/CH_3OH	methanol
Me_6TREN	tris[2-(dimethyl)aminoethyl]amine
NAlkPMI	*N*-alkyl-2-pyridylmethanimine
NMR	nuclear magnetic resonance
NPMI	*N*-alkyl-2- pyridylmethanimine
OSET	outer sphere electron transfer
PMDETA	*N,N,N',N'',N''*-pentamethyldiethylenetriamine
TDAPA	tris(2-(dimethylamino)phenyl)amine
TEMPO	2,2,6,6-tetramethylpiperidin-1-oxyl
TPMA	tris(2-pyridylmethyl)amine
TPEDA	*N,N,N',N'*-tetrakis(2-pyridylmethyl)ethylenediamine
TMC ATRA	transition metal catalyzed atom transfer radical addition
Tp^x	trispyrazolyl borate
UV-Vis	ultraviolet-visible spectroscopy
V-70	2,2'-azobis(4-methoxy-2,4-dimethylvaleronitrile

Chapter 1.

INTRODUCTION AND BACKGROUND[†]

1.1 The Origins of Atom Transfer Radical Addition- "Peroxide Effect"

The origins of atom transfer radical addition (ATRA) can be traced back to 1937 when Kharasch and co-workers discovered " the peroxide effect" which accounted for anti-Markovnikov addition of HBr to unsymmetrical alkenes in the presence of peroxide initiators.[1] The generally accepted mechanism for this reaction involves free-radical intermediates as outlined in Scheme 1.1.1. Soon after the discovery of the "peroxide effect" it was recognized that a variety of substrates such as hydrocarbons,

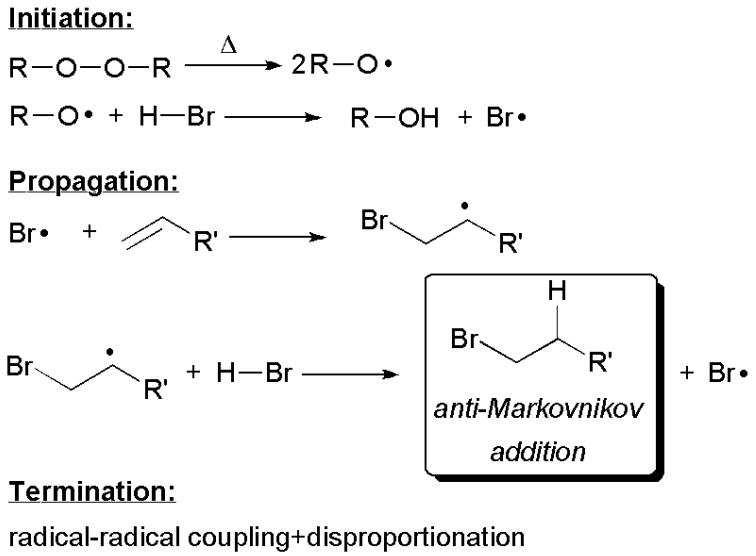

Scheme 1.1.1. Anti-Markovnikov addition of HBr to unsymmetrical alkenes in the presence of peroxide initiators.

[†] Reproduced in part with permission from Eckenhoff, W.T.; Pintauer, T. *Cat. Rev. – Sci. Eng.* **2010**, *51*(1), 1-59. Copyright 2010 Taylor & Francis Group, LLC.

polyhalogenated alkanes, alcohols, ethers, amines, aldehydes, ketones, aliphatic acids and esters, and compounds of sulfur, phosphorous, silicon, tin and germanium can be used in the radical addition to alkenes. In particular, Kharasch investigated the addition of polyhalogenated alkanes (CBr_4, CCl_4, CBr_3Cl and CCl_3Br) to alkenes in the presence of free-radical initiators or light (Scheme 1.1.2), in a reaction that is today widely referred to as the *Kharasch addition* or *atom transfer radical addition (ATRA)*.[2, 3] Very high yields

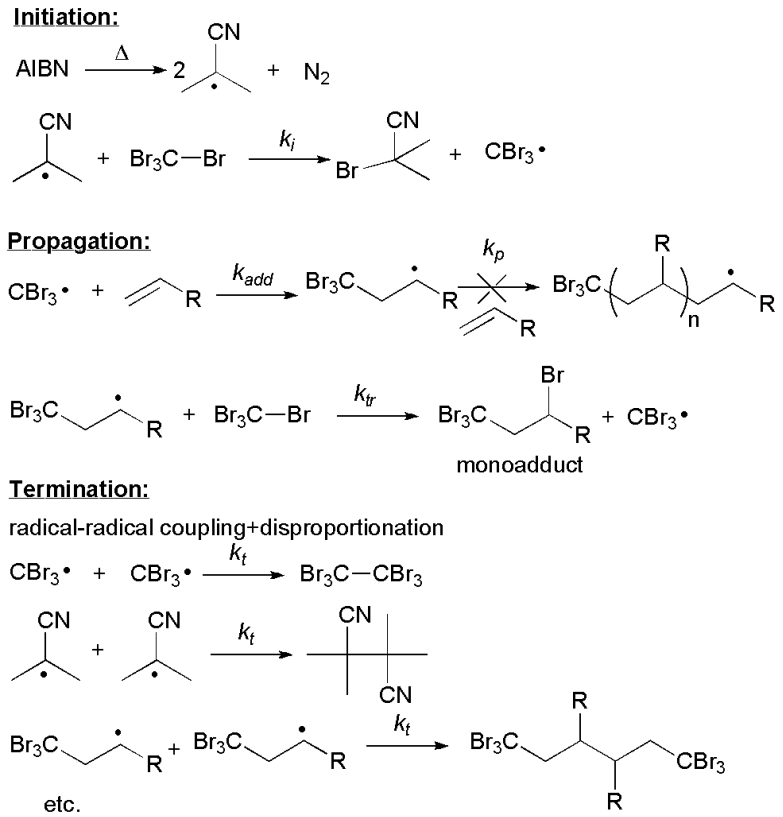

Scheme 1.1.2. Kharasch addition of CBr_4 to alkene in the presence of free-radical initiator AIBN.

of the monoadduct were obtained in the case of simple α-olefins (1-hexene, 1-octene and 1-decene), but were significantly decreased for more reactive monomers such as styrene, methyl acrylate and methyl methacrylate. The principal reason for the decreased yield of

the monoadduct was radical-radical coupling and repeating radical addition to alkene to generate oligomers and polymers. Although, radical-radical termination reactions by coupling and disproportionation could be suppressed by decreasing the radical concentration ($R_t \propto [\text{radicals}]^2$), telomerization reactions could not be avoided due to the low chain transfer constant (k_{tr}/k_p, Scheme 1.1.2). The research was thus shifted in a direction of finding means to selectively control the product distribution.

1.2 Fundamentals of Transition Metal Catalyzed Atom Transfer Addition

The principal drawback of non-transition metal catalyzed ATRA was the inability to control the chain transfer constant (k_{tr}/k_p, Scheme 1.1.2). This resulted in significantly lower yields of the monoadduct for monomers that are highly active in free-radical polymerization such as styrene, methyl acrylate, methyl methacrylate and acrylonitrile (Table 1.2.1). Clearly, a search for a better halogen atom transfer agent was needed.

Table 1.2.1. Chain transfer constants for CCl_4 in free-radical polymerization at 60 ^{o}C.[4]

Alkene	k_{tr} / $M^{-1}s^{-1}$	k_p / $M^{-1}s^{-1}$	k_{tr}/k_p
ethylene	259	16	16.2
1-hexene	320	22	14.5
vinyl acetate	2400	2300	1.04
acrylonitrile	0.17	1960	0.0000865
methyl acrylate	0.26	2090	0.000124
methyl methacrylate	0.12	515	0.000233
styrene	1.8	165	0.0109

In 1956, Minisci et. al. attempted thermal polymerization of acrylonitrile in CCl_4 and $CHCl_3$ in a steel autoclave and observed considerable amounts of monoadduct (CCl_3-CH_2-CHClCN with CCl_4 and $CHCl_2$-CH_2-CHClCN with $CHCl_3$).[5] These results were unexpected because the chain transfer constants (k_{tr}/k_p) of CCl_4 (Table 1.2.1) and $CHCl_3$ are not high enough to prevent polymerization of acrylonitrile. In 1961, on the grounds of analogous redox haloalkylations of acrylonitrile, the same authors proposed a mechanism in which iron chlorides (arising from corrosion of the autoclave) played a major role in this process by increasing the chain transfer constant.[6-11] This reaction marked the beginning of transition metal catalyzed ATRA. Since the seminal report by Minisci et. al., a number of species were found to be particularly active in ATRA process and they included the complexes of Cu, Fe, Ru and Ni,[12-17] as well as metal oxides[18, 19] and zero valent metals such as Cu(0)[20, 21] and Fe(0).[22-24] Great progress has been made in not just controlling the product selectivity, but also in utilizing a variety of halogenated compounds (alkyl and aryl halides, [10, 25, 26] *N*-chloroamines, [10] alkylsulfonyl halides[27-32] and polyhalogenated compounds[27, 32-34]). Furthermore, it was also demonstrated that a variety of alkenes (styrene, alkyl acrylates and acrylonitrile) could be used as the source of reactive unsaturation. Therefore, transition metal catalyzed (TMC) ATRA became broadly applicable synthetic tool.[13-15, 35, 36]

Based on chemo-, regio-, and stereoselectivity, it is generally accepted that the mechanism of TMC ATRA involves free radical intermediates.[10, 27] The proposed mechanism in the case of copper complexes is shown in Scheme 1.2.1. Homolytic cleavage of an alkyl halide bond by a copper(I) complex generates a corresponding copper(II) complex and an organic radical ($k_{a,1}$). The radical may terminate (k_t) or add to

an alkene (k_{add}) in an inter- or intramolecular fashion or it can abstract the halogen atom from the copper(II) complex and return to the original dormant alkyl halide species ($k_{d,1}$). If the abstraction of the halogen atom occurs after the first addition to an alkene, the desired monoadduct will be formed ($k_{d,2}$). This step regenerates the corresponding

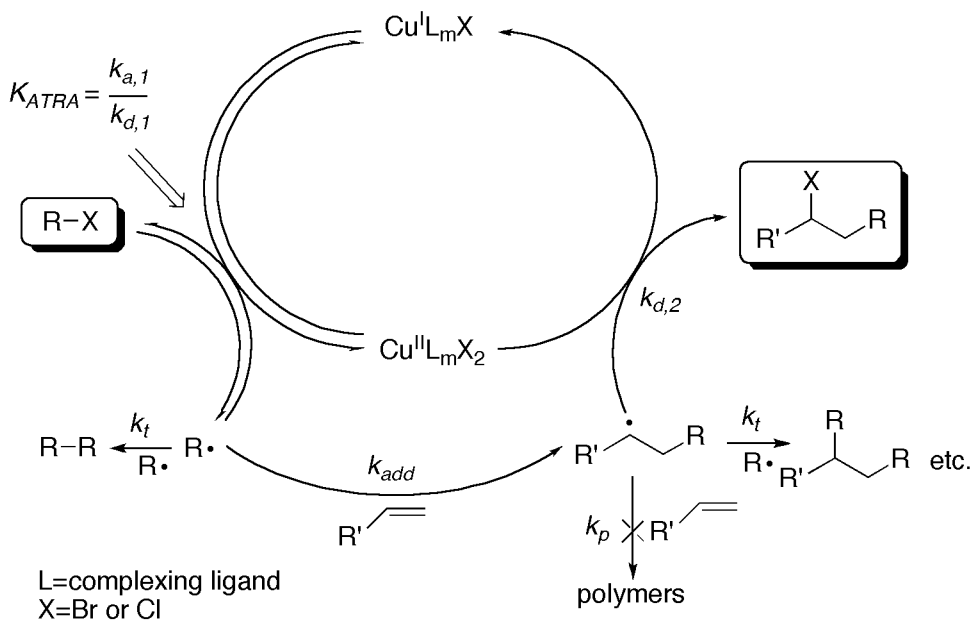

Scheme 1.2.1. Proposed mechanism for copper catalyzed ATRA.

copper(I) complex and therefore completes the catalytic cycle. There are several guidelines that should be followed in order to increase chemoselectivity of the monoadduct. Firstly, the radical concentration must be low in order to suppress radical termination reactions (rate constants of activation [$k_{a,1}$ and $k_{a,2}$]<<rate constants of deactivation [$k_{d,1}$ and $k_{d,2}$]). Secondly, further activation of the monoadduct should be avoided ($k_{a,1}$>>$k_{a,2}$, ideally $k_{a,2}$≈0). Lastly, formation of oligomers should be suppressed, indicating that the rate of deactivation ($k_{d,2}$[$Cu^{II}L_mX$]) should be much larger than the rate of propagation (k_p[alkene]). Alkyl halides for copper catalyzed ATRA are typically chosen such that if addition occurs, then the newly formed radical is much less stabilized

than the initial radical and will essentially irreversibly react with a copper(II) complex to form an inactive monoadduct. TMC ATRA reactions can also be conducted intramolecularly when alkyl halide and alkene functionalities are part of the same molecule. Intramolecular TMC ATRA or atom transfer radical cyclization (ATRC) is a very attractive synthetic tool because it enables the synthesis of functionalized ring systems that can be used as starting materials for the preparation of complex organic molecules.[15, 37] Furthermore, halide functionality in the resulting product can be very beneficial because it can be easily reduced, eliminated, displaced, converted to a Grignard reagent, or if desired serve as a further radical precursor. The use of copper mediated ATRC in organic synthesis has been reviewed recently and some illustrative examples will be discussed later in this chapter.[15, 36-39]

1.3 Fundamentals of Transition Metal Catalyzed Atom Transfer Radical Polymerization

In 1995, a new class of controlled/"living" radical polymerization method was reported by the groups of Matyjaszewski[40] and Sawamoto.[41] This new process named atom transfer radical polymerization (ATRP),[40] has had a tremendous impact on the synthesis of macromolecules with well-defined compositions, architectures and functionalities.[42-58] ATRP has been successfully mediated by a variety of metals, including those from groups IV (Ti[59]), VI (Mo[60-62]), VII (Re[63]), VIII (Fe[64-67], Ru[41, 68] and Os[69, 70]), IX (Rh[71]and Co[72]), X (Ni[73, 74] and Pd[75]) and XI (Cu[40, 53, 76]). Copper complexes have been the most thoroughly investigated in ATRP and are perhaps the most efficient

catalysts based on broad range of monomers and applicability to diverse reaction media. Copper catalyzed ATRP is mechanistically similar to ATRA with the exception that the reaction conditions are modified in such a way that more than one addition step occurs.

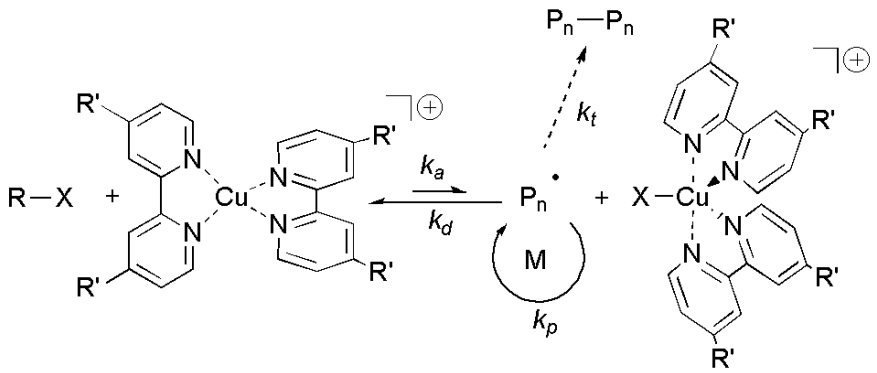

Scheme 1.3.1. Proposed mechanism for copper(I)/2,2'-bipyridine catalyzed ATRP.

As indicated in Scheme 1.3.1, a homolytic cleavage of an alkyl halide bond (RX) by a copper(I) bipyridine complex generates an alkyl radical and a corresponding copper(II) bipyridine complex. The newly formed radicals can initiate polymerization by addition across a double bond of a vinyl monomer, propagate, terminate by either coupling or disproportionation, or be reversibly deactivated by the copper(II) bipyridine complex. In ATRP, formation of radicals is reversible and stationary radical concentration is low because the equilibrium between the activation (k_a) and deactivation (k_d) processes, $K_{ATRP}=k_a/k_d$, is strongly shifted to the left-hand side ($k_a<<k_d$). This in turn minimizes radical termination reactions and enables synthesis of polymers with predetermined molecular weights, narrow molecular weight distributions and high functionalities.[43] Copper catalyzed ATRP is well suited for the preparation of (*co*)polymers with controlled topologies, including star- and comb-like polymers, as well as branched, hyperbranched, dendritic, network, and cyclic type structures.[52] The basic strategies for producing polymeric materials by ATRP are illustrated in Figure 1.3.1.

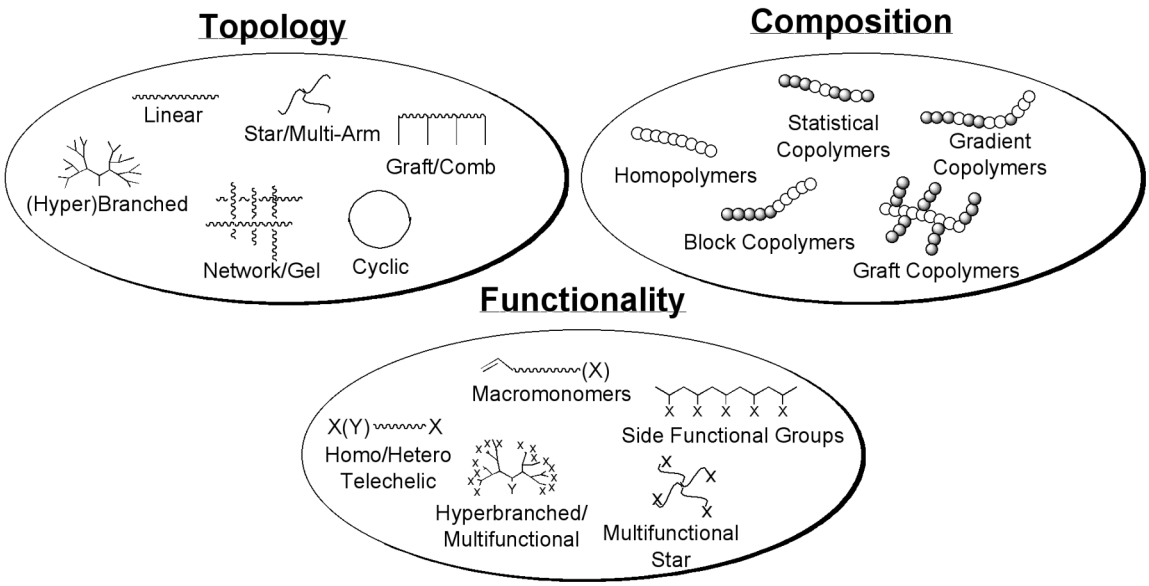

Figure 1.3.1. Schematic representation of polymers with controlled topology, composition and functionality synthesized using copper catalyzed ATRP.

1.4 Transition Metal Catalyzed Atom Transfer Radical Addition in Organic Synthesis

The efficient synthesis of cyclic systems continues to be an important area of modern organic chemistry. The increasingly common methodology for the formation of such cyclic systems involves free radical cyclization protocols[35, 77-79] in particular due to the pioneering work of Giese (tin hydride mediated radical addition to olefins),[80] Barton (radical decarboxylation and deoxygenation)[81, 82] and Curran (iodine atom transfer radical reactions).[83] The majority of such reactions are typically mediated by organotin or organosilane reagents as illustrated in Scheme 1.4.1. Perhaps, apart from high toxicity of organotin reagents, the main disadvantage of these methods is that they are reductive in nature. In other words, the resulting cyclized product looses the halogen group functionality and is therefore not suitable for further functionalization. Additionally, the

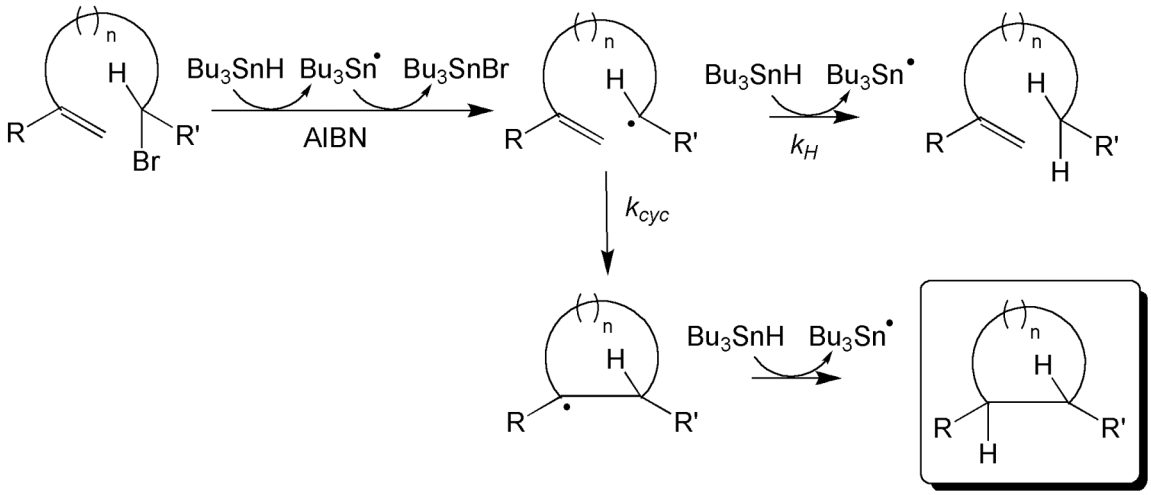

Scheme 1.4.1. Free radical cyclization mediated by nBu$_3$SnH.

Table 1.4.1. Copper catalyzed cyclization of unsaturated trichloroesters.

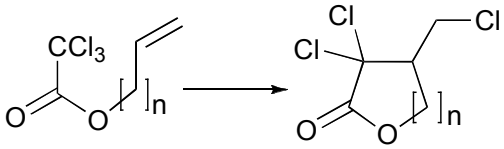

catalyst (mol %)	n	solvent	T (^{o}C)	time (h)	conv. (%)	yield (%)	Ref.
CuCl (2)	1	MeCN	110	16	72	34	38
CuCl (2)	1	^{i}PrOH	110	16	21	3	38
CuCl (2)	1	^{t}BuOH	110	16	40	19	38
CuCl (20)	1	MeCN	110	16	97	59	38
CuCl (30)	1	MeCN	110	16	98	95	38
Cu_2O (2)	1	MeCN	110	16	49	27	38
$Cu(NO_3)_2$ (2)	1	MeCN	110	16	68	47	38
CuCl/PMDETA (10)	1	DCE	80	12-48	/	48	36
CuCl/TPEDA (10)	2	DCE	80	12-48	/	99	36
CuCl/TPMA (3)	2	DCE	80	12-48	/	90	36
CuCl/bpy (30)	3	DCE	84	18	100	60	84
CuCl/bpy (30)	3	DCE	130	2.5	100	58	84
CuCl/TPEDA (10)	3	DCE	80	12-48	/	53	36
CuCl/TPMA (10)	3	DCE	80	12-48	/	53	36
CuCl/TPEDA (10)	4	DCE	80	12-48	/	51	36
CuCl/TPMA (10)	4	DCE	80	12-48	/	70	36

DCE=1,2-dichloroethane, PMDETA= *N*, *N*, *N'*, *N''*, *N''*-pentamethyldiethyelenetriamine, bpy=2,2'-bipyridine, TPEDA= *N*,*N*,*N'*,*N'*-tetrakis(2-pyridylmethyl)ethylenediamine, TPMA= tris[(2-pyridyl)methyl]amine. For ligand structures refer to Scheme 1.5.2.

competition between radical cyclization (k_{cyc}[R$^{\bullet}$], Scheme 1.4.1) and trapping by hydrogen atom abstraction (k_H[R$^{\bullet}$][nBu$_3$SnH], Scheme 1.4.1) typically results in the

mixture of products, unless slow addition of organotin or organosilane reagents is employed. Transition metal catalyzed atom transfer radical addition (TMC ATRA) is another convenient method for the construction of various ring systems.[15] The first successful example of copper mediated ATRC reaction included the synthesis of trichlorinated γ-lactones from readily accessible alkenyl trichloroacetates (Table 1.4.1).[38, 85] The reaction was highly selective, but required elevated temperatures (110-130 °C) and large amounts of copper catalyst (20-30 mol% relative to substrate). Some improvements have been achieved utilizing tetradentate nitrogen based ligands such as tris(2-pyridylmethyl)amine (TPMA) and tris[2-(*N*,*N*-dimethylamino)ethyl]amine (Me_6TREN) (*vide infra*), resulting in a decrease in the amount of required catalyst (3-10 mol% relative to substrate) and reaction temperature (80 °C).[36, 84, 86, 87] A range of crown

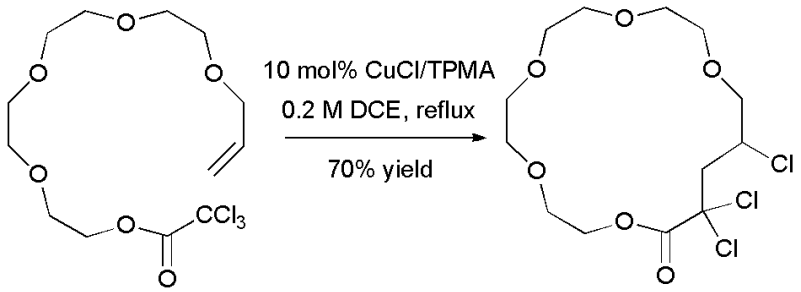

Scheme 1.4.2. Synthesis of crown ethers using copper catalyzed ATRC.

ethers have also been synthesized using this methodology (Scheme 1.4.2).[36] TMC ATRA is also suitable for the synthesis of various functionalized β- and γ-lactams. In general, the cyclization of α-*N*-allylcarbamoyl radicals is a difficult process requiring high temperatures, primarily due to the high barrier to rotation around amide bond. As indicated in Scheme 1.4.3, only the *anti* conformer can cyclize and *N*-protecting groups typically regulate the *syn*-*anti* equilibrium.[88] Cyclizations of γ-lactam precursors in the

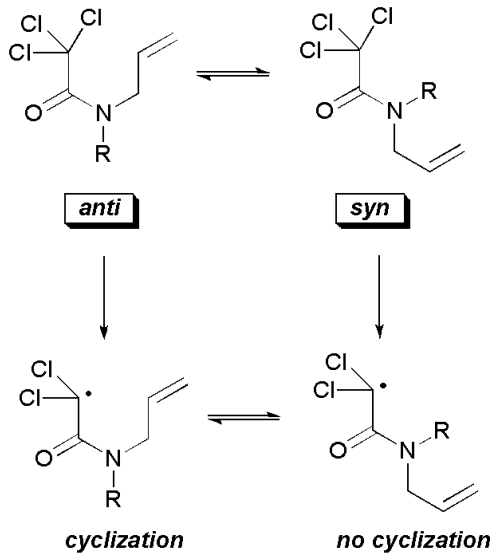

Scheme 1.4.3. *Syn-anti* equilibrium in cyclization of α-*N*-allylcarbamoyl radicals.

presence of only $Cu^{I}Cl$ required elevated reaction temperatures (80-140°C).[89-92] However, efficient cyclizations were achieved at temperatures as low as 25°C when suitable complexing ligands such as 2,2-bipyridine (bpy) (Table 1.4.2), [89] *N*-alkyl-2-pyridylmethanimine (NPMI)[93] or tris[2-(*N*,*N*-dimethylamino)ethyl]amine (Me_6TREN)[92, 94, 95] were used. As will be discussed in the next section, the role of complexing ligand in these systems is not only to increase the solubility of the copper complex in the reaction medium, but also to regulate the equilibrium constant for atom transfer ($K_{ATRA}=k_{a,1}/k_{d,1}$, Scheme 1.2.1). Copper(I) chloride in conjunction with 2,2'-bipyridine was also found to efficiently catalyze ATRC of several α-chloroglycine derivatives with a 3-alkenyl substituent at nitrogen (Scheme 1.4.4).[96] These reactions proceeded via 2-aza-5-alken-1-yl radicals as intermediates which bear an electron-withdrawing carbonyl substituent at the radical center and at nitrogen. The cyclized products resembled proline, an important amino acid needed for the production of collagen and cartilage.

Table 1.4.2. Synthesis of γ-lactams using copper catalyzed ATRC.[89]

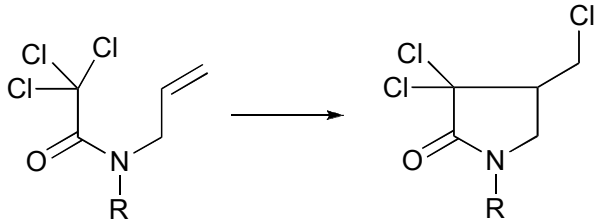

catalyst (mol %)	R	solvent	T (°C)	time (h)	yield (%)
CuCl (30)	Bn	MeCN	80	18	68
CuCl/bpy (30)	Bn	CH_2Cl_2	RT	1	98
CuCl (30)	Ts	MeCN	RT	24	97
CuCl/bpy (5)	Ts	CH_2Cl_2	RT	0.2	91
CuCl (30)	Boc	MeCN	80	4	80
CuCl/bpy (30)	Boc	CH_2Cl_2	RT	2	78

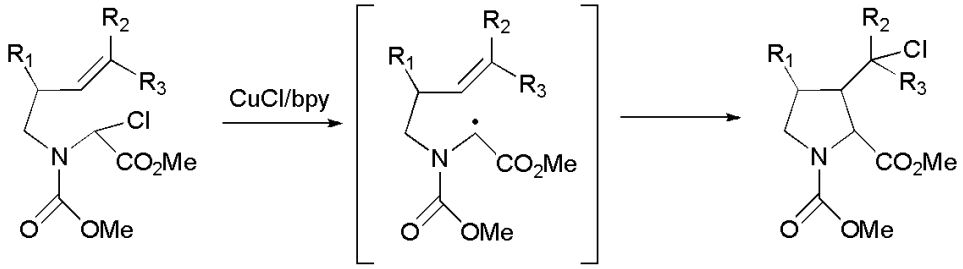

Scheme 1.4.4. Copper catalyzed ATRC of α-chloroglycine derivatives to 3-(1-chloroalkyl)-substituted prolines.

Lastly, copper(I) complexes with nitrogen based ligands have been shown to be quite effective in catalyzing sequentially both ATRA and ATRC. In the case of ATRC followed by ATRA, substrates are typically chosen such that intermolecular addition reactions are slower than intramolecular ones. Some representative examples of these cascade type reactions are illustrated in Scheme 1.4.5.[39, 97]

In summary, copper catalyzed ATRA and ATRC reactions can be utilized in the synthesis of various substrates that can be used as building blocks for the construction of complex molecules and natural products. Until recently, one of the principal drawbacks

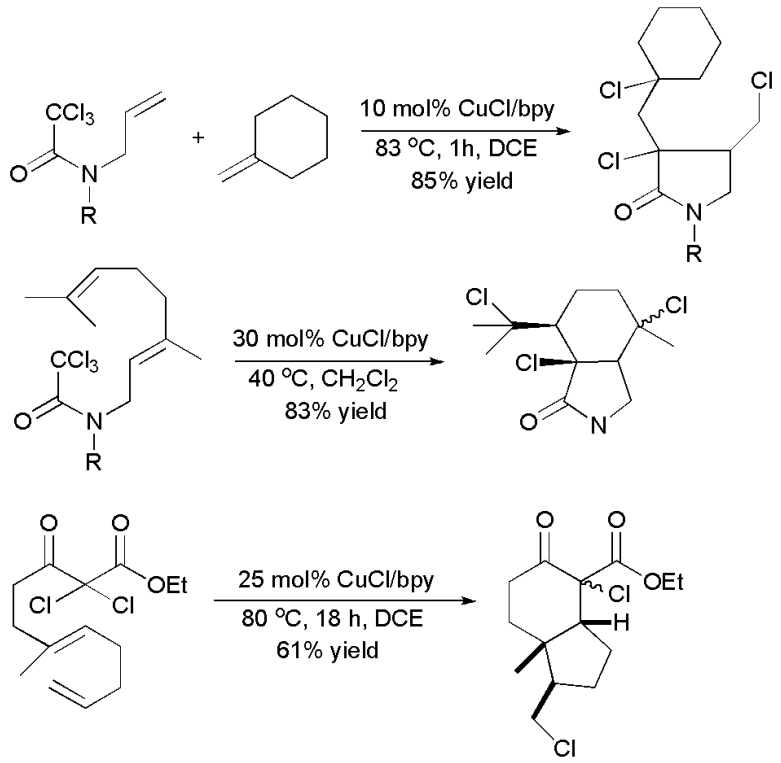

Scheme 1.4.5. Sequential ATRA and ATRC reactions catalyzed by CuCl/bpy complex.

of these useful synthetic tools remained the large amount of copper complex needed to achieve high selectivity towards the desired target compound (typically 5-30 mol% relative to substrate). This obstacle caused serious problems in product separation and catalyst regeneration, making both processes environmentally unfriendly and expensive. In order to better understand factors that led to the development of novel methodologies that can be used to drastically reduce the amount of copper catalysts in ATRA and ATRC, it is necessary to carefully define and examine the components and characteristics of both systems. In the next two sections, mechanistic and structural understanding of copper catalyzed ATRA/ATRC will be discussed.

1.5 Basic Components of Transition Metal Catalyzed Atom Transfer Radical Addition

Transition metal catalyzed atom transfer radical addition (ATRA) is a multicomponent system, composed of an alkene, an alkyl halide and a transition metal complex. Typical alkenes that are used in ATRA include simple α-olefins (1-hexene, 1-octene and 1-decene), styrenes, meth(acrylates) and acrylonitrile. Initiators, on the other hand, are commonly polyhalogenated alkanes,[27, 32-34] benzylic halides,[10, 25, 26] *N*-haloamines,[10] α-halonitriles,[98, 99] α-haloacetates[34, 100], α-haloaldehydes[20, 101, 102] and alkylsulfonyl halides[27-32] (Scheme 1.5.1).

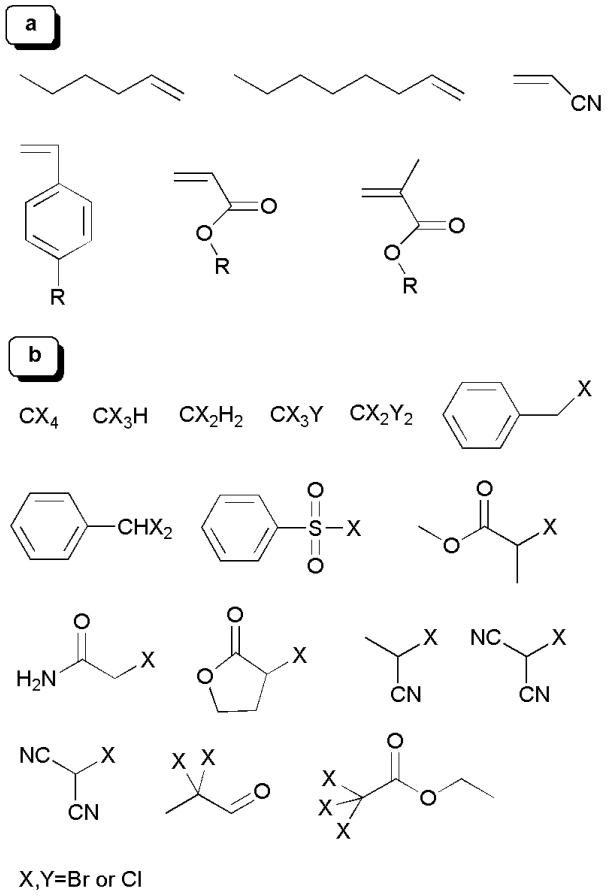

Scheme 1.5.1. Examples of alkenes (a) and alkyl halides (b) commonly used in copper mediated ATRA.

Transition metal complex is perhaps the most important component of the catalytic system because it regulates dynamic equilibrium between the dormant (alkyl halide) and propagating species (radicals). For copper catalyzed ATRA this is typically achieved utilizing bidentate (2,2'-bipyridine (bpy)[84, 86, 87] and *N*-alkyl-2-pyridylmethanimine (NAlkPMI)[15, 37, 92, 103-107]), tridentate (*N*, *N*, *N'*, *N''*, *N''*-pentamethyldiethyelenetriamine (PMDETA)[108-110] and trispyrazolyl borate (Tp^x)[111, 112]), tetradentate (1,1,4,7,10,10-hexamethyltriethylenetetramine (HMTETA)[36], tris[2-(dimethylaminoethyl]amine (Me_6TREN)[92, 95, 103] and tris[(2-pyridyl)methyl]amine (TPMA)[36, 113]) and multidentate (*N*,*N*,*N'*,*N'*-tetrakis(2-pyridylmethyl)ethylenediamine (TPEDA)[36, 113]) nitrogen based complexing ligands (Scheme 1.5.2).

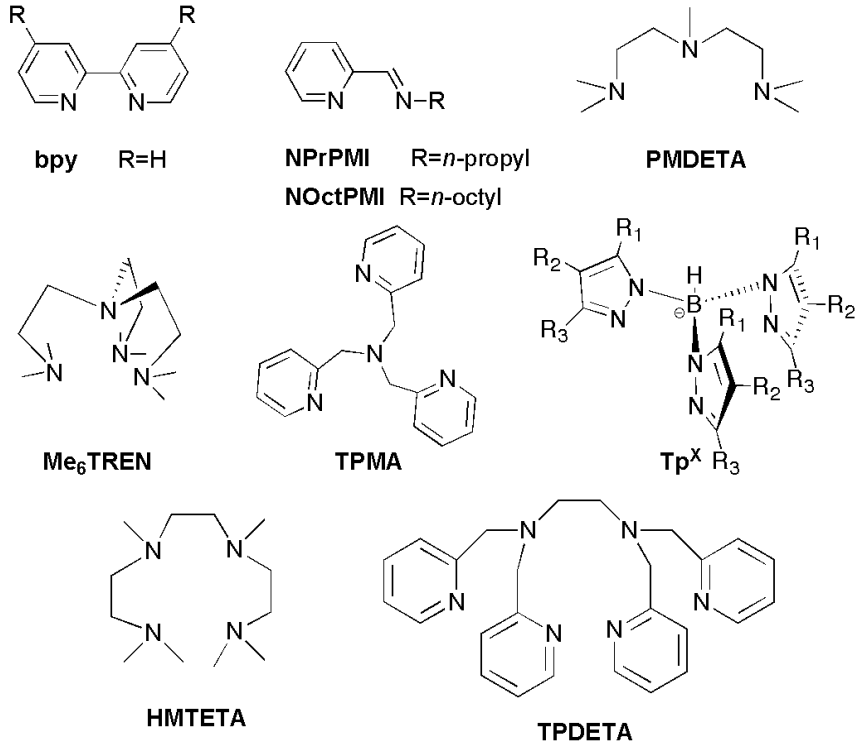

Scheme 1.5.2. Structures of nitrogen based ligands commonly used in copper catalyzed ATRA.

1.6 Kinetics of Copper Catalyzed Atom Transfer Radical Addition

According to the proposed mechanism outlined in Scheme 1.2.1, the rate of alkene consumption in copper catalyzed ATRA is given by the following equation:

$$-\frac{d[alkene]}{dt} = k_{add}[R^{\bullet}][alkene]$$

Neglecting termination reactions due to the persistent radical effect,[114-119] monoadduct activation by assuming that $k_{a,2}\approx 0$ and using a fast equilibrium approximation, the radical concentration ($[R^{\bullet}]$) in the system is given by:

$$[R^{\bullet}] = \frac{k_{a,1}[Cu^{I}L_{m}X][RX]}{k_{d,1}[Cu^{II}L_{m}X_{2}]}$$

Combining these two expression gives the following rate law for copper catalyzed ATRA:

$$-\frac{d[alkene]}{dt} = \frac{k_{a,1}k_{add}[Cu^{I}L_{m}X][RX][alkene]}{k_{d,1}[Cu^{II}L_{m}X_{2}]} = \frac{K_{ATRA}k_{add}[Cu^{I}L_{m}X][RX][alkene]}{[Cu^{II}L_{m}X_{2}]}$$

where $K_{ATRA}=k_{a,1}/k_{d,1}$. Therefore, the rate of alkene consumption in copper catalyzed ATRA depends on the equilibrium constant for atom transfer (K_{ATRA}), concentrations of alkyl halide ([RX]) and alkene, addition rate constant of alkene (k_{add}), and the ratio of concentrations of activator ($Cu^{I}L_{m}X$) and deactivator ($Cu^{II}L_{m}X_{2}$). If the radical concentration in the system is constant, a plot of $\ln([alkene]_0/[alkene]_t)$ vs. time should give a straight line with the apparent equilibrium constant for atom transfer being equal to $K_{ATRA}^{app}=K_{ATRA}/[Cu^{II}L_{m}X_{2}]=\text{slope}/k_{add}[RX]_0[Cu^{I}]_0$.

1.7 Equilibrium Constants for Atom Transfer Radical Addition

The equilibrium constant for ATRA, $K_{ATRA}=k_{a,1}/k_{d,1}$, provides critical information about the position of dynamic equilibrium between dormant and active species during addition (Scheme 1.2.1). As stated above, the relative magnitude of K_{ATRA} can be easily accessed from the rate of alkene consumption using $\ln([M]_0/[M]_t)$ vs. t plots which provide values for the apparent equilibrium constant $K_{ATRA}^{app}=K_{ATRA}/[Cu^{II}L_mX_2]$. More accurate values can be obtained from model studies using modified analytical solution of the persistent radical effect[114] originally developed by Fischer[115-117] and Fukuda[118]:

$$F(Cu^{II}L_mX_2) = 2k_tK_{ATRA}{}^2t + \frac{1}{3[Cu^{I}L_mX]_0}$$

For the simplest case when the initial concentration of the activator $[Cu^{I}L_mX]_0=C_0$ is equal to the initial concentration of the alkyl halide $[RX]_0=I_0$, the function $F(Cu^{II}L_mX_2)$ can be calculated as:

$$F(Cu^{II}L_mX_2) = \frac{C_0{}^2}{3(C_0-Y)^3} - \frac{C_0}{(C_0-Y)^2} + \frac{1}{C_0-Y}$$

where Y is equal to the concentration of the deactivator $[Cu^{II}L_mX_2]$. Therefore, a plot of $F(Cu^{II}L_mX_2)$ vs. time should give a straight line once the equilibrium is established and K_{ATRA} can be calculated from the slope, $K_{ATRA}=(\text{slope}/2k_t)^{1/2}$. Although this methodology has never been applied to copper catalyzed ATRA, it has been extensively used in mechanistically similar atom transfer radical polymerization (ATRP). Values of K_{ATRP}

measured for various alkyl halides and $Cu^{I}L_{m}X$ complexes commonly used in ATRP and ATRA are summarized in Table 1.7.1.

The values of K_{ATRP} reported in Table 1.7.1 illustrate the strong effect of complexing ligand, halogen and alkyl groups. For ethyl 2-bromoisobutyrate (EBriB), relative values of K_{ATRP} increase in the order bpy (1) < PMDETA (20) < TPMA (2500) < Me_6TREN (40, 000). Furthermore, the value of K_{ATRP} for $Cu^{I}Br$/TPMA and EBriB (9.65×10^{-6}) is approximately 30 times larger than for MBrP (3.25×10^{-7}), indicating that

Table 1.7.1. Values of K_{ATRP} for $Cu^{I}X$/L complexes measured in CH_3CN at 22 ^{o}C.

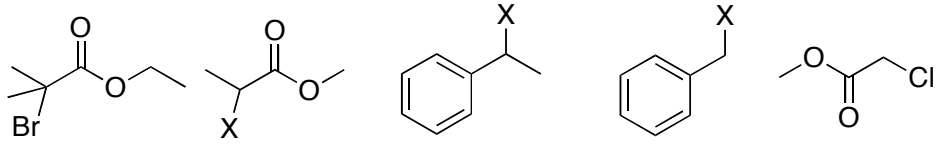

EBrIB | **MBrP (X=Br) MClP (X=Cl)** | **PEBr (X=Br) PECl (X=Cl)** | **BzBr (X=Br) BzCl (X=Cl)** | **MClAc**

Ligand	$Cu^{I}X$	Initiator	K_{ATRP}	Ref.
bpy	$Cu^{I}Br$	EBriB	3.93×10^{-9}	114
PMDETA	$Cu^{I}Br$	EBriB	7.46×10^{-8}	114
TPDETA	$Cu^{I}Br$	EBriB	2.00×10^{-6}	120
TPMA	$Cu^{I}Br$	EBriB	9.65×10^{-6}	114
	$Cu^{I}Br$	PEBr	4.58×10^{-6}	114
	$Cu^{I}Cl$	PECl	8.60×10^{-7}	114
	$Cu^{I}Br$	BzBr	6.78×10^{-7}	114
	$Cu^{I}Br$	MBrP	3.25×10^{-7}	114
	$Cu^{I}Cl$	MClP	4.28×10^{-8}	114
Me_6TREN	$Cu^{I}Br$	EBrIB	1.54×10^{-4}	121
	$Cu^{I}Cl$	MClAc	3.30×10^{-6}	121

tertiary alkyl halides are more reactive than secondary ones. Lastly, the values of K_{ATRP} for RBr are approximately 6 to 10 times larger than those for Cl-based systems. These differences indicate that the C-Br bond is relatively weaker than the C-Cl bond in comparison to Cu^{II}-Br and Cu^{II}-Cl bonds.

1.8 Activation and Deactivation Rate Constants for Atom Transfer Radical Addition

1.8.1 Activation Rate Constants

Prior to the development of an analytical solution of the persistent radical effect for transition metal mediated ATRA and ATRP, the activity of the catalyst was typically accessed by independently measuring the activation (k_a) and deactivation (k_d) rate constants. Activation rate constants in copper catalyzed ATRA are typically determined from model studies in which a copper(I) complex is reacted with alkyl halide in the presence of radical trapping agents such as TEMPO.[122-124] Rates are determined by monitoring the rate of disappearance of alkyl halide in the presence of a large excess of the activator (Cu^IL_mX) and TEMPO. Under such pseudo-first order conditions, the activation rate constant can be calculated from $\ln([RX]_0/[RX]_t)$ vs. t plots (slope=-$k_a[Cu^IL_mX]_0$).

In one of the earlier studies, the activation rate constants for the reaction between various substituted sulfonyl chlorides and copper(I) chloride in acetonitrile at 110 ^oC were found to obey the Hammett's equation (Table 1.8.1).[125, 126] These results indicated that the homolytic cleavage of the C-Cl bond was the rate determining step during ATRA, consistent with the mechanism discussed in Scheme 1.2.1. In a related study, thermodynamic parameters derived from the activation rate constants for the reaction between chlorobenzene and $FeCl_2$ in acetonitrile revealed the large negative entropies of the activation, which suggested the formation of an ordered activation complex in the transition state (Table 1.8.2).[127] This was in agreement with the inner sphere electron

Table 1.8.1. Rate constants for atom transfer from sulfonyl chlorides to $Cu^{I}Cl$ in CH_3CN ($RSO_2Cl + Cu^{I}Cl \rightarrow RSO_2^{\cdot} + Cu^{II}Cl_2$) in the presence of styrene at 110 °C.[125, 126]

R	k_a ($Lmol^{-1}s^{-1}$)
p-$OMeC_6H_4$	5.73×10^{-2}
p-MeC_6H_4	6.43×10^{-2}
C_6H_5	8.93×10^{-2}
p-ClC_6H_4	1.12×10^{-1}
p-BrC_6H_4	1.14×10^{-1}
p-$NO_2C_6H_4$	1.99×10^{-1}

Table 1.8.2. Activation rate constants (k_a) and thermodynamic parameters for the reaction $RCCl_3 + FeCl_2 \rightarrow RCCl_2^{\cdot} + Fe^{III}Cl_3$ in CH_3CN.[127]

R	T (°C)	k_a ($M^{-1}s^{-1}$)	$\Delta H^{\neq}$ ($kcalmol^{-1}$)	$\Delta S^{\neq}$ ($calmol^{-1}K^{-1}$)
C_6H_5	34	$(5.63\pm0.03)\times10^{-3}$	14.5±0.5	-21.6±2
$C_6H_5C(O)$	36	$(1.45\pm0.08)\times10^{-3}$	14.4±0.4	-24.9±1
$C_6H_5OC(O)$	34	$(0.52\pm0.01)\times10^{-3}$	12.5±0.8	-32.9±2.5

transfer (ISET) mechanism proceeding by the bimolecular reaction. Similar results were also obtained using $CpCr(CO)_3$ complex (Table 1.8.3).[128]

By far, the vast majority of activation rate constants for alkyl halides were determined following the discovery of copper catalyzed ATRP.[42, 122-124] The activation rate constants were found to strongly depend on the structures of complexing ligand, alkyl halide, solvent and temperature. In a recent study of a variety of copper(I) complexes with nitrogen-based ligands, values of k_a were found to span more than six

Table 1.8.3. Activation rate constants (k_a) and thermodynamic parameters for the reaction $RBr + CpCr(CO)_3 \rightarrow R^{\cdot} + CpCr(CO)_3Br$ in toluene.[128]

RBr	T (K)	k_a ($M^{-1}s^{-1}$)	$\Delta H^{\neq}$ ($kcalmol^{-1}$)	$\Delta S^{\neq}$ ($calmol^{-1}K^{-1}$)
$BrCH_2CO_2Me$	274	$(1.71\pm0.22)\times10^{-4}$	16.8±1.8	-14±6
	296	$(1.77\pm0.34)\times10^{-3}$		
$BrCH_2CN$	246	$(1.56\pm0.36)\times10^{-3}$	13.8±2.1	-15±6
	263	$(1.05\pm0.26)\times10^{-2}$		
p-NO_2-$C_6H_4CH_2Br$	263	$(2.20\pm0.41)\times10^{-2}$	14.1±3.4	-13±10
	280	$(1.08\pm0.25)\times10^{-1}$		

orders of magnitude (Table 1.8.4).[129] Generally, the activation rate constant in ATRP/ATRA will depend on the topology of the complexing ligand (cyclic~linear<branched), the nature of the N-ligand (aryl amine<aryl imine<alkyl amine~pyridine), steric bulk around the metal center and the linking unit between the nitrogen atoms (C4<<C3<C2) or the "bite" angle.

Table 1.8.4. Activation rate constants for various ligands with ethyl-2-bromoisobutyrate (EBrIB) in the presence of $Cu^{I}Br$ in CH_3CN at 35 ^{o}C.[129]

Ligand	k_a **(Lmol^{-1}s^{-1})**
bpy	0.066
PMDETA	2.7
TPMA	62
Me_6TREN	450

Compounds that contain halogen atoms activated by trihalomethyl, dihalomethyl, α-carbonyl, phenyl, vinyl or cyano groups make efficient ATRP and ATRA initiators. The reactivity of these initiators can be correlated with bond dissociation energy (BDE)[130] and generally depends on:

- degree of initiator substitution (primary<secondary<tertiary)
- leaving atom/group (Cl<Br<I)
- radical stabilizing groups (-Ph~C(O)OR<<CN)

Representative examples are shown in Figure 1.8.1.

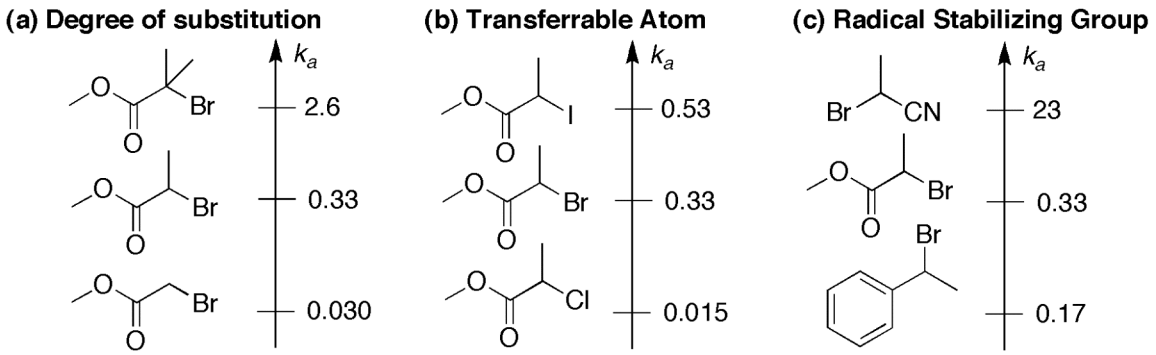

Figure 1.8.1. Values of k_a ($M^{-1}s^{-1}$) in ATRA/ATRP for various initiators with $Cu^{I}X$/PMDETA (X=Br,Cl or I) measured in CH_3CN at 35 ^{o}C.

1.8.2 Deactivation Rate Constants

Deactivation rate constants (k_d, Scheme 1.2.1) have been much less studies in ATRA. The principal reason is the lack of experimental techniques for measuring relatively fast deactivation process, which is typically on the order of 1.0×10^{8}-1.0×10^{9} $M^{-1}s^{-1}$. Kochi et. al. have determined deactivation rate constants for 5-hexenyl and cyclopropylmethyl radicals in the presence of copper(II) halides and pseudohalides,[131-133] taking into account the known rates of radical rearrangement that are readily accessible from pulse laser photolysis measurements.[134] Results are summarized in Table 1.8.5. Relatively large values of the measured rate constants suggested that the deactivation process occurred through an atom rather than electron transfer process, consistent with the mechanism proposed in Scheme 1.2.1.

The rate constants of deactivation (k_d) can also be determined in a competitive clock reaction using TEMPO as a radical trap, as demonstrated for 1-phenylethyl radicals

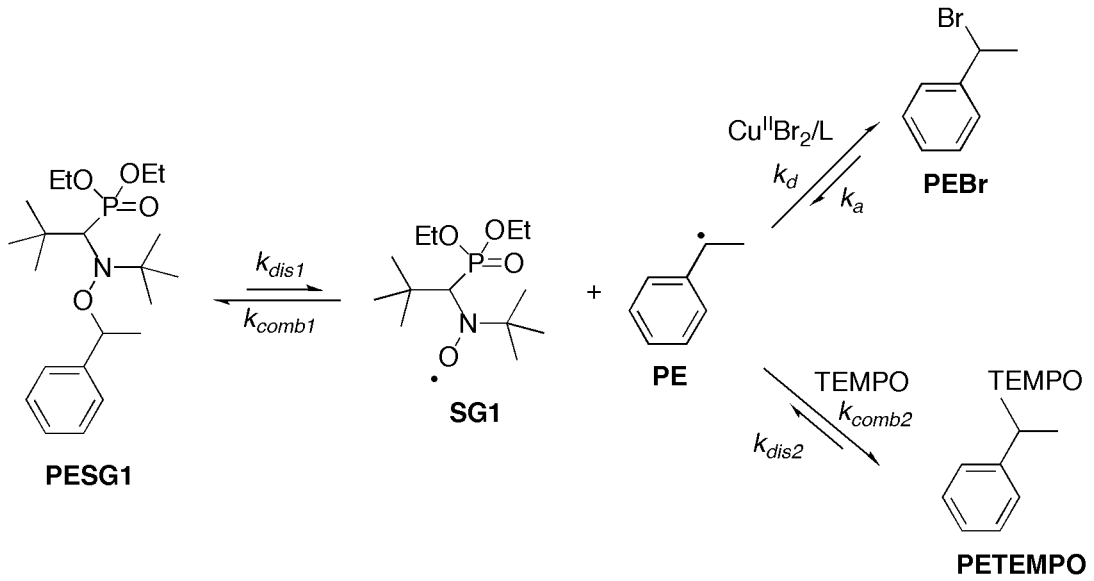

Scheme 1.8.1. Model reactions for deactivation rate constant measurements.

in mechanistically similar ATRP.[123] 1-Phenylethyl radical in this model system was generated by thermal decomposition of 1-(*N*,*N*-(2-methylpropyl-1)(1-deithylphosphono-2,2-dimethyl-propyl-1-)-*N*-oxyl)-1-phenylethane (PESG1) alkoxyamine (Scheme 1.8.1). Results are summarized in Table 1.8.6. In the deactivation process, $Cu^{II}Br_2$/dNbpy complex was more active in ethyl acetate than in acetonitrile. Deactivation was also slower with $Cu^{II}Cl_2$ than $Cu^{II}Br_2$ complexes. Furthermore, the $Cu^{II}Br_2$/dNbpy complex appeared to have higher activity than either $Cu^{II}Br_2$/PMDETA or $Cu^{II}Br_2$/Me_6TREN. In a related study, activation and deactivation rate constants in ATRP for copper complexes with a series of tridentate nitrogen based ligands were determined and correlated with

Table 1.8.5. Rate constants of deactivation (k_d) of 5-hexenyl and cyclopropylmethyl radicals by copper(II) halides and pseudohalides at 25 °C in CH_3CN.[131-133]

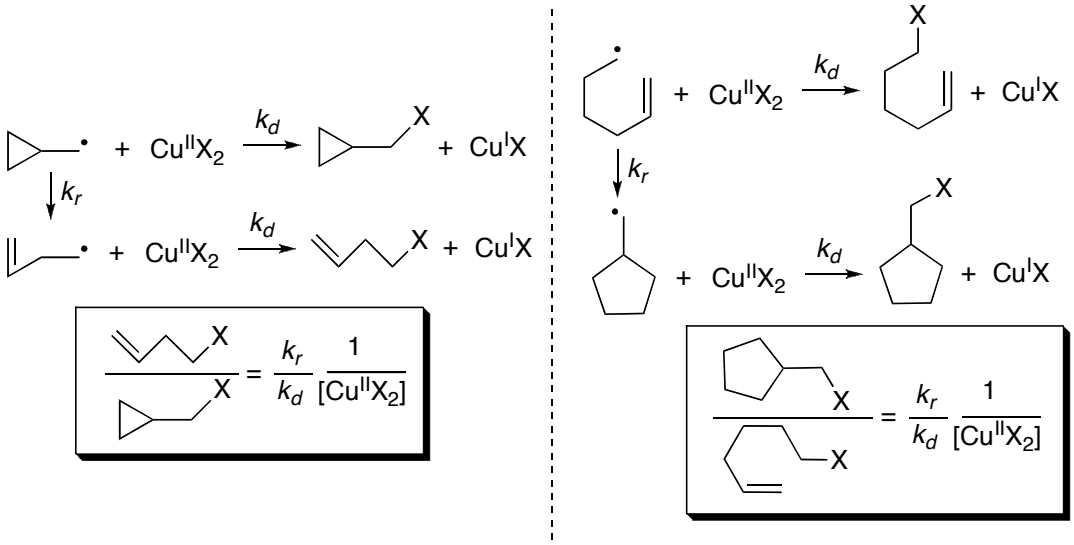

Radical	Copper(II)[a]	k_r/k_d[b]	k_d ($M^{-1}s^{-1}$)
5-hexenyl	$Cu^{II}(NCS)_2$	3.9×10^{-4}	2.6×10^{8}
cyclopropylmethyl	$Cu^{II}(NCS)_2$	2.7×10^{-1}	3.6×10^{8}
5-hexenyl	$Cu^{II}Cl_2$	4.0×10^{-4}	2.0×10^{8}
cyclopropylmethyl	$Cu^{II}Cl_2$	9.2×10^{-2}	1.1×10^{9}
5-hexenyl	$Cu^{II}Br_2$	4.0×10^{-4}	2.0×10^{8}
cyclopropylmethyl	$Cu^{II}Br_2$	2.3×10^{-2}	4.3×10^{9}

[a]$[Cu^{II}X_2]$=1.0 M. [b]k_r(5-hexenyl radicals)=1.0×10^{5} s^{-1} and k_r(cyclopropylmethyl radicals)=1.0×10^{8} s^{-1}.[134]

Table 1.8.6. Deactivation rate constants (k_d) for 1-phenylethyl radicals measured under various conditions at 75 °C.[123]

Complex	Solvent	$k_d/M^{-1}s^{-1}$
$Cu^{II}Br_2$/dNbpy	CH_3CN	2.5×10^{7}
$Cu^{II}Br_2$/PMDETA	CH_3CN	6.1×10^{7}
$Cu^{II}Br_2/Me_6TREN$	CH_3CN	1.4×10^{7}
$Cu^{II}Br_2$/2dNbpy	ethyl acetate	2.4×10^{8}
$Cu^{II}Cl_2$/2dNbpy	CH_3CN	4.3×10^{6}

Table 1.8.7. Structure-activity study of tridentate nitrogen based ligands in copper catalyzed ATRP.[a]

Ligand	Red. Potential (mV)	k_a ($M^{-1}s^{-1}$)	k_d ($M^{-1}s^{-1}$)
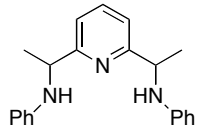	200	2.0×10^{-6}	7.2×10^{7}
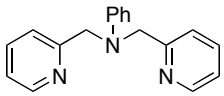	70	1.4×10^{-3}	9.1×10^{6}
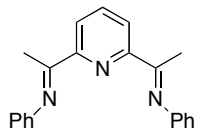	65	4.0×10^{-4}	7.9×10^{6}
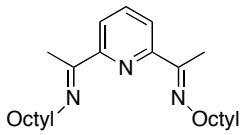	-110	1.4×10^{-2}	3.1×10^{6}
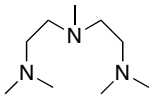	-155	1.0×10^{-1}	6.1×10^{6}
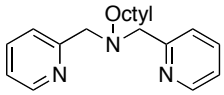	-175	6.6×10^{-1}	3.3×10^{6}
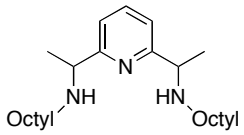	-220	5.0×10^{-2}	4.2×10^{5}
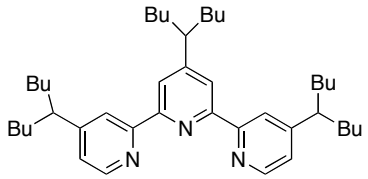	-240	4.2×10^{-1}	4.1×10^{5}

[a]Activation (k_a, 35 °C, CH_3CN) and deactivation (k_d, 75 °C, CH_3CN) rate constants were determined for 1-phenylethyl bromide (1-PEBr) and 1-(*N*,*N*-(2-methylpropyl-1)-(1-diethylphosphono-2,2-dimethylpropyl-1-)-*N*-oxyl)-1-phenylethane (PESG1), respectively.

redox potentials.[135] The study found that more reducing copper catalysts formed faster activating copper(I) and slower deactivating copper(II) species (Table 1.8.7). The rate of activation was dependent on the nature of nitrogen binding site in the ligand. Generally, the activation rate constant increased for ligands with alkyl amine or pyridine complexing sites. Furthermore, the phenyl substituted ligands formed very slow activating and fast deactivating catalysts. Slower deactivation rate constants were found for catalysts with a central pyridine unit in the ligand than for catalysts derived from ligands with a central amine unit. In general, the activity of tridentate nitrogen based ligands decreased in the following order: alkyl amine~pyridine>alkyl imine>>aryl imine> aryl amine.

With recent advances in determination of the equilibrium constant for atom transfer ($K_{ATRA}=k_a/k_d$), deactivation rate constants ($k_d=k_a/K_{ATRA}$) can now be easily obtained for a variety of alkyl halides from readily accessible activation rate constants (k_a).[114] The presented methodologies for the determination of activation (k_a), deactivation (k_d) and overall equilibrium constant for ATRA (K_{ATRA}) can be easily applied for catalyst screening, and also provide crucial information necessary for the design of highly active catalysts (*vide infra*).

1.9 Structural Understanding of Copper Catalyzed Atom Transfer Radical Addition

Structural characterization of transition metal complexes involved in catalysis is essential for understanding of the reaction mechanism and can provide invaluable information regarding catalyst design and performance. In ATRA and ATRP reactions,

the catalyst typically consists of a transition metal accompanied by a complexing ligand and counterion, which can form a covalent or ionic bond with the metal center. An efficient catalyst should be able to expand its coordination sphere and oxidation number upon halogen atom abstraction from an alkyl halide (ATRA) or dormant polymer species (ATRP). Additionally, the catalyst should not participate in any side reactions, as they would result in lowering of the catalytic activity. Concurrent reactions which can occur during the ATRA or ATRP process include: (a) monomer, solvent or radical coordination to the metal center, (b) oxidation/reduction of radicals to radical cations/anions, respectively, (c) β-halogen abstraction, and (d) disproportionation (Scheme 1.9.1).[42, 55-58, 136, 137]

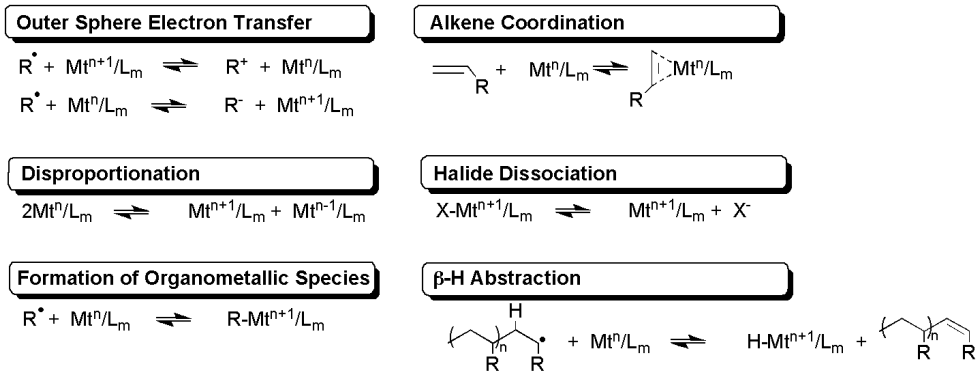

Scheme 1.9.1. Possible side reactions in transition metal catalyzed ATRA/ATRP.

Structural features of copper(I) and copper(II) complexes with monodentate, bidentate and tridentate nitrogen based ligands (Scheme 1.5.2) have been reviewed recently.[55] In this section, we will concentrate on recent advances in structural characterization of highly ATRA and ATRP active copper complexes with tetradentate (tris[2-(dimethylaminoethyl]amine (Me_6TREN)[92, 95, 103, 138-140] and tris[(2-pyridyl)methyl]amine (TPMA)[36, 113, 140-142]) and multidentate (*N*,*N*,*N'*,*N'*-tetrakis(2-pyridylmethyl)ethylene-diamine (TPEDA)[36, 113, 120]) nitrogen based ligands. As discussed

in the previous section, the high activity of these complexes can be explained in terms of increased values of the activation rate constants (k_a, Table 1.8.4) and the equilibrium constant for atom transfer (K_{ATRA} or K_{ATRP}, Table 1.7.1), when compared to other copper(I) complexes with bidentate and tridentate nitrogen based ligands.[57,114,120,123,143,144]

1.9.1 Structural Features of Copper(I) Complexes

Structures of copper(I) complexes with tetradentate tris[2-(dimethylaminoethyl]amine (Me_6TREN) ligand are very rare.[55] The principal problem in their isolation lies in the fact that they are extremely air and moisture sensitive. Schindler and coworkers have successfully isolated and structurally characterized a $[Cu^I(Me_6TREN)][ClO_4]$ complex.[145] The solid state X-ray structure of the complex (Figure 1.9.1) indicated that copper(I) cation is coordinated by four nitrogen atoms of Me_6TREN ligand (Cu^I-N(equatorial)=2.122(7) Å and Cu^I-N(axial)=2.200(14) Å).

Formally, this complex can be best described as trigonal pyramidal in geometry due to the weak coordination of the perchlorate anion (Cu^I-O=3.53(1) Å) to the copper(I)

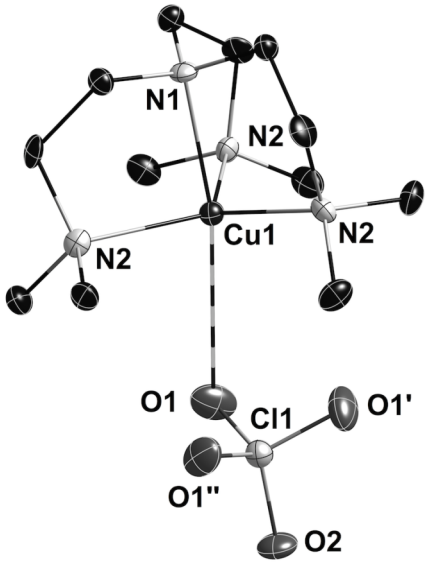

Figure 1.9.1. Molecular structure of $[Cu^I(Me_6TREN)][ClO_4]$.

center. In the case of $Cu^{I}Br/Me_6TREN$ complex, EXAFS studies have indicated several possible structures in solution which included $[Cu^{I}(Me_6TREN)][Br]$, $[Cu^{I}(Me_6TREN)][Cu^{I}Br_2]$ and $Cu^{I}(Me_6TREN)'Br$ (Me_6TREN' denotes a tricoordinate Me_6TREN).[56, 145-147] These structures were based on the validated assumption that the maximum coordination number of copper(I) should not exceed four.[148]

The TPMA ligand generally coordinates to the copper(I) center in a tetradentate fashion, similarly to Me_6TREN.[149-152] Due to the rigid ligand geometry and the tendency of copper(I) to adopt tetrahedral geometry, the axial Cu^{I}-N bond length is typically elongated and the fifth coordination site occupied by a monodentate ligand such as CH_3CN. The role of counterion coordination (in particular Br^- and Cl^-) in these complexes still remains very unclear. Recently, we were able to isolate and structurally characterize neutral $Cu^{I}(TPMA)Cl$[153] and $Cu^{I}(TPMA)Br$[154] complexes. To our surprise,

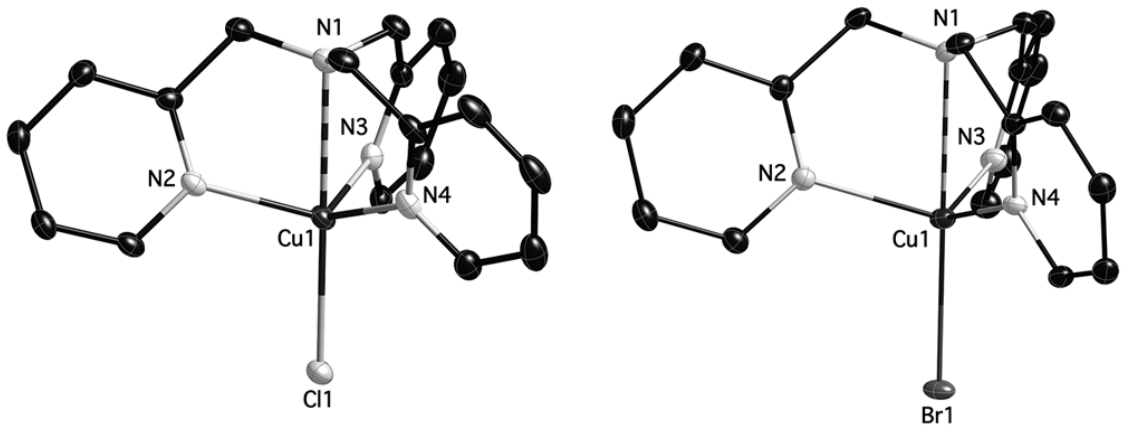

Figure 1.9.2. Molecular structures of $Cu^{I}(TPMA)Cl$ and $Cu^{I}(TPMA)Br$ complexes.[†]

both complexes contained coordinated halide anions (Figure 1.9.2). In $Cu^{I}(TPMA)Cl$, the copper(I) ion was coordinated by four nitrogen atoms with bond lengths of

[†] Structural features of copper(I) complexes with the TPMA ligand will be discussed in detail in Chapters 2,3, and 4.

2.0704(11), 2.0833(11) and 2.0888(11) Å for the equatorial Cu^I-N and 2.4366(11) Å for the axial Cu^I-N bonds, and a chlorine atom with a bond length of 2.3976(4) Å. The molecular structure of Cu^I(TPMA)Br was similar to the structure of Cu^I(TPMA)Cl and the complex was also found to be pseudo-pentacoordinated in the solid state due to the coordination of TPMA (Cu^I-N_{eq}=2.1024(15), 2.0753(15), 2.0709(15) Å, Cu^I-N_{ax}=2.4397(14) Å) and bromine atom to the copper(I) center (Cu^I-Br=2.5088(3) Å). The axial elongation of Cu^I-N bond was not induced by the coordination of Br^- and Cl^- anions to $[Cu^I(TPMA)]^+$ cations, because similar elongations have been observed in $[Cu^I(TPMA)(CH_3CN)][A]$ (A=ClO_4^-, PF_6^- and BPh_4^-) complexes.[155] These results indicate that halide anions are very weakly coordinated to $[Cu^I(TPMA)]^+$ cations. Therefore, from the mechanistic point of view, activation in the ATRA/ATRP process with copper complexes containing TPMA ligand proceeds with either (a) prior dissociation of halide anion from Cu^I(TPMA)X complex (X=Br^- and Cl^-) or (b) dissociation of X^- from the corresponding $Cu^{II}(TPMA)X_2$, to generate the deactivator $[Cu^{II}(TPMA)X][X]$.

Multidentate nitrogen based ligand *N,N,N',N'*-tetrakis(2-pyridylmethyl)ethylenediamine (TPEDA) has been successfully used in copper mediated ATRA and ATRP reactions.[36, 120] It forms a highly active complex in conjunction with Cu^IBr, which effectively catalyzes controlled/"living" radical polymerizations of methyl acrylate, methyl methacrylate and styrene using very low concentrations of the copper complex (6-8 ppm). The molecular structure of Cu^IBr/TPEDA in the solid state indicated the formation of binuclear $Cu^I_2Br_2$(TPEDA) complex (Figure 1.9.3). In $Cu^I_2Br_2$(TPEDA), each copper(I) center was coordinated by two nitrogen atoms from pyridyl groups (Cu^I-

N=2.024 and 2.057 Å), one tertiary amine nitrogen atom (Cu^I-N=2.336 Å) and a bromine atom (Cu^I-Br=2.327 Å), resulting in a distorted tetrahedral geometry. In solution, Cu^IBr/TPEDA was found to equilibrate between binuclear and mononuclear complexes.

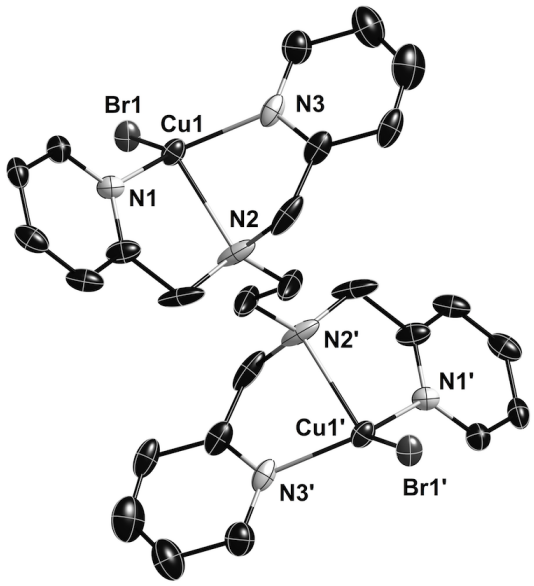

Figure 1.9.3. Molecular structure of binuclear $Cu^I_2Br_2$(TPDETA) complex.

1.9.2 Structural Features of Copper(II) Complexes

Copper(II) complexes that are generated during ATRA and ATRP processes are essential for the deactivation step (i.e. reversible halogen atom abstraction from a copper(II) complex by radicals to generate dormant alkyl halide species and a copper(I) complex, Scheme 1.2.1). The simplest structural parameter that can be correlated with the kinetics of the deactivation process is the Cu^{II}-Br bond length.[120, 146, 153, 154] The strength of this bond can be used as a crude estimate to evaluate deactivation rate constant (k_d), which is responsible for low radical concentration in ATRA and ATRP systems.

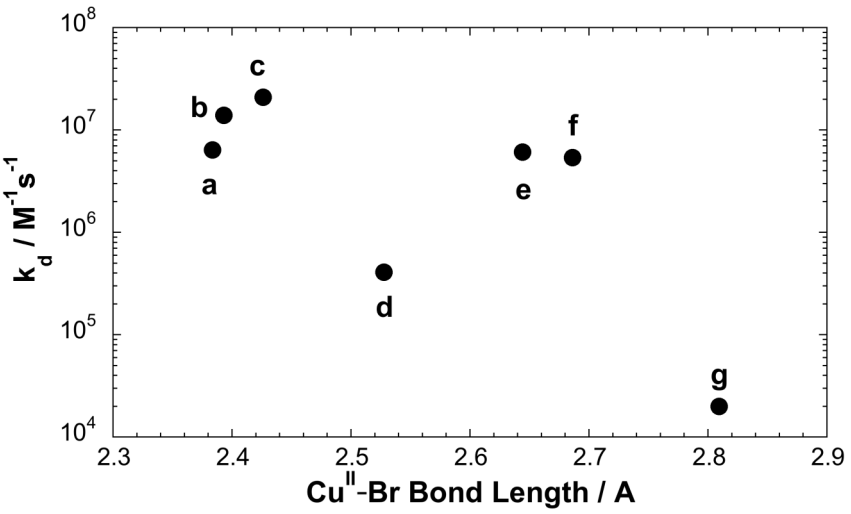

Figure 1.9.4. A plot of Cu^{II}-Br bond length vs. deactivation rate constant (k_d) for a series of copper(II) complexes commonly used in ATRA and ATRP.

Figure 1.9.4 shows the comparison between Cu^{II}-Br bond length and deactivation rate constant for copper(II) complexes with nitrogen based ligands. Structures of the complexes are shown in Figure 1.9.5. As indicated in Figure 1.9.4, there is no direct correlation between the length of the Cu^{II}-Br bond and the deactivation rate constant. It appears that the weaker or longer Cu^{II}-Br bond length is not the only factor that effects the deactivation ([Cu^{II}(Me_4CYCLAM)Br][Br] [k_d=2.0×10^4 $M^{-1}s^{-1}$ and Cu^{II}-Br=2.8092(6) Å] vs. [Cu^{II}(Me_6TREN)Br][Br] [k_d=1.4×10^7 $M^{-1}s^{-1}$ and Cu^{II}-Br=2.393(3) Å]). The structural reorganization of copper(II) complex upon bromine atom abstraction by a corresponding radical is another important process that needs to be taken into account.

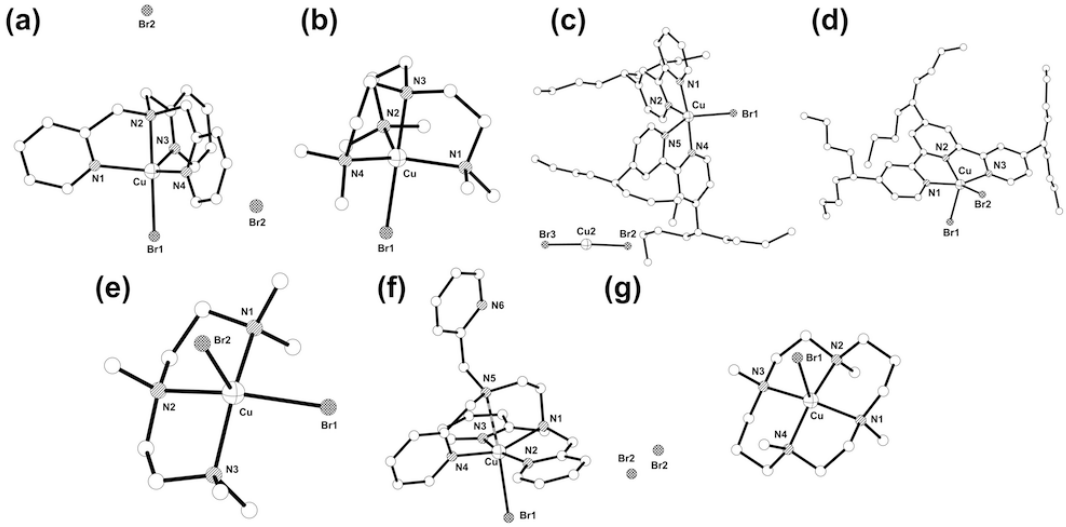

Figure 1.9.5. Molecular structures of [Cu^{II}(TPMA)Br][Br] (a), [Cu^{II}(Me_6TRENBr][Br] (b), [Cu^{II}(dNbpy)$_2$Br][Br] (c), Cu^{II}(tNtpy)Br_2 (d), Cu^{II}(PMDETA)Br_2 (e), [Cu^{II}(TPEDA)Br][Br] (f) and [Cu^{II}(Me_4CYCLAM)Br][Br] (g).

For example, structural features of Cu^{I}(TPMA)Br (Figure 1.9.2) and [Cu^{II}(TPMA)Br][Br][†] (Figure 1.9.5) complexes, which represent activator and deactivator, respectively, are very similar from the point of view of TPMA coordination.[153, 154] In Cu^{I}(TPMA)Br complex, the average Cu^{I}-N_{eq} bond length is 0.0100 Å longer than in the [Cu^{II}(TPMA)Br][Br]. The N_{ax}-Cu-N_{eq} angles are very similar in both complexes, while the average angle in the plane N_{ax}-Cu-N_{ax} is slightly larger in [Cu^{II}(TPMA)Br][Br] (117.53(3)^{o}) than in Cu^{I}(TPMA)Br (113.51(10)^{o}). The only more pronounced difference in TPMA coordination to the copper center can be seen in shortening of Cu-N_{ax} bond length by approximately 0.400 Å on going from Cu^{I}(TPMA)Br to [Cu^{II}(TPMA)Br][Br]. Similar observations were also made in the case of Cu^{I}(TPMA)Cl and [Cu^{II}(TPMA)Cl][Cl] complexes, in which the shortening of Cu-N_{ax} bond length was determined to be 0.389 Å.[153] Therefore, from the structural point of

[†] Structural features of copper(II) complexes with the TPMA ligand will be discussed in detail in chapters 2,3, and 4.

view, the high activity of $Cu^{I}(TPMA)X$ (X=Br^{-} and Cl^{-}) and $[Cu^{II}(TPMA)X][X]$ complexes in ATRA and ATRP can be explained by minimal entropic rearrangement when $Cu^{I}(TPMA)X$ complex homolytically cleaves the R-X bond to generate $[Cu^{II}(TPMA)X][X]$.

1.10 Towards "Greening" of Copper Catalyzed Atom Transfer Radical Addition and Cyclization

Transition metal catalyzed atom transfer radical addition (ATRA) or Kharasch addition,[2, 3, 12-15, 35] despite being discovered nearly 40 years before tin mediated radical addition to olefins[80] and iodine atom transfer radical reaction,[83] is still not fully utilized as a technique in free radical synthesis. As aforementioned, one of the principal reasons for small participation of ATRA in complex molecule and natural product syntheses until recently, remained the large amount of transition metal complex needed to achieve high selectivity towards the desired target compound (5-30 mol% relative to substrate). Such large amounts of catalyst were required in order to compensate for the accumulation of the deactivator (transition metal complex in the higher oxidation state), as a result of unavoidable and often diffusion controlled radical-radical coupling reactions ($k_t \approx 2.0\times10^{9}$ $M^{-1}s^{-1}$). Various methodologies have been developed to overcome this problem and they include: (a) the design of solid supported catalysts, (b) the use of biphasic systems containing fluorous solvents, (c) the use of highly active copper(I) complexes based on ligand design and (d) catalyst regeneration in the presence of environmentally benign reducing agents. These methodologies are discussed in detail in the following sections.

1.10.1 Solid Supported Catalysis

While solid-supported catalysis does not necessarily result in the reduction of the overall copper concentration in ATRA and ATRC, it does in theory allow for catalyst recycling, making this method highly attractive. The success of solid-supported catalysis will largely depend on the accessibility of the immobilized metal catalyst. In other words, active catalyst sites must be readily approachable by not only alkyl halides, but also resulting radicals. In mechanistically similar atom transfer radical polymerization (ATRP), this represents a major problem because the large "living" polymer chains cannot easily diffuse to the solid support.[58, 156-164] However, small molecule synthesis should not be limited by this problem and thus ATRA and ATRC reactions could in theory be successful with solid supported catalyst. Three types of solid supports have been investigated thus far: cross-linked silica, cross-linked polystyrene and JandaJel™.[15, 165, 166]

The first example of solid supported ATRC was performed with a silica supported copper catalyst.[15, 165] The complexing ligand *N*-propyl-2-pyridylmethanimine tethered to silica was easily synthesized by condensing pyridine-2-carboxaldehyde with aminopropyl functionalized silica (Scheme 1.10.1). The catalytic activity of this ligand, in conjunction

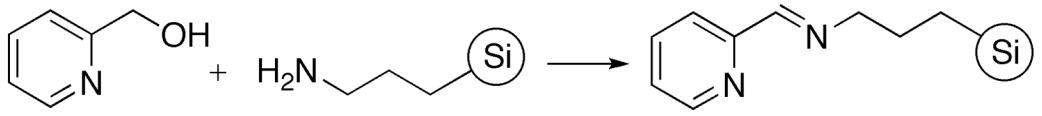

Scheme 1.10.1. Synthesis of a typical silica supported *N*-propyl-2-pyridylmethanimine ligand.

with $Cu^{I}Br$ and $Cu^{I}Cl$, was tested in ATRC of a range of activated and unactivated 2-haloacetamides (Table 1.10.1). Excellent yields of the 5-*exo*-*trig* cyclic products were

obtained for all substrates after 18-48 hours in dichloroethane at reflux using 30 mol% of the catalyst. Furthermore, the activity of copper(I) supported catalyst closely matched the homogeneous environment using structurally similar *N*-butyl-2-pyridylmethanimine ligand.[93, 94]

The catalyst efficiency in this process decreased with each successive run because of the accumulation of the deactivator (Cu^{II} species). This was also visually observed by a distinct color change of the solid support from brown (Cu^{I}) to green (Cu^{II}). Leeching of

Table 1.10.1. ATRC of haloacetamides catalyzed by silica supported copper(I)/*N*-propyl-2-pyridylmethanimine complex.[15, 165]

Entry	Substrate	Product	Time (hr)	Yield (%)
1	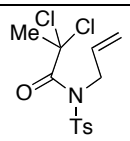	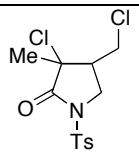	18	94
2	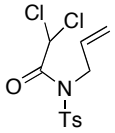	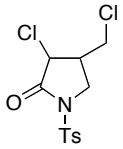	24	96
3	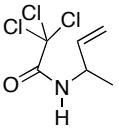	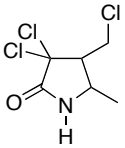	48	75
4	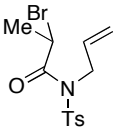	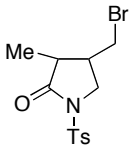	24	92
5	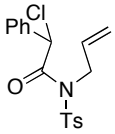	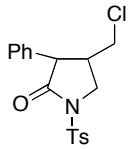	22	94
6	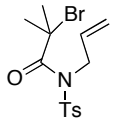	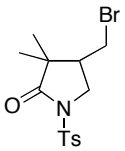	24	92
7	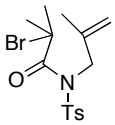	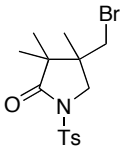	36	90

the catalyst was not detected by ICP-MS and the copper content in solution remained constant after three independent runs.

In a related study, a series of nitrogen based ligands bound to polystyrene and JandaJel™ supports were investigated in copper catalyzed 5-*exo-trig*, 5-*exo-dig*, 4-*exo-trig* and 5-*endo-trig* ATRC reactions to yield nitrogen heterocycles similar to those shown in Table 1.10.1.[166] Generally, it was found that the type of solid support had negligible effect on the efficiency and selectivity of the cyclization. However, both were found to strongly depend on the nature of complexing ligand used. For example, 5-*exo-trig* cyclization of haloacetamides (entries 1, 3 and 6, Table 1.10.1) proceeded more rapidly with *N*-alkyl-2-pyridylmethanimine ligands than with PMDETA or Me_6TREN. These results were explained in terms of catalyst leaching, which was confirmed experimentally. Similar to the earlier study,[165] catalyst efficiency also significantly decreased upon recycling because of the accumulation of the copper(II) complex.

1.10.2 Biphasic Systems

Historically, liquid-liquid biphasic systems have been utilized in synthetic processes to allow for simple work-up by taking advantage of the differences in miscibility. The most commonly used combinations are aqueous biphasic systems, which consist of water as one phase and either hydrocarbons or other low polarity solvents as the other. The aqueous phase may contain a dissolved reagent of catalyst. The drawback of a water/hydrocarbon system is it's inherent limitation to non-water sensitive reagents.[167, 168] The method of fluorous biphasic systems was first demonstrated by Horvath and Rabai as an environmentally friendly and water-free approach to catalyst recycling.[169] Fluorous solvents, such as perfluorinated alkanes, ethers, and tertiary

amines are non-polar in nature, but have a low solubility in most hydrocarbon solvents. When a biphasic system of this nature is heated under pressure, the two phases become miscible and the reaction proceeds under homogeneous conditions. After cooling, the two solvents again become immiscible, allowing the catalyst to be easily separated from the products. In the seminal work done by Horvath and Rabai, hydroformylation reactions were performed with rhodium catalysts dissolved in the fluorous solvent, which provided more solubility for alkenes as compared to the previously used aqueous systems. Catalyst leaching was not detected in the hydrocarbon layer and subsequent reactions were performed with the same catalyst solution with negligible differences difference in product yields.[169]

Fluorous biphasic systems were applied to ATRA and ATRC reactions in an effort to reduce catalyst loadings and allow for complete metal extraction from the reaction mixture.[113] In this work, perfluorinated analogues of PMDETA and Me_6TREN were synthesized as ligands for copper catalyzed ATRC of pent-4-enyl trichloroacetate to yield eight membered ring lactone (Scheme 1.10.2).[86, 87, 170]

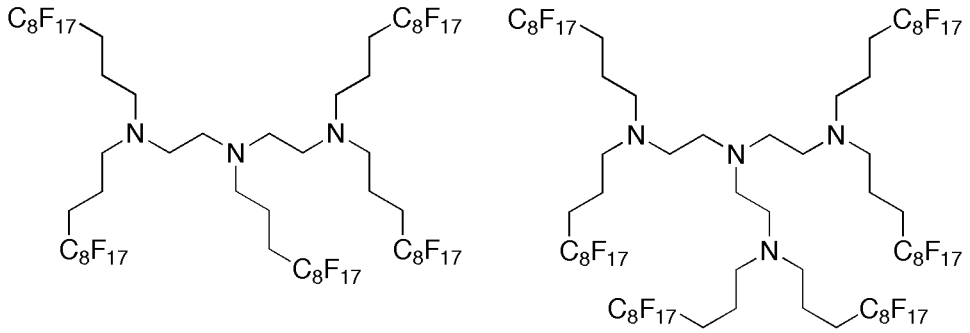

Scheme 1.10.2. Perfluorinated derivatives of PMDETA and Me_6TREN.

Fluorous biphasic reactions were performed in a mixture of perfluoroheptane, trifluorotoluene and 1,2-dichloroethane at 80 ^{o}C (Table 1.10.2). The reaction kinetics of the fluorous biphasic systems were found to be considerably slower than the analogous

reaction with $Cu^{I}Cl$/PMDETA in non-fluorinated solvents. In 20 hours, yields of less than 50% were obtained with catalyst concentrations of 1 mol % relative to the substrate.

Table 1.10.2. Conversion of trichloroester under homogeneous and fluorous biphasic conditions.

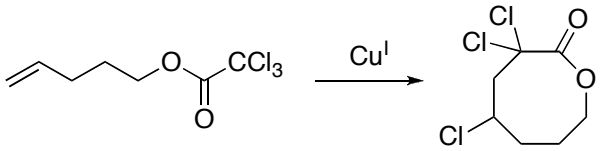

Catalyst[a]	Catayst ratio (mol%)	Lactone yield (%)	Time (h)
Homogeneous Catalysis			
$Cu^{I}Cl$/PMDETA	1	50	10
$Cu^{I}Cl$/PMDETA/Fe	1	99	10
Heterogeneous Catalysis			
$Cu^{I}Cl$/PMDETA$_F$	1	34	20
$Cu^{I}Cl$/Me$_6$TREN$_F$	1	48	20
$Cu^{I}Cl$/PMDETA$_F$	5	88	20
$Cu^{I}Cl$/Me$_6$TREN$_F$	5	97	10
$Cu^{I}Cl$/PMDETA$_F$/Fe	1	91	20
$Cu^{I}Cl$/PMDETA$_F$/Fe	5	99	10
$Cu^{I}Cl$/Me$_6$TREN$_F$/Fe	1	98	20
$Cu^{I}Cl$/Me$_6$TREN$_F$/Fe	5	99	10

[a]Metal to ligand stoichiometry was 1:1, for structures of PMDETA$_F$ and Me$_6$TREN$_F$ refer to Scheme 1.10.2. When added, iron powder was in 10:1 ratio relative to copper catalyst.

These yields doubled with an increase in catalyst loading to 5 mol%. Marked improvement was also reported when 10 equivalents of iron powder relative to the catalyst were used. The role of iron in this system was to reduce copper(II) to copper(I) complex, which was needed to homolytically cleave the alkyl halide bond. Additionally, catalyst recycling in the fluorous phase was tested four times without a noticeable difference in the product yield, provided that iron powder was present in the system.

1.10.3 Development of Highly Active Ligands in Copper Catalyzed Atom Transfer Radical Addition

Another approach to decreasing the copper concentration in ATRA and ATRC reactions is through the use of highly active complexing ligands. While much of the work in this area has been done for copper catalyzed ATRP,[42, 57, 70, 120, 121, 129, 137, 143, 171-175] the results are directly applicable to both ATRA and ATRC. The complexing ligand, in conjunction with copper, is essential for all of these processes because it regulates the dynamic equilibrium for atom transfer ($K_{ATRA\ or\ ATRP}=k_a/k_d$, Scheme 1.5.2).[55, 56] As mentioned earlier in the article, the activity of a certain ligand in ATRA/ATRP process is typically determined by measuring the activation (k_a), deactivation (k_d) and overall

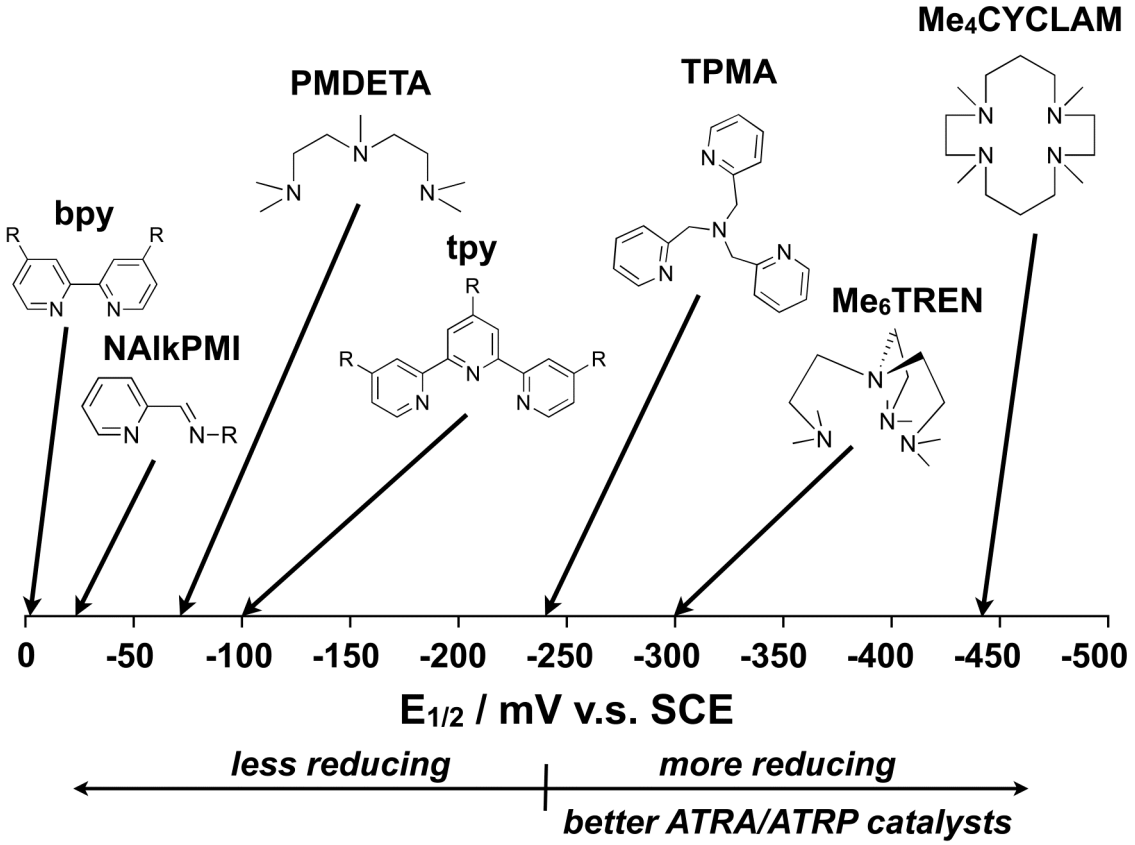

Figure 1.10.1. Redox potentials ($E_{1/2}$ vs. SCE) for copper complexes with neutral nitrogen based ligands commonly used in ATRA and ATRP.

equilibrium constant for atom transfer ($K_{ATRA\ or\ ATRP}$).[114, 123, 129, 135, 143, 144, 171] Also, for complexes that have similar "halidophilicities" or equilibrium constants for halide anion coordination to the copper(II) center, the redox potential can be used as a measure of catalyst activity.[143, 176] This was demonstrated in linear correlation between K_{ATRP} and $E_{1/2}$ values for a series of copper(I) complexes with nitrogen based ligands.[114, 135, 176, 177] Generally, more reducing copper(I) complexes are also better catalysts for ATRA/ATRP (Figure 1.10.1). Currently, the most active ligands in copper mediated ATRA/ATRP are neutral tetradentate and multidentate nitrogen based ligands tris[2-(dimethylaminoethyl]amine (Me_6TREN)[92, 95, 103, 138-140], tris[(2-pyridyl)methyl]amine (TPMA)[36, 113, 140-142], *N*,*N*,*N'*,*N'*-tetrakis(2-pyridylmethyl)ethylenediamine (TPEDA)[36, 113, 120], 1,4,8,11-tetraaza-1,4,8,11-tetramethylcyclotetradecane ($Me_4CYCLAM$)[178], and dimethylated 1,8-ethylene cross bridged 1,4,8,11-tetraazacyclotetradecane (DMCBCy)[121] (Scheme 1.5.2). Additionally, copper(I) complexes containing monoanionic trispyrazolyl borate ligands have also been shown to be very effective catalysts in ATRA and ATRC.[111, 112]

1.11 Highly Efficient Copper Catalyzed Atom Transfer Radical Addition and Cyclization Reactions in the Presence of Reducing Agents

1.11.1 Regeneration of Catalyst in Atom Transfer Radical Addition

Until recently, one of the major drawbacks of transition metal catalyzed ATRA remained the large amount of catalyst required to achieve high selectivity towards the desired target compound (as high as 30 mol% relative to alkene).[179] This obstacle caused serious problems in product separation and catalyst regeneration, making the process environmentally unfriendly and expensive. The principal reason for the need of high catalyst concentration is that radical termination reactions lead to the irreversible accumulation of persistent radical or deactivator ($Cu^{II}L_mX_2$ complex) under typical ATRA conditions. In other words, if the initial catalyst concentration is too low, all of the activator (Cu^{I} complex) will eventually be consumed as a persistent radical and the addition will only reach limited conversions.

Originally, the solution to this problem has been found for copper catalyzed atom transfer radical polymerization (ATRP),[40, 179-186] and was subsequently applied first to ruthenium[187] and then copper[153, 154, 188] catalyzed ATRA reactions. In all of these processes, the activator (transition metal complex in the lower oxidation state) is continuously regenerated from deactivator (transition metal complex in the higher oxidation state) in the presence of reducing agents such as phenols, glucose, ascorbic acid, hydrazine, tin(II) 2-ethylhexanoate, magnesium, and free radical initiators (Scheme 1.11.1). Such regeneration compensates for unavoidable radical-radical coupling

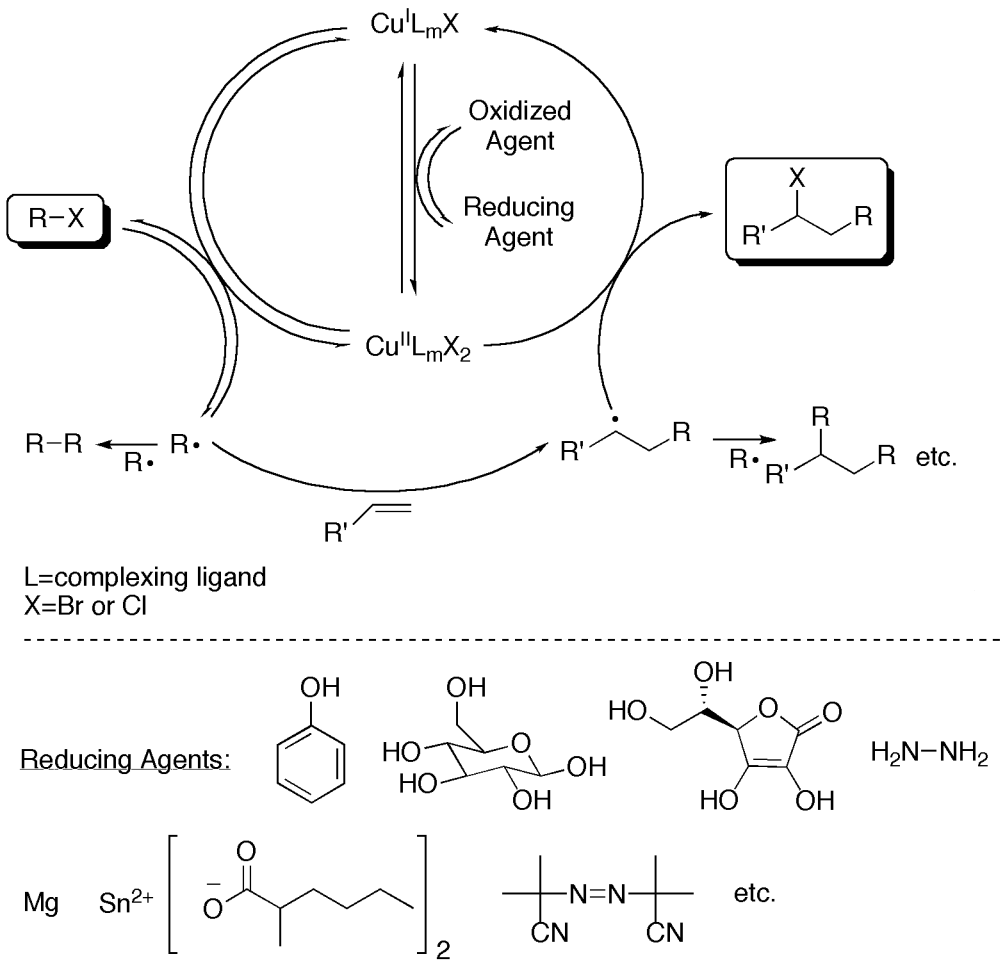

Scheme 1.11.1. Proposed mechanism for copper(I) regeneration in ATRA in the presence of reducing agents.

reactions, enabling a significant reduction in the amount of metal catalyst. When applied to ATRA of CCl_4 to alkenes catalyzed by $Cp^*Ru^{III}Cl_2(PPh_3)$ complex in the presence of AIBN, TONs as high as 44500 were obtained.[187] Even more impressive TONs were achieved with CBr_4 and $[Cu^{II}(TPMA)Br][Br]$ (TPMA=tris(2-pyridylmethyl)amine) complex (as high as 160000), enabling efficient ATRA reactions in the presence of as low as 5 ppm of copper.[154] Previous TONs for copper catalyzed ATRA ranged between 0.1 and 10.[15, 179] Since the seminal reports by our,[153] and the research group of Severin,[187] this method of catalyst regeneration in ATRA has attracted considerable

academic interest,[150, 179, 188-195] and was even successfully applied to intramolecular ATRA or atom transfer radical cyclization (ATRC) reactions.[111, 194-196] The following sections describe synthetic applications and kinetic features of this novel catalytic system.

1.11.2 Highly Efficient Copper Catalyzed Atom Transfer Radical Addition in the Presence of Free-Radical Initiators as Reducing Agents[†]

Highly efficient copper-mediated ATRA in the presence of AIBN was first reported in the addition of CCl_4 and $CHCl_3$ to 1-hexene, 1-octene, styrene, and methyl acrylate.[153] In this seminal work, Cu^I(TPMA)Cl complex was chosen because of its high activity in ATRA and ATRP reactions.[15, 55, 56, 60, 120, 129, 138, 143, 147, 179, 197] However, the conversion of only 2% was observed after 24 h at 60 ^oC in ATRA of CCl_4 to 1-hexene when the ratio of catalyst to alkene was 1:10,000. This result was not surprising because the low catalyst-to-CCl_4 ratio resulted in complete deactivation of the catalyst. In other words, because of irreversible radical-radical termination reactions, Cu^I(TPMA)Cl was converted to [Cu^{II}(TPMA)Cl][Cl]. This situation was changed by the addition of an external radical source such as AIBN. The slow decomposition of AIBN provided constant source of radicals, which continuously reduced [Cu^{II}(TPMA)Cl][Cl] to Cu^I(TPMA)Cl complex. Indeed, when the above reaction was conducted in the presence of 5.0 mol% AIBN (relative to the alkene), 88% conversion of 1-hexene was observed after 24 h with the main product being the desired monoadduct (yield=72%, Table 1.11.1). Increasing the catalyst concentration, under the same reaction conditions,

---

[†] ATRA of polyhalogenated methanes to alkenes with Cu^I(TPMA)Cl will be discussed in detail in Chapters 2 and 3.

Table 1.11.1. ATRA of polychlorinated compounds to alkenes catalyzed by Cu^{I}(TPMA)Cl in the presence of AIBN.[a]

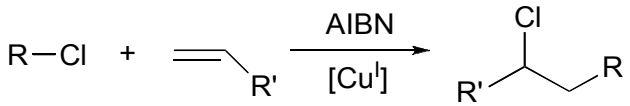

Alkene	RCl	$[Alkene]_0/[Cu^I]_0$	Yield (%)	TON
1-hexene	CCl_4	10000:1	72	7200
		5000:1	98	4900
1-octene	CCl_4	10000:1	67	6700
		5000:1	87	4350
styrene	CCl_4	1000:1	42	420
		500:1	54	270
		250:1	85	212
methyl acrylate	CCl_4	1000:1	60	600
1-hexene	$CHCl_3$	1000:1	56	560
1-octene	$CHCl_3$	500:1	49	245
styrene	$CHCl_3$	1000:1	58	580
methyl acrylate	$CHCl_3$	1000:1	63	630

[a] All reactions were performed in toluene at 60°C for 24 h with $[R\text{-}Cl]_0$:$[alkene]_0$=4.0. The yield is based on the formation of monoadduct and was determined by ^{1}H NMR using toluene as internal standard or column chromatography. The conversion of alkene for all substrates ranged from 85-100%.

resulted in a complete conversion of 1-hexene and increase in the yield of monoadduct (98%). Similar results were also obtained with 1-octene. The TONs in these experiments ranged between 4900-7200 (1-hexene) and 4350-6700 (1-octene), and were by far the highest obtained for copper catalyzed ATRA of CCl_4 to alkenes.[15, 179] The efficient regeneration of the copper(I) complex by AIBN suggested that ATRA reactions could also be conducted using air stable [Cu^{II}(TPMA)Cl][Cl] complex, which was confirmed experimentally.

To test the applicability of this new methodology for copper(I) regeneration in ATRA, additional experiments were conducted using other alkenes as well as alkyl halides (Table 1.11.1). Relatively high yields of the monoadduct were obtained in the ATRA of CCl_4 to styrene and methyl acrylate, but with much higher catalyst loadings. At the Cu^{I}(TPMA)Cl to styrene ratio of 1:250, complete conversion of styrene was

observed after 24 hours and monoadduct was obtained in 85% yield. Further increase in the ratio of styrene to Cu^{I}(TPMA)Cl still resulted in quantitative conversion of styrene, however, more pronounced decrease in the yield of monoadduct was observed. The decrease in the yield of monoadduct was mostly due to the formation of oligomers/polymers. Similar results were also obtained for methyl acrylate. The experiments with less active $CHCl_3$ also worked reasonably well. Relatively high yields were obtained for all alkenes investigated at $[alkene]_0$:$[Cu^{I}]_0$ ratios between 500 and 1000.

Encouraged by the results, we have conducted additional experiments in the presence of [Cu^{II}(TPMA)Br][Br] complex and polybrominated compounds.[154] This selection of the catalyst and alkyl halide should result in a significant improvement in the

Table 1.11.2. ATRA of polybrominated compounds to alkenes catalyzed by [Cu^{II}(TPMA)Br][Br] in the presence of AIBN.[a]

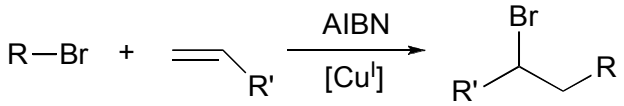

Alkene	RBr	$[Alk.]_0$:$[Cu^{II}]_0$	% Conv.	% Yield	TON
methyl acrylate	CBr_4	200,000:1	~100	81(76)[b]	1.6×10^5
		100,000:1	~100	94	9.4×10^4
styrene	CBr_4	200,000:1	~100	95(86)[b]	1.9×10^5
		100,000:1	99	99	9.9×10^4
methyl acrylate	$CHBr_3$	5,000:1	~100	23(21)[b]	1.1×10^3
		1,000:1	~100	57	5.7×10^2
		500:1	~100	66	3.3×10^2
styrene	$CHBr_3$	5,000:1	~100	77	3.9×10^3
		1,000:1	~100	92	9.2×10^2
1-hexene	$CHBr_3$	10,000:1	67	61(59)[b]	6.1×10^3
1-octene	$CHBr_3$	10,000:1	75	69(54)[b]	6.9×10^3
1-decene	$CHBr_3$	10,000:1	74	63(64)[b]	6.3×10^3

[a]All reactions were performed in bulk at 60°C for 24 hours with $[R\text{-}Br]_0$:$[alkene]_0$:$[AIBN]_0$=4:1:0.05, except reactions with CBr_4 which were performed in CH_3CN. [b]Isolated yield after column chromatography.

catalytic activity because Cu-Br and C-Br bonds are much weaker than the corresponding chloride analogues.[130, 198] Indeed, truly remarkable results were obtained (Table 1.11.2). The activity of $[Cu^{II}(TPMA)Br][Br]$ complex in ATRA of polybrominated compounds to alkenes in the presence of AIBN, based on catalyst loadings, conversion of alkene, and the yield of monoadduct, was approximately 10 times higher than the activity of $[Cu^{II}(TPMA)Cl]Cl]$.[153] Also, for comparable monomers and alkyl halides, its activity exceeded the activity of the $[Cp^*Ru^{III}Cl_2(PPh_3)]$ complex.[187] $[Cu^{II}(TPMA)Br][Br]$, in conjunction with AIBN, effectively catalyzed ATRA reactions of polybrominated compounds to alkenes with concentrations between 5 and 100 ppm, which was by far the lowest number achieved in any metal mediated ATRA. [15, 36, 179, 199-201]

AIBN is not a particularly suitable reducing agent for alkenes with high propagation rate constants in free radical polymerization such as methyl acrylate (MA) ($k_{p,60}=2.8\times10^4$ $M^{-1}s^{-1}$), butyl acrylate (BA) ($k_{p,60}=3.1\times10^4$ $M^{-1}s^{-1}$), vinyl acetate (VA) ($k_{p,60}=7.9\times10^3$ $M^{-1}s^{-1}$) and styrene (sty) ($k_{p,60}=3.3\times10^2$ $M^{-1}s^{-1}$).[202] ATRA of these alkenes in the presence of AIBN at 60°C yielded significant amounts of polymers/telomers unless high copper loadings and/or large excess of alkyl halide (4 eq. relative to alkene) were used.[153, 154, 188] The principal reason for the difficulty in controlling the formation of single addition adduct was not inefficient catalyst regeneration or further activation of the monoadduct, but rather competing polymerization initiated by the presence of AIBN. The potential solution to this problem is to utilize redox-reducing agents that do not generate free radicals, such as magnesium.[194] However, the presence of magnesium as a reducing agent is less desired because it increases the total metal concentration in the system. An alternative solution is to utilize low temperature free radical initiators such as

Table 1.11.3. Ambient-temperature ATRA of polyhalogenated compounds to alkenes catalyzed by $[Cu^{II}(TPMA)X][X]$ (X=Cl^- and Br^-) in the presence of free-radical initiator V-70 as a reducing agent.

Alkene[a]	Product	R-X	$[Alk]_0:[Cu^{II}]_0$	% Yield[b]	TON[c]
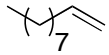	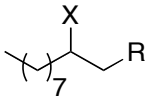	CCl_4	2000:1	80	1600
			1000:1	93	930
		CBr_4	50000:1	88	17500
			10000:1	~100	4600
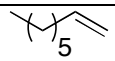	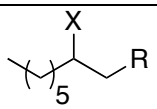	CCl_4	2000:1	84	1680
			1000:1	97	970
		CBr_4	50000:1	93	18500
			10000:1	~100	4400
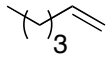	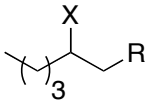	CCl_4	2000:1	85	1750
			1000:1	96	960
		CBr_4	50000:1	93	14500
			10000:1	98	3400
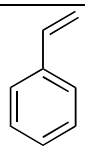	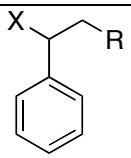	CCl_4	500:1	51	255
		CBr_4	2000:1	57	560
			200:1	91	124
		$CHBr_3$	1000:1	70	700
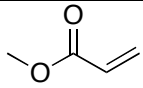	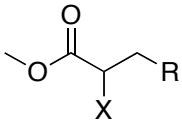	CCl_4	2000:1	62	1240
			1000:1	84	840
		CBr_4	50000:1	63	4400
			10000:1	82	330
		$CHBr_3$	1000:1	48	480
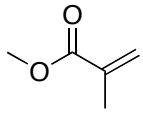	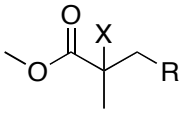	CCl_4	2000:1	44	880
			1000:1	66	660
		CBr_4	20000:1	63	7200
			10000:1	62	6300
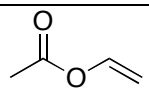	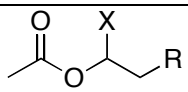	CCl_4	2000:1	70	1220
			1000:1	94	780
		CBr_4	5000:1	84	2500
			1000:1	44	610

[a]All reactions were performed in CH_3CN at ambient temperature (22±2°C) for 24 hours with $[RX]_0:[alkene]_0:[V\text{-}70]_0$=1:1:0.05, except reactions with 1-decene which were performed in 1,2-dichloroethane. [b]Yield is based on the formation of monoadduct and was determined by ^1H NMR spectroscopy using anisole (styrene) or 1,4-dimethoxybenzene (all other alkenes) as internal standards. [c]TONs were calculated taking into account the percent yield of monoadduct for ATRA reactions conducted in the absence of $[Cu^{II}(TPMA)X][X]$ (see ref. [188]).

2,2'-azobis(4-methoxy-2,4-dimethyl valeronitrile) (V-70) that could be used at ambient temperatures and easily, together with radical decomposition products, removed from reaction mixtures. At ambient temperatures, free radical polymerization of highly active

monomers (3.0×10^2 $s^{-1}<k_p$[alkene]$<1.8\times10^3$ s^{-1}), as a result of decrease in propagation rate constants ($k_{p,25}$(MA)=1.3×10^4 $M^{-1}s^{-1}$, $k_{p,25}$(BA)=1.5×10^4 $M^{-1}s^{-1}$, $k_{p,25}$(VA)=3.4×10^3 $M^{-1}s^{-1}$ and $k_{p,25}$(sty)=87 $M^{-1}s^{-1}$)[202] is expected to compete with a halide transfer (1.8×10^3 $s^{-1}<k_{d,2}[Cu^{II}L_mX_2]<1.8\times10^5$ s^{-1}) to a much lesser extent.[203] Consequently, provided efficient regeneration of the copper(I) complex, substantially higher yields of the desired monoadduct could be obtained. Indeed, at ambient temperatures, V-70 has been shown to be a very effective reducing agent for ATRA, enabling selective formation of the monoadduct with a-olefins and highly active alkenes such as methyl acrylate, methyl methacrylate and vinyl acetate (Table 1.11.3).[188] Very recently, copper complexes with tris-pyrazolylborate ligands have been shown to be effective without a reducing agent at low catalysts concentrations (0.33-0.02 mol%) in ATRA of several alkenes and alkyl halides. Small amounts of acetonitrile were employed as a weakly coordinating ligand to saturate the coordination sphere of copper for alkyl halide cleavage, thus lowering the overall radical concentration and preventing the accumulation of copper(II).[204]

1.11.3 Kinetic Studies of Copper Catalyzed Atom Transfer Radical Addition

The main function of the reducing agent in transition metal catalyzed ATRA is to continuously regenerate the activator (transition metal complex in the lower oxidation state), which is needed to homolytically cleave the alkyl halide bond (Scheme 1.11.1).[153, 154, 179, 180, 187, 194, 205, 206] In the absence of a reducing agent, the rate of alkene consumption in ATRA depends on: (a) the equilibrium constant for atom transfer ($K_{ATRA}=k_{a,1}/k_{d,1}$), (b) concentrations of alkyl halide ([RX]) and alkene, (c) addition rate constant of alkene (k_{add}), and (d) the ratio of concentrations of activator ($Cu^{I}L_mX$) and deactivator

($Cu^{II}L_mX_2$). If the radical concentration in the system is constant, a plot of $\ln([\text{alkene}]_0/[\text{alkene}]_t)$ vs. time should give a straight line with the apparent equilibrium

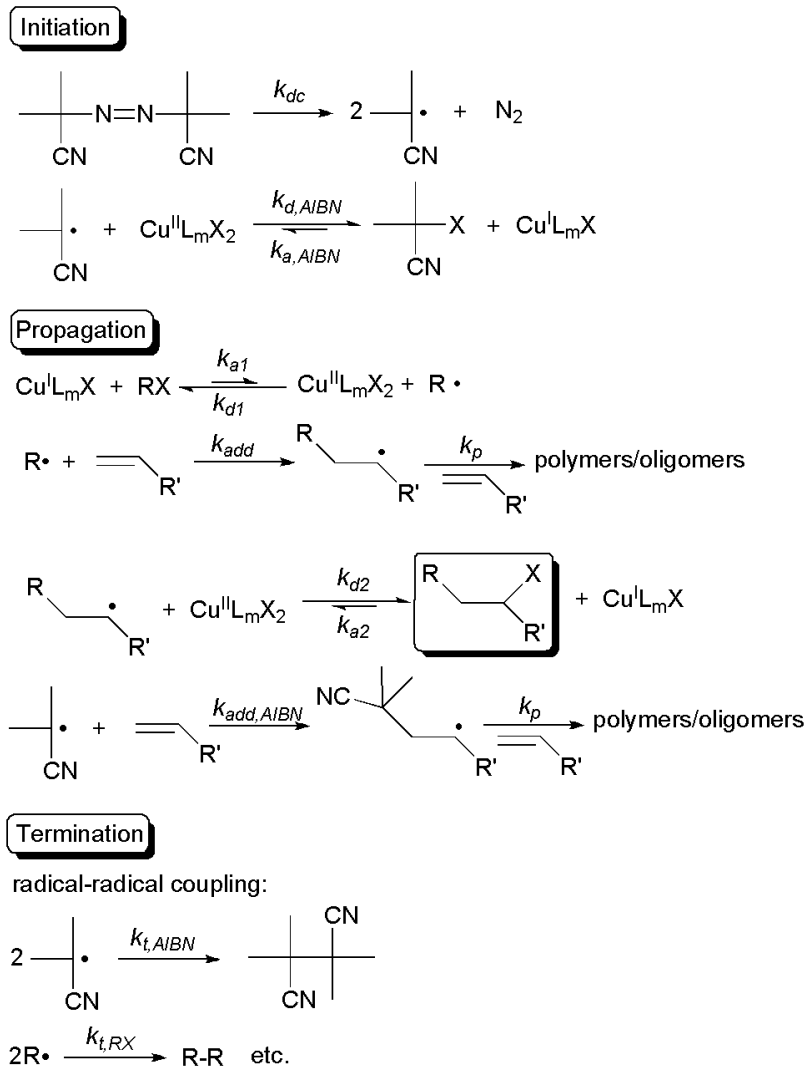

Scheme 1.11.2. Initiation, propagation and termination steps in copper catalyzed ATRA in the presence of free-radical initiator AIBN.

constant for atom transfer being equal to $K_{ATRA}^{app}=K_{ATRA}/[Cu^{II}L_mX_2]=\text{slope}/k_{add}[RX]_0[Cu^{I}]_0$. The reaction kinetics in the presence of free radical reducing agent such as AIBN appear to be rather complex. The principal reason is the incorporation of additional reactions steps that involve AIBN. These steps

are: (a) decomposition of AIBN to generate free radicals, (b) reduction of copper(II) to copper(I) in the presence of AIBN and (c) free radical polymerization of alkene initiated by AIBN. The elementary reactions for these processes are shown in Scheme 1.11.2. The rate of disappearance of alkene (neglecting monoadduct re-activation by assuming that $k_{a2}\approx 0$) is given by the following expression:

$$-\frac{d[alkene]}{dt} = k_{add}[R^{\bullet}][alkene] + k_{add,AIBN}[I^{\bullet}][alkene] + k_p[I-Alk^{\bullet}][alkene]$$

where the first term corresponds to ATRA process and the second and third ones to free-radical polymerization initiated by AIBN (I· denotes radicals formed from the decomposition of AIBN and I-Alk· radicals formed in subsequent additions of I· to alkene). In free radical polymerization, the number of molecules reacting in the initiation step is far less than the number in the propagation step for a process producing high molecular weight polymer. To a very close approximation the former can be neglected and the polymerization rate is given simply by the rate of propagation. Therefore, the above equation can be simplified to:

$$-\frac{d[alkene]}{dt} = k_{add}[R^{\bullet}][alkene] + k_p[I^{\bullet}][alkene]$$

If we combine the equilibrium expressions for copper(I) regeneration and activation/deactivation of alkyl halide (RX), the radical concentration (R·) in the system is equal to:

$$\frac{[Cu^{I}L_mX][I-X]}{[Cu^{II}L_mX_2][I^{\bullet}]} = \frac{k_{d,AIBN}}{k_{a,AIBN}} = \frac{1}{K_{ATRA,AIBN}}$$

$$\frac{[Cu^{II}L_mX_2][R^{\bullet}]}{[Cu^{I}L_mX][R-X]} = \frac{k_{a,1}}{k_{d,1}} = K_{ATRA,RX}$$

$$[R^{\bullet}] = \frac{K_{ATRA,RX}}{K_{ATRA,AIBN}}\frac{[R-X]}{[I-X]}[I^{\bullet}]$$

Substituting this expression into the original equation for the rate of disappearance of alkene in ATRA yields:

$$-\frac{d[alkene]}{dt} = k_{add}\frac{K_{ATRA,RX}}{K_{ATRA,AIBN}}\frac{[R-X]}{[I-X]}[I^{\bullet}][alkene] + k_p[I^{\bullet}][alkene]$$

This equation is not directly usable because it contains a term for the concentration of radicals [I·]. However, using steady-state approximation, this concentration can be easily determined by assuming that the rate of initiation is equal to the rate of termination. In other words:

$$\frac{d[I^{\bullet}]}{dt} = 2k_{dc}[AIBN] = 2k_t[I^{\bullet}]^2 \approx 0$$

$$[I^{\bullet}] = \sqrt{\frac{k_{dc}}{k_t}[AIBN]}$$

Final substitution of the expression for [I·] gives the rate of disappearance of alkene in copper catalyzed ATRA containing free-radical initiator as a reducing agent:

$$-\frac{d[alkene]}{dt} = \sqrt{\frac{k_{dc}}{k_t}[AIBN]}\left(k_{add}\frac{K_{ATRA,RX}}{K_{ATRA,AIBN}}\frac{[R-X]}{[I-X]} + k_p\right)[alkene]$$

From this equation, it is apparent that the rate depends not only on the concentrations of alkene, RX and I-X, but also on the equilibrium constants $K_{ATRA,RX}$ and $K_{ATRA,AIBN}$, addition (k_{add}) and propagation (k_p) rate constants for alkene, as well as decomposition (k_{dc}) and termination (k_t) rate constants for AIBN. Surprisingly, the rate of alkene consumption is not dependent on the concentrations of copper(I) and copper(II) complexes. Several experimental results are fully consistent with these observations.

For alkenes that have low propagation rate constants in free radical polymerization, such as simple α-olefins (1-hexene, 1-octene and 1-decene), high yields of monoadduct can be obtained using low copper(II) concentrations.[153, 154, 188] The

catalytic activity for α-olefins appears to be relatively independent on the concentration of AIBN. However, increase in the concentration of AIBN generally increases the reaction rate.[207] For ATRA of CCl_4 to 1-octene catalyzed by $[Cu^{II}(TPMA)Cl][Cl]$, the apparent reaction order was 0.36 with respect to AIBN, which is close to 0.5 predicted from the above derived rate law. Similarly, the reaction order with respect to AIBN was found to be 0.49 in the case of styrene. Furthermore, for ATRA of CCl_4 to 1-octene, styrene, and methyl acrylate, the apparent rate constant of the reaction was found to be relatively independent on the

Table 1.11.4. Values of k_{obs} (s^{-1}) for the ATRA of CCl_4 to alkenes with varying concentrations of $[Cu^{II}(TPMA)Cl][Cl]$.[a]

$[alkene]_0:[Cu^{II}]_0$ ratio	1-octene	styrene	methyl acrylate
100:1	2.0×10^{-4}	3.7×10^{-5}	2.3×10^{-4}
500:1	1.6×10^{-4}	1.2×10^{-5}	4.3×10^{-4}
1000:1	1.3×10^{-4}	0.7×10^{-5}	5.9×10^{-4}

[a] $[olefin]_0/[CCl_4]_0/[AIBN]_0 = 1:4:0.05$; $[alkene]_0 = 0.95M$.

concentration of copper(II) complex (Table 1.11.4). In a related study, the rates of polymerization in ICAR (initiators for continuous activator regeneration) ATRP of styrene mediated by copper(II) bromide complexes with Me_6TREN, TPMA, PMDETA and dNbpy in the presence of AIBN were very similar,[180] despite large differences in the equilibrium constants for atom transfer in CH_3CN at 35 °C (K_{ATRP} (ethyl 2- bromoisobutyrate)=1.54×10^{-4}, 9.65×10^{-6}, 7.46×10^{-8} and 3.93×10^{-9}, respectively).[114] These results indicate that regardless of the choice of catalyst, the ratio of equilibrium constants $K_{ATRA,RX}/K_{ATRA,AIBN}$ should remain nearly constant.

So far, we have discussed kinetic features of copper catalyzed ATRA in the presence of free-radical initiators from the point of view of reaction rates or alkene consumption. Another important aspect that needs to be addressed is product

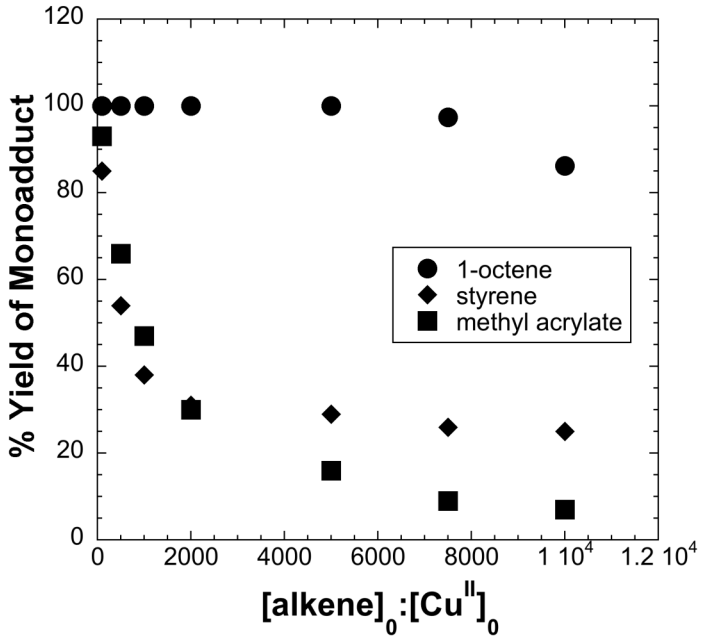

Figure 1.11.1. Effect of $[Cu^{II}(TPMA)Cl][Cl]$ on ATRA of CCl_4 to alkenes in the presence of AIBN.

selectivity. The concentration of deactivator ($Cu^{II}L_mX_2$) plays a crucial role. In order to achieve a high yield of the desired monoadduct, the rate of radical trapping ($k_{d,2}[Cu^{II}L_mX_2]$) should be much higher than the rate of free radical polymerization (k_p[alkene]). This is illustrated in Figure 1.11.1. For simple α-olefins such as 1-octene, the catalyst regeneration was efficient using alkene to copper(II) ratios as low as 10000:1. However, a more pronounced effect of the catalyst loading on alkene conversion and the yield of monoadduct was observed in the case of methyl acrylate and styrene. For styrene, a relatively high yield of the monoadduct was obtained at much higher catalyst loadings (100:1). A further increase in the ratio of styrene to

copper(II) still resulted in quantitative conversions, however, a more pronounced decrease in the yield of monoadduct was observed. The decrease in the yield of monoadduct was mostly due to the formation of polymers as a result of competing radical polymerization initiated by AIBN. This effect was even more pronounced in the case of methyl acrylate. As aforementioned, competing free radical polymerization for highly active alkenes can be suppresed using low temperature free-radical initiators such as 2,2'-azobis(4-methoxy-2,4-dimethyl valeronitrile) or V-70.[188]

1.12 Highly Efficient Copper Catalyzed Atom Transfer Radical Cyclization in the Presence of Reducing Agents

1.12.1 Intramolecular ATRC

In our recent study, intermolecular ATRA of polyhalogenated compounds to alkenes were successfully catalyzed using ppm amounts of copper(II) complexes with TPMA ligand in the presence of free-radical diazo initiators as reducing agents.[153, 154, 179, 188, 206] The logical extension of this methodology is to conduct intramolecular ATRA or atom transfer radical cyclization (ATRC) reactions. Such reactions are synthetically more attractive because they enable the synthesis of functionalized ring systems that can be used as starting materials in the preparation of complex organic molecules.

The methodology used to regenerate activator in ATRA originally developed for Ru[187] and Cu[153, 154] catalysts has been successfully utilized in a range of 5-*exo-trig* and 5-*exo-dig* ATRC reactions of bromoacetamides using 0.1-1 mol% of Cu^{I}(TPMA)Br or [Cu^{II}(TPMA)Br][Br] complexes (Table 1.12.1).[196] The presence of AIBN as a reducing agent enabled a 30-300 fold reduction in the amount of catalyst previously reported for

such cyclizations.[15, 93-95, 103, 166] Very recently, the $Cp^*RuCl_2(PPh_3)$ complex has been shown to be effective in ATRC in the presence of Mg as a reducing agent, producing lactones, lactams, and furans in excellent yields (Scheme 1.12.1).[194, 195]

Table 1.12.1. ATRC of bromoacetamides catalyzed by copper complexes with TPMA ligand in the presence of AIBN.[a]

Substrate	Product	Solvent	T (°C)	Yield (%)
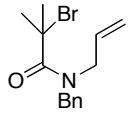	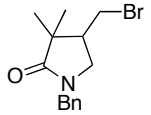	CH_2Cl_2 CH_2Cl_2 Toluene	50 50 110	84 97[b] 87
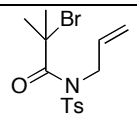	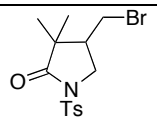	CH_2Cl_2	50	95
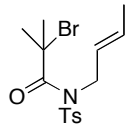	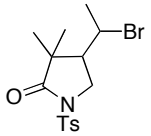	CH_2Cl_2	50	100
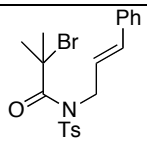	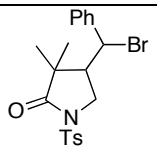	CH_2Cl_2	50	99
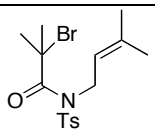	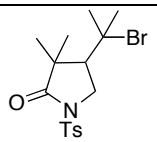	CH_2Cl_2	50	99
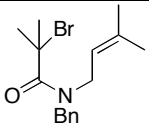	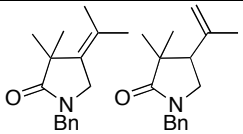	CH_2Cl_2 Toluene	50 110	13[b] 88[b] (1:2)
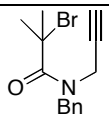	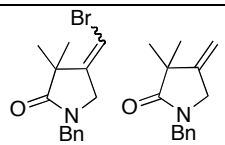	CH_2Cl_2 Toluene	50 110	30 (3:2) 67 (1:1)
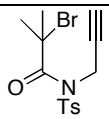	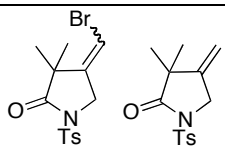	CH_2Cl_2 Toluene	50 110	33 (1:2) 67 (1:1)
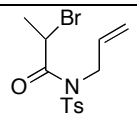	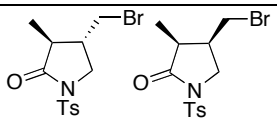	Toluene	110	90 (4:1)

[a]Reactions were performed with $[substrate]_0:[Cu^I \text{ or } Cu^{II}]_0:[AIBN]_0$ = 1:0.01:0.10 for 24 h. [b]$CuBr_2$/TPMA complex was used. Ref. [196]

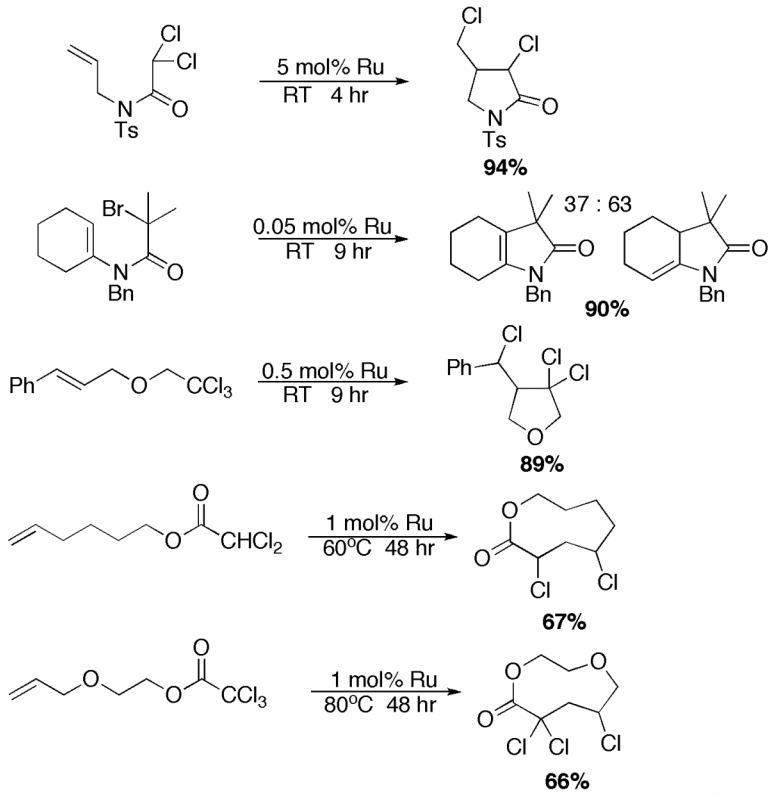

Scheme 1.12.1. Ring closing ATRC reactions catalyzed by $Cp^{*}RuCl_2(PPh_3)$ in the presence of Mg as a reducing agent.

1.12.2 Atom Transfer Sequential Radical Addition/Cyclization Processes

The principal advantages of the methodology for catalyst regeneration in ATRC are two fold. On one hand, the presence of reducing agents enables a significant reduction in the amount of metal catalyst. Such reduction is very beneficial because it increases the radical annulation efficiency by decreasing the rate of radical trapping by the deactivator, compared to the rate of radical ring closure. On the other hand, the rate constant of deactivation can be further controlled through ligand design. Apart from the successful use of reducing agents in Cu and Ru catalyzed ATRC reactions discussed above,[111, 194-196] examples of atom transfer sequential radical addition/cyclization processes are very rare. In a preliminary study, we have reported on copper catalyzed

addition of polyhalogenated compounds to 1,5-hexadiene and 1,7-octadiene using AIBN.[208] These cascade type reactions were catalyzed using copper(II) concentrations as low as 0.01 mol% (relative to diene), however, the cyclic products were difficult to control as a result of slow rates for ring closure. For 1,5-hexadiene, in addition to the

Table 1.12.2. ATRA of CCl_4 to 1,6-dienes followed by sequential ATRC catalyzed by copper(I) homoscorpionate ($Cu^{I}Tp^{X}$) and $[Cu^{II}(TPMA)Cl][Cl]$ complexes in the presence of free-radical initiators and Mg as reducing agents.[111, 209]

1,6-Diene	Product	Catalyst[a]	T/°C	Red. Agent	$[Diene]_0$: $[Cu^{II}]_0$(mol%)	Yield (%)	*cis*:*trans*
	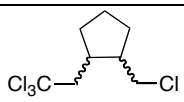	$CuTp^{t\text{-}Bu,Me}$	30	-	100:1 (1.0)	59	87:13
		$CuTp^{Cy,4Br}$	30	-	100:1 (1.0)	62	84:16
		$[Cu^{II}(TPMA)Cl][Cl]$	60	AIBN	5000:1 (0.02)	95(83)[c]	84:16
			30	V-70	2500:1 (0.04)	92	85:15
			RT[b]	V-70	2500:1 (0.04)	87	86:14
	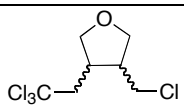	$CuTp^{t\text{-}Bu,Me}$	30	Mg	100:1 (1.0)	>99	86:14
		$CuTp^{Cy,4Br}$	30	Mg	100:1 (1.0)	>99	82:18
		$[Cu^{II}(TPMA)Cl][Cl]$	60	AIBN	2000:1 (0.05)	89(70)[c]	80:20
			30	V-70	1000:1 (0.1)	91	79:21
			RT[b]	V-70	1000:1 (0.1)	80	87:13
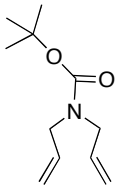	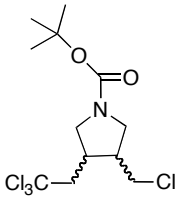	$CuTp^{t\text{-}Bu,Me}$	30	Mg	100:1 (1.0)	95	87:13
		$CuTp^{Cy,4Br}$	30	Mg	100:1 (1.0)	90	83:17
		$[Cu^{II}(TPMA)Cl][Cl]$	60	AIBN	5000:1 (0.02)	96	74:26
			60	AIBN	10000:1 (0.01)	91(75)[c]	66:34
			30	V-70	5000:1 (0.02)	87	64:36
			RT[b]	V-70	5000:1 (0.02)	77	56:44
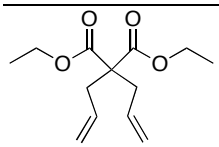	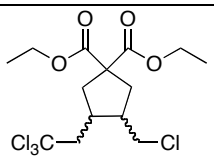	$CuTp^{t\text{-}Bu,Me}$	30	Mg	100:1 (1.0)	>99	93:7
		$CuTp^{Cy,4Br}$	30	Mg	100:1 (1.0)	>99	90:10
		$[Cu^{II}(TPMA)Cl][Cl]$	60	AIBN	5000:1 (0.02)	~100	86:14
			60	AIBN	10000:1 (0.01)	89(80)[c]	84:16
			30	V-70	5000:1 (0.02)	90	91:9
			RT[b]	V-70	5000:1 (0.02)	81	86:14
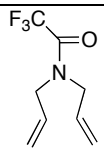	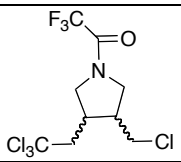	$[Cu^{II}(TPMA)Cl][Cl]$	60	AIBN	5000:1 (0.02)	90(77)[c]	81:19
			60	AIBN	10000:1 (0.01)	73	84:16
			30	V-70	1000:1 (0.1)	95	73:27
			RT[b]	V-70	1000:1 (0.1)	87	73:27

[a]Reactions with $[Cu^{II}(TPMA)Cl][Cl]$ were performed in CH_3OH for 24 h with $[CCl_4]_0$:$[diene]_0$:[AIBN or V-70]$_0$=1.25:1:0.05, $[diene]_0$=1.0 M. Reactions with $Cu^{I}Tp^{X}$ were performed in benzene-d_6 for 24 h with $[1,6\text{-diene}]_0$:$[CCl_4]$=1:100:400. The yield is based on the formation of 5-*exo*-*trig* product (*cis* and *trans*) and was determined by ^{1}H NMR using toluene or 1,4-dimethoxybenzene as internal standard (relative errors are ±15%). [b]RT=22±2 °C. [c]Isolated yield after column chromatography for the large scale reaction.

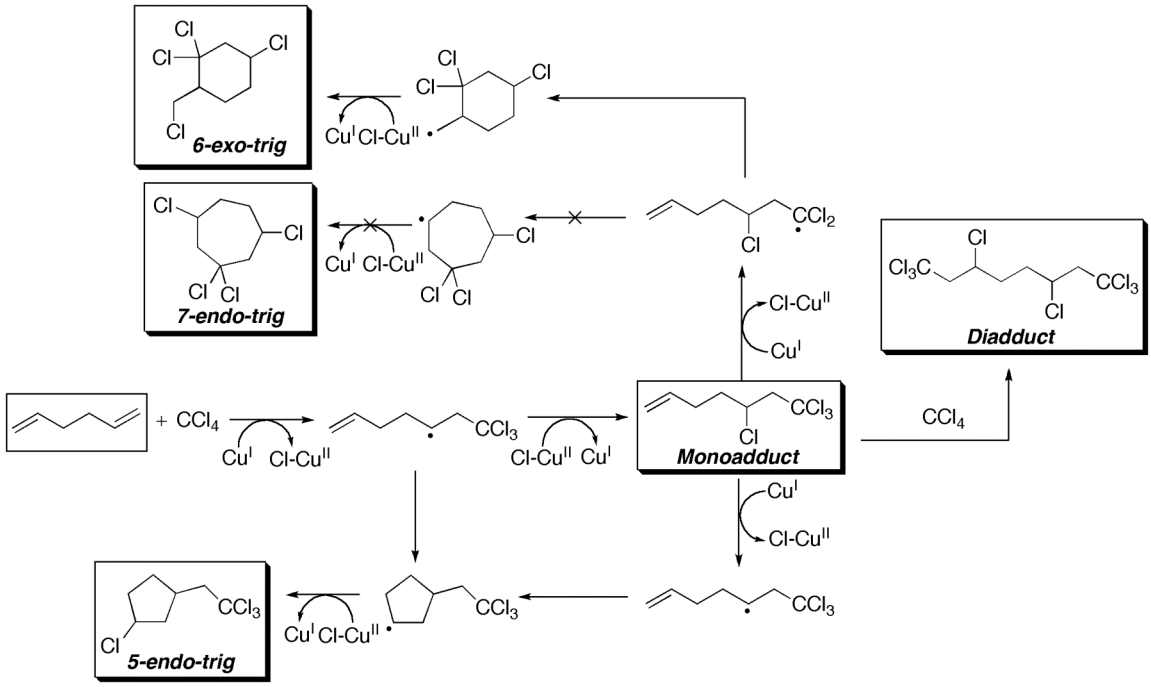

Scheme 1.12.2. Observed products in ATRC of CCl_4 to 1,5-hexadiene catalyzed by $[Cu^{II}(TPMA)Cl][Cl]$ in the presence of AIBN.

desired 5-*endo-trig* cyclic product, we have also observed the formation of the monoadduct, diadduct and 6-*exo-trig* product. The latter one was formed as a result of further monoadduct activation (Scheme 1.12.2). 7-*Endo trig* product was not observed under any reaction conditions. Similar problems in controlling the yields of cyclic products were also observed for 1,7-octadiene. Very recently, copper homoscorpionate complexes[112] have been utilized in the addition of CCl_4 to 1,6-dienes to yield 1,2-disubstituted cyclopentanes.[111] Quantitative yields of the products were obtained using 1 mol % of the catalyst in the presence of magnesium as a reducing agent (Table 1.12.2).

1,6-Dienes are excellent candidates to further expand the methodology for catalyst regeneration originally developed for ATRA[153, 154] because the addition of radicals generated from alkyl halides results in a formation of 5-hexenyl radicals, which are known to undergo very fast and selective 5-*exo-trig* mode of cyclization ($k_{exo\text{-}trig}\approx10^5$

s^{-1}, $k_{exo\text{-}trig}/k_{endo\text{-}trig}\approx100$).[134] Assuming that the rate constant of deactivation for copper(II) complexes with highly active TPMA ligand in ATRA is on the order of 10^8 $M^{-1}s^{-1}$,[153, 154, 179] the rate of radical ring closure (resulting in 5-*exo-trig* cyclic product) will approach the rate of radical trapping (resulting in the formation of halogen terminated open chain monoadduct and diadduct) at copper(II) concentrations on the order of 1.0×10^{-3} M (0.1 mol% relative to diene when $[diene]_0$=1.0 M, Scheme 1.12.3). Therefore, in theory, the selective formation of 5-*exo-trig* cyclic product could be obtained using much lower copper(II) concentrations, provided that a reducing agent is present in the system. The reducing agent continuously regenerates copper(I) from the copper(II) complex, which accumulates in the system as a result of unavoidable radical-radical termination reactions.[153, 154]

AIBN (2,2′-azobis(isobutyronitrile)) or V-70 (2,2'- azobis(4-methoxy-2,4-dimethyl valeronitrile)) initiated ATRA of CCl_4 to 1,6-heptadiene in the absence of a catalyst resulted in ~20% yield of the 5-*exo-trig* cyclic product. For all other dienes investigated, no cyclic products were observed. However, when $[Cu^{II}(TPMA)Cl][Cl]$ complex was used in conjunction with the free-radical diazo initiator, truly remarkable results were obtained (Table 1.12.2).[209] In the presence of AIBN at 60 ^oC, cyclic products derived from the addition of CCl_4 to 1,6-heptadiene, diallyl ether and *N*,*N*-diallyl-2,2,2-trifluoroacetamide were synthesized in nearly quantitative yields using as low as 0.02 mol% of the catalyst (relative to diene). On the other hand, excellent results with *tert*-butyl-*N*,*N*-diallylcarbamate and diethyl diallylmalonate were also achieved using even smaller amounts of the catalyst (0.01 mol%). These results indicate nearly a 100 fold reduction in catalyst loading over the methodology that utilizes copper(I)

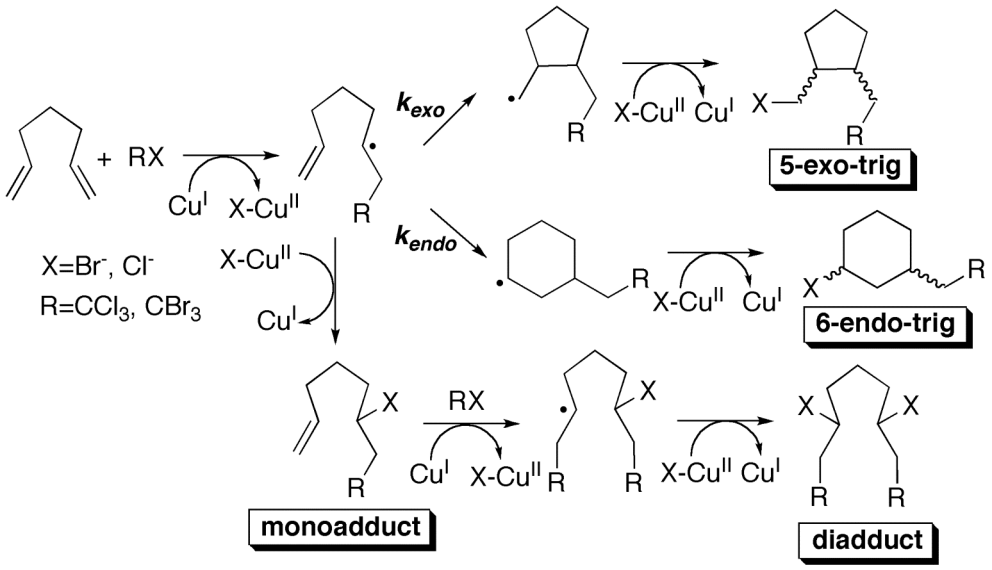

Scheme 1.12.3. ATRC pathways in the addition of polyhalogenated compounds to 1,6-heptadienes catalyzed by copper complexes.

homoscorpionate complexes and Mg as the reducing agent.[111] Furthermore, as indicated in Table 1.12.2, cyclization reactions were also quite efficient at ambient temperature when V-70 was used as a reducing agent. Regardless of the choice of diene, reaction temperature or free-radical reducing agent, 1,2-disubstituted cyclopentanes showed a strong preference for the formation of the *cis*-product, which was also observed in similar free radical cyclizations that do not utilize transition metal complexes as halogen transfer agents.[210-212]

1.13 Conclusions And Future Outlook

In summary, copper catalyzed ATRA and ATRC reactions can be utilized in the synthesis of various substrates that can be used as building blocks for the construction of complex molecules. Until recently, one of the principal drawbacks of these useful synthetic tools remained the large amount of copper catalyst needed to achieve high selectivity towards the desired target compound (typically 5-30 mol% relative to substrate). This obstacle caused serious problems in product separation and catalyst regeneration, making both processes environmentally unfriendly and expensive. The amount of copper catalyst can be dramatically decreased in the presence of free-radical diazo initiators as reducing agents. The role of reducing agent in ATRA and ATRC is to continuously regenerate the activator (copper(I) complex) from the deactivator (copper(II) complex). As a result, single addition adducts in copper mediated ATRA and ATRC reactions can be synthesized using very low concentrations of copper catalysts (5-100 pm). It is envisioned that the recent developments in this area could have important industrial implications on the synthesis of small organic molecules, natural products and pharmaceutical drugs.

1.14 References

(1) Kharasch, M. S.; Engelmann, H.; Mayo, F. R., The Peroxide Effect in the Addition of Reagents to Unsaturated Compounds. XV. The Addition of Hydrogen Bromide to 1- and 2-Bromo and Chloro-Propenes. *J. Org. Chem.* **1937,** *2*, 288-302.

(2) Kharasch, M. S.; Jensen, E. V.; Urry, W. H., Addition of Carbon Tetrachloride and Chloroform to Olefins. *Science* **1945,** *102*(2640), 128-128.

(3) Kharasch, M. S.; Jensen, E. V.; Urry, W. H., Addition of Derivatives of Chlorinated Acetic Acid to Olefins. *J. Am. Chem. Soc.* **1945,** *67*, 1626-1626.

(4) Odian, G., *Principles of Polymerization*. 4th ed.; John Wiley & Sons: Hoboken, 2004.

(5) De Malde, M.; Minisci, F.; Pallini, U.; Volterra, E.; Quilico, A., Reactions between acrylonitriles and aliphatic halogen derivatives. *Chim. Ind. (Milan)* **1956,** *38*, 371-382.

(6) Minisci, F., Radical Reactions in Solution. Dipolar Character of Free Radicals from Decomposition of Organic Peroxides. *Gazz. Chim. Ital.* **1961,** *91*, 386-389.

(7) Minisci, F.; Pallini, U., Radical reactions in solution. Haloalkylation of acrylic acid derivatives. *Gazz. Chim. Ital.* **1961,** *91*, 1030-1036.

(8) Minisci, F.; Galli, R., Influence of the Electrophilic Character on the Reactivity of Free Radicals in Solution. Reactivity of Alkoxy, Hydroxy, Alkyl, and Azido Radicals in the Presence of Olefins. *Tetrahedron Lett.* **1962**, 533-538.

(9) Minisci, F.; Galli, R., Addition of N-Chloroamines to Styrene and Butadiene, Catalyzed by Iron and Copper Salts. *Chim. Ind. (Milan)* **1963,** *45*(11), 1400-1401.

(10) Minisci, F., Free-Radical Additions to Olefins in the Presence of Redox Systems. *Acc. Chem. Res.* **1975,** *8*(5), 165-171.

(11) Minisci, F.; Cecere, M.; Galli, R., Oxidation of Carbon Free Radicals in the Presence of Cu and Fe Salts. New Synthesis of Nitro Derivatives and Nitric Esters. *Gazz. Chim. Ital.* **1963,** *93*, 1288-1294.

(12) Iqbal, J.; Bhatia, B.; Nayyar, N. K., Transition Metal-Promoted Free-Radical Reactions in Organic Synthesis: The Formation of Carbon-Carbon Bonds *Chem. Rev.* **1994,** *94*(2), 519-564.

(13) Gossage, R. A.; Van De Kuil, L. A.; Van Koten, G., Diaminoarylnickel(II) "Pincer" Complexes: Mechanistic Considerations in the Kharasch Addition Reaction, Controlled Polymerization, and Dendrimeric Transition Metal Catalysts. *Acc. Chem. Res.* **1998,** *31*(7), 423-431.

(14) Severin, K., Ruthenium Catalysts for the Kharasch Reaction. *Curr. Org. Chem.* **2006,** *10*(2), 217-224.

(15) Clark, A. J., Atom Transfer Radical Cyclisation Reactions Mediated by Copper Complexes. *Chem. Soc. Rev.* **2002,** *31*(1), 1-11.

(16) Nagashima, H., Radical Reactions. In *Ruthenium in Organic Synthesis*, Murahashi, S.-I., Ed. Wiley-VCH: Weinheim, 2004; pp 333-343.

(17) Delaude, L.; Demonceau, A.; Noels, A. F., Ruthenium Promoted Radical Processes Toward Fine Chemistry. In *Topics in Organometallic Chemistry*, Bruneau, C.; Dixneuf, P. H., Eds. Springer: Berlin, 2004; Vol. 11, pp 155-171.

(18) Hajek, M.; Silhavy, P.; Malek, J., Free Radical Addition Reactions Initiated by Metal Oxides. XI. Metal-Oxide Induced Redox Chain Addition of Tetrachloromethane to a Carbon-Carbon Double Bond. *Collection Czechoslov. Chem. Commun.* **1980,** *45*, 3488-3501.

(19) Hajek, M.; Silhavy, P.; Malek, J., Free Radical Addition Reactions Initiated by Metal Oxides. XII. Catalytic Activity of Copper Oxides and Chlorides in the Redox Chain Addition of Tetrachloromethane to Styrene. *Collection Czechoslov. Chem. Commun.* **1980,** *45*, 3502-3509.

(20) Steiner, E.; Martin, P.; Bellius, D., Metal-Catalyzed Radical Addition of Polyhalogenated Compounds to Olefins. Part 2. A New Simple Synthesis of 2,3,5-Trichloropyridine. *Helv. Chim. Acta* **1982,** *65*, 983-985.

(21) Metzger, J. O.; Mahler, R., Radical Additions of Activated Haloalkanes to Alkenes Initiated by Electron Transfer from Copper in Solvent-Free Systems. *Angew. Chem. Int. Ed.* **1995,** *34*, 902-904.

(22) Bellesia, F.; Forti, L.; Ghelfi, F.; Pagnoni, U. M., The CuBr/Fe(0) Promoted Radical Addition of Methyl 2-Bromo-2-Chlorocarboxylates to Olefins. *Synth. Commun.* **1997,** *27*, 961-971.

(23) Forti, L.; Ghelfi, F.; Libertini, E.; Pagnoni, U. M., Halogen Atom Transfer Radical Addition of α-Polychloro Esters to Olefins Promoted by Fe(0) Filings. *Tetrahedron* **1997,** *53*, 17761-17768.

(24) Forti, L.; Ghelfi, F.; Pagnoni, U. M., Fe(0) Initiated Halogen Atom Transfer Radical Addition of Methyl 2-Br-2-Cl-Carboxylates to Olefins. *Tetrahedron Lett.* **1996,** *37*, 2077-2078.

(25) Baban, J. A.; Roberts, B. P., An Electron Spin Resonance Study of Alkyl Radical Addition to Diethyl Vinylphosphonate. *J. Chem. Soc. Perkin Trans.* **1981,** *1*, 161-166.

(26) Caronna, T.; Citterio, A.; Ghirardini, M.; Minisci, F., Nucleophilic Character of Alkyl Radicals. XIII. Absolute Rate Constants for the Addition of Alkyl Radicals to Acrylonitrile and Methyl Acrylate. *Tetrahedron* **1977,** *33*, 793-796.

(27) Asscher, M.; Vofsi, D., Chlorine Activation by Redox-Transfer. Part I. The Reaction Between Aliphatic Amines and Carbon Tetrachloride. *J. Chem. Soc.* **1961**, 2261-2264.

(28) Sinnreich, J.; Asscher, M., Redox-Transfer. VII. Addition of Ethylene and Butadiene to Functionally Substituted Aromatic Sulfonyl Chlorides. *J. Chem. Soc. Perkin Trans.* **1972,** *1*, 1543-1545.

(29) Kamigata, N.; Sawada, H.; Kobayashi, M., Reactions of Arenesulfonyl Chlorides with Olefins Catalyzed by a Ruthenium(II) Complex. *J. Org. Chem.* **1983,** *48*, 3793-3796.

(30) Block, E.; Aslam, M.; Eswarakrishman, V.; Gebreyes, K.; Hutchinson, J.; Iyer, R. S.; Laffitte, J. A., α-Haloalkanesulfonyl Bromides in Organic Synthesis. 5. Versatile Reagents for the Synthesis of Conjugated Polyenes, Enones, and 1,3-Oxathiole 1,1-Dioxides. *J. Am. Chem. Soc.* **1986,** *108*, 4568-4580.

(31) Amiel, Y., The Thermal and the Copper-Catalyzed Addition of Sulfonyl Bromides to Phenylacetylene. *J. Org. Chem.* **1974,** *39*, 3867-3870.

(32) Truce, W. E.; Wolf, G. C., Adducts of Sulfonyl Iodides with Acetylenes. *J. Org. Chem.* **1971,** *36*, 1727-1732.

(33) Freidlina, R. K.; Velichko, F. K., Synthetic Applications of Homolytic Addition and Telomerization Reactions of Bromine-Containing Addends with Unsaturated Compounds Containing Electron-Withdrawing Substituents. *Synthesis* **1977,** *3*, 145-154.

(34) Julia, M.; Sasussine, L.; Thuillier, G. I., Addition du Chloroacetate de Methyle sur les Olefines. *J. Organomet. Chem.* **1979,** *174*, 359-366.

(35) Curran, D. P., *Comprehensive Organic Synthesis*. Pergamon: New York, 1992; p 715.

(36) De Campo, F.; Lastecoueres, D.; Verlhac, J.-B., New Copper(I) and Iron(II) Complexes for Atom Transfer Radical Macrocyclization Reactions. *J. Chem. Soc., Perkin Trans. 1* **2000,** (4), 575-580.

(37) Clark, A. J.; Battle, G. M.; Bridge, A., Efficient β-Lactam Synthesis via 4-exo Atom Tranfer Radical Cyclization Using CuBr(tripyridylamine) Complexe. *Tetrahedron Lett.* **2001,** *42*, 4409-4412.

(38) Nagashima, H.; Seki, K.; Ozaki, N.; Wakamatsku, H.; Itoh, K.; Tomo, Y.; Tsuyi, J., Transition-Metal-Catalyzed Radical Cyclization: Copper-Catalyzed Cyclization of Allyl Trichloroacetates to Trichlorinated γ-Lactones. *J. Org. Chem.* **1990,** *55*, 985-990.

(39) Yang, D.; Yan, Y.-L.; Zheng, B.-F.; Gao, Q.; Zhu, N.-Y., Copper(I)-Catalyzed Chlorine Atom Transfer Radical Cyclization Reactions of Unsaturated α-Chloro β-Keto Esters. *Org. Lett.* **2006,** *8*(25), 5757-5760.

(40) Wang, J.-S.; Matyjaszewski, K., Controlled/"Living" Radical Polymerization. Atom Transfer Radical Polymerization in the Presence of Transition-Metal Complexes. *J. Am. Chem. Soc.* **1995,** *117*(20), 5614-5615.

(41) Kato, M.; Kamigaito, M.; Sawamoto, M.; Higashimura, T., Polymerization of Methyl Methacrylate with the Carbon Tetrachloride/Dichlorotris-(triphenylphosphine)ruthenium(II)/Methylaluminum Bis(2,6-di-tert-butylphenoxide) Initiating System: Possibility of Living Radical Polymerization. *Macromolecules* **1995,** *28*(5), 1721-1723.

(42) Braunecker, W. A.; Matyjaszewski, K., Controlled/Living Radical Polymerization: Features, Developments and Perspectives. *Prog. Polym. Sci.* **2007,** *32*, 93-146.

(43) Coessens, V.; Pintauer, T.; Matyjaszewski, K., Functional Polymers by Atom Transfer Radical Polymerization. *Prog. Polym. Sci.* **2001,** *26*(3), 337.

(44) Kamigaito, M.; Ando, T.; Sawamoto, M., Metal-Catalyzed Living Radical Polymerization. *Chem. Rev.* **2001,** *101*(12), 3689-3745.

(45) Matyjaszewski, K., *Controlled Radical Polymerization (ACS Symp. Ser. 685)*. ACS: Washington, DC, 1998; p 483.

(46) Matyjaszewski, K., *Controlled/Living Radical Polymerization. Progress in ATPR, NMP and RAFT (ACS Symp. Ser. 768)*. ACS: Washington, DC., 2000; p 484.

(47) Matyjaszewski, K., *Advances in Controlled/Living Radical Polymerization (ACS Symp. Ser. 854)*. ACS: Washington, DC., 2003.

(48) Matyjaszewski, K., Controlling Polymer Structures by Atom Transfer Radical Polymerization and other Controlled/Living Radical Polymerizations *Macromol. Symp.* **2003,** *195*, 25-31.

(49) Matyjaszewski, K., Macromolecular Engineering: From Rational Design Through Precise Macromolecular Synthesis and Processing to Targeted Macroscopic Material Properties *Prog. Polym. Sci.* **2005,** *30*(8-9), 858-875.

(50) Matyjaszewski, K., *Controlled Radical Polymerization. From Synthesis to Materials (ACS Symp. Ser. 944)*. ACS: Washington, DC., 2006.

(51) Matyjaszewski, K.; Davis, T. P., *Handbook of Radical Polymerization*. Wiley: Hoboken, 2002.

(52) Matyjaszewski, K.; Gnanou, Y.; Leibler, L., *Macromolecular Engineering-Precise Synthesis, Materials Properties, Applications*. Willey-VCH: Weinheim, 2007.

(53) Matyjaszewski, K.; Xia, J., Atom Transfer Radical Polymerization. *Chem. Rev.* **2001,** *101*(9), 2921-2990.

(54) Patten, T. E.; Matyjaszewski, K., Copper(I)-Catalyzed Atom Transfer Radical Polymerization. *Acc. Chem. Res.* **1999,** *32*(10), 895-903.

(55) Pintauer, T.; Matyjaszewski, K., Structural Aspects of Copper Catalyzed Atom Transfer Radical Polymerization. *Coord. Chem. Rev.* **2005,** *249*(11-12), 1155-1184.

(56) Pintauer, T.; McKenzie, B.; Matyjaszewski, K., Toward Structural and Mechanistic Understanding of Transition Metal-Catalyzed Atom Transfer Radical Processes *ACS Symp. Ser.* **2003,** *854*, 130-147.

(57) Tsarevsky, N. V.; Braunecker, W. A.; Vacca, A.; Gans, P.; Matyjaszewski, K., Competitive Equilibria in Atom Transfer Radical Polymerization. *Macromol. Symp.* **2007,** *248*, 60-70.

(58) Tsarevsky, N. V.; Matyjaszewski, K., "Green" Atom Transfer Radical Polymerization: From Process Design to Preparation of Well-Defined Environmentally Friendly Polymeric Materials. *Chem. Rev.* **2007,** *107*, 2270-2299.

(59) Kabachii, Y. A.; Kochev, S. Y.; Bronstein, L. M.; Blagodatskikh, I. B.; Valetsky, P. M., Atom Transfer Radical Polymerization with Ti(III) Halides and Alkoxides. *Polym. Bull.* **2003,** *50*, 271-278.

(60) Le Grognec, E.; Claverie, J.; Poli, R., Radical Polymerization of Styrene Controlled by Half-Sandwich Mo(II)/Mo(IV) Complexes: all Basic Mechanisms are Possible. *J. Am. Chem. Soc.* **2001,** *123*, 9513-9524.

(61) Brandts, J. A. M.; van de Geijn, P.; van Faassen, E. E.; Boersma, J.; van Koten, G., Controlled Radical Polymerization of Styrene in the Presence of Lithium Molybdate(V) Complexes and Benzylic Halides. *J. Organomet. Chem.* **1999,** *584*, 246-253.

(62) Maria, S.; Stoffelbach, F.; Matta, J.; Darran, J.-C.; Richard, P.; Poli, R., The Radical Trap in Atom Transfer Radical Polymerization need not be Thermodynamically Stable. A Study of the $MoX_3(PMe_3)_3$ Catalysts. *J. Am. Chem. Soc.* **2005,** *127*, 5946-5956.

(63) Kotani, Y.; Kamigaito, M.; Sawamoto, M., Re(V) Mediated Living Radical Polymerization of Styrene: $ReO_2I(PPh_3)_2$/R-I Initiating Systems. *Macromolecules* **1999,** *32*, 2420-2424.

(64) Matyjaszewski, K.; Wei, M.; Xia, J.; McDermott, N. E., Controlled/"Living" Radical Polymerization of Styrene and Methyl Methacrylate Catalyzed by Iron Complexes. *Macromolecules* **1997,** *30*, 8161-8164.

(65) Ando, T.; Kamigaito, M.; Sawamoto, M., Iron(III) Chloride Complex for Living Radical Polymerization of Methyl Methacrylate. *Macromolecules* **1997,** *30*, 4507-4510.

(66) O'Reilly, R. K.; BGibson, V. C.; White, A. J. P.; Williams, D. J., Five-coordinate Iron(III) Complexes Bearing Tridentate Nitrogen Donor Ligands as Catalysts for Atom Transfer Radical Polymerization. *Polyhedron* **2004,** *23*, 2921-2928.

(67) Teodorescu, M.; Gaynor, S.; Matyjaszewski, K., Halide Anions as Ligands in Iron-Mediated Atom Transfer Radical Polymerization. *Macromolecules* **2000,** *33*, 2335-2339.

(68) Simal, F.; Demonceau, A.; Noels, A. F., Highly Efficient Ruthenium-Based Catalytic Systems for Controlled Free Radical Polymerization of Vinyl Monomers. *Angew. Chem. Int. Ed. Eng.* **1999,** *38*, 538-540.

(69) Braunecker, W. A.; Itami, Y.; Matyjaszewski, K., Osmium Mediated Radical Polymerization. *Macromolecules* **2005,** *38*, 9402-9404.

(70) Braunecker, W. A.; Brown, W. C.; Morelli, B. C.; Tang, W.; Poli, R.; Matyjaszewski, K., Origin of Activity in Cu-, Ru-, and Os-Mediated Radical Polymerization. *Macromolecules* **2007,** *40*(24), 8576-8585.

(71) Percec, V.; Barboiu, B.; Neumann, A.; Ronda, J. C.; Zhao, M., Metal-Catalyzed "Living" Radical Polymerization of Styrene Initiated with Arenesulfonyl Chlorides. From Heteregeneous to Homogeneous Catalysis. *Macromolecules* **1996,** *29*, 3665-3668.

(72) Wang, B.; Zhuang, Y.; Luo, X.; Xu, S.; Zhou, X., Controlled/"Living" Radical Polymerization of MMA Catalyzed by Cobaltocene. *Macromolecules* **2003,** *36*, 9684-9686.

(73) Granel, C.; Dubois, P.; Jerome, R.; Teyssie, P., Controlled Radical Polymerization of Methacrylic Monomers in the Presence of a Bis(ortho-chelated) Arylnickel(II) Complex and Different Activated Alkyl Halides. *Macromolecules* **1996,** *29*, 8576-8582.

(74) Uegaki, H.; Kotani, Y.; Kamigaito, M.; Sawamoto, M., Nickel Mediated Living Radical Polymerization of Methyl Methacrylate. *Macromolecules* **1997,** *30*(2249-2253).

(75) Lecomte, P.; Drapier, I.; Dubois, P.; Teyssie, P.; Jerome, R., Controlled Radical Polymerization of Methyl Methacrylate in the Presence of Palladium Acetate, Triphenylphosphine and Carbon Tetrachloride. *Macromolecules* **1997,** *30*, 7631-7633.

(76) Patten, T. E., Polymers with Very Low Polydispersities from Atom Transfer Radical Polymerization. *Science* **1996,** *272*, 866-868.

(77) Curran, D. P., The Design and Application of Free Radical Chain Reactions in Organic Synthesis. Part 2. *Synthesis* **1988,** *7*, 489-513.

(78) Curran, D. P., The Design and Application of Free Radical Chain Reactions in Organic Synthesis. Part 1. *Synthesis* **1988,** *6*, 417-439.

(79) Jasperse, C. P.; Curran, D. P.; Fevig, T. L., Radical Reactions in Natural Product Synthesis. *Chem. Rev.* **1991,** *91*, 1237-1286.

(80) Giese, B., Syntheses with Radicals. Carbon-Carbon Coupling via Organotin and -Mercury Compounds. *Angew. Chem.* **1985,** *97*, 555-567.

(81) Barton, D. H. R.; Crich, D.; Motherwell, W. B., New and Improved Methods for the Radical Decarboxylation of Acids. *J. Chem. Soc. Chem. Comm.* **1983,** *17*, 939-941.

(82) Barton, D. H. R.; McCombie, S. W., New Method for the Deoxygenation of Secondary Alcohols. *J. Chem. Soc. Perkin Trans. 1* **1975**, 1574-1585.

(83) Curran, D. P.; Chen, M.-H.; Dooseop, K., Atom-Transfer Cyclization. A Novel Isomerization of Hex-5-ynyl Iodides to Iodomethylene Cyclopentanes. *J. Am. Chem. Soc.* **1986,** *108*, 2489-2490.

(84) Pirrung, F., Hiemstra, Henk, Speckamp, N., Synthesis of Medium-sized Lactones by the Copper(I)Chloride/ 2,2'-Bipyridine-Catalyzed Cyclization of Di- and Trichloroacetates. *Tetrahedron* **1994,** *50*(43), 12415-12442.

(85) Nagashima, H.; Wakamatsku, H.; Itoh, K.; Tomo, Y.; Tsuji, J., New Regio- and Stereoselective Preparation of Trichlorinated γ-Butyrolactones by Copper Catalyzed Cyclization of Allyl Trichloroacetates. *Tetrahedron Lett.* **1983,** *23*, 2395-2398.

(86) Pirrung, F. O. H.; Hiemstra, H.; Speckamp, W. N.; Kaptein, B.; Schoemaker, H. E., Synthesis of Enetiometrically Pure Eight- and Nine- Membered Lactones by Copper(I) Chloride/2,2'-Bipyridine-Catalyzed Cyclization. *Synthesis* **1995,** *4*, 458-472.

(87) Pirrung, F. O. H.; Hiemstra, H.; Kaptein, B.; Sobrino, M. E. M.; Petra, D. G. I.; Schoemaker, H. E.; Speckamp, W. N., Diastereoselective Synthesis of Medium-Sized Lactones by Cu(bpy)Cl Catalyzed Cyclization of Trichloroacetates. *Synlett.* **1993,** *10*, 739-740.

(88) Iwamatsu, S.; Matsubara, K.; Nagashima, H., Synthetic Studies of cis-3α-Aryloctahydroindole Derivatives by Copper-Catalyzed Cyclization of N-Allyltrichloroacetamides: Facile Construction of Benzylic Quaternary Carbons by Carbon-Carbon Bond-Forming Reactions. *J. Org. Chem.* **1999,** *64*, 9625-9631.

(89) Nagashima, H.; Ozaki, N.; Ishii, M.; Seki, K.; Washiyama, M.; Itoh, K., Transition Metal-Catalyzed Radical Cyclizations: A Low-Temperature Process for the Cyclization of N-Protected N-Allyltrichloroacetamides to Trichlorinated γ-Lactams and Application to the Stereoselective Preparation of α,β-Disubstituted γ-Lactams. *J. Org. Chem.* **1993,** *58*, 464-470.

(90) Nagashima, H.; Wakamatsku, H.; Itoh, K., A Novel Preparative Method for γ-Butyrolactams via Carbon-Carbon Bond Formation: Copper- or Ruthenium-Catalyzed Cyclization of N-Allyltrichloroacetamides. *J. Chem. Soc., Chem. Commun.* **1984**, 652-653.

(91) Nagashima, H.; Ara, H.; Wakamatsku, H.; Itoh, K., Stereoselective Preparation of Bicyclic Lactams by Copper- or Ruthenium-Catalyzed Cyclization of N-Allyltrichloroacetamides: a Novel Entry to Pyrrolidine Alkaloid Skeletons. *J. Chem. Soc., Chem. Comm.* **1985**, 518-519.

(92) Clark, A. J.; De Campo, F.; Deeth, R. J.; Filik, R. P.; Gatard, S.; Hunt, N. A.; Lastecoueres, D.; Thomas, G. H.; Verlhac, J.-B.; Wongtap, H., Atom Transfer Radical Cyclizations of Activated and Unactivated *N*-Allylhaloacetamides and *N*-Homoallylhaloacetamides Using Chiral and Non-Chiral Copper Complexes. *J. Chem. Soc., Perkin Trans. 1* **2000**, 671-680.

(93) Clark, A. J.; Duncalf, D. J.; Filik, R. P.; Haddleton, D. M.; Thomas, G. H.; Wongtap, H., N-Alkyl-2-Pyridylmethanimines as Tuneable Alternatives to Bipyridine Ligands in Copper Mediated Atom Transfer Radical Cyclization. *Tetrahedron Lett.* **1999,** *40*, 3807-3810.

(94) Clark, A. J.; Filik, R. P.; Thomas, G. H., Ligand Geometry Effects in Copper Mediated Atom Transfer Radical Cyclisations. *Tetrahedron Lett.* **1999,** *40*, 4885-4888.

(95) Clark, A. J.; Dell, C. P.; Ellard, J. M.; Hunt, N. A.; McDonagh, J. P., Efficient Room Temperature Copper(I) Mediated 5-Endo Radical Cyclizations. *Tetrahedron Lett.* **1999,** *40*(49), 8619-8623.

(96) Udding, J. H.; Tujip, C. J. M.; Hiemstra, H.; Speckamp, W. N., Transition Metal-Catalyzed Chlorine Transfer Cyclizations of Carbon-Centered Glycine Radicals; a Novel Synthetic Route to Cyclic α-Amino Acids. *Tetrahedron* **1999,** *50*(6), 1907-1918.

(97) Iwamatsu, S.; Kondo, H.; Matsubara, K.; Nagashima, H., Copper-Catalyzed Facile Carbon-Carbon Bond Forming Reactions at the α-Position of α,α,γ-Trichlorinated γ-Lactams. *Tetrahedron* **1999,** *55*, 1687-1706.

(98) Miniotte, H. G.; Hubert, A. J.; Teyssie, P., The Role of Copper(I) Complexes in the Selective Formation of Oxazoles from Unsaturated Nitriles and Diazoesters. *J. Organomet. Chem.* **1975,** *88*, 115-120.

(99) Julia, M.; Thuillier, G.; Saussine, L., Additions D'Chloronitriles sur les Olefines par Catalyse Redox. *J. Organomet. Chem.* **1979,** *177*, 211-220.

(100) Murai, S.; Sonoda, N.; Tsutsumi, S., Copper Salts Induced Addition of Ethyl Trichloroacetate to Olefins. *J. Org. Chem.* **1964,** *31*(9), 3000-3003.

(101) Pierre, M.; Eginhard, S.; Streith, J.; Winkler, T.; Bellus, D., Metal-Catalyzed Additions of Organic Polyhalides to Olefins. 4. Convenient Approaches to Heterocycles via Copper-Catalyzed Additions of Organic Polyhalides to Activated Olefins. *Tetrahedron* **1985,** *41*(19), 4057-4078.

(102) Bellius, D., Copper-Catalyzed Additions of Organic Polyhalides to Olefins: a Versatile Synthetic Tool. *Pure Appl. Chem.* **1985,** *57*, 1827-1838.

(103) Clark, A. J.; Battle, G. M.; Heming, A. M.; Haddleton, D. M.; Bridge, A., Ligand Electronic Effects on Rates of Copper Mediated Atom Transfer Radical Cyclisation and Polymerisation. *Tetrahedron Lett.* **2001,** *42*, 2003-2005.

(104) Haddleton, D. M.; Crossman, M. C.; Hunt, K. H., Reactivity ratios in MMA copolymerizations. *Macromolecules* **1997,** *30*, 3992-3995.

(105) Haddleton, D. M.; Duncalf, D. J.; Kukulj, D.; Crossman, M. C.; Jackson, S. G.; Bon, S. A. F.; Clark, A. J.; Schooter, A. J., *N*-Alkyl-Pyridylmethanimine Copper(I) Complexes. *Eur. J. Inorg. Chem.* **1998**, 1799-1806.

(106) Haddleton, D. M.; Jasieczek, C. B.; Hannon, M. J.; Shooter, A. J., Atom Transfer Radical Polymerization of Methyl Methacrylate Initiated by Alkyl Bromide and 2-Pyridinecarbaldehyde Imine Copper(I) Complexes. *Macromolecules* **1997,** *30*(7), 2190-2193.

(107) Lad, J.; Harrison, S.; Mantovani, G.; Haddleton, D. M., Copper Mediated Living Radical Polymerisation: Interactions Between Monomer and Catalyst. *Dalton. Trans.* **2003**, 4175-4180.

(108) Bendetti, M.; Forti, L.; Ghelfi, F.; Pagnoni, U. M.; Ronzoni, R., Halogen Atom Transfer Radical Cyclization of *N*-Allyl-*N*-benzyl-2,2-dihaloamides to 2-Pyrrolidinones, Promoted by Fe(0)-$FeCl_3$ or CuCl-TMEDA. *Tetrahedron* **1997,** *53*, 14031-14042.

(109) Ghelfi, F.; Bellesia, F.; Forti, L.; Ghirardini, G.; Grandi, R.; Libertini, E.; Montemaggi, M. C.; Pagnoni, U. M.; Pinetti, A.; De Buyck, D., The Influence of Benzylic Protection and Allylic Substituents on the CuCl-TMEDA Catalyzed Rearrangement of *N*-Allyl-*N*-benzyl-2,2-dihaloamides to γ-Lactams. Application to the Stereoselective Synthesis of Pilolactam. *Tetrahedron* **1999,** *55*(18), 5839-5852.

(110) Ghelfi, F.; Parsons, A. F., *N*,*N*-(Dimethylamino)-2-Pyrrolidinones from the Rearrangement of *N*-Allyl-*N*′,*N*′-Dimethyl-2,2-dichlorohydrazides Promoted by CuCl-*N*,*N*,*N*′,*N*′-Tetramethylethylenediamine. *J. Org. Chem.* **2000,** *65*(19), 6249-6253.

(111) Munoz-Molina, J. M.; Belderrain, T. R.; Perez, P. J., Copper-Catalyzed Synthesis of 1,2-Disubstituted Cyclopentanes from 1,6-Dienes by Ring-Closing Kharasch Addition of Carbon Tetrachloride. *Adv. Synth. Catal.* **2008,** *350*, 2365-2372.

(112) Munoz-Molina, J. M.; Caballero, A.; Diaz-Requejo, M. M.; Trofimenko, S.; Belderrain, T. R.; Perez, P. J., Copper-Homoscorpionate Complexes as Active Catalysts for Atom Transfer Radical Addition to Olefins. *Inorg. Chem.* **2007,** *46*, 7725-7730.

(113) De Campo, F.; Lastecoueres, D.; Vincent, J.-M.; Verlhac, J.-B., Copper(I) Complexes Mediated Cyclization Reaction of Unsaturated Ester under Fluoro Biphasic Procedure. *J. Org. Chem.* **1999,** *64*, 4969-4971.

(114) Tang, W.; Tsarevsky, N. V.; Matyjaszewski, K., Determination of Equilibrium Constants for Atom Transfer Radical Polymerization. *J. Am. Chem. Soc.* **2006,** *128*(5), 1598-1604.

(115) Fischer, H., Persistents Radicals. *J. Am. Chem. Soc.* **1986,** *108*, 3925-3927.

(116) Fischer, H., Persistent Radical Effect. *J. Polym. Sci. Part A:Polym. Chem.* **1999,** *37*(13), 1885-1901.

(117) Fischer, H., Persistent Radical Effect. *Chem. Rev.* **2001,** *101*(12), 3581-3610.

(118) Goto, A.; Fukuda, T., Kinetics of Living Radical Polymerization. *Prog. Polym. Sci.* **2004,** *29*, 329-385.

(119) Studer, A., The Persistent Radical Effect in Organic Synthesis. *Chem. Eur. J.* **2001,** *7*(6), 1159-1164.

(120) Tang, H.; Arulsamy, N.; Radosz, M.; Shen, Y.; Tsarevsky, N. V.; Braunecker, W. A.; Tang, W.; Matyjaszewski, K., Highly Active Copper-Based Catalyst for Atom Transfer Radical Polymerization. *J. Am. Chem. Soc.* **2006,** *128*(50), 16277-16285.

(121) Tsarevsky, N. V.; Braunecker, W. A.; Tang, W.; Brook, S. J.; Matyjaszewski, K.; Weismann, G. R., Copper Based ATRP Catalysts of Very High Activity Derived from Dimethyl Crossbridged Cyclam. *J. Mol. Catal. A: Chem* **2006,** *257*, 132-140.

(122) Goto, A.; Fukuda, T., Determination of the Activation Rate Constants of Alkyl Halide Initiators for Atom-Transfer Radical Polymerization. *Macromol. Rapid Commun.* **1999,** *20*, 633-636.

(123) Matyjaszewski, K.; Paik, H.-j.; Zhou, P.; Diamanti, S. J., Determination of Activation and Deactivation Rate Constants of Model Compounds in Atom Transfer Radical Polymerization. *Macromolecules* **2001,** *34*(15), 5125-5131.

(124) Ohno, K.; Goto, A.; Fukuda, T.; Xia, J.; Matyjaszewski, K., Kinetic Studies on the Activation Process in an ATRP. *Macromolecules* **1998,** *31*, 2699-2701.

(125) Orochov, A.; Asscher, M.; Vofsi, D., Redox-Transfer. VI. Determination of the Hammett ρ-Constant for the Oxidation of Cuprous Chloride by Aromatic Sulfonyl Chlorides. *J. Chem. Soc.* **1969**, 255-259.

(126) Or, A.; Asscher, M.; Vofsi, D., Redox Transfer. VIII. Addition of Benzenesulfonyl Chloride and Carbon Tetrachloride to Substituted Styrenes. Kinetic Study. *J. Chem. Soc. Perkin Trans.* **1972,** *7*, 1000-1002.

(127) Cornia, A.; Folli, U.; Sbardellati, S.; Taddei, F., Electron Transfer in the Reactions of Organic Trichloromethyl Derivatives with Iron(II) Chloride. *J. Chem. Soc. Perkin Trans.* **1993,** *10*, 1847-1853.

(128) Huber, T. A.; Macartney, D. H.; Baird, M. C., Kinetics and Mechanisms of Halogen Abstraction Reactions of the 17-Electron, Metal-Centered Radical $CpCr(CO)_3$ with Organic Halides. *Organometallics* **1995,** *14*(2), 592-602.

(129) Tang, W.; Matyjaszewski, K., Effects of Ligands on the Activation Rate Constants in ATRP. *Macromolecules* **2006,** *39*, 4953-4959.

(130) Gillies, M. B.; Matyjaszewski, K.; Norrby, P.-O.; Pintauer, T.; Poli, R.; Richard, P. A., A DFT Study of R-X Bond Dissociation Enthaplies of Relevance to the Initiation Process in Atom Transfer Radical Polymerization. *Macromolecules* **2003,** *36*, 8551-8559.

(131) Jenkins, C. L.; Kochi, J. K., Homolytic and Ionic Mechanisms in the Ligand-Transfer Oxidation of Alkyl Radicals by Copper(II) Halides and Pseudohalides. *J. Am. Chem. Soc.* **1972,** *94*(3), 856-865.

(132) Jenkins, C. L.; Kochi, J. K., Solvolytic Routes via Alkylcopper Intermediates in the Electron-Transfer Oxidation of Alkyl Radicals. *J. Am. Chem. Soc.* **1972,** *94*, 843-855.

(133) Kochi, J. K., *Free Radicals*. John Wiley & Sons: New York, 1973; Vol. 1.

(134) Togo, H., *Advanced Free Radical Reactions for Organic Synthesis*. Elsevier: Amsterdam, 2004.

(135) Matyjaszewski, K.; Gobelt, B.; Paik, H.-j.; Horwitz, C. P., Tridentate Nitrogen-Based Ligands in Cu-Based ATRP: A Structure-Activity Study. *Macromolecules* **2001,** *34*(3), 430-440.

(136) Matyjaszewski, K., Radical Nature of Cu-Catalyzed Controlled Radical Polymerizations (Atom Transfer Radical Polymerization). *Macromolecules* **1998,** *31*(15), 4710-4717.

(137) Tsarevsky, N. V.; Braunecker, W. A.; Matyjaszewski, K., Electron Transfer Reactions Relevant to Atom Transfer Radical Polymerization. *J. Organomet. Chem.* **2007,** *692*, 3212-3222.

(138) Xia, J.; Gaynor, S. G.; Matyjaszewski, K., Controlled/"Living" Radical Polymerization. Atom Transfer Radical Polymerization of Acrylates at Ambient Temperature. *Macromolecules* **1998,** *31*(17), 5958-5959.

(139) Xia, J.; Matyjaszewski, K., Multidentate nitrogen based ligands. *Macromolecules* **1999,** *32*, 2434-2437.

(140) Xia, J.; Zhang, X.; Matyjaszewski, K., The Effects of Ligands on Copper Mediated Atom Transfer Radical Polymerization. In *Transition Metal Catalysis in Macromolecular Design*, Boffa, L. S.; Novak, B. M., Eds. Am. Chem. Soc.: Washington, D. C., 2000; Vol. 760, pp 207-223.

(141) Xia, J.; Matyjaszewski, K., Controlled/"Living" Radical Polymerization. Atom Transfer Radical Polymerization Using Multidentate Amine Ligands. *Macromolecules* **1997,** *30*, 7697-7700.

(142) Xia, J.; Zhang, X.; Matyjaszewski, K., The effect of ligands on copper-mediated atom transfer radical polymerization. *ACS Symposium Series* **2000,** *760*(Transition Metal Catalysis in Macromolecular Design), 207-223.

(143) Tang, W.; Kwak, Y.; Braunecker, W.; Tsarevsky, N. V.; Coote, M. L.; Matyjaszewski, K., Understanding Atom Transfer Radical Polymerization: Effect of Ligand and Initiator Structures on the Equilibrium Constants *J. Am. Chem. Soc.* **2008,** *130*(132), 10702-10713.

(144) Matyjaszewski, K.; Nanda, A. K.; Tang, W., Effect of [Cu^{II}] on the Rate of Activation in ATRP. *Macromolecules* **2005,** *38*, 2015-2018.

(145) Becker, M.; Heinemann, F. W.; Schindler, S., Reversible Binding of Dioxygen by a Copper(I) Complex with Tris(2-dimethylaminoethyl)amine (Me_6tren) as a Ligand. *Chem. Eur. J.* **1999,** *5*(11), 3124-3129.

(146) Kickelbick, G.; Pintauer, T.; Matyjaszewski, K., Structural Comparison of Cu^{II} Complexes in Atom Transfer Radical Polymerization. *New. J. Chem.* **2002,** *26*(4), 462-468.

(147) Pintauer, T.; Reinohl, U.; Feth, M.; Bertagnolli, H.; Matyjaszewski, K., Extended X-ray Absorption Fine Structure Study of Copper(I) and Copper(II) Complexes in Atom Transfer Radical Polymerization. *Eur. J. Inorg. Chem.* **2003,** (11), 2082-2094.

(148) Wilkinson, G., *Comprehensive Coordination Chemistry*. Pergamon Press: New York, 1987; Vol. 5.

(149) Karlin, K. D.; Zubieta, J., *Copper Coordination Chemistry: Biochemical and Inorganic Perspectives*. Adenine Press: New York, 1983.

(150) Maiti, D.; Sarjeant, A. A. N.; Itoh, S.; Karlin, K. D., Suggestion of an Organometallic Intermediate in an Intramolecular Dechlorination Reaction Involvning Copper(I) and $ArCH_2Cl$ Moiety. *J. Am. Chem. Soc.* **2008,** *130*(17), 5644-5645.

(151) Tyeklar, Z.; Jacobson, R. R.; Wei, N.; Murthy, N. N.; Zubieta, J.; Karlin, K. D., Reversible Reaction of Dioxygen (and Carbon Monoxide) with a Copper(I) Complex. X-Ray Structures of Relevant Mononuclear Cu(I) Precursor Adducts and the Trans-(μ -1,2-peroxo)dicopper(II) Product *J. Am. Chem. Soc.* **1993,** *115*(7), 2677-2689.

(152) Zhang, C. X.; Kaderli, S.; Costas, M.; Kim, E.-I.; Neuhold, Y.-M.; Karlin, K. D.; Zuberbuhler, A. D., Copper(I)-Dioxygen Reactivity of $[(L)Cu^{I}]^{+}$ (L=Tris(2-pyridylmethyl)amine): Kinetic/Thermodynaimc and Spectroscopic Studies Concerning the Formation of $Cu\text{-}O_2$ and $Cu_2\text{-}O_2$ Aducts as a Function of Solvent Medium and 4-Pyridyl Ligand Substituent Variations. *Inorg. Chem.* **2003,** *42*, 1807-1824.

(153) Eckenhoff, W. T.; Pintauer, T., Atom Transfer Radical Addition in the Presence of Catalytic Amounts of Copper(I/II) Complexes with Tris(2-pyridylmethyl)amine. *Inorg. Chem.* **2007,** *46*(15), 5844-5846.

(154) Eckenhoff, W. T.; Garrity, S. T.; Pintauer, T., Highly Efficient Copper Mediated Atom Transfer Radical Addition (ATRA) in the Presence of Reducing Agent. *Eur. J. Inorg. Chem.* **2008**, 563-571.

(155) Eckenhoff, W. T.; Pintauer, T., Structural Comparison of Copper(I) Complexes with Tris(2-pyridylmethyl)amine (TPMA) in Atom Transfer Radical Addition (ATRA). *Polym. Prepr. (Am. Chem. Soc. Div. Polym. Chem.)* **2008,** *49(2)*, 282-283.

(156) Kickelbick, G.; Paik, H.-J.; Matyjaszewski, K., Immobilization of the Copper Catalyst in Atom Transfer Radical Polymerization. *Macromolecules* **1999,** *32*, 2941-2947.

(157) Haddleton, D. M.; Duncalf, D. J.; Kukulj, D.; Radigue, A. P., 3-Aminopropyl Silica Supported Living Radical Polymerization of Methyl Methacrylate: Dichlorotris(triphenylphosphine)ruthenium(II) Mediated Atom Transfer Polymerization. *Macromolecules* **1999,** *32*(15), 4769-4775.

(158) Shen, Y.; Zhu, S.; Zeng, F.; Pelton, R. H., Atom Transfer Radical Polymerization of Methyl Methacrylate by Silica Gel Supported Copper Bromide/Multidentate Amine. *Macromolecules* **2000,** *33*, 5427-5431.

(159) Shen, Y.; Zhu, S.; Zeng, F.; Pelton, R. H., Supported Atom Transfer Radical Polymerization of Methyl Methacrylate Mediated by CuBr-Tetraethyl Diethylenetriamine Grafted onto Silica Gel. *J. Polym. Sci. Part A:Polym. Chem.* **2001,** *39*, 1051-1059.

(160) Shen, Y.; Zhu, S.; Pelton, R. H., Packed Column Reactor for Continuous Atom Transfer Radical Polymerization: Methyl Methacrylate Polymerization Using Silica Gel Supported Catalyst. *Macromol. Rapid Commun.* **2000,** *21*, 956-959.

(161) Duquesne, E.; Degee, P.; Habimana, J.; Dubois, P., Supported Nickel Bromide Catalyst for Atom Transfer Radical Polymerization (ATRP) of Methyl Methacrylate. *Chem. Commun.* **2004**, 640-641.

(162) Duquesne, E.; Habimana, J.; Degee, P.; Dubois, P., Nickel-Catalyzed Supported ATRP of Methyl Methacrylate Using Crosslinked Polystyrene Triphenylphosphine as Ligand. *Macromolecules* **2005,** *38*(24), 9999-10006.

(163) Duquesne, E.; Labruyere, C.; Habimana, J.; Degee, P.; Dubois, P., Copper-Based Supported Catalyst for the Atom Transfer Radical Polymerization of Methyl Methacrylate: How can Activity and Control be Tuned up? *J. Polym. Sci. Part A:Polym. Chem.* **2005,** *44*(2), 744-756.

(164) Hong, S. C.; Matyjaszewski, K., Fundamentals of Supported Catalysts for Atom Transfer Radical Polymerization (ATRP) and Application of an Immobilized/Soluble Hybrid Catalyst System to ATRP. *Macromolecules* **2002,** *35*, 7592-7605.

(165) Clark, A. J.; Filik, R. P.; Haddleton, D. M.; Radigue, A. P.; J., S. C.; Thomas, G. H.; E., S. M., Solid-Supported Catalysts for Atom-Transfer Radical Cyclization of 2-Haloacetamides. *J. Org. Chem.* **1999,** *64*, 8954-8957.

(166) Clark, A. J.; Geden, J. V.; Thom, S., Solid Support Copper Catalysts for Atom Transfer Radical Cyclizations: Assessment of Support Type and Ligand Structure on Catalyst Performance in the Synthesis of Nitrogen Heterocycles. *J. Org. Chem.* **2006,** *71*(4), 1471-1479.

(167) Herrmann, W. A., Water-Soluble Ligands, Metal Complexes, and Catalysts: Synergism of Homogeneous and Heterogeneous Catalysis. *Angew. Chem. Int. Ed. Engl.* **1993,** *32*, 1524.

(168) Joo, F.; Toth, Z., Catalysis by Water-Soluble Phosphine Complexes of Transition Metal Ions in Aqueous and Two-Phase Media. *J. Mol. Cat.* **1980,** *8*, 369-383.

(169) Horvath, I. T.; Rabai, J., Facile Catalyst Separation Without Water: Fluorous Biphase Hydroformylation of Olefins. *Science* **1994,** *266*, 72-75.

(170) De Campo, F.; Lastecoueres, D.; Verlhac, J.-B., New and Improved Catalysts for Transition Metal Catalysed Radical Reactions. *Chem. Commun.* **1998**, 2117-2118.

(171) Tang, W.; Matyjaszewski, K., Effects of Initiator Structure on Activation Rate Constants in ATRP. *Macromolecules* **2007,** *40*(6), 1858-1863.

(172) Lin, C. Y.; Coote, M. L.; Gennaro, A.; Matyjaszewski, K., Ab Initio Evaluation of the Thermodynamic and Electrochemical Properties of Alkyl Halides and Radicals and Their Mechanistic Implications for Atom Transfer Radical Polymerization *J. Am. Chem. Soc.* **2008,** *130*(138), 12762-12774.

(173) Pintauer, T.; Zhou, P.; Matyjaszewski, K., General Method for Determination of the Activation, Deactivation, and Initiation Rate Constants in Transition Metal-Catalyzed Atom Transfer Radical Processes. *J. Am. Chem. Soc.* **2002,** *124*(28), 8196-8197.

(174) Braunecker, W. A.; Pintauer, T.; Tsarevsky, N. V.; Kickelbick, G.; Matyjaszewski, K., Towards Understanding Monomer Coordination in Atom Transfer Radical Polymerization: Synthesis of $[Cu^{I}(PMDETA)(\pi\text{-}M)][BPh_4]$ (M = Methyl Acrylate, Styrene, 1-Octene and Methyl Methacrylate) and Structural Studies by FT-IR, ^{1}H NMR Spectroscopy and X-ray Crystallography. *J. Organomet. Chem.* **2005,** *690*(4), 916-924.

(175) Braunecker, W. A.; Tsarevsky, N. V.; Pintauer, T.; Gil, R. R.; Matyjaszewski, K., Quantifying Vinyl Monomer Coordination to CuI in Solution and the Effect of Coordination on Monomer Reactivity in Atom Transfer Radical Copolymerization. *Macromolecules* **2005,** *38*(10), 4081-4088.

(176) Qiu, J.; Matyjaszewski, K.; Thounin, L.; Amatore, C., Cyclic Voltammetric Studies of Copper Complexes Catalyzing Atom Transfer Radical Polymerization. *Macromol. Chem. Phys.* **2000,** *201*, 1625-1631.

(177) Matyjaszewski, K., From Atom Transfer Radical Addition to Atom Transfer Radical Polymerization. *Curr. Org. Chem.* **2002,** *6*, 67-82.

(178) Konak, C.; Ganchev, B.; Teodorescu, M.; Matyjaszewski, K.; Kopeckova, P.; Kopecek, J., Poly[*N*-(2-hydroxypropyl)methacrylamide-block-*n*-butyl acrylate] micelles in water/DMF mixed solvents. *Polymer* **2002,** *43*(13), 3735-3741.

(179) Pintauer, T.; Matyjaszewski, K., Atom Transfer Radical Addition and Polymerization Reactions Catalyzed by ppm Amounts of Copper Complexes. *Chem. Soc. Rev.* **2008,** *37*, 1087-1097.

(180) Matyjaszewski, K.; Jakubowski, W.; Min, K.; Tang, W.; Huang, J.; Braunecker, W. A.; Tsarevsky, N. V., Diminishing Catalyst Concentration in Atom Transfer Radical Polymerization with Reducing Agents. *Proc. Natl. Acad. Sci. U.S.A.* **2006,** *103*, 15309-15314.

(181) Jakubowski, W.; Matyjaszewski, K., Activator Generated by Electron Transfer for Atom Transfer Radical Polymerization. *Macromolecules* **2005,** *38*, 4139-4146.

(182) Jakubowski, W.; Matyjaszewski, K., Activators Regenerated by Electron Transfer for Atom-Transfer Radical Polymerization of (Meth)acrylates and Related Block Copolymers. *Angew. Chem. Int. Ed.* **2006,** *45*(27), 4482-4486.

(183) Jakubowski, W.; Min, K.; Matyjaszewski, K., Activators Regenerated by Electron Transfer for Atom Transfer Radical Polymerization of Styrene *Macromolecules* **2006,** *39*(1), 39-45.

(184) Matyjaszewski, K.; Dong, H.; Jakubowski, W.; Pietrasik, J.; Kusumo, A., Grafting from Surfaces for "Everyone": ARGET ATRP in the Presence of Air. *Langmuir* **2007,** *23*(8), 4528-4531.

(185) Min, K.; Gao, H.; Matyjaszewski, K., Preparation of Homopolymers and Block Copolymers in Miniemulsion by ATRP Using Activators Generated by Electron Transfer. *J. Am. Chem. Soc.* **2005,** *127*, 3825-3830.

(186) Min, K.; Gao, H.; Matyjaszewski, K., Use of Ascorbic Acid as Reducing Agent for Synthesis of Well-Defined Polymers by ARGET ATRP. *Macromolecules* **2007,** *40*, 1789-1791.

(187) Quebatte, L.; Thommes, K.; Severin, K., Highly Efficient Atom Transfer Radical Addition Reactions with a Ru^{III} Complex as a Catalyst Precursor. *J. Am. Chem. Soc.* **2006,** *128*(23), 7440-7441.

(188) Pintauer, T.; Eckenhoff, W. T.; Ricardo, C.; Balili, M. N. C.; Biernesser, A. B.; Noonan, S. J.; Taylor, M. J. W., Highly Efficient, Ambient-Temperature Copper-Catalyzed Atom-Transfer Radical Addition (ATRA) in the Presence of Free-Radical Initiator (V-70) as a Reducing Agent. *Chem. Eur. J.* **2009,** *15*, 38-41.

(189) Blackman, A. G., Tripodal Tetraamine Ligands Containing Three Pyridine Units: The Other Polypyridyl Ligands *Eur. J. Inorg. Chem.* **2008**, 2633-2647.

(190) Diaz-Alvarez, A. E.; Crochet, P.; Zablocka, M.; Duhayon, C.; Cadierno, V.; Majoral, J. P., Developing the Kharasch Reaction in Aqueous Media: Dinuclear Group 8 and 9 Catalysts Containing the Bridging Cage Ligand tris(1,2-dimethylhydrazino)diphosphane. *Eur. J. Inorg. Chem.* **2008**, 786-794.

(191) Iizuka, Y.; Li, Z. M.; Satoh, K.; Karnigaito, M.; Okamoto, Y.; Ito, J.; Nishiyama, H., Chiral (-)-DIOP Ruthenium Complexes for Asymmetric Radical Addition and Living Radical Polymerization Reactions. *Eur. J. Org. Chem.* **2007**, 782-791.

(192) Lundgren, R. J.; Rankin, M. A.; McDonald, R.; Stradiotto, M., Neutral, Cationic, and Zwitterionic Ruthenium(II) Atom Transfer Radical Addition Catalysts Supported by P,N-Substituted Indene or Indenide Ligands *Organometallics* **2008,** *27*(2), 254-258.

(193) Oe, Y.; Uozumi, Y., Highly Efficient Heterogeneous Aqueous Kharasch Reaction with an Amphiphilic Resin-Supported Ruthenium Catalyst *Adv. Synth. Catal.* **2008,** *350*(11-12), 1771-1775.

(194) Thommes, K.; Icli, B.; Scopelliti, R.; Severin, K., Atom-Transfer Radical Addition (ATRA) and Cyclization (ATRC) Reactions Catalyzed by a Mixture of $[RuCl_2Cp^*(PPh_3)]$ and Magnesium. *Chem. Eur. J.* **2007,** *13*(24), 6899-6907.

(195) Wolf, J.; Thommes, K.; Brie, O.; Scopelliti, R.; Severin, K., Dinuclear Ruthenium Ethylene Complexes: Synthesis, Structures, and Catalytic Applications in ATRA and ATRC Reactions. *Organometallics* **2008,** *27*, 4464-4474.

(196) Clark, A. J.; Wilson, P., Copper Mediated Atom Transfer Radical Cyclizations with AIBN. *Tetrahedron Lett.* **2008,** *49*, 4848-4850.

(197) Xia, J.; Matyjaszewski, K., Controlled/"Living" Radical Polymerization. Atom Transfer Radical Polymerization Catalyzed by Copper(I) and Picolylamine Complexes. *Macromolecules* **1999,** *32*(8), 2434-2437.

(198) Luo, Y.-R., *Handbook of Bond Dissociation Energies in Organic Compounds*. CRC Press: Boca Raton FL., 2003.

(199) Quebatte, L.; Haas, M.; Solari, E.; Scopelliti, R.; Nguyen, Q. T.; Severin, K., Combinatorial Catalysis with Bimetallic Complexes: Robust and Efficient Catalysts for Atom-Transfer Radical Additions. *Angew. Chem., Int. Ed.* **2004,** *43*(12), 1520-1524.

(200) Quebatte, L.; Haas, M.; Solari, E.; Scopelliti, R.; Nguyen, Q. T.; Severin, K., Atom-Transfer Radical Reactions Under Mild Conditions with $[\{RuCl_2(1,3,5\text{-}C_6H_3iPr_3)\}_2]$ and PCy_3 as the Catalyst Precursors. *Angew. Chem., Int. Ed.* **2005,** *44*(7), 1084-1088.

(201) Quebatte, L.; Solari, E.; Scopelliti, R.; Severin, K., A Bimetallic Ruthenium Ethylene Complex as a Catalyst Precursor for the Kharasch Reaction. *Organometallics* **2005,** *24*(7), 1404-1406.

(202) Beuermann, S.; Buback, M., Rate Coefficients of Free-Radical Polymerization Deduced from Pulsed Laser Experiments. *Prog. Polym. Sci.* **2002,** *27*, 191-254.

(203) Koelsch, C. F.; Boekelheide, V., Coupling of a,B-unsaturated compounds with diazonium salts. *J. Am. Chem. Soc.* **1944,** *66*(3), 412-415.

(204) Munoz-Molina, J. M.; Belderrain, T. R.; Perez, P. J., An Efficient, Selective, and Reducing Agent-Free Copper Catalyst for the Atom-Transfer Radical Addition of Halo Compounds to Activated Olefins *Inorg. Chem.* **2010,** *49*(2), 642-645.

(205) Eckenhoff, W. T.; Manor, B. C.; Pintauer, T., New Tetradentate Ligand Tris-[(3,5-dimethyl-1H-pyrazol-1-yl)methyl]amine (TDPMA) for Atom Transfer Radical Addition (ATRA). *Polym. Prepr. (Am. Chem. Soc. Div. Polym. Chem.)* **2008,** *49(2)*, 213-214.

(206) Pintauer, T., Atom Transfer Radical Addition (ATRA) Catalyzed by ppm Amounts of Copper Complexes. *Polym. Prepr. (Am. Chem. Soc. Div. Polym. Chem.)* **2008,** *49(2)*, 12-13.

(207) Balili, M. N. C.; Pintauer, T., Kinetic Studies of Copper Catalyzed Atom Transfer Radical Addition of Carbon Tetrachloride to Alkenes in the Presence of Reducing Agents. *Polym. Prepr. (Am. Chem. Soc., Div. Polym. Chem.)* **2008,** *49(2)*, 161-162.

(208) Ricardo, C. L.; Pintauer, T., Atom Transfer Radical Cascade Reactions in the Presence of Catalytic Amounts of Copper(II) Complexes with Tris(2-pyridylmethyl)amine. *Polym. Prepr. (Am. Chem. Soc. Div. Polym. Chem.)* **2008,** *49(2)*, 14-15.

(209) Ricardo, C.; Pintauer, T., Copper Catalyzed Atom Transfer Radical Cascade Reactions in the Presence of Free-Radical Diazo Initiators as Reducing Agents. *Chem. Commun.* **2009,** *in press*.

(210) Brace, N. O., Cyclization Reactions of 6-Hepten-2-yl Radicals, 1-Trichloromethyl-6-hepten-2-yl Radicals, and Related Compounds. *J. Org. Chem.* **1967,** *32*, 2711-2718.

(211) Beckwith, A. L. J.; Schiesser, C. H., Regio- and Stereo-Selectivity of Alkenyl Radical Ring Closure: A Theoretical Study. *Tetrahedron* **1985,** *41*, 3925-3941.

(212) Spellmeyer, D. C.; Houk, K. N., Force-Field Model for Intramolecular Radical Additions. *J. Org. Chem.* **1987,** *52*, 959-974.

Chapter 2.

ATOM TRANSFER RADICAL ADDITION IN THE PRESENCE OF CATALYTIC AMOUNTS OF COPPER(I/II) COMPLEXES WITH TRIS(2-PYRIDYLMETHYL)AMINE[†]

Highly efficient atom transfer radical addition (ATRA) of polyhalogenated compounds to alkenes catalyzed by copper(I/II) complexes with tris(2-pyridylmethyl)amine (TPMA) in the presence of radical initiator (AIBN) was reported.

2.1 Introduction

The addition of halogenated compounds to carbon-carbon double (or triple) bonds through a radical process is one of the fundamental reactions in organic chemistry.[1] It was first reported in the early 1940s in which the halogenated methanes were directly added to olefinic bonds.[2] The process was initiated by small amounts of diacyl peroxides or by light. This reaction became known as the Kharasch addition or atom transfer radical addition (ATRA).[3] However, soon after its discovery, it was realized that the use of the Kharasch addition reaction was rather limited because of radical-radical couplings to form alkanes and repeating radical addition to alkene to generate oligomers and polymers. The research was thus shifted in a direction of finding means to selectively control the product distribution. This was achieved by utilizing transition metal complexes which are much more effective halogen transfer agents than alkyl

---

[†] Reproduced in part with permission from Eckenhoff, W.T.; Pintauer, T. *Inorg. Chem.* **2007**, *46*(15), 5844-5846. Copyright 2007 American Chemical Society

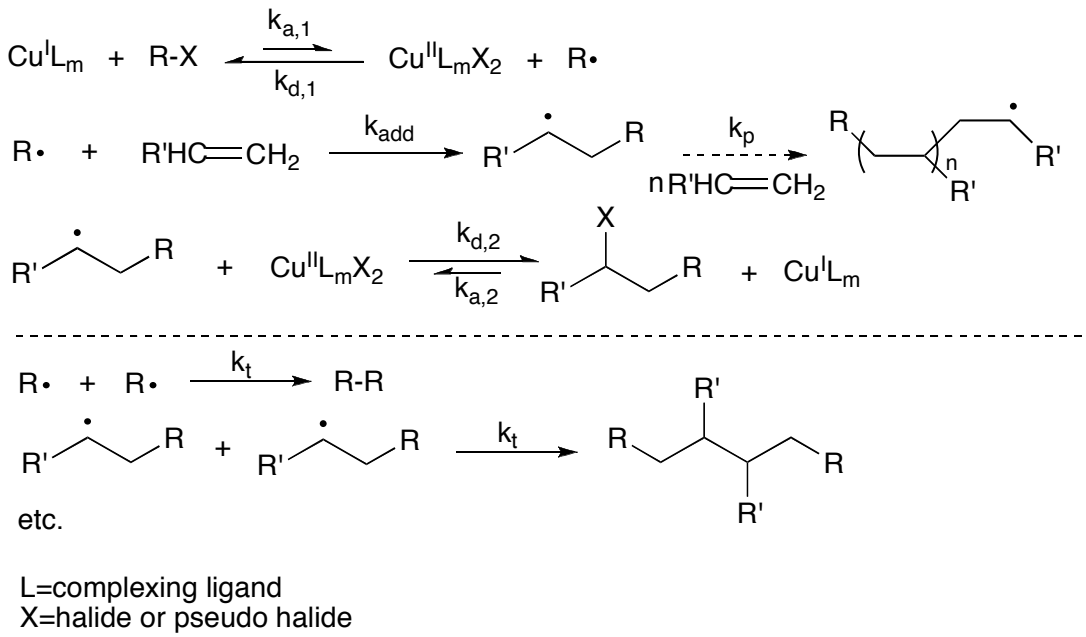

Scheme 2.1.1. Proposed mechanism for copper catalyzed ATRA.

halides. A number of species were found to be particularly effective and they included the complexes of Ru, Fe, Cu and Ni.[4-7]

It is generally accepted that the mechanism of copper catalyzed ATRA involves free radical intermediates (Scheme 2.1.1).[8, 9] Homolytic cleavage of the alkyl halide bond (R-X) by the copper(I) complex generates an alkyl radical $R^{\bullet}$ and the corresponding copper(II) complex. The radical $R^{\bullet}$ adds across the double bond of an olefin, terminates by radical coupling or disproportionation, or abstracts the halogen from the copper(II) complex. The key to increase the chemoselectivity of the monoadduct lies in the radical generating step. In order to achieve high selectivity, the following guidelines need to be met: (a) radical concentration must be low in order to suppress radical termination reactions (rate of activation ($k_{a,1}$ and $k_{a,2}$)<<rate of deactivation ($k_{d,1}$ and $k_{d,2}$)), (b) further activation of the monoadduct should be avoided ($k_{a,1}$>>$k_{a,2}$) and (c) the formation of

oligomers/polymers should be suppressed (rate of transfer ($k_{d,2}[Cu^{II}L_mX]$)>>rate of propagation (k_p[alkene])).

Although transition metal catalyzed ATRA can be applied to a variety of halogenated substrates and alkenes, one of the principal drawbacks of this useful synthetic tool is the amount of catalyst required to achieve the high selectivity towards the monoadduct. In copper catalyzed ATRA, the amount of catalyst typically ranges from 10-30 mol% relative to alkene and/or halogenated compound.[7] As a result, the separation of the catalyst from the reaction mixture is often tedious and difficult. The solution to this problem has recently been found for atom transfer radical polymerization (ATRP),[10, 11] which originated from ATRA. This new process, termed initiators for continuous activator regeneration (ICAR),[12] utilizes copper(II) complexes which are continuously reduced to copper(I) complexes in the presence of phenols, glucose, hydrazine and radical initiators. With ICAR ATRP, controlled synthesis of poly(styrene) and poly(methyl methacrylate) can be implemented with catalyst concentration between 10 and 50 ppm. This technique has recently been utilized with great success in ATRA reactions catalyzed by $[Cp^*Ru^{III}Cl_2(PPh_3)]$ complex.[13] However, to the best of our knowledge, it has never been applied to copper mediated ATRA.

2.2 ATRA of polychlorinated methanes across alkenes

In this section, we report on the characterization and high activity of $Cu^{I}Cl$ and $Cu^{II}Cl_2$ complexes with tris(2-pyridylmethyl)amine (TPMA) in ATRA reactions of polyhalogenated compounds to alkenes in the presence of 2,2'-azobis(2-methylpropionitrile) (AIBN). The tetradentate nitrogen based ligand tris(2-pyridylmethyl)amine (TPMA) was chosen for this study because its complexation to

$Cu^{I}X$ (X=Br or Cl) results in a formation of one of the most active catalysts in copper mediated ATRP.[14-16] Despite the fact that $Cu^{I}Cl$/TPMA complex is a highly active catalyst in ATRP, the conversion of only 2% was observed after 24 hours at 60 ^{o}C in ATRA of CCl_4 to 1- hexene when the ratio of catalyst to olefin was 1:10000. This result is not surprising because the low catalyst/CCl_4 ratio resulted in a complete deactivation of the catalyst. In other words, due to the irreversible radical coupling reactions (Scheme 2.1.1), $Cu^{I}Cl$/TPMA complex was converted to $Cu^{II}Cl_2$/TPMA. In the absence of $Cu^{I}Cl$/TPMA, 3% conversion of 1-hexene was observed resulting in the formation of oligomers/polymers.

Table 2.2.1. ATRA of polychlorinated compounds to alkenes catalyzed by Cu^{I}(TPMA)Cl in the presence of AIBN.[a]

Entry	Alkene	RCl	$[Alkene]_0/[Cu^{I}]_0$	Yield (%)	TON
1	1-hexene	CCl_4	10000:1	72	7200
2			5000:1	98	4900
3	1-octene	CCl_4	10000:1	67	6700
4			5000:1	87	4350
5	styrene	CCl_4	1000:1	42	420
6			500:1	54	270
7			250:1	85	212
8	methyl acrylate	CCl_4	1000:1	60	600
9	1-hexene	$CHCl_3$	1000:1	56	560
10	1-octene	$CHCl_3$	500:1	49	245
11	styrene	$CHCl_3$	1000:1	58	580
12	methyl acrylate	$CHCl_3$	1000:1	63	630

[a]All reactions were performed in toluene at 60 ^{o}C for 24 h with $[R\text{-}Cl]_0$:$[alkene]_0$=4.0. The yield is based on the formation of monoadduct and was determined by ^{1}H NMR using toluene as internal standard or column chromatography. The conversion of alkene for all substrates ranged from 85-100%.

This situation can be changed by the addition of external radical source such as AIBN. The slow decomposition of AIBN provides constant source of radicals, which continuously reduce $Cu^{II}Cl_2$/TPMA complex to $Cu^{I}Cl$/TPMA (Appendix A).[12] Indeed, when the above reaction was conducted in the presence of 5.0 mol% AIBN (relative to

the olefin), 88% conversion of 1-hexene was observed after 24 h with the main product being the desired monoadduct (yield=72%, entry 1, Table 2.2.1). Increasing the catalyst concentration (entry 2), under the same reaction conditions, resulted in a complete conversion of 1-hexene and increase in the yield of monoadduct (98%). Similar results were also obtained with 1-octene (entries 3 and 4). The TONs in these experiments ranged between 4900-7200 (1-hexene) and 4350-6700 (1-octene), and are the highest so far obtained for copper catalyzed ATRA of CCl_4 to olefins. Previously reported TONs ranged between 0.1 and 10.[7, 17] The efficient regeneration of the copper(I) complex by AIBN suggests that ATRA reactions can also be conducted using $Cu^{II}Cl_2$/TPMA complex, which we have confirmed experimentally. In the case when the starting catalyst is $Cu^{II}Cl_2$/TPMA, the process can be termed reverse ATRA, in analogy with well known reverse ATRP developed by Matyjaszewski.[11, 18]

To test the applicability of this new methodology for copper(I) regeneration in ATRA, additional experiments were conducted using other alkenes as well as alkyl halides. Relatively high yields of monoadduct were obtained in ATRA of CCl_4 to styrene (entry 5-7) and methyl acrylate (entry 8), but with much higher catalyst loadings. At the $Cu^{I}Cl$/TPMA to styrene ratio of 1:250 (entry 7), complete conversion of styrene was observed after 24 hours and monoadduct was obtained in 85% yield. Further increase in the ratio of styrene to $Cu^{I}Cl$/TPMA (entries 5 and 6) still resulted in quantitative conversion of styrene, however, more pronounced decrease in the yield of monoadduct was observed. The decrease in the yield of monoadduct was mostly due to the formation of oligomers/polymers. Similar results were also obtained for methyl acrylate. The experiments with less active $CHCl_3$ substrate also worked reasonably well. Relatively

high yields were obtained for all alkenes investigated at $[alkene]_0:[Cu^I]_0$ ratios between 500 and 1000 (entry 9-12).

The catalytic activity of Cu^ICl/TPMA complex in AIBN mediated ATRA reported in this study is lower than the activity of recently reported Ru^{II} and Ru^{III} complexes which were capable of catalyzing ATRA reactions of CCl_4 to olefins with TONs as high as 44500. However, despite the superiority of ruthenium in intermolecular ATRA reactions,[13, 19, 20] we believe that the success of this new methodology for catalyst regeneration can be applied to atom transfer radical cyclization reactions (ATRC), which are predominantly conducted using copper(I) complexes.[7]

2.3 Structural Features of $[Cu^I(TPMA)Cl]$ and $[Cu^{II}(TPMA)Cl][Cl]$

The structural features of highly ATRP and now ATRA active Cu^IX/TPMA (X=Cl and Br) complexes are still not fully understood.[21] Typically, TPMA coordinates to the copper(I) complex in a tetradentate fashion,[22] similarly to structurally related tris[2-(N,N-dimethylamino)ethyl]amine (Me_6TREN).[21, 23] However, the role of halide counterion in these complexes is also very unclear. For example, in the case of Cu^IBr/Me_6TREN complex, EXAFS studies have indicated several possible structures in solution which included $[Cu^I(Me_6TREN)][Br]$, $[Cu^I(Me_6TREN)][Cu^IBr_2]$ and $[Cu^I(Me_6TREN')Br]$ (Me_6TREN' denotes a tricoordinated Me_6TREN). These structures were based on the validated assumption that the maximum coordination number of copper(I) should not exceed four.[24]

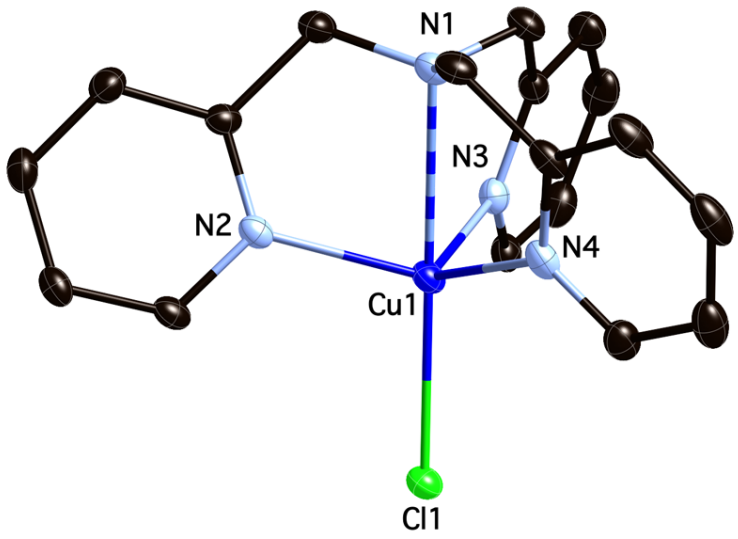

Figure 2.3.1. Molecular structure of Cu^{I}(TPMA)Cl, shown with 30% probability displacement ellipsoids. H atoms have been omitted for clarity.

Shown in Figure 2.3.1is the molecular structure of Cu^{I}(TPMA)Cl complex, which was obtained by slow crystallization of Cu^{I}Cl/TPMA from THF/EtOH at -35 ^{o}C. Surprisingly, the geometry of the complex is distorted trigonal bipyramidal. The copper(I) ion is coordinated by four nitrogen atoms with bond lengths of 2.0704(11), 2.0833(11) and 2.0888(11) Å for the equatorial Cu-N and 2.4366(11) Å for the axial Cu-N bonds and a chlorine atom with a bond length of 2.3976(4) Å. Furthermore, the copper(I) atom lies 0.534(6) Å below the least squares plane derived from N1, N2 and N3, towards the chloride ion.

The corresponding deactivator [Cu^{II}(TPMA)Cl][Cl] can be synthesized from $Cu^{II}Cl_2$ and TPMA, or alternatively Cu^{I}(TPMA)Cl and a large excess of halogenated compound (CCl_4, $CHCl_3$, etc.). In [Cu^{II}(TPMA)Cl][Cl] (Figure 2.3.2), the Cu^{II} atom is coordinated by four nitrogen atoms (Cu^{II}-N_{eq}=2.0759(8) Å and Cu^{II}-N_{ax}=2.0481(14) Å)) from TPMA ligand and a chlorine atom (Cu^{II}-Cl=2.2369(4) Å). The overall geometry of the complex is distorted trigonal bipyramidal and the copper(II) atom is positioned

0.335(3) Å below the least squares plane derived from the equatorial nitrogen atoms in TPMA. The molecule possesses crystallographic 3-fold symmetry with respect to the Cu-Cl1 or Cu-N1 vector. The structures of Cu^{I}(TPMA)Cl and [Cu^{II}(TPMA)Cl][Cl], from

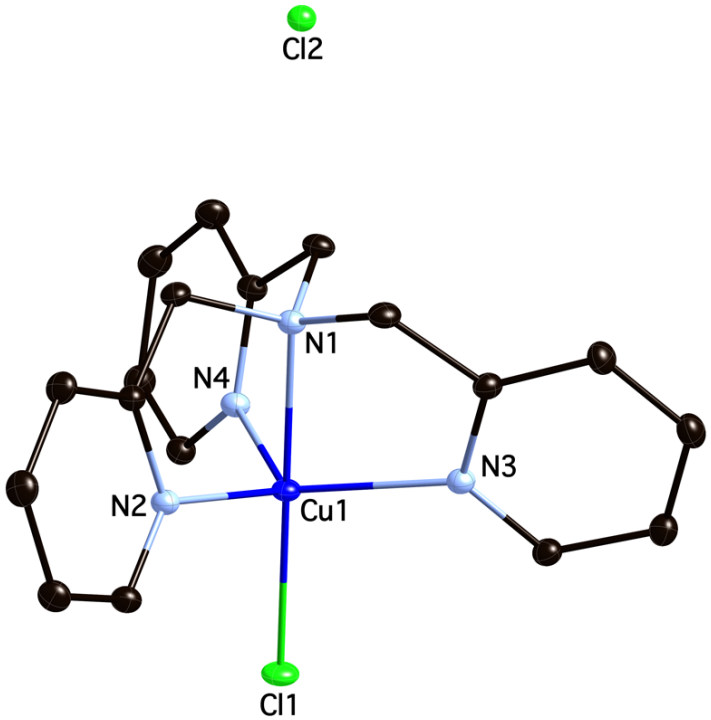

Figure 2.3.2. Molecular structure of [Cu^{II}(TPMA)Cl][Cl], shown with 30% probability displacement ellipsoids. H atoms have been omitted for clarity.

the point of view of TPMA coordination, are very similar. In Cu^{I}(TPMA)Cl complex, the average Cu^{I}-N_{eq} bond length is approximately 0.0050 Å longer than in [Cu^{II}(TPMA)Cl][Cl]. The angles in the plane N_{ax}-Cu-N_{ax} are slightly smaller in Cu^{I}(TPMA)(Cl) (111.13(4)-116.60(4)^{o}) than in [Cu^{II}(TPMA)Cl][Cl] (117.447(12)^{o}), while the N_{ax}-Cu-N_{eq} angles are very similar. The only more pronounced difference in the TPMA coordination to the copper center can be seen in the shortening of Cu-N_{ax} bond length on going from Cu^{I}(TPMA)Cl (2.4366(11) Å) to [Cu^{II}(TPMA)Cl][Cl] (2.0481(14) Å). From the structural point of view, we believe that the high activity of TPMA ligand

in ATRA/ATRP can be explained by the fact that the minimum entropic rearrangement is required when Cu^{I}(TPMA)Cl complex homolytically cleaves R-Cl bond to generate the corresponding [Cu^{II}(TPMA)Cl][Cl] complex. At the present moment, it is the unclear what is the role of Cl^{-} coordination to the [Cu^{I}(TPMA)]$^{+}$ cation (Cu^{I}-Cl=2.3976(4)Å). The most reasonable explanation is that the activation in ATRA/ATRP process proceeds with either prior dissociation of Cl^{-} from Cu^{I}(TPMA)Cl complex or dissociation of Cl^{-} from the corresponding Cu^{II}(TPMA)Cl_2 to generate the deactivator [Cu^{II}(TPMA)Cl][Cl]. Both possibilities are currently under investigation.

2.4 Conclusions

In summary, characterization and high activity of $Cu^{I}Cl$ and $Cu^{II}Cl_2$ complexes with TPMA in ATRA of polyhalogenated compounds to alkenes was reported. This methodology utilized AIBN which provided external source of radicals for continuous regeneration of copper(I) complex. The TONs for 1-hexene (7200) and 1-octene (6700) are the highest so far reported for copper catalyzed ATRA of CCl_4 to olefins. The outlined procedure can potentially be used to decrease the amount of copper catalyst in other ATRA and ATRC reactions.

2.5 Experimental Part

General Procedures - All chemicals were purchased from commercial sources and used as received. Tris(2-pyridylmethyl)amine (TPMA) was synthesized according to literature procedures.[25] Solvents (methylene chloride, pentane, acetonitrile and toluene) were degassed and deoxygenated using Innovative Technology solvent purifier. Methanol was distilled and deoxygenated by bubbling argon for 30 minutes prior to use. All

manipulations were performed under argon atmosphere in a dry box (<1.0 ppm of O_2 and <0.5 ppm of H_2O) or using standard Schlenk line techniques. ^{1}H NMR spectra were obtained using Bruker Avance 400 MHz spectrometer and chemical shifts are given in ppm relative to residual solvent peaks (C_6D_6, 7.16 ppm; $CDCl_3$, 7.26 ppm; $(CD_3)_2CO$, 2.09 ppm). IR spectra were recorded in the solid state or solution using Nicolet Smart Orbit 380 FT-IR spectrometer (Thermo Electron Corporation). Elemental analyses for C, H and N were obtained from Midwest Microlab, LLC.

X-ray Crystal Structure Determination - The X-ray intensity data were collected at 150 K using graphite-monochromated Mo Kα radiation (λ=0.71073 Å) on a Bruker Smart Apex II CCD diffractometer. Data reduction included absorption corrections by the multiscan method using SADABS.[26] Crystal data and experimental conditions are given in Table 1. Structures were solved by direct methods and refined by full-matrix least squares using SHELXTL 6.1 bundled software package.[27] The H atoms were positioned geometrically (aromatic C-H=0.93 Å, methylene C-H=0.97 Å and methyl C-H=0.96 Å) and treated as riding atoms during subsequent refinement, with U_{iso}(H)=1.2U_{eq}(C) or 1.5U_{eq}(methyl C). The methyl groups were allowed to rotate about their local threefold axes. ORTEP-3 for Windows was used to generate molecular graphics.[28]

Synthesis of Cu^I(TPMA)Cl - Cu^I(TPMA)Cl. Cu^ICl (0.100 g, 1.01 mmol) and TPMA (0.293 g, 1.01 mmol) were dissolved in 1.0 mL of EtOH and the mixture stirred under argon for 15 min. THF (1.0 mL) was then added and the solution placed in a refrigerator at -35 ^oC inside the dry box. After 48 h, orange needles were formed, which were

filtered, washed several times with pentane and dried under vacuum to yield 0.286 g (73%) of Cu^{I}(TPMA)Cl. ^{1}H NMR ($(CD_3)_2CO$, 300 MHz, 213 K): δ8.98 (d, J=4.4 Hz, 3H), δ7.79 (dt, J_1=7.6 Hz, J_2=1.6 Hz, 3H), δ7.37 (d, J=7.6 Hz, 3H), δ7.32 (t, J=6.0 Hz, 3H), δ3.92 (s, 6H). Anal. Calcd. for $C_{18}H_{18}ClCuN_4$: C, 55.52; H, 4.66; N, 14.39. Found: C, 55.84; H, 4.60; N, 14.35.

Synthesis of [Cu^{II}(TPMA)Cl][Cl] - Dichloromethane (2 mL) was added to a round bottom flask containing $Cu^{II}Cl_2$ (0.100 g, 0.744 mmol) and tris(2-pyridylmethyl)amine (TPMA) (0.216 g , 0.744 mol). The reaction mixture was stirred at room temperature for 30 minutes and product precipitated by the slow addition of pentane. Green powder was then filtered, washed with 2×10 mL of pentane and dried under vacuum to yield 0.302 g (96%) of [Cu^{II}(TPMA)Cl][Cl]. Anal. Calcd. for $C_{18}H_{18}Cl_2CuN_4$: C, 50.89; H, 4.27; N, 13.19. Found: C, 50.71; H, 4.34; N, 13.25. FT-IR (solid): cm^{-1}, 3364m, 1606s, 1479s, 1436s, 1306m, 1262m, 1094m, 1049m, 1020s, 955w, 841w, 765m. Crystals suitable for X-ray analysis were obtained by slow diffusion of diethyl ether into an acetonitrile solution of the copper(II) complex at room temperature.

General Procedure for the ATRA of CCl_4/$CHCl_3$ to Alkenes - In a typical experiment, the stock solution (0.05 M) of Cu^{I}Cl/TPMA was prepared by dissolving 0.0990 g (1.00 mmol) of Cu^{I}Cl and 0.290 g (1.00 mmol) of tris(2-pyridylmethyl)amine (TPMA) in 20.0 mL of MeOH. To a 5 ml Schlenk flask was then added 700 µL (8.72 mmol) of chloroform or 841 µL (8.72 mmol) of carbon tetrachloride, 500 µL toluene, 0.0179 g (0.109 mmol) of AIBN and 2.18 mmol of olefin. The catalyst solution was then

added at the desired catalyst/alkene ratio. The flask was sealed and stirred at 60 ^{o}C for 24 hours. The conversion of the alkene was determined by ^{1}H NMR using toluene as internal standard. The yield of the monoadduct was determined using either ^{1}H NMR or column chromatography (20/80 vol. ethyl acetate and hexane for styrene and methyl acrylate and hexane for 1-hexene and 1-octene).

General Procedure for the Reverse ATRA of $CCl_4/CHCl_3$ to Alkenes - The procedure for the ATRA in the presence of $Cu^{I}Cl$/TPMA was used except that the stock solution (0.05 M) of $Cu^{II}Cl_2$/TPMA was prepared by dissolving 0.134 g (1.00 mmol) of $Cu^{II}Cl_2$ and 0.290 g (1.00 mmol) of tris(2-pyridylmethyl)amine (TPMA) in 20.0 mL of MeOH.

Reduction of [Cu^{II}(TPMA)Cl][Cl] in the presence of AIBN - [Cu^{II}(TPMA)Cl][Cl] (0.0085 g, 0.0200 mmol) was dissolved in 10.0 mL of degassed CH_3CN and 0.328 g (2.00 mmol, 100 eq.) of AIBN added. The green solution was then heated at 80 ^{o}C for 3 hours. During heating, the solution slowly changed color from green to orange. The UV-Vis spectrum of the reaction mixture after 3 hours indicated complete disappearance of [Cu^{II}(TPMA)Cl][Cl] complex. Furthermore, the resulting spectrum (after dilution) was identical to Cu^{I}(TPMA)Cl complex, which was synthesized by reacting $Cu^{I}Cl$ with the stoichiometric amount of TPMA ligand.

2.6 References

(1) Curran, D. P., The Design and Application of Free Radical Chain Reactions in Organic Synthesis. Part 1. *Synthesis* **1988,** (6), 417-439.

(2) Kharasch, M. S.; Jensen, E. V.; Urry, W. H., Addition of Carbon Tetrachloride and Chloroform to Olefins. *Science* **1945,** *102*(2640), 128.

(3) Curran, D. P., *Comprehensive Organic Synthesis*. Pergamon: New York, 1992; p 715.

(4) Iqbal, J.; Bhatia, B.; Nayyar, N. K., Transition Metal Promoted Free Radical Reactions in Organic Synthesis: The Formation of Carbon-Carbon Bonds. *Chem. Rev.* **1994,** *94*(2), 519-564.

(5) Severin, K., Ruthenium Catalysts for the Kharasch Reaction. *Curr. Org. Chem.* **2006,** *10*, 217-224.

(6) Gossage, R. A.; Van De Kuil, L. A.; Van Koten, G., Diaminoarylnickel(II) "Pincer" Complexes: Mechanistic Considerations in the Kharasch Addition Reaction, Controlled polymerization, and Dendrimeric Transition Metal Catalysts. *Acc. Chem. Res.* **1998,** *31*(7), 423-431.

(7) Clark, A. J., Atom Transfer Radical Cyclisation Reactions Mediated by Copper Complexes. *Chem. Soc. Rev.* **2002,** *31*(1), 1-11.

(8) Minisci, F., Free-Radical Additions to Olefins in the Presence of Redox Systems. *Acc. Chem. Res.* **1975,** *8*(5), 165-171.

(9) Asscher, M.; Vosfsi, D., Chlorine Activation by Redox-transfer. Part I. The Reaction Between Aliphatic Amines and Carbon Tetrachloride. *J. Chem. Soc.* **1961**, 2261-2264.

(10) Wang, J. S.; Matyjaszewski, K., Controlled/"Living" Radical Polymerization. Atom Transfer Radical Polymerization in the Presence of Transition-Metal Complexes. *J. Am. Chem. Soc.* **1995,** *117*(20), 5614-5615.

(11) Matyjaszewski, K.; Xia, J., Atom Transfer Radical Polymerization. *Chem. Rev.* **2001,** *101*(9), 2921-2990.

(12) Matyjaszewski, K.; Jakubowski, W.; Min, K.; Tang, W.; Huang, J.; Braunecker, W.; Tsarevsky, N., Diminishing Catalyst Concentration in Atom Transfer Radical Polymerization with Reducing Agents. *Proc. Nat. Acad. Sci.* **2006,** *103*(42), 15309-15314.

(13) Quebatte, L.; Thommes, K.; Severin, K., Highly Efficient Atom Transfer Radical Addition Reactions with a RuIII Complex as a Catalyst Precursor. *J. Am. Chem. Soc.* **2006,** *128*(23), 7440-7441.

(14) Xia, J.; Gaynor, S. G.; Matyjaszewski, K., Controlled/"Living" Radical Polymerization. Atom Transfer Radical Polymerization of Acrylates at Ambient Temperature. *Macromolecules* **1998,** *31*(17), 5958-5959.

(15) Xia, J.; Matyjaszewski, K., Controlled/"Living" Radical Polymerization. Atom Transfer Radical Polymerization Catalyzed by Copper(I) and Picolylamine Complexes. *Macromolecules* **1999,** *32*(8), 2434-2437.

(16) Tang, H.; Arulsamy, N.; Radosz, M.; Shen, Y.; Tsarevsky, N. V.; Braunecker, W. A.; Tang, W.; Matyjaszewski, K., Highly Active Copper-Based Catalyst for Atom Transfer Radical Polymerization. *J. Am. Chem. Soc.* **2006,** *128*(50), 16277-16285.

(17) De Campo, F.; Lastecoueres, D.; Verlhac, J. B., New Copper(I) and Iron(II) Complexes for Atom Transfer Radical Macrocyclisation Reactions. *J. Chem. Soc. Perkin Trans. 1* **2000,** *4*, 575-580.

(18) Xia, J.; Matyjaszewski, K., Homogeneous Reverse Atom Transfer Radical Polymerization of Styrene Initiated by Peroxides. *Macromolecules* **1999,** *32*(16), 5199-5202.

(19) Quebatte, L.; Haas, M.; Solari, E.; Scopelliti, R.; Nguyen, Q. T.; Severin, K., Atom Transfer Radical Reactions Under Mild Conditions with [{RuCl2(1,3,5-C6H3iPr3)}2] and PCy3 as the Catalyst Precursors. *Angew. Chem., Int. Ed.* **2005,** *44*(7), 1084-1088.

(20) Quebatte, L.; Haas, M.; Solari, E.; Scopelliti, R.; Nguyen, Q. T.; Severin, K., Combinatorial catalysis with bimetallic complexes: robust and efficient catalysts for atom-transfer radical additions. *Angew. Chem., Int. Ed.* **2004,** *43*(12), 1520-1524.

(21) Pintauer, T.; Matyjaszewski, K., Structural Aspects of Copper Catalyzed Atom Transfer Radical Polymerization. *Coord. Chem. Rev.* **2005,** *249*(11-12), 1155-1184.

(22) Karlin, K. D.; Zubieta, J., *Copper Coordination Chemistry: Biochemical and inorganic Perspective*. Adenine Press: New York, 1983.

(23) Kickelbick, G.; Pintauer, T.; Matyjaszewski, K., Structural comparison of CuII complexes in atom transfer radical polymerization. *New J. Chem.* **2002,** *26*(4), 462-468.

(24) Wilkinson, G., *Comprehensive Coordination Chemistry*. Pergamon Press: New York, 1987; Vol. 5.

(25) Tyeklar, Z.; Jacobson, R. R.; Wei, N.; Murthy, N. N.; Zubieta, J.; Karlin, K. D., Reversible reaction of dioxygen (and carbon monoxide) with a copper(I) complex. X-ray structures of relevant mononuclear Cu(I) precursor adducts and the trans-(.mu.-1,2-peroxo)dicopper(II) product. *J. Am. Chem. Soc.* **1993,** *115*(7), 2677-2689.

(26) Sheldrick, G. M., *SADABS Version 2.03*. University of Gottingen, Germany: 2002.

(27) Sheldrick, G. M., *SHELXTL 6.1,Crystallographic Computing System*. Bruker Analytical X-Ray System: Madison, WI, 2000.

(28) Faruggia, L. J., ORTEP-3 for Windows. *J. Appl. Cryst.* **1997,** *30 (5, Pt. 1)*, 565.

Chapter 3.

HIGHLY EFFICIENT COPPER MEDIATED ATOM TRANSFER RADICAL ADDITION (ATRA) IN THE PRESENCE OF REDUCING AGENT[†]

Synthesis, characterization and exceptional activity of Cu^{I}(TPMA)Br (TPMA = tris(2-pyridylmethyl)amine) and [Cu^{II}(TPMA)Br][Br] complexes in ATRA reactions of polybrominated compounds to alkenes in the presence of reducing agent (AIBN) was reported. [Cu^{II}(TPMA)Br][Br], in conjunction with AIBN, effectively catalyzed ATRA reactions of CBr_4 and $CHBr_3$ to alkenes with concentrations between 5 and 100 ppm, which is the lowest number achieved in copper mediated ATRA. The molecular structure of Cu^{I}(TPMA)Br indicated that the complex was pseudo pentacoordinated in the solid state due to the coordination of TPMA (Cu^{I}-N = 2.1024(15), 2.0753(15), 2.0709(15) and 2.4397(14) Å) and bromide anion to the copper(I) center (Cu^{I}-Br = 2.5088(3) Å). Variable temperature ^{1}H NMR and cyclic voltammetry studies confirmed the equilibrium between Cu^{I}(TPMA)Br and [Cu^{I}(TPMA)(CH_3CN)][Br], indicating some degree of halide anion dissociation in solution. The coordination of bromide anion to [Cu^{I}(TPMA)]$^{+}$ cation resulted in a formation of much more reducing Cu^{I}(TPMA)Br complex ($E_{1/2}$ = -720 mV vs. Fc/Fc^{+}) than the corresponding ClO_4^{-} ($E_{1/2}$ = -422 mV vs. Fc/Fc^{+}), PF_6^{-} ($E_{1/2}$ = -421 mV vs. Fc/Fc^{+}), and BPh_4^{-} ($E_{1/2}$ = -397 mV vs. Fc/Fc^{+}) analogues. In [Cu^{II}(TPMA)Br][Br], the Cu^{II} atom was coordinated by four nitrogen atoms (Cu^{II}-N_{eq} = 2.073(2) Å and Cu^{II}-N_{ax} = 2.040(3) Å) from TPMA ligand and a bromine atom (Cu^{II}-Br =

[†] Reproduced in part with permission from Eckenhoff, W.T.; Pintauer, T. *Eur. J. Inorg. Chem.* **2008**, (4), 563-571. Copyright 2008 Wiley-VCH Verlag GmbH & Co.

2.3836(6) Å). The overall geometry of the complex was distorted trigonal bipyramidal. Cu^{I}(TPMA)Br and [Cu^{II}(TPMA)Br][Br] complexes showed similar structural features from the point of view of TPMA coordination. The only more pronounced difference in the TPMA coordination to the copper center was observed in the shortening of Cu-N_{ax} bond length by approximately 0.400 Å on going from Cu^{I}(TPMA)Br to [Cu^{II}(TPMA)Br][Br].

3.1 Introduction

The addition of halogenated compounds to carbon-carbon double (or triple) bonds through a radical process is one of the fundamental reactions in organic chemistry.[1, 2] It was first reported in the early 1940s in which halogenated methanes were directly added to olefinic bonds in the presence of radical initiators or light.[3, 4] Today, this reaction is known as the Kharasch addition or atom transfer radical addition (ATRA),[5] and it is typically catalyzed by transition metal complexes of Ru, Fe, Ni and Cu.[6-9] Although

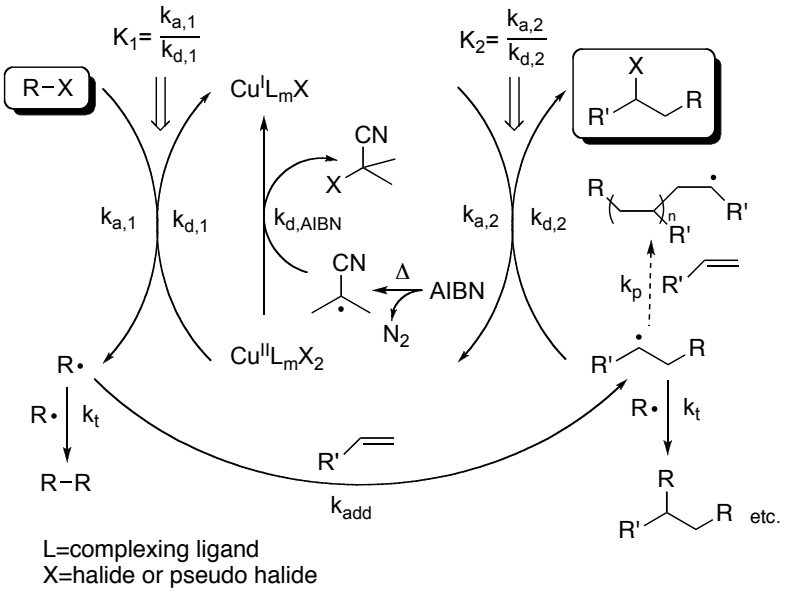

Scheme 3.1.1. Proposed mechanism for copper(I) regeneration in the presence of reducing agent (AIBN) during ATRA process.

transition metal catalyzed ATRA can be applied to a variety of halogenated substrates and alkenes, one of the principal drawbacks of this useful synthetic tool until recently remained the large amount of catalyst required to achieve the high selectivity towards monoadduct. The solution to this problem has been found for atom transfer radical polymerization (ATRP),[10-21] which originated from ATRA. These new processes termed initiators for continuous activator regeneration (ICAR)[22] and activators regenerated by electron transfer (ARGET)[23, 24] utilize copper(II) complexes which are continuously reduced to copper(I) complexes in the presence of phenols, glucose, ascorbic acid, hydrazine, tin(II) 2-ethylhexanoate and radical initiators. With ICAR ATRP, controlled synthesis of poly(styrene) and poly(methyl methacrylate) can be implemented with catalyst concentrations between 10 and 50 ppm.[22] This technique for catalyst regeneration has recently been utilized with great success in ATRA reactions catalyzed by $[Cp^{*}Ru^{III}Cl_2(PPh_3)]$ complex.[25, 26] In the case of ATRA of CCl_4 to olefins in the presence of AIBN, TON's as high as 44500 were obtained.[25] We have also applied this technique in copper mediated ATRA utilizing Cu^{I}(TPMA)Cl and $[Cu^{II}(TPMA)Cl][Cl]$ complexes (TPMA = tris(2-pyridylmethyl)amine).[27] TPMA ligand was chosen for the study because its complexation to $Cu^{I}X$ (X = Cl or Br) results in a formation of one of the most active catalysts in copper mediated ATRP.[28-30] The maximum activity in the addition of CCl_4 to alkenes was achieved with the catalyst to olefin ratio of 1:10,000, resulting in TON's of 7,200 for 1-hexene and 6,700 for 1-octene.

The underlying principle of catalyst regeneration in the presence of reducing agent in ATRA is shown in Scheme 3.1.1. The mechanism is modified from the well-established free radical mechanism operating in metal catalyzed ATRA reactions.[7, 31-34]

In order to increase the chemoselectivity towards the monoadduct, the following general guidelines need to be met: (a) radical concentration must be low in order to suppress radical termination reactions (activation rate constant ($k_{a,1}$ and $k_{a,2}$)<<deactivation rate constant ($k_{d,1}$ and $k_{d,2}$)), (b) further activation of the monoadduct should be avoided ($k_{a,1}$>>$k_{a,2}$) and (c) the formation of oligomers/polymers should be suppressed (rate of transfer ($k_{d,2}$[$Cu^{II}L_mX$])>>rate of propagation (k_p[alkene])). If a large excess of alkyl halide is used relative to copper(I) complex, the equilibrium $K_1 = k_{a,1}/k_{d,1}$ will be shifted towards the right hand side and, as a result of irreversible radical coupling reactions, all of the copper(I) complex will be converted to the corresponding copper(II) complex. To compensate for this unavoidable side reaction in ATRA, a reducing agent such as radical initiator 2,2'-azobis(2-methylpropionitrile) (AIBN) is added to the reaction mixture. Slow decomposition of AIBN provides a constant source of radicals, which continuously reduce copper(II) to copper(I) complex. Copper(I) complex is needed for the activation of alkyl halide (R-X). Furthermore, the efficient regeneration of the copper(I) complex by reducing agent enables ATRA reactions to be conducted starting with the air stable copper(II) complex.[27] Similar observations were also made in the case of [$Cp^*Ru^{III}Cl_2(PPh_3)$] complex.[25, 26] The outlined methodology to decrease the amount of metal catalyst in ATRA reactions could have a significant impact in radical syntheses of natural products, pharmaceutical drugs and other complex molecules, which are currently predominantly conducted utilizing stoichiometric amounts of organotin and organosilane reagents.[35-37] In conjunction with the reduced amount of metal catalyst, the other potential advantage of transition metal catalyzed ATRA is that the resulting product

contains a halide group, which can be easily reduced, eliminated, displaced or converted to a Grignard reagent.

In this chapter, we report on the synthesis, characterization and exceptional activity of Cu^{I}(TPMA)Br and [Cu^{II}(TPMA)Br][Br] complexes in ATRA reactions of polybrominated compounds to alkenes in the presence of reducing agent (AIBN).

3.2 ATRA of $CHBr_3$ and CBr_4 to alkenes

Addition of CBr_4 to simple olefins (1-hexene, 1-octene and 1-decene) in the presence of reducing agent AIBN, but without the Cu^{I}(TPMA)Br complex, proceeded very efficiently at 60 ^{o}C and the desired monoadduct was formed in quantitative yields (Table 3.2.1). These results are not surprising because of the known ability of CBr_4 to function as a very efficient chain transfer agent.[38, 39] In the case of methyl acrylate (entry 4) and styrene (entry 5), quantitative conversions were also observed, however, the decreased yield of the monoadduct was mostly due to the formation of oligomers/polymers as a result of the presence of free radical initiator. Similar reactions

Table 3.2.1. Addition of polybrominated compounds to alkenes in the presence of AIBN.

Entry[a]	Alkene	RBr	% Conversion	% Yield
1	1-hexene	CBr_4	~100	~100
2	1-octene	CBr_4	~100	~100
3	1-decene	CBr_4	~100	~100
4	methyl acrylate	CBr_4	~100	32
5	styrene	CBr_4	99	72
6	1-hexene	$CHBr_3$	10	8
7	1-octene	$CHBr_3$	9.5	9
8	1-decene	$CHBr_3$	11	8
9	methyl acrylate	$CHBr_3$	99	0
10	styrene	$CHBr_3$	41	0

[a]All reactions were performed in CH_3CN at 60 ^{o}C for 24 hours with $[R\text{-}Br]_0$:$[alkene]_0$:$[AIBN]_0$=4:1:0.05. The yield is based on the formation of monoadduct and was determined by ^{1}H NMR using anisole or toluene as internal standard.

in the presence of $CHBr_3$ yielded very low amounts of the monoadduct in the case of 1-hexene (8%, entry 6), 1-octene (9%, entry 7) and 1-decene (8%, entry 8) or none in the case of methyl acrylate (entry 9) and styrene (entry 10). For the latter two alkenes, the major products were oligomers/polymers. In the absence of AIBN, ATRA of CBr_4 and $CHBr_3$ with the Cu^{I}(TPMA)Br to alkene ratios between 1:500 and 1:10,000 did not yield the desired monoadduct, despite the high activity of the complex in ATRP.[28-30] The principle reason was the complete deactivation of the copper(I) complex to the corresponding copper(II) complex, consistent with the proposed mechanism shown in Scheme 3.1.1.

3.3 ATRA of $CHBr_3$ and CBr_4 to alkenes catalyzed by [Cu^{II}(TPMA)Br][Br] in the presence of AIBN

Shown in Table 3.3.1 are the results for the ATRA of polybrominated compounds to alkenes catalyzed by [Cu^{II}(TPMA)Br][Br] complex in the presence of a reducing agent AIBN. The reaction conditions were optimized in such a way as to achieve maximum conversion of the alkene and high yield of the monoadduct. For methyl acrylate, a significant improvement in the yield of the monoadduct was achieved using [Cu^{II}(TPMA)Br][Br] to methyl acrylate ratios of 1:200,000 (81%, entry 1) and 1:100,000 (94%, entry 2). Furthermore, using identical reaction conditions, the complete conversion of styrene was also achieved with the main product being the desired monoadduct (95% entry 3 and 99% entry 4). These results clearly indicate that the slow decomposition of AIBN provides a constant source of radicals, which continuously

reduce [Cu^{II}(TPMA)Br][Br] complex to Cu^{I}(TPMA)Br, which is needed to homolytically cleave the R-Br bond.

As indicated in Table 3.3.1, the methodology for copper(I) regeneration in ATRA in the presence of reducing agent AIBN worked very well for less active bromoform. Relatively high yields of monoadduct were obtained in ATRA of $CHBr_3$ to methyl-

Table 3.3.1. ATRA of polybrominated compounds to alkenes catalyzed by [Cu^{II}(TPMA)Br][Br] in the presence of AIBN.

Entry[a]	Alkene	R-Br	$[Alk.]_0$:$[Cu^{II}]_0$	% Conv.	% Yield[b]
1	methyl acrylate	CBr_4	200,000:1	~100	81(76)[c]
2			100,000:1	~100	94
3	styrene	CBr_4	200,000:1	~100	95(86)[c]
4			100,000:1	99	99
5	methyl acrylate	$CHBr_3$	10,000:1	~100	11(11)[c]
6			5,000:1	~100	23
7			1,000:1	~100	57
8			500:1	~100	66
9	styrene	$CHBr_3$	10,000:1	~100	70
10			5,000:1	~100	77
11			1,000:1	~100	92
12	1-hexene	$CHBr_3$	10,000:1	~100	61(59)[c]
13	1-octene	$CHBr_3$	10,000:1	67	69(54)[c]
14	1-decene	$CHBr_3$	10,000:1	75	63(64)[c]
				74	

[a]All reactions were performed in bulk at 60°C for 24 hours with $[R\text{-}Br]_0$:$[alkene]_0$:$[AIBN]_0$=4:1:0.05, except reactions for entries 1-4 which were performed in CH_3CN. [b]The yield is based on the formation of monoadduct and was determined by ^1H NMR using anisole or toluene as internal standard. [c]Isolated yield after column chromatography.

acrylate (entry 7 and 8) and styrene (entry 10 and 11), but with much higher catalyst loadings. Further decrease in the amount of catalyst for both monomers resulted in a decrease in the yield of the monoadduct. The decrease in the yield of monoadduct was mostly due to the formation of oligomers/polymers, which can be attributed to (a) insufficient trapping of radicals generated from AIBN by the copper(II) complex and (b) further activation of the monoadduct by the copper(I) complex (more pronounced in the

case of methyl acrylate). In the ATRA of $CHBr_3$ to 1-hexene (entry 12), 1-octene (entry 13) and 1-decene (entry 14), moderate yields of the monoadduct can be attributed to incomplete alkene conversions. Furthermore, the conversions of the alkene for entries 12-14 were relatively independent on the copper(II):alkene ratios between 1:500 and 1:10,000, indicating that the rate of addition of $CHBr_2^{\cdot}$ radicals to alkenes is slow. ATRA of $CHBr_3$ to alkenes (entries 5-14, Table 3.3.1) yielded similar results in acetonitrile, indicating that an increase in solvent polarity did not significantly alter the catalytic performance of $[Cu^{II}(TPMA)Br][Br]$.

The activity of $[Cu^{II}(TPMA)Br][Br]$ complex in ATRA of polybrominated compounds to alkenes in the presence of AIBN, based on catalyst loading, conversion of alkene and the yield of monoadduct, is approximately 10 times higher than the activity of previously reported $[Cu^{II}(TPMA)Cl]Cl]$ in the ATRA of polychlorinated compounds to alkenes. Also, for comparable monomers and alkyl halides, its activity is very close to the activity of $[Cp^{*}Ru^{III}Cl_2(PPh_3)]$ complex.[25] $[Cu^{II}(TPMA)Br][Br]$, in conjunction with AIBN, effectively catalyzes ATRA reactions of polybrominated compounds to alkenes with concentrations between 5 and 100 ppm, which is by far the lowest number achieved in copper mediated ATRA.[9, 27, 40, 41]

3.4 Synthesis and characterization of $Cu^{I}(TPMA)Br$

The high activity of $[Cu^{I}(TPMA)Br]$ and $[Cu^{II}(TPMA)Br][Br]$ complexes in ATRA can be explained in terms of increased values of the activation rate constant ($k_{a,1}$, Scheme 3.1.1) and the equilibrium constant for atom transfer ($K_1=k_{a,1}/k_{d,1}$, Scheme 3.1.1), when compared to other copper(I) complexes with bidentate and tridentate nitrogen based ligands and different counterions.[42-45] The structural features of highly ATRP and now

ATRA active $Cu^{I}X$/TPMA (X = Cl and Br) complexes are still not fully understood.[46] TPMA typically coordinates to the copper(I) complex in a tetradentate fashion, similarly to structurally related tris[2-(*N*,*N*-dimethylamino)ethyl]amine (Me_6TREN).[47, 48] However, the role of counterion in these complexes is also very unclear. For example, in the crystal structure of $[Cu^{I}(Me_6TREN)][ClO_4]$,[48] the copper(I) atom was found to be distorted trigonal bipyramidal and it was coordinated by four nitrogen atoms from Me_6TREN ligand (Cu^{I}-N_{eq} = 2.122(7) A and Cu^{I}-N_{ax} = 2.200(14) A) and an oxygen atom from ClO_4^- anion (Cu^{I}-O = 3.53(1) A). In the case of $Cu^{I}Br/Me_6TREN$ complex, EXAFS studies have indicated several possible structures in solution which included $[Cu^{I}(Me_6TREN)][Br]$, $[Cu^{I}(Me_6TREN)][Cu^{I}Br_2]$ and $[Cu^{I}(Me_6TREN')Br]$ (Me_6TREN' denotes a tricoordinated Me_6TREN).[46, 49-51] These structures were based on the validated assumption that the maximum coordination number of copper(I) should not exceed

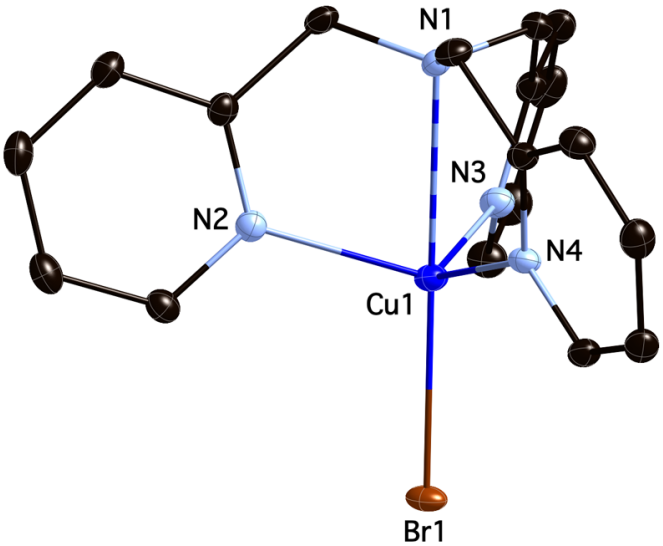

Figure 3.4.1. Molecular structure of Cu^{I}(TPMA)Br, shown with 30% thermal probability ellipsoids. H atoms have been omitted for clarity. Selected distances [Å] and angles [°]: Cu1-N1 2.4397(14), Cu1-N2 2.1024(15), Cu1-N3 2.0753(15), Cu1-N4 2.0709(15), Cu1-Br1 2.5088(3), N4-Cu1-N3 120.51(6), N4-Cu1-N2 112.40(6), N3-Cu1-N2 107.61(6), N4-Cu1-N1 75.37(5), N3-Cu1-N1 74.86(5), N2-Cu1-N1 74.80(5), N1-Cu1-Br1 179.14(3).

four.[52] Recently, we have isolated a neutral Cu^{I}(TPMA)Cl complex, which was surprisingly pseudo pentacoordinated.[27] The copper(I) ion was coordinated by four nitrogen atoms with bond lengths of 2.0704(11), 2.0833(11) and 2.0888(11) Å for the equatorial Cu-N and 2.4366(11) Å for the axial Cu-N bonds and a chlorine atom with a bond length of 2.3976(4) Å.

Shown in Figure 3.4.1 is the molecular structure of Cu^{I}(TPMA)Br complex, which was obtained by slow crystallization of Cu^{I}Br/TPMA from THF/EtOH at -35 ^{o}C. The copper(I) center is also pseudo pentacoordinated and the geometry of the complex is distorted trigonal bipyramidal. The copper(I) atom is coordinated by four nitrogen atoms with bond lengths of 2.1014(15), 2.0753(15), and 2.0709(15) Å for the equatorial Cu-N and 2.4397(14) Å for the axial Cu-N bonds and a bromine atom with a bond length of 2.5088(3) Å. Furthermore, the copper(I) atom lies 0.538(6) Å below the least squares plane derived from N2, N3 and N4, towards the bromide ion. The molecule possesses near (noncrystallographic) 3-fold symmetry with respect to the Cu-Br1 or Cu-N1 vector.

^{1}H NMR spectrum of Cu^{I}(TPMA)Br complex in $(CD_3)_2CO$ at room temperature (Figure 3.4.2) is very broad , indicating a fluxional system. However, on cooling to 220 K, the resonances due to the coordinated TMPA ligand become very well resolved. Only one set of resonances for the protons in TPMA ligands were observed which is consistent with near 3-fold symmetry observed in the solid state structure of Cu^{I}(TPMA)Br complex. Since TPMA coordinates to the copper(I) center through four nitrogen atoms, hydrogen atoms that are close to the coordinated nitrogen atoms should be significantly deshielded relative to the free ligand. This was indeed observed. The chemical shift of

hydrogen atom next to the nitrogen atom in pyridine ring (H_1, Figure 3.4.2) at 220 K moves approximately 0.60 ppm downfield relative to free TPMA. Such downfield shift

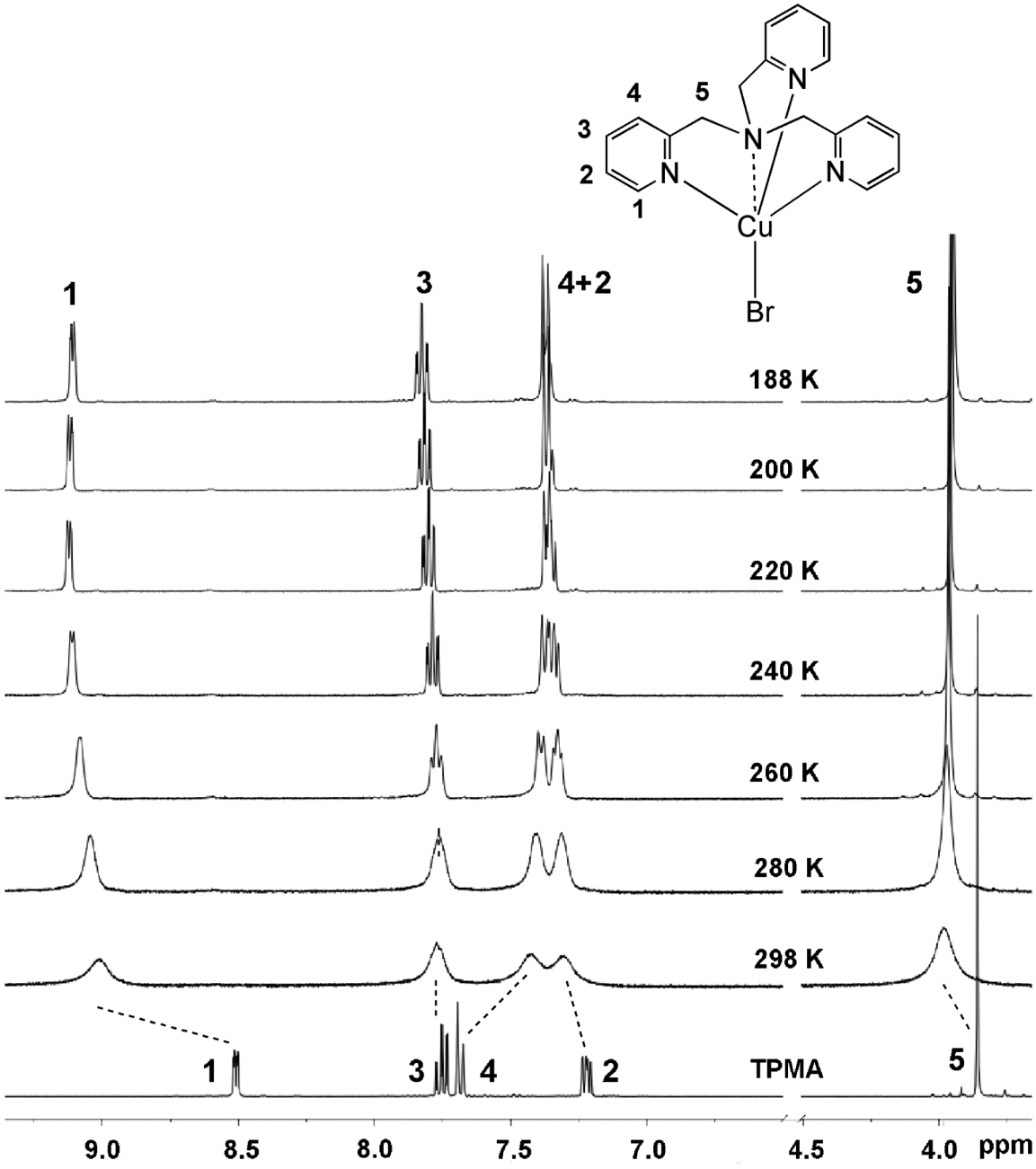

Figure 3.4.2. Variable temperature ^{1}H NMR spectra (400 MHz, $(CD_3)_2CO$) of Cu^I(TPMA)Br complex.

in proton resonances between 0.50 and 0.70 ppm is typically observed in copper(I) complexes with nitrogen based ligands.[53-56] Similarly, the downfield shift of methylene protons in TPMA (H_5, Figure 3.4.2) by 0.10 ppm also indicates coordination. A much smaller downfield shift for methylene protons (H_5) when compared to H_1 in coordinated TPMA is also consistent with the solid state structure of Cu^I(TPMA)Br complex. In Cu^I(TPMA)Br, the distance between the central nitrogen atom and the copper(I) center is on average 0.360 Å longer than the distance between the copper(I) center and the nitrogen atom from pyridine ring. Consequently, the deshielding effect for methylene protons (H_5) should be less than for pyridine proton (H_1), which was observed. The resonances for H_2 and H_3 protons in Cu^I(TPMA)Br are only slightly shielded upon coordination ($\Delta\delta$ = 0.12 and 0.05 ppm, respectively). Furthermore, the resonance for H_4 proton moves approximately 0.32 ppm upfield upon TPMA coordination to the copper(I) center.

The broadened resonances in the solution ^{1}H NMR spectra of Cu^I(TPMA)Br (260-298 K) in $(CD_3)_2CO$ could be induced by the occurrence of the fluxional processes such as ligand dissociation, which are well known in copper(I) complexes with nitrogen-containing ligands.[57-59] In the case of tetradentate TPMA ligand, the dissociation and association of the pyridine nitrogen atoms has been proposed in the previous studies, as well as the possibility for the formation of dimers in which each copper(I) ion is ligated with two pyridine nitrogens and one tertiary amine nitrogen atom of a single TPMA and one pyridine nitrogen atom of the second adjacent TPMA ligand.[60, 61] The ^{1}H NMR spectra of Cu^I(TPMA)Br in Figure 3.4.2 are not consistent with the dimer formation because such coordination environment would result in two chemically inequivalent

methylene groups. Furthermore, the association/dissociation of the pyridine atoms in TPMA ligand (Scheme 3.4.1) appears to be the minor dynamic process because significant deshielding effects would have been observed in the variable temperature ^{1}H NMR studies. For example, the chemical shift of the hydrogen atom next to the nitrogen atom in pyridine ring of TPMA ligand (H_1, Figure 3.4.2) becomes deshielded by approximately 0.10 ppm in the temperature range 298-188 K. In order to test the possibility for Br^- dissociation from the Cu^I(TPMA)Br complex, NMR experiments were performed in the presence of externally added source of Br^- anions, such as tetrabutylammonium bromide (TBABr). In the presence of 1.0 eq. of TBABr, room temperature ^{1}H NMR spectrum of Cu^I(TPMA)Br appeared sharper and resembled the spectrum of Cu^I(TPMA)Br at 260 K in the absence of TBABr. This indicates that the broadening in the ^{1}H NMR spectra of Cu^I(TPMA)Br (260-298 K) could be induced by the dissociation of Br^- anions to generate $[Cu^I(TPMA)]^+[Br]^-$. Furthermore, variable temperature experiments performed in CD_3CN (230-298 K) also indicated halide anion dissociation. Additionally, in the case of Cu^I(TPMA)Br complex in CD_3CN (99% D), we were able to observe the proton resonance for the coordinated CD_3CN, which progressively shifted from 2.13 ppm (298 K) to 2.35 ppm (230 K). At 230 K, only four resonances for the coordinated TPMA ligand were observed, indicating the formation of

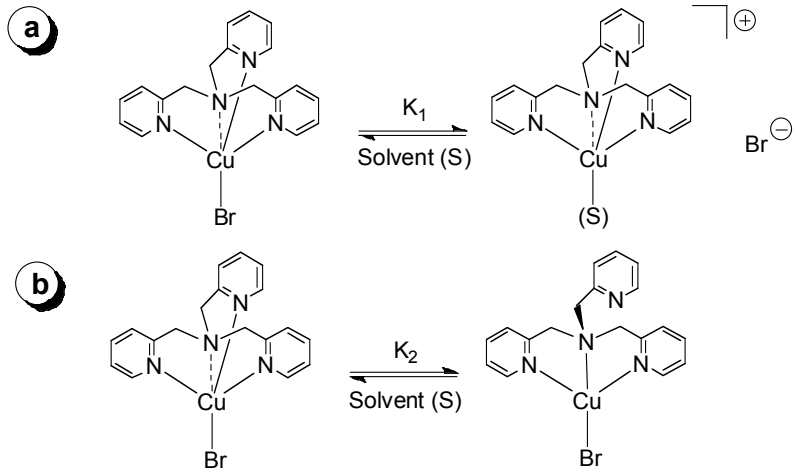

Scheme 3.4.1. Proposed equilibria for Cu^{I}(TPMA)Br involving (a) halide anion and (b) pyridine nitrogen association/dissociation.

[Cu^{I}(TPMA)(CH_3CN)][Br] complex in solution (Scheme 3.4.1). Copper(I) complexes with TPMA ligand and its derivatives containing acetonitrile as the fifth ligand have been previously observed and structurally characterized.[60] Quantifying the temperature and solvent dependence on the equilibrium constant for bromide anion dissociation from Cu^{I}(TPMA)Br complex is subject to future investigation in our laboratories. The study could provide much needed information in an ongoing debate on the nature of the atom transfer radical addition and polymerization from the point of view of concerted inner-

Table 3.4.1. Cyclic voltammetry data for copper(I) complexes in CH_3CN.

Complex[a]	Supp. Elect.	$E_{1/2}$ (mV)	ΔE_p (mV)	i_{pa}/i_{pc}
[Cu^{I}(TPMA)][BPh_4]	TBA-BPh_4	-397	107	1.17
	TBA-Br	-699	109	0.94
[Cu^{I}(TPMA)][ClO_4]	TBA-ClO_4	-422	94	0.95
	TBA-Br	-706	97	0.92
[Cu^{I}(TPMA)][PF_6]	TBA-PF_6	-421	88	0.94
	TBA-Br	-711	88	0.91
Cu^{I}(TPMA)Br	TBA-Br	-720	93	1.08
Cu^{I}(TPMA)Cl	TBACl	-742	111	1.16

[a]Potentials are reported versus Fc/Fc^{+} and were measured under the same electrochemical cell conditions.

sphere electron transfer process (ISET) or a two step process with an outer-sphere electron transfer (OSET).[11, 62, 63]

In order to further examine the coordination of bromide anion to the Cu^{I}(TPMA)Br complex, cyclic voltammetry experiments were performed. Cyclic voltammetry has been extensively used in probing the catalytic activity of copper(I)

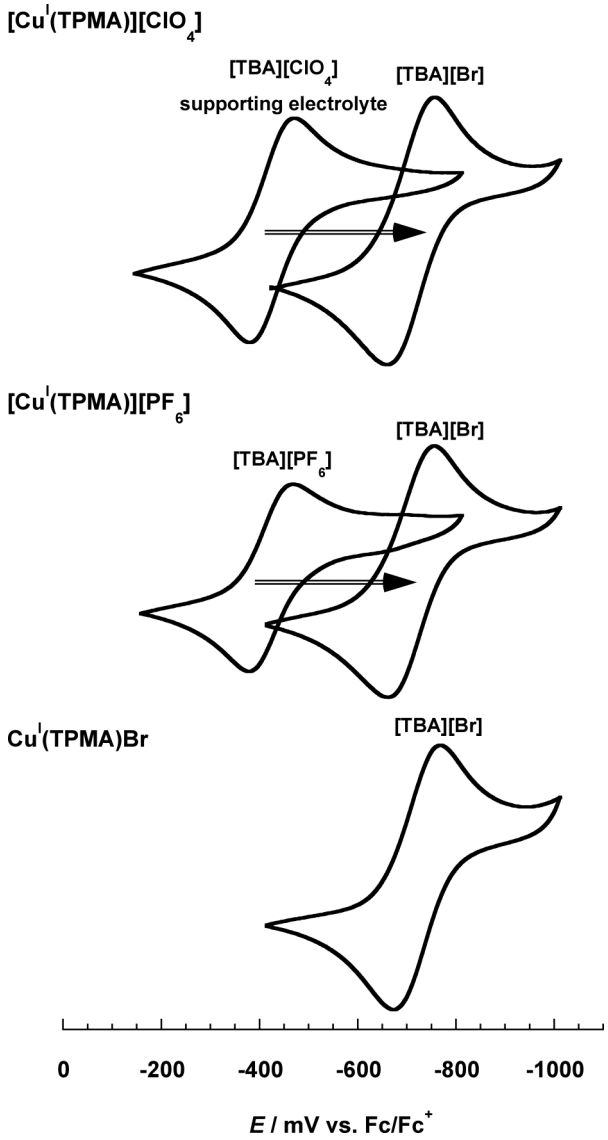

Figure 3.4.3. Cyclic voltammograms of [Cu^{I}(TPMA)][A] (A = ClO_4^-, PF_6^- and Br^-) in the presence of different supporting electrolytes in CH_3CN at room temperature. Spectra are presented with respect to Fc/Fc^+ couple.

complexes in ATRP/ATRA because the redox potential can be correlated with the equilibrium constant for atom transfer (K_{ATRA} or K_{ATRP}, Scheme 3.1.1).[44, 46, 50, 64] Shown in Figure 3.4.3 are cyclic voltammograms of [Cu^{I}(TPMA)][A] (A = ClO_4^-, PF_6^- and Br^-) complexes in the presence of different supporting electrolytes in CH_3CN at room temperature. The electrochemical data are given in Table 3.4.1. The copper(I) complexes display single quasi-reversible redox behavior with i_{pa}/i_{pc} varying from 0.91 to 1.17.

Peak separations were all close to 100 mV at a scan rate of 100 mV/s. The Cu^{II}/Cu^{I} reduction potentials measured for the copper(I) complexes are reported relative to the ferrocene-ferrocenium couple which was used as an external reference. The redox potentials for [Cu^{I}(TPMA)][ClO_4]/TBA-ClO_4 (supporting electrolyte), [Cu^{I}(TPMA)][PF_6]/TBA-PF_6, and [Cu^{I}(TPMA)][BPh_4]/TBA-BPh_4 were determined to be $E_{1/2}$= -422 mV (ΔE_p = 94 mV), $E_{1/2}$ = -421 mV (ΔE_p=88 mV), $E_{1/2}$ = -397 mV (ΔE_p=107 mV) in CH_3CN, respectively. Changing the supporting electrolyte to TBA-Br resulted in the shifting of cyclic voltammograms for both complexes by approximately 300 mV ($E_{1/2}$ = -706 mV (ΔE_p = 97 mV) for ClO_4^-, $E_{1/2}$ = -711 mV (ΔE_p = 88 mV) for PF_6^-, and $E_{1/2}$ = -699 mV (ΔE_p = 109 mV) for BPh_4^- complex, respectively). Furthermore, as indicated in Figure 3.4.3, the voltammograms for ClO_4^- and PF_6^- complexes were nearly identical to the cyclic voltammogram of Cu^{I}(TPMA)Br complex using TBA-Br as the supporting electrolyte ($E_{1/2}$ = -720 mV (ΔE_p = 93 mV). Therefore, for both complexes, it is apparent that the bromide anion has coordinated to the [Cu^{I}(TPMA)]$^+$ cation forming Cu^{I}(TPMA)Br complex, confirming the reverse of the equilibrium shown in Scheme 3.4.1. These results also indicate that the coordination of bromide anion to

$[Cu^{I}(TPMA)]^{+}$ cation results in a formation of much more reducing $Cu^{I}(TPMA)Br$ complex, when compared to ClO_4^-, PF_6^-, and BPh_4^- analogues. Since previous studies by Matyjaszewski et. al.[44, 46, 50, 64] have indicated that the K_{ATRP} or K_{ATRA} equilibrium constants correlate linearly with the $E_{1/2}$ values of the copper complexes (provided that copper(II) complexes have similar "halidophilicities" (K_{HP}) or the equilibrium constants for the heterolytic dissociation of the halide anion), one can assume that $Cu^{I}(TPMA)Br$ complex should be a better catalyst for ATRA/ATRP, then $[Cu^{I}(TPMA)][ClO_4]$ or $[Cu^{I}(TPMA)][PF_6]$. However, in the ATRA of $CHBr_3$ and CBr_4 to alkenes catalyzed by $[Cu^{I}(TPMA)][A]$ (A=ClO_4^-, PF_6^- and Br^-) similar catalytic activities were obtained. Therefore, apart from the redox potentials, additional factors must also contribute towards the equilibrium constant for atom transfer.

3.5 Synthesis and characterization of $[Cu^{II}(TPMA)Br][Br]$

The corresponding deactivator, $[Cu^{II}(TPMA)Br][Br]$ was synthesized by reacting $Cu^{II}Br_2$ with the stoichiometric amount of TPMA. The same complex can be alternatively prepared by reacting $Cu^{I}(TPMA)Br$ with excess alkyl halide (CBr_4 or $CHBr_3$). Shown in Figure 3.5.1 is the molecular structure of $[Cu^{II}(TPMA)Br][Br]$ complex. In $[Cu^{II}(TPMA)Br[Br]$, the Cu^{II} atom is coordinated by four nitrogen atoms (Cu^{II}-N_{eq} = 2.073(2) Å and Cu^{II}-N_{ax} = 2.040(3) Å)) from TPMA ligand and a bromine atom (Cu^{II}-Br = 2.3836(6) Å). The overall geometry of the complex is distorted trigonal bipyramidal and the copper(II) atom is positioned 0.329(3) Å below the least squares plane derived from the equatorial nitrogen atoms in TPMA. The N1, Cu1 and Br1 atoms lie on crystallographic threefold rotation axis.

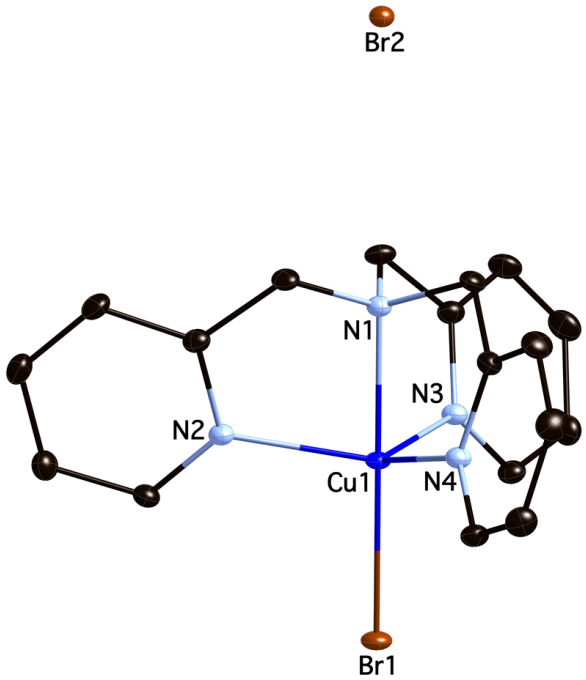

Figure 3.5.1. Molecular structure of [Cu^{II}(TPMA)Br][Br], shown with 30% probability displacement ellipsoids. H atoms have been omitted for clarity. Symmetry codes: (i) –*y*+1/2, -*z*+1, *x*+1/2 and (ii) *z*-1/2, -*x*+1/2, -*y*+1. Selected distances [Å] and angles [^{o}]: Cu1-N1 2.040(3), Cu1-N2 2.073(2), Cu1-Br1 2.3836(6), N1-Cu1-N2 80.86(5), N2-Cu1-$N2^{i}$ 117.53(3), N1-Cu1-Br1 180.00(5).

From the point of view of TPMA coordination, the structures of Cu^{I}(TPMA)Br and [Cu^{II}(TPMA)Br][Br] are very similar. In Cu^{I}(TPMA)Br complex, the average Cu^{I}-N_{eq} bond length is 0.0100 Å longer than in [Cu^{II}(TPMA)Br][Br]. The N_{ax}-Cu-N_{eq} angles are very similar in both complexes, while the average angle in the plane N_{ax}-Cu-N_{ax} is slightly larger in [Cu^{II}(TPMA)Br][Br] (117.53(3)^{o}) than in Cu^{I}(TPMA)Br (113.51(10)^{o}). The only more pronounced difference in the TPMA coordination to the copper center can be seen in the shortening of Cu-N_{ax} bond length by approximately 0.400 Å on going from Cu^{I}(TPMA)Br to [Cu^{II}(TPMA)Br][Br]. Similar observations were also made in the case of Cu^{I}(TPMA)Cl and [Cu^{II}(TPMA)Cl][Cl] complexes, in which the shortening of Cu-N_{ax} bond length on going from copper(I) to copper(II) complex was determined to be 0.389

Å.[27] From the structural point of view, the high activity of Cu^{I}(TPMA)Br and [Cu^{II}(TPMA)Br][Br] complexes in ATRA, can be explained by the fact that minimum entropic rearrangement is required when Cu^{I}(TPMA)Br complex homolytically cleaves R-Br bond to generate [Cu^{II}(TPMA)Br][Br]. At the present moment, it is the unclear what is the role of Br^{-} coordination to the [Cu^{I}(TPMA)]$^{+}$ cation (Cu^{I}-Br = 2.5088(3) Å). The most reasonable explanation is that the activation in ATRA/ATRP process proceeds with either prior dissociation of Br^{-} from Cu^{I}(TPMA)Br complex or dissociation of Br^{-} from the corresponding Cu^{II}(TPMA)Br_2 to generate the deactivator [Cu^{II}(TPMA)Br][Br]. As a part of an ongoing investigation in our laboratories, detailed kinetic measurements and cyclic voltammetry studies are being conducted in order to further investigate the equilibrium for Br^{-} coordination to the [Cu^{I}(TPMA)$^{+}$ cation in Cu^{I}(TPMA)Br complex and its effect on catalytic activity and reaction mechanism.

3.6 Conclusions

In summary, synthesis, characterization and high activity of Cu^{I}Br and $Cu^{II}Br_2$ complexes with TPMA in ATRA of polybrominated compounds to alkenes was reported. The methodology utilized AIBN, which provided external source of radicals for continuous regeneration of the copper(I) complex. [Cu^{II}(TPMA)Br][Br], in conjunction with AIBN, effectively catalyzed ATRA reactions of CBr_4 and $CHBr_3$ to alkenes with concentrations between 5 and 100 ppm, which is the lowest number achieved in copper mediated ATRA. Molecular structure of Cu^{I}(TPMA)Br indicated that the complex was pseudo pentacoordinated in the solid state due to the coordination of bromide anion to the copper(I) center (Cu^{I}-Br=2.5088(3) Å). Variable temperature ^{1}H NMR and cyclic voltammetry studies confirmed the equilibrium between Cu^{I}(TPMA)Br and

$[Cu^{I}(TPMA)(S)][Br]$ (S = solvent) complexes, indicating halide anion dissociation in solution. The extent of dissociation was depended on the solvent polarity and temperature. In $[Cu^{II}(TPMA)Br[Br]$, the Cu^{II} atom was coordinated by four nitrogen atoms (Cu^{II}-N_{eq} = 2.073(2) Å and Cu^{II}-N_{ax} = 2.040(3) Å)) from TPMA ligand and a bromine atom (Cu^{II}-Br = 2.3836(6) Å). The overall geometry of the complex was distorted trigonal bipyramidal. $Cu^{I}(TPMA)Br$ and $[Cu^{II}(TPMA)Br][Br]$ complexes showed similar structural features for the point of view of TPMA coordination. The only more pronounced difference in the TPMA coordination to the copper center was observed in the shortening of Cu-N_{ax} bond length by approximately 0.400 Å on going from $Cu^{I}(TPMA)Br$ to $[Cu^{II}(TPMA)Br][Br]$. Apart from the detailed structural and mechanistic studies of this interesting catalytic system, we are presently utilizing the outlined procedure to decrease the amount of copper catalyst in synthetically more attractive atom transfer radical cyclization (ATRC) reactions.

3.7 Experimental Part

General Procedures - All chemicals were purchased from commercial sources and used as received. Tris(2-pyridylmethyl)amine (TPMA) was synthesized according to literature procedures.[65] Solvents (methylene chloride, pentane, acetonitrile and toluene) were degassed and deoxygenated using Innovative Technology solvent purifier. All monomers were degassed by bubbling argon for 30 minutes and stored in the dry box. Methanol was distilled and deoxygenated by bubbling argon for 30 minutes prior to use. All manipulations were performed under argon atmosphere in a dry box (<1.0 ppm of O_2 and <0.5 ppm of H_2O) or using standard Schlenk line techniques. ^{1}H NMR spectra were obtained using Bruker Avance 300 and 400 MHz spectrometers and chemical shifts are

given in ppm relative to residual solvent peaks (C_6D_6, 7.16 ppm; $CDCl_3$, 7.26 ppm; $(CD_3)_2CO$, 2.05 ppm). IR spectra were recorded in the solid state or solution using Nicolet Smart Orbit 380 FT-IR spectrometer (Thermo Electron Corporation). Elemental analyses for C, H and N were obtained from Midwest Microlab, LLC.

Synthesis of Cu^I(TPMA)Br - Cu^IBr (25.0 mg, 0.174 mmol) and TPMA (50.0 mg, 0.174 mmol) were dissolved in 2 mL of EtOH/THF (50%/50% vol.) and slow crystallization at -35 ^oC afforded orange crystals. The supernatant liquid was decanted and the crystals washed with 2×10 mL *n*-pentane and dried under vacuum to yield 47 mg (63%) of Cu^I(TPMA)Br. ^1H NMR ($(CD_3)_2CO$, 300 MHz, 220 K): δ9.10 (d, J=4.2 Hz, 3H), δ7.81 (dt, J_1=7.7 Hz, J_2=1.8 Hz, 3H), δ7.36 (d, J=7.8 Hz, 3H), δ7.32 (m, 3H), δ3.94 (s, 6H). Anal Calcd. for $C_{18}H_{18}BrCuN_4$ (433.81): C, 49.84; H, 4.18; N, 12.91. Found: C, 49.55; H, 4.09; N, 12.65.

Synthesis of [Cu^{II}(TPMA)Br][Br] - Dichloromethane (2 mL) was added to a round bottom flask containing $Cu^{II}Br_2$ (0.878 g, 3.93 mmol) and tris(2-pyridylmethyl)amine (TPMA) (1.141 g, 3.93 mmol). The reaction mixture was stirred at room temperature for 30 minutes and product precipitated by the slow addition of *n*-pentane. The supernatant liquid was decanted and the green powder was washed with 2×10 mL of *n*- pentane and dried under vacuum to yield 1.93 g (96%) of [Cu^{II}(TPMA)Br][Br]. Anal. Calcd. for $C_{18}H_{18}Br_2CuN_4$ (513.72): C, 42.08; H, 3.53; N, 10.91. Found: C, 42.06; H, 3.55; N, 10.72. FT-IR (solid): cm^{-1}, 3048w, 2932w, 2864w, 1602m, 1470m, 1434m, 1299m, 1155w, 1091m, 1016m, 792s, 648m. Crystals suitable for x-ray analysis were obtained

by slow diffusion of diethyl ether into an acetonitrile solution of the complex at room temperature.

Catalyst solutions - Two catalyst solutions were made using dilution flasks to accommodate the various catalyst loadings. Catalyst solution A was made by dissolving 25.7 mg of [Cu(TPMA)Br][Br] in 5.00 mL of acetonitrile to give a 0.01M solution. Catalyst solution B was made in two steps by first dissolving 25.7 mg of [Cu(TPMA)Br][Br] in 10.00 mL of acetonitrile to give a 0.005M solution. 1.00 mL of this 0.005M solution was then diluted to 10.00 mL of acetonitrile to yield a 0.0005M catalyst solution.

ATRA of $CHBr_3$ to alkenes - To a 5 mL Schlenk flask was added 282.0 μL (3.22 mmol) bromoform, which was dissolved in 500 μL of acetonitrile. To this solution was added 0.805 mmol of alkene, 6.6 mg (40.3 μmol) of AIBN, and 15.0 μL of toluene in the case of 1-hexene, 1-octene, and 1-decene or anisole in the case of styrene and methyl acrylate. The catalyst solution A was then added at the desired alkene/catalyst ratio between 500:1 and 10,000:1. The flask was then sealed under argon and stirred at 60 ^{o}C for 24 hours. The conversion of the alkene and the yield of the monoadduct was determined by ^{1}H NMR using internal standard. Column chromatography was used to determine isolated yields (10% ethyl acetate in hexanes for styrene and methyl acrylate and hexane for 1-hexene, 1-octene, and 1-decene).

ATRA of CBr_4 to alkenes - Carbon tetrabromide (1.067 g, 3.22 mmol) was placed in a 5 mL Schlenk flask and dissolved in 500.0 μL of acetonitrile. To this solution was added 0.805 mmol of alkene, 6.6 mg (40.3 μmol) of AIBN, and 15.0 μL of toluene in the case

of 1-hexene, 1-octene, and 1-decene or anisole in the case of styrene and methyl acrylate. The catalyst solution B was then added at the desired alkene/catalyst ratio between 100,000:1 and 200,000:1. The flask was then sealed under argon and stirred at 60 ^{o}C for 24 hours. The conversion of the alkene and the yield of the monoadduct was determined by ^{1}H NMR using internal standard. Column chromatography was used to determine isolated yields (10% ethyl acetate in hexanes for styrene and methyl acrylate and hexane for 1-hexene, 1-octene, and 1-decene).

X-ray crystal structure determination - The X-ray intensity data were collected at 150 K using graphite-monochromated Mo Kα radiation (λ=0.71073 Å) on a Bruker Smart Apex II CCD diffractometer. Data reduction included absorption corrections by the multiscan method using SADABS.[66] Crystal data and experimental conditions are given in Table 4. Structures were solved by direct methods and refined by full-matrix least squares using SHELXTL 6.1 bundled software package.[67] The H atoms were positioned geometrically (aromatic C-H=0.93 Å, methylene C-H = 0.97 Å and methyl C-H = 0.96 Å) and treated as riding atoms during subsequent refinement, with U_{iso}(H)=1.2U_{eq}(C) or 1.5U_{eq}(methyl C). The methyl groups were allowed to rotate about their local threefold axes. ORTEP-3 for Windows was used to generate molecular graphics.[68] Crystallographic data (excluding structure factors) for the structures reported in this article have been deposited with Cambridge Crystallographic Data Center as supplementary publications nos. CCDC-649993 (Cu^{I}(TPMA)Br) and CCDC-649992 ([Cu^{II}(TPMA)Br][Br]). Copies of the data can be obtained free of charge on application

to CCDC, 12 Union Road, Cambridge CB21EZ, UK (fax(+44)1223-336-033; e-mail: deposit@ccdc.cam.ac.uk).

Cyclic voltammetry - Electrochemical measurements were carried out using Bioanalytical Systems (BAS) model CV-50W in a dry box. Cyclic voltammograms were recorded with a standard three-electrode system consisting of a Pt-wire working electrode, a standard calomel reference electrode, and a Pt-wire auxiliary electrode. Tetrabutyammonium perchlorate (TBA-ClO_4), tetrabutylammonium hexafluorophosphate (TBA-PF_6), Tetrabutyammonium tetraphenylborate (TBA-BPh_4), tetrabutylammonium chloride (TBA-Cl) and tetrabutylammonium bromide (TBA-Br) were used as the supporting electrolyte, and all voltammograms were externally referenced to ferrocene. As such, the potentials are reported with respect to Fc/Fc+ couple, without junction correction. All cyclic voltammograms were simulated digitally to obtain the half-wave potentials.

3.8 References

(1) Curran, D. P., The Design and Application of Free Radical Chain Reactions in Organic Synthesis. Part 1. *Synthesis* **1988,** *6*, 417-439.

(2) Curran, D. P., The Design and Application of Free Radical Chain Reactions in Organic Synthesis. Part 2. *Synthesis* **1988,** *7*, 489-513.

(3) Kharasch, M. S.; Jensen, E. V.; Urry, W. H., Addition of Carbon Tetrachloride and Chloroform to Olefins. *Science* **1945,** *102*(2640), 128.

(4) Kharasch, M. S.; Jensen, E. V.; Urry, W. H., Addition of Derivatives of Chlorinated Acetic Acid to Olefins. *J. Am. Chem. Soc.* **1945,** *67*, 1626.

(5) Curran, D. P., *Comprehensive Organic Synthesis*. Pergamon: New York, 1992; p 715.

(6) Iqbal, J.; Bhatia, B.; Nayyar, N. K., Transition Metal-Promoted Free-Radical Reactions in Organic Synthesis: The Formation of Carbon-Carbon Bonds. . *Chem. Rev.* **1994,** *94*(2), 519-564.

(7) Severin, K., Ruthenium catalysts for the Kharasch reaction. *Curr. Org. Chem.* **2006,** *10*(2), 217-224.

(8) Gossage, R. A.; Van De Kuil, L. A.; Van Koten, G., Diaminoarylnickel(II) "Pincer" Complexes: Mechanistic Considerations in the Kharasch Addition Reaction, Controlled polymerization, and Dendrimeric Transition Metal Catalysts. *Acc. Chem. Res.* **1998,** *31*(7), 423-431.

(9) Clark, A. J., Atom Transfer Radical Cyclisation Reactions Mediated by Copper Complexes. *J. Chem. Soc. Rev* **2002,** *31*(1), 1-11.

(10) Wang, J. S.; Matyjaszewski, K., Controlled/"Living" Radical Polymerization. Atom Transfer Radical Polymerization in the Presence of Transition-Metal Complexes. . *J. Am. Chem. Soc.* **1995,** *117*(20), 5614-5615.

(11) Matyjaszewski, K.; Xia, J., Atom transfer radical polymerization. *Chem. Rev.* **2001,** *101*(9), 2921-2990.

(12) Matyjaszewski, K., *Controlled Radical Polymerization (ACS Symp. Ser. 685)*. ACS: Washington, DC, 1998; p 483.

(13) Matyjaszewski, K., *Controlled/Living Radical Polymerization. Progress in ATPR, NMP and RAFT (ACS Symp. Ser. 768)*. ACS: Washington, DC., 2000; p 484.

(14) Coessens, V.; Pintauer, T.; Matyjaszewski, K., Functional polymers by atom transfer radical polymerization. *Prog. Polym. Sci.* **2001,** *26*(3), 337.

(15) Matyjaszewski, K.; Davis, T. P., *Handbook of Radical Polymerization*. Wiley: Hoboken, 2002.

(16) Matyjaszewski, K., *Advances in Controlled/Living Radical Polymerization (ACS Symp. Ser. 854)*. ACS: Washington, DC., 2003.

(17) Matyjaszewski, K., Controlling polymer structures by atom transfer radical polymerization and other controlled/living radical polymerizations. . *Macromol. Symp.* **2003,** *195*, 25-31.

(18) Matyjaszewski, K., Macromolecular engineering: From rational design through precise macromolecular synthesis and processing to targeted macroscopic material properties. . *Prog. Polym. Sci.* **2005,** *30*(8-9), 858-875.

(19) Matyjaszewski, K., *Controlled Radical Polymerization. From Synthesis to Materials (ACS Symp. Ser. 944)*. ACS: Washington, DC., 2006.

(20) Patten, T. E.; Matyjaszewski, K., Copper(I)-Catalyzed Atom Transfer Radical Polymerization. *Acc. Chem. Res.* **1999,** *32*(10), 895-903.

(21) Kamigaito, M.; Ando, T.; Sawamoto, M., Metal-Catalyzed Living Radical Polymerization. *Chem. Rev.* **2001,** *101*(12), 3689-3745.

(22) Matyjaszewski, K.; Jakubowski, W.; Min, K.; Tang, W.; Huang, J.; Braunecker, W. A.; Tsarevsky, N. V., Diminishing Catalyst Concentration in Atom Transfer Radical Polymerization with Reducing Agents. *Proc. Natl. Acad. Sci. U.S.A.* **2006,** *103*, 15309-15314.

(23) Jakubowski, W.; Matyjaszewski, K., Activators Regenerated by Electron Transfer for Atom-Transfer Radical Polymerization of (Meth)acrylates and Related Block Copolymers. *Angew. Chem. Int. Ed.* **2006,** *45*(27), 4482-4486.

(24) Jakubowski, W.; Min, K.; Matyjaszewski, K., Activators Regenerated by Electron Transfer for Atom Transfer Radical Polymerization of Styrene. . *Macromolecules* **2006,** *39*(1), 39-45.

(25) Quebatte, L.; Thommes, K.; Severin, K., Highly Efficient Atom Transfer Radical Addition Reactions with a RuIII Complex as a Catalyst Precursor. *J. Am. Chem. Soc.* **2006,** *128*(23), 7440-7441.

(26) Thommes, K.; Icli, B.; Scopelliti, R.; Severin, K., Atom-Transfer Radical Addition (ATRA) and Cyclization (ATRC) Reactions Catalyzed by a Mixture of [RuCl2Cp*(PPh3)] and Magnesium. *Chem. Eur. J.* **2007,** *13*(24), 6899-6907.

(27) Eckenhoff, W. T.; Pintauer, T., Atom Transfer Radical Addition in the Presence of Catalytic Amounts of Copper(I/II) Complexes with Tris(2-pyridylmethyl)amine. *Inorg. Chem.* **2007,** *46*(15), 5844-5846.

(28) Xia, J.; Gaynor, S. G.; Matyjaszewski, K., Controlled/"Living" Radical Polymerization. Atom Transfer Radical Polymerization of Acrylates at Ambient Temperature. *Macromolecules* **1998,** *31*(17), 5958-5959.

(29) Xia, J.; Matyjaszewski, K., Controlled/"Living" Radical Polymerization. Atom Transfer Radical Polymerization Catalyzed by Copper(I) and Picolylamine Complexes. *Macromolecules* **1999,** *32*(8), 2434-2437.

(30) Tang, H.; Arulsamy, N.; Radosz, M.; Shen, Y.; Tsarevsky, N. V.; Braunecker, W. A.; Tang, W.; Matyjaszewski, K., Highly Active Copper-Based Catalyst for Atom Transfer Radical Polymerization. *J. Am. Chem. Soc.* **2006,** *128*(50), 16277-16285.

(31) Minisci, F., Free-Radical Additions to Olefins in the Presence of Redox Systems. *Acc. Chem. Res.* **1975,** *8*(5), 165-171.

(32) Asscher, M.; Vofsi, D., Chlorine Activation by Redox-Transfer. Part I. The Reaction Between Aliphatic Amines and Aarbon Tetrachloride. *J. Chem. Soc.* **1961**, 2261-2264.

(33) Delaude, L.; Demonceau, A.; Noels, A. F., Ruthenium Promoted Radical Processes Toward Fine Chemistry. In *Topics in Organometallic Chemistry*, Bruneau, C.; Dixneuf, P. H., Eds. Springer: Berlin, 2004; Vol. 11, pp 155-171.

(34) Nagashima, H., Radical Reactions. In *Ruthenium in Organic Synthesis*, Murahashi, S.-I., Ed. Wiley-VCH: Weinheim, 2004; pp 333-343.

(35) Jasperse, C. P.; Curran, D. P.; Fevig, T. L., Radical Reactions in Natural Product Synthesis. *Chem. Rev.* **1991,** *91*, 1237-1286.

(36) Giese, B., *Angew. Chem.* **1985,** *97*, 555.

(37) Curran, D. P.; Chen, M.-H.; Spletzer, E.; Seong, C. M.; Chang, C.-T., *J. Am. Chem. Soc.* **1986,** *108*, 6384.

(38) Brandrup, J.; Immergut, E. H.; Gulke, E. A., *Polymer Handbook*. Wiley-Interscience: New York, 1999.

(39) Eastmond, G. C., The Kinetics of Free Radical Polymerization of Vinyl Monomers in Homogeneous Solutions. In *Comphrehensive Chemical Kinetics*, Bamford, C. H.; Tipper, C. F. H., Eds. American Elsevier: New York, 1976; Vol. 14A.

(40) De Campo, F.; Lastecoueres, D.; Verlhac, J.-B., New copper(I) and iron(II) complexes for atom transfer radical macrocyclization reactions. *J. Chem. Soc., Perkin Trans. 1* **2000,** (4), 575-580.

(41) Munoz-Molina, J. M.; Caballero, A.; Diaz-Requejo, M. M.; Trofimenko, S.; Belderrain, T. R.; Perez, P. J., Copper-Homoscorpionate Complexes as Active Catalysts for Atom Transfer Radical Addition to Olefins. *Inorg. Chem.* **2007,** *46*, 7725-7730.

(42) Tang, W.; Tsarevsky, N. V.; Matyjaszewski, K., Determination of Equilibrium Constants for Atom Transfer Radical Polymerization. *J. Am. Chem. Soc.* **2006,** *128*(5), 1598-1604.

(43) Matyjaszewski, K.; Paik, H.-j.; Zhou, P.; Diamanti, S. J., Determination of Activation and Deactivation Rate Constants of Model Compounds in Atom Transfer Radical Polymerization. *Macromolecules* **2001,** *34*(15), 5125-5131.

(44) Matyjaszewski, K.; Gobelt, B.; Paik, H.-j.; Horwitz, C. P., Tridentate Nitrogen-Based Ligands in Cu-Based ATRP: A Structure-Activity Study. *Macromolecules* **2001,** *34*(3), 430-440.

(45) Schellekens, M. A. J.; de Wit, F.; Klumperman, B., Effect of the Copper Counterion on the Activation Rate Parameter in Atom Transfer Radical Polymerization. *Macromolecules* **2001,** *34*(23), 7961-7966.

(46) Pintauer, T.; Matyjaszewski, K., Structural Aspects of Copper Catalyzed Atom Transfer Radical Polymerization. *Coord. Chem. Rev.* **2005,** *249*(11-12), 1155-1184.

(47) Karlin, K. D.; Zubieta, J., *Copper Coordination Chemistry: Biochemical and Inorganic Perspectives*. Adenine Press: New York, 1983.

(48) Becker, M.; Heinemann, F. W.; Schindler, S., Reversible binding of dioxygen by a copper(I) complex with tris(2-dimethylaminoethyl)amine (Me6tren) as a ligand. *Chem. Eur. J.* **1999,** *5*(11), 3124-3129.

(49) Kickelbick, G.; Pintauer, T.; Matyjaszewski, K., Structural comparison of CuII complexes in atom transfer radical polymerization. *New. J. Chem.* **2002,** *26*(4), 462-468.

(50) Pintauer, T.; McKenzie, B.; Matyjaszewski, K., Toward structural and mechanistic understanding of transition metal-catalyzed atom transfer radical processes. . *ACS Symp. Ser.* **2003,** *854*, 130-147.

(51) Pintauer, T.; Reinohl, U.; Feth, M.; Bertagnolli, H.; Matyjaszewski, K., Extended X-ray absorption fine structure study of copper(I) and copper(II) complexes in atom transfer radical polymerization. *Eur. J. Inorg. Chem.* **2003,** (11), 2082-2094.

(52) Wilkinson, G., *Comprehensive Coordination Chemistry*. Pergamon Press: New York, 1987; Vol. 5.

(53) Munakata, M.; Kitagawa, S.; Kosome, S.; Asahara, A., Studies of copper(I) olefin complexes. Formation constants of copper olefin complexes with 2,2'-bipyridine, 1,10-phenanthroline, and their derivatives. . *Inorg. Chem.* **1986,** *25*(15), 2622-2627.

(54) Thompson, J. S.; Swiatek, R. M., Copper(I) complexes with unsaturated small molecules. Synthesis and properties of monoolefin and carbonyl complexes. *Inorg. Chem.* **1985,** *24*(1), 110-113.

(55) Kitagawa, S.; Munakata, M., Binuclear copper(I) complexes which reversibly react with carbon monoxide. 1. Di-μ -halogeno-bis(2,2'-bipyridine)dicopper(I) and its derivatives. . *Inorg. Chem.* **1981,** *20*(7), 2261-2267.

(56) Kitagawa, S.; Munakata, M.; Miyaji, N., New mixed-ligand copper(I) complexes with 2,2'-bipyridine and their NMR spectra. . *Inorg. Chem.* **1982,** *21*(10), 3842-3843.

(57) Mealli, C.; Arcus, C. A.; Wilkinson, J. L.; Marks, T. J.; Ibers, J. A., *J. Am. Chem. Soc.* **1976,** *98*, 711-718.

(58) Coggin, D. K.; Gonzalez, J. A.; Kook, A. M.; Stanbury, D. M.; Wilson, L. J., *Inorg. Chem.* **1991,** *30*, 1115-1125.

(59) Carrier, S. M.; Ruggiero, C. E.; Houser, R. P.; Tolman, W. B., *Inorg. Chem.* **1993,** *32*, 4889-4899.

(60) Zhang, C. X.; Kaderli, S.; Costas, M.; Kim, E.-I.; Neuhold, Y.-M.; Karlin, K. D.; Zuberbuhler, A. D., Copper(I)-Dioxygen Reactivity of [(L)CuI]+ (L=Tris(2-pyridylmethyl)amine): Kinetic/Thermodynaimc and SPectroscopic Studies Concerning the Formation of Cu-O2 and Cu2-O2 Aducts as a Function of Solvent Medium and 4-Pyridyl Ligand Substituent Variations. *Inorg. Chem.* **2003,** *42*, 1807-1824.

(61) Tyeklar, Z.; Jacobson, R. R.; Wei, N.; Murthy, N. N.; Zubieta, J.; Karlin, K. D., Reversible Reaction of O2 (and CO) with a Copper(I) Complex. X-ray Strucutres of Relevant Mononuclear Cu(I) Precursor Aducts and the trans-(u-1,2-Peroxo)dicopper(II) Product. *J. Am. Chem. Soc.* **1993,** *115*, 2677-2689.

(62) Tsarevsky, N. V.; Matyjaszewski, K., "Green" Atom Transfer Radical Polymerization: From Process Design to Preparation of Well-Defined Environmentally Friendly Polymeric Materials. *Chem. Rev.* **2007,** *107*, 2270-2299.

(63) Braunecker, W. A.; Matyjaszewski, K., Controlled/Living Radical Polymerization: Features, Developments and Perspectives. *Prog. Polym. Sci.* **2007,** *32*, 93-146.

(64) Qiu, J.; Matyjaszewski, K.; Thounin, L.; Amatore, C., Cyclic Voltammetric Studies of Copper Complexes Catalyzing Atom Transfer Radical Polymerization. *Macromol. Chem. Phys.* **2000,** *201*, 1625-1631.

(65) Tyeklar, Z.; Jacobson, R. R.; Wei, N.; Murthy, N. N.; Zubieta, J.; Karlin, K. D., Reversible reaction of dioxygen (and carbon monoxide) with a copper(I) complex. X-ray structures of relevant mononuclear Cu(I) precursor adducts and the trans-(μ -1,2-peroxo)dicopper(II) product. . *J. Am. Chem. Soc.* **1993,** *115*(7), 2677-2689.

(66) Sheldrick, G. M., *SADABS Version 2.03*. University of Gottingen: Germany, 2002.

(67) Sheldrick, G. M., *SHELXTL 6.1,Crystallographic Computing System*. Bruker Analytical X-Ray System: Madison, WI, 2000.

(68) Faruggia, L. J., ORTEP-3 for Windows. *J. Appl. Cryst.* **1997,** *30 (5, Pt. 1)*, 565.

Chapter 4.

AMBIENT TEMPERATURE COPPER CATALYZED ATRA REACTIONS IN THE PRESENCE OF FREE RADICAL INITIATOR (V-70) AS A REDUCING AGENT[†]

Highly efficient ambient temperature copper catalyzed ATRA of polyhalogenated compounds to alkenes in the presence of free radical initiator 2,2'-azobis(4-methoxy-2,4-dimethyl valeronitrile) (V-70) was reported. V-70 has been shown to be very effective reducing agent, enabling selective formation of the ATRA product with highly active monomers such as methyl acrylate, methyl methacrylate and vinyl acetate using as low as 0.002 mol% of copper.

4.1 Introduction

The addition of halogenated compounds to carbon-carbon double (or triple) bonds through a radical process is one of the fundamental reactions in organic chemistry.[1] It was first reported in the early 1940s in which halogenated alkenes were directly added to olefinic bonds in the presence of free radical initiators or light.[2] Today, this reaction is known as the Kharasch addition or atom transfer radical addition (ATRA), and it is typically catalyzed by transition metal complexes of Ru, Fe, Ni and Cu.[3-6] Transition metal catalyzed ATRA, despite being discovered nearly 40 years before widely used tin mediated radical addition to olefins[7] and iodine atom transfer radical addition,[8] is still not

---

[†] Reproduced in part with permission from Pintauer, T.; Eckenhoff, W.T.; Ricardo, C.; Balili, M.N.C.; Biernesser, A.B.; Noonan, S.T.; Taylor, M.J.W. *Chem. Eur. J.* **2009**, *15*(1), 38-41. Copyright 2008 Wiley-VCH Verlag GmbH & Co.

fully utilized as a technique in organic synthesis. Until recently, the principal reason for small participation of ATRA in complex molecule and natural product syntheses remained the large amount of transition metal needed to achieve high selectivity towards the desired target compound (typically 5-30 mol% relative to alkene).[3, 9] This obstacle caused serious problems in product separation and catalyst regeneration, making the process environmentally unfriendly and expensive.

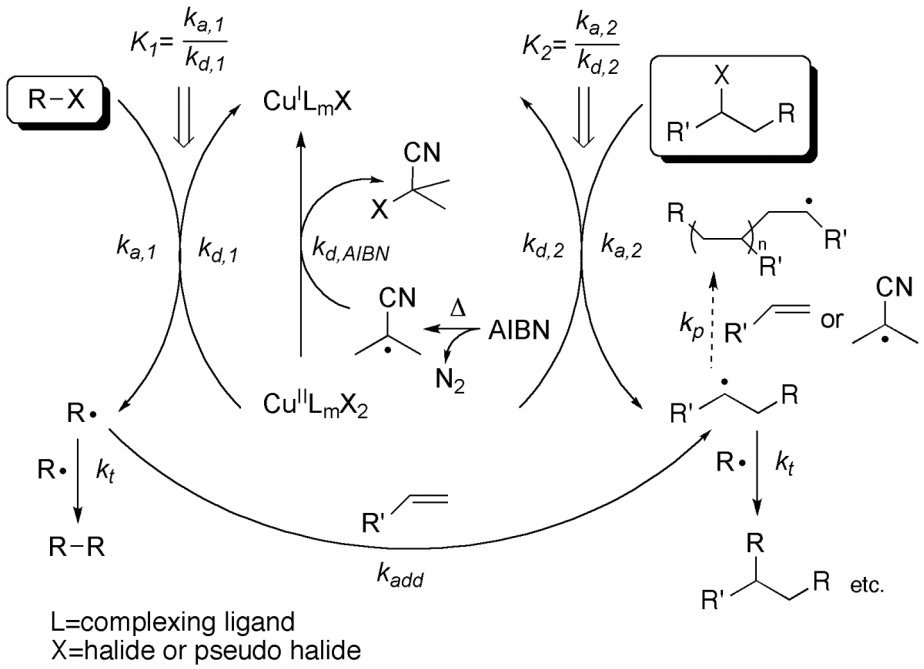

Scheme 4.1.1. Proposed mechanism for copper(I) regeneration in the presence of reducing agent (AIBN) during ATRA process.

Originally, the solution to this problem has been found for copper catalyzed atom transfer radical polymerization (ATRP),[3, 10, 11] and was subsequently applied first to ruthenium[12] and then copper[13, 14] catalyzed ATRA reactions. In all of these processes, the activator (transition metal complex in the lower oxidation state) is continuously regenerated from deactivator (transition metal complex in the higher oxidation state) in

the presence of reducing agents such as phenols, glucose, ascorbic acid, hydrazine, tin(II) 2-ethylhexanoate magnesium and free radical initiators (Scheme 4.1.1).[3] When applied to ATRA of CCl_4 to alkenes catalyzed by $Cp^*Ru^{III}Cl_2(PPh_3)$ complex in the presence of AIBN, TONs as high as 44500 were obtained.[12] Even more impressive TONs were achieved with CBr_4 and $[Cu^{II}(TPMA)Br][Br]$ (TPMA=tris(2-pyridylmethyl)amine) complex (as high as 160000), enabling efficient ATRA reactions in the presence of as little as 5 ppm of copper.[13] Since the seminal reports by our[14] and the research group of Severin,[12] this method of catalyst regeneration in ATRA has attracted considerable academic interest,[15-22] and was even successfully applied to intramolecular ATRA or atom transfer radical cyclization (ATRC) reactions.[21-23]

In our initial studies, AIBN was successfully utilized as a reducing agent in copper catalyzed ATRA of polyhalogenated compounds to alkenes at 60 ^oC.[13, 14] Excellent results were obtained in the case of simple a-olefins (1-hexene, 1-decene and 1-octene), as well as methyl acrylate and styrene. However, this method of catalyst regeneration was completely unsuccessful for monomers with high propagation rate constants such as methyl acrylate (MA) ($k_{p,60}=2.8\times10^4$ $M^{-1}s^{-1}$), butyl acrylate (BA) ($k_{p,60}=3.1\times10^4$ $M^{-1}s^{-1}$), vinyl acetate (VA) ($k_{p,60}=7.9\times10^3$ $M^{-1}s^{-1}$) and styrene (sty) ($k_{p,60}=3.3\times10^2$ $M^{-1}s^{-1}$).[24] Copper catalyzed ATRA of these monomers in the presence of AIBN at 60 ^oC yielded exclusively polymers. The principal reason for the lack of formation of the desired single addition adduct was not inefficient catalyst regeneration or further activation of the monoadduct, but rather competing polymerization initiated by the presence of AIBN (Scheme 4.1.1). The potential solution to this problem is to utilize redox-reducing agents that do not generate free radicals, such as magnesium.[21] However,

the presence of magnesium as a reducing agent is less desired because it increases the total metal concentration in the system. An alternative solution is to utilize low temperature free radical initiators that could be used at ambient temperatures and easily, together with radical decomposition products, removed from reaction mixtures. At ambient temperatures, free radical polymerization of highly active monomers (3.0×10^2 s^{-1}<k_p[alkene]<1.8×10^3 s^{-1}), as a result of decrease in propagation rate constants ($k_{p,25}$(MA)=1.3×10^4 $M^{-1}s^{-1}$, $k_{p,25}$(BA)=1.5×10^4 $M^{-1}s^{-1}$, $k_{p,25}$(VA)=3.4×10^3 $M^{-1}s^{-1}$ and $k_{p,25}$(sty)=87 $M^{-1}s^{-1}$)[24] is expected to compete with a halide transfer (1.8×10^3 s^{-1} <$k_{d,2}$[$Cu^{II}L_mX_2$]<1.8×10^5 s^{-1}) to a much lesser extent.[25] Consequently, provided efficient regeneration of the copper(I) complex, substantially higher yields of the desired monoadduct could be obtained.

In this chapter, we report on highly efficient ambient temperature copper catalyzed ATRA of polyhalogenated compounds to alkenes in the presence of free radical initiator 2,2'-azobis(4-methoxy-2,4-dimethyl valeronitrile) (V-70) as a reducing agent.

4.2 ATRA with Using V-70 as a Reducing Agent

The addition of polyhalogenated compounds (in particular CBr_4 and CCl_4) to alkenes could proceed only in the presence of free radical initiator, because of their known ability to function as very efficient chain-transfer agents.[26, 27] As indicated in Table 4.2.1 (entries 3,7 and 11), V-70 ambient temperature initiated Kharasch addition reactions proceeded with reasonably high yields only in the case of CBr_4 and simple a-olefins. However, the obtained yields of the monoadduct (53-64 %) were significantly lower than the yields obtained at 60°C in the presence of AIBN (96-100%).[13]

Furthermore, the formation of monoadduct was observed in the V-70 initiated free radical addition of CBr_4 to styrene (entry 15), methyl acrylate (entry 19) and vinyl acetate (entry 27) and $CHBr_3$ to methyl acrylate (entry 20) and methyl methacrylate (entry 24), albeit with much smaller yields. For these highly active monomers, the discrepancies between the alkene conversion and percent yield were mostly due to competing free radical polymerization.

Table 4.2.1. Ambient temperature Kharasch addition of polyhalogenated compounds to alkenes in the presence of V-70.

Entry[a]	Alkene	R-X	% Conv.	% Yield[b]
1	1-decene	CCl_4	5	0
2		$CHCl_3$	3	0
3		CBr_4	55	53
4		$CHBr_3$	3	0
5	1-octene	CCl_4	8	0
6		$CHCl_3$	1	0
7		CBr_4	57	56
8		$CHBr_3$	5	0
9	1-hexene	CCl_4	4	0
10		$CHCl_3$	3	0
11		CBr_4	66	64
12		$CHBr_3$	4	0
13	styrene	CCl_4	18	1
14		$CHCl_3$	26	0
15		CBr_4	32	29
16		$CHBr_3$	37	0
17	methyl acrylate	CCl_4	88	0
18		$CHCl_3$	83	0
19		CBr_4	96	38
20		$CHBr_3$	51	37
21	methyl methacrylate	CCl_4	86	0
22		$CHCl_3$	83	0
23		CBr_4	91	8
24		$CHBr_3$	96	14
25	vinyl acetate	CCl_4	18	16
26		$CHCl_3$	11	0
27		CBr_4	30	27
28		$CHBr_3$	6	0

[a] All reactions were performed in CH_3CN at 22±2 °C for 24 hours with $[RX]_0$:$[alkene]_0$:$[V\text{-}70]_0$=1:1:0.05.
[b] Yield is based on the formation of monoadduct and was determined by ^1H NMR spectroscopy.

When $[Cu^{II}(TPMA)X][X]$ ($X=Cl^-$ (for RCl) or Br^- (for RBr)) was added to the reaction mixture at ambient temperature, truly remarkable results were obtained (Table 4.2.2). For ATRA of CCl_4 to α-olefins (1-decene, 1-octene and 1-hexene), excellent yields of the monoadduct were obtained using Cu^{II} to alkene ratio of 1:1000 (entries 1, 8, and 15). Further decrease in catalyst loading to 1:2000 (0.05 mol %) still resulted in high conversions and excellent yields of the monoadduct. Even more impressive results were obtained in ATRA of CBr_4 to 1-decene (entries 4-6), 1-octene (entries 11-13) and 1-hexene (entries 18-20) using as low as 0.002 mol% of copper (20 ppm relative to alkene). On the other hand, $CHCl_3$ and $CHBr_3$ were found to be quite inactive in ATRA reactions with α-olefins at ambient temperatures, at catalyst loadings as high as 10 mol%.

As aforementioned, ATRA of polyhalogenated compounds to monomers that are highly active in free radical polymerization was not very successful at 60 ^oC when AIBN was used as radical initiator. As a result of very high propagation rate constants for monomers such as methyl acrylate, methyl methacrylate, acrylonitrile or vinyl acetate, copper catalyzed ATRA in the presence of AIBN as a reducing agent at 60 ^oC yielded exclusively polymers. The results at ambient temperatures using V-70 as a reducing agent were quite different. In ATRA of CCl_4 (entry 22) and CBr_4 (entry 27) to styrene, monoadduct was obtained in nearly quantitative yields using between 0.2 and 0.5 mol% of copper catalyst. ATRA reactions with styrene were also quite successful with less active $CHCl_3$ (entries 25-26) and $CHBr_3$ (30-31). Similarly, dramatic improvements were also observed in ATRA of CCl_4 and CBr_4 to methyl acrylate (entries 32-33 and 34-36) and methyl methacrylate (entries 39-40 and 41-42). For both monomers, ATRA of CCl_4 and CBr_4 proceeded very efficiently at ambient temperature using catalyst loadings as

Table 4.2.2. Ambient temperature ATRA of polyhalogenated compounds to alkenes catalyzed by $[Cu^{II}(TPMA)X][X]$ (X=Cl^- and Br^-) in the presence of free radical initiator V-70 as a reducing agent.

Entry[a]	Alkene	R-X	$[Alkene]_0:[Cu^{II}]_0$	% Conv./%Yield[c]	TON[d]
1	1-decene	CCl_4	1000:1 (0.1)[b]	93/93	930
2			2000:1 (0.05)	81/80	1600
3		$CHCl_3$	10:1 (10)	1/0	/
4		CBr_4	10000:1 (0.01)	~100/99	4600
5			20000:1 (0.005)	96/89	7200
6			50000:1 (0.002)	92/88	17500
7		$CHBr_3$	100:1 (1)	2/2	2
8	1-octene	CCl_4	1000:1 (0.1)	99/97	970
9			2000:1 (0.05)	87/84	1680
10		$CHCl_3$	10:1 (10)	2/0	/
11		CBr_4	10000:1 (0.01)	~100/~100	4400
12			20000:1 (0.005)	96/94	7600
13			50000:1 (0.002)	92/93	18500
14		$CHBr_3$	100:1 (1)	3/2	2
15	1-hexene	CCl_4	1000:1 (0.1)	96/96	960
16			2000:1 (0.05)	86/85	1700
17		$CHCl_3$	10:1 (10)	4/0	/
18		CBr_4	10000:1 (0.01)	~100/98	3400
19			20000:1 (0.005)	98/96	6400
20			50000:1 (0.002)	96/93	14500
21		$CHBr_3$	100:1 (1)	4/4	4
22	styrene	CCl_4	500:1 (0.2)	54/51	255
23			1000:1 (0.1)	33/31	310
24			2000:1 (0.05)	22/24	480
25		$CHCl_3$	100:1 (1)	60/48	48
26			200:1 (0.5)	51/39	78
27		CBr_4	200:1 (0.5)	96/91	124
28			2000:1 (0.05)	64/57	560
29			10000:1 (0.01)	49/46	1700
30		$CHBr_3$	1000:1 (0.1)	86/70	700
31			2000:1 (0.05)	82/61	1220
32	methyl acrylate	CCl_4	1000:1 (0.1)	~100/84	840
33			2000:1 (0.05)	~100/62	1240
34		CBr_4	10000:1 (0.01)	~100/82	4400
35			20000:1 (0.005)	~100/70	6400
36			50000:1 (0.002)	~100/63	12500
37		$CHBr_3$	1000:1 (0.1)	64/48	480
38			2000:1 (0.05)	47/39	780
39	methyl methacrylate	CCl_4	1000:1 (0.1)	~100/66	660
40			2000:1 (0.05)	87/44	880
41		CBr_4	10000:1 (0.01)	~100/71	6300
42			20000:1 (0.005)	~100/44	7200
43		$CHBr_3$	1000:1 (0.1)	94/8	/
44			2000:1 (0.05)	96/5	/
45	vinyl acetate	CCl_4	1000:1 (0.1)	96/94	780
46			2000:1 (0.05)	80/70	1220
47		CBr_4	1000:1 (0.1)	95/88	610
48			2000:1 (0.05)	87/87	1200
49			5000:1 (0.02)	80/77	2500
50		$CHBr_3$	100:1 (1)	7/6	6
51			200:1 (0.5)	3/3	6

[a]All reactions were performed in CH_3CN at ambient temperature (22±2°C) for 24 hours with $[RX]_0:[alkene]_0:[V\text{-}70]_0$=1:1:0.05, except reactions for entries 1-7 which were performed in 1,2-dichloroethane. [b]mol% of copper relative to alkene. [c]Yield is based on the formation of monoadduct and was determined by ^1H NMR spectroscopy. [d]TONs were calculated taking into account the percent yield of monoadduct for ATRA reactions conducted in the absence of $[Cu^{II}(TPMA)X][X]$ (see Table 4.2.1).

low as 0.1 and 0.005 mol%, respectively. As evident from Table 4.2.2 (entries 37-38) ATRA of $CHBr_3$ to methyl acrylate also yielded the desired monoadduct with 0.1 and 0.05 mol% of copper. Furthermore, $CHBr_3$ was quite inactive alkyl halide in copper catalyzed ATRA of methyl methacrylate (entries 43-44). Although high monomer conversions were obtained, they were mostly attributed to polymer formation. For details on product characterization, see Appendix C.

The methodology for catalyst regeneration in copper mediated ATRA in the presence of V-70 as a reducing agent also worked very well in the addition of CCl_4 and CBr_4 to highly active vinyl acetate. For CCl_4 (entries 45-46) and CBr_4 (entries 47-49), quantitative yields of the monoadduct were obtained using as little as 0.1 and 0.02 mol% of copper catalyst, respectively. However, similarly to methyl methacrylate, ATRA of $CHBr_3$ to vinyl acetate (entries 50-51) was also quite unsuccessful even when high copper concentrations were used (0.5-1.0 mol%).

4.3 Conclusions

In summary, highly efficient ambient temperature ATRA of polyhalogenated compounds to alkenes catalyzed by $[Cu^{II}(TPMA)X][X]$ ($X=Br^-$ and Cl^-) complexes in the presence of 2,2'-azobis(4-methoxy-2,4-dimethyl valeronitrile) (V-70) was reported. V-70 has been shown to be very effective reducing agent for this process, enabling selective formation of the monoadduct with highly active monomers such as methyl acrylate, methyl methacrylate and vinyl acetate.

4.4 Experimental Section

Materials - All chemicals were purchased from commercial sources and used as received. Tris(2-pyridylmethyl)amine (TPMA) was synthesized according to literature procedures.[28] All solvents were used as received. ^{1}H NMR spectra were obtained using Bruker Avance 400 MHz spectrometer and chemical shifts are given in ppm relative to residual solvent peaks (C_6D_6, 7.16 ppm; $CDCl_3$, 7.26 ppm; $(CD_3)_2CO$, 2.09 ppm). IR spectra were recorded in the solid state or solution using Nicolet Smart Orbit 380 FT-IR spectrometer (Thermo Electron Corporation).

Synthesis of [Cu^{II}(TPMA)Cl][Cl] - Dichloromethane (2 mL) was added to a round bottom flask containing $Cu^{II}Cl_2$ (0.100 g, 0.744 mmol) and tris(2-pyridylmethyl)amine (TPMA) (0.216 g , 0.744 mol). The reaction mixture was stirred at room temperature for 30 minutes and product precipitated by the slow addition of pentane. Green powder was then filtered, washed with 2 x 10 mL of pentane and dried under vacuum to yield 0.302 g (96%) of [Cu^{II}(TPMA)Cl][Cl]. Anal. Calcd. for $C_{18}H_{18}Cl_2CuN_4$: C, 50.89; H, 4.27; N, 13.19. Found: C, 50.71; H, 4.34; N, 13.25. FT-IR (solid): cm^{-1}, 3364m, 1606s, 1479s, 1436s, 1306m, 1262m, 1094m, 1049m, 1020s, 955w, 841w, 765m.

General Procedure for ATRA of Polyhalogenated Compounds to Alkenes Using [Cu^{II}]$_0$:[Alkene]$_0$ Ratios Between 1:1000 and 1:50000 - ATRA reactions were performed in disposable 5.0 mm NMR tubes equipped with a plastic cap. In a typical

experiment, alkene (1.11 x 10^{-3} mol, V(methyl acrylate)=100 μL, V(1-octene)=174 μL, V(methyl methacrylate)=120 μL, V(vinyl acetate)=103 μL, V(styrene)=127 μL, V(1-hexene)=140 μL and V(1-decene)=210 μL) was dissolved in 400 μL of acetonitrile. The appropriate alkyl halide was then added to the solution (1.0 eq., 1.11 x 10^{-3} mol, V(CCl_4)=107 μL, V($CHCl_3$)=88.8 μL, m(CBr_4)=0.368 g and V($CHBr_3$)=97 μL), followed by 2,2'-azobis(4-methoxy-2,4-dimethyl valeronitrile) (V-70) (0.0171 g, 5.55 x 10^{-5} mol) and internal standard (anisole for styrene and 1,4-dimethoxybenzene for all other alkenes). After the desired amount of copper(II) was added (for 0.02 M [Cu^{II}(TPMA)X][X] in CH_3CN: 1000:1 (V=55 μL), 2000:1 (V=28 μL) and 5000:1 (V=11 μL and for 0.01 M [Cu^{II}(TPMA)X][X] in CH_3CN: 10000:1 (V=11 μL), 20000:1 (V=5.5 μL) and 50000:1 (V=2.2μL)) , the NMR tube was flushed with argon for 30 seconds, sealed with a plastic cap and teflon tape and left at room temperature (22±2°C) for 24 hours. The conversion of alkene and the percent yield of monoadduct were determined using ^{1}H NMR spectroscopy.

General Procedure for ATRA of Polyhalogenated Compounds to Alkenes Using [Cu^{II}]$_0$:[Alkene]$_0$ Ratios Between 1:100 and 1:500 - Similar procedure to the one above was used, except that the volume of initially added acetonitrile was adjusted for the volume already added with the catalyst solution. For 0.02 M [Cu^{II}(TPMA)X][X] in CH_3CN: 100:1 (V(cat)=555 μL, V(CH_3CN)=0), 200:1 (V(cat)=280 μL, V(CH_3CN)=120 μL) and 500:1 (V(cat)=111 μL, V(CH_3CN)=289 μL).

4.5 References

(1) Curran, D. P., *Comprehensive Organic Synthesis*. Pergamon: New York, 1992; p 715.

(2) Kharasch, M. S.; Jensen, E. V.; Urry, W. H., Addition of Carbon Tetrachloride and Chloroform to Olefins. *Science* **1945,** *102*(2640), 128-128.

(3) Pintauer, T.; Matyjaszewski, K., Atom Transfer Radical Addition and Polymerization Reactions Catalyzed by ppm Amounts of Copper Complexes. *Chem. Soc. Rev.* **2008,** *37*, 1087-1097.

(4) Gossage, R. A.; Van De Kuil, L. A.; Van Koten, G., Diaminoarylnickel(II) "Pincer" Complexes: Mechanistic Considerations in the Kharasch Addition Reaction, Controlled Polymerization, and Dendrimeric Transition Metal Catalysts. *Acc. Chem. Res.* **1998,** *31*(7), 423-431.

(5) Iqbal, J.; Bhatia, B.; Nayyar, N. K., Transition Metal-Promoted Free-Radical Reactions in Organic Synthesis: The Formation of Carbon-Carbon Bonds *Chem. Rev.* **1994,** *94*(2), 519-564.

(6) Severin, K., Ruthenium Catalysts for the Kharasch Reaction. *Curr. Org. Chem.* **2006,** *10*(2), 217-224.

(7) Giese, B., Syntheses with Radicals. Carbon-Carbon Coupling via Organotin and -Mercury Compounds. *Angew. Chem.* **1985,** *97*, 555-567.

(8) Curran, D. P.; Chen, M.-H.; Dooseop, K., Atom-Transfer Cyclization. A Novel Isomerization of Hex-5-ynyl Iodides to Iodomethylene Cyclopentanes. *J. Am. Chem. Soc.* **1986,** *108*, 2489-2490.

(9) Clark, A. J., Atom Transfer Radical Cyclisation Reactions Mediated by Copper Complexes. *Chem. Soc. Rev.* **2002,** *31*(1), 1-11.

(10) Matyjaszewski, K.; Jakubowski, W.; Min, K.; Tang, W.; Huang, J.; Braunecker, W. A.; Tsarevsky, N. V., Diminishing Catalyst Concentration in Atom Transfer Radical Polymerization with Reducing Agents. *Proc. Natl. Acad. Sci. U.S.A.* **2006,** *103*, 15309-15314.

(11) Wang, J.-S.; Matyjaszewski, K., Controlled/"Living" Radical Polymerization. Atom Transfer Radical Polymerization in the Presence of Transition-Metal Complexes. *J. Am. Chem. Soc.* **1995,** *117*(20), 5614-5615.

(12) Quebatte, L.; Thommes, K.; Severin, K., Highly Efficient Atom Transfer Radical Addition Reactions with a Ru^{III} Complex as a Catalyst Precursor. *J. Am. Chem. Soc.* **2006,** *128*(23), 7440-7441.

(13) Eckenhoff, W. T.; Garrity, S. T.; Pintauer, T., Highly Efficient Copper Mediated Atom Transfer Radical Addition (ATRA) in the Presence of Reducing Agent. *Eur. J. Inorg. Chem.* **2008**, 563-571.

(14) Eckenhoff, W. T.; Pintauer, T., Atom Transfer Radical Addition in the Presence of Catalytic Amounts of Copper(I/II) Complexes with Tris(2-pyridylmethyl)amine. *Inorg. Chem.* **2007,** *46*(15), 5844-5846.

(15) Blackman, A. G., Tripodal Tetraamine Ligands Containing Three Pyridine Units: The Other Polypyridyl Ligands *Eur. J. Inorg. Chem.* **2008**, 2633-2647.

(16) Diaz-Alvarez, A. E.; Crochet, P.; Zablocka, M.; Duhayon, C.; Cadierno, V.; Majoral, J. P., Developing the Kharasch Reaction in Aqueous Media: Dinuclear Group 8 and 9 Catalysts Containing the Bridging Cage Ligand tris(1,2-dimethylhydrazino)diphosphane. *Eur. J. Inorg. Chem.* **2008**, 786-794.

(17) Iizuka, Y.; Li, Z. M.; Satoh, K.; Karnigaito, M.; Okamoto, Y.; Ito, J.; Nishiyama, H., Chiral (-)-DIOP Ruthenium Complexes for Asymmetric Radical Addition and Living Radical Polymerization Reactions. *Eur. J. Org. Chem.* **2007**, 782-791.

(18) Lundgren, R. J.; Rankin, M. A.; McDonald, R.; Stradiotto, M., Neutral, Cationic, and Zwitterionic Ruthenium(II) Atom Transfer Radical Addition Catalysts Supported by P,N-Substituted Indene or Indenide Ligands *Organometallics* **2008,** *27*(2), 254-258.

(19) Maiti, D.; Sarjeant, A. A. N.; Itoh, S.; Karlin, K. D., Suggestion of an Organometallic Intermediate in an Intramolecular Dechlorination Reaction Involvning Copper(I) and ArCH2Cl Moiety. *J. Am. Chem. Soc.* **2008,** *130*(17), 5644-5645.

(20) Oe, Y.; Uozumi, Y., Highly Efficient Heterogeneous Aqueous Kharasch Reaction with an Amphiphilic Resin-Supported Ruthenium Catalyst *Adv. Synth. Catal.* **2008,** *350*(11-12), 1771-1775.

(21) Thommes, K.; Icli, B.; Scopelliti, R.; Severin, K., Atom-Transfer Radical Addition (ATRA) and Cyclization (ATRC) Reactions Catalyzed by a Mixture of [$RuCl_2Cp^*(PPh_3)$] and Magnesium. *Chem. Eur. J.* **2007,** *13*(24), 6899-6907.

(22) Wolf, J.; Thommes, K.; Brie, O.; Scopelliti, R.; Severin, K., Dinuclear Ruthenium Ethylene Complexes: Synthesis, Structures, and Catalytic Applications in ATRA and ATRC Reactions. *Organometallics* **2008,** *27*, 4464-4474.

(23) Clark, A. J.; Wilson, P., Copper Mediated Atom Transfer Radical Cyclizations with AIBN. *Tet. Lett.* **2008,** *49*, 4848-4850.

(24) Beuermann, S.; Buback, M., Rate Coefficients of Free-Radical Polymerization Deduced from Pulsed Laser Experiments. *Prog. Polym. Sci.* **2002,** *27*, 191-254.

(25) Koelsch, C. F.; Boekelheide, V., Coupling of a,B-unsaturated compounds with diazonium salts. *J. Am. Chem. Soc.* **1944,** *66*(3), 412-415.

(26) Brandrup, J.; Immergut, E. H.; Gulke, E. A., *Polymer Handbook*. Wiley-Interscience: New York, 1999.

(27) Eastmond, G. C., The Kinetics of Free Radical Polymerization of Vinyl Monomers in Homogeneous Solutions. In *Comphrehensive Chemical Kinetics*, Bamford, C. H.; Tipper, C. F. H., Eds. American Elsevier: New York, 1976; Vol. 14A.

(28) Tyeklar, Z.; Jacobson, R. R.; Wei, N.; Murthy, N. N.; Zubieta, J.; Karlin, K. D., Reversible reaction of dioxygen (and carbon monoxide) with a copper(I) complex. X-ray structures of relevant mononuclear Cu(I) precursor adducts and the trans-(.mu.-1,2-peroxo)dicopper(II) product. *J. Am. Chem. Soc.* **1993,** *115*(7), 2677-2689.

Chapter 5.

ATOM TRANSFER RADICAL ADDITION (ATRA) MEDIATED BY COPPER COMPLEXES WITH THE TRIS(2-DIMETHYLAMINOETHYL)AMINE (ME_6TREN) LIGAND IN THE PRESENCE OF AIBN AS A REDUCING AGENT

Copper catalyzed atom transfer radical addition (ATRA) and cyclization (ATRC) reactions typically utilize neutral nitrogen based complexing ligands. In previous studies for mechanistically similar atom transfer radical polymerization (ATRP), the equilibrium constant for atom transfer ($K_{ATRA}=k_a/k_d$) was found to correlate linearly with redox potentials for copper complexes. Generally, tetradentate nitrogen based ligands such as TPMA (tris(2-pyridylmethyl)amine) and Me_6TREN (tris2-dimethylaminoethyl)amine) were found to be particularly active for atom transfer radical processes based on relatively low values for K_{ATRA}, as a result of high activation rate constants (k_a). Such high activity is an important requirement for ATRA and ATRC processes that utilize reducing agents to continuously regenerate the activator (copper(I) complex) from the corresponding deactivator (copper(II) complex). Additionally, in catalyst regeneration techniques, copper complexes should be particularly stable and not undergo side reactions such as ligand dissociation, protonation, alkene coordination or dissociation of halide anions.

In this chapter, we focus on the evaluation of Me_6TREN ligand in copper catalyzed ATRA in the presence of the free-radical initiator AIBN (2,2′-azobis(isobutyronitrile)). The addition of carbon tetrachloride to 1-hexene, 1-octene and *cis*-cyclooctene proceeded

efficiently to yield 89, 85 and 85% of the monoadduct, respectively, using a catalyst to alkene ratio of 2500:1. For alkenes that readily undergo free radical polymerization, such as methyl acrylate, catalyst loadings as high as 0.4 mol-% were required. Furthermore, modest yields of the monoadduct were obtained with less active alkyl halides (chloroform and bromoform) using 250:1 and 500:1 ratios of copper(II) to alkene. Interestingly, the addition of carbon tetrachloride to *cis*-cyclooctene produced only 1-chloro-4-(trichloromethyl)-cyclooctene, while carbon tetrabromide yielded 75:25 ratio of 1,2 to 1,4-regioisomers.

The activity of $[Cu^{II}(Me_6TREN)X][X]$ ($X=Br^-$ and Cl^-) complexes in ATRA in the presence of AIBN was additionally probed by adding excess free ligand, a source of halide anions and triphenylphosphine. The results indicated that disproportionation is a likely cause for the lower activity of Me_6TREN as compared to TPMA.

5.1 Introduction

Discovered by Kharasch in 1945, atom transfer radical addition (ATRA) is a fundamental reaction for the formation of carbon-carbon bonds starting from alkyl halides and alkenes.[1-3] The reaction is typically initiated by peroxides, diazo compounds or light. Initially, ATRA was limited to the addition of polyhalogenated alkanes to alkenes that do not readily undergo free radical polymerization such as α-olefins. However, the realization that transition metal complexes could act as a better halogen atom transfer agent than alkyl halides, and additionally catalyze ATRA through a reversible redox process, expanded the scope of this simple organic transformation.[4-8]

These catalysts provided better selectivity towards the monoadduct by reducing the overall radical concentration, thus suppressing side reactions such as radical termination and oligomerization/polymerization. Complexes of Cu, Fe, Ru, and Ni were found to be particularly active for a variety of alkyl halides and alkenes.[9-21] However, metal-mediated ATRA systems required large concentrations of the catalyst in order to obtain high yields of the monoadduct (typically between 5 and 30 mol% relative to alkene). This was mostly due to radical termination reactions, which resulted in accumulation of the deactivator (transition metal complex in the higher oxidation state). Similar problems were also encountered in synthetically more useful intramolecular version of ATRA, also commonly known as atom transfer radical cyclization (ATRC).[22-33] The use of solid supported catalysts[26, 34, 35] and biphasic fluorous systems[36] were examined as solutions to catalyst recycling and recovery, but were met with only limited success. Although, the catalyst in such systems could be easily separated from the reaction mixture, the problem of recycling due to the accumulation of the deactivator species still remained.

The most effective method of diminishing catalyst concentration in ATRA is that of in situ catalyst regeneration in the presence of free radical diazo initiators (e.g. 2,2′-azobis(2-methylpropionitrile) (AIBN)) or magnesium. This method was originally developed for mechanistically similar atom transfer radical polymerization (ATRP)[37-40], and was subsequently applied first to Ru[41-47] and then Cu[48-61] based ATRA. In all of these processes, the deactivator (transition metal complex in the higher oxidation state) is constantly reduced to the activator (transition metal complex in the lower oxidation state). The proposed mechanism for copper catalyzed ATRA in the presence of the free

radical diazo initiator AIBN is shown in Scheme 5.1.1. Radicals generated from thermal decomposition of AIBN partially reduce copper(II) to a corresponding copper(I)

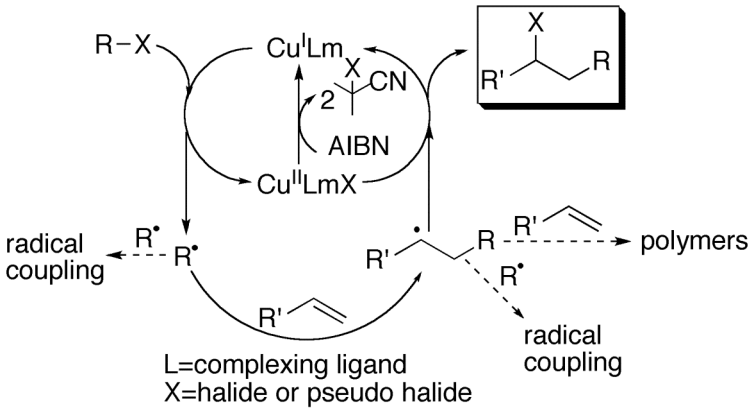

Scheme 5.1.1. Proposed ATRA mechanism in the presence of AIBN as a reducing agent.

complex. The copper(I) complex starts a catalytic cycle by homolytically cleaving an alkyl halide bond to produce an alkyl radical that adds across a carbon-carbon double bond of an alkene. The generated secondary radical then irreversibly abstracts halogen atom from the copper(II) complex to form a desired monoadduct. This step regenerates the activator or copper(I) complex, completing the catalytic cycle. As indicated in Scheme 5.1.1, the competing side reactions in this process include radical terminations by coupling or disproportionation, as well as repeating radical additions to alkene to form oligomers/polymers.

Catalyst regeneration has been shown to be highly successful when used in copper mediated ATRA systems, producing the highest turn-over-numbers (TON) observed for this process.[51, 54, 61] Using [Cu^{I}(TPMA)Cl] (TPMA = tris(2-pyridylmethyl)amine) and AIBN, TONs as high as 7200 were achieved in the addition of CCl_4 to 1-hexene,[50] and even more notable results were obtained with [Cu^{II}(TPMA)Br][Br] in the addition of CBr_4 to methyl acrylate and styrene with TONs of 162,000 and 190,000 respectively.[49]

Controlling the single addition to highly reactive alkenes (vinyl acetate, methyl methacrylate, methyl acrylate, and styrene), which polymerize rapidly in the presence of free radical initiators, has historically been a challenge for ATRA. By performing the reactions at room temperature using 2,2'-azobis(4-methoxy-2,4-dimethylvaleronitrile) (V-70) and $[Cu^{II}(TPMA)X][X]$ (X=Cl or Br), the addition of polyhalogenated methanes proceeded efficiently with $[Cu^{II}]_0 << 0.1$ mol% relative to alkene.[53] Copper(I) complexes with anionic trispyrazolylborate (homoscorpionate) ligands were also recently shown to be effective in ATRA systems without the use of reducing agents. In this case, small amounts of acetonitrile were used to coordinatively saturate copper in the lower oxidation state, suppressing the oxidation by alkyl halide.[58, 59] This process reduced the overall radical concentration and thus minimized accumulation of the deactivator (copper(II)

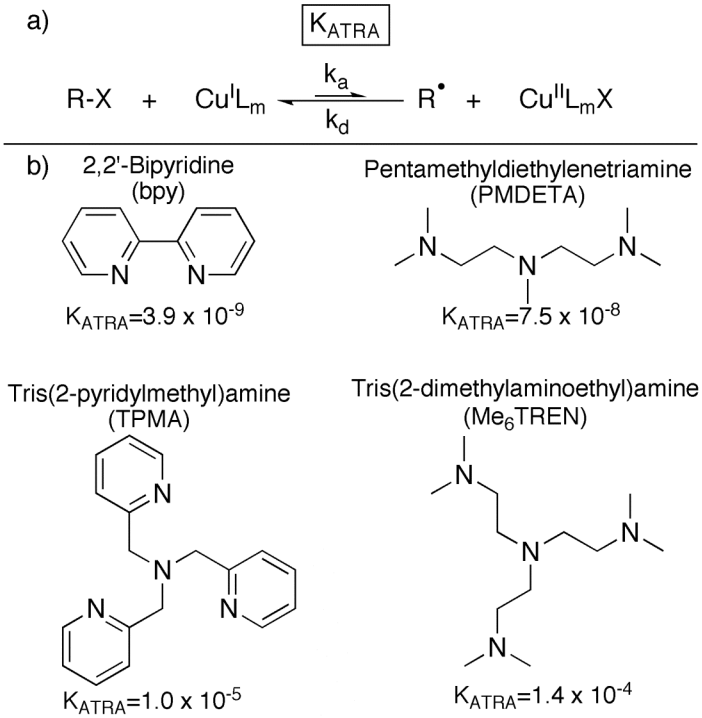

Scheme 5.1.2. a) ATRA equilibrium and b) common ligands used in atom transfer radical addition/polymerization reactions and their equilibrium constants measured for EtBriB in the presence of $Cu^{I}Br$ in CH_3CN at 22°C.

complex). The methodology for catalyst regeneration in the presence of reducing agents was also extended towards more complex organic synthesis with the addition of CCl_4 to 1,6-heptadiene derivatives followed by sequential ATRC to yield substituted cyclopentanes in a single step with the lowest catalyst loadings reported so far.[56, 57] Recently, monoadducts formed via Ru mediated ATRA and ATRC in the presence of magnesium powder as a reducing agent were utilized in a second reaction to synthesize cyclopropane rings via dehalogenation.[44] These examples are a visible indicator that this methodology is on a trajectory to potentially become a "greener" alternative to currently available synthetic processes for such organic transformations.

The success of ATRA in the presence of reducing agents using copper complexes with TPMA ligand encouraged us to seek more active ligands for this process. According to the well established correlation of equilibrium constants and activity in ATRP, tris((2-dimethylamino)ethyl)amine (Me_6TREN) was projected to be an even more potent ligand for copper catalyzed ATRA. Me_6TREN was first introduced for ATRP of acrylates under ambient conditions where it was indeed shown to have exceptionally high activity when complexed to Cu^IBr[62-65] and was subsequently extended to ATRC reactions of bromoacetimides with excellent results compared to other nitrogen-based ligands.[66, 67] In this chapter, we describe the use of copper(II) complexes with Me_6TREN ligand for the ATRA of polyhalogented methanes to various alkenes and the structural characterization of these complexes.

5.2 ATRA Mediated by Copper Complexes with Me_6TREN Ligand

The activity of copper complexes with the Me_6TREN ligand was first evaluated in ATRA of polychlorinated- and polybrominated methanes to a variety of alkenes (Table 5.2.1). Overall, catalysis with $[Cu^{II}(Me_6TREN)X][X]$ (X=Cl,Br) in the presence of AIBN was found to be less active than it's pyridyl counterpart, tris(pyridylmethyl)amine (TPMA). At alkene to catalyst ratios of 2500:1, ATRA of CCl_4 to 1-hexene, 1-octene, and *cis*-cyclooctene achieved yields between 85-89% (entries 2, 4, & 6). Much better yields of monoadduct were obtained at higher catalyst loadings (entries 1, 3, & 5). Poor control was attained

Table 5.2.1. Reactions of polyhalogenated methanes with various alkenes[a] catalyzed by $[Cu^{II}(Me_6TREN)X][X]$ (X=Cl,Br), in the presence of AIBN.

Entry	Alkene	$[Alkene]_0$:$[Cu]_0$	R-X	Conv.(%)/Yield(%)
1	1-hexene	1000:1	CCl_4	100/100
2	1-hexene	2500:1	CCl_4	89/89
3	1-octene	1000:1	CCl_4	99/99
4	1-octene	2500:1	CCl_4	85/85
5	*cis*-cyclooctene	1000:1	CCl_4	95/95
6	*cis*-cyclooctene	2500:1	CCl_4	85/85
7	methyl acrylate	250:1	CCl_4	100/67
8	1-hexene	250:1	$CHCl_3$	51/51
9	1-octene	250:1	$CHCl_3$	46/46
10	*cis*-cyclooctene	250:1	$CHCl_3$	26/26
11	styrene	250:1	$CHCl_3$	77/40
12	methyl acrylate	250:1	$CHCl_3$	100/32
13	1-hexene	500:1	$CHBr_3$	46/46
14	1-octene	500:1	$CHBr_3$	39/39
15	*cis*-cyclooctene	500:1	$CHBr_3$	37/37
16	styrene	250:1	$CHBr_3$	98/80
17	styrene	500:1	$CHBr_3$	93/69
18	methyl acrylate	250:1	$CHBr_3$	100/51
19	methyl acrylate	1000:1	CBr_4	100/87

[a]Reactions run at 60°C for 24 hr in CH_3CN. $[Alkene]_0$:$[R\text{-}X]_0$:$[AIBN]_0$=1:1.1:0.05. $[Alkene]_0$ = 1.34 M (CBr_4 reactions expanded in volume, [M]=1.13 M). Yield and conversion were determined by ^1H NMR.

in the case of the addition of CCl_4 to methyl acrylate, which required a higher catalyst loading in order to suppress competing free radical polymerization (entry 7). The additions of chloroform to all alkenes were found to produce low yields of monoadduct (entries 8-12) due to slower activation on account of stronger C-Cl bonds as compared to CCl_4. Free radical polymerization of alkene is mainly responsible for the high conversions and low yields observed in the case of styrene and methyl acrylate. Similar results were observed with reactions of bromoform to alkenes with the exception of styrene (entries 13-15). In these cases, nearly complete conversion of styrene and monoadduct yields as high as 80% and 69% were observed in entries 16 and 17, respectively.

Due to the large chain transfer constant of carbon tetrabromide, ATRA reactions to most alkenes proceeded efficiently in the absence of copper catalyst, with the exception of methyl acrylate, which polymerized rapidly, affording only 12% The addition of $[Cu^{II}(Me_6TREN)Br][Br]$ to ATRA reactions of CBr_4 and methyl acrylate at 12% yield, where using a 1000:1 ratio of alkene to catalyst increased the product yield to 87% (entry 19).

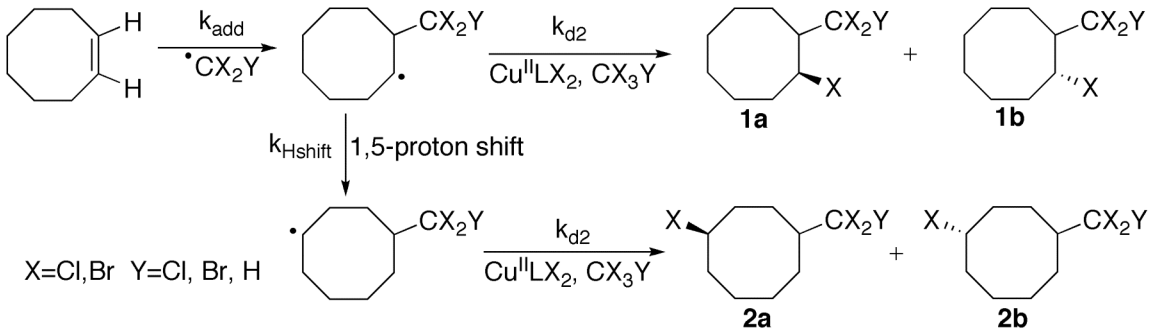

Scheme 5.2.1. Formation of enantiomers from the addition of polyhalogenated methanes to cyclooctene mediated by $[Cu^{II}(Me_6TREN)X][X]$ or by free radicals generated by the decomposition of AIBN.

The addition of CCl_4, $CHCl_3$, and $CHBr_3$ to *cis*-cyclooctene was found to produce a 1,4-regioisomer product (2a, 2b), resulting from a proton shift occurring after the addition of $R^{\bullet}$ across the carbon-carbon double bond (Scheme 5.2.1) (For the molecular structure of cis-1-Chloro-4-(trichloromethyl)-cyclooctane, see Appendix D). This product arises in cases where the rate constant of deactivation, either by another alkyl halide or by copper catalyst, is less than the rate constant of proton transfer. The 1,2-regioisomer (1a, 1b) was not detected in any of the above cases, which is consistent with previously published results where initiation was achieved by thermal or photoinitiated means.[68, 69] However, in a separate study, the use of $[RuCl_2PPh_3]$ was shown to produce greater yields of the 1,2-regioisomers at higher concentrations (15.3 mol%).[70]

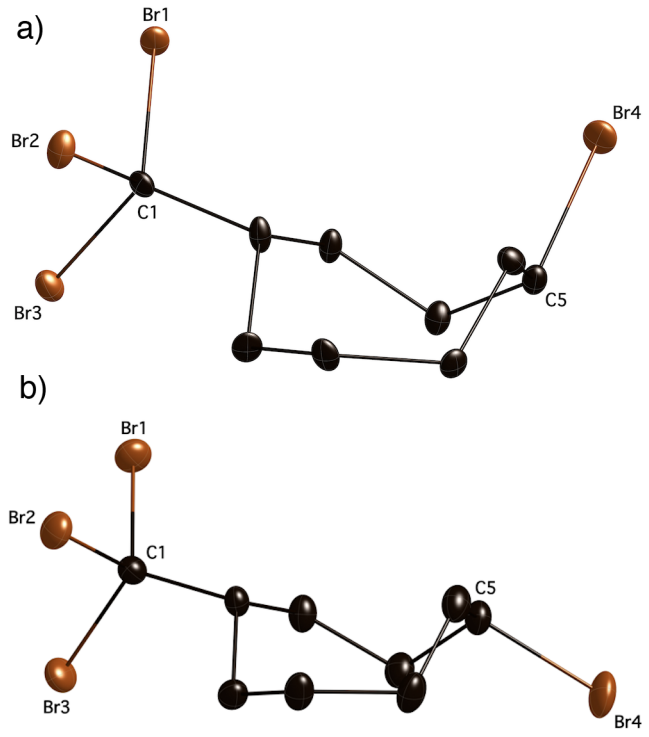

Figure 5.2.1. Molecular structures of *cis*-1-Bromo-4-(tribromomethyl)cyclooctane (a) and *trans*-1-Bromo-4-(tribromomethyl)cyclooctane (b) collected at 150K, shown with 50% probability displacement ellipsoids. H-atoms omitted for clarity. Selected bond distances [Å] for a) Br1-C1 1.951(7), Br2-C1 1.942(7), Br3-C1 1.954(7), Br4-C5 1.992(7). For b) Br1-C1 1.958(2), Br2-C1 1.960(2), Br3-C1 1.944(2), Br4-C5 1.988(2).

Carbon tetrabromide adds to *cis*-cyclooctene with nearly quantitative yields in the presence of AIBN but interestingly, the major reaction product was found to be 1-bromo-2-(tribromomethyl)cyclooctane (1a, 1b) and the minor product 1-bromo-4-(tribromomethyl)cyclooctane (2a, 2b) with a 75:25 ratio respectively (Scheme 5.2.1). Each regioisomer consisted of a 50:50 ratio of diastereomers, which is typical for radical additions and resonance signals for all four products were easily detectable by ^{1}H NMR (Appendix D). These products were separated by column chromatography using pentane and products 2a and 2b were found to crystallize separately from chloroform at -10°C (Figure 5.2.1).

The drastic difference in product distribution as compared to CCl_4 and $CHBr_3$ indicates that the alkyl halide plays an important role in radical trapping (k_{d2}, Scheme 5.1.1). CBr_4 is well known to be a highly efficient chain transfer agent and thus it is able to trap the generated radical on the cyclooctane ring before proton transfer is possible (k_{HShift}, Scheme 5.2.1). To further investigate this possibility, bromotrichloromethane was used in ATRA to *cis*-cyclooctene in identical conditions because it should have a deactivating ability between that of CCl_4 and CBr_4. The product distribution in this case consisted of a 52:48 ratio of products 1a and 1b relative to 2a and 2b, supporting the claim that the product composition depends greatly on the chain transfer constant of the alkyl halide.

5.3 Optimization of [Cu(Me$_6$TREN)Cl][Cl] Mediated ATRA Reactions

Available electrochemical and kinetic data on copper complexes with Me$_6$TREN indicate that they should be considerably more active than corresponding complexes with

the TPMA ligand. Possible reasons for this lack of activity could include: i) ligand dissociation ii) halide dissociation or iii) complex disproportionation. Alkyl amine ligands are well known to be weaker binding ligands as compared to pyridine based ligands, so ligand dissociation was investigated first. Although copper(II) complexes with Me_6TREN ligand are quite stable, the corresponding copper(I) complexes are less stable.[71] By adding excess amounts of Me_6TREN ligand, the equilibrium of dissociation could be shifted toward the complexed and more active copper(I) complex. No significant effect was observed in the case of CCl_4 and 1-octene up to 20 equivalents of excess ligand in overall product yield (Table 5.3.1). Reactions of styrene and CCl_4 showed a very slight decrease in yield with increasing ligand concentration. The reactions with methyl acrylate were most affected by the excess ligand, where addition of additional ligand inhibited free radical polymerization of methyl acrylate and thus

Table 5.3.1. Effect of added ligand, tetrabutylammonium chloride (TBA-Cl), triphenylphosphine (PPh_3), and copper metal on ATRA reactions.[a]

Alkene	$[Alkene]_0$: $[Cu]_0$	$[L]_0$: $[Cu]_0$	Conv.(%)/ Yield(%)	$[TBA\text{-}Cl]_0$: $[Cu]_0$	Conv.(%)/ Yield(%)	$[PPh_3]_0$: $[Cu]_0$	Conv.(%)/ Yield(%)
1-octene	5000:1	1	69/69	0	69/69	0	69/69
1-octene	5000:1	2	59/59	1	62/62	1	54/54
1-octene	5000:1	6	60/60	5	43/43	5	37/37
1-octene	5000:1	11	58/58	10	53/53	10	22/22
1-octene	5000:1	21	54/54	20	52/52	20	16/16
styrene	250:1	1	60/22	0	60/22	0	60/22
styrene	250:1	2	65/25	1	63/23	1	57/13
styrene	250:1	6	62/21	5	60/18	5	48/0
styrene	250:1	11	63/18	10	57/16	10	47/0
styrene	250:1	21	68/16	20	52/12	20	47/0
methyl acrylate	250:1	1	100/66	0	100/66	0	100/66
methyl acrylate	250:1	2	100/66	1	100/70	1	100/51
methyl acrylate	250:1	6	97/57	5	100/68	5	100/0
methyl acrylate	250:1	11	86/40	10	100/66	10	100/0
methyl acrylate	250:1	21	76/32	20	99/55	20	100/0

[a]ATRA reactions run at 60°C for 24 hr in CH_3CN. L=Me_6TREN. Excess ligand, TBA-Cl, and PPh_3 added in solution of CH_3CN. $[Alkene]_0$:$[CCl_4]_0$: $[AIBN]_0$=1:1.1:0.05. $[Alkene]_0$ = 1.34 M. Yield and conversion determined by ^1H NMR.

reduced conversion from 100% to 76% and yield from 65% to 32% respectively. In each case where a large excess of ligand was used, precipitation of $[HN(CH_2CH_2NH(CH_3)_2][Cl_4]$ was observed, likely arising from a reaction between alkyl halide and the excess ligand. Interestingly, conversion of 1-octene was measured in ATRA reactions with CCl_4 and 1, 6 and 21 equivalents of ligand relative to copper, which showed increasing deviations from linearity with ligand concentration (Figure 5.3.1). Initial rates of conversion were found to be higher with more equivalents of Me_6TREN and then levelled off after ~3 hours. In the case of 1:1 ligand to copper ratio, 9% conversion is observed, compared to 20% and 37% with 6 and 21 equivalents, respectively.

This behaviour is typical of ATRA systems with a large excess of copper(I) and could be explained by the propensity of Me_6TREN to act as a reducing agent. To test this hypothesis, UV-Vis was employed to monitor the equilibrium ratio of copper(I) to copper(II) complexes in the presence of AIBN. When only a single equivalent of ligand is added to $CuCl_2$, only 10% of the copper(II) was found to be reduced to copper(I), even after six days. However, upon addition of 21 equivalents of ligand, all of the copper(II) complex was found to be reduced to copper(I). This indicates that Me_6TREN could indeed participate in the reduction of copper(II).

The possibility of chloride dissociation was also examined (Table 5.3.1) by addition of tetrabutylammonium chloride (TBA-Cl). The addition of TBA-Cl was found to have an overall negative effect on ATRA yields. For the addition of 1-octene to CCl_4, yields of monoadduct decreased from 69% to 52% in the presence of 20 equivalents TBA-Cl.

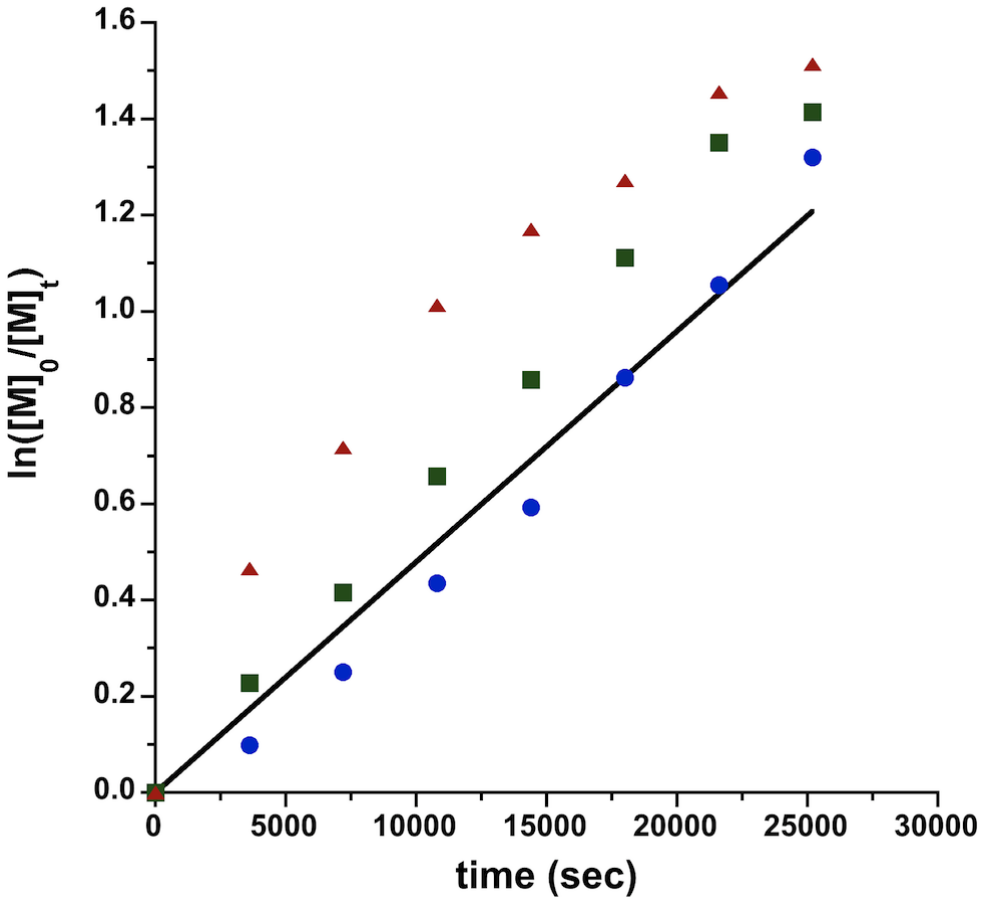

Figure 5.3.1. First order kinetic plots of 1-octene conversion with CCl_4 with ligand to copper ratios of 1:1 (●), 6:1 (■), and 21:1 (▲). Reactions were run at 60°C in CH_3CN. $[1\text{-octene}]_0$:$[CCl_4]_0$:$[AIBN]_0$:$[Cu]_0$=500:550:25:1. $[1\text{-octene}]_0$=1.34 M.

Similarly, styrene showed a decrease in yield from 22% to 12% when 20 equivalents of TBA-Cl was used, accompanied by decreased conversion from 66% to 52%. In the addition of CCl_4 to methyl acrylate in the presence of 20 eq. of TBA-Cl, nearly quantitative conversions were observed. However, the yields of the desired monoadduct were found to decrease from 66% to 55%, respectively. These findings are mirrored by the kinetic monitoring of 1-octene conversion with CCl_4 (Figure 5.3.2). The k_{obs} in these reactions was found to decrease from 5.0 x 10^{-5}, to 4.5 x 10^{-5}, to 4.1 x 10^{-5} M^1 s^{-1} with 1,

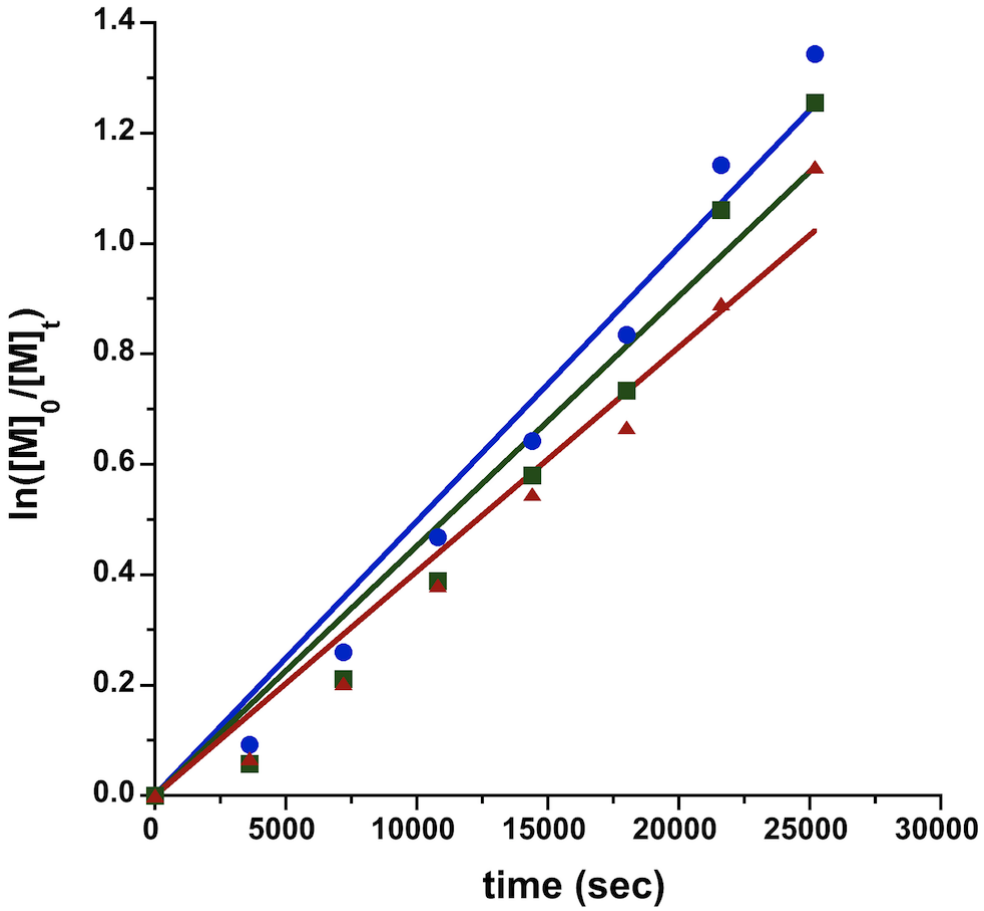

Figure 5.3.2. First order kinetic plots of 1-octene conversion with CCl_4 with TBA-Cl to $[Cu^{II}(Me_6TREN)Cl][Cl]$ ratios of 0:1 (●), 5:1 (■), and 20:1 (▲). Reactions were run at 60°C in CH_3CN. $[1\text{-octene}]_0$:$[CCl_4]_0$:$[AIBN]_0$:$[Cu]_0$=500:550:25:1. $[1\text{-octene}]_0$=1.34 M.

5 and 20 equivalents of TBA-Cl. This decreased activity is most likely due to the formation of complexes which are not active in ATRA systems.

Ligand dissociation was found to be unlikely as a cause of low activity in ATRA systems, so disproportionation, which is known to occur readily with copper(I) Me_6TREN complexes, was investigated next. Neutral phosphines, such as PPh_3 and $P(OBu)_3$ have been shown to stabilize copper complexes from this process. Both phosphines were found to produce very similar results when added to ATRA systems of 1-octene, styrene, and methyl acrylate and CCl_4 reactions and thus only data for PPh_3 are

shown. The yield of monoadduct in the case of 1-octene was found to drastically decrease in the presence of more than 10 equivalents of PPh_3. Under such conditions, it mimicked the Kharasch addition in the presence of AIBN only, indicating the complete inactivity of the copper complex to catalyze ATRA. Product yields in both styrene and methyl acrylate were reduced to negligible amounts by the addition of more than 10 equivalents of PPh_3 relative to copper. The reason for this decreased yield could be coordinative saturation of the copper complex or the formation of less active complexes.

ATRA reactions were also performed in DMF, MeOH, and MeOH/H_2O aside from CH_3CN. Disproportionation is known to occur more rapidly in more polar solvents and thus would have a more noticeable effect on ATRA reactions. ATRA reactions of CCl_4 to 1-octene and methyl acrylate were both found to be negatively affected by a medium of increased polarity. At a catalyst loading of 500:1, 1-octene was previously shown to produce quantitative yields of monoadduct in CH_3CN, but was found to produce a mere 50% yield in both MeOH and DMF. These were further decreased upon addition of water. A similar trend was noted for methyl acrylate, which was showed total conversion in each solvent, but yields of monoadduct decreased from 67% in CH_3CN, to 52% and 37% in MeOH and DMF respectively. The increased polarity of the reaction medium decreased yields in all cases, which can be explained by increased disproportionation or halide dissociation. However, dissociation of halide in the copper(II) state would manifest as reduced deactivation capability of the complex, which would be observed as a large disparity between conversion and yield in the case of 1-octene. In the above experiments for 1-octene, conversion and yields were found to be equal, thus halide dissociation is not likely to be the main issue with reduced yields,

although experiments can be carried out in which excess halide is added to these systems to confirm this.

In conclusion, [Cu^{II}(Me_6TREN)X][X] (X=Cl,Br) complexes were found to be efficient catalysts for ATRA in the presence of AIBN as a reducing agent for a variety of alkenes with several polyhalogenated methanes. However, the activity of these complexes was not as high as expected and all attempts to increase product yields were found to produce the opposite effect.

5.4 Molecular Structure Determination of Complexes

The copper(II) complexes, [Cu(Me_6TREN)Cl][Cl] (**1**) and [Cu(Me_6TREN)Br][Br] (**2**), used as catalysts for ATRA were synthesized and characterized by single crystal x-ray diffraction. Both complexes were found to possess a distorted trigonal pyramidal

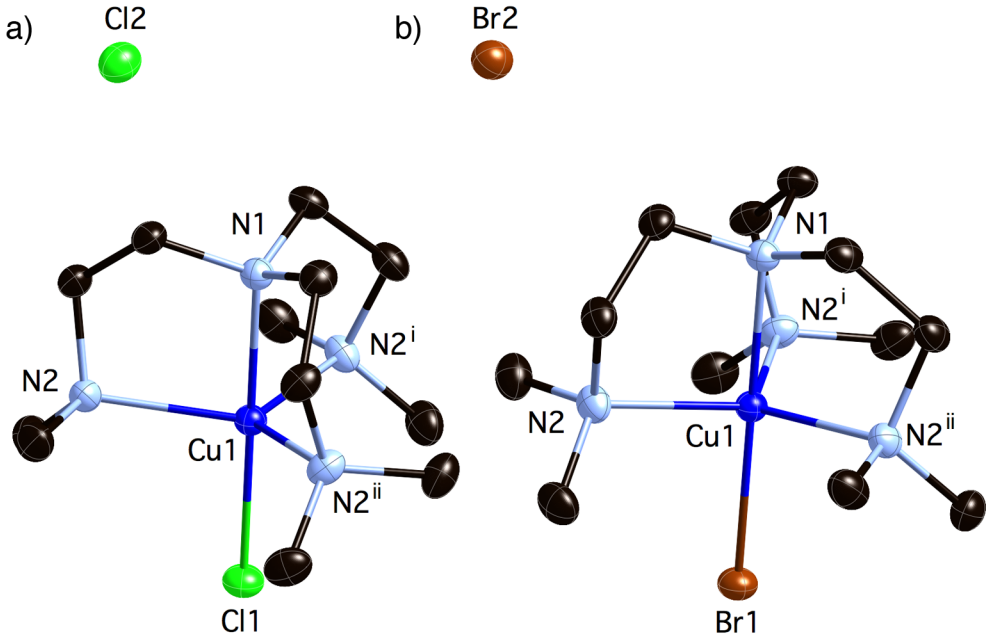

Figure 5.4.1. Molecular structures of a) [Cu^{II}(Me_6TREN)Cl][Cl] **(1)**: symmetry codes: 1. -z+3/2,-x+1,y+1/2 2. -y+1,z-1/2,-x+3/2 and b) [Cu^{II}(Me_6TREN)Br][Br] **(2)**: symmetry codes: 1. y,z,x 2. z,x,y collected at 150K shown with 50% thermal probability ellipsoids. H-atoms omitted for clarity.

Table 5.4.1. Selected bond distances (Å) and angles (°) for complexes $[Cu^{II}(Me_6TREN)Cl][Cl]$ **(1)** and $[Cu^{II}(Me_6TREN)Br][Br]$ **(2)**.[a]

Parameter	1	2
Cu-N1	2.0545(15)	2.046(2)
Cu-N2	2.1489(9)	2.1527(13)
Cu-X	2.2589(5)	2.4016(4)
N1-Cu-N2	84.62(3)	84.81(4)
N2-Cu-X	95.38(3)	95.19(4)
N2-Cu-N2^{i}	119.132(8)	119.191(11)
N1-Cu-X	180.00(2)	180.00(4)

[a] X=Cl for complex **1** and Br from complex **2**.

geometry with perfect C_3 symmetry (Figure 5.4.1). Each complex is coordinated by four nitrogen atoms and either a chloride (**1**) or bromide (**2**) anion. The axial Cu-N bonds in both complexes were close to 2.05 Å and the equatorial bonds were slightly longer, approximately 2.15 Å (Table 5.4.1). The Cu-Cl and Cu-Br bond lengths was found to be 2.2589(5) and 2.4016(4) Å respectively. All of the angles in the coordination spheres of both molecules are close to a typical trigonal bipyramidal geometry. A non-coordinating chloride and bromide was present in both complex **1** and **2,** respectively.Additionally, the structures reported herein are in close agreement with a previously reported structure for $[Cu(Me_6TREN)Br][Br]$[72,73] and $[Cu(Me_6TREN)Cl_{0.63}/Br_{0.37}][Br]$[74] as well as similar copper complexes with tetradentate nitrogen based ligands.[75-77]

Only a few examples of copper(I) complexes with the Me_6TREN ligand have known molecular structures[78, 79] due to their propensity to disproportionate, even in acetonitrile at reduced temperatures. To prevent this, a single equivalent of PPh_3 was added to a solution of $[Cu^{I}(CH_3CN)_4][ClO_4]$ before addition of Me_6TREN. Salt metathesis with BPh_4^- allowed for faster crystallization. No disproportionation was observed and the resulting material was air stable. The molecular structure of complex **3**,

$[Cu^{I}(Me_6TREN)PPh_3][BPh_4]$, was found to be distorted tetrahedral around copper(I) ion, where one arm of the Me_6TREN ligand was displaced by PPh_3 (Figure 5.2.1). Three

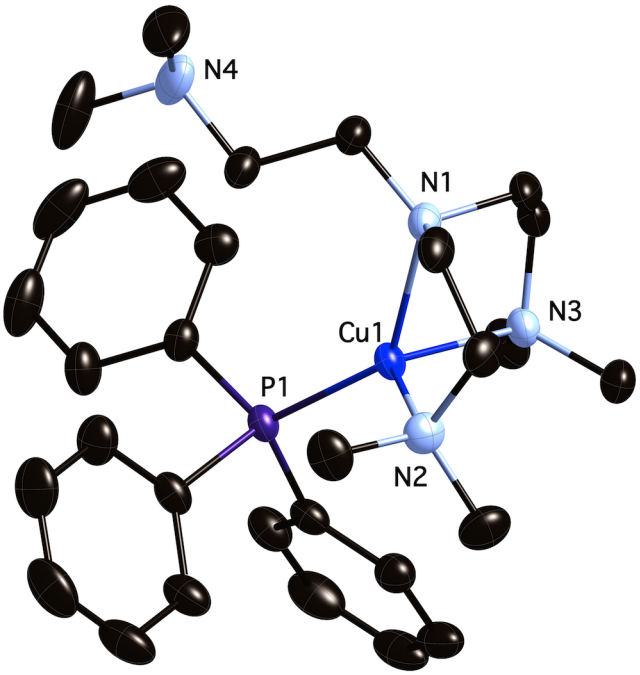

Figure 5.4.2. Molecular structure of $[Cu^{I}(Me_6TREN)PPh_3][BPh_4]$ (3) collected at 150K shown with 50% probability displacement ellipsoids. H-atoms omitted for clarity. Selected bond distances [Å] and angles [°]: Cu1-N1 2.1450(14), Cu1-N2 2.1753(17), Cu1-N3 2.1865(18), Cu1-P1 2.1910(5), N1-Cu1-N2 85.79(6), N1-Cu1-N3 83.87(6), N2-Cu1-N3 113.40(8), N1-Cu1-P1 136.92(4), N2-Cu1-P1 111.80(6), N3-Cu1-P1 119.80(4).

nitrogen atoms from the Me_6TREN ligand were found to be coordinated at distances of 2.1450(14), 2.1753(17), 2.1865(18) Å and a phosphorus atom from PPh_3 at 2.1910(5) Å. The addition of PPh_3 to the complex greatly increases steric bulk around copper, which apparently forced an arm of the Me_6TREN ligand away from copper in a similar fashion to previously reported structures with the TPMA ligand.[75, 80]

From the solid-state structure of **3**, the Me_6TREN ligand appears to coordinate in the same manner as the pentamethyldiethylenetriamine (PMDETA) ligand, so solution state

studies were performed by ^{1}H NMR to probe the structure (Figure 5.4.3). At room temperature, only a single peak is observed for the -N-CH_3 groups of the ligand at 2.20 ppm and two signals for the methylene protons at 3.04 and 2.68 ppm. All three signals

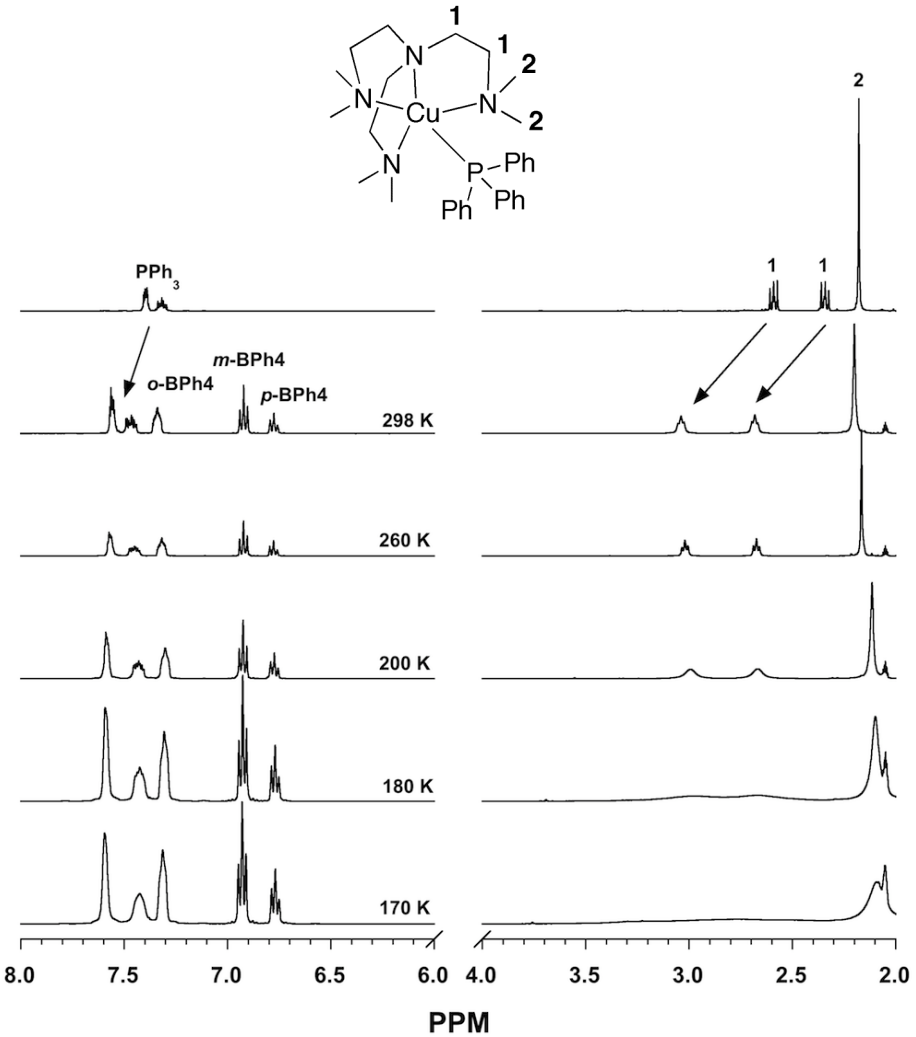

Figure 5.4.3. Variable temperature ^{1}H NMR (400 MHz, acetone-*d*6) of $[Cu^I(Me_6TREN)PPh_3][BPh_4]$ (3).

showed a downfield shift relative to the free ligand (2.56 and 2.31 ppm for methylene and 2.16 ppm for methyl), consistent with coordination to copper. Upon cooling, the signals for Me_6TREN broaden until finally at 170K the signals for the methylene protons coalesced and the singlet for the methyl protons becomes greatly broadened at 2.09 ppm.

The observed broadening and chemical shift toward the free ligand support the rapiddissociation/association of at least one ligand arm. The sample could not be cooled further as a solution in order to observe the splitting of signals into free and complexed ligand arms. Peaks corresponding to PPh_3 (7.57-7.55 ppm and 7.49-7.44 ppm) and BPh_4^- (7.33, 6.92, and 6.77 ppm) were observed to show very little change as a result of cooling. It is clear from these results that a rapid exchange of the ligand arms was occurring in solution, which would explain why Me_6TREN, even in the presence of one equivalent of PPh_3, would still retain characteristics of a tetradentate ligand.

5.5 Conclusions

Copper(II) complexes with the Me_6TREN ligand were thoroughly investigated as catalysts for ATRA in the presence of AIBN as a reducing agent. These complexes were found to catalyze the addition of CCl_4, $CHCl_3$, CBr_4, and $CHBr_3$ to a series of alkenes with good efficiency, albeit lower than expected due to their large ATRA equilibrium constants. Thus, attempts to increase their activity towards ATRA were probed by addressing ligand/halide dissociation and disproportionation equilibriums. Although the catalytic efficiency could not be increased, complex disproportionation at elevated reaction temperatures was found to be most likely the cause for the reduced activity.

The reactions of CCl_4 to *cis*-cyclooctene was found to produce solely the 1-chloro-4-(trichloromethyl)cyclooctane as a result of intramolecular proton transfer. Interestingly, CCl_3Br and CBr_4 produced both the 1,2- and 1,4-regioisomers in 48:52 and 75:25 ratios, respectively, when reacted with *cis*-cyclooctene. This observation indicated

that the product distribution is governed by the chain transfer ability of the alkyl halide and not transition state geometric differences.

The molecular structures of $[Cu^{II}(Me_6TREN)Cl][Cl]$ and $[Cu^{II}(Me_6TREN)Br][Br]$ were determined and found to be nearly isostructural with distorted trigonal bipyramidal geometries with perfect C_3 symmetry. A rare example of a copper(I) complex with Me_6TREN was prepared using PPh_3 to stabilize the complex against disproportionation. The molecular structure of $[Cu^{I}(Me_6TREN)PPh_3][BPh_4]$ was found to be distorted tetrahedral as a result of the dissociation of a single ligand arm. ^1H NMR confirmed that although the ligand is highly fluxional, it retains C_3 symmetry at higher temperatures.

5.6 Experimental Part

Materials - All chemicals were purchased from commercial sources and used as received. Tetrakis(acetonitrile)copper(I) perchlorate[81] was synthesized according to literature procedures. *Warning: Although we have experienced no problems, perchlorate metal salts are potentially explosive and should be handled with care.* All manipulations involving copper(I) complexes were performed under argon in the dry box (<1.0 ppm O_2 and <0.5 ppm H_2O) or using standard Schlenk line techniques. Solvents (pentane, acetonitrile, acetone, and diethyl ether) were degassed and deoxygenated using an Innovative Technology solvent purifier. Methanol was vacuum distilled and deoxygenated by bubbling argon for 30 min prior to use. Synthesis of copper(II) complexes were performed in ambient conditions and solvents were used as received.

NMR spectroscopy - ^{1}H NMR spectra were obtained using Bruker Avance 400 and 500 MHz spectrometers and chemical shifts are given in ppm relative to residual solvent peaks [$CDCl_3$ δ 7.26 ppm; $(CD_3)_2CO$ δ 2.05 ppm]. iNMR and kaleidagraph software was used to generate images NMR spectra. Temperature calibrations were performed using a pure methanol sample.

X-ray Crystal Structure Determination - The X-ray intensity data were collected at 150K using graphite-monochromated Mo-*K* radiation (0.71073 Å) with a Bruker Smart Apex II CCD diffractometer. Data reduction included absorption corrections by the multi-scan method using SADABS.[82] Structures were solved by direct methods and refined by full matrix least squares using SHELXTL 6.1 bundled software package.[83] The H-atoms were positioned geometrically (aromatic C-H 0.93, methylene C-H 0.97, and methyl C-H 0.96) and treated as riding atoms during subsequent refinement, with $U_{iso}(H) = 1.2U_{eq}(C)$ or $1.5U_{eq}$(methyl C). The methyl groups were allowed to rotate about their local threefold axes. ORTEP-3 for windows[84] and Crystal Maker 7.2 were used to generate molecular graphics.

Infrared Spectroscopy - IR spectra were recorded in the solid state using Nicolet Smart Orbit 380 FT-IR spectrometer (Thermo Electron Corporation).

Elemental Analysis for C, H, and N - Elemental analyses for C, H, and N were obtained from Midwest Microlabs, LLC.

General Procedures for ATRA Reactions - In a vial was combined: 0.033g AIBN (0.20 mmol), p-methoxybenzene (internal standard), 4.03 mmol alkene (630 μL 1-octene, 525 μL *cis*-cyclooctene, 500 μL 1-hexene, 462 μL styrene, 362 μL methyl acrylate), and 4.43 mmol alkyl halide (430 uL CCl_4, 355 uL $CHCl_3$, 387 uL $CHBr_3$, 1.470g CBr_4). Solvent was then added (acetonitrile, methanol, dimethylformamide) so that total volume in the reaction mixture was 2.20 mL with 1-hexene, 1-octene, and *cis*-cyclooctene or 1.39 mL for styrene or methyl acrylate reactions (additives, such as TBA-Cl, PPh_3, or Me_6TREN, were added in solution (32.2 mM for 1-octene reactions and 645.0 mM for styrene and methyl acrylate reactions) and diluted to the proper amount of solvent). The solution in the vial was then divided equally into 5 NMR tubes (439 μL for 1-hexene, 1-octene and *cis*-cyclooctene reactions and 278 μL for styrene and methyl acrylate reactions). A 0.01 M solution of $[Cu^{II}(Me_6TREN)X][X]$ (X=Cl, Br) in acetonitrile, methanol, or dimethylformamide was added in the following quantities for various catalyst loadings: 250:1 – 322 μL, 500:1 – 161 μL, 1000:1 – 81 μL, 2500:1 – 32 μL, 5000:1 – 16 μL, 10,000:1 – 8 μL. The total volume in the NMR tubes was then adjusted by the addition of solvent so that [alkene] = 1.34 M. Reaction tubes were flushed with argon for 30 seconds and were sealed with a plastic NMR tube cap and wrapped in Teflon tape and run at 60°C for 24 hr.

Synthesis of Tris(2-dimethylaminoethyl)amine (Me_6TREN) - Tris((2-dimethylamino)ethyl)amine was synthesized according to published procedures.[85, 86] Density was experimentally determined to be 0.860 g/mL. ^{1}H-NMR (400 MHz, $CDCl_3$,

298K): δ 2.52 (dd, J = 8.7, 6.2 Hz, 6H), 2.29 (dd, J = 8.7, 6.1 Hz, 6H), 2.14 (s, 18H). ^{13}C-NMR (101 MHz; $CDCl_3$, 298K): δ 57.12 (s, 3C), 52.71 (s, 3C), 45.55 (s, 6C).

[Cu^{II}(Me$_6$TREN)Cl][Cl] - $CuCl_2$ (0.50 g, 3.71 mmol) was dissolved in methylene chloride and Me_6TREN (0.860 g, 1 mL, 3.71 mmol) was added. The blue solution was stirred at RT for 15 minutes. The complex was precipitated by addition of 50 mL of petroleum ether. The blue powder was collected by filtration and dried under vacuum (1.326 g, 98%). Anal. Calcd. for $C_{12}H_{30}N_4CuCl_2$ (364.85): C, 39.50; H, 8.29; N, 15.36. Found: C, 38.81; H, 7.97; N, 14.98.

[Cu^{II}(Me$_6$TREN)Br][Br] - $CuBr_2$ (0.83 g, 3.71 mmol) was dissolved in methylene chloride and Me_6TREN (0.860 g, 1 mL, 3.71 mmol) was added. The green solution was stirred at RT for 15 minutes. The complex was precipitated by addition of 50 mL of petroleum ether. The green powder was collected by filtration and dried under vacuum (1.326 g, 98%). Anal. Calcd. for $C_{12}H_{30}N_4CuBr_2$ (453.75): C, 31.76; H, 6.66; N, 12.35. Found: C, 31.40; H, 6.46; N, 12.20.

[Cu^{I}(Me$_6$TREN)PPh$_3$][BPh$_4$] - $Cu^{I}(CH_3CN)_4ClO_4$ (100 mg, 3.06 x 10^{-4} mol) and PPh_3 (80 mg, 3.06 x 10^{-4} mol) were dissolved in 3 mL MeOH. Me_6TREN (70 mg, 82 μL, 3.06 x 10^{-4} mol) was added, followed by $NaBPh_4$ (105 mg, 3.06 x 10^{-4} mol). A colorless powder began to precipitate immediately. The solution was left at1-35°C overnight to complete precipitation. The methanol was removed and the powder was redissolved in 3 mL acetone and crystallized by slow diffusion of diethyl ether. (0.213 g collected, 80%).

^{1}H-NMR (400 MHz, acetone-*d*6, 298K): δ 7.57-7.55 (m, 9H), 7.49-7.44 (m, 6H), 7.36-7.32 (m, 8H), 6.92 (t, *J* = 7.4 Hz, 8H), 6.79-6.76 (m, 4H), 3.04 (t, *J* = 5.4 Hz, 6H), 2.68 (t, *J* = 5.6 Hz, 6H), 2.20 (s, 18H). Anal. Calcd. for $C_{54}H_{65}BCuN_4P$ (875.45): C, 74.08; H, 7.48; N, 6.40. Found: C, 74.99; H, 8.65; N, 6.87.

5.7 References

(1) Kharasch, M. S.; Engelmann, H.; Mayo, F. R., The Peroxide Effect in the Addition of Reagents to Unsaturated Compounds. XV. The Addition of Hydrogen Bromide to 1- and 2-Bromo and Chloro-Propenes. *J. Org. Chem.* **1937,** *2*, 288-302.

(2) Kharasch, M. S.; Jensen, E. V.; Urry, W. H., Addition of Carbon Tetrachloride and Chloroform to Olefins. *Science* **1945,** *102*(2640), 128-128.

(3) Kharasch, M. S.; Jensen, E. V.; Urry, W. H., Addition of Derivatives of Chlorinated Acetic Acid to Olefins. *J. Am. Chem. Soc.* **1945,** *67*, 1626-1626.

(4) De Malde, M.; Minisci, F.; Pallini, U.; Volterra, E.; Quilico, A., Reactions between acrylonitriles and aliphatic halogen derivatives. *Chim. Ind. (Milan)* **1956,** *38*, 371-382.

(5) Minisci, F., Radical Reactions in Solution. Dipolar Character of Free Radicals from Decomposition of Organic Peroxides. *Gazz. Chim. Ital.* **1961,** *91*, 386-389.

(6) Minisci, F., Free-Radical Additions to Olefins in the Presence of Redox Systems. *Acc. Chem. Res.* **1975,** *8*(5), 165-171.

(7) Minisci, F.; Cecere, M.; Galli, R., Oxidation of Carbon Free Radicals in the Presence of Cu and Fe Salts. New Synthesis of Nitro Derivatives and Nitric Esters. *Gazz. Chim. Ital.* **1963,** *93*, 1288-1294.

(8) Minisci, F.; Pallini, U., Radical reactions in solution. Haloalkylation of acrylic acid derivatives. *Gazz. Chim. Ital.* **1961,** *91*, 1030-1036.

(9) Asscher, M.; Vosfsi, D., Chlorine Activation by Redox-transfer. Part I. The Reaction Between Aliphatic Amines and Carbon Tetrachloride. *J. Chem. Soc.* **1961**, 2261-2264.

(10) Asscher, M.; Vosfsi, D., Chlorine Activation by Redox-transfer. Addition of Carbon Tetrachloride and Chloroform to Olefins. *Chem. Ind.* **1962**, 209-210.

(11) Asscher, M.; Vosfsi, D., Chlorine Activation by Redox-transfer. Part III. The "Abnormal" Addition of Chloroform to Olefins. *J. Chem. Soc.* **1963**, 3921-3927.

(12) Bellius, D., Copper-Catalyzed Additions of Organic Polyhalides to Olefins: a Versatile Synthetic Tool. *Pure Appl. Chem.* **1985,** *57*, 1827-1838.

(13) Burton, D. J.; Kehoe, L. J., Copper chloride-ethanolamine catalyzed addition of polyhaloalkanes to 1-octene. *J. Org. Chem.* **1970,** *35*(5), 1339-1342.

(14) Forti, L.; Ghelfi, F.; Pagnoni, U. M., Fe(0) Initiated Halogen Atom Transfer Radical Addition of Methyl 2-Br-2-Cl-Carboxylates to Olefins. *Tetrahedron Lett.* **1996,** *37*, 2077-2078.

(15) Gossage, R. A.; Van De Kuil, L. A.; Van Koten, G., Diaminoarylnickel(II) "Pincer" Complexes: Mechanistic Considerations in the Kharasch Addition Reaction, Controlled Polymerization, and Dendrimeric Transition Metal Catalysts. *Acc. Chem. Res.* **1998,** *31*(7), 423-431.

(16) Iqbal, J.; Bhatia, B.; Nayyar, N. K., Transition Metal-Promoted Free-Radical Reactions in Organic Synthesis: The Formation of Carbon-Carbon Bonds *Chem. Rev.* **1994,** *94*(2), 519-564.

(17) Murai, S.; Sonoda, N.; Tsutsumi, S., Copper Salts Induced Addition of Ethyl Trichloroacetate to Olefins. *J. Org. Chem.* **1964,** *31*(9), 3000-3003.

(18) Quebatte, L.; Haas, M.; Solari, E.; Scopelliti, R.; Nguyen, Q. T.; Severin, K., Combinatorial Catalysis with Bimetallic Complexes: Robust and Efficient Catalysts for Atom-Transfer Radical Additions. *Angew. Chem., Int. Ed.* **2004,** *43*(12), 1520-1524.

(19) Quebatte, L.; Haas, M.; Solari, E.; Scopelliti, R.; Nguyen, Q. T.; Severin, K., Atom-Transfer Radical Reactions Under Mild Conditions with $[\{RuCl_2(1,3,5\text{-}C_6H_3iPr_3)\}_2]$ and PCy_3 as the Catalyst Precursors. *Angew. Chem., Int. Ed.* **2005,** *44*(7), 1084-1088.

(20) Quebatte, L.; Solari, E.; Scopelliti, R.; Severin, K., A Bimetallic Ruthenium Ethylene Complex as a Catalyst Precursor for the Kharasch Reaction. *Organometallics* **2005,** *24*(7), 1404-1406.

(21) Severin, K., Ruthenium Catalysts for the Kharasch Reaction. *Curr. Org. Chem.* **2006,** *10*(2), 217-224.

(22) Clark, A. J., Atom Transfer Radical Cyclisation Reactions Mediated by Copper Complexes. *Chem. Soc. Rev.* **2002,** *31*(1), 1-11.

(23) Clark, A. J.; Battle, G. M.; Bridge, A., Efficient β-Lactam Synthesis via 4-exo Atom Tranfer Radical Cyclization Using CuBr(tripyridylamine) Complexe. *Tetrahedron Lett.* **2001,** *42*, 4409-4412.

(24) Clark, A. J.; Battle, G. M.; Heming, A. M.; Haddleton, D. M.; Bridge, A., Ligand Electronic Effects on Rates of Copper Mediated Atom Transfer Radical Cyclisation and Polymerisation. *Tetrahedron Lett.* **2001,** *42*, 2003-2005.

(25) Clark, A. J.; Dell, C. P.; Ellard, J. M.; Hunt, N. A.; McDonagh, J. P., Efficient Room Temperature Copper(I) Mediated 5-Endo Radical Cyclizations. *Tetrahedron Lett.* **1999,** *40*(49), 8619-8623.

(26) Clark, A. J.; Filik, R. P.; Haddleton, D. M.; Radigue, A. P.; J., S. C.; Thomas, G. H.; E., S. M., Solid-Supported Catalysts for Atom-Transfer Radical Cyclization of 2-Haloacetamides. *J. Org. Chem.* **1999,** *64*, 8954-8957.

(27) De Campo, F.; Lastecoueres, D.; Verlhac, J.-B., New Copper(I) and Iron(II) Complexes for Atom Transfer Radical Macrocyclization Reactions. *J. Chem. Soc., Perkin Trans. 1* **2000,** (4), 575-580.

(28) Iwamatsu, S.; Kondo, H.; Matsubara, K.; Nagashima, H., Copper-Catalyzed Facile Carbon-Carbon Bond Forming Reactions at the α-Position of α,α,γ-Trichlorinated γ-Lactams. *Tetrahedron* **1999,** *55*, 1687-1706.

(29) Iwamatsu, S.; Matsubara, K.; Nagashima, H., Synthetic Studies of cis-3α-Aryloctahydroindole Derivatives by Copper-Catalyzed Cyclization of N-Allyltrichloroacetamides: Facile Construction of Benzylic Quaternary Carbons by Carbon-Carbon Bond-Forming Reactions. *J. Org. Chem.* **1999,** *64*, 9625-9631.

(30) Lee, G. M.; Weinreb, S. M., Transition Metal Catalyzed Intramolecular Cyclizations of (Trichloromethyl)alkenes. *J. Org. Chem.* **1990,** *55*, 1281-1285.

(31) Nagashima, H.; Wakamatsku, H.; Itoh, K.; Tomo, Y.; Tsuji, J., New Regio- and Stereoselective Preparation of Trichlorinated γ-Butyrolactones by Copper Catalyzed Cyclization of Allyl Trichloroacetates. *Tetrahedron Lett.* **1983,** *23*, 2395-2398.

(32) Udding, J. H.; Tujip, C. J. M.; Hiemstra, H.; Speckamp, W. N., Transition Metal-Catalyzed Chlorine Transfer Cyclizations of Carbon-Centered Glycine Radicals; a Novel Synthetic Route to Cyclic α-Amino Acids. *Tetrahedron* **1999,** *50*(6), 1907-1918.

(33) Udding, J. H.; Tujip, C. J. M.; van Zanden, N. A.; Hiemstra, H.; Speckamp, W. N., Transition Metal-Catalyzed, Chlorine-Transfer Radical Cyclizations of 2-(3-Alken-1-oxy)-2-Chloroacetates. Formal Total Synthesis of Avenaciolide and Isoavenaciolide. *J. Org. Chem.* **1994,** *59*, 1993-2003.

(34) Clark, A. J.; Geden, J. V.; Thom, S., Solid Support Copper Catalysts for Atom Transfer Radical Cyclizations: Assessment of Support Type and Ligand Structure on Catalyst Performance in the Synthesis of Nitrogen Heterocycles. *J. Org. Chem.* **2006,** *71*(4), 1471-1479.

(35) Oe, Y.; Uozumia, Y., Highly Efficient Heterogeneous Aqueous Kharasch Reaction with an Amphiphilic Resin-Supported Ruthenium Catalyst *Adv. Synth. Catal.* **2008,** *350*, 1771-1775.

(36) De Campo, F.; Lastecoueres, D.; Vincent, J.-M.; Verlhac, J.-B., Copper(I) Complexes Mediated Cyclization Reaction of Unsaturated Ester under Fluoro Biphasic Procedure. *J. Org. Chem.* **1999,** *64*, 4969-4971.

(37) Jakubowski, W.; Matyjaszewski, K., Activators Regenerated by Electron Transfer for Atom-Transfer Radical Polymerization of (Meth)acrylates and Related Block Copolymers. *Angew. Chem.* **2006,** *118*, 4594-4598.

(38) Jakubowski, W.; Min, K.; Matyjaszewski, K., Activators Regenerated by Electron Transfer for Atom Transfer Radical Polymerization of Styrene *Macromolecules* **2006,** *39*(1), 39-45.

(39) Matyjaszewski, K.; Jakubowski, W.; Min, K.; Tang, W.; Huang, J.; Braunecker, W. A.; Tsarevsky, N. V., Diminishing Catalyst Concentration in Atom Transfer Radical Polymerization with Reducing Agents. *Proc. Natl. Acad. Sci. U.S.A.* **2006,** *103*, 15309-15314.

(40) Wang, J.-S.; Matyjaszewski, K., Controlled/"Living" Radical Polymerization. Atom Transfer Radical Polymerization in the Presence of Transition-Metal Complexes. *J. Am. Chem. Soc.* **1995,** *117*(20), 5614-5615.

(41) Fernández-Zúmel, M. A.; Thommes, K.; Kiefer, G.; Sienkiewicz, A.; Pierzchala, K.; Severin, K., Atom-Transfer Radical Addition Reactions Catalyzed by RuCp* Complexes: A Mechanistic Study. *Chem. Eur. J.* **2009,** *15*(43), 11601-11607.

(42) Quebatte, L.; Thommes, K.; Severin, K., Highly Efficient Atom Transfer Radical Addition Reactions with a Ru^{III} Complex as a Catalyst Precursor. *J. Am. Chem. Soc.* **2006,** *128*(23), 7440-7441.

(43) Thommes, K.; Icli, B.; Scopelliti, R.; Severin, K., Atom-Transfer Radical Addition (ATRA) and Cyclization (ATRC) Reactions Catalyzed by a Mixture of $[RuCl_2Cp^*(PPh_3)]$ and Magnesium. *Chem. Eur. J.* **2007,** *13*(24), 6899-6907.

(44) Thommes, K.; Kiefer, G.; Scopelliti, R.; Severin, K., Olefin Cyclopropanation by a Sequential Atom-Transfer Radical Addition and Dechlorination in the Presence of a Ruthenium Catalyst. *Angew. Chem. Int. Ed.* **2009,** *48*(43), 8115-8119.

(45) Wolf, J.; Thommes, K.; Brie, O.; Scopelliti, R.; Severin, K., Dinuclear Ruthenium Ethylene Complexes: Synthesis, Structures, and Catalytic Applications in ATRA and ATRC Reactions. *Organometallics* **2008,** *27*, 4464-4474.

(46) Lundgren, R. J.; Rankin, M. A.; McDonald, R.; Stradiotto, M., Neutral, Cationic, and Zwitterionic Ruthenium(II) Atom Transfer Radical Addition Catalysts Supported by P,N-Substituted Indene or Indenide Ligands *Organometallics* **2008,** *27*(2), 254-258.

(47) Nair, R. P.; Kim, T. H.; Frost, B. J., Atom Transfer Radical Addition Reactions of CCl_4, $CHCI_3$, and p-Tosyl Chloride Catalyzed by $Cp'Ru(PPh_3)(PR_3)Cl$ Complexes. *Organometallics* **2009,** *28*(16), 4681-4688.

(48) Balili, M. N. C.; Pintauer, T., Persistent Radical Effect in Action: Kinetic Studies of Copper-Catalyzed Atom Transfer Radical Addition in the Presence of Free-Radical Diazo Initiators as Reducing Agents. *Inorg. Chem.* **2009,** *48*, 9018-9026.

(49) Eckenhoff, W. T.; Garrity, S. T.; Pintauer, T., Highly Efficient Copper Mediated Atom Transfer Radical Addition (ATRA) in the Presence of Reducing Agent. *Eur. J. Inorg. Chem.* **2008**, 563-571.

(50) Eckenhoff, W. T.; Pintauer, T., Atom Transfer Radical Addition in the Presence of Catalytic Amounts of Copper(I/II) Complexes with Tris(2-pyridylmethyl)amine. *Inorg. Chem.* **2007,** *46*(15), 5844-5846.

(51) Eckenhoff, W. T.; Pintauer, T., Copper Catalyzed Atom Transfer Radical Addition (ATRA) and Cyclization (ATRC) Reactions in the Presence of Reducing Agents. *Cat. Rev. Sci. Eng.* **2010,** *52*, 1-59.

(52) Pintauer, T., "Greening" of Copper Catalyzed Atom Transfer Radical Addition (ATRA) and Cyclization (ATRC) Reactions. *ACS Symp. Ser.* **2009,** *1023*, 63-84.

(53) Pintauer, T.; Eckenhoff, W. T.; Ricardo, C.; Balili, M. N. C.; Biernesser, A. B.; Noonan, S. J.; Taylor, M. J. W., Highly Efficient, Ambient-Temperature Copper-Catalyzed Atom-Transfer Radical Addition (ATRA) in the Presence of Free-Radical Initiator (V-70) as a Reducing Agent. *Chem. Eur. J.* **2009,** *15*, 38-41.

(54) Pintauer, T.; Matyjaszewski, K., Atom Transfer Radical Addition and Polymerization Reactions Catalyzed by ppm Amounts of Copper Complexes. *Chem. Soc. Rev.* **2008,** *37*, 1087-1097.

(55) Pintauer, T.; Matyjaszewski, K., Structural and Mechanistic Aspects of Copper Catalyzed Atom Transfer Radical Polymerization. *Top. Organomet. Chem.* **2009,** *26*, 221-251.

(56) Ricardo, C.; Pintauer, T., Copper Catalyzed Atom Transfer Radical Cascade Reactions in the Presence of Free-Radical Diazo Initiators as Reducing Agents. *Chem. Commun.* **2009**, 3029-3031.

(57) Muñoz-Molina, J. M.; Belderraín, T. R.; Pérez, P. J., Copper-Catalyzed Synthesis of 1,2-Disubstituted Cyclopentanes from 1,6-Dienes by Ring-Closing Kharasch Addition of Carbon Tetrachloride. *Adv. Synth. Catal.* **2008,** *350*, 2365-2372.

(58) Muñoz-Molina, J. M.; Belderraín, T. R.; Pérez, P. J., An Efficient, Selective, and Reducing Agent-Free Copper Catalyst for the Atom-Transfer Radical Addition of Halo Compounds to Activated Olefins. *Inorg. Chem.* **2010,** *49*(2), 642-645.

(59) Muñoz-Molina, J. M.; Caballero, A.; Díaz-Requejo, M. M.; Trofimenko, S.; Belderraín, T. R.; Pérez, P. J., Copper-Homoscorpionate Complexes as Active Catalysts for Atom Transfer Radical Addition to Olefins. *Inorg. Chem.* **2007,** *46*, 7725-7730.

(60) Balili, M. N. C.; Pintauer, T., Kinetic Studies of the Initiation Step in Copper Catalyzed Atom Transfer Radical Addition (ATRA) in the Presence of Free Radical Diazo Initiators as Reducing Agents. *Inorg. Chem.* **2010,** *49*(12), 5642-5649.

(61) Pintauer, T., Catalyst Regeneration in Transition-Metal-Mediated Atom-Transfer Radical Addition (ATRA) and Cyclization (ATRC) Reactions. *Eur. J. Inorg. Chem.* **2010**, 2449-2460.

(62) Xia, J.; Gaynor, S. G.; Matyjaszewski, K., Controlled/"Living" Radical Polymerization. Atom Transfer Radical Polymerization of Acrylates at Ambient Temperature. *Macromolecules* **1998,** *31*(17), 5958-5959.

(63) Tang, W.; Matyjaszewski, K., Effect of Ligand Structure on Activation Rate Constants in ATRP. *Macromolecules* **2006,** *39*(15), 4953-4959.

(64) Matyjaszewski, K.; Jakubowski, W.; Min, K.; Tang, W.; Huang, J.; Braunecker, W.; Tsarevsky, N., Diminishing Catalyst Concentration in Atom Transfer Radical Polymerization with Reducing Agents. *Proc. Nat. Acad. Sci.* **2006,** *103*(42), 15309-15314.

(65) Queffelec, J.; Gaynor, S. G.; Matyjaszewski, K., Optimization of Atom Transfer Radical Polymerization Using Cu(I)/Tris(2-(dimethylamino)ethyl)amine as a Catalyst. *Macromolecules* **2000,** *33*(23), 8629-8639.

(66) Clark, A. J.; Filik, R. P.; Thomas, G. H., Ligand Geometry Effects in Copper Mediated Atom Transfer Radical Cyclisations. *Tetrahedron Lett.* **1999,** *40*(26), 4885-4888.

(67) Clark, A. J.; Battle, G. M.; Bridge, A., Efficient β-Lactam Synthesis via 4-exo Atom Transfer Radical Cyclisation using CuBr(tripyridylamine) complex. *Tetrahedron Lett.* **2001,** *42*(26), 4409-4412.

(68) Dneprovskii, A. S.; Ermoshkin, A. A.; Kasatochkin, A. N.; Boyarskii, V. P., Addition of Bromotrichloromethane and tetrachloromethane to cis-Cyclooctene, Cyclohexene, and Norbornadiene in the presence of Palladium(II) Complexes. *Russ. J. Org. Chem.* **2003,** *39*(7), 994-1007.

(69) Traynham, J. G.; Couvillon, T. M., Radical additions of Cl-CCl3 to cis-cyclooctene. *J. Am. Chem. Soc.* **1967,** *89*(13), 3205-3211.

(70) Matsumoto, H.; Nakano, T.; Takasu, K.; Nagai, Y., Radical reactions in the coordination sphere. 4. Addition of carbon tetrachloride to cis-cyclooctene catalyzed by dichlorotris(triphenylphosphine)ruthenium(II). *J. Org. Chem.* **1978,** *43*(9), 1734-1736.

(71) Tsarevsky, N.; Braunecker, W.; Vacca, A.; Gans, P.; Matyjaszewski, K., Competitive Equilibria in Atom Transfer Radical Addition. *Macromol. Symp.* **2007,** *248*, 60-70.

(72) Di Vaira, M.; Orioli, P. L., Crystal structure of tris(2-dimethylaminoethyl)amine nickel(II) and copper(II) bromides. *Acta Cryst. Sec. B.* **1968,** *24*(4), 595-599.

(73) Pintauer, T.; Matyjaszewski, K., Structural Aspects of Copper Catalyzed Atom Transfer Radical Polymerization. *Coord. Chem. Rev.* **2005,** *249*(11-12), 1155-1184.

(74) Baisch, U.; Poli, R., Copper(I/II) and cobalt(II) coordination chemistry of relevance to controlled radical polymerization processes. *Polyhedron* **2008,** *27*, 2175-2185.

(75) Eckenhoff, W. T.; Pintauer, T., Structural Comparison of Copper(I) and Copper(II) Complexes with Tris(2-pyridylmethyl)amine Ligand in Atom Transfer Radical Addition. *Inorg. Chem.* **2010,** *ASAP*.

(76) Eckenhoff, W. T.; Garrity, S. T.; Pintauer, T., Highly Efficient Copper-Mediated Atom Transfer Radical Addition (ATRA) in the Presence of a Reducing Agent. *Eur. J. Inorg. Chem.* **2008,** (4), 563-571.

(77) Eckenhoff, W. T.; Pintauer, T., Atom Transfer Radical Addition in the Presence of Catalytic Amounts of Copper(I/II) Complexes with Tris(2-pyridylmethyl)amine *Inorg. Chem.* **2007,** *46*(15), 5844-5846.

(78) Wurtele, C.; Sander, O.; Lutz, V.; Waitz, T.; Tuczek, F.; Schindler, S., Aliphatic C-H Bond Oxidation of Toluene Using Copper Peroxo Complexes That Are Stable at Room Temperature. *J. Am. Chem. Soc.* **2009,** *131*(22), 7544-7545.

(79) Becker, M.; Heinemann, F. W.; Schindler, S., Reversible Binding of Dioxygen by a Copper(I) Complex with Tris(2-dimethylaminoethyl)amine (Me6tren) as a Ligand *Chem. Eur. J.* **1999,** *5*(11), 3124-3129.

(80) Tyeklar, Z.; Jacobson, R. R.; Wei, N.; Murthy, N. N.; Zubieta, J.; Karlin, K. D., Reversible reaction of dioxygen (and carbon monoxide) with a copper(I) complex. X-ray structures of relevant mononuclear Cu(I) precursor adducts and the trans-(.mu.-1,2-peroxo)dicopper(II) product. *J. Am. Chem. Soc.* **1993,** *115*(7), 2677-2689.

(81) Munakata, M.; Kitagawa, S.; Asahara, A.; Masuda, H., Crystal structure of bis(2,2'-bipyridine)copper(I) perchlorate. *Bull. Chem. Soc. Jpn.* **1987,** *60*(5), 1927-1929.

(82) Sheldrick, G. M., *SADABS Version 2.03*. University of Gottingen, Germany: 2002.

(83) Sheldrick, G. M., *SHELXTL 6.1,Crystallographic Computing System*. Bruker Analytical X-Ray System: Madison, WI, 2000.

(84) Faruggia, L. J., ORTEP-3 for Windows. *J. Appl. Cryst.* **1997,** *30 (5, Pt. 1)*, 565.

(85) Ciampolini, M.; Nardi, N., Five-coordinated high-spin complexes of bivalent cobalt, nickel, and copper with tris(2-dimethylaminoethyl)amine. . *Inorg. Chem.* **1966,** *5*(1), 41-44.

(86) Cohen, N. A.; Tillman, E. S.; Thakur, S.; Smith, J. R.; Eckenhoff, W. T.; Pintauer, T., Effect of the Ligand in Atom Transfer Radical Polymerization Reactions Initiated by Photodimers of 9-bromoanthracene. *Macromol. Chem. Phys.* **2009,** *210*(3-4), 263-268.

Chapter 6.

STRUCTURAL COMPARISON OF COPPER(I) AND COPPER(II) COMPLEXES WITH TRIS(2-PYRIDYL-METHYL)AMINE LIGAND[†]

Copper(I) complexes with tris(2-pyridylmethyl)amine (TPMA) ligand were synthesized and characterized in order to examine the effect of counter anions (Br^-, ClO_4^-, and BPh_4^-), as well as auxiliary ligands (CH_3CN, 4,4'-dipyridyl, and PPh_3) on the molecular structures in both solid state and solution. Partial dissociation of one of the pyridyl arms in TPMA was not observed when small auxiliary ligands such as CH_3CN or Br^- were coordinated to copper(I), but was found to occur with larger ones such as PPh_3 or 4,4'-dipyridyl. All complexes were found to adopt a distorted tetrahedral geometry, with the exception of $[Cu^I(TPMA)][BPh_4]$, which was found to be trigonal pyramidal due to stabilization via a long cuprophilic interaction with a bond length of 2.8323(12) Å. Copper(II) complexes with the general formula $[Cu^{II}(TPMA)X][Y]$ (X=Cl^-, Br^- and Y=ClO_4^-, BPh_4^-), were also synthesized in order to examine the effect of different counter-ions on the geometry of $[Cu^{II}(TPMA)X]^+$ cation, and were found to be isostructural with previously reported $[Cu^{II}(TPMA)X][X]$ (X= Cl^- or Br^-) complexes.

[†] Reproduced with permission from Eckenhoff, W.T.; Pintauer, T. *Inorg. Chem.* **2010**, *49*(22), 10617-10626. Copyright 2010 American Chemical Society.

6.1 Introduction and Background

Tris(2-pyridylmethyl)amine (TPMA) is a widely used neutral tripodal nitrogen based ligand that has been complexed to a wide variety of transition metals. Currently, the Cambridge Crystallographic Database contains over 350 structures with metals spanning from group 1 to 13 of the periodic table, including many cases from the lanthanide and actinide series. TPMA is an excellent chelator that typically coordinates

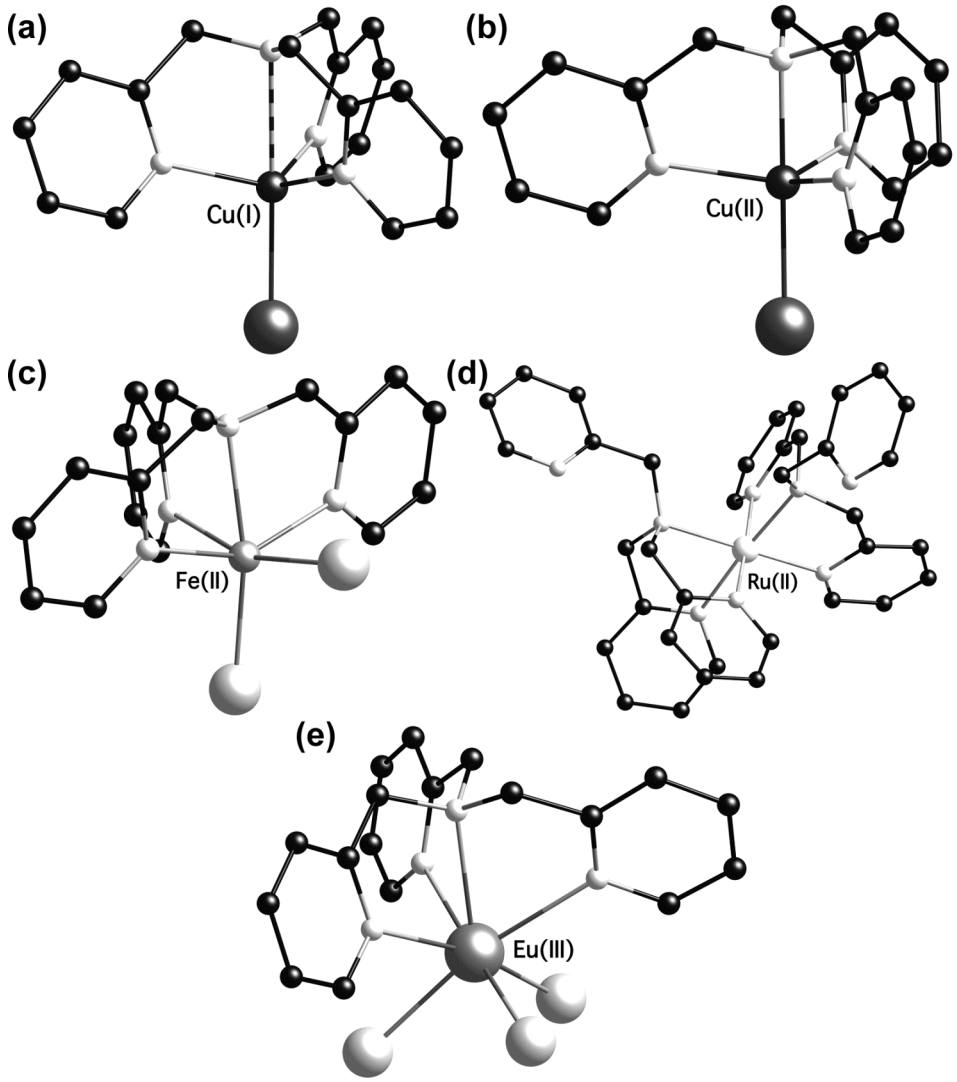

Figure 6.1.1. Examples of different transition metal complexes containing coordinated TPMA ligand; (a) $Cu^{I}(TPMA)Br$,[1] (b) $[Cu^{II}(TPMA)Br][Br]$,[1] (c) $Fe^{II}(TPMA)Cl_2$,[2] (d) $[Ru^{II}(TPMA)_2][PF_6]_2$,[3] and (e) $Eu^{III}(TPMA)Cl_3$.[4]

to a metal in a tetradentate fashion. However, in some cases, tridentate coordination achieved by pyridyl nitrogen arm dissociation has also been observed. Some representative structures of copper(I and II),[1] iron(II),[2] ruthenium(II)[3] and europium(III)[4] complexes with TPMA ligand are shown in Figure 6.1.1.

Over the past few years, TPMA has received considerable attention as a ligand of choice in copper complexes that mimic certain metalloenzymes of relevance to oxygen activation.[5-13] Also, on the other hand, it's complexes with copper have been shown to be among the most active in atom transfer radical addition (ATRA)[14-16] and polymerization (ATRP).[17, 18] Both processes originated from well known Kharasch addition in which polyhalogenated compounds were added to alkenes via free-radical means.[19-21] Recent studies have also indicated that TPMA is superior complexing ligand in ATRA[1, 15, 16, 22-32] and ATRP[26, 33-36] that utilize reducing agents. The role of reducing agent in both systems is to continuously regenerate the activator species (copper(I) complex) from the corresponding deactivator (copper(II) complex). The latter one accumulates in the

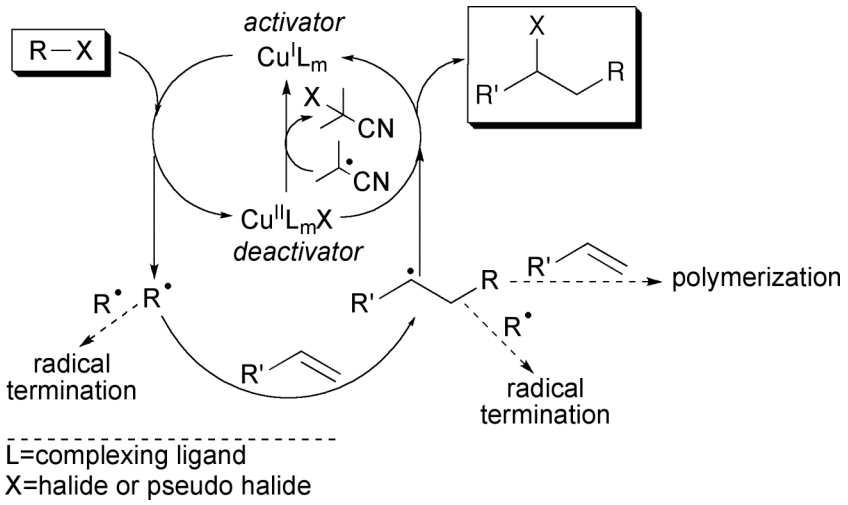

Scheme 6.1.1. Proposed mechanism for copper catalyzed ATRA in the presence of free radical diazo initiator (AIBN).

system as a result of unavoidable and often diffusion controlled radical-radical termination reactions. This is schematically illustrated in Scheme 6.1.1 in the case of simple ATRA additions. ATRP is mechanistically similar process with the exception that the structures of the starting alkyl halide and alkene (or monomer) are modified in such a way that multiple activation/deactivation cycles can occur. As a result, these synthetically useful reactions for the syntheses of small organic molecules and well-defined polymers can now be conducted using ppm amounts of copper.

Despite a significant effort devoted to the use of copper(I) and copper(II) complexes with TPMA ligand in synthetic aspects of ATRA and ATRP, structural and mechanistic studies of this active catalytic system still need further investigation. Recently, the molecular structures of Cu^{I}(TPMA)Cl and Cu^{I}(TPMA)Br were elucidated and surprisingly, taking into account the tetradentate nature of TPMA ligand, the copper(I) centers were found to contain coordinated halide anions (Figure 6.1.1.a).[1, 23, 37] While these complexes can be seen as pseudo-pentacoordinated, they were formally described as distorted tetrahedral due to the elongated Cu-N axial bond. It was further hypothesized that the high activity of Cu^{I}(TPMA)X and the corresponding [Cu^{II}(TPMA)X][X] (X=Br^{-} or Cl^{-}) complexes in ATRA can be explained by the fact that minimum entropic rearrangement was required upon oxidation and reduction. However, the presence of coordinated halide anions raised further questions regarding the catalytic mechanism of ATRA, which was conventionally described as an inner sphere electron transfer (ISET).[17, 38-41] The outer sphere electron transfer (OSET) mechanism,[17, 38, 39, 41] while theoretically feasible, was recently probed by extensive ab initio calculations, which concluded that OSET was approximately 12 orders of magnitude slower than the

ISET, clearly making this an unlikely scenario. Therefore, ISET process for copper(I) halide complexes with TPMA ligand would require an open coordination site, and is most likely preceded by either dissociation of the halide anion or one arm of the TPMA, as indicated in Scheme 6.1.2.

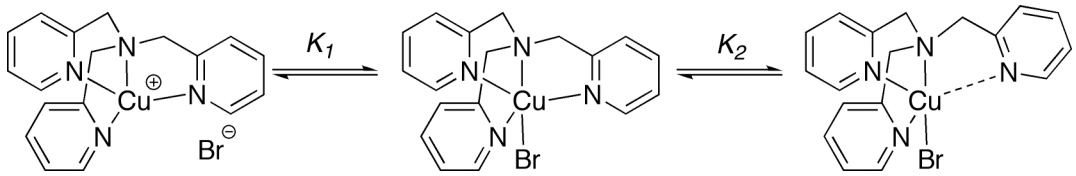

Scheme 6.1.2. Proposed equilibria for Cu^{I}(TPMA)Br involving bromide anion and pyridine nitrogen association/dissociation.

Dynamic behavior of Cu^{I}(TPMA)X (X=Br^{-} and Cl^{-}) was further probed by ^{1}H NMR spectroscopy, which confirmed that the most probable structure in solution was in fact a monomer with chemically equivalent pyridyl arms.[1, 37] Coordination of a solvent molecule, such as acetone, could theoretically also produce a symmetrical monomeric structure, but no evidence was found to suggest this. Hence, bromide anion was assumed to be the coordinating auxiliary ligand. Isolation of a dimeric complex, $[Cu^{I}(TPMA)]_2[ClO_4]_2$,[42] was achieved in the absence of a coordinating solvent or ligand and the variable temperature ^{1}H NMR showed, as expected, all three pyridyl arms as chemically distinct. This also suggested that the bromide anion was bound to copper in solution in the case of Cu^{I}(TPMA)Br, thus preventing dimer formation. Similar conclusions were also drawn for Cu^{I}(TPMA)Cl complex.

To further investigate the role of the anion, copper(I and II) complexes were synthesized with a variety of counter-ions such as perchlorate (ClO_4^{-}), hexafluorophosphate (PF_6^{-}), and tetraphenylborate (BPh_4^{-}). However, complexes with

these "non-coordinating" anions were found to less reducing by approximately 300 mV, when compared to their halide analogues.[1] These results also indicated that such complexes should be substantially less active in ATRA systems based on the linear correlation of $E_{1/2}$ values with the equilibrium constant for atom transfer (K_{ATRA}).[17, 27, 43-46] Clearly, the counter-ion in the copper(I) state, which was previously thought to be merely a spectator ion, plays an important role in the reaction mechanism.

In this chapter, copper(I and II) complexes with TPMA ligand were synthesized and counter-ion and coordinating ligand effects on the catalyst structure in the solid state and solution examined.

6.2 Solid State Structural Studies of Copper(I) Complexes

Following the structural elucidation of Cu^{I}(TPMA)Cl and Cu^{I}(TPMA)Br, it was immediately observed that these complexes were pseudo-pentacoordinated in the solid state due to the coordination of halide anions to the copper(I) centers.[1, 23] These results were not expected, particularly taking into account the strong preference for copper(I) complexes to adopt tetrahedral geometry and the tetradentate nature of the TPMA ligand. However, after careful examination, it was observed that the copper-amine ($Cu\text{-}N_{am}$) bond length in both complexes was slightly elongated at approximately 2.4 Å, when compared to a typical Cu-N bond (2.0-2.1 Å). Additionally, the copper atom in each complex was positioned below the least-squares-plane (LSP) derived from three pyridyl nitrogen atoms by approximately 0.53 Å. Therefore, copper(I) halide complexes

containing TPMA ligand can be best described as formally being distorted tetrahedral in geometry, as a result of this elongation.

It was initially hypothesized that the elongation was the result of large halide anion coordinated to copper on the opposing axial site.[42] To test this, $[Cu^{I}(TPMA)CH_3CN][BPh_4]$ (**1**) was synthesized via salt metathesis of $Cu^{I}(TPMA)Br$ with $NaBPh_4$ in acetonitrile (Figure 6.2.1). The axial Cu1-N_{am} bond in **1** was found to be elongated with a bond length of 2.4109(10) Å and the Cu-N_{py} bonds ranged from

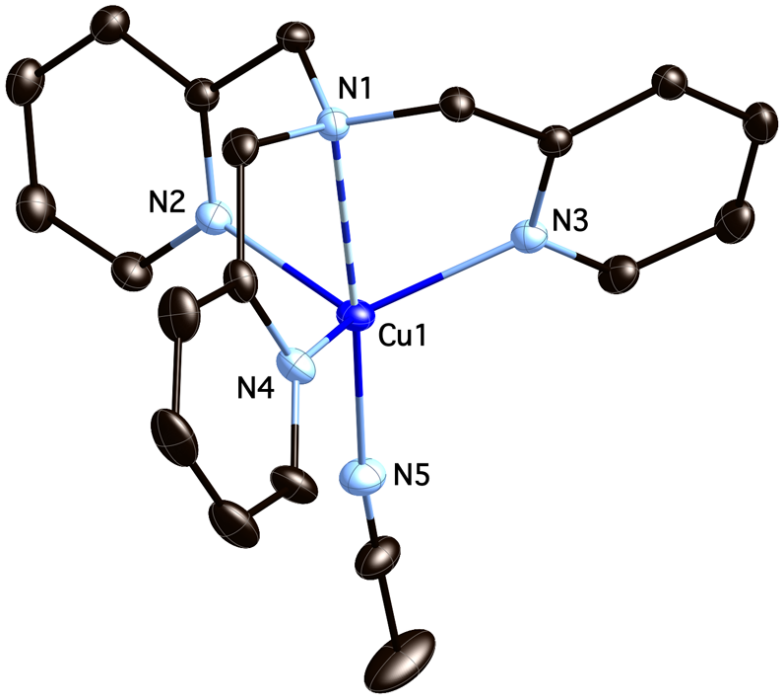

Figure 6.2.1. Molecular structure of $[Cu^{I}(TPMA)CH_3CN][BPh_4]$ (**1**) at 150K, shown with 50% probability displacement ellipsoids. H-atoms and counter anion have been omitted for clarity. Selected distances [Å] and angles [°]: Cu1-N1 2.4109(10), Cu1-N2 2.1031(10), Cu1-N3 2.1114(11), Cu-N4 2.0624(10), Cu1-N5 1.9914(11), N1-Cu1-N2 74.47(4), N1-Cu1-N3 74.04(4), N1-Cu1-N4 76.08(3), N1-Cu1-N5 175.94(4), N2-Cu1-N3 109.44(4), N2-Cu1-N4 115.97(4), N2-Cu1-N5 104.02(5), N3-Cu1-N4 114.92(4), N3-Cu1-N5 103.19(5), N4-Cu1-N5 107.90(5).

2.0624(10) to 2.1114(11) Å. These results are in good agreement with previously characterized Cu^{I}(TPMA)Cl and Cu^{I}(TPMA)Br complexes.[1, 23] Also, on the other hand, the copper(I) center was positioned below the LSP derived from N2, N3, and N4 towards the acetonitrile by 0.545(6) Å. The same distances in Cu^{I}(TPMA)Cl and Cu^{I}(TPMA)Br were found to be 0.534(6) Å and 0.538(6) Å, respectively.[1, 23] The discussed Cu-N bond lengths in **1** also compare very well with previously reported complexes of similar structure (Table 6.2.1).[11-13, 47, 48]

Table 6.2.1. Structural comparison of copper(I) complexes with TPMA containing halide anions or monodentate R-C≡N ligands. Bond lengths are given in angstroms (Å) and angles in degrees (^{o}).

Complex[a]	Cu-N_{am}	Cu-N_{py}[b]	Cu-N_{AN}	N_{am}-Cu-N_{AN}	Cu-$LSP_{N,py}$	Ref.
$[Cu^{I}(L)(AN)][BPh_4]$	2.4109(10)	2.0923(18)	1.9914(11)	175.94(4)	0.545(6)	c
$[Cu^{I}(L)(AN)][ClO_4]$	2.43(1)	2.09(2)	1.99(1)	179.5(5)	0.545(6)	47
$[Cu^{I}(L')(AN)][PF_6]$	2.439(8)	2.110(11)	1.999(9)	174.9(2)	0.569(6)	13
Cu^{I}(L)Cl	2.4366(11)	2.0808(19)	/	/	0.534(6)	23
Cu^{I}(L)Br	2.4397(14)	2.0825(26)	/	/	0.538(6)	1

[a]L=TPMA, L'= methyl-6-((bis(2-pyridinylmethyl)amino) methyl)pyridine-3-carboxylate, AN=CH_3CN. [b]Average Cu-N(pyridine) bond length. [c] This work.

In complex **1**, Cu1-N5 bond was the shortest bond in the coordination sphere with a bond distance of 1.9914(11) Å. The N_{am}-Cu1-N_{py} angles were found to be acute as a result, ranging from 74.04(4)^{o} to 76.08(3)^{o}. The larger bond angles between the copper atom and pyridine/acetonitrile nitrogen atoms (N_{py}-Cu-N_{py} and N_{py}-Cu-N5) were between 103.19(4)^{o} and 115.97(4)^{o}. The coordinated acetonitrile molecule was nearly linear (C-N-C bond angle=178.68(6)^{o}) and bent by 11.79(6)^{o} from the Cu-N5 bond towards the N4 pyridine ring. With this exception, $[Cu^{I}(TPMA)(CH_3CN)]^{+}$ cation had near perfect (non-crystallographic) C_3 symmetry. In the unit cell, the absence of available heteroatoms

resulted in only weak C---H-C interactions between TPMA ligands, which ranged between 2.823(6) and 2.898(6) Å (Appendix E).

Due to the axial elongation observed in **1**, the nature of the auxiliary ligand can therefore be ruled out as causing Cu-N_{am} elongation that was previously observed in copper(I) halide complexes with TPMA ligand. Although the preferred geometry for copper(I) is tetrahedral, the rigid structure of TPMA restricts such an arrangement. The elongation of the Cu-N_{am} bond and the long distance of copper to the LSP derived from nitrogen atoms in pyridine rings is likely the result of a distorted-tetrahedral geometry comprising of three nitrogen atoms from TPMA and the auxiliary ligand coordinated in the fourth site.

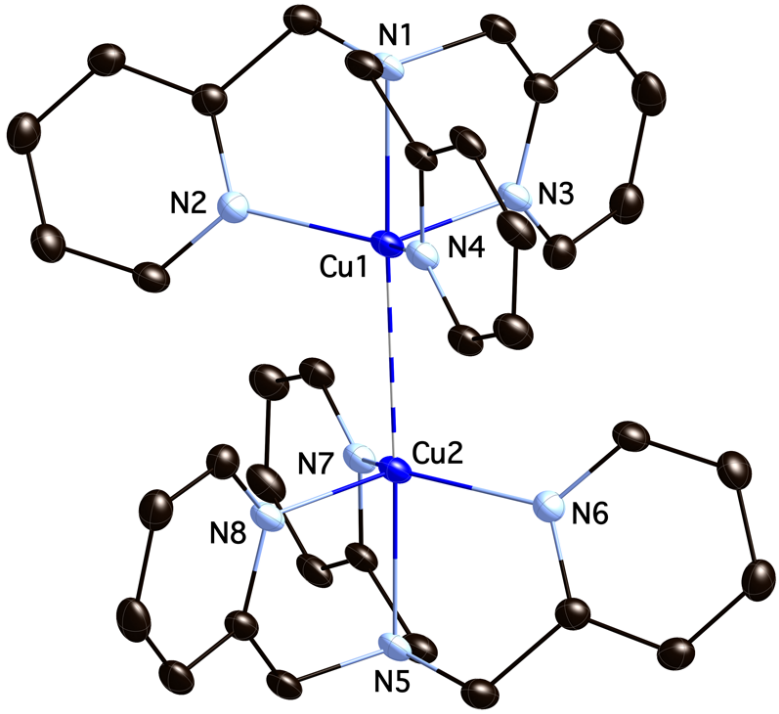

Figure 6.2.2. Molecular structure of [Cu^{I}(TPMA)][BPh_4] (**2**) at 150K, shown with 50% probability displacement ellipsoids. H-atoms and counter anion have been omitted for clarity. Selected distances [Å] and angles [°]: Cu1-N1 2.211(3), Cu1-N2 2.042(4), Cu1-N3 2.037(4), Cu1-N4 2.036(4), Cu1-Cu2 2.8323(12), N1-Cu1-N2 80.73(13), N1-Cu1-N3 82.08(14), N1-Cu1-N4 81.39(14), N2-Cu1-N3 117.83(15), N2-Cu1-N4 117.49(14), N3-Cu1-N4 118.10(15), Cu1-Cu2-N5 177.73(10).

When the synthesis of **1** was repeated in methanol, which does not readily coordinate to copper, $[Cu^{I}(TPMA)][BPh_4]$ (**2**) was isolated. Complex **2** was surprisingly found to have a slightly distorted trigonal pyramidal geometry stabilized by a weak cuprophilic interaction at 2.8323(12) Å (Figure 6.2.2). The axial Cu-N_{am} bond (2.211(3) Å) was found to be shorter than in the previous examples of copper(I) TPMA complexes (Table 6.2.1) and the three equatorial Cu-N_{py} bonds were statistically equivalent with lengths of 2.042(4), 2.037(4), and 2.036(4) Å. In conjunction with the shorter Cu-N_{am}

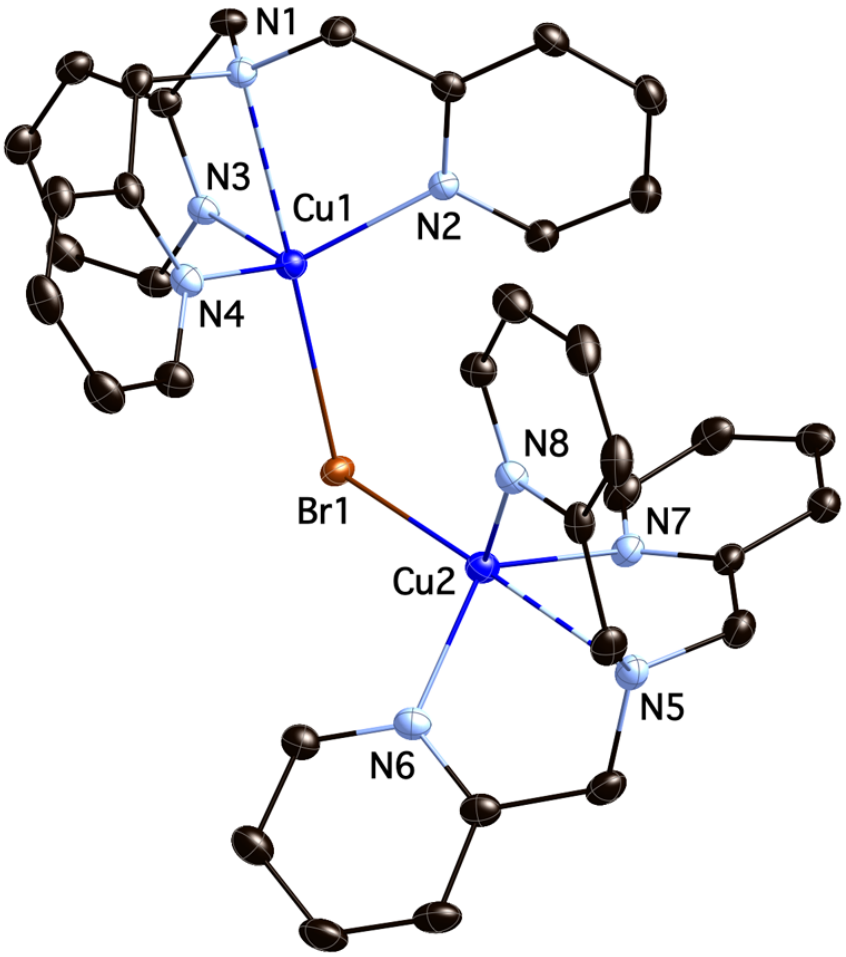

Figure 6.2.3. Molecular structure of $[(Cu^{I}(TPMA))_2\text{-}\mu\text{-}Br][BPh_4]_2$ (**3**) at 150K, shown with 50% probability displacement ellipsoids. H-atoms and counter anion have been omitted for clarity. Selected distances [Å] and angles [°]: Cu1-N1 2.429(2), Cu1-N2 2.067(2), Cu1-N3 2.131(2), Cu1-N4 2.065(2), Cu1-Br1 2.5228(4), N1-Cu1-N2 76.00(7), N1-Cu1-N3 74.08(7), N1-Cu1-N4 75.28(8), N2-Cu1-N3 107.70(8), N4-Cu1-N2 111.32(8), N4-Cu1-N3 121.61(8), Cu1-Br1-Cu2 117.456(13).

bond length, the copper atom in **2** was displaced to a lesser extent (0.304 Å) from the LSP derived from nitrogen atoms in pyridine rings. The two $[Cu^{I}(TPMA)]^{+}$ cations stabilized by a cuprophilic interaction were arranged in such a way that the pyridyl rings were staggered to achieve minimal steric interference. Weak intermolecular C-H---C interactions were also observed in the crystal lattice ranging from 2.74-2.99(6) Å (Appendix E).

The salt metathesis of $Cu^{I}(TPMA)Br$ with half equivalent of $NaBPh_4$ formed $[(Cu^{I}(TPMA)_2\text{-}\mu\text{-}Br][BPh_4]$ (**3**) (Figure 6.2.3). The formation of **3** was also observed in the synthesis of **2**, unless the by-product NaBr was rapidly removed from the reaction mixture. Complex **3** exhibited a highly unusual structure where two $[Cu^{I}(TPMA)]^{+}$ cations were bridged by a single bromide anion, creating two pseudo-pentacoordinated moieties each with a distorted tetrahedral geometry. The remaining charge was balanced by a non-coordinating BPh_4^{-} anion. The two sides of the large cation were quite similar and the pyridyl rings of TPMA were arranged in a pseudo staggered conformation to minimize steric hindrance partially imposed by the Cu1-Br-Cu2 angle (117.46(1)^{o}). The average Cu1-N_{am} bond in **3** was determined to be 2.424(2) Å, which was in good agreement with previously isolated $Cu^{I}(TPMA)Cl$[23] and $Cu^{I}(TPMA)Br$[1] complexes. Similarly, the average Cu1-N_{py} bonds ranged from 2.062(2) to 2.112(2) Å. The Cu-Br bond lengths in **3** (2.5228(4) and 2.5564(4) Å) were slightly longer when compared to $[Cu^{I}(TPMA)Br]$ (2.5088(3) Å), which was presumably a result of the bridging of two Cu^{I} centers. Distorted tetrahedral geometry of Cu1 and Cu2 atoms in $[(Cu^{I}(TPMA)_2\text{-}\mu\text{-}Br]^{+}$ cation was further evident by relatively large displacement from the LSP derived from pyridine nitrogen atoms (0.537(6) and 0.499(6) Å, respectively). Lastly, the crystal

structure of **3** was stabilized by a series of weak C-H---C (2.814(6)-2.887(6) Å) and dipole N---H-C (2.643(6) Å) interactions (Appendix E).

A very different structure was observed when $[Cu^{I}(CH_3CN)_4][ClO_4]$ was reacted with 1 eq. of TPMA in methanol. Instead of a long cuprophilic interaction between two monomeric $[Cu^{I}(TPMA)]^{+}$ cations, the dimer $[Cu^{I}(TPMA)]_2[ClO_4]_2*CH_3OH$ (**4**) was isolated in the solid state. Presumably, copper(I)/TPMA complex rearranged into a dimer via pyridyl arm dissociation and coordination to a second copper(I) center, and vice versa (Figure 6.2.4). Based on a Cambridge Crystallographic Database search, only one other complex with a structurally similar 6-Ph-TPMA (1-(6-phenylpyridin-2-yl)-*N*,*N*-bis(pyridin-2-ylmethyl)methanamine) ligand and PF_6^- counter-ion has been reported.[49]

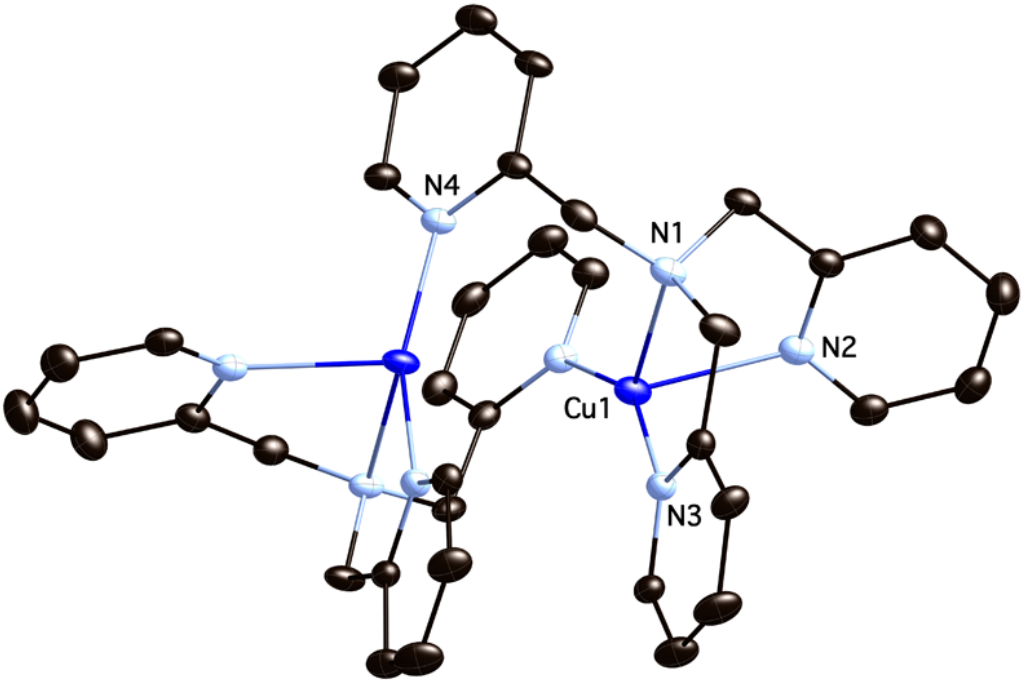

Figure 6.2.4. Molecular structure of $[Cu^{I}(TPMA)]_2[ClO_4]_2$ (**4**) at 150K, shown with 50% probability displacement ellipsoids. H-atoms, counter anions, and solvent molecules have been omitted for clarity. Selected distances [Å] and angles [°]: Cu1-N1 2.2590(13), Cu1-N2 1.9909(12), Cu1-N3 2.2213(16), Cu1-N4 1.9593(13), N1-Cu1-N2 81.87(5), N1-Cu1-N3 75.63(5), N1-Cu1-N4 123.01(5), N2-Cu1-N3 95.25(5), N2-Cu1-N4 150.49(6), N3-Cu1-N4 105.68(6).

Each copper(I) center in **4** was coordinated to four nitrogen atoms with bond lengths of 2.2590(13), 1.9909(12), 2.2213(16), and 1.9593(13) Å, respectively. The bond angles between the copper(I) center and N2, N3, and N4 atoms (75.63(5)^o, 81.87(5)^o, and 95.25(5)^o, respectively) indicated distortions from ideal tetrahedral geometry. Furthermore, the larger angles in this complex were associated with the bridging pyridine N4 atom (N3-Cu1-N4 105.68(6)^o, N1-Cu1-N4 123.01(5)^o, and N2-Cu1-N4 150.49(6)^o). The molecular structure of $[Cu^I(TPMA)]_2[ClO_4]_2*CH_3OH$ was stabilized by weak C-H---C contacts between TPMA ligands with distances ranging from 2.806(6) to 2.994(6) Å. Additionally, weak Cl-O---H-C and Cl-O---H-O interactions were detected between ClO_4^- counter-ion and TPMA ligand (2.562(6)-2.627(6) Å), and ClO_4^- and CH_3OH solvate (2.403(6)-2.678(6) Å) (Appendix E).

While changing the anion in copper(I) complexes with the TPMA ligand has produced a wide variety of molecular structures with different degrees of steric hindrance around the copper(I) center, preliminary studies have indicated that such variations had small effect on the reaction rate in ATRA containing free radical diazo initiators as reducing agents. Recent kinetic studies of this process revealed that the rate of alkene consumption was dependent on the concentration and rate of decomposition of the radical initiator, but independent on the concentration of the copper catalyst.[22, 32, 50] Therefore, more precise kinetic data could be provided by careful measurements of the activation ($Cu^I+RX \rightarrow Cu^{II}X+R\cdot$) and deactivation ($Cu^{II}X+R\cdot \rightarrow Cu^I+RX$) rate constants, which are currently being conducted in our laboratories. If the activation in ATRA catalyzed by copper(I)/TPMA complexes is proceeding via an inner sphere electron transfer and does not increase in the presence of non-coordinating anions, then it is possible that arm

dissociation from TPMA could create an open coordination site necessary for the homolytic cleavage of the carbon-halide bond. By coordinating ligands of different steric bulk to $[Cu^{I}(TPMA)][BPh_4]$ (**2**), this possibility could be structurally examined. The bidentate bridging ligand 4,4'-dipyridyl (4,4'-dipy) was added to complex **2** as a slightly larger alternative to acetonitrile. Several equivalents of the ligand were used to obtain X-ray quality crystals and two complexes were identified in the unit cell, the bridged $[(Cu^{I}(TPMA)_2(4,4'\text{-dipy})][BPh_4]$ (**5**) (Figure 6.2.5) and $[Cu^{I}(TPMA)(4,4'\text{-dipy})][BPh_4]$ (**6**) (Figure 6.2.6). The coordination of 4,4'-dipyridyl sterically forced dissociation of one arm of TPMA ligand in both cases, resulting in a distorted tetrahedral geometry. The N_{am}-Cu1-$N_{4,4'\text{-dipy}}$ bond angle was more skewed in complex **6** (141.14(9)^{o}) which resulted in displacement of N9 pyridyl nitrogen atom further away from copper(I) center (Cu1-

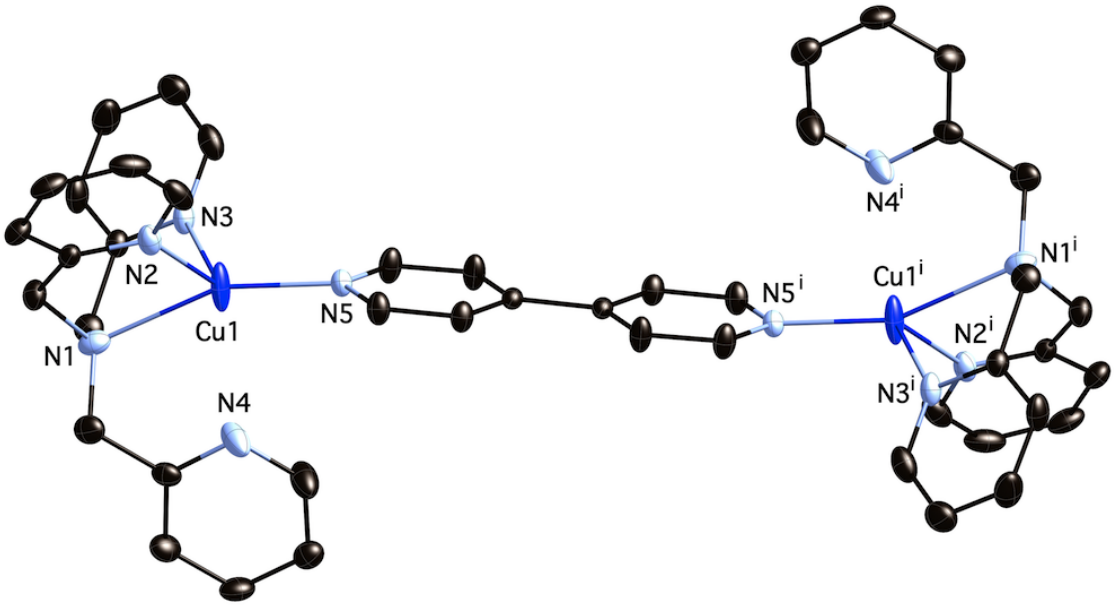

Figure 6.2.5. Molecular structure of $[(Cu^{I}(TPMA))_2dipy][BPh_4]_2$ (**5**) at 150K, shown with 50% probability displacement ellipsoids. H-atoms and counter anions have been omitted for clarity. Selected distances [Å] and angles [^{o}]: Cu1-N1 2.325(3), Cu1-N2 2.052(3), Cu1-N3 2.085(2), Cu1---N4 2.523(6), Cu1-N5 1.998(2), N1-Cu1-N2 78.59(9), N1-Cu1-N3 77.53(9), N1-Cu1-N5 157.08(9), N2-Cu1-N3 102.06(9), N2-Cu1-N5 118.82(9), N3-Cu1-N5 110.33(9).

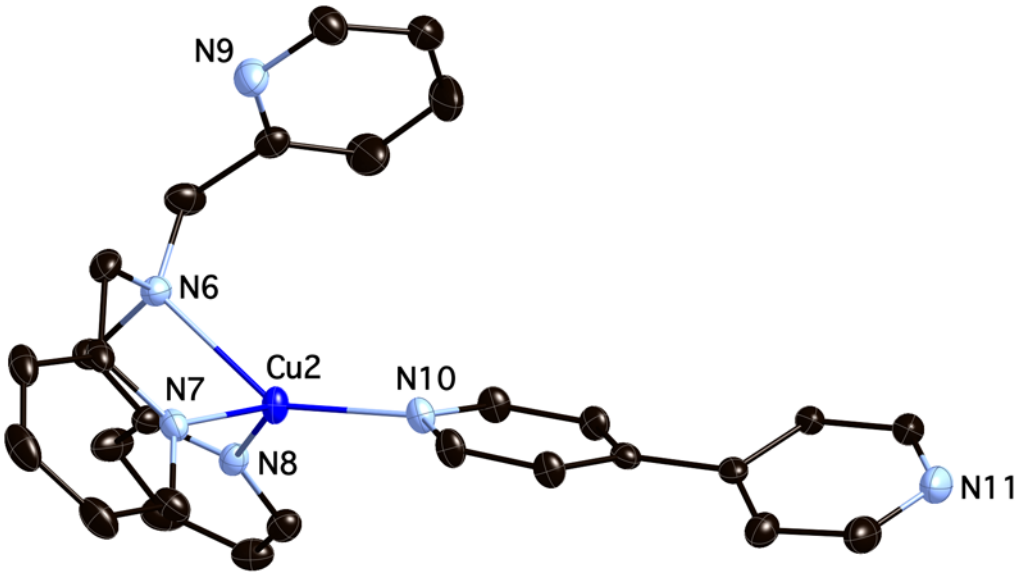

Figure 6.2.6. Molecular structure of [Cu^{I}(TPMA)dipy][BPh_4] (**6**) at 150K, shown with 50% probability displacement ellipsoids. H-atoms and counter anions have been omitted for clarity. Selected distances [Å] and angles [^{o}]: Cu2-N6 2.248(2), Cu2-N7 2.065(2), Cu2-N8 2.043(2), Cu2-N10 1.970(2), N6-Cu2-N7 78.60(9), N6-Cu2-N8 80.75(9), N6-Cu2-N10 141.14(9), N7-Cu2-N8 116.98(9), N7-Cu2-N10 118.09(9), N8-Cu2-N10 115.09(9).

N9=4.360(6) Å), in contrast to complex **5** (157.08(9)^{o}) where the ousted nitrogen atom appeared to be weakly interacting with copper (Cu1-N4=2.523(6) Å). In addition, the alkyl amine-copper bond was also shorter in **6** (Cu2-N6=2.248(2) Å) than in **5** (Cu1-N1=2.325(3) Å). In both complexes, the remaining copper-pyridyl nitrogen bonds from TPMA ligand were relatively unchanged (2.052(3) and 2.085(2) Å for **5**; 2.065(2) and 2.043(2) Å for **6**), and the distance to 4,4'-dipyridyl was also similar (1.998(2) and 1.970(2) Å, respectively). Furthermore, coordinated 4,4'-dipyridyl was found to be planar in complex **5**, and slightly twisted in **6** with a torsion angle of 24.76(6)^{o}. The free 4,4'-dipyridyl molecule found in the structure served to stabilize the crystal packing via weak N···H-C dipole interactions at 2.707(6) Å (Appendix E). Additionally, the non-coordinating N11 in **6** was found to weakly interact with the copper atom of adjacent

molecule at the distance of 3.438(6) Å, which could explain the non-planarity of 4,4'-dipyridyl discussed above. It is also interesting to note that both **5** and **6** appear to be much more air stable than the corresponding copper(I) complexes with halide anions and/or acetonitrile.

To study the outcome of larger monodentate ligand complexation to $[Cu^{I}(TPMA)][BPh_4]$, triphenylphosphine (PPh_3) was used to synthesize $[Cu^{I}(TPMA)(PPh_3)][BPh_4]$ (**7**). The coordination of PPh_3 had even larger effect on arm dissociation of TPMA ligand than 4,4'-dipyridyl, displacing the N4 pyridyl atom by

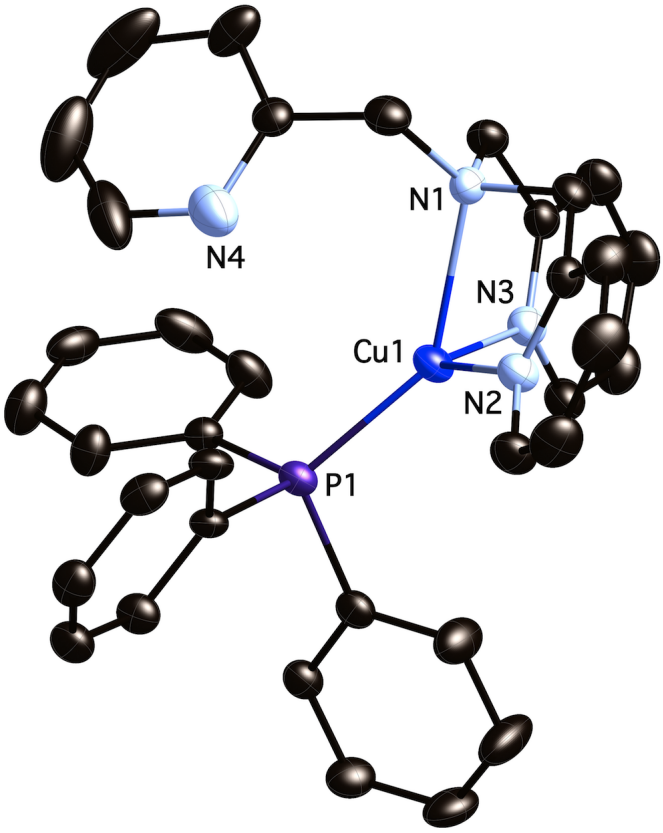

Figure 6.2.7. Molecular structure of $[Cu^{I}(TPMA)PPh_3][BPh_4]$ (**7**) at 150K, shown with 50% probability displacement ellipsoids. H-atoms and counter anions have been omitted for clarity. Selected distances [Å] and angles [°]: Cu1-N1 2.214(3), Cu1-N2 2.073(3), Cu1-N3 2.114(3), Cu1-P1 2.1853(12), N1-Cu1-N2 80.81(12), N1-Cu1-N3 78.63(13), N2-Cu1-N3 117.13(13), N1-Cu1-P1 141.65(9), P1-Cu1-N2 119.74(10), P1-Cu1-N3 112.79(10).

3.258(6) Å (Figure 6.2.7). As a result, complex **7** was distorted tetrahedral in geometry and the complexation to copper(I) center occurred through the aliphatic (Cu1-N1=2.2089(14) Å) and two pyridine (Cu1-N2=2.0661(14) Å and Cu1-N3=2.1083(15) Å) nitrogen atoms of TPMA, and phosphorous atom from PPh_3 (Cu1-P1=2.1852(5) Å). The structural features of **7** were similar to $[Cu^I(TPMA)(PPh_3)][PF_6]$, with the exception that in the latter complex the nitrogen atom from the displaced arm in TPMA was pointing away from copper (Cu-N=6.530(2) Å).[13] This could be attributed to much smaller N1-Cu1-P1 bond angle (127.8^o) when compared to **7** (141.78(4)^o). Nevertheless, the Cu-N4 bond distance in **7** (3.258(6) Å) was longer than the sum of Van der Waals radii (2.95 Å), indicating negligible interactions between the displaced pyridyl nitrogen atom and copper. Intermolecular interactions observed in the unit cell included only weak C-H---C contacts ranging from 2.809 to 2.850(6) Å (Appendix E).

The auxiliary ligands used in the above discussed complexes (acetonitrile, 4,4'-dipyridyl, and triphenylphosphine) are all strong σ-donors, but vary drastically in terms of steric bulk. Therefore, these monodentate ligands should have different effects on

Table 6.2.2. Structural comparison of complexes 1, 5, 6, and 7 with the general formula $[Cu^I(TPMA)L][BPh_4]$ (L= CH_3CN, 4,4'-dipyridyl, or PPh_3). Selected bond lengths are given in angstroms (Å) and the cone angle in degrees (^{o}).

Complex	**1**	**5**	**6**	**7**
L_{aux}	*CH_3CN*	*4,4-dipy*	*4,4'-dipy*	*PPh_3*
Cu-N_{am}	2.4109(10)	2.325(3)	2.248(2)	2.214(3)
Cu-$N_{py,1}$	2.1031(10)	2.052(3)	2.065(2)	2.073(3)
Cu-$N_{py,2}$	2.1114(11)	2.085(2)	2.053(2)	2.114(3)
Cu-$N_{py,3}$	2.0624(10)	2.523(6)	4.360(5)	3.327(6)
Cu-L_{aux}	1.9914(11)	1.998(2)	1.970(2)	2.1853(12)
N_{am}-Cu-L_{aux}	175.94(4)	157.08(9)	141.14(9)	141.65(9)
Cone angle[a]	37.8	86.5	87.4	138.8

[a]Cone angle was calculated for the auxiliary ligand.

TPMA coordination in copper(I) complexes. In order to quantitatively assess the steric bulk of each ligand, cone angles[51] were calculated from the molecular structures using a previously reported method.[52] As indicated in Table 6.2.2, acetonitrile in complex **1** was found to have a cone angle of 37.80^{o}, which did not result in arm dissociation of the TPMA ligand. However, the larger 4,4'dipyridyl, with a cone angle of 86.46^{o} in **5** and 87.26^{o} in **6**, displaced one of the pyridine rings in TPMA by 3.824 and 4.305 Å, respectively (the distance was calculated between the copper(I) atom and centroid point derived from nitrogen and carbon atoms in the pyridine ring). The effect was also observed for triphenylphosphine (cone angle=141.72^{o}) in complex **7**, in which the same distance was determined to be 4.217 Å. Although there appears to be no direct correlation between the cone angle and pyridine ring displacement from the copper(I) center, it is apparent that the latter does to some extend depend on the steric bulk of the auxiliary ligand. Studies on the effect of these monodentate ligands on catalytic activity in ATRA are currently underway in our laboratories.

6.3 Solution Studies of Copper(I) Complexes

Variable temperature ^{1}H NMR spectroscopy was used to probe structures of copper(I) complexes with TPMA ligand in solution. This technique was previously shown to be useful in examining the structure of Cu^{I}(TPMA)Br,[1] which was found to be highly symmetrical and monomeric in solution, as indicated by chemically equivalent pyridine rings (Figure 6.3.1.a). A very similar ^{1}H NMR spectrum was also observed for [Cu^{I}(TPMA)(CH_3CN)][BPh_4] (**1**) (Appendix E). In **1**, a singlet for acetonitrile was shifted downfield by approximately 1.6 ppm in acetone-d_6 upon cooling from 298 K to

180 K, indicating a deshielding effect as a result of coordination. On the other hand, $[Cu^{I}(TPMA)]_2[ClO_4]*CH_3OH$ (**4**), exhibited four broad resonances at room temperature similar to $Cu^{I}(TPMA)Br$, suggesting the structure was also monomeric (Figure 6.3.1.b). Interestingly, upon cooling to 185K, evidence for dimer formation consistent with the

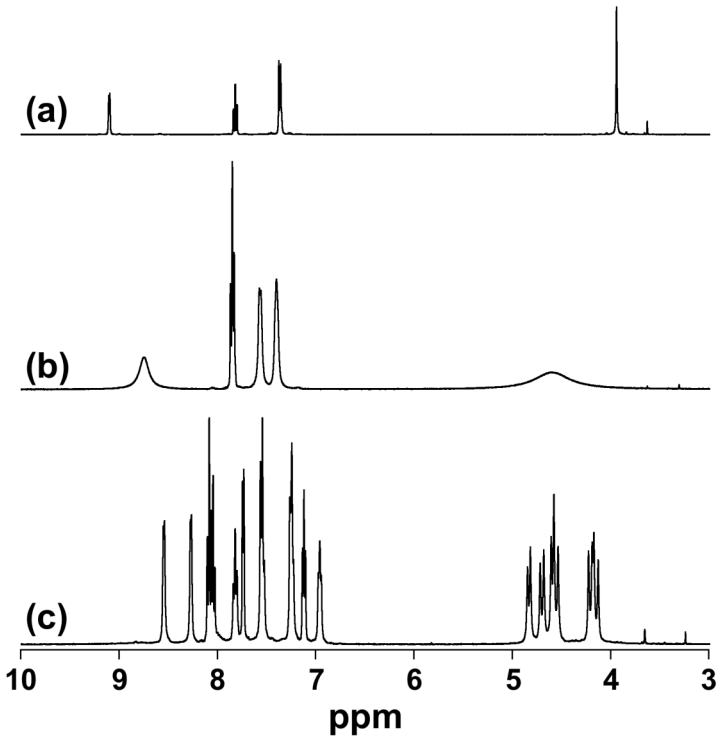

Figure 6.3.1. ^1H NMR spectra (400 MHz, $(CD_3)_2CO$) of $[Cu^{I}(TPMA)Br]$ at 180K (a), $[Cu^{I}(TPMA)][ClO_4]$ at 298K (b), and $[Cu^{I}(TPMA)]_2[ClO_4]_2$ at 185K (c).

solid state structure was clearly observed by the emergence of three sets of unequal peaks between 8.54 and 6.95 ppm for the pyridyl and 4.82 and 4.17 ppm for the methylene protons (Figure 6.3.1.c). When the same complex was dissolved in acetonitrile-d_3, only peaks corresponding to the monomer were observed, indicating the formation of $[Cu^{I}(TPMA)(CD_3CN)][ClO_4]$. Similarly, at room temperature $[Cu^{I}(TPMA)][BPh_4]$ (**2**) also exhibited a monomeric structure resembling **1**. However, upon cooling to 180K, the peaks associated with the dimer formation clearly emerged in relatively equal proportions

relative to the monomer. Therefore, it is likely that an equilibrium between the monomer and dimer exists in solution for complex **2** as shown in Scheme 6.3.1.

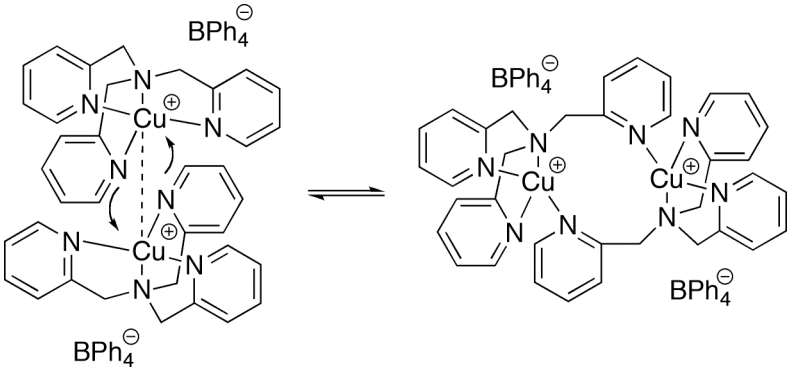

Scheme 6.3.1. Equilibrium between monomeric [Cu(TPMA)][BPh_4] and dimeric [Cu(TPMA)]$_2$[BPh_4]$_2$ in the absence of a coordinating solvent.

The ^{1}H NMR spectrum for [(Cu^I(TPMA)$_2$-μ-Br][BPh_4] (**3**) showed five peaks for TPMA at 9.17, 7.78, 7.40, 7.08, and 4.03 ppm (Appendix E). This suggested that the complex had highly symmetrical structure in solution, which was inconsistent with the solid state in which two [Cu^I(TPMA)]$^+$ cations were bridged by bromide anion at an angle of 117.46(1)^o. We ruled out the possibility for dissociation because it would have

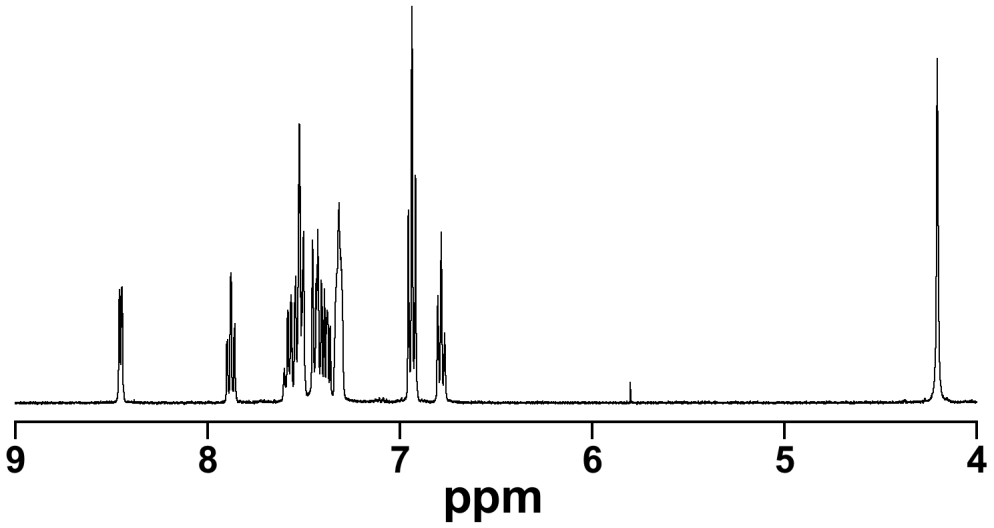

Figure 6.3.2. ^{1}H NMR (400 MHz, 180K, $(CD_3)_2CO$) spectrum of [Cu^I(TPMA)PPh_3][BPh_4] (**7**).

resulted in the formation of Cu^{I}(TPMA)Br, [Cu^{I}(TPMA)][BPh_4] and [Cu^{I}(TPMA)]$_2$[BPh_4]$_2$, which was not observed experimentally using low temperature ^{1}H NMR studies. Similarly to **1** and **3**, [Cu^{I}(TPMA)(PPh_3)][BPh_4] (**7**) also showed five resonances for TPMA ligand, indicating that in solution all three pyridyl arms were symmetrically coordinated to the copper(I) center (Figure 6.3.2). However, the chemical shift of the proton in close proximity to the pyridyl nitrogen showed a significant upfield shift (8.46 ppm), in contrast to **1** (8.65 ppm) or Cu^{I}(TPMA)Br (9.10 ppm), which was presumably the result of σ-donation from the coordinated triphenylphosphine. This was also confirmed by ^{31}P{^{1}H} NMR which showed a downfield shift of 8.9 ppm relative to free phosphine.

6.4 Solid-State Structural Studies of Copper(II) Complexes

ATRA is commonly performed starting with the copper(II) complex or deactivator due to its oxidative stability. When such a complex is reduced in the presence of radicals generated by the decomposition of initiator such as AIBN, the copper(I) or activator is formed which starts the catalytic cycle by homolytically cleaving an alkyl halide bond. In order to investigate the counter-ion effect on the structure of copper(II) complexes with TPMA ligand [Cu^{II}(TPMA)Cl][ClO_4] (**8**), [Cu^{II}(TPMA)Cl][BPh_4] (**9**), [Cu^{II}(TPMA)Br][ClO_4] (**10**), and [Cu^{II}(TPMA)Br][BPh_4] (**11**) where synthesized by salt methathesis of previously reported [Cu^{II}(TPMA)X][X] (X=Br^- or Cl^-) complexes.[1, 23] Although **8** and **9** were crystallographically quite different from [Cu^{II}(TPMA)Cl][Cl],

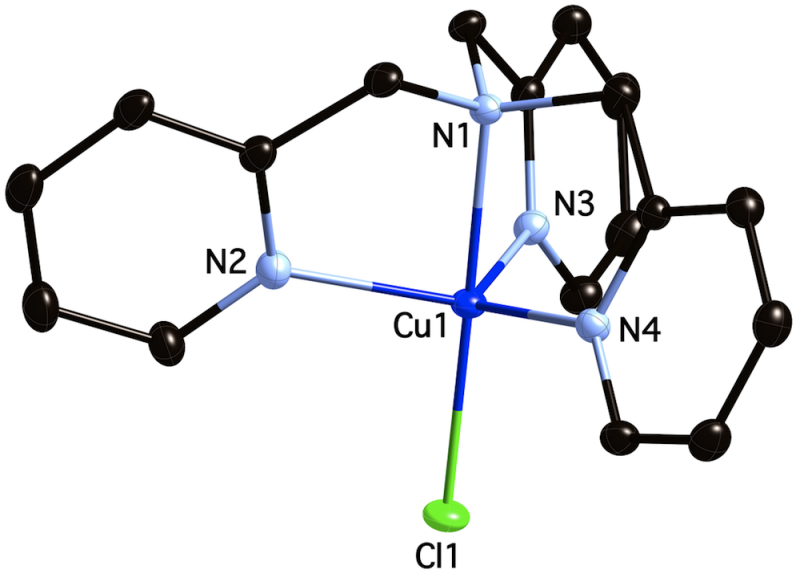

Figure 6.4.1. Molecular structure of $[Cu^{II}(TPMA)Cl][ClO_4]$ (**8**) at 150K, shown with 50% probability displacement ellipsoids. H-atoms and counter anion have been omitted for clarity.

Table 6.4.1. Structural comparison of $[Cu^{II}(TPMA)Cl[A]$ complexes (A=Cl^-, ClO_4^- (**8**) and BPh_4^- (**9**). Bond lengths are given in angstroms (Å) and angles in degrees (^{o}).

	$[Cu^{II}(TPMA)Cl][Cl]^a$	**8**^{b}	**9**^{b}
Cu1-N1$_{ax}$	2.0481(14)	2.0413(15)	2.0550(9)
Cu1-N2$_{eq}$	2.0759(8)	2.1115(16)	2.0870(11)
Cu1-N3$_{eq}$	2.0759(8)	2.0567(16)	2.0512(10)
Cu1-N4$_{eq}$	2.0759(8)	2.0292(16)	2.0312(11)
Cu1-N$_{eq,av.}$^{c}	2.0759(8)	2.0658(28)	2.0564(18)
Cu1-Cl1	2.2369(4)	2.2390(5)	2.2333(3)
N1-Cu1-N2	80.71(2)	81.05(7)	80.88(4)
N1-Cu1-N3	80.71(2)	80.63(6)	82.38(4)
N1-Cu1-N4	80.71(2)	81.97(6)	81.56(4)
N2-Cu1-N3	117.447(12)	108.44(6)	110.43(4)
N3-Cu1-N4	117.447(12)	126.20(6)	127.53(4)
N4-Cu1-N2	117.447(12)	118.43(6)	115.71(4)
Cl1-Cu1-N2	99.29(2)	99.23(5)	99.47(3)
Cl1-Cu1-N3	99.29(2)	99.88(5)	97.26(3)
Cl1-Cu1-N4	99.29(2)	97.33(5)	98.49(3)
Cl1-Cu1-N1	180.000(19)	179.29(5)	179.58(3)

^{a}Ref. 23. ^{b}This work. Values for complex **8** are averaged from two molecules in the asymmetric unit. ^{c}Average Cu-N equatorial bond length.

the $[Cu^{II}(TPMA)Cl]^+$ cations were nearly identical in both cases (Table 6.4.1). Each copper(II) cation in **8** and **9** was distorted trigonal bipyramidal in geometry, as a result of coordination of four nitrogen atoms from TPMA ligand and one chlorine atom. (Figure 6.4.1). The Cu^{II}-Cl bonds in **8** (2.2390(5) Å) and **9** (2.2341(3) Å) were very similar to the corresponding chloride complex (2.2369(4) Å). Furthermore, the copper(II) atom in complexes **8** and **9** was displaced from the LSP derived from nitrogen atoms in pyridine rings by 0.317(6) (averaged) and 0.299(6) Å respectively, which also compared well with $[Cu^{II}(TPMA)Cl][Cl]$ (0.335(6) Å). Complexes **8** and **9** lacked perfect crystallographic 3-fold symmetry with respect to Cu-Cl or Cu-N_{am} vector observed in $[Cu^{II}(TPMA)Cl][Cl]$, which was presumably due to the presence of more bulky ClO_4^- and BPh_4^- counter-ions. However, the cations in each case had nearly perfect (non-crystallographic) C_3 symmetry. The intermolecular interactions in **8** consisted mostly of O···H-C dipole interactions between the perchlorate counter-ion and the TPMA ligand, which ranged from 2.396(6) to 2.694(6) Å. Weak Cl---H-C attractions between the coordinated chloride and the TPMA ligand in the adjacent molecule were also observed ranging from 2.793(6) to 2.860(6) Å (Appendix E). On the other hand, the crystal structure of complex **9** was stabilized by weak C-H---C contacts involving the anion, TPMA, and a solvent acetonitrile with distances ranging from 2.669(6) to 2.884(6) Å. Lastly, two Cl---H-C interactions were also detected between the chlorine atom and TPMA with distances of 2.857(6) and 2.840(6) Å, respectively (Appendix E).

The corresponding bromide complexes, $[Cu^{II}(TPMA)Br][ClO_4]$ (**10**) and $[Cu^{II}(TPMA)Br][BPh_4]$ (**11**), were found to be structurally similar to the chlorides **8**, **9**, and $[Cu^{II}(TPMA)Cl][Cl]$ discussed above (Figure 6.4.2). The cations lacked perfect

crystallographic 3-fold symmetry observed in [Cu^{II}(TPMA)Br][Br],[1] but pyridine rings in coordinated TPMA ligand were nearly symmetrical with respect to C_3 rotation. From the point of view of TPMA coordination, these complexes were also comparable to

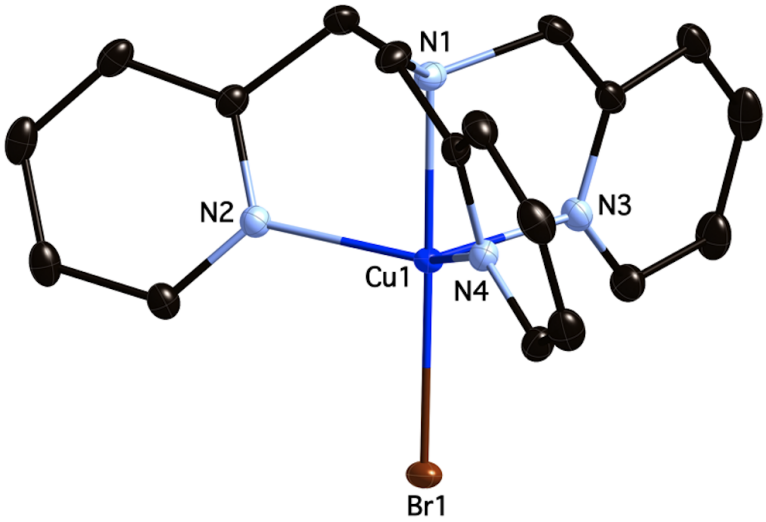

Figure 6.4.2. Molecular structure of [Cu^{II}(TPMA)Br][ClO_4] (**10**) at 150K, shown with 50% probability displacement ellipsoids. H-atoms and counter anion have been omitted for clarity.

previously discussed **8** and **9**. While the typical Cu^{II}-Cl bond length in **8** and **9** was close to 2.23 Å, the Cu^{II}-Br bond distance in **10** and **11** was found to be longer as a result of the larger atomic radii of bromine atom (2.3765(3) and 2.3711(2) Å, respectively). The copper(II) atom was displaced from the LSP by 0.330(6) (averaged) in complex **10** and 0.299(6) Å in **11**, which compared well with the bromide complex (0.329(6) Å) (Table 6.4.2). No other significant differences in the structures were observed.

Additionally, intermolecular interactions in **10** and **11** were found to closely resemble **8** and **9**. The crystal structure of **10** was stabilized be predominately strong C-H---O dipole forces at distances ranging from 2.429(6) to 2.620(6) Å, and two weaker C-

H---Br dipole contacts (2.963(6)-2.987(6)) Å. Furthermore, one van der Waals C-H---C interaction between coordinated TPMA ligands was found to exist at 2.875(6) Å (see supporting information). In the crystal structure of **11**, weak C-H---C contacts ranging

Table 6.4.2. Selected bond lengths [Å] and angles [°] for [Cu^{II}(TPMA)Br][A] (A=Br, ClO_4^- (10) and BPh_4^- (11)) complexes.

Complex	**[Cu^{II}(TPMA)Br][Br]**[a]	**10**[b]	**11**[b]
Cu1-$N1_{ax}$	2.040(3)	2.0387(17)	2.0534(11)
Cu1-$N2_{eq}$	2.073(2)	2.0642(18)	2.0545(12)
Cu1-$N3_{eq}$	2.073(2)	2.0515(17)	2.0328(12)
Cu1-$N4_{eq}$	2.073(2)	2.1163(18)	2.0909(12)
Cu1-$N_{eq,av.}$[c]	2.073(2)	2.0773(31)	2.0594(21)
Cu1-Br1	2.3836(6)	2.3765(3)	2.3711(2)
N1-Cu1-N2	80.86(5)	80.36 (7)	82.32(5)
N1-Cu1-N3	80.86(5)	81.44(7)	81.55(5)
N1-Cu1-N4	80.86(5)	81.03(7)	80.98(5)
N2-Cu1-N3	117.53(3)	124.95(7)	128.21(5)
N3-Cu1-N4	117.53(3)	117.89(7)	115.28(5)
N4-Cu1-N2	117.53(3)	109.80(7)	110.17(5)
Br1-Cu1-N2	99.14(5)	100.44(5)	97.55(3)
Br1-Cu1-N3	99.14(5)	97.76(5)	98.68(3)
Br1-Cu1-N4	99.14(5)	99.03(5)	98.89(4)
Br1-Cu1-N1	180.00(5)	179.11(5)	179.77(3)

[a]Ref. 1. [b]This work. Values for complex **10** are averaged for two molecules in the asymmetric unit. [c]Average Cu-N equatorial bond length.

from 2.703(6) to 2.892(6) Å, as well as weak C-H---Br dipole interactions at 2.951(6) and 2.921(6) were observed Å (Appendix E).

In solution, **8**, **9**, **10**, and **11** were found to have similar UV-Vis spectra (λ_{max}≈960 nm, ε_{max}≈190 $Lmol^{-1}cm^{-1}$), indicating negligible interactions of anions with the copper(II) centers, consistent with the solid state studies discussed above.

6.5 Conclusions

In conclusion, the effects of counter-ions (Cl^-, Br^-, ClO_4^-, and BPh_4^-) and auxiliary ligands (Cl^-, Br^-, CH_3CN, 4,4'-dipyridyl, and PPh_3) on the structures of copper(I) and copper(II) complexes with TPMA ligand were investigated. Copper(I)/TPMA complexes with Br^- and CH_3CN were found to be distorted tetrahedral in geometry and each copper(I) center was coordinated by an auxiliary monodentate ligand and three nitrogen atoms from pyridyl rings. In these complexes, the axial elongation of Cu^I-N_{am} bond (~2.4 Å) was observed, indicating not only the rigidity of TPMA ligand, but also the strong preference for copper(I) to adopt four coordinated geometry. In the absence of monodentate ligand, two structures were observed. A monomeric trigonal pyramidal $[Cu^I(TPMA)][BPh_4]$ complex was characterized in the solid state, which was stabilized by a weak cuprophilic interaction (2.8323(12) Å). On the other hand, $[Cu^I(TPMA)]_2[ClO_4]_2$ was found to be dimeric in which dissociated pyridyl arms of TPMA ligand bridged two copper(I) centers. In copper(I) complexes containing larger auxiliary ligands such as 4,4'-dipyridyl or PPh_3, a pyridyl arm of TPMA ligand was found to partially or totally dissociate. These complexes were all monomeric in the solid state, with the exception of $[(Cu^I(TPMA))_2(4,4'\text{-dipy})][BPh_4]_2$ in which 4,4'-dipyridyl ligand bridged two $[Cu^I(TPMA)]^+$ cations.

Copper(II) complexes with the general formula $[Cu^{II}(TPMA)X][Y]$ ($X=Cl^-$, Br^- and $Y=ClO_4^-$, BPh_4^-) were synthesized and characterized in the solid state in order to investigate the counter-ion effect on the structure of $[Cu^{II}(TPMA)X]^+$. In each complex, the copper(II) atom was found to be distorted trigonal bipyramidal in geometry with

nearly perfect C_3 symmetry for coordinated TPMA ligand. The average Cu^{II}-N bond distances were found to range between 2.03 and 2.12 Å, consistent with previous studies.

6.6 Experimental Part

General Procedures - All chemicals were purchased from commercial sources and used as received. Tris(2-pyridylmethyl)amine (TPMA)[53] and $[Cu^{I}(CH_3CN)_4][ClO_4]$[54] were synthesized according to literature procedures. Although we have experienced no problems, perchlorate metal salts are potentially explosive and should be handled with care. All manipulations involving copper(I) complexes were performed under argon atmosphere in the dry box (<1.0 ppm O_2 and <0.5 ppm H_2O), or using standard Schlenk line techniques. Solvents (pentane, acetonitrile, acetone, and diethyl ether) were degassed and deoxygenated using an Innovative Technology solvent purifier. Methanol was vacuum distilled and deoxygenated by bubbling argon for 30 min prior to use. Synthesis of copper(II) complexes were performed in ambient conditions and solvents were used as received. ^{1}H NMR spectra were obtained using Bruker Avance 400 and 500 MHz spectrometers and chemical shifts are given in ppm relative to residual solvent peaks ($CDCl_3$ δ7.26 ppm; $(CD_3)_2CO$ δ2.05 ppm; CD_3CN δ1.96 ppm). ^{31}P NMR was referenced externally with 85% H_3PO_4 in D_2O at δ0. iNMR software and Kaleidagraph was used to generate images of NMR spectra. Temperature calibrations were performed using a pure methanol sample. IR spectra were recorded in the solid state using Nicolet Smart Orbit 380 FT-IR spectrometer (Thermo Electron Corporation). Elemental analyses for C, H, and N were obtained from Midwest Microlabs, LLC.

X-ray Crystal Structure Determination - The X-ray intensity data were collected at 150K using graphite-monochromated Mo-K radiation (0.71073 Å) with a Bruker Smart Apex II CCD diffractometer. Data reduction included absorption corrections by the multi-scan method using SADABS.[55] Structures were solved by direct methods and refined by full matrix least squares using SHELXTL 6.1 bundled software package.[56] The H-atoms were positioned geometrically (aromatic C-H 0.93, methylene C-H 0.97, and methyl C-H 0.96) and treated as riding atoms during subsequent refinement, with U_{iso}(H) = 1.2U_{eq}(C) or 1.5U_{eq}(methyl C). The methyl groups were allowed to rotate about their local threefold axes. ORTEP-3 for windows[57] and Crystal Maker 7.2 were used to generate molecular graphics.

[Cu^{I}(TPMA)(CH_3CN)][BPh_4] (1) - TPMA (89.0 mg, 0.306 mmol) was dissolved in 2 mL of methanol followed by addition of [$Cu^{I}(CH_3CN)_4$][ClO_4] (100 mg, 0.306 mmol), resulting in a yellow solution. $NaBPh_4$ (105 mg, 0.306 mmol) was then added to the reaction mixture, which resulted in immediate precipitation of a yellow powder. The crude product was filtered, thoroughly washed with methanol, and re-dissolved in acetonitrile, resulting in a red solution. [Cu^{I}(TPMA)(CH_3CN)][BPh_4] was precipitated as an orange powder by slow addition of diethyl ether (yield =137 mg, 62%). X-ray quality crystals were obtained by crystallization in acetonitrile via slow diffusion of diethyl ether. ^{1}H NMR ($(CD_3)_2CO$, 400 MHz, 180K): δ9.17 (d, J = 4.7 Hz, 3H), δ7.77 (td, J = 7.6, 1.5 Hz, 3H), δ7.39 (d, J = 7.8 Hz, 4H), δ7.30 (m, 4H), δ7.10 (m, 3H), δ6.92 (t, J = 7.3 Hz, 4H), δ6.76 (t, J = 7.2 Hz, 2H), δ4.03 (s, 6H), δ 3.54 (s, 3H). FT-IR (solid): ν (cm^{-1})= 3058 (m), 1599 (m), 1573 (w), 1475 (m), 1434 (m), 1367 (w), 1269 (w), 1153

(w), 1051 (w), 974 (w), 841 (w), 764 (m), 746 (m), 733 (s), 704 (s), 611 (s). Anal. Calcd. for $C_{44}H_{41}N_5CuB$ (714.17): C, 74.00; H, 5.79; N, 9.81. Found C, 73.89; H, 6.01; N, 9.67.

[Cu^I(TPMA)][BPh$_4$] (2) - TPMA (89.0 mg, 0.306 mmol) was dissolved in 2 mL of methanol followed by addition of [Cu^I(CH$_3$CN)$_4$][ClO$_4$] (100 mg, 0.306 mmol), resulting in a yellow solution. NaBPh$_4$ (105 mg, 0.306 mmol) was then added to the reaction mixture which resulted in immediate precipitation of a yellow powder. The crude product was washed thoroughly with methanol to yield 156 mg (76%) of [Cu^I(TPMA)][BPh$_4$]. Crystals suitable for X-ray diffraction were obtained in acetone via slow diffusion of diethyl ether. ^{1}H NMR ((CD$_3$)$_2$CO, 400 MHz, 298K): δ8.67 (s, 3H), δ7.82 (td, J = 7.7, 1.3 Hz, 3H), δ7.43 (d, J = 7.8 Hz, 3H), δ7.38-7.33 (m, 12H), δ6.92 (t, J = 7.4 Hz, 7H), δ6.77 (t, J = 7.2 Hz, 4H), δ4.15 (bs, 6H). FT-IR (solid): ν(cm^{-1}) = 3053(w), 2982(w), 1601(m), 1475(m), 1427(m), 1269(w), 1134(w), 1101(w), 762(m), 733(s), 702(s), 611(m), 501(w). Anal. Calcd. for $C_{42}H_{38}N_4CuB$ (673.14): C, 74.94; H, 5.69; N, 8.32. Found: C, 74.63; H, 5.66; N, 8.13.

[(Cu^I(TPMA))$_2$-μ-Br][BPh$_4$] (3) - Cu^I(TPMA)Br (100 mg, 0.231 mmol), previously synthesized according to published procedures,[1] was dissolved in 5 mL of methanol followed by addition of half an equivalent of NaBPh$_4$ (39.4 mg, 0.115 mmol). Although the precipitation of yellow powder occurred immediately, it quickly dissolved back into the reaction mixture, resulting in the formation of an orange solution. Upon slow addition of diethyl ether or THF, [(Cu^I(TPMA))$_2$-μ-Br][BPh$_4$] precipitated as a red-orange powder (yield = 81.0 mg, 32%). X-ray quality crystals were obtained in acetone

via slow diffusion of diethyl ether. ^{1}H NMR ($(CD_3)_2CO$, 400 MHz, 180K): δ9.17 (d, J = 3.8 Hz, 6H), δ7.78 (t, J = 7.4 Hz, 6H), δ7.40 (d, J = 7.7 Hz, 6H), δ7.31 (m, 8H), δ 7.08 (m, 6H), δ6.92 (m, 8H), δ6.76 (m, 4H), δ4.03 (bs, 12H). FT-IR (solid): ν (cm^{-1}) = 3051(w), 2982(w), 2885(w), 2843(w), 1597(m), 1566(w), 1473(m), 1427(m), 1365(w), 1315(w), 1150(m), 1049(m), 975(w), 894(w), 758(s), 725(s), 706(s), 613(m), 501(m). Anal Calcd. for $C_{60}H_{56}N_8Cu_2BrB$ (1106.95): C, 65.10; H, 5.10; N, 10.12. Found: C, 65.00; H, 5.19; N, 10.15.

*$[Cu^I(TPMA)]_2[ClO_4]_2$*CH_3OH (4)* - $[Cu^I(CH_3CN)_4][ClO_4]$ (50.0 mg, 0.153 mmol) and TPMA (44.4 mg, 0.153 mmol) were dissolved in 1.0 mL of methanol. The vial was then sealed and placed in the freezer for two days, after which yellow crystals suitable for X-ray analysis were obtained (yield = 48.0 mg, 35 %). ^{1}H NMR ($(CD_3)_2CO$, 400 MHz, 185K): δ8.54 (d, J=4.4 Hz, 2H), δ8.26 (d, J=4.4 Hz, 2H), δ8.06 (m, 4 H), δ7.81 (t, J=7.2, 2H), δ7.73 (d, J=5.2, 2H), δ7.54 (pt, J=7.6, 4H), δ7.24 (pt, J=2.6, 4H), δ7.11 (t, J=6.0, 2H), δ6.95 (t, J=6.0, 2H), δ4.82 (d, J=11.6, 2H), δ4.69 (d, J=14.4, 2H), δ4.57 (m, J=14.0, 4H), δ4.17 (dd, J=23.1, 16.2 Hz, 4H). FT-IR (solid): ν (cm^{-1}) = 3068 (w), 2881 (w), 2359 (w), 2159 (w), 1600 (m), 1547 (w), 1477 (m), 1435 (m), 1082 (s), 724 (m), 620 (m). Anal. Calcd. for $C_{36}H_{36}N_8Cu_2Cl_2O_8$ (906.72): C, 47.69; H, 4.00; N, 12.36. Found: C, 47.72; H, 4.29; N, 12.27.

$[(Cu^I(TPMA))_2(4,4'\text{-dipy})][BPh_4]_2$ (5) and $[Cu^I(TPMA)(4,4'\text{-dipy})][BPh_4]$ (6) - $[Cu^I(TPMA)][BPh_4]$ (135 mg, 0.201 mmol) was dissolved in 10.0 mL of acetone followed by addition of 5 equivalents of 4,4'-dipyridyl (156 mg, 1.00 mmol), which

resulted in a dark red solution. Crystals of X-ray quality were obtained in acetone by slow diffusion of diethyl ether, and contained both $[(Cu^{I}(TPMA))_2(4,4'\text{-dipy})][BPh_4]_2$ and $[Cu^{I}(TPMA)(4,4'\text{-dipy})][BPh_4]$ in the asymmetric unit.

$[Cu^{I}(TPMA)(PPh_3)][BPh_4]$ (7) - $[Cu^{I}(TPMA)][BPh_4]$ (100 mg, 0.149 mmol) was dissolved in 3.0 mL of acetone and PPh_3 (39.0 mg, 0.149 mmol) was added, which resulted in a light yellow solution. Crystallization occurred immediately, producing colorless crystals suitable for X-ray analysis (yield = 109 mg, 78%). ^{1}H NMR ($(CD_3)_2CO$, 400 MHz, 180K): δ8.46 (d, J = 4.4 Hz, 3H), δ7.88 (td, J = 7.7, 1.6 Hz, 3H), δ7.54 (m, 10H), δ7.39 (m, 11H), δ7.30 (m, 8H), δ6.92 (t, J = 7.4 Hz, 8H), δ6.76 (t, J = 7.1 Hz, 4H), δ4.17 (bs, 6H). ^{31}P NMR ($(CD_3)_2CO$, 162 MHz, 220K): δ 2.88. FT-IR (solid): ν (cm^{-1}) = 3051(w), 2997(w), 1581(w), 1477(m), 1434(m), 1265(w), 1095(w), 841(w), 733(s), 702(s), 609(m), 498(m). Anal. Calcd. for $C_{60}H_{53}BCuN_4P$ (935.42): C, 77.04; H, 5.71; N, 5.99. Found: C, 76.69; H, 5.70; N, 5.92.

$[Cu^{II}(TPMA)Cl][ClO_4]$ (8) - $[Cu^{II}(TPMA)Cl][Cl]$ (50.0 mg, 0.118 mmol), synthesized by previously reported methods,[23] was dissolved in 5.0 mL of methylene chloride and $NaClO_4$ (14.4 mg, 0.118 mmol) added. After stirring overnight, NaCl was filtered from the solution and blue powder precipitated by slow addition of pentane. $[Cu^{II}(TPMA)Cl][ClO_4]$ was collected by filtration and dried under vacuum (yield = 34.0 mg, 59 %). Crystals suitable for X-ray analysis were obtained in acetonitrile by slow diffusion of diethyl ether. FT-IR (solid): ν (cm^{-1}) = 3066(w), 2935(w), 1608(m), 1574(w), 1477(m), 1435(m), 1308(w), 1265(w), 1076(s), 764(m), 621(s). Anal. Calcd.

for $C_{18}H_{18}N_4CuCl_2O_4$ (488.81): C, 44.23; H, 3.71; N, 11.46. Found: C, 44.25; H, 3.76; N, 11.41.

*[Cu^{II}(TPMA)Cl][BPh$_4$]*CH$_3$CN (9)* - [Cu^{II}(TPMA)Cl][Cl] (50.0 mg, 0.118 mmol), synthesized by previously reported methods,[23] was dissolved in 3.0 mL of methanol followed by the addition of $NaBPh_4$ (40.3 mg, 0.118 mmol). Precipitation of a green powder occurred immediately. The crude product was washed with methanol, collected by filtration, and dried under vacuum to yield 64.5 mg (77%) of [Cu^{II}(TPMA)Cl][BPh$_4$]. Crystals of [Cu^{II}(TPMA)Cl][BPh$_4$]*CH$_3$CN suitable for X-ray analysis were obtained in acetonitrile by slow diffusion of diethyl ether. FT-IR (solid): ν (cm^{-1}) = 3054(w), 2989(w), 2931(w), 1605(m), 1574(w), 1477(m), 1427(m), 1261(m), 1022(m), 737(s), 710(s), 613(m), 505(w). Anal. Calcd. for $C_{44}H_{41}N_5CuClB$ (749.64): C, 70.50; H, 5.51; N, 9.34. Found: C, 70.35; H, 5.63; N, 9.36.

[Cu^{II}(TPMA)Br][ClO$_4$] (10) - [Cu^{II}(TPMA)Br][Br] (100 mg, 0.195 mmol), synthesized by previously reported methods,[1] was dissolved in 5.0 mL of methylene chloride and $NaClO_4$ (23.9 mg, 0.195 mmol) added. After stirring overnight, NaBr was removed from the reaction mixture by filtration and blue powder precipitated by slow addition of pentane. [Cu^{II}(TPMA)Br][ClO$_4$] was collected by filtration and dried under vacuum (yield = 50.0 mg, 47%). Crystals suitable for X-ray analysis were obtained in acetonitrile by slow diffusion of diethyl ether. FT-IR (solid) ν (cm^{-1}) = 3066(w), 1608(w), 1477(m), 1308(m), 1265(w), 1080(s), 652(m), 621(s), 505(m). Anal. Calcd. for

$C_{18}H_{18}N_4CuClBrO_4$ (533.26): C, 40.54; H, 3.40; N, 10.51. Found: C, 40.54; H, 3.39; N, 10.45.

*[Cu^{II}(TPMA)Br][BPh$_4$]*CH$_3$CN (11)* - [Cu^{II}(TPMA)Br][Br] (100 mg, 0.193 mmol), synthesized by previously reported methods,[1] was dissolved in 3.0 mL of methanol and $NaBPh_4$ (66.0 mg, 0.193 mmol) added. Green powder which precipitated immediately was washed with methanol, collected by filtration, and dried under vacuum to yield 95.0 mg (65 %) of [Cu^{II}(TPMA)Br][BPh$_4$]. Crystals of [Cu^{II}(TPMA)Br][BPh$_4$]*CH$_3$CN suitable for X-ray analysis were obtained in acetonitrile by slow diffusion of diethyl ether. FT-IR (solid): ν (cm^{-1}) = 3055(w), 2997(w), 2931(w), 1605(m), 1574(m), 1477(m), 1427 (m), 1261(m), 1022(m), 733(s), 706(s), 613(m), 505(m). Anal. Calcd. for $C_{44}H_{41}N_5CuBBr$ (794.09): C, 66.55; H, 5.20; N, 8.82. Found: C, 66.47; H, 5.16; N, 8.79.

6.7 References

(1) Eckenhoff, W. T.; Garrity, S. T.; Pintauer, T., Highly Efficient Copper Mediated Atom Transfer Radical Addition (ATRA) in the Presence of Reducing Agent. *Eur. J. Inorg. Chem.* **2008**, 563-571.

(2) Mandon, D.; Machkour, A.; Goetz, S.; Welter, R., *Inorg. Chem.* **2002,** *41*, 5364-5372.

(3) Bjernemose, J.; Hazell, A.; McKenzie, C. J.; Mahon, M. F.; Nielsena, L. P.; Raithby, P. R.; Simonsen, O.; Toftlund, H.; Wolny, J. A., *Polyhedron* **2003,** *22*, 875-885.

(4) Wietzke, R.; Mazzanti, M.; Latour, J. M.; Pecaut, J.; Cordier, P. Y.; Madic, C., *Inorg. Chem.* **1998,** *37*, 6690-6697.

(5) Baldwin, M. J.; Ross, P. K.; Pate, J. E.; Tyeklar, Z.; Karlin, K. D.; Solomon, E. I., Spectroscopic and Theoretical Studies of an End-On Peroxide-Bridged Coupled Binuclear Copper(II) Model Complex of Relevance to the Active Sites in Hemocyanin and Tyrosinase *J. Am. Chem. Soc.* **1991,** *113*(23), 8671-8679.

(6) Fry, H. C.; Scaltrito, D. V.; Karlin, K. D.; Meyer, G. J., The Rate of O2 and CO Binding to a Copper Complex, Determined by a "Flash-and-Trap" Technique, Exceeds that for Hemes. *J. Am. Chem. Soc.* **2003,** *125*(39), 11866-11871.

(7) Karlin, K. D.; Hayes, J. C.; Juen, S.; Hutchinson, J. P.; Zubieta, J., Tetragonal vs. Trigonal Coordination in Copper (II) Complexes with Tripodal Ligands: Structures and Properties of [Cu(C23H24N4)Cl]PF6 and [Cu(C18H18N4)Cl]PF6. *Inorg. Chem.* **1982,** *21*(11), 4106-4108.

(8) Karlin, K. D.; Nanthakumar, A.; Fox, S.; Murthy, N. N.; Ravi, N.; Huynh, B. H.; Orosz, R. D.; Day, E. P., X-ray Structure and Physical Properties of the Oxo-Bridged Complex [(F8-TPP)Fe-O-Cu(TMPA)]+, F8-TPP = Tetrakis(2,6-difluorophenyl)porphyrinate(2-), TMPA = Tris(2-pyridylmethyl)amine: Modeling the Cytochrome c Oxidase Fe-Cu Heterodinuclear Active Site. *J. Am. Chem. Soc.* **1994,** *116*(11), 4753-4763.

(9) Karlin, K. D.; Wei, N.; Jung, B.; Kaderli, S.; Niklaus, P.; Zuberbuhler, A. D., Kinetics and Thermodynamics of Formation of Copper-Dioxygen Adducts: Oxygenation of Mononuclear Copper(I) Complexes Containing Tripodal Tetradentate Ligands *J. Am. Chem. Soc.* **1993,** *115*(21), 9506-9514.

(10) Karlin, K. D.; Zubieta, J., *Copper Coordination Chemistry: Biochemical and Inorganic Perspectives*. Adenine Press: New York, 1983.

(11) Wei, N.; Lee, D.; Murthy, N. N.; Tyeklar, Z.; Karlin, K. D.; Kaderli, S.; Jung, B.; Zuberbuehler, A. D., Kinetic Preference without Thermodynamic Stabilization in the Intra- vs Intermolecular Formation of Copper-Dioxygen Complexes. *Inorg. Chem.* **1994,** *33*(21), 4625-4626.

(12) Wei, N.; Murthy, N. N.; Chen, Q.; Zubieta, J.; Karlin, K. D., Copper(I)/Dioxygen Reactivity of Mononuclear Complexes with Pyridyl and Quinolyl Tripodal Tetradentate Ligands: Reversible Formation of Cu:O2 = 1:1 and 2:1 Adducts. *Inorg. Chem.* **1994,** *33*(9), 1953-1965.

(13) Tyeklar, Z.; Jacobson, R. R.; Wei, N.; Murthy, N. N.; Zubieta, J.; Karlin, K. D., Reversible Reaction of Dioxygen (and Carbon Monoxide) with a Copper(I) Complex. X-Ray Structures of Relevant Mononuclear Cu(I) Precursor Adducts and the Trans-(μ -1,2-peroxo)dicopper(II) Product *J. Am. Chem. Soc.* **1993,** *115*(7), 2677-2689.

(14) Clark, A. J., Atom Transfer Radical Cyclisation Reactions Mediated by Copper Complexes. *Chem. Soc. Rev.* **2002,** *31*(1), 1-11.

(15) Eckenhoff, W. T.; Pintauer, T., Copper Catalyzed Atom Transfer Radical Addition (ATRA) and Cyclization (ATRC) Reactions in the Presence of Reducing Agents. *Cat. Rev. Sci. Eng.* **2010,** *52*, 1-59.

(16) Pintauer, T., Catalyst Regeneration in Transition-Metal-Mediated Atom-Transfer Radical Addition (ATRA) and Cyclization (ATRC) Reactions. *Eur. J. Inorg. Chem.* **2010**, 2449-2460.

(17) Matyjaszewski, K.; Xia, J., Atom Transfer Radical Polymerization. *Chem. Rev.* **2001,** *101*(9), 2921-2990.

(18) Wang, J.-S.; Matyjaszewski, K., Controlled/"Living" Radical Polymerization. Atom Transfer Radical Polymerization in the Presence of Transition-Metal Complexes. *J. Am. Chem. Soc.* **1995,** *117*(20), 5614-5615.

(19) Kharasch, M. S.; Engelmann, H.; Mayo, F. R., The Peroxide Effect in the Addition of Reagents to Unsaturated Compounds. XV. The Addition of Hydrogen Bromide to 1- and 2-Bromo and Chloro-Propenes. *J. Org. Chem.* **1937,** *2*, 288-302.

(20) Kharasch, M. S.; Jensen, E. V.; Urry, W. H., Addition of Carbon Tetrachloride and Chloroform to Olefins. *Science* **1945,** *102*(2640), 128-128.

(21) Kharasch, M. S.; Jensen, E. V.; Urry, W. H., Addition of Derivatives of Chlorinated Acetic Acid to Olefins. *J. Am. Chem. Soc.* **1945,** *67*, 1626-1626.

(22) Balili, M. N. C.; Pintauer, T., Persistent Radical Effect in Action: Kinetic Studies of Copper-Catalyzed Atom Transfer Radical Addition in the Presence of Free-Radical Diazo Initiators as Reducing Agents. *Inorg. Chem.* **2009,** *48*, 9018-9026.

(23) Eckenhoff, W. T.; Pintauer, T., Atom Transfer Radical Addition in the Presence of Catalytic Amounts of Copper(I/II) Complexes with Tris(2-pyridylmethyl)amine. *Inorg. Chem.* **2007,** *46*(15), 5844-5846.

(24) Pintauer, T., "Greening" of Copper Catalyzed Atom Transfer Radical Addition (ATRA) and Cyclization (ATRC) Reactions. *ACS Symp. Ser.* **2009,** *1023*, 63-84.

(25) Pintauer, T.; Eckenhoff, W. T.; Ricardo, C.; Balili, M. N. C.; Biernesser, A. B.; Noonan, S. J.; Taylor, M. J. W., Highly Efficient, Ambient-Temperature Copper-Catalyzed Atom-Transfer Radical Addition (ATRA) in the Presence of Free-Radical Initiator (V-70) as a Reducing Agent. *Chem. Eur. J.* **2009,** *15*, 38-41.

(26) Pintauer, T.; Matyjaszewski, K., Atom Transfer Radical Addition and Polymerization Reactions Catalyzed by ppm Amounts of Copper Complexes. *Chem. Soc. Rev.* **2008,** *37*, 1087-1097.

(27) Pintauer, T.; Matyjaszewski, K., Structural and Mechanistic Aspects of Copper Catalyzed Atom Transfer Radical Polymerization. *Top. Organomet. Chem.* **2009,** *26*, 221-251.

(28) Ricardo, C.; Pintauer, T., Copper Catalyzed Atom Transfer Radical Cascade Reactions in the Presence of Free-Radical Diazo Initiators as Reducing Agents. *Chem. Commun.* **2009**, 3029-3031.

(29) Muñoz-Molina, J. M.; Belderraín, T. R.; Pérez, P. J., Copper-Catalyzed Synthesis of 1,2-Disubstituted Cyclopentanes from 1,6-Dienes by Ring-Closing Kharasch Addition of Carbon Tetrachloride. *Adv. Synth. Catal.* **2008,** *350*, 2365-2372.

(30) Muñoz-Molina, J. M.; Belderraín, T. R.; Pérez, P. J., An Efficient, Selective, and Reducing Agent-Free Copper Catalyst for the Atom-Transfer Radical Addition of Halo Compounds to Activated Olefins. *Inorg. Chem.* **2010,** *49*(2), 642-645.

(31) Muñoz-Molina, J. M.; Caballero, A.; Díaz-Requejo, M. M.; Trofimenko, S.; Belderraín, T. R.; Pérez, P. J., Copper-Homoscorpionate Complexes as Active Catalysts for Atom Transfer Radical Addition to Olefins. *Inorg. Chem.* **2007,** *46*, 7725-7730.

(32) Balili, M. N. C.; Pintauer, T., Kinetic Studies of the Initiation Step in Copper Catalyzed Atom Transfer Radical Addition (ATRA) in the Presence of Free Radical Diazo Initiators as Reducing Agents. *Inorg. Chem.* **2010,** *49*(12), 5642-5649.

(33) Jakubowski, W.; Matyjaszewski, K., Activator Generated by Electron Transfer for Atom Transfer Radical Polymerization. *Macromolecules* **2005,** *38*, 4139-4146.

(34) Jakubowski, W.; Matyjaszewski, K., Activators Regenerated by Electron Transfer for Atom-Transfer Radical Polymerization of (Meth)acrylates and Related Block Copolymers. *Angew. Chem. Int. Ed.* **2006,** *45*(27), 4482-4486.

(35) Jakubowski, W.; Min, K.; Matyjaszewski, K., Activators Regenerated by Electron Transfer for Atom Transfer Radical Polymerization of Styrene *Macromolecules* **2006,** *39*(1), 39-45.

(36) Matyjaszewski, K.; Jakubowski, W.; Min, K.; Tang, W.; Huang, J.; Braunecker, W. A.; Tsarevsky, N. V., Diminishing Catalyst Concentration in Atom Transfer Radical Polymerization with Reducing Agents. *Proc. Natl. Acad. Sci. U.S.A.* **2006,** *103*, 15309-15314.

(37) Hsu, S. C.; Chien, S. S.; Chen, H. H.; Chiang, M. Y., Synthesis and Characterization of Copper(I) Complexes Containing Tris(2-pyridylmethyl)amine Ligand. *J. Chin. Chem. Soc.* **2007,** *54*(3), 685-692.

(38) Kochi, J. K., *Free Radicals*. John Wiley & Sons: New York, 1973; Vol. 1.

(39) Lin, C. Y.; Coote, M. L.; Gennaro, A.; Matyjaszewski, K., Ab Initio Evaluation of the Thermodynamic and Electrochemical Properties of Alkyl Halides and Radicals and Their Mechanistic Implications for Atom Transfer Radical Polymerization *J. Am. Chem. Soc.* **2008,** *130*(138), 12762-12774.

(40) Matyjaszewski, K., Radical Nature of Cu-Catalyzed Controlled Radical Polymerizations (Atom Transfer Radical Polymerization). *Macromolecules* **1998,** *31*(15), 4710-4717.

(41) Tsarevsky, N. V.; Braunecker, W. A.; Matyjaszewski, K., Electron Transfer Reactions Relevant to Atom Transfer Radical Polymerization. *J. Organomet. Chem.* **2007,** *692*, 3212-3222.

(42) Eckenhoff, W. T.; Manor, B. C.; Pintauer, T., New Tetradentate Ligand Tris-[(3,5-dimethyl-1H-pyrazol-1-yl)methyl]amine (TDPMA) for Atom Transfer Radical Addition (ATRA). *Polym. Prepr. (Am. Chem. Soc. Div. Polym. Chem.)* **2008,** *49(2)*, 213-214.

(43) Matyjaszewski, K.; Gobelt, B.; Paik, H.-j.; Horwitz, C. P., Tridentate Nitrogen-Based Ligands in Cu-Based ATRP: A Structure-Activity Study. *Macromolecules* **2001,** *34*(3), 430-440.

(44) Qiu, J.; Matyjaszewski, K.; Thounin, L.; Amatore, C., Cyclic Voltammetric Studies of Copper Complexes Catalyzing Atom Transfer Radical Polymerization. *Macromol. Chem. Phys.* **2000,** *201*, 1625-1631.

(45) Tang, W.; Kwak, Y.; Braunecker, W.; Tsarevsky, N. V.; Coote, M. L.; Matyjaszewski, K., Understanding Atom Transfer Radical Polymerization: Effect of Ligand and Initiator Structures on the Equilibrium Constants *J. Am. Chem. Soc.* **2008,** *130*(132), 10702-10713.

(46) Tang, W.; Tsarevsky, N. V.; Matyjaszewski, K., Determination of Equilibrium Constants for Atom Transfer Radical Polymerization. *J. Am. Chem. Soc.* **2006,** *128*(5), 1598-1604.

(47) Lim, B. S.; Holm, R. H., Molecular Heme-Cyanide-Copper Bridged Assemblies: Linkage Isomerism, Trends in CN Values, and Relation to the Heme-a3/CuB Site in Cyanide-Inhibited Heme-Copper Oxidases. *Inorg. Chem.* **1988,** *37*, 4898-4908.

(48) Xu, X.; Maresca, K. J.; Das, D.; Zahn, S.; Zubieta, J.; Canary, J. W., Crystal-Driven Distortion of Ligands in Copper Coordination Complexes : Conformational Pseudo-Enantiomers *Chem. Eur. J.* **2002,** *8*(24), 5679-5683.

(49) Jensen, M. P.; Que, E. L.; Shan, X.; Rybak-Akimova, E.; Que, L. J., Spectroscopic and Kinetic Studies of the reaction of [CuI(6-PhTPA)]+ with O2. *J. Chem. Soc. Dalton Trans.* **2006,** *29*, 3523-3527.

(50) Balili, M. N. C.; Pintauer, T., Kinetic Studies of Copper Catalyzed Atom Transfer Radical Addition of Carbon Tetrachloride to Alkenes in the Presence of Reducing Agents. *Polym. Prepr. (Am. Chem. Soc., Div. Polym. Chem.)* **2008,** *49(2)*, 161-162.

(51) Tolman, C. A., Steric effects of phosphorus ligands in organometallic chemistry and homogeneous catalysis. *Chem. Rev.* **1977,** *77*(3), 313-348.

(52) Muller, T.; Mingos, M. P., Determination of the Tolman cone angle from crystallographic parameters and a statistical analysis using the Crystallographic Data Base. *Trans. Met. Chem.* **1995,** *20*(6), 533-539.

(53) Britovsek, G.; England, J.; White, A., Non-Heme Iron(II) Complexes Containing Tripodal Tetradentate Nitrogen Ligands and Their Application in Alkane Oxidaion Catalysis. *Inorg. Chem.* **2005,** *44*(22), 8125-8134.

(54) Munakata, M.; Kitagawa, S.; Asahara, A.; Masuda, H., Synthesis and Crystal Structure of [Cu(CH3CN)4][ClO4]. *Bull. Chem. Soc. Jpn.* **1987,** *60*, 1927-1929.

(55) Sheldrick, G. M., *SADABS Version 2.03*. University of Gottingen: Germany, 2002.

(56) Sheldrick, G. M., *SHELXTL 6.1,Crystallographic Computing System*. Bruker Analytical X-Ray System: Madison, WI, 2000.

(57) Faruggia, L. J., ORTEP-3 for Windows. *J. Appl. Cryst.* **1997,** *30 (5, Pt. 1)*, 565.

Chapter 7.

MECHANISTIC INVESTIGATION OF ATOM TRANSFER RADICAL ADDITION (ATRA) CATALYZED BY COPPER COMPLEXES WITH TRIS(2-PYRIDYLMETHYL)AMINE (TPMA) LIGAND

The ability of metal complexes to catalyze atom transfer radical addition (ATRA) has been known for over 50 years. Recently, the molecular structure of [Cu^{I}(TPMA)Cl] (TPMA=tris(2-pyridylmethyl)amine), which is one of the most active complexes for ATRA in the presence of 2,2'-azobis(isobutyronitrile) (AIBN) as a reducing agent, was found to be pseudo-pentacoordinated in the solid state due to coordination of a chloride anion to the copper(I) center. This raised questions about the reaction mechanism if the same structure was found in solution. The effect of the counter-ion on the solution state structure of copper(I) complexes with TPMA ligand was investigated by cyclic voltammetry, ^{1}H NMR spectroscopy and through ATRA kinetics. The halide was found to have a strong affinity for the copper(I) complex and thus TPMA dissociation was targeted as a possible means of the opening of a coordination site required for widely accepted inner sphere electron transfer (ISET) mechanism. Rate constants for complete TPMA displacement were measured at different temperatures in order to determine thermodynamic parameters and $\Delta G^{\ddagger}$ for this exchange was found to be 43.25 KJ (10.34 kcal), with $\Delta H^{\ddagger}$ and $\Delta S^{\ddagger}$ being equal to 2.96 KJ and -60.0 J K^{-1}, respectively. The fluxional nature of the TPMA ligand, coupled with the strong affinity of halides to copper(I), suggested that partial TPMA dissociation is the most likely route for the opening of a coordination site. To support this claim, addition of up to two equivalents of

triphenylphosphine (PPh_3) were found to have no effect on ATRA. Furthermore, the tris(2-(dimethylamino)phenyl)amine (TDAPA) ligand was also utilized in ATRA reactions as a tetradentate ligand with structural similarities to both TPMA and Me_6TREN (tris2-dimethylaminoethyl)amine), which are highly active for ATRA. However, these complexes were found to have poor activity in ATRA reactions, most likely due to the lack of fluxionality of the ligand as compared to TPMA and Me_6TREN.

7.1 Introduction

The atom transfer radical addition (ATRA) is a facile technique for the formation of carbon-carbon bonds, originating from the Kharasch addition,[1, 2] typically catalyzed by Cu or Ru complexes.[3-12] ATRA has long been accepted to proceed via a radical mechanism (Scheme 7.1.1),[10, 13] where an alkyl halide can be homolytically cleaved ($k_{a,1}$) by a metal complex in the lower oxidation state (activator), generating an alkyl radical

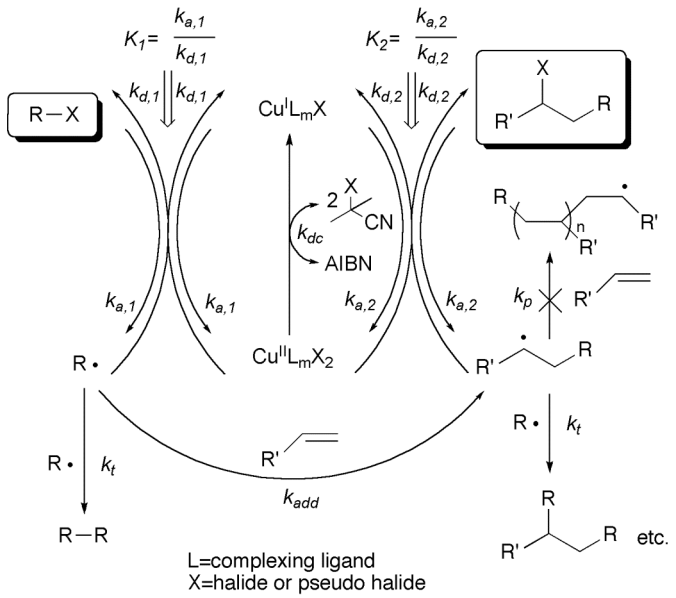

Scheme 7.1.1. ATRA mechanism in the presence of a copper catalyst and AIBN as a reducing agent

and metal complex in the higher oxidation state (deactivator). The alkyl radical can either undergo the reverse reaction ($k_{d,1}$), generating the dormant alkyl halide and activator species, terminate with another alkyl radical (k_t), or add across an alkene (k_{add}), forming a secondary radical. The secondary radical can terminate (k_t), add across another alkene forming oligomers (k_p), or be trapped by the deactivator species ($k_{d,2}$), forming the desired monoadduct. To achieve good yields of the monoadduct: (i) the deactivation rate constants should be greater than activation rate constants ($k_{a,1}$ $k_{a,2}$ << $k_{d,1}$ $k_{d,2}$), which lowers the overall radical concentration, decreasing radical terminations, (ii) reactivation of the monoadduct should be avoided by carefully choosing alkyl halide/alkene combinations so that $k_{a,2}\approx 0$, and (iii) the rate of deactivation should be sufficiently larger than the rate of propagation ($k_{d,2}[Cu^{II}]>>k_p[\text{alkene}]$).[14] Recently, the use of reducing agents, such as 2,2' azobis(isobutyronitrile) (AIBN),[15-25] 2,2'-azobis(4-methoxy-2,4-dimethyl valeronitrile) (V-70),[26] magnesium,[27-33] and ascorbic acid,[34] have been used to regenerate the activator species state due to an accumulation of the deactivator species allowing for drastic reductions in the amount of metal required to control the reaction.

The catalytic mechanism of ATRA is widely accepted to proceed via inner-sphere electron transfer (ISET).[35-38] The ISET process in ATRA requires the alkyl halide to come within bonding distance of the activator species where the halide forms pseudo-bonds with the alkyl group and metal. The bond between the alkyl group and halide is then homolytically cleaved generating the oxidized metal and alkyl radical (Scheme 7.1.2). One of the most highly active copper catalysts for this transformation is $[Cu^{I}(TPMA)X]$ (X=Cl,Br/TPMA=tris(2-pyridylmethyl)amine) and the solid state molecular structure of these complexes was recently found to be pseudo-

pentacoordinated with both TPMA and halide coordinated.[17, 18, 39] When the solution state structure was probed, the complex was observed to be fluxional at room temperature, although the complex was clearly observed to have C_3 symmetry, suggesting halide association in solution. Copper(I) complexes without a halide or other coordinating ligand have been shown to dimerize in an unsymmetrical manner.[40] The possibility of halide coordination in solution was surprising because such a complex is typically described as coordinatively saturated and thus dissociation of a ligand must occur for an ISET process, raising the possibility of an outer sphere electron transfer (OSET). The OSET mechanism for ATRA can be described as proceeding via

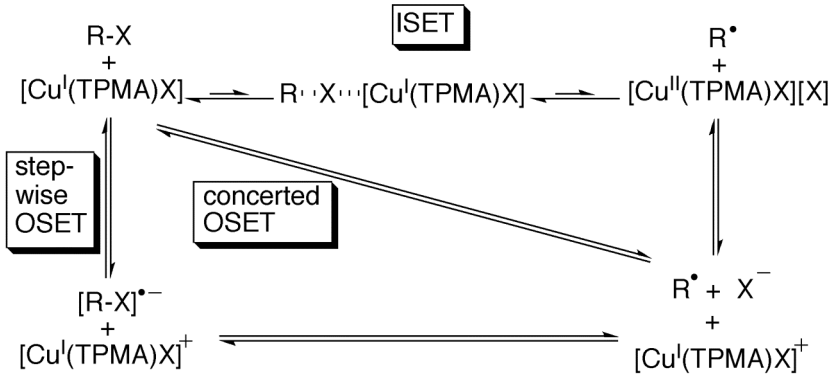

Scheme 7.1.2. Possible mechanisms of electron transfer from the copper complex to alkyl halide to generate the oxidized complex and alkyl radical.

concerted or stepwise pathways. The OSET process takes place in one concerted step, in which the transition metal complex is oxidized and the alkyl halide forms an alkyl radical and halide anion by dissociative electron transfer. The halide then eventually coordinates to the metal. The stepwise mechanism describes the formation of a radical anion on the alkyl halide after oxidation of the metal complex, subsequently followed by cleavage into radical and halide anion (Scheme 7.1.2). All three pathways yield the exact same products and thus can only be ruled out by examination of activation barriers. Extensive

ab initio calculations were performed in order to determine the activation enthalpies for each process in the gas phase and solution phase (DMF and CH_3CN) and thus estimate a rate constant for OSET using bromoacetonitrile for the alkyl halide and $Cu^{I/II}$/TPMA complex for electron transfer.[41] Using calculated standard reduction potentials of bromoacetonitrile, it was determined that adiabatic reduction of the alky halide to a radical anion would have a large enthalpic penalty (20.3 kcal mol^{-1}), which is significantly larger than for the concerted process or ISET. The activation rate constant for the concerted mechanism was calculated as 10^{-9} M^{-1} s^{-1} by using the standard reduction potential of bromoacetonitrile, the experimentally determined reduction potential for $Cu^{I/II}$/TPMA, and the bond dissociation energy of C-Br in bromoacetonitrile. Compared to the known activation rate constants of ISET, OSET via concerted pathway was found to have a lower rate constant by 10^{-11} M^{-1} s^{-1}, supporting the notion that ISET is strongly favored.[41] Clearly, further studies into the catalytic mechanism of alkyl halide cleavage by [Cu^{I}(TPMA)X] complexes were warranted. In this chapter, the role of the counter-ion, the possibility of halide and TPMA dissociation, and phosphine inhibition were examined in order to provide more information on that nature of the ATRA mechanism.

7.2 Role of the Counter-ion in ATRA

Following the realization that the counter-ion in copper(I) complexes with TPMA ligand drastically affects not only the electrochemistry,[17] but also the molecular structure,[40] the role of these anions in the ATRA mechanism were investigated. It was

expected, with such a large difference in reduction potential, that ATRA reactions of various alkenes with CCl_4 using $[Cu^{II}(TPMA)Cl][Y]$ ($Y=ClO_4^-$, PF_6^-, and BPh_4^-) as catalysts would be far less active than previously used catalysts ($Y=Cl^-$) for ATRA. Surprisingly, when these complexes were used in ATRA with AIBN as a reducing agent, no differences in monoadduct conversion or yield were detected after 24 hr with a variety

Table 7.2.1. Examination of effect of anion in ATRA reactions with CCl_4.[a]

Complex	Alkene	$[Alkene]_0$: $[Cu]_0$	CH_3CN		CH_3OH	
			Conv.	Yield	Conv.	Yield
[Cu(TPMA)Cl][Cl]	1-hexene	5000:1	100%	100%	100%	100%
[Cu(TPMA)Cl][ClO_4]			100%	100%	100%	100%
[Cu(TPMA)Cl][PF_6]			100%	100%	100%	100%
[Cu(TPMA)Cl][BPh_4]			100%	100%	100%	100%[b]
[Cu(TPMA)Cl][Cl]	1-octene	5000:1	99%	99%	99%	99%
[Cu(TPMA)Cl][ClO_4]			99%	99%	99%	99%
[Cu(TPMA)Cl][PF_6]			99%	99%	99%	99%
[Cu(TPMA)Cl][BPh_4]			95%	95%	97%	97%[b]
[Cu(TPMA)Cl][Cl]	styrene	500:1	85%	60%	100%	65%
[Cu(TPMA)Cl][ClO_4]			85%	62%	100%	68%
[Cu(TPMA)Cl][PF_6]			92%	67%	100%	67%
[Cu(TPMA)Cl][BPh_4]			81%	59%	100%	72%[b]
[Cu(TPMA)Cl][Cl]	methyl acrylate	500:1	100%	62%	100%	69%
[Cu(TPMA)Cl][ClO_4]			100%	60%	100%	73%
[Cu(TPMA)Cl][PF_6]			100%	70%	100%	76%
[Cu(TPMA)Cl][BPh_4]			100%	65%	100%	71%[b]

[a] Reactions performed at 60°C in CH_3CN or CH_3OH, $[alkene]_0$:$[CCl_4]_0$:$[AIBN]_0$=1:1:0.05, $[alkene]_0$=2.10 M. Conversion and yield were calculated by ^1H NMR using 1,4-dimethoxybenzene and internal standard. [b] [Cu(TPMA)Cl][BPh_4] was added in a solution of acetone.

of alkenes (Table 7.2.1). It has previously been shown that reaction kinetics of ATRA in the presence of reducing agents are rather complicated.[16, 25] When a free radical initiator is used as a reducing agent, the rate of alkene consumption is governed by the rate of decomposition of the free radical source and not by the copper concentration. However, product selectivity was shown to be directly correlated to the activity of the catalyst,

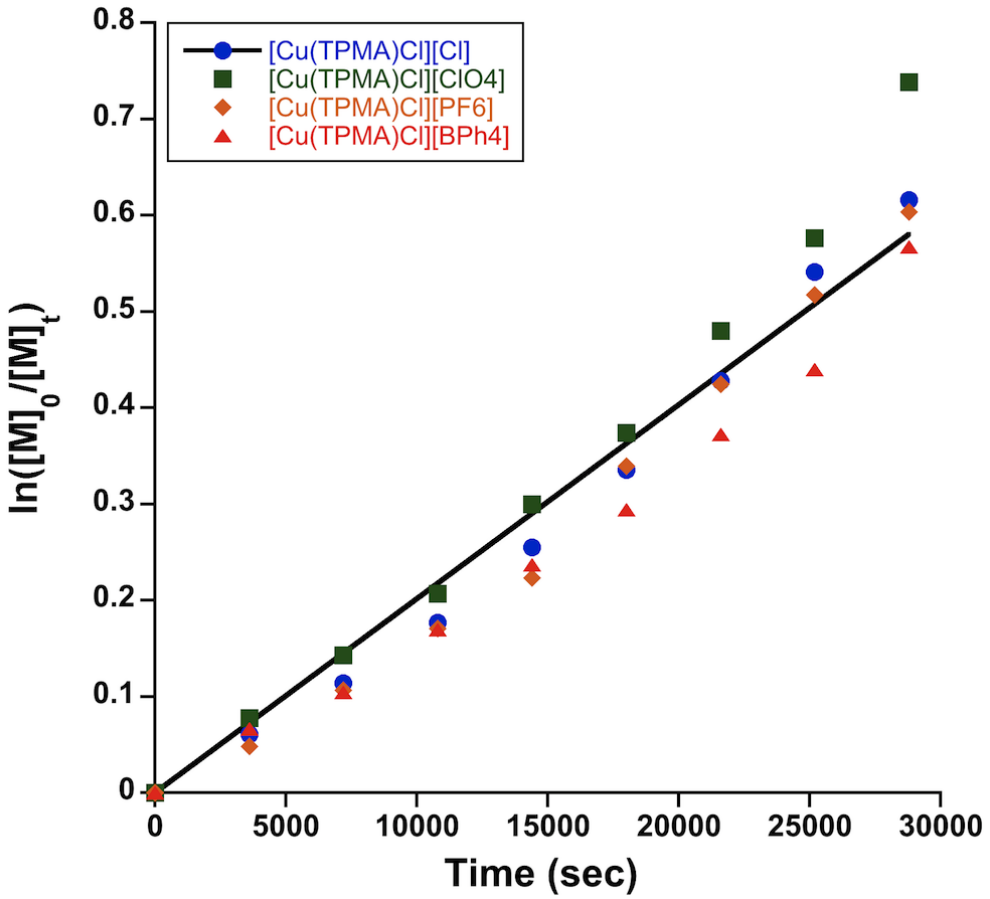

Figure 7.2.1. First order kinetic plot for ATRA of CCl_4 to 1-octene catalyzed by [Cu(TPMA)Cl][Y] (Y=Cl^- (●), ClO_4^- (■), BPh_4^- (▲), PF_6^- (◆)) in the presence of AIBN. $[alkene]_0$:$[CCl_4]_0$:$[AIBN]_0$:$[Cu^{II}]_0$=5000:5000:250:1, $[alkene]_0$=2.10 M.

especially with alkenes that readily polymerize in the presence of free radicals. However, using $[Cu^{II}(TPMA)Cl][Y]$, nearly quantitative conversions were achieved in the addition of CCl_4 to both 1-hexene and 1-octene at a 5000:1 alkene to copper ratio. In the case of styrene and methyl acrylate, yields ~65% were observed at a 500:1 ratio, all of which is consistent with ATRA catalyzed by $Cu^{I}(TPMA)Cl$.[18] Additionally, reactions performed in the absence of coordinating ligands and solvents (i.e. methanol and non-coordinating anions) showed no difference in product yield, but a slight increase in conversion was

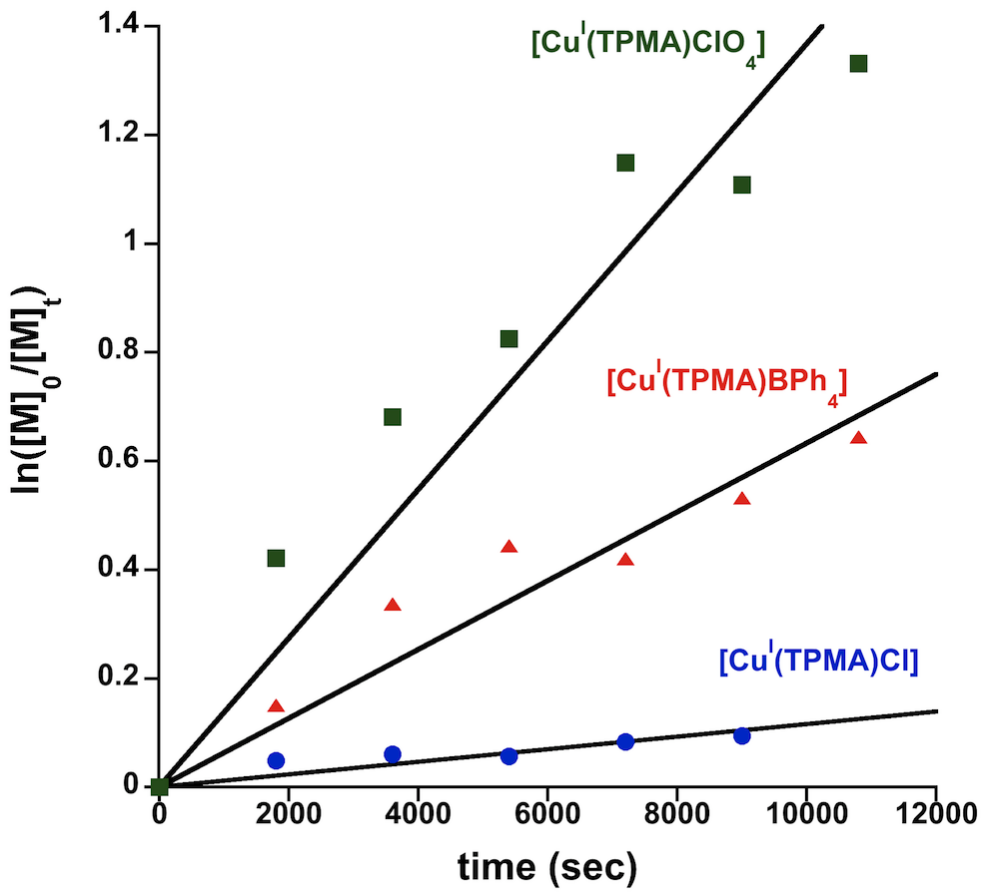

Figure 7.2.2. First order kinetic plot for ATRA of CCl_4 to 1-octene catalyzed by [Cu(TPMA)Cl][Y] (Y=Cl^- (●), ClO_4^- (■), BPh_4^- (▲)). $[alkene]_0$:$[CCl_4]_0$:$[Cu]_0$=50:50:1, $[alkene]_0$=2.10 M.

observed in the case of CCl_4 and styrene, likely due to a polarity effect. As expected, no difference was found in the observed reaction rates, where the k_{obs} for the conversion of 1-octene was found to be ~2 x 10^{-5} $M^{-1}s^{-1}$ (Figure 7.2.1). However, in the absence of AIBN and higher concentrations of catalyst, we found that ATRA of CCl_4 and methyl acrylate with complexes containing non-coordinating counter-ions had significantly larger values of k_{obs} than with Cu^I(TPMA)Cl (Figure 7.2.2). The perchlorate complex was found to have the largest k_{obs} (1.37 x 10^{-4} $M^{-1}s^{-1}$), followed by the tetraphenylborate complex (6.33 x 10^{-5} $M^{-1}s^{-1}$), with the slowest being the chloride complex (1.16 x 10^{-5} M^{-1} s^{-1}). This difference in activity supports the theory that ATRA will proceed faster when

the coordination sphere of copper has an open coordination site, which does not require ligand dissociation. We expected to see a similar effect in the values of equilibrium

Table 7.2.2. Equilibrium constants for [Cu^I(TPMA)Y] (Y=Cl^-, ClO_4^-, and BPh_4^-).[a]

Complex	K_{ATRA} (10^{-7})
[Cu^I(TPMA)Cl]	2.21(±0.069)
[Cu^I(TPMA)ClO_4]	4.65(±0.027)
[Cu^I(TPMA)BPh_4]	4.48(±0.072)

[a] Equilibrium constants measured using benzyl bromide in the presence of Cu^IBr in CH_3CN at 22 °C

constant for [Cu^I(TPMA)Y] (Y=Cl^-, ClO_4^-, and BPh_4^-), but the difference was found to be marginal, ranging from 2.21 x 10^{-7} to 4.65 x 10^{-7} $M^{-1}s^{-1}$ (Table 7.2.2, Appendix F).

In order for these complexes to have equal activity in ATRA systems with AIBN, they must proceed via similar catalytic processes, where the presence of a coordinating anion is inconsequential. We hypothesized that this could proceed along two different pathways: halide dissociation or partial TPMA dissociation, both of which could adequately explain the observed fluxionality of [Cu^I(TPMA)Br]. If the halide dissociated in the case of [Cu^I(TPMA)Cl], the complex would act in a similar manner to complexes with non- coordinating anions, in which the copper(I) center might be stabilized by

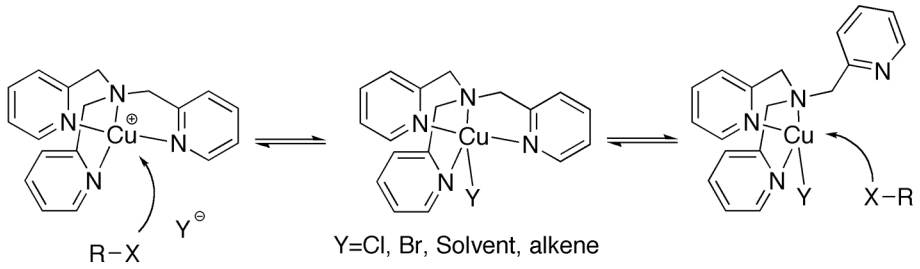

Scheme 7.2.1. Possible pathways for alkyl halide to oxidize coordinatively saturated copper(I) center with the TPMA ligand.

solvent or alkene, both of which are in large excess relative to copper. Alternatively, exchange of partial TPMA dissociation is also a likely route, in the event that an arm of TPMA dissociates from the copper center (Scheme 7.2.1).

7.3 Halide Dissociation

We began by examining the possibility of halide dissociation. It was previously reported that the ^{1}H NMR spectra of [Cu^{I}(TPMA)X] (X=Cl,Br) were highly fluxional at room temperature.[17, 39] Addition of 1, 2, 5 and 10 equivalents of TBA-Br to a solution of [Cu^{I}(TPMA)Br] was found to produce a spectra of TPMA with well defined peaks, which was originally thought to arise from the dissociation equilibrium of Br^{-} being shifted to

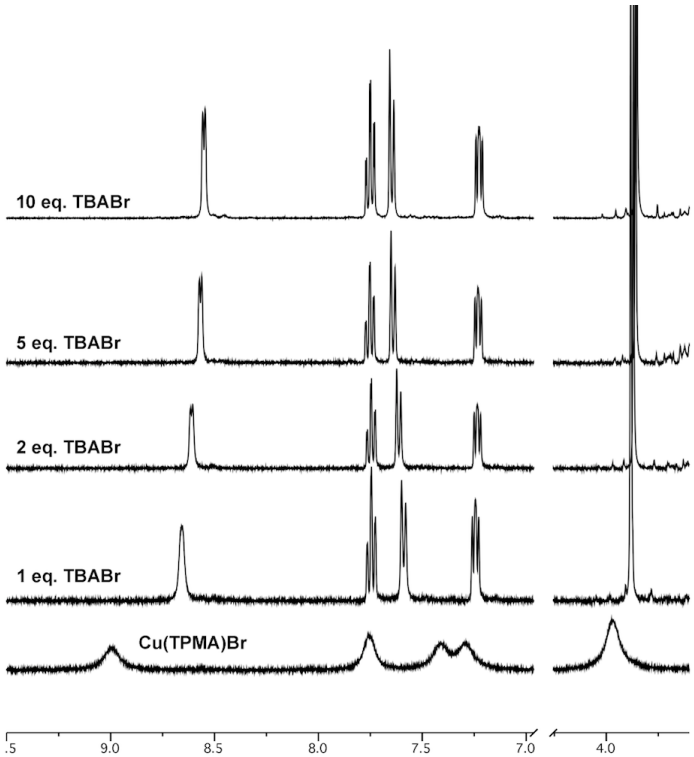

Figure 7.3.1. Effect of TBA-Br on ^{1}H NMR spectra of [Cu^{I}(TPMA)Br] (400 MHz, 298K, acetone-*d*6)

the complexed form due to the presence of excess Br^{-} (Figure 7.3.1). However, it was observed that this improved spectra was actually the result of an equilibrium of TPMA displacement and formation of [Cu^{I}Br$_{2}$][TBA] or other copper halide complexes being shifted toward dissociated TPMA. In addition, when [Cu^{I}(TPMACl] was observed in cyclic voltammetry in large excesses of TBA-Cl, the formation of [Cu^{I}Cl$_{2}$][TBA] was

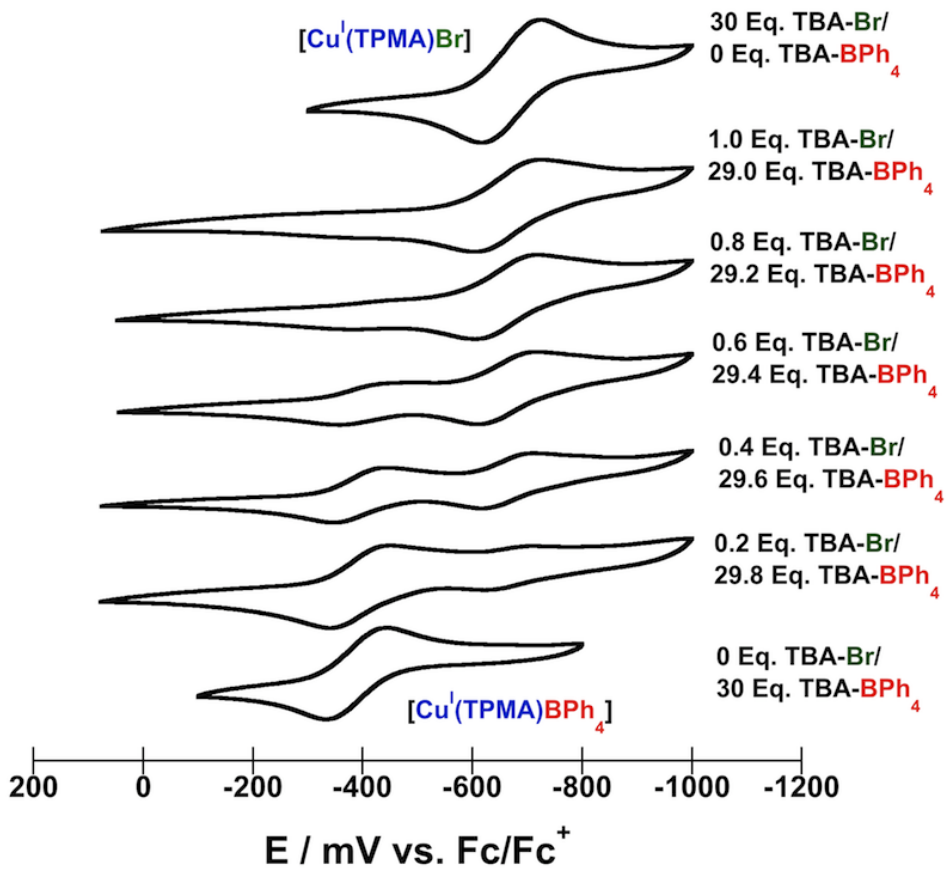

Figure 7.3.2. Effect of TBA-Br on the redox potential of $Cu^{I}(TPMA)BPh_4$ with TBA-BPh_4 as supporting electrolyte. Scan rate = 100 mV/s, waves reported with respect to Fc/Fc^+ couple.

observed at -98 mV as a minor wave compared to [Cu^{I}(TPMA)Cl] (Appendix F), which shows that total TPMA displacement by X^- (X=Cl,Br) is only significant in large excesses of TBA-X on the NMR timescale. It was previously shown that cyclic voltammetry of [Cu^{I}(TPMA)Y] (Y= ClO_4^-, BPh_4^- and PF_6^-) gave identical $E_{1/2}$ values as [Cu^{I}(TPMA)Br] or [Cu^{I}(TPMA)Cl] when they were performed with 30 Eq. TBA-Br or TBA-Cl, respectively, as supporting electrolytes.

This experiment was repeated with by titrating TBA-Br with [$Cu^{I}(TPMA)BPh_4$] using TBA-BPh_4 as the supporting electrolyte (Figure 7.3.2). Nearly quantitative conversion of [$Cu^{I}(TPMA)BPh_4$] to [Cu^{I}(TPMA)Br] was observed with only a single

equivalent of TBA-Br, which shows the strong affinity of Br^- to copper(I) in solution. Furthermore, the presence of a dimer was previously shown by ^1H NMR at low temperatures when a non-coordinating counter-ion was used in acetone-*d*6,[40] which is not observed in ^1H NMR spectra where halides or other ligands are present, even at low temperatures, indicating that the association of any coordinating substrate prevents this process from occurring.

A plausible explanation for the large difference in redox potential between copper(I) complexes with halides versus complex counter-ions, is the stability of the corresponding copper(II) complex, which is generated by oxidation during electrochemical measurements. Recently reported log β values (β=stability constant, *vide infra*) for $Cu^{II}(Me_6TREN)^{2+}$ (27.2±0.1) and $[Cu^{II}(Me_6TREN)Cl]^+$ (33.8±0.1) show how the halide has a great stabilizing effect for a copper(II) species with a similar tetradentate ligand.[42] The following equation shows how the redox potential is related to the relative stabilization of the Cu^{II} state compared to the Cu^{I} state, with the complexing ligand, L:[37,38]

$$\beta^m = \frac{[Cu^m L]}{[Cu^m][L]};\ m = I\ or\ II$$

$$E \approx E^0 + \frac{RT}{F}\left(\ln\frac{[Cu^{II}]_{total}}{[Cu^{I}]_{total}} - \ln\frac{\beta^{II}}{\beta^{I}}\right)$$

Using the provided stability constants for the corresponding copper(I) complexes with and without halides, the difference in β^{II}/β^{I} is approximately four orders of magnitude. Such a large difference in complex stability is most likely the cause for decreased redox potential observed for $Cu^{I}(TPMA)^+$ complexes with ClO_4^-, BPh_4^-, and PF_6^- anions.

Table 7.3.1. Conductivity values for $[Cu^{I}(TPMA)Y]$ ($Y=Cl^-, Br^-, ClO_4^-, BPh_4^-$) in CH_3CN[a]

Complex	Conductivity (μS/cm)
$[Cu^{I}(TPMA)Cl]$	2.64(±0.007)
$[Cu^{I}(TPMA)Br]$	3.01(±0.028)
$[Cu^{I}(TPMA)ClO_4]$	5.50(±0.064)
$[Cu^{I}(TPMA)BPh_4]$	6.29(±0.021)

[a] measured in drybox (O_2<0.5 ppm), $[Cu^{I}]$=1.0 mM.

Finally, dissociation of the anion would result in increased ionic character of the copper complex, which can be measured by solution conductivity. The conductivity of solutions with copper(I) complexes with the TPMA ligand to be 2.64 μS/cm with chloride and 3.01 μS/cm with bromide (Table 7.3.1). The values of conductivity were found to be approximately doubled when using perchlorate (5.50 μS/cm) or tetraphenylborate (6.29 μS/cm), indicating that the halide complexes have less ionic character. However, the presence of conductivity in the case of the halide complexes also suggests that there is some dissociation of anion in these cases.

7.4 Dissociation of TPMA

After ruling out halide dissociation as the mechanism for the opening of a coordination site due to their affinity to copper(I) complexes in solution, dissociation of TPMA was investigated. Partial dissociation of TPMA is well documented in the solid state, particularly when a bulky ligand was coordinated to the fifth site.[39, 40, 43] In solution, ^1H NMR spectrum of $[Cu^{I}(TPMA)X]$ (X=Cl,Br) was found to be fluxional, showing broad signals for TPMA protons. To confirm that the observed fluxionality of the TPMA ligand on copper(I) was the result of TPMA dissociation, one equivalent of TPMA was added to a solution of $[Cu^{I}(TPMA)Br]$ in acetone-*d*6. (Figure 7.4.1). The ^1H

NMR spectrum at room temperature was found to be slightly sharpened as compared to Cu^{I}(TPMA)Br, showing 5 broad signals. Three signals, those most affected by copper coordination, were found to completely coalesce at 226K and signals for free TPMA and complexed TPMA were easily distinguishable at lower temperatures (peaks at 3.56 ppm in spectrum E and 3.71 ppm in spectrum F are from a solvent impurity). From these NMR spectra, rate constants of TPMA dissociation were calculated[44] at several temperatures and plotted by Eyring's equation to extract thermodynamic parameters (Figure 7.4.2). The $\Delta H^{\ddagger}$, $\Delta S^{\ddagger}$, and $\Delta G^{\ddagger}$ for this exchange was found to be 2.96 KJ, -60.0 J K^{-1} and 43.25 KJ respectively. This indicates that TPMA is quite labile and thus partial

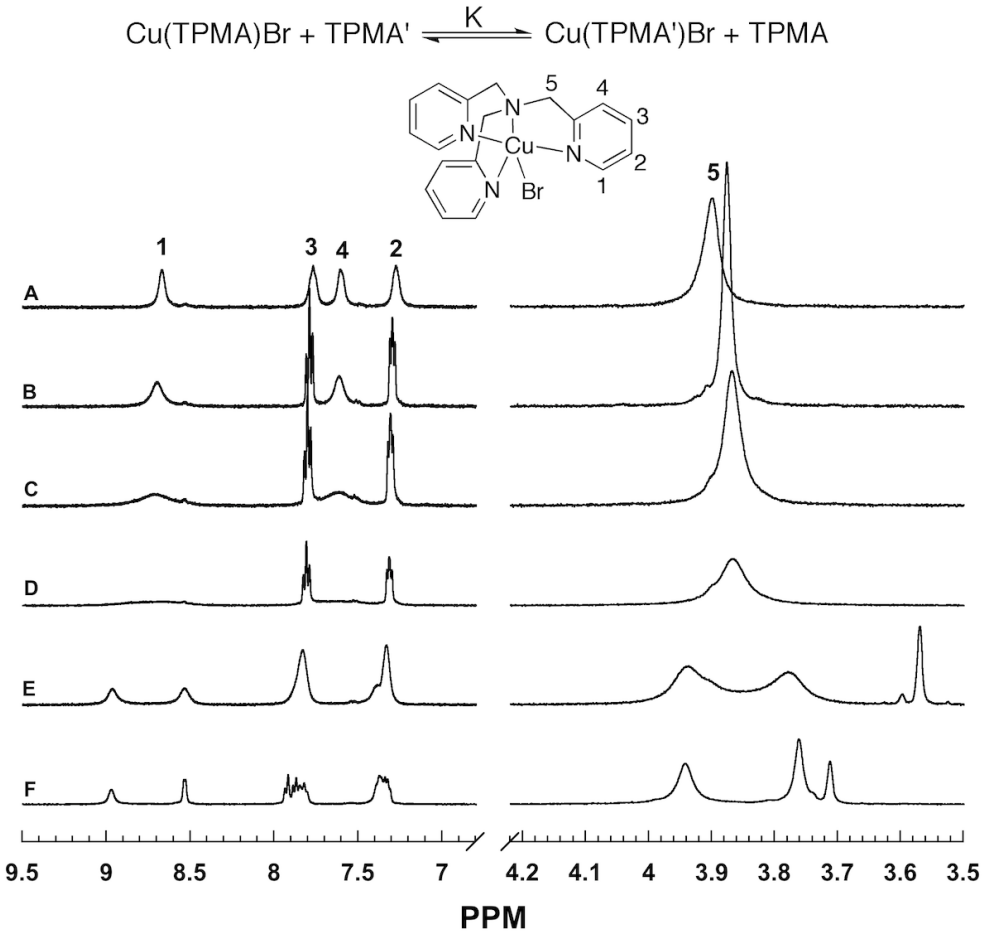

Figure 7.4.1. Variable temperature ^{1}H NMR of [Cu^{I}(TPMA)Br] with 1.0 eq TPMA (400 MHz, acetone-*d*6). **A)** 280K **B)** 250K **C)** 235K **D)** 226K **E)** 200K **F)** 185K.

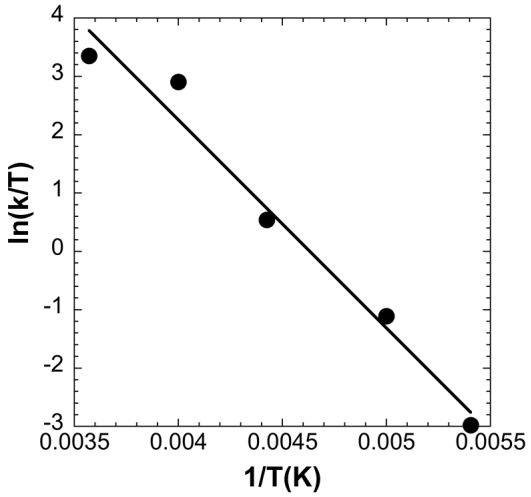

Figure 7.4.2. Eyring plot of TPMA exchange rate constants.

dissociation is a likely mechanism for the activation step of ATRA. However, it is important to note the importance of the TPMA ligand for activity in ATRA systems. ATRA with $Cu^{I}Br$ and $Cu^{I}Cl$ at the low concentrations used in this study was not found to produce monoadduct in quantities greater than can be attributed to free radical chain transfer initiated by AIBN (~20% with CCl_4 and 1-hexene).

7.5 Phosphine Inhibition

To investigate if ATRA can still proceed when the fifth coordination site is blocked by a large, strongly binding ligand, triphenyl phosphine (PPh_3), was added to the reaction mixtures in various concentrations. PPh_3 is known to bind to copper complexes with the TPMA ligand, especially when a non-coordinating anion is used. The molecular structure of $[Cu(TPMA)PPh_3][BPh_4]$ has previously been reported with a dissociated ligand arm,[40, 43] but ^{1}H NMR studies have indicated that all three pyridyl arms and PPh_3 are bound or in a fast exchange in solution making it an ideal complex to test whether ATRA will proceed efficiently as a result of partial TPMA dissociation. ATRA with several alkenes

Table 7.5.1. ATRA reactions of CCl_4 with $Cu^I(TPMA)BPh_4$ in the presence of PPh_3.[a]

		Conversion(yield) (%)			
Alkene	**$[Alkene]_0$:$[Cu]_0$**	**0 Eq. PPh_3**	**2 Eq. PPh_3**	**20 Eq. PPh_3**	**40 Eq. PPh_3**
1-hexene	5000:1	100(100)	100(100)	84(84)	38(38)
1-octene	5000:1	100(100)	100(100)	71(71)	22(22)
styrene	1000:1	46(31)	37(24)	0(0)	-
methyl acrylate	1000:1	50(100)	49(1000)	35(100)	-

[a]Reactions performed at 60°C in CH_3CN, $[alkene]_0$:$[CCl_4]_0$:$[AIBN]_0$=1:1:0.05, $[alkene]_0$=2.39 M. Conversion and yield were calculated by ^1H NMR using 1,4-dimethoxybenzene as an internal standard.

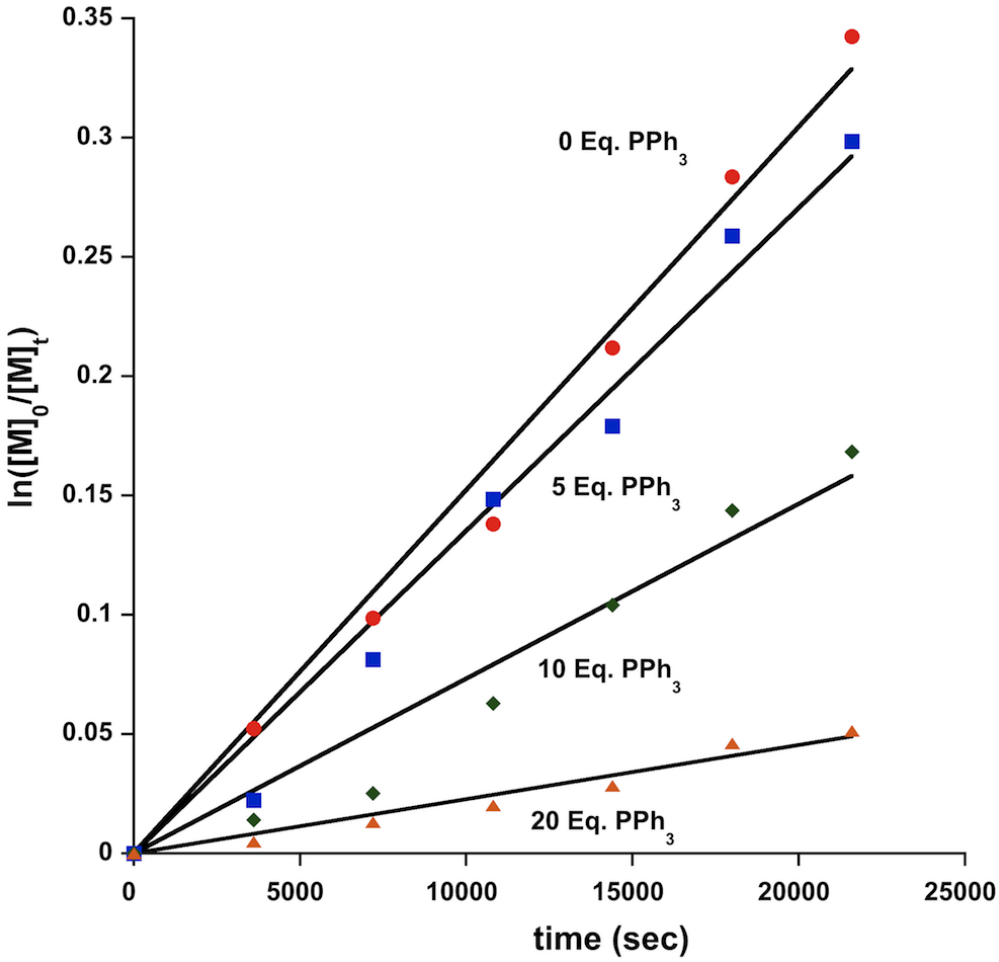

Figure 7.5.1. First order kinetic plots of ATRA of CCl_4 and 1-octene mediated by $[Cu^{II}(TPMA)Cl][Y]$ (Y=Cl^-, BPh_4^-) in the presence of 0 (●), 5 (■), 10 (◆) and 20 (▲) equivalents of PPh_3. Reactions performed at 60°C in CH_3CN, $[1\text{-octene}]_0$:$[CCl_4]_0$:$[AIBN]_0$[:$Cu]_0$= 500:500:25:1, $[alkene]_0$=2.39 M. Conversion and yield were calculated by ^1H NMR using 1,4-dimethoxybenzene as an internal standard.

in the presence of 1-10 eq. of PPh_3 proceeded efficiently in the case of 1-hexene and 1-octene (Table 7.5.1). However, a negative effect was observed for product yields in the cases of styrene and methyl acrylate, where polymers can be formed by poor trapping or free radical initiation by the decomposition of AIBN. Increased concentrations of PPh_3 were even found to have a detrimental effect on the conversion of α-olefins. These results were reflected in kinetic monitoring of 1-octene conversion, where the observed rate decreased from 1.5×10^{-5} M^{-1} s^{-1} without PPh_3 to 1.4×10^{-5} $M^{-1}s^{-1}$, 7.3×10^{-6} $M^{-1}s^{-1}$, 2.3×10^{-6} $M^{-1}s^{-1}$ with 5, 10, and 20 eq., respectively (Figure 7.5.1). Similar results were found when tributyl phosphite ($P(OBu)_3$) was added, but 4,4'-dipyridyl, which has also been shown to bind $[Cu^I(TPMA)BPh_4]$,[40] was found to have no effect up to 40 equivalents relative to copper. We found that addition of PPh_3 in low with the TPMA ligand has no appreciable effect on conversion of alkene but only on product selectivity, which agrees with previously reported kinetics of copper catalyzed ATRA in the presence of free radical reducing agents. At elevated concentrations of PPh_3, the formation of $Cu(PPh_3)_x$ (x=3 or 4) is likely. Complexes of this type, ($[Cu^I(PPh_3)_3CH_3CN][ClO_4]$, $[Cu^I(PPh_3)_3][BPh_4]$, $[Cu^I(PPh_3)_3(PPh_3)][BPh_4]$) were synthesized (Appendix F) and were found to have no activity in ATRA systems and thus a decrease of conversion in these cases is expected even though a copper complex is present.

7.6 ATRA with Tris(2-(dimethylamino)phenyl)amine Ligand

The tetradentate ligand tris(2-(dimethylamino)phenyl)amine (TDAPA) is structurally similar to TPMA and Me_6TREN ligands, which are among the most active

ligands for ATRA (Scheme 7.6.1). Initially, it was rationalized that the TDAPA ligand would also show high activity in ATRA systems when complexed to $CuCl_2$ and $CuBr_2$. However, very poor activity of TDAPA/$CuCl_2$ was observed in the addition of CCl_4 to 1-hexene, 1-octene, styrene and methyl acrylate.

The addition of CCl_4 to 1-hexene and 1-octene, which produces nearly quantitative yields with [Cu^{II}(TPMA)Cl][Cl] at catalyst loadings as low as 5000:1, was observed to achieve very low yields (~25%) with [Cu^{II}(TDAPA)Cl][Cl] at with catalyst loadings as

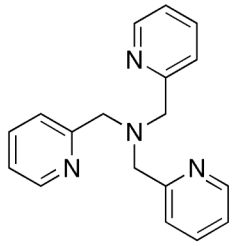

Tris(2-pyridylmethyl)amine
(TPMA)

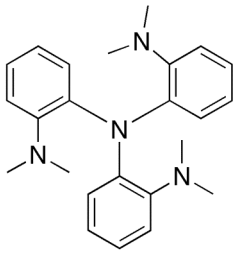

Tris(2-(dimethylamino)phenyl)amine
(TDAPA)

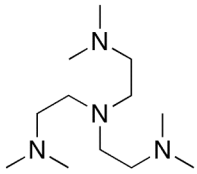

Tris(2-(dimethylamino)ethyl)amine
(Me_6TREN)

Scheme 7.6.1. Structurally similar tetradentate nitrogen-based ligands

Table 7.6.1. ATRA of CCl_4 to alkenes with [Cu^{II}(TDAPA)Cl][Y] (Y=Cl^-, BF_4^-, BPh_4^-) in the presence of AIBN.[a]

Alkene	Anion	Conv.(Yield)(%)
1-hexene	Cl^-	24(24)
1-octene		25(25)
styrene		41(7)
methyl acrylate		100(1)
1-hexene	BF_4^-	49(49)
1-octene		59(59)
styrene		50(35)
methyl acrylate		100(10)
1-hexene	BPh_4^-	60(60)
1-octene		45(45)

[a]Reactions performed at 60°C in CH_3CN, $[alkene]_0$:$[CCl_4]_0$:$[AIBN]_0$:$[Cu]_0$=250:250:12.5:1, $[alkene]_0$=2.39 M. Conversion and yield were calculated by ^{1}H NMR using 1,4-dimethoxybenzene as an internal standard.

high as 250:1 (Table 7.6.1). The high conversions in the case of styrene and methyl acrylate are due to free radical polymerization, presumably initiated by AIBN, and monoadduct yields in both cases were very low. The ATRA results with $[Cu^{II}(TDAPA)Cl][Cl]$ are equal to those achieved in the absence of catalyst via free radical initiation of CCl_4 by AIBN. Upon examination of the ligand structure, it was hypothesized that the phenyl substituent on the ligand backbone reduced lability of the ligand because of steric constraints and the lack of free rotation possible about the ligand arm and thus when the complex has a strongly coordinating anion, activation is very slow. This assumption was validated by replacing the anion with BPh_4- and BF_4-, which showed improvements in ATRA yields for both 1-hexene and 1-octene (45%-60%) under identical conditions. However, the use of a non-coordinating counter-ion still does not

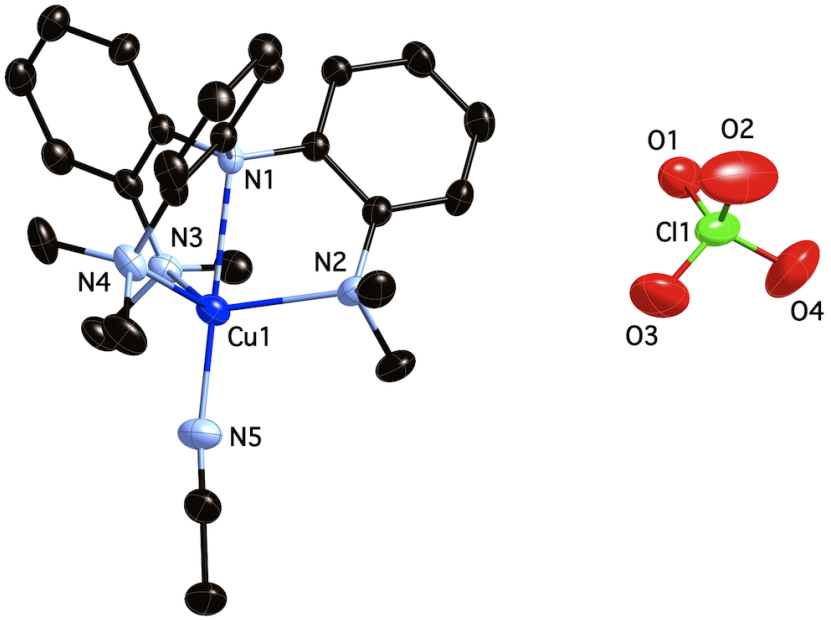

Figure 7.6.1. Molecular structure of $[Cu^{I}(TDAPA)CH_3CN][ClO_4]$ collected at 150 K, shown at 50% probability ellipsoids with H-atoms omitted for clarity. Selected bond distances [Å] and angles[°]: Cu1-N1 2.372(2), Cu1-N2 2.234(2), Cu1-N3 2.267(3), Cu1-N4 2.206(2), Cu1-N5 1.953(3), N1-Cu1-N2 75.69(8), N1-Cu1-N3 75.03(8), N1-Cu1-N4 75.77(8), N1-Cu1-N5 175.49(11), N2-Cu1-N3 115.86(9), N2-Cu1-N4 113.40(9), N3-Cu1-N4 112.57(9), N2-Cu1-N5 103.09(12), N3-Cu1-N5 101.90(12), N4-Cu1-N5 108.60(11)

increase activity to the level of TPMA or Me_6TREN complexes, suggesting that partial ligand dissociation maybe be essential for tetradentate ligands.

To rule out the possibility of weak coordination of TDAPA ligand to copper(I) salts, the molecular structure of $[Cu^I(TDAPA)CH_3CN][ClO_4]$ was obtained (Figure 7.6.1, Appendix F). The copper(I) center was found to be coordinated in a distorted tetrahedral geometry by N2, N3, N4, and N5 with Cu-N bond lengths of 2.234(2), 2.267(3), 2.206 (2), and 1.953(3) Å. The Cu-N1 distance was found to be elongated to 2.372(2) Å, similar to copper(I) complexes with the TPMA ligand. The angles about Cu1, excluding N1, are all close to that for a regular tetrahedron. Due to the preferred tetrahedral geometry of copper(I) complexes and the ligand geometry which forces N1 to be within bonding distance of copper, $[Cu^I(TDAPA)CH_3CN][ClO_4]$ is best described as pseudo-pentacoordinated. The Cu1-N bond lengths for N2, N3, and N4 are all slightly longer than are typically seen for $[Cu^I(TPMA)CH_3CN]$ (~2.1 Å), which is presumably due to the rigidity of the ligand backbone preventing further torsion of the arm to allow closer coordination. Copper(II) complexes with TDAPA ligand were found to adopt a similar trigonal bipyramidyl geometry, similar to that with TPMA ligands.[45] Thus, the molecular structures of copper(I) and copper(II) complexes provides little evidence for reduced ATRA activity except that the ligand is clearly more rigid, which supports the claim that fluxionality for copper complexes with tetradentate ligands is required for good activity in ATRA.

The solution state structure of $[Cu^I(TDAPA)CH_3CN][ClO_4]$ was probed by ^1H NMR spectroscopy for a comparison of fluxionality with the corresponding TPMA complex. At room temperature, the signals for phenyl and acetonitrile protons were

observed to be broadened and shifted downfield from the free ligand, indicating coordination and fluxionality at these positions. However, a sharp peak was observed for the methyl protons upfield of the free ligand. These protons would be expected to be affected to the greatest extent by a dissociation/association equilibrium due to their proximity to the binding site. The disparity of fluxionality between the phenyl protons and the methyl protons suggests that the cause of fluxionality of the phenyl protons is not due to ligand displacement.

7.7 Conclusions

The catalytic mechanism of ATRA in the presence of the tetradentate ligand TPMA was examined because recently [Cu^{I}(TPMA)X] (X=Cl,Br) complexes were found to be pseudo-pentacoordinated in the solid state as a result of halide coordination. Two possible pathways for an alkyl halide to oxidize a coordinatively saturated copper(I) complex, halide dissociation or partial TPMA dissociation, were considered. Halides were found to be highly cuprophilic by cyclic voltammetry and ^{1}H NMR, suggesting that dissociation is not likely. The TPMA ligand was observed to be fluxional by ^{1}H NMR and rate constants for total displacement were measured in order to calculate thermodynamic parameters ($\Delta G^{\ddagger}$=43.25 KJ mol^{-1}). To test this, PPh_3 was added to ATRA reactions to coordinatively saturate the copper(I) complex but was found to have little effect until large excesses were used indicating that partial TPMA dissociation is likely as a mechanism for alkyl halide cleavage. Inhibition in the presence of large excesses of free PPh_3 was due to the formation of copper phosphine complexes, which were not active in ATRA. Finally, the tris(2-(dimethylamino)phenyl)amine ligand was also examined as a ligand for ATRA, but was found to have very low activity. The most

likely reason for this is the lack of fluxionality of the ligand arms to create a coordination site for alkyl halide cleavage.

7.8 Experimental Part

Materials - All chemicals were purchased from commercial sources and used as received. Tris(2-pyridylmethyl)amine[46] and tetrakis(acetonitrile)copper(I) perchlorate[47] were synthesized according to literature procedures. Although we have experienced no problems, perchlorate metal salts are potentially explosive and should be handled with care. All manipulations involving copper(I) complexes were performed under argon in the dry box (<1.0 ppm O_2 and <0.5 ppm H_2O) or using standard Schlenk line techniques. Solvents (pentane, acetonitrile, acetone, and diethyl ether) were degassed and deoxygenated using an Innovative Technology solvent purifier. Methanol was vacuum distilled and deoxygenated by bubbling argon for 30 min prior to use. Synthesis of copper(II) complexes were performed in ambient conditions and solvents were used as received.

General Procedure for ATRA with Different Counter-ions in the Presence of AIBN- In a vial, 3.22 mmol alkene was combined with 310 μL CCl_4 (3.22 mmol), 26.4 mg AIBN (0.16 mmol), and an appropriate amount of CH_3CN so the total volume was 1.22 mL (for 1-hexene or 1-octene) of 0.896 mL (for styrene or methyl acrylate). *p*-methoxybenzene was added as an internal standard. The reaction mixture was then

divided equally into four NMR tubes (5 mm) and different volumes of copper complex from a 0.01 M solution in CH_3CN was added. The volumes were then adjusted with CH_3CN so the total volume was 384 μL and the [alkene]= 2.10 M in each reaction tube. The tubes were then flushed with argon for 30 sec, capped with a standard plastic NMR tube cap, and finally sealed with Teflon tape. The reactions were then left to sit in a 60°C oil bath for 24 hr. Upon completion, the reactions were analyzed for conversion and yield by ^{1}H NMR.

General Procedure for ATRA with Different Counter-ions without Reducing Agents - In a vial in a drybox (O_2 < 0.5 ppm), 580 μL methyl acrylate (6.44 mmol) was combined with 622 μL CCl_4 (6.44 mmol), 1.87 mL CH_3CN, 0.0644 mmol of copper(I) complex, and 0.0644 mmol of copper(II) complex. *p*-methoxybenzene was added as an internal standard and [alkene]= 2.10 M. The reaction mixture was then divided equally into eight NMR tubes (5 mm), capped with a standard plastic NMR tube cap, and sealed with Teflon tape. The reactions were then left to sit in a 60°C oil bath and removed at timed intervals. Upon completion, the reactions were analyzed for conversion and yield by ^{1}H NMR.

Phosphine Inhibition Reactions - In a vial, 4.03 mmol alkene was combined with 388 μL CCl_4 (4.03 mmol), 33.1 mg AIBN (0.20 mmol), 80 μL of 0.01 M solution in CH_3CN of [Cu(TPMA)Cl][Y] (where Y=Cl, BPh_4) (8 x 10^{-7} mol), and an appropriate volume of CH_3CN so the total volume was 1.18 mL. *p*-methoxybenzene was added as an internal standard. The reaction mixture was then divided equally into five NMR tubes (5 mm)

and different volumes of inhibitor (PPh_3, $P(OBu)_3$, 4,4'-dipyridyl) from a 0.05 M solution in CH_3CN were added. The volumes were then adjusted by adding CH_3CN in order to make each reaction mixture 2.21 M in alkene. The tubes were then flushed with argon for 30 sec, capped with a standard plastic NMR tube cap, and finally sealed with Teflon tape. The reactions were then left to sit in a 60°C oil bath for 24 hr. Upon completion, the reactions were analyzed for conversion and yield by ^{1}H NMR.

Calculation of Equilibrium Constant of TPMA Dissociation - In a drybox with argon atmosphere (O_2<0.5 ppm), Cu(TPMA)Br and 1.0 equivalents of TPMA were dissolved in acetone-*d*6 and sealed in an air tight 5mm NMR tube and observed by variable temperature ^{1}H NMR. Using previously reported methods,[44] the rate constant was measured at each temperature and plotted using the Eyring equation to extract thermodynamic parameters.

Measurement of Equilibrium Constants for Copper Complexes - In a drybox, 3.0 mL of a 5 mM solution of [Cu^I(TPMA)Y] (Y=Cl, ClO_4, PF_6) (1.5 x 10^{-5} mol), was added to a quartz cuvette with a septum. Once the airtight cuvette was removed from the drybox, 1.7 μL (1.5 x 10^{-5} mol) of degassed benzyl chloride was added. The solution was shaken vigorously and the absorbance was measured by UV-vis at 958 nm for three hours. K_{ATRA} was calculated using previously published procedures,[48].

Synthesis of [Cu^I(TDAPA)CH_3CN][ClO_4] – In a drybox, 50.0 mg (0.13 mmol) tris(2-(dimethylamino)phenyl)amine (TDAPA) was dissolved in 5.0 mL acetonitrile, followed

by addition of 44.0 mg (0.13 mmol) $[Cu^{I}(CH_3CN)_4][ClO_4]$ and stirred until dissolved. 10.0 mL of diethyl ether was added and the solution left at -35ºC overnight. 40.2 mg (52% yield) of white powder was collected by filtration. Slow evaporation of diethyl ether into a concentrated solution afforded colorless crystals suitable for X-ray analysis. ^{1}H NMR ($(CD_3)_2CO$, 400 MHz, 296K): δ7.49-7.22 (m, 12H), δ3.13 (bs, 3H), δ2.28 (s, 18H). C, 53.97; H, 5.75; N, 12.10. Found: C, 53.75; H, 5.66; N, 12.03.

NMR spectroscopy - ^{1}H NMR spectra were obtained using Bruker Avance 400 and 500 MHz spectrometers and chemical shifts are given in ppm relative to residual solvent peaks [$CDCl_3$ δ 7.26 ppm; $(CD_3)CO$ δ 2.05 ppm; CD_3CN δ 1.96 ppm]. ^{31}P NMR was referenced externally with 85% H_3PO_4 in D_2O at δ 0. iNMR and KaleidaGraph software was used to generate images of NMR spectra. Temperature calibrations were performed using a pure methanol sample.

X-ray Crystal Structure Determination - The X-ray intensity data were collected at 150K using graphite-monochromated Mo-*K* radiation (0.71073 Å) with a Bruker Smart Apex II CCD diffractometer. Data reduction included absorption corrections by the multi-scan method using SADABS.[49] Structures were solved by direct methods and refined by full matrix least squares using SHELXTL 6.1 bundled software package.[50] The H-atoms were positioned geometrically (aromatic C-H 0.93, methylene C-H 0.97, and methyl C-H 0.96) and treated as riding atoms during subsequent refinement, with $U_{iso}(H) = 1.2U_{eq}(C)$ or $1.5U_{eq}$(methyl C). The methyl groups were allowed to rotate about their local threefold axes. ORTEP-3 for windows[51] and Crystal Maker 7.2 were

used to generate molecular graphics.

Conductivity - Conductivity measurements were performed using a VWR© Traceable Bench/Portable Conductivity Meter (23226-505) in a drybox (O_2<0.5 ppm) using 1 mM solutions of copper complex in acetonitrile.

Infrared Spectroscopy - IR spectra were recorded in the solid state using Nicolet Smart Orbit 380 FT-IR spectrometer (Thermo Electron Corporation).

Elemental Analysis for C, H, and N - Elemental analyses for C, H, and N were obtained from Midwest Microlabs, LLC.

Cyclic voltammetry - Electrochemical measurements were carried out using Bioanalytical Systems (BAS) model CV-50W in a dry box. Cyclic voltammograms were recorded with a standard three-electrode system consisting of a Pt-wire working electrode, a standard calomel reference electrode, and a Pt-wire auxiliary electrode. Tetrabutyammonium perchlorate (TBA-ClO_4), tetrabutylammonium tetraphenylborate (TBA-BPh_4), tetrabutylammonium chloride (TBA-Cl), and tetrabutylammonium bromide (TBA-Br) were used as the supporting electrolyte, and all voltammograms were externally referenced to ferrocene. As such, the potentials are reported with respect to Fc/Fc+ couple, without junction correction. All cyclic voltammograms were simulated digitally to obtain the half-wave potentials.

7.9 References

(1) Kharasch, M. S.; Jensen, E. V.; Urry, W. H., Addition of Carbon Tetrabromide and Bromoform to Olefins. *J. Am. Chem. Soc.* **1946,** *68*(1), 154-155.

(2) Kharasch, M. S.; Jensen, E. V.; Urry, W. H., Addition of Carbon Tetrachloride and Chloroform to Olefins. *Science* **1945,** *102*(2640), 128.

(3) Severin, K., Ruthenium Catalysts for the Kharasch Reaction. *Curr. Org. Chem.* **2006,** *10*, 217-224.

(4) Quebatte, L.; Scopelliti, R.; Severin, K., Atom Transfer Radical Additions with the Cationic Half-Sandwich Complex [Cp*Ru(pPh3h(CH3CN)]OTf *Eur. J. Inorg. Chem.* **2005,** (16), 3353-3358.

(5) Quebatte, L.; Haas, M.; Solari, E.; Scopelliti, R.; Nguyen, Q. T.; Severin, K., Combinatorial catalysis with bimetallic complexes: robust and efficient catalysts for atom-transfer radical additions. *Angew. Chem., Int. Ed.* **2004,** *43*(12), 1520-1524.

(6) Clark, A. J., Atom Transfer Radical Cyclisation Reactions Mediated by Copper Complexes. *Chem. Soc. Rev.* **2002,** *31*(1), 1-11.

(7) Clark, A. J.; Dell, C. P.; Ellard, J. M.; Hunt, N. A.; McDonagh, J. P., Efficient Room Temperature Copper(I) Mediated 5-endo Radical Cyclisation. *Tetrahedron Lett.* **1999,** *40*(49), 8619-8623.

(8) Bland, W. J.; Davis, R.; Durrant, J.; Jim, L. A., The Mechanism of the Addition of Tetrahaloalkanes to Alkenes in the Presence of [RuCl2(PPh3)3] *J. Organomet. Chem.* **1984,** *267*, C45-C48.

(9) Nagashima, H.; Wakamatsu, H.; Itoh, K.; Tomo, Y.; Tsuji, J., New Regio- and Stereoselective Preparation of Trichlorinated l-Butyrolactones by Copper Catalyzed Cyclization of Allyl Trichloroacetates. *Tetrahedron Lett.* **1983,** *24*(23), 2395-2398.

(10) Minisci, F., Free-Radical Additions to Olefins in the Presence of Redox Systems. *Acc. Chem. Res.* **1975,** *8*(5), 165-171.

(11) Asscher, M.; Vosfsi, D., Chlorine Activation by Redox-transfer. Part II. The Addition of Carbon Tetrachloride to Olefins. *J. Chem. Soc.* **1963**, 1887-1896.

(12) Asscher, M.; Vosfsi, D., Chlorine Activation by Redox-transfer. Part III. The "Abnormal" Addition of Chloroform to Olefins. *J. Chem. Soc.* **1963**, 3921-3927.

(13) Curran, D. P., The Design and Application of Free Radical Chain Reactions in Organic Synthesis. Part 2. *Synthesis* **1988,** (7), 489-513.

(14) Pintauer, T.; Matyjaszewski, K., Structural Aspects of Copper Catalyzed Atom Transfer Radical Polymerization. *Coord. Chem. Rev.* **2005,** *249*(11-12), 1155-1184.

(15) Pintauer, T., "Greening" of copper catalyzed atom transfer radical addition (ATRA) and cyclization (ATRC) reactions. *ACS Symp. Ser.* **2009,** *1023*, 63-84.

(16) Eckenhoff, W. T.; Pintauer, T., Copper Catalyzed Atom Transfer Radical Addition (ATRA) and Cyclization (ATRC) Reactions in the Presence of Reducing Agents. *Cat. Rev. - Sci. Eng.* **2009,** *51*(1), 1-59.

(17) Eckenhoff, W. T.; Garrity, S. T.; Pintauer, T., Highly Efficient Copper-Mediated Atom Transfer Radical Addition (ATRA) in the Presence of a Reducing Agent. *Eur. J. Inorg. Chem.* **2008,** (4), 563-571.

(18) Eckenhoff, W. T.; Pintauer, T., Atom Transfer Radical Addition in the Presence of Catalytic Amounts of Copper(I/II) Complexes with Tris(2-pyridylmethyl)amine *Inorg. Chem.* **2007,** *46*(15), 5844-5846.

(19) Quebatte, L.; Thommes, K.; Severin, K., Highly Efficient Atom Transfer Radical Addition Reactions with a RuIII Complex as a Catalyst Precursor. *J. Am. Chem. Soc.* **2006,** *128*(23), 7440-7441.

(20) Nair, R. P.; Kim, T. H.; Frost, B. J., Atom Transfer Radical Addition Reactions of CCl4, CHCl3, and p-Tosyl Chloride Catalyzed by Cp'Ru(PPh3)(PR3)Cl Complexes. *Organometallics* **2009,** *28*(16), 4681-4688.

(21) Lundgren, R. J.; Rankin, M. A.; McDonald, R.; Stradiotto, M., Neutral, Cationic, and Zwitterionic Ruthenium(II) Atom Transfer Radical Addition Catalysts Supported by P,N-Substituted Indene or Indenide Ligands. *Organometallics* **2008,** *27*(2), 254-258.

(22) Pintauer, T., Catalyst Regeneration in Transition-Metal-Mediated Atom-Transfer Radical Addition (ATRA) and Cyclization (ATRC) Reactions *Eur. J. Inorg. Chem.* **2010,** *17*, 2449-2460.

(23) Balili, M. N. C.; Pintauer, T., Kinetic Studies of the Initiation Step in Copper Catalyzed Atom Transfer Radical Addition (ATRA) in the Presence of Free Radical Diazo Initiators as Reducing Agents *Inorg. Chem.* **2010,** *49*(12), 5642-5649.

(24) Ricardo, C.; Pintauer, T., Copper catalyzed atom transfer radical cascade reactions in the presence of free-radical diazo initiators as reducing agents. *Chem. Comm.* **2009,** (21), 3029-3031.

(25) Balili, M. N. C.; Pintauer, T., Persistent Radical Effect in Action: Kinetic Studies of Copper-Catalyzed Atom Transfer Radical Addition in the Presence of Free-Radical Diazo Initiators as Reducing Agents. *Inorg. Chem.* **2009,** *48*(18), 9018-9026.

(26) Pintauer, T.; Eckenhoff, W. T.; Ricardo, C.; Balili, M. N. C.; Biernesser, A. B.; Noonan, S. T.; Taylor, M. J. W., Highly Efficient Ambient-Temperature Copper-Catalyzed Atom-Transfer Radical Addition (ATRA) in the Presence of Free-Radical Initiator (V-70) as a Reducing Agent *Chem. Eur. J.* **2009,** *15*(1), 38-41.

(27) Thommes, K.; Severin, K., Olefin Cyclopropanations via Sequential Atom Transfer Radical-Dechlorination Reactions. *Chimia* **2010,** *64*(3), 188-190.

(28) Wolf, J.; Thommes, K.; Briel, O.; Scopelliti, R.; Severin, K., Dinuclear Ruthenium Ethylene Complexes: Syntheses, Structures, and Catalytic Applications in ATRA and ATRC Reactions. *Organometallics* **2008,** *27*(17), 4464-4474.

(29) Munoz-Molina, J. M.; Belderrain, T. R.; Perez, P. J., Copper-Catalyzed Synthesis of 1,2-Disubstituted Cyclopentanes from 1,6-Dienes by Ring-Closing Kharasch Addition of Carbon Tetrachloride *Adv. Synth. Catal.* **2008,** *350*, 2365-2372.

(30) Fernández-Zúmel, M. A.; Kiefer, G.; Thommes, K.; Scopelliti, R.; Severin, K., Ruthenium vs. Osmium Complexes as Catalysts for Atom Transfer Radical Addition Reactions *Eur. J. Inorg. Chem.* **2010,** (23), 3596-3601.

(31) Thommes, K.; Kiefer, G.; Scopelliti, R.; Severin, K., Olefin Cyclopropanation by a Sequential Atom-Transfer Radical Addition and Dechlorination in the Presence of a Ruthenium Catalyst. *Angew. Chem. Int. Ed.* **2009,** *48*(43), 8115-8119.

(32) Fernandez-Zumel, M. A.; Thommes, K.; Kiefer, G.; Sienkiewicz, A.; Pierzchala, K.; Severin, K., Atom-Transfer Radical Addition Reactions Catalyzed by RuCp* Complexes: A Mechanistic Study *Chem. Eur. J.* **2009,** *15*(43), 11601-11607.

(33) Thommes, K.; Icli, B.; Scopelliti, R.; Severin, K., Atom Transfer Radical Addition (ATRA) and Cyclization (ATRC) Reactions Catalyzed by a Mixture of [RuCl2Cp*(PPh3)] and Magnesium. *Chem. Eur. J.* **2007,** *13*(24), 6899-6907.

(34) Taylor, M. J. W.; Eckenhoff, W. T.; Pintauer, T., Copper Catalyzed Atom Transfer Radical Addition (ATRA) and Cyclization Reactions in the Presence of Environmentally Benign Ascorbic Acid as a Reducing Agent. *Dalton Trans.* **2010,** *In Press*.

(35) Matyjaszewski, K., Radical Nature of Cu-Catalyzed Controlled Radical Polymerizations (Atom Transfer Radical Polymerization). *Macromolecules* **1998,** *31*(15), 4710-4717.

(36) Matyjaszewski, K.; Xia, J., Atom Transfer Radical Polymerization. *Chem. Rev.* **2001,** *101*(9), 2921-2990.

(37) Tsarevsky, N.; Braunecker, W. A.; Vacca, A.; Gans, P.; Matyjaszewski, K., Competitive Equilibria in Atom Transfer Radical Polymerization. *Macromol. Symp.* **2007,** *248*, 60-70.

(38) Tsarevsky, N.; Braunecker, W. A.; Matyjaszewski, K., Electron Transfer Reactions Relevant to Atom Transfer Radical Polymerization. *J. Organomet. Chem.* **2007,** *692*(15), 3212-3222.

(39) Hsu, S. C.; Chien, S. S.; Chen, H. H.; Chiang, M. Y., Synthesis and Characterization of Copper(I) Complexes Containing Tris(2-pyridylmethyl)amine Ligand. *J. Chin. Chem. Soc.* **2007,** *54*(3), 685-692.

(40) Eckenhoff, W. T.; Pintauer, T., Structural Comparison of Copper(I) and Copper(II) Complexes with Tris(2-pyridylmethyl)amine Ligand in Atom Transfer Radical Addition. *Inorg. Chem.* **2010,** *49*(22), 10617-10626.

(41) Lin, C. Y.; Coote, M. L.; Gennaro, A.; Matyjaszewski, K., Ab Initio Evaluation of the Thermodynamic and Electrochemical Properties of Alkyl Halides and Radicals and Their Mechanistic Implications for Atom Transfer Radical Polymerization. *J. Am. Chem. Soc.* **2008,** *130*(38), 12762-12774.

(42) Bortolamei, N.; Isse, A. A.; Di Marco, V. B.; Gennaro, A.; Matyjaszewski, K., Thermodynamic Properties of Copper Complexes Used as Catalysts in Atom Transfer Radical Polymerization. *Macromolecules* **2010,** *43*(22), 9257-9267.

(43) Tyeklar, Z.; Jacobson, R. R.; Wei, N.; Murthy, N. N.; Zubieta, J.; Karlin, K. D., Reversible reaction of dioxygen (and carbon monoxide) with a copper(I) complex. X-ray structures of relevant mononuclear Cu(I) precursor adducts and the trans-(.mu.-1,2-peroxo)dicopper(II) product. *J. Am. Chem. Soc.* **1993,** *115*(7), 2677-2689.

(44) Crabtree, R. H., Physical Methods in Organometallic Chemistry. In *The Organometallic Chemistry of the Transition Metals*, 4 ed.; John Wiley & Sons Inc.: Hoboken, NJ, 2005; pp 275-296.

(45) Chu, L.; Hardcastle, K. I.; MacBeth, C. E., Transition Metal Complexes Supported by a Neutral Tetraamine Ligand Containing N,N-dimethylaniline Units. *Inorg. Chem.* **2010**.

(46) Britovsek, G.; England, J.; White, A., Non-Heme Iron(II) Complexes Containing Tripodal Tetradentate Nitrogen Ligands and Their Application in Alkane Oxidaion Catalysis. *Inorg. Chem.* **2005,** *44*(22), 8125-8134.

(47) Munakata, M.; Kitagawa, S.; Asahara, A.; Masuda, H., Crystal structure of bis(2,2'-bipyridine)copper(I) perchlorate. *Bull. Chem. Soc. Jpn.* **1987,** *60*(5), 1927-1929.

(48) Fischer, H., The Persistent Radical Effect: A Principle for Selective Radical Reactions and Living Radical Polymerizations. *Chem. Rev.* **2001,** *101*, 3581-3610.

(49) Sheldrick, G. M., *SADABS Version 2.03*. University of Gottingen, Germany: 2002.

(50) Sheldrick, G. M., *SHELXTL 6.1,Crystallographic Computing System*. Bruker Analytical X-Ray System: Madison, WI, 2000.

(51) Faruggia, L. J., ORTEP-3 for Windows. *J. Appl. Cryst.* **1997,** *30 (5, Pt. 1)*, 565.

Appendix A.

A.1 Product Characterization

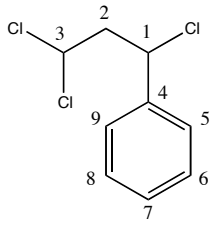

(1,3,3-Trichloropropyl)benzene. ^{1}H NMR ($CDCl_3$, 300 MHz, RT): δ7.41 (m, 5H, C5-C9), δ5.82 (dd, 1H, J_1=8.3 Hz, J_2=5.0 Hz, C3), δ5.09 (dd, 1H, J_1=9.3, J_2=5.1 Hz, C1), δ2.99 (m, 1H, C2), δ2.79 (m, 1H, C2).

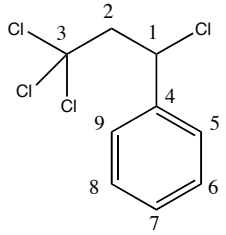

(1,3,3,3-Tetrachloropropyl)benzene. ^{1}H NMR ($CDCl_3$, 300 MHz, RT): δ7.64 (m, 5H, C4-C9), δ5.31 (t, 1H, J=6.0 Hz, C1), δ3.60 (m, 2H, C2).

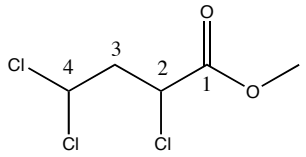

Methyl-2,4,4-trichlorobutanoate. ^{1}H NMR ($CDCl_3$, 300 MHz, RT): δ5.91 (dd, 1H, J_1=8.7 Hz, J_2=4.5 Hz, C4), δ5.42 (dd, 1H, J_1=9.6 Hz, J_2=4.8 Hz, C2), δ3.82 (s, 3H, O-CH_3), δ2.83 (m, 2H, C3).

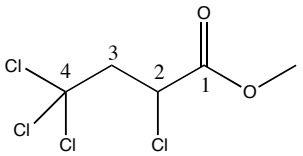

Methyl-2,4,4,4-tetrachlorobutanoate. ^{1}H NMR ($CDCl_3$, 300 MHz, RT): δ4.61 (dd, 1H, J_1=8.1 Hz, J_2=3.6 Hz, C2), δ3.82 (s, 3H, O-CH_3), δ2.83 (dd, 2H, J_1=15.2 Hz, J_2=3.8 Hz, C3).

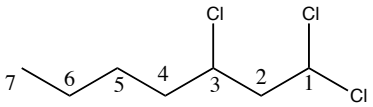

1,1,3-trichloroheptane. ^{1}H NMR ($CDCl_3$, 300 MHz, RT): δ6.03 (t, 1H, *J*=6.6 Hz, C1), δ4.11 (m, 1H, C3), δ2.56 (t, 2H, *J*=6.8 Hz, C2), δ1.75 (m, 2H, C4), δ1.39 (m, 4H, C5-C6), δ0.98 (t, 3H, *J*=6.9Hz, C7).

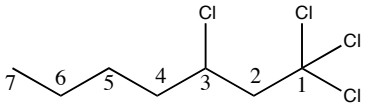

1,1,1,3-tetrachloroheptane. ^{1}H NMR ($CDCl_3$, 300 MHz, RT): δ4.26 (m, 1H, C3), δ3.20 (m, 2H, C2), δ1.87 (m, 2H, C4), δ1.45 (m, 4H, C5-C6), δ0.98 (t, 3H, *J*=6.9, C7).

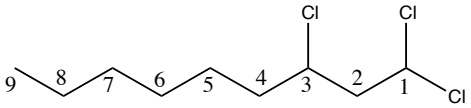

1,1,3-trichlorononane. ^{1}H NMR ($CDCl_3$, 300 MHz, RT): δ5.97 (t, 1H, *J*=6.6 Hz, C1), δ4.07 (q, 1H, *J*=6.3 Hz, C3), δ2.53 (t, 2H, *J*=6.7 Hz, C2), δ1.77 (m, 2H, C4), δ1.30 (m, 8H, C5-C8), δ0.89 (t, 3H, *J*=6.9 Hz, C9).

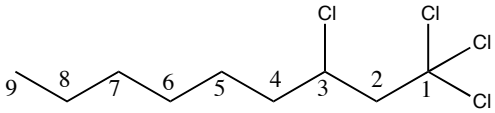

1,1,1,3-tetrachlorononane. ^{1}H NMR ($CDCl_3$, 300 MHz, RT): δ4.26 (m, 1H, H3), δ3.20 (m, 2H, C2), δ1.85 (m, 2H, C4), δ1.35 (m, 8H, C5-C8), δ0.90 (t, 3H, *J*=6.9 Hz, C9).

A.2 Crystallographic Data

Table A.2.1. Crystallographic data and experimental data for [Cu^I(TPMA)Cl].

	[Cu^I(TPMA)Cl]
Formula	$C_{18}H_{18}ClCuN_4$
Color	orange
Shape	rhomboid
Formula Weight	389.35
Crystal System	monoclinic
Space Group	c2/c
Temp (K)	150K
Cell Constants	
***a*, Å**	24.968(2)
***b*, Å**	12.9711(12)
***c*, Å**	12.5678(11)
α, deg	90
β, deg	114.7060(10)
γ, deg	90
V, $Å^3$	3697.6(6)
Formula units/unit cell	8
Dcal'd, gcm^{-3}	1.399
μ, mm^{-1}	1.332
F(000)	1600
Diffractometer	Bruker Smart ApexII
Radiation, graphite monochr.	Mo Kα (λ=0.71073 Å)
Crystal size, mm	0.250 x 0.132 x 0.082
θ range, deg	1.80< θ <25.52
Range of *h,k,l*	±30, ±15, ±15
Reflections collected/unique	14977/3435
R_{int}	0.0357
Refinement Method	Full Matrix Least-Squares on F^2
Data/Restraints/Parameters	3435/0/217
GOF on F^2	1.066
Final R indices [I>2σ(I)]	R_1=0.0821 wR_2=0.2431
R indices (all data)	R_1=0.1013 wR_2=0.2648
Max. Resid. Peaks (e*$Å^{-3}$)	4.360 and -0.406

Table A.2.2. Atomic coordinates (x 10^4) and equivalent isotropic displacement parameters (A^2 x 10^3) for [Cu^{I}(TPMA)Cl]. U(eq) is defined as one third of the trace of the orthogonalized Uij tensor.

	x	y	z	U(eq)
Cu(1)	6559(1)	3694(1)	6484(1)	26(1)
N(4)	7401(1)	3979(1)	7727(1)	25(1)
N(2)	6999(1)	4850(1)	5536(1)	25(1)
N(1)	6021(1)	5001(1)	6049(1)	26(1)
N(3)	6497(1)	2902(1)	4999(1)	26(1)
C(10)	8182(1)	3647(1)	9598(1)	32(1)
C(6)	7714(1)	4772(1)	7592(1)	25(1)
C(3)	6504(1)	5466(1)	4768(1)	30(1)
C(5)	7440(1)	5408(1)	6484(1)	30(1)
C(2)	7227(1)	4126(1)	4940(1)	29(1)
C(4)	6059(1)	5678(1)	5276(1)	26(1)
C(1)	6786(1)	3276(1)	4381(1)	28(1)
C(7)	7638(1)	3429(1)	8721(1)	27(1)
C(11)	8498(1)	4473(1)	9454(1)	37(1)
C(8)	6688(1)	2889(1)	3290(1)	37(1)
C(9)	6113(1)	2133(1)	4540(1)	33(1)
C(13)	5601(1)	5165(1)	6451(1)	31(1)
C(12)	8264(1)	5038(1)	8437(1)	33(1)
C(14)	5216(1)	5989(1)	6105(1)	37(1)
C(16)	5683(1)	6523(1)	4885(1)	33(1)
C(17)	5992(1)	1717(1)	3449(1)	40(1)
C(18)	6285(1)	2106(1)	2818(1)	43(1)
C(15)	5256(1)	6675(1)	5308(2)	41(1)
Cl(1)	6155(1)	2519(1)	7435(1)	36(1)

Table A.2.3. Bond lengths [Å] and angles [deg] for [Cu^{I}(TPMA)Cl].

Cu(1)-N(4)	2.0704(11)
Cu(1)-N(3)	2.0833(11)
Cu(1)-N(1)	2.0888(11)
Cu(1)-Cl(1)	2.3976(4)
Cu(1)-N(2)	2.4366(11)
N(4)-C(6)	1.3418(17)
N(4)-C(7)	1.3482(16)
N(2)-C(5)	1.4413(17)
N(2)-C(2)	1.4530(17)
N(2)-C(3)	1.4548(16)
N(1)-C(4)	1.3425(17)
N(1)-C(13)	1.3504(17)
N(3)-C(9)	1.3370(19)
N(3)-C(1)	1.3477(17)
C(10)-C(7)	1.380(2)
C(10)-C(11)	1.384(2)
C(10)-H(10)	0.9300
C(6)-C(12)	1.3891(19)
C(6)-C(5)	1.5215(18)
C(3)-C(4)	1.5124(19)
C(3)-H(3A)	0.9700
C(3)-H(3B)	0.9700
C(5)-H(5A)	0.9700
C(5)-H(5B)	0.9700
C(2)-C(1)	1.510(2)
C(2)-H(2A)	0.9700
C(2)-H(2B)	0.9700
C(4)-C(16)	1.3917(19)
C(1)-C(8)	1.3874(19)
C(7)-H(7)	0.9300
C(11)-C(12)	1.380(2)
C(11)-H(11)	0.9300
C(8)-C(18)	1.379(2)
C(8)-H(8)	0.9300
C(9)-C(17)	1.391(2)
C(9)-H(9)	0.9300
C(13)-C(14)	1.380(2)
C(13)-H(13)	0.9300
C(12)-H(12)	0.9300
C(14)-C(15)	1.375(2)
C(14)-H(14)	0.9300
C(16)-C(15)	1.383(2)
C(16)-H(16)	0.9300
C(17)-C(18)	1.375(2)
C(17)-H(17)	0.9300
C(18)-H(18)	0.9300
C(15)-H(15)	0.9300
N(4)-Cu(1)-N(3)	116.60(4)
N(4)-Cu(1)-N(1)	113.20(4)
N(3)-Cu(1)-N(1)	111.13(4)
N(4)-Cu(1)-Cl(1)	103.63(3)

N(3)-Cu(1)-Cl(1)	104.00(3)
N(1)-Cu(1)-Cl(1)	107.09(3)
N(4)-Cu(1)-N(2)	75.13(4)
N(3)-Cu(1)-N(2)	75.35(4)
N(1)-Cu(1)-N(2)	74.90(4)
Cl(1)-Cu(1)-N(2)	177.99(3)
C(6)-N(4)-C(7)	117.86(11)
C(6)-N(4)-Cu(1)	119.98(8)
C(7)-N(4)-Cu(1)	122.03(9)
C(5)-N(2)-C(2)	115.32(11)
C(5)-N(2)-C(3)	115.11(11)
C(2)-N(2)-C(3)	114.43(10)
C(5)-N(2)-Cu(1)	104.16(7)
C(2)-N(2)-Cu(1)	101.72(7)
C(3)-N(2)-Cu(1)	103.68(8)
C(4)-N(1)-C(13)	117.58(12)
C(4)-N(1)-Cu(1)	119.62(9)
C(13)-N(1)-Cu(1)	122.63(9)
C(9)-N(3)-C(1)	118.26(12)
C(9)-N(3)-Cu(1)	122.25(10)
C(1)-N(3)-Cu(1)	118.69(9)
C(7)-C(10)-C(11)	118.38(13)
C(7)-C(10)-H(10)	120.8
C(11)-C(10)-H(10)	120.8
N(4)-C(6)-C(12)	122.20(12)
N(4)-C(6)-C(5)	117.83(11)
C(12)-C(6)-C(5)	119.95(12)
N(2)-C(3)-C(4)	112.62(10)
N(2)-C(3)-H(3A)	109.1
C(4)-C(3)-H(3A)	109.1
N(2)-C(3)-H(3B)	109.1
C(4)-C(3)-H(3B)	109.1
H(3A)-C(3)-H(3B)	107.8
N(2)-C(5)-C(6)	112.99(11)
N(2)-C(5)-H(5A)	109.0
C(6)-C(5)-H(5A)	109.0
N(2)-C(5)-H(5B)	109.0
C(6)-C(5)-H(5B)	109.0
H(5A)-C(5)-H(5B)	107.8
N(2)-C(2)-C(1)	110.61(11)
N(2)-C(2)-H(2A)	109.5
C(1)-C(2)-H(2A)	109.5
N(2)-C(2)-H(2B)	109.5
C(1)-C(2)-H(2B)	109.5
H(2A)-C(2)-H(2B)	108.1
N(1)-C(4)-C(16)	122.40(13)
N(1)-C(4)-C(3)	117.89(11)
C(16)-C(4)-C(3)	119.60(12)
N(3)-C(1)-C(8)	121.52(14)
N(3)-C(1)-C(2)	116.71(11)
C(8)-C(1)-C(2)	121.77(13)
N(4)-C(7)-C(10)	123.24(13)
N(4)-C(7)-H(7)	118.4
C(10)-C(7)-H(7)	118.4
C(12)-C(11)-C(10)	119.13(13)
C(12)-C(11)-H(11)	120.4

C(10)-C(11)-H(11)	120.4
C(18)-C(8)-C(1)	119.70(15)
C(18)-C(8)-H(8)	120.2
C(1)-C(8)-H(8)	120.2
N(3)-C(9)-C(17)	123.02(15)
N(3)-C(9)-H(9)	118.5
C(17)-C(9)-H(9)	118.5
N(1)-C(13)-C(14)	122.99(14)
N(1)-C(13)-H(13)	118.5
C(14)-C(13)-H(13)	118.5
C(11)-C(12)-C(6)	119.19(14)
C(11)-C(12)-H(12)	120.4
C(6)-C(12)-H(12)	120.4
C(15)-C(14)-C(13)	119.04(14)
C(15)-C(14)-H(14)	120.5
C(13)-C(14)-H(14)	120.5
C(15)-C(16)-C(4)	119.03(14)
C(15)-C(16)-H(16)	120.5
C(4)-C(16)-H(16)	120.5
C(18)-C(17)-C(9)	118.45(15)
C(18)-C(17)-H(17)	120.8
C(9)-C(17)-H(17)	120.8
C(17)-C(18)-C(8)	119.04(14)
C(17)-C(18)-H(18)	120.5
C(8)-C(18)-H(18)	120.5
C(14)-C(15)-C(16)	118.95(14)
C(14)-C(15)-H(15)	120.5
C(16)-C(15)-H(15)	120.5

Table A.2.4. Anisotropic displacement parameters (A^2 x 10^3) for [Cu^{I}(TPMA)Cl]. The anisotropic displacement factor exponent takes the form: -2 pi^2 [h^2 a*^2 U11 + ... + 2 h k a* b* U12]

	U11	U22	U33	U23	U13	U12
Cu(1)	32(1)	26(1)	22(1)	1(1)	12(1)	-1(1)
N(4)	30(1)	23(1)	21(1)	1(1)	11(1)	1(1)
N(2)	31(1)	23(1)	22(1)	4(1)	12(1)	4(1)
N(1)	28(1)	28(1)	21(1)	-2(1)	9(1)	-1(1)
N(3)	33(1)	25(1)	21(1)	2(1)	12(1)	3(1)
C(10)	37(1)	36(1)	21(1)	1(1)	11(1)	10(1)
C(6)	31(1)	25(1)	23(1)	-1(1)	14(1)	1(1)
C(3)	37(1)	29(1)	25(1)	9(1)	14(1)	7(1)
C(5)	37(1)	25(1)	30(1)	4(1)	15(1)	-4(1)
C(2)	35(1)	32(1)	28(1)	5(1)	19(1)	5(1)
C(4)	28(1)	24(1)	23(1)	0(1)	7(1)	1(1)
C(1)	36(1)	26(1)	23(1)	5(1)	14(1)	10(1)
C(7)	36(1)	25(1)	23(1)	2(1)	14(1)	4(1)
C(11)	31(1)	49(1)	27(1)	-5(1)	7(1)	0(1)
C(8)	57(1)	35(1)	26(1)	4(1)	23(1)	12(1)
C(9)	42(1)	26(1)	29(1)	-1(1)	13(1)	1(1)
C(13)	30(1)	39(1)	25(1)	-6(1)	11(1)	-3(1)
C(12)	32(1)	36(1)	31(1)	-5(1)	13(1)	-7(1)
C(14)	28(1)	44(1)	39(1)	-10(1)	14(1)	0(1)
C(16)	29(1)	28(1)	38(1)	4(1)	9(1)	3(1)
C(17)	50(1)	29(1)	31(1)	-5(1)	6(1)	4(1)
C(18)	67(1)	35(1)	22(1)	-3(1)	13(1)	14(1)
C(15)	33(1)	35(1)	52(1)	-2(1)	12(1)	7(1)
Cl(1)	48(1)	33(1)	27(1)	3(1)	16(1)	-9(1)

Table A.2.5. Hydrogen coordinates (x 10^4) and isotropic displacement parameters (A^2 x 10^3) for [Cu^{I}(TPMA)Cl].

	x	y	z	U(eq)
H(10)	8332	3248	10270	38
H(3A)	6309	5107	4033	36
H(3B)	6650	6116	4612	36
H(5A)	7261	6020	6643	36
H(5B)	7749	5630	6251	36
H(2A)	7593	3831	5492	35
H(2B)	7309	4487	4348	35
H(7)	7425	2876	8819	32
H(11)	8863	4646	10034	45
H(8)	6893	3156	2878	45
H(9)	5918	1865	4971	40
H(13)	5569	4702	6986	37
H(12)	8472	5591	8320	39
H(14)	4935	6079	6406	45
H(16)	5719	6978	4348	40
H(17)	5719	1187	3152	48
H(18)	6212	1846	2084	52
H(15)	4999	7233	5057	50

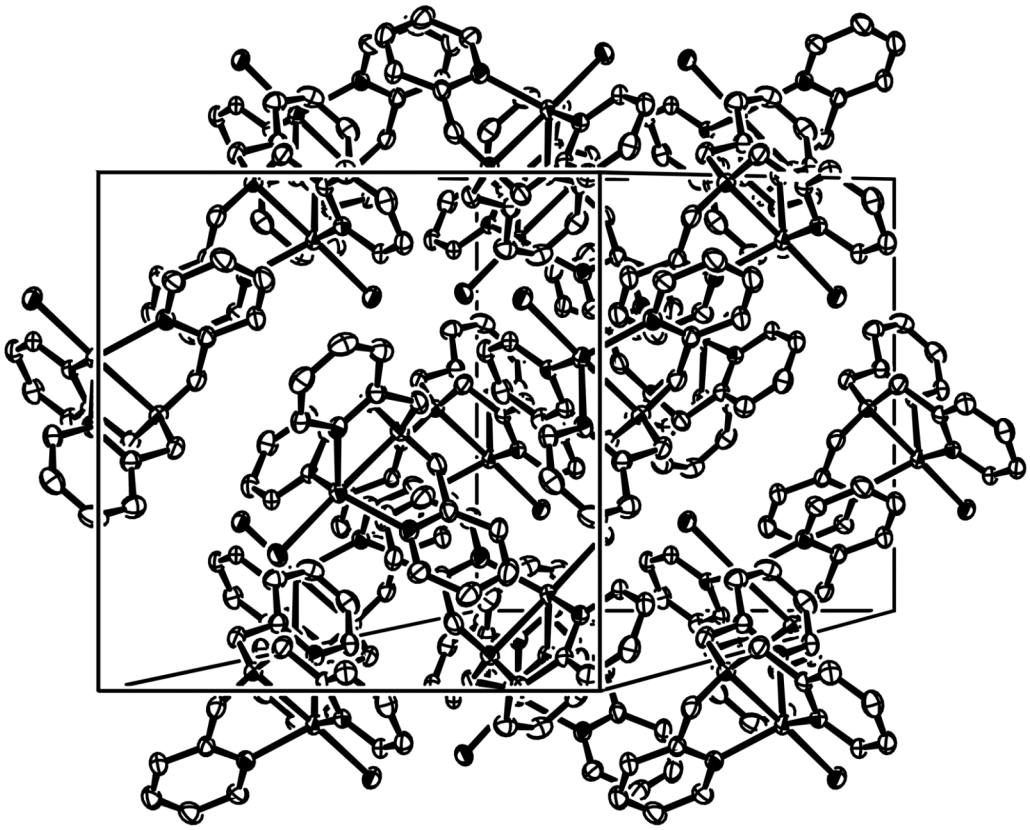

Figure A.2.1. Packing diagram of [Cu^{I}(TPMA)Cl] viewed along the c-axis.

Table A.2.6. Crystallographic data and experimental data for $[Cu^{II}(TPMA)Cl][Cl]$.

	$[Cu^{II}(TPMA)Cl][Cl]$
Formula	$C_{18}H_{18}Cl_2CuN_4$
Color	green
Shape	rhomboid
Formula Weight	424.81
Crystal System	cubic
Space Group	P 21 3
Temp (K)	150K
Cell Constants	
***a*, Å**	12.41570 (10)
***b*, Å**	12.41570 (10)
***c*, Å**	12.41570 (10)
α, deg	90
β, deg	90
γ, deg	90
V, $Å^3$	1913.88(3)
Formula units/unit cell	4
Dcal'd, gcm^{-3}	1.474
μ, mm^{-1}	1.428
F(000)	868
Diffractometer	Bruker Smart ApexII
Radiation, graphite monochr.	Mo Kα (λ=0.71073 Å)
Crystal size, mm	0.460 x 0.360 x 0.186
θ range, deg	2.32< θ <32.79
Range of *h,k,l*	±18, ±18, ±18
Reflections collected/unique	35485/2342
R_{int}	0.0306
Refinement Method	Full Matrix Least-Squares on F^2
Data/Restraints/Parameters	2342/0/76
GOF on F^2	1.054
Final R indices [I>2σ(I)]	R_1=0.0170 wR_2=0.0455
R indices (all data)	R_1=0.0184 wR_2=0.0460
Max. Resid. Peaks (e*$Å^{-3}$)	0.266 and -0.220

Table A.2.7. Atomic coordinates (x 10^4) and equivalent isotropic displacement parameters (A^2 x 10^3) for [Cu^{II}(TPMA)Cl][Cl]. U(eq) is defined as one third of the trace of the orthogonalized Uij tensor.

	x	y	z	U(eq)
C(1)	8357(1)	4756(1)	250(1)	20(1)
Cu(1)	8127(1)	3127(1)	1873(1)	17(1)
Cl(2)	800(1)	5800(1)	9200(1)	18(1)
Cl(1)	7087(1)	2087(1)	2913(1)	26(1)
N(1)	9079(1)	4079(1)	921(1)	17(1)
N(2)	7105(1)	4439(1)	1696(1)	18(1)
C(3)	6916(1)	6117(1)	763(1)	23(1)
C(5)	5696(1)	5657(1)	2183(1)	23(1)
C(2)	7426(1)	5136(1)	924(1)	18(1)
C(6)	6250(1)	4692(1)	2308(1)	20(1)
C(4)	6038(1)	6384(1)	1403(1)	25(1)

Table A.2.8. Bond lengths [Å] and angles [deg] for [Cu^{II}(TPMA)Cl][Cl].

C(1)-N(1)	1.4842(11)
C(1)-C(2)	1.5031(14)
C(1)-H(1A)	0.9700
C(1)-H(1B)	0.9700
Cu(1)-N(1)	2.0481(14)
Cu(1)-N(2)#1	2.0759(8)
Cu(1)-N(2)#2	2.0759(8)
Cu(1)-N(2)	2.0759(8)
Cu(1)-Cl(1)	2.2369(4)
N(1)-C(1)#1	1.4842(11)
N(1)-C(1)#2	1.4843(11)
N(2)-C(6)	1.3432(12)
N(2)-C(2)	1.3520(12)
C(3)-C(2)	1.3869(14)
C(3)-C(4)	1.3893(16)
C(3)-H(3)	0.9300
C(5)-C(4)	1.3903(15)
C(5)-C(6)	1.3910(14)
C(5)-H(5)	0.9300
C(6)-H(6)	0.9300
C(4)-H(4)	0.9300
N(1)-C(1)-C(2)	109.29(8)
N(1)-C(1)-H(1A)	109.8
C(2)-C(1)-H(1A)	109.8
N(1)-C(1)-H(1B)	109.8
C(2)-C(1)-H(1B)	109.8
H(1A)-C(1)-H(1B)	108.3
N(1)-Cu(1)-N(2)#1	80.71(2)
N(1)-Cu(1)-N(2)#2	80.71(2)
N(2)#1-Cu(1)-N(2)#2	117.448(12)
N(1)-Cu(1)-N(2)	80.71(2)
N(2)#1-Cu(1)-N(2)	117.447(12)
N(2)#2-Cu(1)-N(2)	117.447(12)
N(1)-Cu(1)-Cl(1)	180.000(19)
N(2)#1-Cu(1)-Cl(1)	99.29(2)
N(2)#2-Cu(1)-Cl(1)	99.29(2)
N(2)-Cu(1)-Cl(1)	99.29(2)
C(1)-N(1)-C(1)#1	111.31(6)
C(1)-N(1)-C(1)#2	111.30(6)
C(1)#1-N(1)-C(1)#2	111.31(6)
C(1)-N(1)-Cu(1)	107.57(6)
C(1)#1-N(1)-Cu(1)	107.57(6)
C(1)#2-N(1)-Cu(1)	107.57(6)
C(6)-N(2)-C(2)	118.96(8)
C(6)-N(2)-Cu(1)	127.34(6)
C(2)-N(2)-Cu(1)	113.45(6)
C(2)-C(3)-C(4)	119.02(9)
C(2)-C(3)-H(3)	120.5
C(4)-C(3)-H(3)	120.5
C(4)-C(5)-C(6)	119.07(10)

C(4)-C(5)-H(5)	120.5
C(6)-C(5)-H(5)	120.5
N(2)-C(2)-C(3)	122.03(9)
N(2)-C(2)-C(1)	114.82(8)
C(3)-C(2)-C(1)	123.14(9)
N(2)-C(6)-C(5)	121.97(9)
N(2)-C(6)-H(6)	119.0
C(5)-C(6)-H(6)	119.0
C(3)-C(4)-C(5)	118.93(9)
C(3)-C(4)-H(4)	120.5
C(5)-C(4)-H(4)	120.5

Symmetry transformations used to generate equivalent atoms:
#1 y+1/2,-z+1/2,-x+1 #2 -z+1,x-1/2,-y+1/2

Table A.2.9. Anisotropic displacement parameters (A^2 x 10^3) for [Cu^{II}(TPMA)Cl][Cl]. The anisotropic displacement factor exponent takes the form: -2 pi^2 [h^2 a*^2 U11 + ... + 2 h k a* b* U12]

	U11	U22	U33	U23	U13	U12
C(1)	21(1)	22(1)	18(1)	6(1)	2(1)	0(1)
Cu(1)	17(1)	17(1)	17(1)	3(1)	3(1)	-3(1)
Cl(2)	18(1)	18(1)	18(1)	1(1)	1(1)	-1(1)
Cl(1)	26(1)	26(1)	26(1)	7(1)	7(1)	-7(1)
N(1)	17(1)	17(1)	17(1)	2(1)	2(1)	-2(1)
N(2)	18(1)	17(1)	18(1)	2(1)	2(1)	-1(1)
C(3)	25(1)	20(1)	25(1)	6(1)	-1(1)	0(1)
C(5)	22(1)	22(1)	25(1)	-2(1)	3(1)	3(1)
C(2)	18(1)	19(1)	18(1)	3(1)	0(1)	-1(1)
C(6)	20(1)	20(1)	19(1)	0(1)	3(1)	-1(1)
C(4)	26(1)	20(1)	31(1)	1(1)	-3(1)	4(1)

Table A.2.10. Hydrogen coordinates (x 10^4) and isotropic displacement parameters (A^2 x 10^3) for [Cu^{II}(TPMA)Cl][Cl].

	x	y	z	U(eq)
H(1A)	8093	4340	-357	24
H(1B)	8752	5370	-27	24
H(3)	7158	6589	234	28
H(5)	5104	5815	2615	28
H(6)	6021	4207	2831	24
H(4)	5686	7039	1312	31

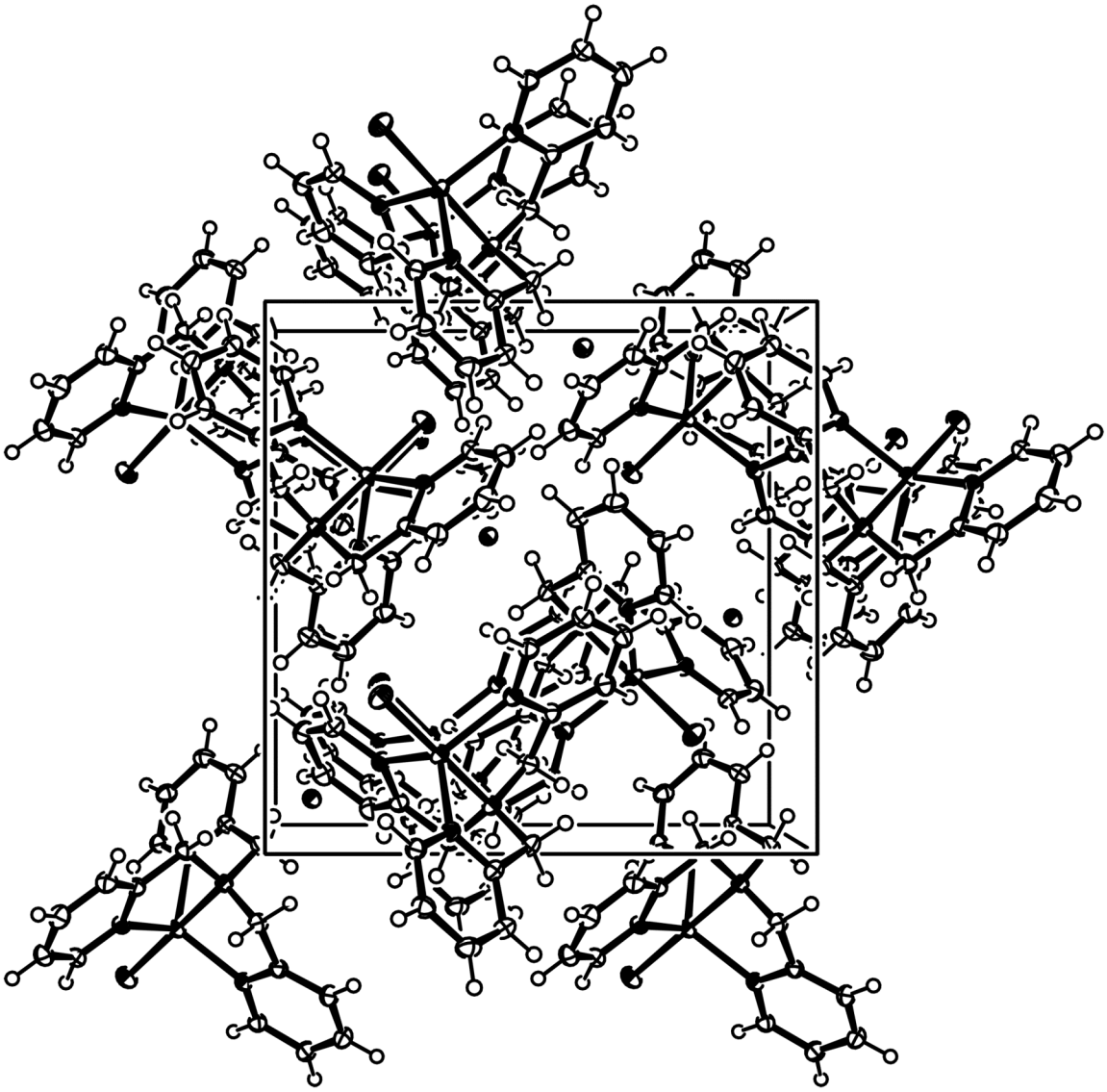

Figure A.2.2. Packing diagram of [Cu^{II}(TPMA)Cl][Cl] viewed along the c-axis.

Appendix B.

B.1 Crystallographic Data

Table B.1.1. Crystallographic data and experimental data for [Cu^I(TPMA)Br]

	[Cu^I(TPMA)Br]
Formula	$C_{18}H_{18}BrCuN_4$
Color	red orange
Shape	rhomboid
Formula Weight	433.81
Crystal System	monoclinic
Space Group	P 21/c
Temp (K)	150K
Cell Constants	
***a*, Å**	10.3042(9)
***b*, Å**	14.2256(12)
***c*, Å**	12.5491(11)
α, deg	90
β, deg	105.5800(10)
γ, deg	90
V, Å^3	1771.9(3)
Formula units/unit cell	4
Dcal'd, gcm^{-3}	1.626
μ, mm^{-1}	3.494
F(000)	872
Diffractometer	Bruker Smart ApexII
Radiation, graphite monochr.	Mo Kα (λ=0.71073 Å)
Crystal size, mm	0.407 x 0.143 x 0.033
θ range, deg	2.05< θ <32.25
Range of *h,k,l*	±15, -20→20, ±18
Reflections collected/unique	23037/6616
R_{int}	0.039
Refinement Method	Full Matrix Least-Squares on F^2
Data/Restraints/Parameters	6616/0/217
GOF on F^2	1.015
Final R indices [I>2σ(I)]	R_1=0.0304 wR_2=0.0621
R indices (all data)	R_1=0.0511 wR_2=0.0680
Max. Resid. Peaks (e*Å^{-3})	0.405 and -0.357

Table B.1.2. Atomic coordinates (x 10^4) and equivalent isotropic displacement parameters (A^2 x 10^3) for [Cu^{I}(TPMA)Br]. U(eq) is defined as one third of the trace of the orthogonalized Uij tensor.

	x	y	z	U(eq)
Br(1)	7635(1)	90(1)	7012(1)	26(1)
Cu(1)	6726(1)	1178(1)	8211(1)	21(1)
N(1)	5855(2)	2221(1)	9401(1)	20(1)
N(2)	8053(2)	2330(1)	8528(1)	21(1)
N(4)	4818(2)	1545(1)	7269(1)	20(1)
C(14)	4157(2)	2267(1)	7578(1)	20(1)
N(3)	6979(2)	447(1)	9684(1)	23(1)
C(6)	8927(2)	2498(1)	7925(2)	24(1)
C(13)	4832(2)	2779(1)	8642(1)	25(1)
C(18)	4217(2)	1110(1)	6309(1)	23(1)
C(1)	7023(2)	2752(1)	10002(1)	25(1)
C(7)	5364(2)	1549(1)	10071(1)	24(1)
C(8)	6376(2)	764(1)	10442(1)	23(1)
C(4)	9559(2)	3975(1)	8793(2)	31(1)
C(17)	2980(2)	1372(1)	5636(2)	26(1)
C(3)	8680(2)	3811(1)	9429(2)	26(1)
C(15)	2917(2)	2578(1)	6936(2)	26(1)
C(5)	9692(2)	3306(1)	8035(2)	30(1)
C(12)	7912(2)	-233(1)	9986(2)	30(1)
C(2)	7947(2)	2978(1)	9280(1)	21(1)
C(9)	6672(2)	391(1)	11503(2)	30(1)
C(16)	2319(2)	2126(1)	5951(2)	29(1)
C(10)	7633(2)	-308(2)	11800(2)	34(1)
C(11)	8273(2)	-620(1)	11034(2)	34(1)

Table B.1.3. Bond lengths [Å] and angles [deg] for [Cu^{I}(TPMA)Br]

Br(1)-Cu(1)	2.5088(3)
Cu(1)-N(4)	2.0709(15)
Cu(1)-N(3)	2.0753(15)
Cu(1)-N(2)	2.1024(15)
Cu(1)-N(1)	2.4397(14)
N(1)-C(1)	1.449(2)
N(1)-C(7)	1.452(2)
N(1)-C(13)	1.453(2)
N(2)-C(2)	1.344(2)
N(2)-C(6)	1.344(2)
N(4)-C(14)	1.346(2)
N(4)-C(18)	1.348(2)
C(14)-C(15)	1.388(2)
C(14)-C(13)	1.516(2)
N(3)-C(12)	1.344(2)
N(3)-C(8)	1.346(2)
C(6)-C(5)	1.380(3)
C(6)-H(6)	0.9300
C(13)-H(13A)	0.9700
C(13)-H(13B)	0.9700
C(18)-C(17)	1.377(3)
C(18)-H(18)	0.9300
C(1)-C(2)	1.515(2)
C(1)-H(1A)	0.9700
C(1)-H(1B)	0.9700
C(7)-C(8)	1.513(3)
C(7)-H(7A)	0.9700
C(7)-H(7B)	0.9700
C(8)-C(9)	1.389(2)
C(4)-C(5)	1.377(3)
C(4)-C(3)	1.379(3)
C(4)-H(4)	0.9300
C(17)-C(16)	1.384(3)
C(17)-H(17)	0.9300
C(3)-C(2)	1.390(2)
C(3)-H(3)	0.9300
C(15)-C(16)	1.383(3)
C(15)-H(15)	0.9300
C(5)-H(5)	0.9300
C(12)-C(11)	1.382(3)
C(12)-H(12)	0.9300
C(9)-C(10)	1.381(3)

C(9)-H(9)	0.9300
C(16)-H(16)	0.9300
C(10)-C(11)	1.377(3)
C(10)-H(10)	0.9300
C(11)-H(11)	0.9300

N(4)-Cu(1)-N(3)	120.51(6)
N(4)-Cu(1)-N(2)	112.40(6)
N(3)-Cu(1)-N(2)	107.61(6)
N(4)-Cu(1)-N(1)	75.37(5)
N(3)-Cu(1)-N(1)	74.86(5)
N(2)-Cu(1)-N(1)	74.80(5)
N(4)-Cu(1)-Br(1)	105.25(4)
N(3)-Cu(1)-Br(1)	104.28(4)
N(2)-Cu(1)-Br(1)	105.43(4)
N(1)-Cu(1)-Br(1)	179.14(3)
C(1)-N(1)-C(7)	114.28(14)
C(1)-N(1)-C(13)	114.31(14)
C(7)-N(1)-C(13)	115.81(15)
C(1)-N(1)-Cu(1)	104.19(10)
C(7)-N(1)-Cu(1)	101.36(10)
C(13)-N(1)-Cu(1)	104.64(10)
C(2)-N(2)-C(6)	117.85(15)
C(2)-N(2)-Cu(1)	119.72(12)
C(6)-N(2)-Cu(1)	122.10(12)
C(14)-N(4)-C(18)	117.51(15)
C(14)-N(4)-Cu(1)	120.25(11)
C(18)-N(4)-Cu(1)	122.17(12)
N(4)-C(14)-C(15)	122.28(16)
N(4)-C(14)-C(13)	118.23(15)
C(15)-C(14)-C(13)	119.43(15)
C(12)-N(3)-C(8)	118.18(16)
C(12)-N(3)-Cu(1)	121.41(13)
C(8)-N(3)-Cu(1)	119.35(12)
N(2)-C(6)-C(5)	122.82(17)
N(2)-C(6)-H(6)	118.6
C(5)-C(6)-H(6)	118.6
N(1)-C(13)-C(14)	113.27(14)
N(1)-C(13)-H(13A)	108.9
C(14)-C(13)-H(13A)	108.9
N(1)-C(13)-H(13B)	108.9
C(14)-C(13)-H(13B)	108.9
H(13A)-C(13)-H(13B)	107.7
N(4)-C(18)-C(17)	123.41(17)
N(4)-C(18)-H(18)	118.3
C(17)-C(18)-H(18)	118.3

N(1)-C(1)-C(2)	111.50(13)
N(1)-C(1)-H(1A)	109.3
C(2)-C(1)-H(1A)	109.3
N(1)-C(1)-H(1B)	109.3
C(2)-C(1)-H(1B)	109.3
H(1A)-C(1)-H(1B)	108.0
N(1)-C(7)-C(8)	110.23(14)
N(1)-C(7)-H(7A)	109.6
C(8)-C(7)-H(7A)	109.6
N(1)-C(7)-H(7B)	109.6
C(8)-C(7)-H(7B)	109.6
H(7A)-C(7)-H(7B)	108.1
N(3)-C(8)-C(9)	121.69(18)
N(3)-C(8)-C(7)	116.15(15)
C(9)-C(8)-C(7)	122.16(17)
C(5)-C(4)-C(3)	119.02(18)
C(5)-C(4)-H(4)	120.5
C(3)-C(4)-H(4)	120.5
C(18)-C(17)-C(16)	118.71(17)
C(18)-C(17)-H(17)	120.6
C(16)-C(17)-H(17)	120.6
C(4)-C(3)-C(2)	118.97(18)
C(4)-C(3)-H(3)	120.5
C(2)-C(3)-H(3)	120.5
C(16)-C(15)-C(14)	119.36(17)
C(16)-C(15)-H(15)	120.3
C(14)-C(15)-H(15)	120.3
C(4)-C(5)-C(6)	119.00(18)
C(4)-C(5)-H(5)	120.5
C(6)-C(5)-H(5)	120.5
N(3)-C(12)-C(11)	122.99(19)
N(3)-C(12)-H(12)	118.5
C(11)-C(12)-H(12)	118.5
N(2)-C(2)-C(3)	122.33(17)
N(2)-C(2)-C(1)	117.20(15)
C(3)-C(2)-C(1)	120.44(16)
C(10)-C(9)-C(8)	119.41(19)
C(10)-C(9)-H(9)	120.3
C(8)-C(9)-H(9)	120.3
C(15)-C(16)-C(17)	118.71(18)
C(15)-C(16)-H(16)	120.6
C(17)-C(16)-H(16)	120.6
C(11)-C(10)-C(9)	119.08(18)
C(11)-C(10)-H(10)	120.5
C(9)-C(10)-H(10)	120.5
C(10)-C(11)-C(12)	118.6(2)

C(10)-C(11)-H(11)	120.7
C(12)-C(11)-H(11)	120.7

Symmetry transformations used to generate equivalent atoms:

Table B.1.4. Anisotropic displacement parameters (A^2 x 10^3) for [Cu^{I}(TPMA)Br]. The anisotropic displacement factor exponent takes the form: -2 pi^2 [h^2 a*^2 U11 + ... + 2 h k a* b* U12]

	U11	U22	U33	U23	U13	U12
Br(1)	37(1)	21(1)	23(1)	-1(1)	15(1)	8(1)
Cu(1)	27(1)	19(1)	18(1)	-2(1)	8(1)	1(1)
N(1)	24(1)	19(1)	17(1)	-4(1)	6(1)	-4(1)
N(2)	23(1)	21(1)	19(1)	0(1)	5(1)	-1(1)
N(4)	24(1)	19(1)	18(1)	-2(1)	9(1)	1(1)
C(14)	26(1)	18(1)	19(1)	0(1)	10(1)	0(1)
N(3)	29(1)	22(1)	19(1)	0(1)	8(1)	0(1)
C(6)	21(1)	29(1)	23(1)	2(1)	6(1)	2(1)
C(13)	31(1)	20(1)	24(1)	-5(1)	9(1)	3(1)
C(18)	29(1)	23(1)	19(1)	-4(1)	10(1)	-3(1)
C(1)	33(1)	24(1)	18(1)	-7(1)	8(1)	-7(1)
C(7)	27(1)	26(1)	21(1)	-5(1)	11(1)	-5(1)
C(8)	29(1)	21(1)	19(1)	-2(1)	8(1)	-7(1)
C(4)	22(1)	28(1)	40(1)	2(1)	4(1)	-6(1)
C(17)	31(1)	31(1)	18(1)	-1(1)	6(1)	-6(1)
C(3)	26(1)	22(1)	30(1)	-3(1)	3(1)	-3(1)
C(15)	27(1)	24(1)	27(1)	1(1)	9(1)	4(1)
C(5)	21(1)	36(1)	34(1)	6(1)	10(1)	-2(1)
C(12)	34(1)	29(1)	28(1)	3(1)	9(1)	3(1)
C(2)	22(1)	21(1)	18(1)	-1(1)	2(1)	-1(1)
C(9)	43(1)	29(1)	20(1)	-1(1)	11(1)	-11(1)
C(16)	26(1)	34(1)	25(1)	5(1)	3(1)	0(1)
C(10)	48(1)	30(1)	20(1)	4(1)	2(1)	-10(1)
C(11)	40(1)	29(1)	30(1)	8(1)	3(1)	2(1)

Table B.1.5. Hydrogen coordinates (x 10^4) and isotropic displacement parameters (A^2 x 10^3) for [Cu^{I}(TPMA)Br].

	x	y	z	U(eq)
H(6)	9020	2049	7411	29
H(13A)	5243	3350	8463	30
H(13B)	4151	2959	9007	30
H(18)	4660	606	6090	28
H(1A)	7515	2391	10639	30
H(1B)	6729	3332	10269	30
H(7A)	4512	1290	9645	28
H(7B)	5215	1864	10714	28
H(4)	10056	4528	8874	37
H(17)	2597	1048	4984	32
H(3)	8579	4250	9949	32
H(15)	2492	3086	7166	31
H(5)	10287	3398	7603	36
H(12)	8335	-452	9466	36
H(9)	6228	610	12008	36
H(16)	1489	2324	5509	35
H(10)	7844	-563	12508	41
H(11)	8934	-1082	11219	41

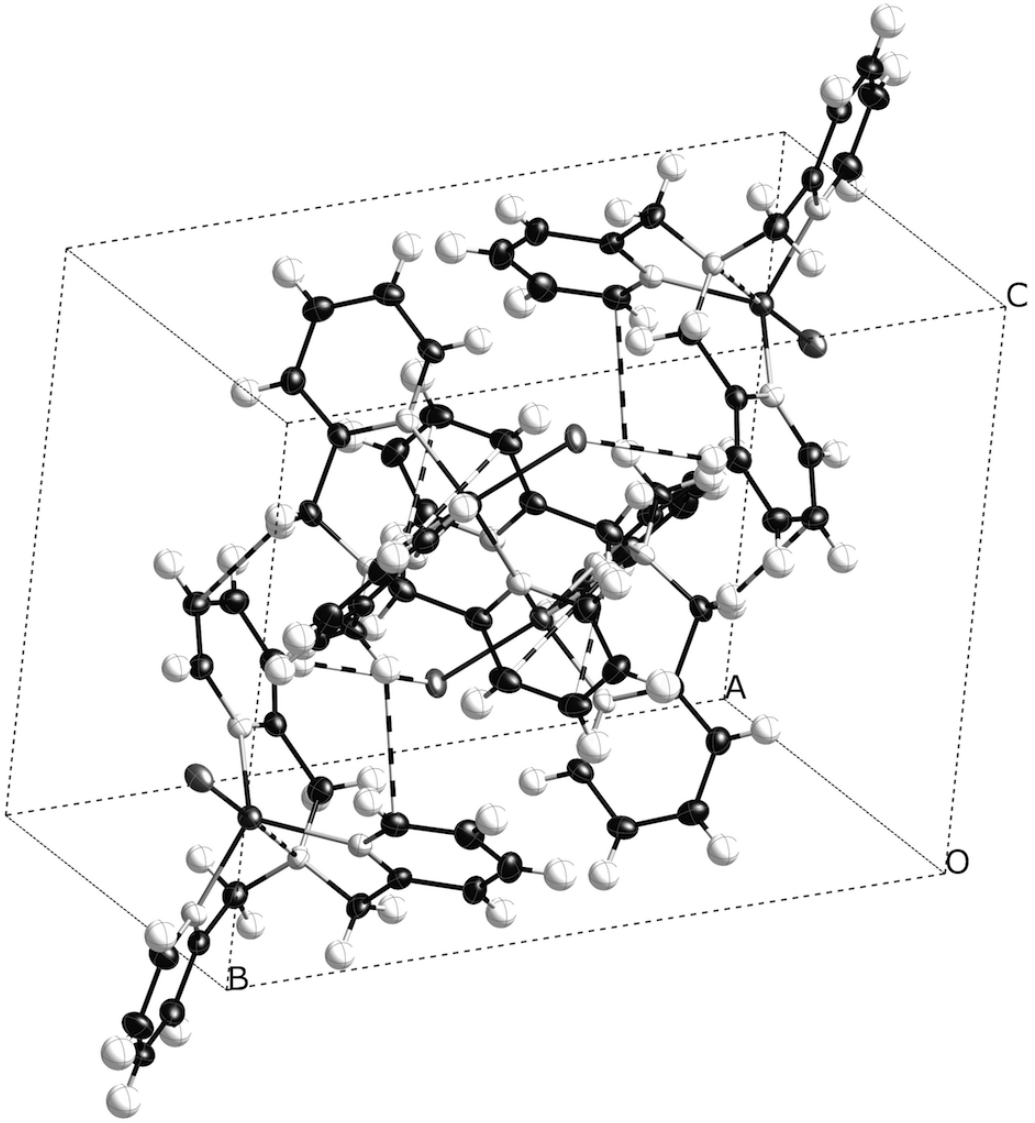

Figure B.1.1. Crystal packing diagram for [Cu^{I}(TPMA)Br]

Table B.1.6. Crystallographic data and experimental data for $[Cu^{II}(TPMA)Br][Br]$

	$[Cu^{II}(TPMA)Br][Br]$
Formula	$C_{18}H_{18}Br_2CuN_4$
Color	green
Shape	rhomboid
Formula Weight	513.72
Crystal System	cubic
Space Group	P 21 3
Temp (K)	150K
Cell Constants	
***a*, Å**	12.6335 (3)
***b*, Å**	12.6335 (3)
***c*, Å**	12.6335 (3)
α, deg	90
β, deg	90
γ, deg	90
V, $Å^3$	2016.37
Formula units/unit cell	4
Dcal'd, gcm^{-3}	1.692
μ, mm^{-1}	5.054
F(000)	1012
Diffractometer	Bruker Smart ApexII
Radiation, graphite monochr.	Mo Kα (λ=0.71073 Å)
Crystal size, mm	0.260 x 0.135 x 0.087
θ range, deg	2.28< θ <32.81
Range of *h,k,l*	±18, -18→19, -19→18
Reflections collected/unique	26426/2460
R_{int}	0.1665
Refinement Method	Full Matrix Least-Squares on F^2
Data/Restraints/Parameters	2460/0/76
GOF on F^2	1.03
Final R indices [I>2σ(I)]	R_1=0.0271 wR_2=0.0637
R indices (all data)	R_1=0.0343 wR_2=0.0649
Max. Resid. Peaks (e*$Å^{-3}$)	0.566 and -0.544

Table B.1.7. Atomic coordinates (x 10^4) and equivalent isotropic displacement parameters (A^2 x 10^3) for [Cu^{II}(TPMA)Br][Br]. U(eq) is defined as one third of the trace of the orthogonalized Uij tensor.

	x	y	z	U(eq)
Br(2)	3329(1)	1671(1)	8329(1)	17(1)
Br(1)	-446(1)	5446(1)	4554(1)	23(1)
Cu(1)	644(1)	4356(1)	5644(1)	16(1)
N(1)	1576(1)	3424(1)	6576(1)	17(1)
C(2)	1566(2)	2381(2)	4953(2)	20(1)
C(1)	2235(2)	2754(2)	5872(2)	21(1)
N(2)	811(2)	3068(2)	4640(2)	18(1)
C(3)	1731(2)	1428(2)	4430(2)	26(1)
C(5)	344(2)	1884(2)	3251(2)	26(1)
C(6)	215(2)	2823(2)	3799(2)	20(1)
C(4)	1109(2)	1172(2)	3578(2)	29(1)

Table B.1.8. Bond lengths [Å] and angles [deg] for [Cu^{II}(TPMA)Br][Br].

Br(1)-Cu(1)	2.3836(6)
Cu(1)-N(1)	2.040(3)
Cu(1)-N(2)#1	2.073(2)
Cu(1)-N(2)	2.073(2)
Cu(1)-N(2)#2	2.073(2)
N(1)-C(1)#1	1.483(3)
N(1)-C(1)	1.483(3)
N(1)-C(1)#2	1.483(3)
C(2)-N(2)	1.349(3)
C(2)-C(3)	1.389(3)
C(2)-C(1)	1.511(3)
C(1)-H(1A)	0.9700
C(1)-H(1B)	0.9700
N(2)-C(6)	1.339(3)
C(3)-C(4)	1.371(4)
C(3)-H(3)	0.9300
C(5)-C(4)	1.383(4)
C(5)-C(6)	1.384(3)
C(5)-H(5)	0.9300
C(6)-H(6)	0.9300
C(4)-H(4)	0.9300
N(1)-Cu(1)-N(2)#1	80.86(5)
N(1)-Cu(1)-N(2)	80.86(5)
N(2)#1-Cu(1)-N(2)	117.53(3)
N(1)-Cu(1)-N(2)#2	80.86(5)
N(2)#1-Cu(1)-N(2)#2	117.52(3)
N(2)-Cu(1)-N(2)#2	117.53(3)
N(1)-Cu(1)-Br(1)	180.00(5)
N(2)#1-Cu(1)-Br(1)	99.14(5)
N(2)-Cu(1)-Br(1)	99.14(5)
N(2)#2-Cu(1)-Br(1)	99.14(5)
C(1)#1-N(1)-C(1)	111.03(13)
C(1)#1-N(1)-C(1)#2	111.03(13)
C(1)-N(1)-C(1)#2	111.03(13)
C(1)#1-N(1)-Cu(1)	107.87(14)
C(1)-N(1)-Cu(1)	107.87(14)
C(1)#2-N(1)-Cu(1)	107.87(14)
N(2)-C(2)-C(3)	121.7(2)
N(2)-C(2)-C(1)	114.8(2)
C(3)-C(2)-C(1)	123.5(2)
N(1)-C(1)-C(2)	108.99(19)

N(1)-C(1)-H(1A)	109.9
C(2)-C(1)-H(1A)	109.9
N(1)-C(1)-H(1B)	109.9
C(2)-C(1)-H(1B)	109.9
H(1A)-C(1)-H(1B)	108.3
C(6)-N(2)-C(2)	118.8(2)
C(6)-N(2)-Cu(1)	127.55(16)
C(2)-N(2)-Cu(1)	113.46(16)
C(4)-C(3)-C(2)	119.4(2)
C(4)-C(3)-H(3)	120.3
C(2)-C(3)-H(3)	120.3
C(4)-C(5)-C(6)	119.4(2)
C(4)-C(5)-H(5)	120.3
C(6)-C(5)-H(5)	120.3
N(2)-C(6)-C(5)	121.9(2)
N(2)-C(6)-H(6)	119.0
C(5)-C(6)-H(6)	119.0
C(3)-C(4)-C(5)	118.8(2)
C(3)-C(4)-H(4)	120.6
C(5)-C(4)-H(4)	120.6

Symmetry transformations used to generate equivalent atoms:
#1 -y+1/2,-z+1,x+1/2 #2 z-1/2,-x+1/2,-y+1

Table B.1.9. Anisotropic displacement parameters (A^2 x 10^3) for [Cu^{II}(TPMA)Br][Br]. The anisotropic displacement factor exponent takes the form: -2 pi^2 [h^2 a*^2 U11 + ... + 2 h k a* b* U12]

	U11	U22	U33	U23	U13	U12
Br(2)	17(1)	17(1)	17(1)	2(1)	-2(1)	2(1)
Br(1)	23(1)	23(1)	23(1)	6(1)	-6(1)	6(1)
Cu(1)	16(1)	16(1)	16(1)	4(1)	-4(1)	4(1)
N(1)	17(1)	17(1)	17(1)	2(1)	-2(1)	2(1)
C(2)	18(1)	20(1)	21(1)	2(1)	1(1)	4(1)
C(1)	18(1)	24(1)	21(1)	1(1)	-2(1)	9(1)
N(2)	19(1)	17(1)	18(1)	2(1)	-2(1)	3(1)
C(3)	30(1)	20(1)	30(1)	-1(1)	0(1)	10(1)
C(5)	30(1)	22(1)	25(1)	-4(1)	-4(1)	-1(1)
C(6)	22(1)	21(1)	18(1)	2(1)	-5(1)	1(1)
C(4)	39(2)	19(1)	29(1)	-4(1)	1(1)	4(1)

Table B.1.10. Hydrogen coordinates (x 10^4) and isotropic displacement parameters (A^2 x 10^3) for [Cu^{II}(TPMA)Br][Br].

	x	y	z	U(eq)
H(1A)	2503	2150	6262	25
H(1B)	2833	3159	5612	25
H(3)	2258	967	4657	32
H(5)	-79	1732	2668	31
H(6)	-302	3298	3577	24
H(4)	1201	532	3227	35

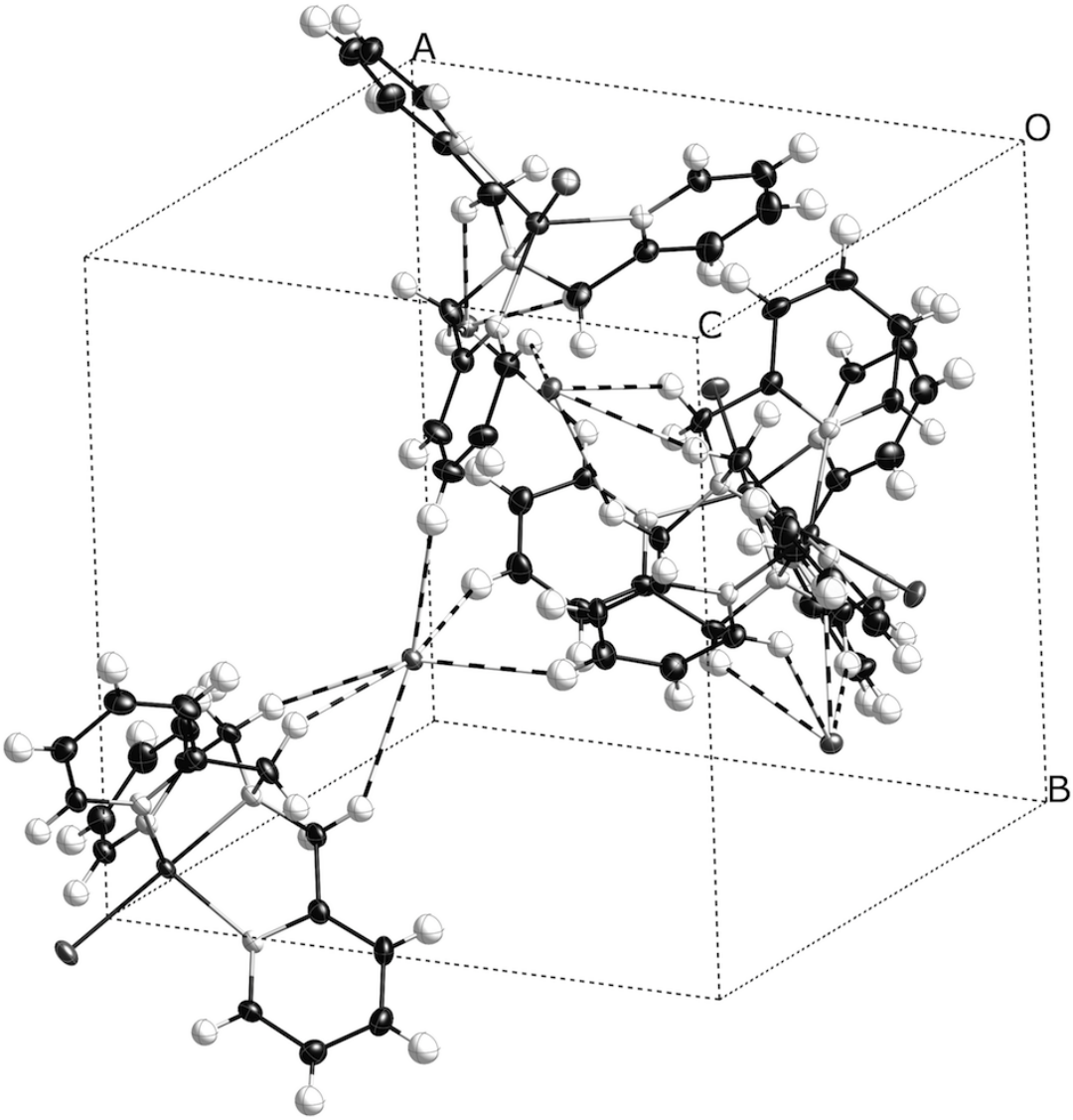

Figure B.1.2. Crystal packing diagram for [Cu^{II}(TPMA)Br][Br]

Appendix C.

C.1. Product Characterization.

^{1}H NMR spectra for all addition products have been reported elsewhere (Eckenhoff, W. T.; Pintauer, T. *Inorg. Chem.* **2007**, *46*, 5844, Eckenhoff, W. T.; Garrity, S. T.; Pintauer, T. *Eur. J. Inorg. Chem.* **2008**, 563-571, Quebatte, L.; Thommes, K.; Severin, K. *J. Am. Chem. Soc.* **2006**, *128*, 7440-7441), except for vinyl acetate and methyl methacrylate.

1,3,3,3-Tetrachloropropylacetate

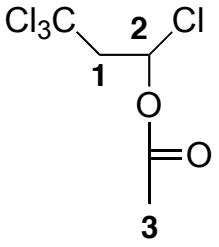

^{1}H NMR (400 MHz; $CDCl_3$): δ6.86 (dd, *J* = 8.2, 2.5 Hz, 1H, *H2*), δ3.58 (dd, *J* = 15.4, 8.2 Hz, 1H, *H1*), δ3.42 (dd, *J* = 15.4, 2.5 Hz, 1H, *H1*), δ2.17 (s, 3H. *H3*).
^{13}C NMR (101 MHz; $CDCl_3$): δ167.99, δ94.10, δ79.27, δ60.91, δ20.88.

1,3,3,3-Tetrabromopropylacetate

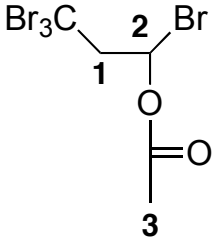

^{1}H NMR (400 MHz; $CDCl_3$): δ6.98 (dd, *J* = 8.7, 2.0 Hz, 1H, *H2*), δ4.04 (dd, *J* = 15.7, 8.7 Hz, 1H, *H1*), δ3.90 (dd, *J* = 15.7, 2.0 Hz, 1H, *H1*), δ2.16 (s, 3H, *H3*).
^{13}C NMR (101 MHz; $CDCl_3$): δ167.65, δ71.20, δ65.20, δ31.57, δ21.13.

Methyl 2,4,4,4-tetrachloro-2-methylbutanoate

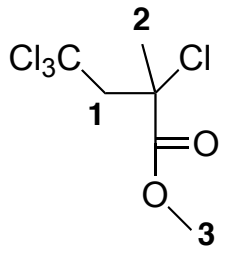

^{1}H NMR (400 MHz; $CDCl_3$): δ3.97 (d, *J* = 15.3 Hz, 1H, *H1*), δ3.80 (s, 3H, *H3*), δ3.44 (d, *J* = 15.3 Hz, 1H, *H1*), δ1.99 (s, 3H, *H2*).
^{13}C NMR (101 MHz; $CDCl_3$): δ170.12, δ94.67, δ64.66, δ62.28, δ53.63, δ26.42.

Methyl 2,4,4,4-tetrabromo-2-methylbutanoate

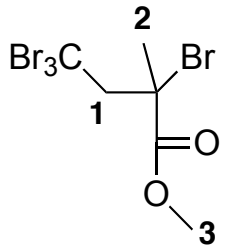

^{1}H NMR (400 MHz; $CDCl_3$): δ4.65 (d, *J* = 15.5 Hz, 1H, *H1*), δ3.90 (d, *J* = 15.5 Hz, 1H, *H1*), δ3.81 (s, 3H, *H3*), δ2.25 (s, 3H, *H2*).
^{13}C NMR (101 MHz; $CDCl_3$): δ170.49, δ65.89, δ57.56, δ53.61, δ31.43, δ26.24.

C.2. NMR Spectra of Products

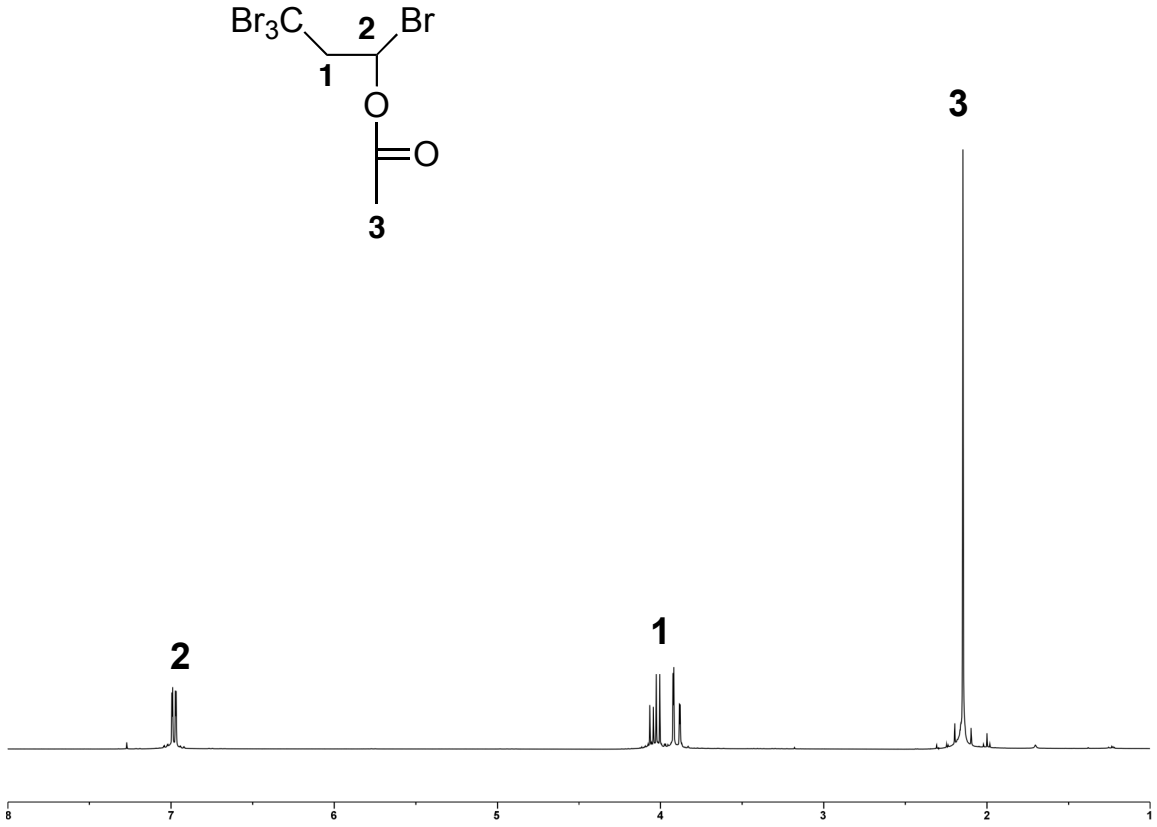

Figure C.2.1. ^{1}H NMR spectrum of 1,3,3,3-Tetrabromopropylacetate (400 MHz, 298K, $CDCl_3$)

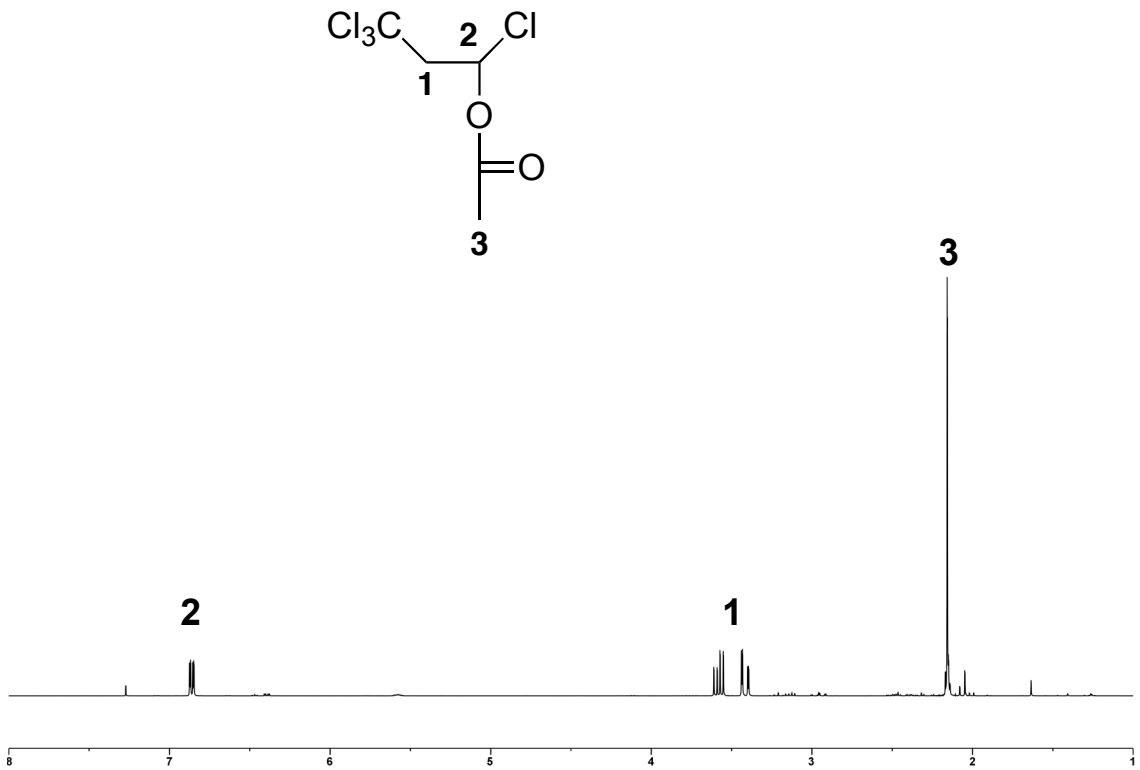

Figure C.2.2. ^{1}H NMR spectrum of 1,3,3,3-Tetrachloropropylacetate (400 MHz, 298K, $CDCl_3$)

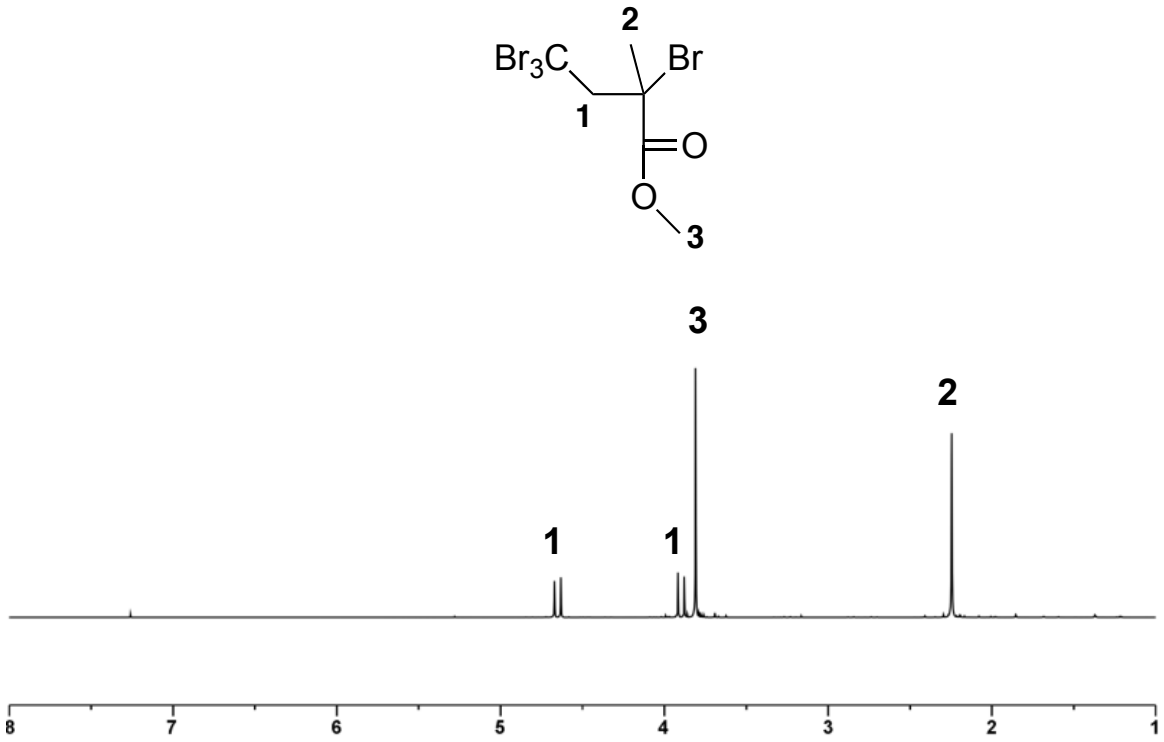

Figure C.2.3. ^{1}H NMR spectrum of methyl 2,4,4,4-tetrabromo-2-methylbutanoate (400 MHz, 298K, $CDCl_3$)

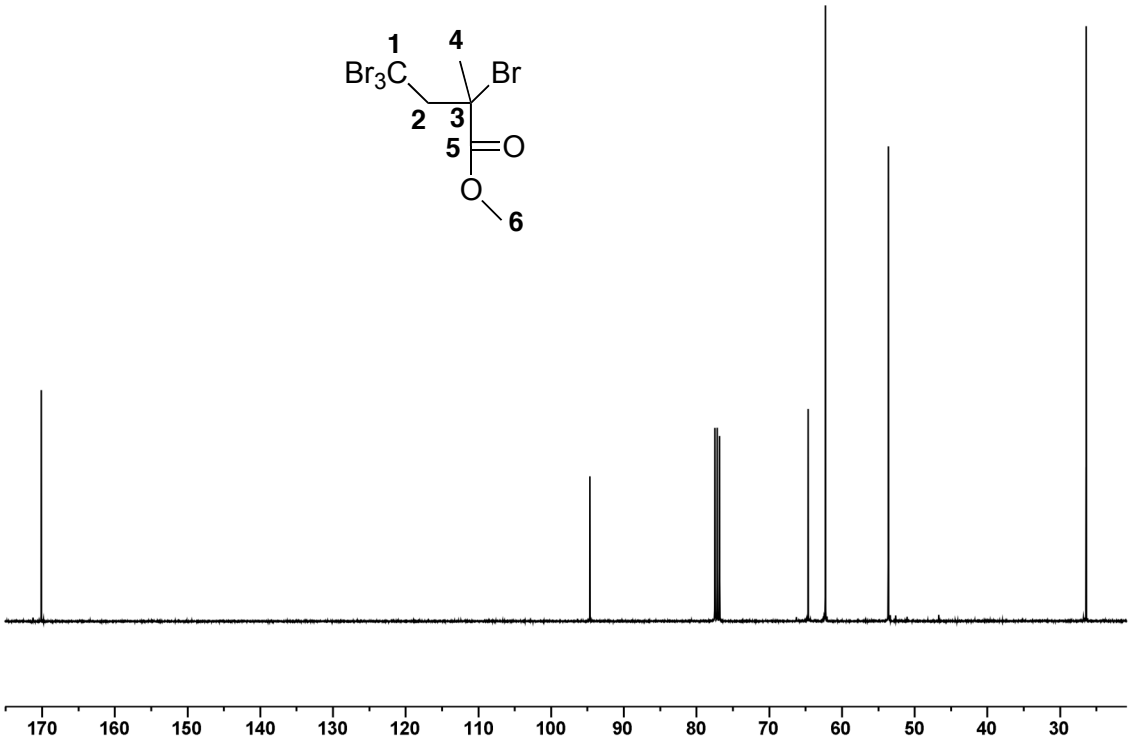

Figure C.2.4. ^{13}C NMR spectrum of methyl 2,4,4,4-tetrabromo-2-methylbutanoate (400 MHz, 298K, $CDCl_3$)

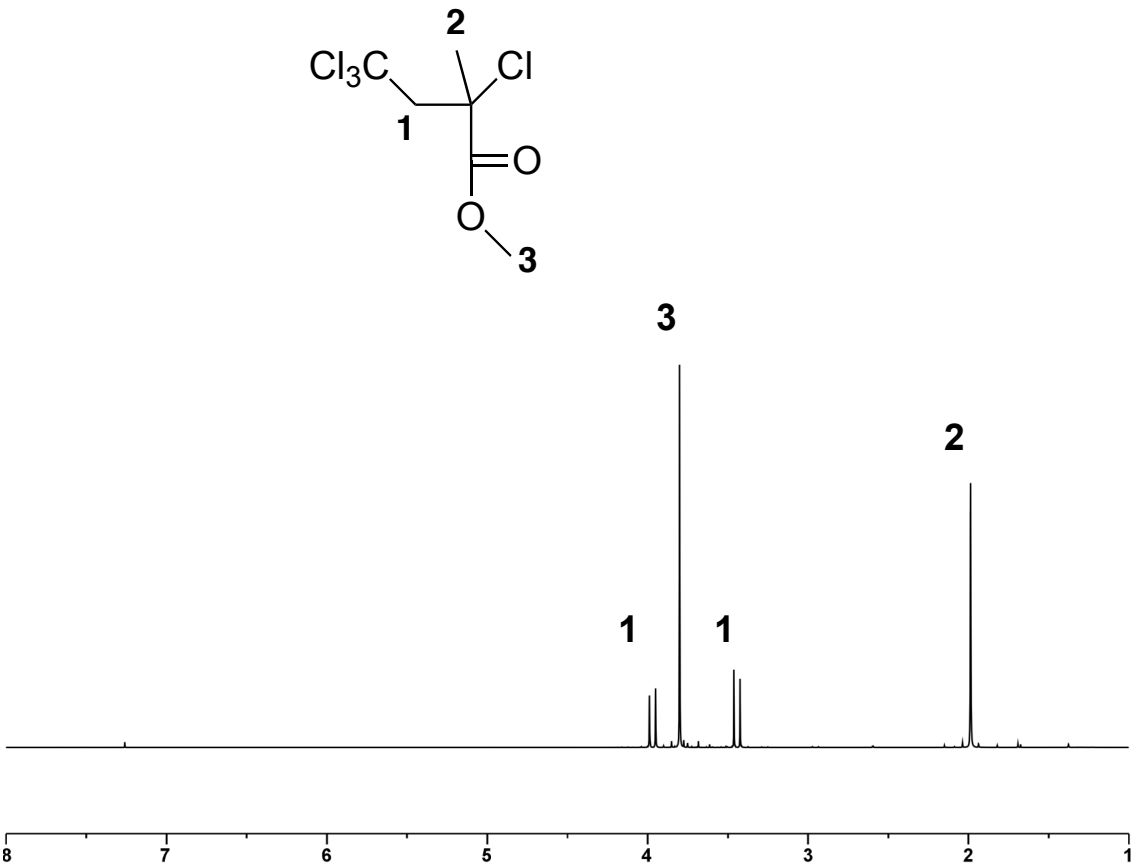

Figure C.2.5. ^{1}H NMR spectrum of methyl 2,4,4,4-tetrachrloro-2-methylbutanoate (400 MHz, 298K, $CDCl_3$)

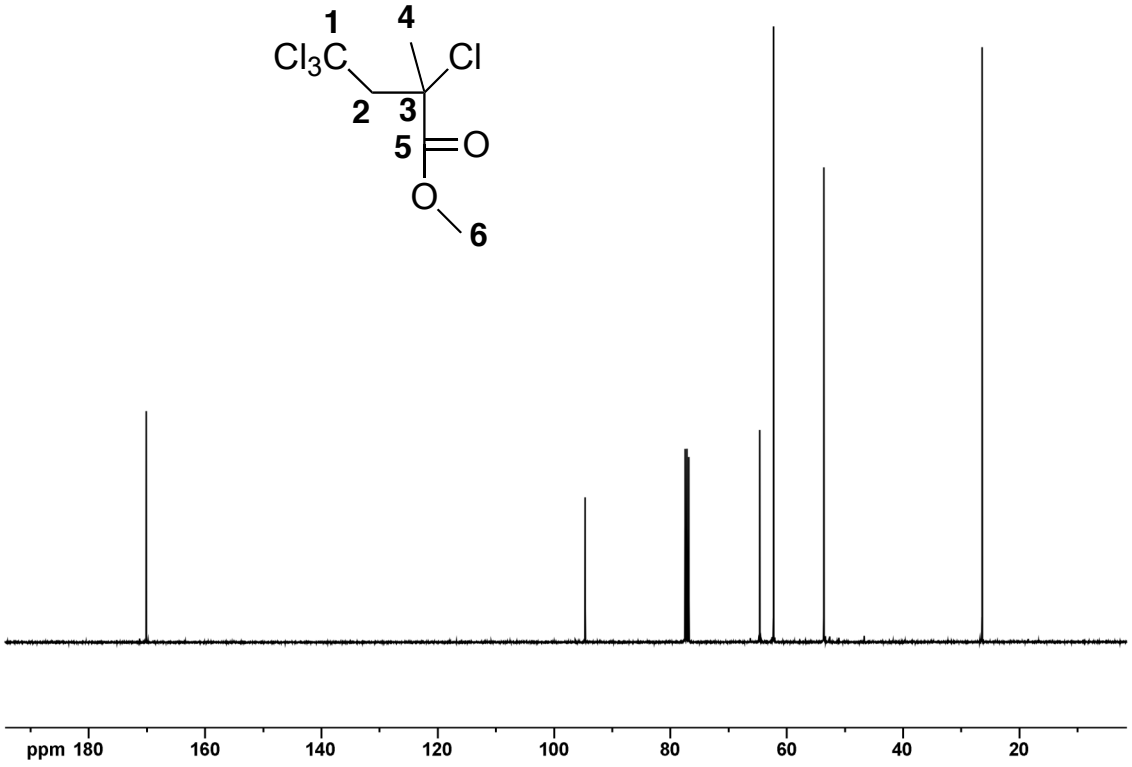

Figure C.2.6. ^{13}C NMR spectrum of methyl 2,4,4,4-tetrachrloro-2-methylbutanoate (400 MHz, 298K, $CDCl_3$)

C.3. Infrared Spectra of Products

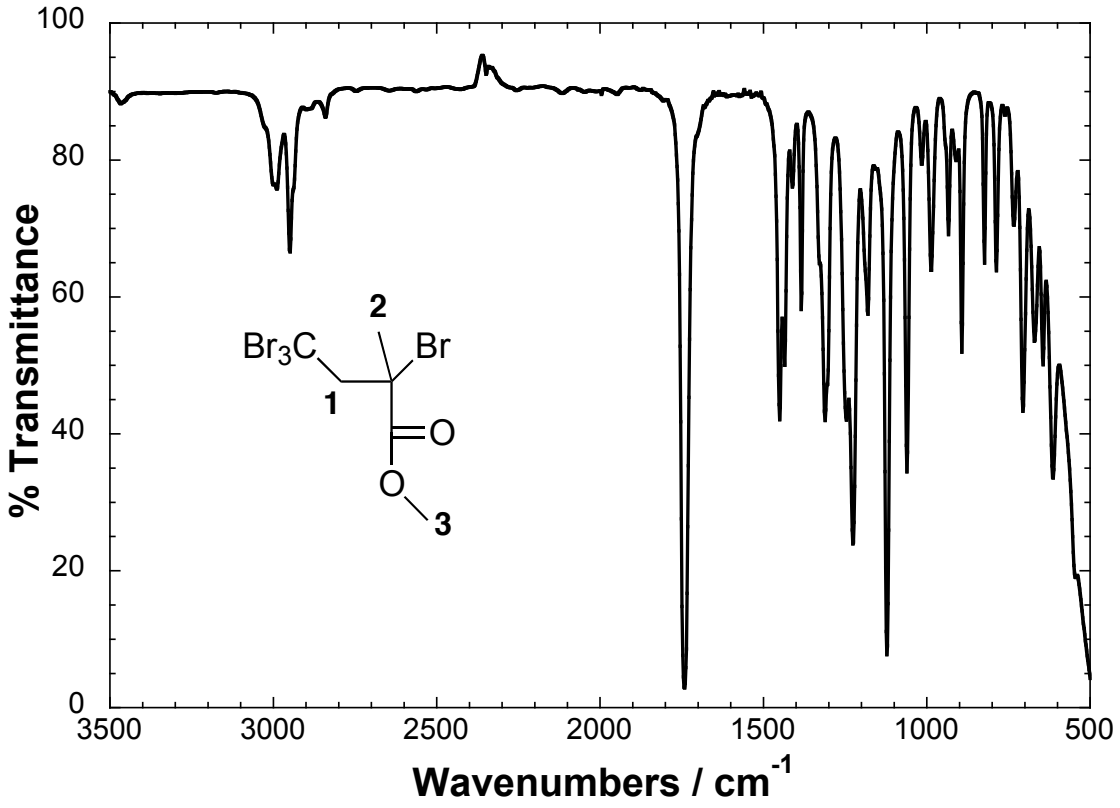

Figure C.3.1. Infrared spectrum of methyl 2,4,4,4-tetrabromo-2-methylbutanoate (ATR, FT-IR)

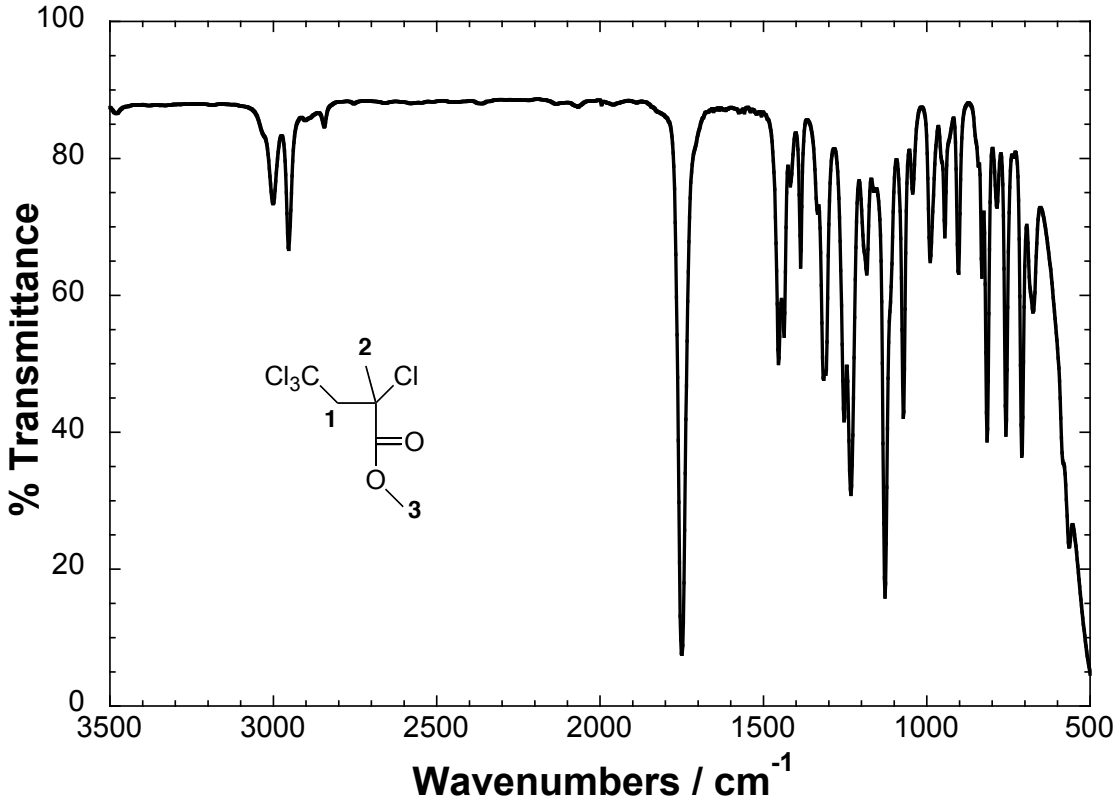

Figure C.3.2. Infrared spectrum of methyl 2,4,4,4-tetrachloro-2-methylbutanoate (ATR, FT-IR)

Appendix D.

D.1. Crystallographic Information for Copper Complexes with Me_6TREN Ligand.

Table D.1.1. Crystallographic and experimental data for complexes **1** and **2**.

	[Cu^{II}(Me_6TREN)Cl][Cl]	**[Cu^{II}(Me_6TREN)Br][Br]**
Formula	$C_{12}H_{30}Cl_2CuN_4$	$C_{12}H_{30}Br_2CuN_4$
Color/Shape	green/rhomboid	green/rhomboid
Formula Weight	364.84	453.76
Crystal System	cubic	cubic
Space Group	P 21 3	P 21 3
Temp (K)	150K	150K
Cell Constants		
***a*, Å**	11.85480 (10)	12.0512 (3)
***b*, Å**	11.85480 (10)	12.0512 (3)
***c*, Å**	11.85480 (10)	12.0512 (3)
α, deg	90	90
β, deg	90	90
γ, deg	90	90
V, $Å^3$	1666.03	1750.21
Formula units/unit cell	4	4
Dcal'd, gcm^{-3}	1.455	1.722
μ, mm^{-1}	1.626	5.808
F(000)	772	916
Diffractometer	Bruker Smart ApexII	Bruker Smart ApexII
Radiation, graphite monochr.	Mo Kα (λ=0.71073 Å)	Mo Kα (λ=0.71073 Å)
Crystal size, mm	0.320 x 0.255 x 0.206	0.258 x 0.223 x 0.129
θ range, deg	2.43< θ <32.77	2.39< θ <32.94
Range of *h,k,l*	±34, ±34, ±35	±35, ±35, ±36
Reflections collected/unique	30664/2038	23236/2153
R_{int}	0.0359	0.0353
Refinement Method	Full Matrix Least-Squares on F^2	Full Matrix Least-Squares on F^2
Data/Restraints/Parameters	2038/0/61	2153/0/60
GOF on F^2	1.155	1.073
Final R indices [I>2σ(I)]	R_1=0.0208 wR_2=0.0553	R_1=0.0185 wR_2=0.0433
R indices (all data)	R_1=0.0221 wR_2=0.0557	R_1=0.0227 wR_2=0.0443
V Max. Resid. Peaks (e*$Å^{-3}$)	0.287 and -0.394	0.434 and -0.177

Table D.2. Crystallographic and experimental data for complex **3**.

	$[Cu^{I}(Me_6TREN)PPh_3][BPh_4]$
Formula	$C_{54}H_{65}BCuN_4P$
Color/Shape	colorless/rhomboid
Formula Weight	875.42
Crystal System	triclinic
Space Group	P -1
Temp (K)	150K
Cell Constants	
***a*, Å**	17.8968(2)
***b*, Å**	17.9299(2)
***c*, Å**	18.4322(2)
α, deg	99.717(10)
β, deg	109.9550(10)
γ, deg	113.8060(10)
V, $Å^3$	4752.43(9)
Formula units/unit cell	4
Dcal'd, gcm^{-3}	1.224
μ, mm^{-1}	0.533
F(000)	1864
Diffractometer	Bruker Smart ApexII
Radiation, graphite monochr.	Mo Kα (λ=0.71073 Å)
Crystal size, mm	0.350 x 0.34 x 0.100
θ range, deg	1.26< θ <29.78
Range of *h,k,l*	±24, ±25, ±25
Reflections collected/unique	79007/26903
R_{int}	0.0356
Refinement Method	Full Matrix Least-Squares on F^2
Data/Restraints/Parameters	26903/0/1111
GOF on F^2	0.898
Final R indices [I>2σ(I)]	R_1=0.0394 wR_2=0.1141
R indices (all data)	R_1=0.0645 wR_2=0.1378
Max. Resid. Peaks (e*$Å^{-3}$)	0.388 and -0.478

D.2. Crystal Packing Diagrams of Copper Complexes with Me_6TREN ligand.

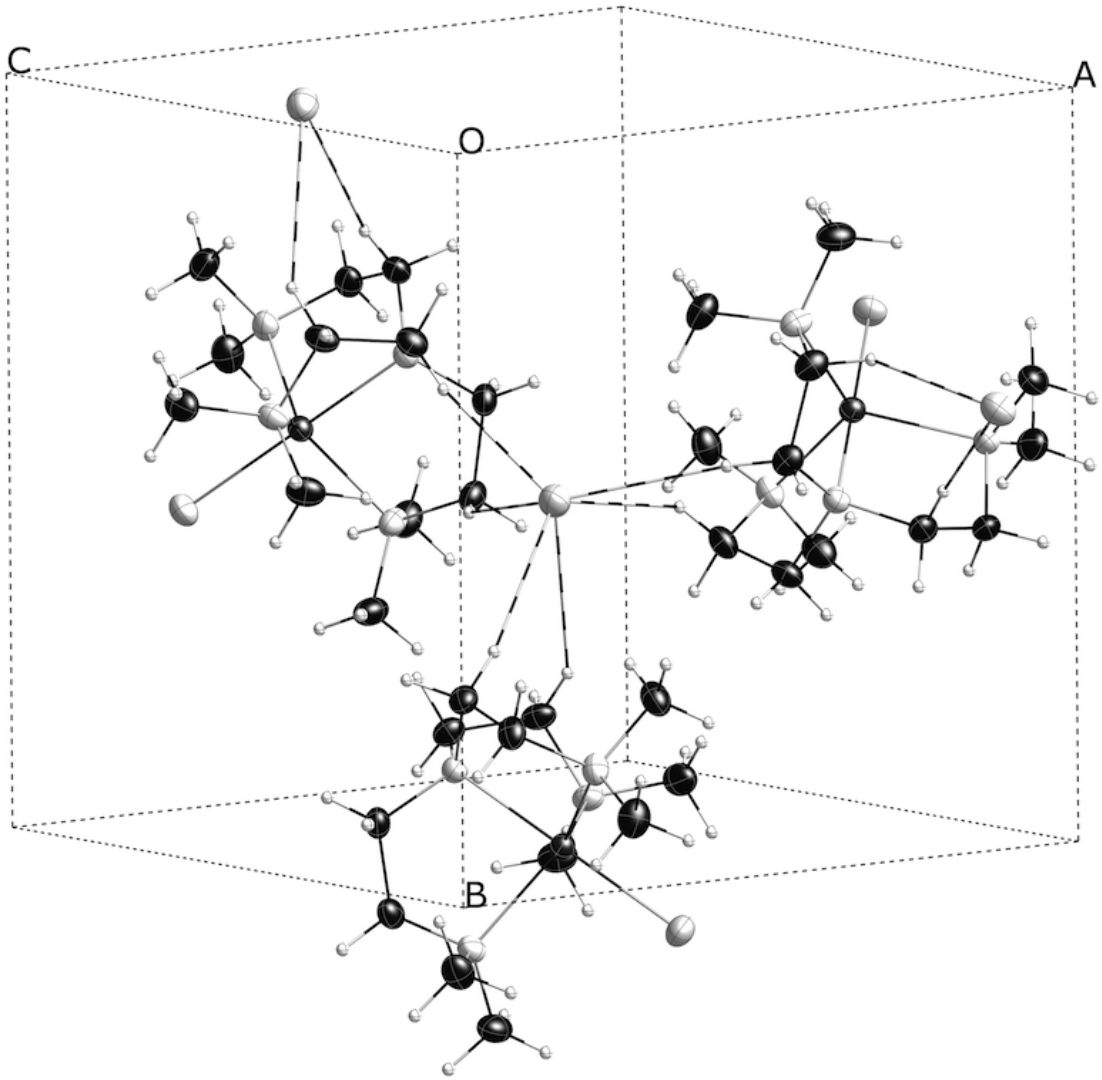

Figure D.2.1. Unit cell packing diagram of $[Cu^{II}(Me_6TREN)Cl][Cl]$ (1) with intermolecular interactions shown with dashed bonds. Only Cl---H-C interactions were detected with distances of 2.733(6) Å (H1B-Cl2) and 2.864(6) Å (H2B-Cl2).

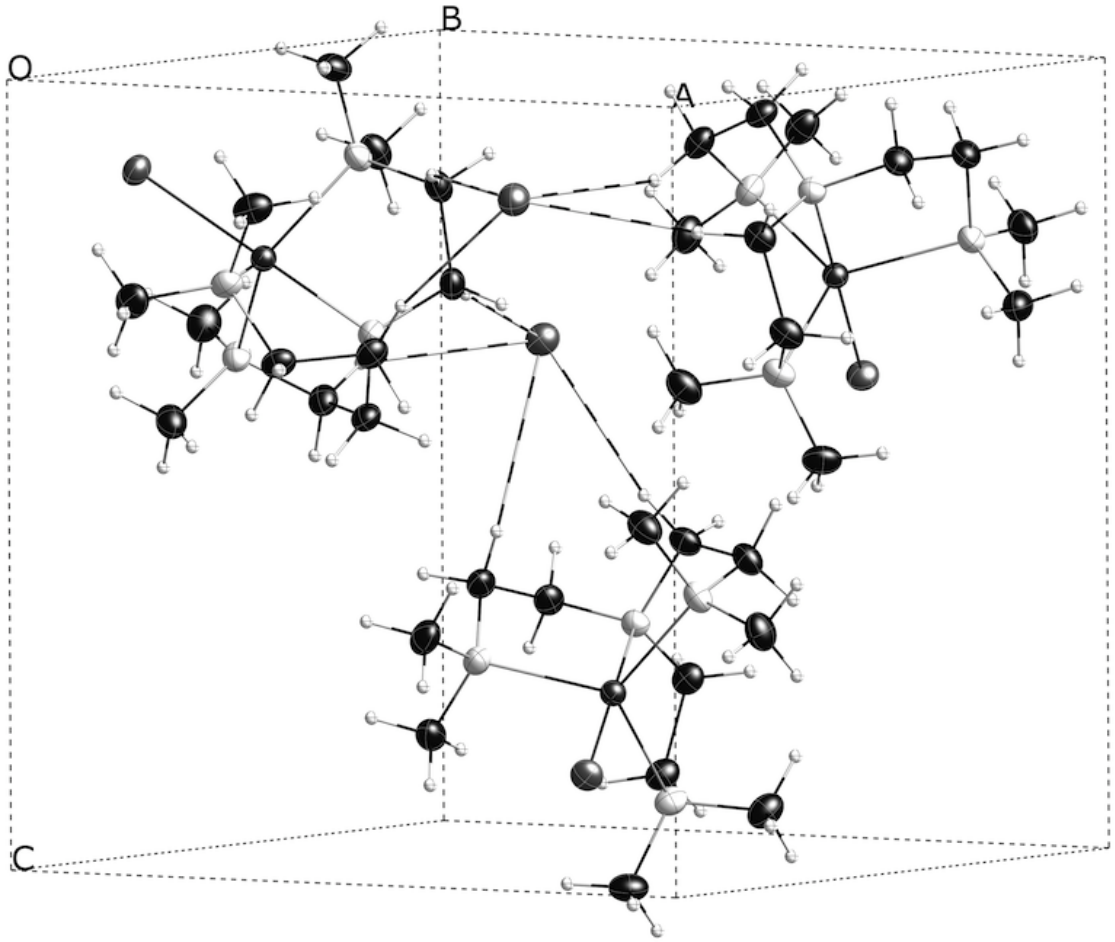

Figure D.2.2. Unit cell packing diagram of $[Cu^{II}(Me_6TREN)Br][Br]$ (2) with intermolecular interactions shown with dashed bonds. Only Br---H-C interactions were detected with distances of 2.838(6) Å (H1A-Br2) and 3.005(6) Å (H2A-Br2).

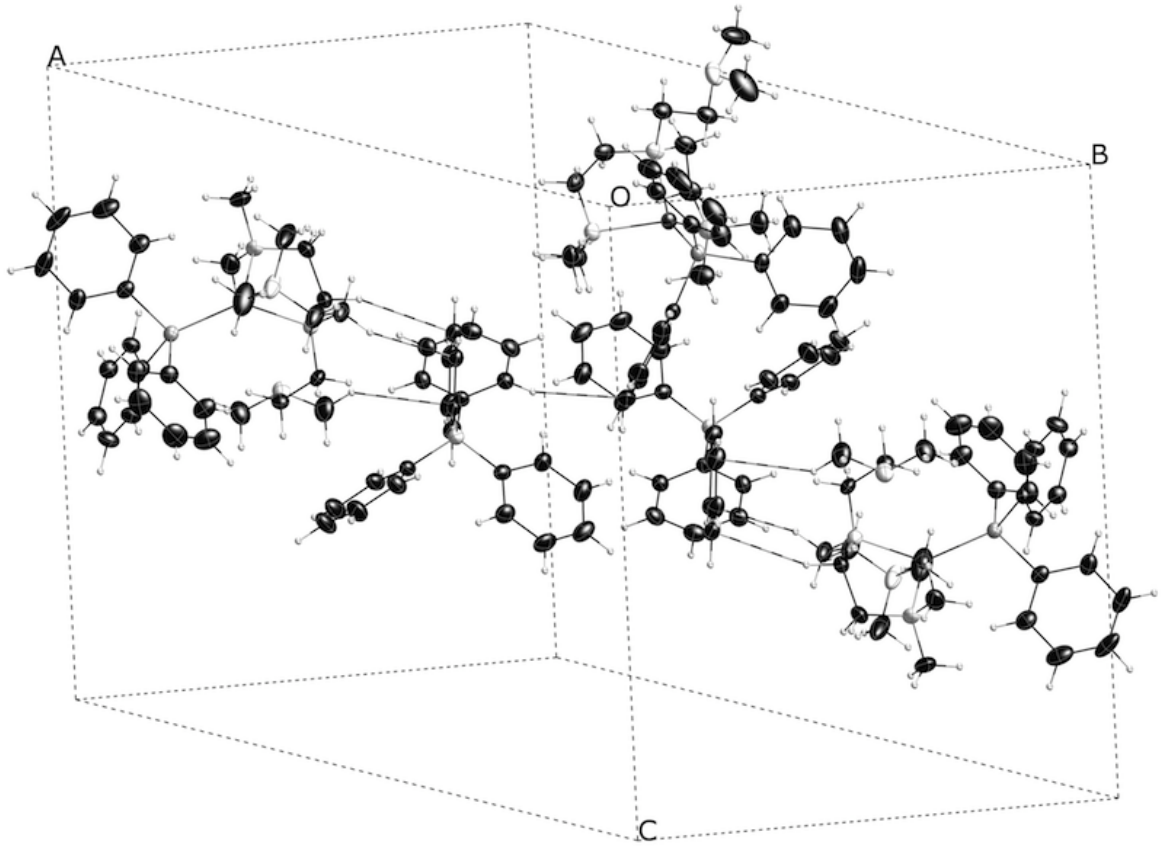

Figure D.2.3. Unit cell packing diagram of $[Cu^{I}(Me_6TREN)PPh_3][BPh_4]$ (3) with intermolecular interactions shown with dashed bonds. Only C---H-C interactions were detected with distances ranging from 2.6579(6) Å to 2.879(6) Å.

D.3. Infrared Spectroscopy of Copper Complexes with Me_6TREN Ligand

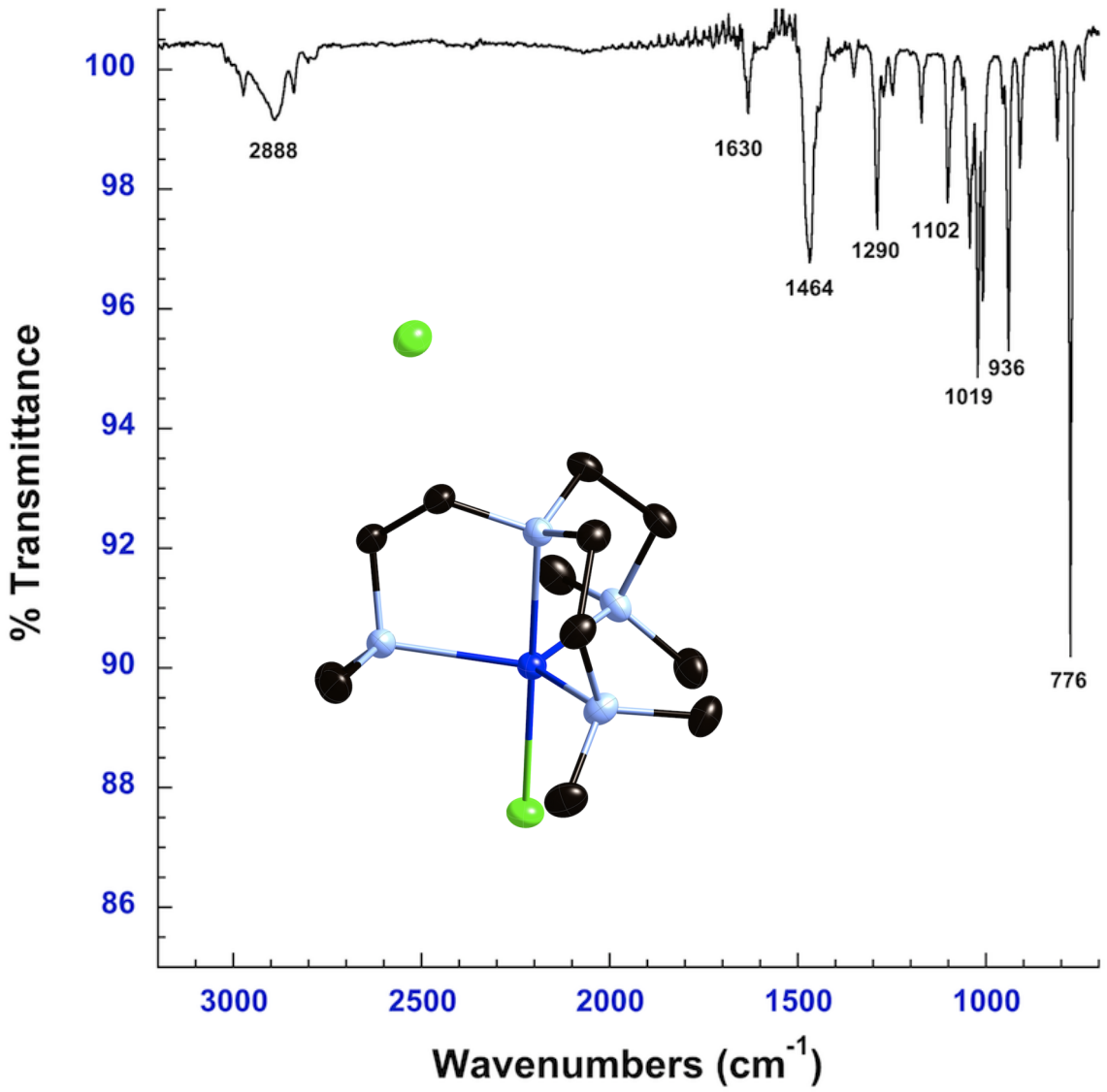

Figure D.3.1. Infrared spectrum for $[Cu^{II}(Me_6TREN)Cl][Cl]$ (**1**) (ATR FT-IR)

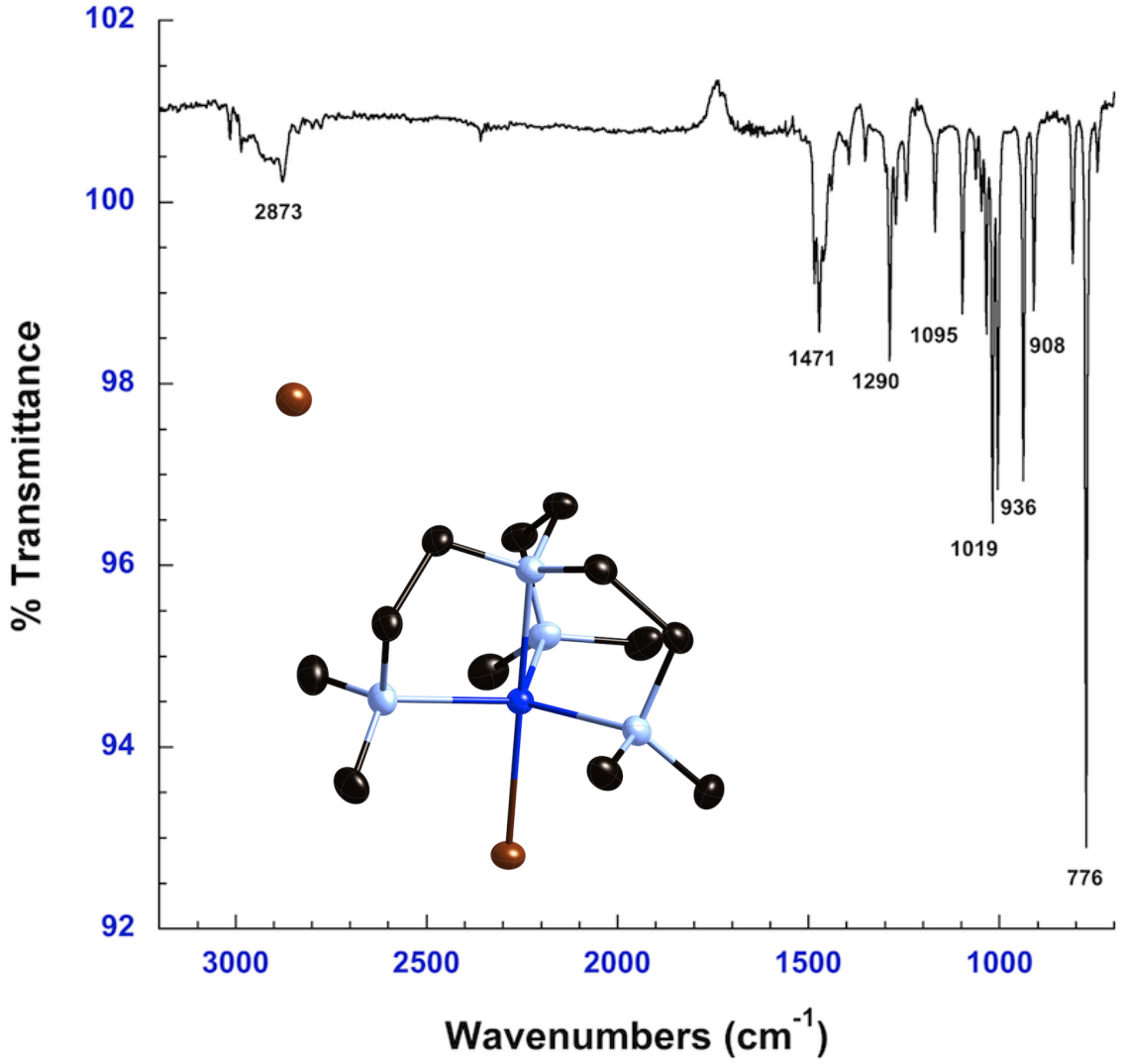

Figure D.3.2. Infrared spectrum for $[Cu^{II}(Me_6TREN)Br][Br]$ (**2**) (ATR FT-IR)

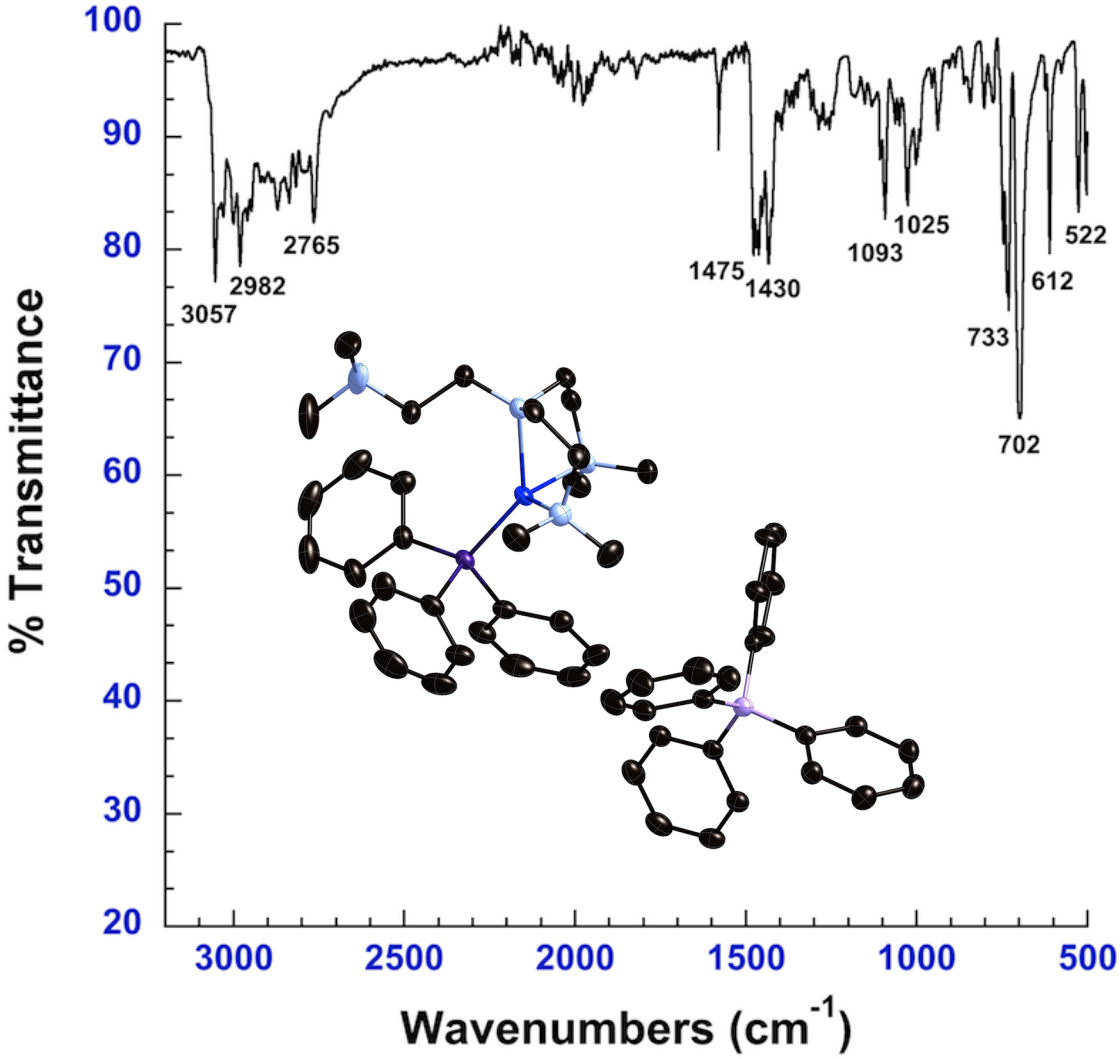

Figure D.3.3. Infrared spectrum for $[Cu^{I}(Me_6TREN)PPh_3][BPh_4]$ (**3**) (ATR FT-IR)

D.4. Crystallographic Information for Monoadducts of *cis*-Cyclooctene

Table D.4.1. Crystallographic and experimental data for *cis*-1-Chloro-4-(trichloromethyl)cyclooctane and *cis*-1-Bromo-4-(trichloromethyl)cyclooctane

	***cis*-1-Cl-4-(CCl_3)cyclooctane**	***cis*-1-Br-4-(CCl_3)cyclooctane**
Formula	$C_9 H_{14} Cl_4$	$C_9 H_{14} Br Cl_3$
Color/Shape	colorless/rhomboid	colorless/rhomboid
Formula Weight	264.00	308.46
Crystal System	triclinic	triclinic
Space Group	P -1	P -1
Temp (K)	150K	150K
Cell Constants		
***a*, Å**	7.3804(2)	7.5398(5)
***b*, Å**	8.8401(2)	8.8709(6)
***c*, Å**	9.3662(2)	9.3096(7)
α, deg	88.6140(10)	89.5290(10)
β, deg	77.9500(10)	78.3550(10)
γ, deg	71.8860(10)	71.4070(10)
V, $Å^3$	567.46(2)	576.97(7)
Formula units/unit cell	2	2
Dcal'd, gcm^{-3}	1.545	1.776
μ, mm^{-1}	0.995	4.21
F(000)	272	308
Diffractometer	Bruker Smart ApexII	Bruker Smart ApexII
Radiation, graphite monochr.	Mo Kα (λ=0.71073 Å)	Mo Kα (λ=0.71073 Å)
Crystal size, mm	0.43 x 0.34 x 0.30	0.27 x 0.22 x 0.10
θ range, deg	2.43 < θ < 32.61	2.24 < θ < 32.53
Range of *h,k,l*	±11, ±13, ±14	±11, -13 12, ±13
Reflections collected/unique	10120/3836	7425/3815
R_{int}	0.0291	0.0148
Refinement Method	Full Matrix Least-Squares on F2	Full Matrix Least-Squares on F2
Data/Restraints/Parameters	3836/0/119	3815/0/118
GOF on F^2	0.777	0.835
Final R indices [I>2σ(I)]	R1=0.0448 wR2=0.1097	R1=0.0376 wR2=0.1186
R indices (all data)	R1=0.0468 wR2=0.1125	R1=0.0480 wR2=0.1282
Max. Resid. Peaks ($e*Å^{-3}$)	0.930 and -0.903	2.186 and -1.098

Table D.4.2 Crystallographic and experimental data for *cis*-1-Bromo-4-(tribromomethyl)cyclooctane and *trans*-1-Bromo-4-(tribromomethyl)cyclooctane

	***cis*-1-Br-4-(CBr_3)cyclooctane**	***trans*-1-Br-4-(CBr_3)cyclooctane**
Formula	$C_9 H_{14} Br_4$	$C_9 H_{14} Br_4$
Color/Shape	colorless/rhomboid	colorless/rhomboid
Formula Weight	441.84	441.84
Crystal System	triclinic	triclinic
Space Group	P -1	P -1
Temp (K)	150K	150K
Cell Constants		
***a*, Å**	7.624(6)	7.32690(10)
***b*, Å**	8.962(7)	9.28220(10)
***c*, Å**	9.546(8)	9.4153(2)
α, deg	88.646(12)	100.6100(10)
β, deg	78.322(11)	92.6440(10)
γ, deg	72.257(10)	98.7340(10)
V, $Å^3$	607.8(9)	620.274(17)
Formula units/unit cell	2	2
Dcal'd, gcm^{-3}	2.414	2.366
μ, mm^{-1}	13.199	12.934
F(000)	416	416
Diffractometer	Bruker Smart ApexII	Bruker Smart ApexII
Radiation, graphite monochr.	Mo Kα (λ=0.71073 Å)	Mo Kα (λ=0.71073 Å)
Crystal size, mm	0.21 x 0.20 x 0.11	0.21 x 0.17 x 0.09
θ range, deg	2.18 < θ < 24.48	2.21 < θ < 32.40
Range of *h,k,l*	±8, ±10, ±11	-11→10, ±13, ±14
Reflections collected/unique	4380/1992	10939/4102
R_{int}	0.043	0.0183
Refinement Method	Full Matrix Least-Squares on F2	Full Matrix Least-Squares on F2
Data/Restraints/Parameters	1992/0/118	4102/0/118
GOF on F^2	0.827	0.654
Final R indices [I>2σ(I)]	R1=0.0403 wR2=0.1101	R1=0.0214 wR2=0.0746
R indices (all data)	R1=0.0525 wR2=0.1187	R1=0.0304 wR2=0.0843
Max. Resid. Peaks (e*$Å^{-3}$)	1.137 and -1.311	1.020 and -0.682

D.5. Molecular Structures of 1-chloro-4-(trichloromethyl)-cyclooctane and 1-bromo-4-(trichloromethyl)cyclooctane.

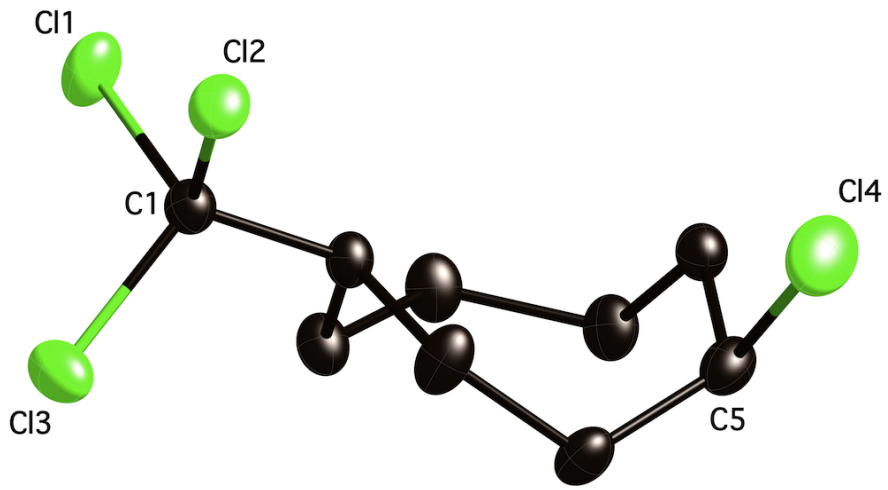

Figure D.5.1. Molecular structure of 1-chloro-4-(trichloromethyl)cyclooctane collected at 150 K, shown at 50% probability ellipsoids with H-atoms omitted for clarity. Selected bond distances [Å]: Cl1-C1 1.7873(12), Cl2-C1 1.7790(12), Cl3-C1 1.7835(12), Cl4-C5 1.8185(13).

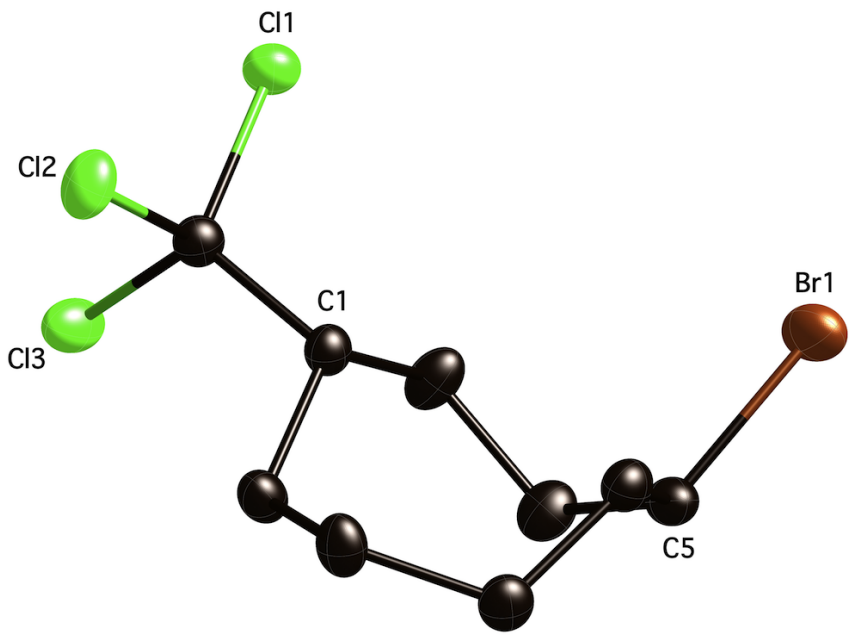

Figure D.5.2. Molecular structure of 1-bromo-4-(trichloromethyl)cyclooctane collected at 150 K, shown at 50% probability ellipsoids with H-atoms omitted for clarity. Selected bond distances [Å]:Br1-C5 1.986(3), Cl2-C1 1.790(3), Cl3-C1 1.788(3), Cl4-C1 1.785(2).

D.6. ^{1}H NMR Spectroscopy Data of Monoadducts for *cis*-Cyclooctene

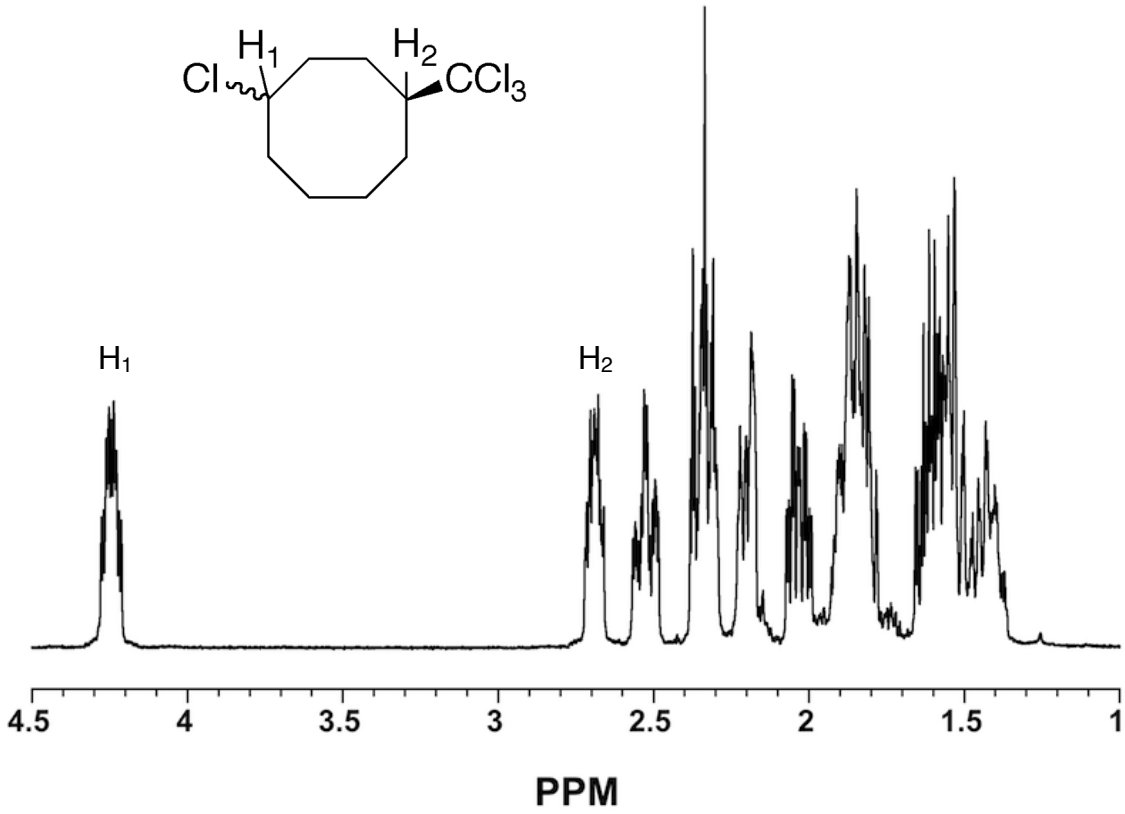

Figure D.6.1. ^{1}H NMR of *rac*-1-Chloro-4-(trichloromethyl)cyclooctane (400 MHz, 298K, $CDCl_3$), both enantiomers were found to have identical ^{1}H NMR spectra.

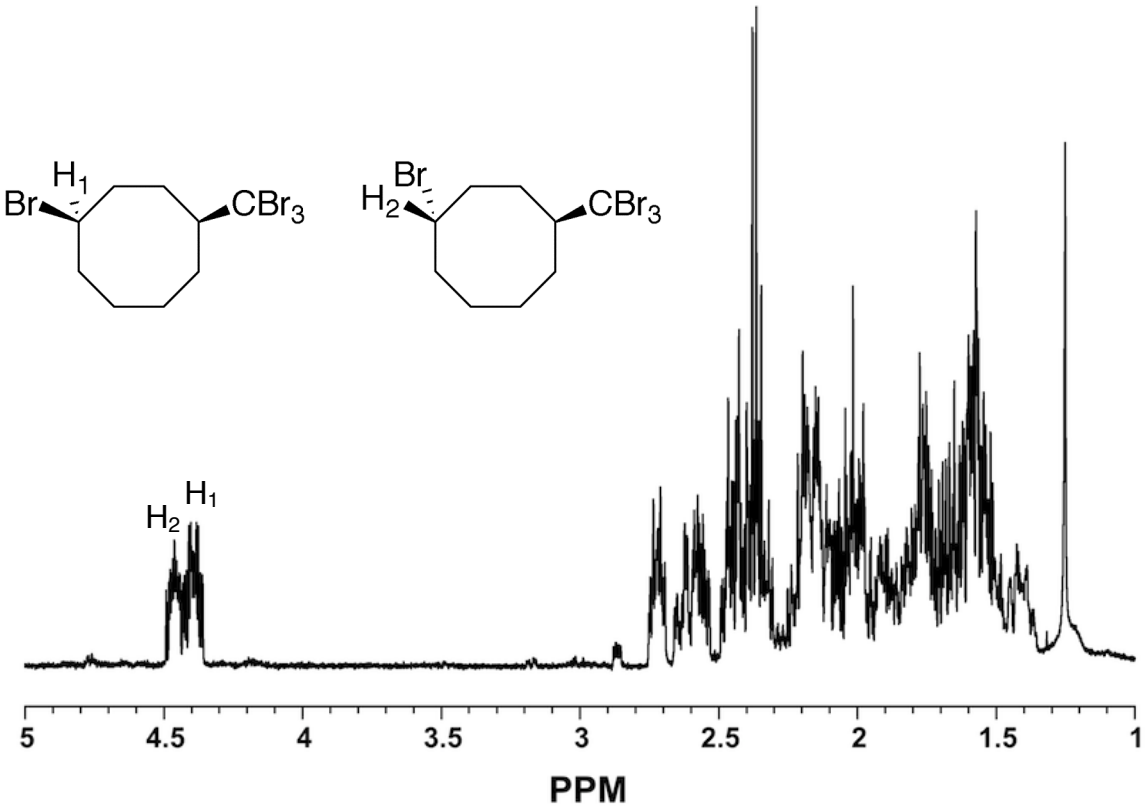

Figure D.6.2. ^{1}H NMR of *rac*-1-Bromo-4-(tribromomethyl)cyclooctane (400 MHz, 298K, $CDCl_3$),), proton assignments were determined by isolation of products.

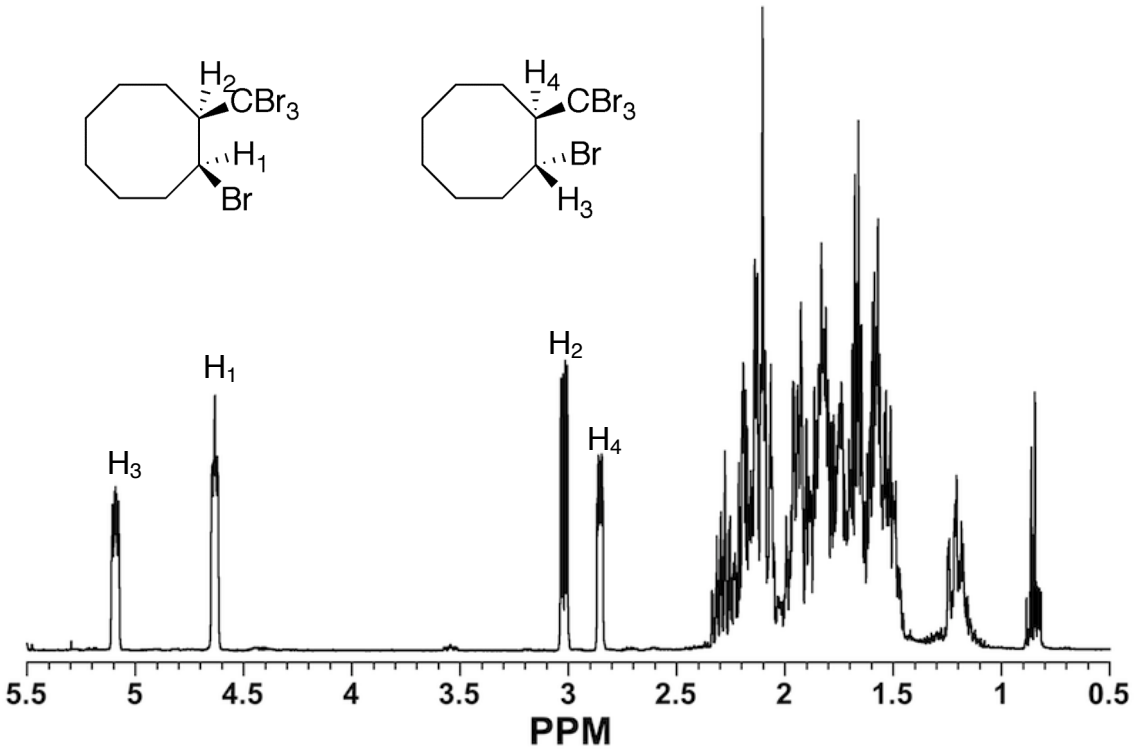

Figure D.6.3. ^{1}H NMR of *rac*-1-Bromo-2-(tribromomethyl)cyclooctane (400 MHz, 298K, $CDCl_3$), proton assignments were determined using ^{1}H NOSEY and ^{1}H COSY NMR.

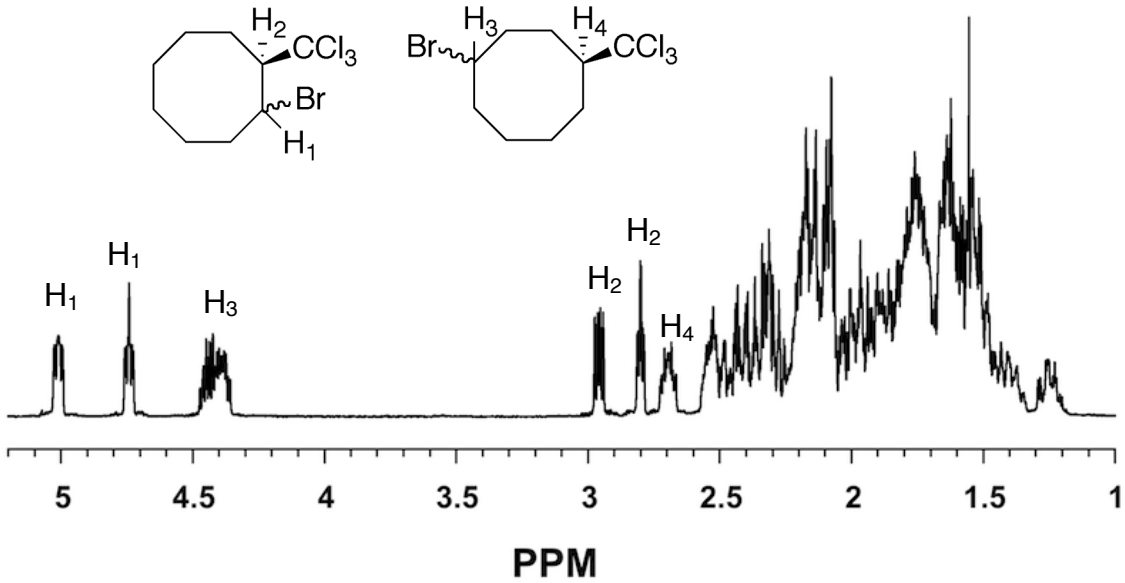

Figure D.6.4. ^{1}H NMR of *rac*-1-Bromo-2-(trichloromethyl)cyclooctane and *rac*-1-Bromo-4-(trichloromethyl)cyclooctane (400 MHz, 298K, $CDCl_3$). Peak assignments for isomers determined by crystallization of 1,4-isomer.

Appendix E.

E.1. Crystallographic Information for Copper Complexes

Table E.1.1. Crystallographic data and experimental data for complexes **1** and **2**.

	$[Cu^{I}(TPMA)CH_3CN][BPh_4]$ (1)	**$[Cu^{I}(TPMA)][BPh_4]$ (2)**
Formula	$C_{44}H_{41}BCuN_5$	$C_{42}H_{38}BCuN_4$
Color/shape	orange/rhomboid	yellow/rhomboids
Formula Weight	714.17	673.11
Crystal System	monoclinic	Triclinic
Space Group	P 21/n	P -1
Temp (K)	150	150
Cell Constants		
***a* (Å)**	13.1779(4)	11.552(4)
***b* (Å)**	12.6607(4)	13.797(5)
***c* (Å)**	22.1937(7)	21.629(7)
α (deg)	90	89.620(5)
β (deg)	91.45	81.377(5)
γ (deg)	90	79.961(5)
V ($Å^3$)	3701.6(2)	3355.6
Formula units/unit cell	4	4
Density calc'd (gcm^{-3})	1.281	1.332
μ (mm^{-1})	0.628	0.688
F(000)	1496	1408
Diffractometer	Bruker Smart ApexII	Bruker Smart ApexII
Radiation, graphite-monochrom.	Mo Kα (λ=0.71073 Å)	Mo Kα (λ=0.71073 Å)
Crystal size (mm)	0.360 x 0.270 x 0.240	0.38 x 0.28 x 0.25
θ range (deg)	1.78< θ <32.63	0.95< θ <25.17
Range of *h,k,l*	±38, ±37, ±65	±13, ±16, ±25
Reflections collected/unique	46448/12714	26263/11912
R_{int}	0.0213	0.0686
Refinement Method	Full Matrix Least-Squares on F^2	Full Matrix Least-Squares on F^2
Data/Restraints/Parameters	12714/0/461	11912/0/865
GOF on F^2	1.026	0.996
Final R indices [I>2σ(I)]	R_1=0.0343 wR_2=0.0897	R_1=0.0698 wR_2=0.1747
R indices (all data)	R_1=0.0480 wR_2=0.0969	R_1=0.1051 wR_2=0.2042
Max. Residual Peaks ($e*Å^{-3}$)	0.394 and -0.340	1.511 and -1.226

Table E.1.2. Crystallographic data and experimental data for complexes **3** and **4**.

	$[(Cu^{I}(TPMA))_2\text{-}\mu Br][BPh_4]$ (3)	**$[Cu^{I}(TPMA)]_2[ClO_4]_2$ *$2CH_3OH$ (4)**
Formula	$C_{60}H_{56}BBrCu_2N_8$	$C_{38}H_{44}Cl_2Cu_2N_8O_{10}$
Color/shape	red/rhomboids	yellow/rhomboids
Formula Weight	1106.95	970.79
Crystal System	monoclinic	monoclinic
Space Group	P 21/n	c2/c
Temp (K)	150	150
Cell Constants		
a (Å)	9.9650(3)	13.7214(3)
b (Å)	15.0762(4)	15.3183(3)
c (Å)	33.9922(9)	19.9249(5)
α (deg)	90	90
β (deg)	91.83	100.8530(10)
γ (deg)	90	90
V ($Å^3$)	5104.2	4113.08
Formula units/unit cell	4	4
Density calc'd (gcm^{-3})	1.441	1.568
μ (mm^{-1})	1.665	1.231
F(000)	2164	2000
Diffractometer	Bruker Smart ApexII	Bruker Smart ApexII
Radiation, graphite-monochrom.	Mo Kα (λ=0.71073 Å)	Mo Kα (λ=0.71073 Å)
Crystal size (mm)	0.35 x 0.20 x 0.12	0.31 x 0.27 x 0.13
θ range (deg)	1.20< θ <28.89	2.01< θ <32.05
Range of h,k,l	±13, ±20, ±46	±20, ±22, ±29
Reflections collected/unique	54423/13420	36177/7038
Rint	0.0452	0.0389
Refinement Method	Full Matrix Least-Squares on F^2	Full Matrix Least-Squares on F^2
Data/Restraints/Parameters	13420/0/649	7038/0/273
GOF on F^2	1.05	1.019
Final R indices [I>2σ(I)]	R_1=0.0390 wR_2=0.0931	R_1=0.0379 wR_2=0.0992
R indices (all data)	R_1=0.0625 wR_2=0.1052	R_1=0.0536 wR_2=0.1103
Max. Residual Peaks ($e^*Å^{-3}$)	0.526 and -0.798	0.697 and -0.464

Table E.1.3. Crystallographic data and experimental data for complexes **5**, **6** and **7**.

	$[Cu^I(TPMA)dipy][BPh_4]$ (5&6)	**$[Cu^I(TPMA)PPh_3][BPh_4]$ (7)**
Formula	$C_{208}H_{184}B_4Cu_4N_{24}$	$C_{60}H_{53}BCuN_4P$
Color/shape	red/rhomboids	yellow/rhomboids
Formula Weight	3317.19	935.38
Crystal System	monoclinic	monclinic
Space Group	P 21/c	P 21/c
Temp (K)	150	150
Cell Constants		
***a*, Å**	9.3559(3)	11.2072(3)
***b*, Å**	15.6108(4)	17.0383(5)
***c*, Å**	57.3203(15)	24.7029(7)
a, deg	90	90
b, deg	91.534(2)	91.338(2)
g, deg	90	90
V, Å3	8368.8	4715.8(2)
Formula units/unit cell	2	4
Density calc'd, gcm^{-3}	1.316	1.317
μ, mm-1	0.567	0.543
F(000)	3472	1960
Diffractometer	Bruker Smart ApexII	Bruker Smart ApexII
Radiation, graphite monochr.	Mo Kα (λ=0.71073 Å)	Mo Kα (λ=0.71073 Å)
Crystal size, mm	0.77 x 0.26 x 0.19	0.350 x 0.160 x 0.150
θ range, deg	0.71< θ <28.02	1.65 < θ < 29.00
Range of *h,k,l*	±12, ±20, ±75	±15, ±23, ±33
Reflections collected/unique	118710/20226	71137/12449
R_{int}	0.0349	0.0526
Refinement Method	Full Matrix Least-Squares on F^2	Full Matrix Least-Squares on F^2
Data/Restraints/Parameters	20226/0/1081	12449/0/604
GOF on F^2	1.130	0.992
Final R indices [I>2σ(I)]	R_1=0.0643 wR_2=0.01382	R_1=0.0418 wR_2=0.1317
R indices (all data)	R_1=0.0776 wR_2=0.1441	R_1=0.0543 wR_2=0.1440
Max. Resid. Peaks (e*$Å^{-3}$)	0.854 and -1.744	0.509 and -0.646

Table E.1.4. Crystallographic data and experimental data for complexes **8** and **9**.

	$[Cu^{II}(TPMA)Cl][ClO_4]$ (8)	**$[Cu^{II}(TPMA)Cl][BPh_4]*CH_3CN$ (9)**
Formula	$C_{18}H_{18}Cl_2CuN_4O_4$	$C_{44}H_{41}BClCuN_5$
Color/shape	blue/rhomboids	blue/rhomboids
Formula Weight	488.80	749.62
Crystal System	monoclinic	monoclinic
Space Group	P 21/c	P 21/c
Temp (K)	150	150
Cell Constants		
***a* (Å)**	14.70460(10)	14.1138(4)
***b* (Å)**	9.28680(10)	17.7509(5)
***c* (Å)**	29.6709(3)	15.0255(4)
α (deg)	90	90
β (deg)	90.7200(10)	100.6670(10)
γ (deg)	90	90
V ($Å^3$)	4051.50(7)	3699.33(18)
Formula units/unit cell	8	4
Density calc'd (gcm^{-3})	1.603	1.346
μ (mm^{-1})	1.375	0.702
F(000)	1992	1564
Diffractometer	Bruker Smart ApexII	Bruker Smart ApexII
Radiation, graphite-monochromated	Mo Kα (λ=0.71073 Å)	Mo Kα (λ=0.71073 Å)
Crystal size (mm)	0.400 x 0.280 x 0.100	0.540 x 0.450 x 0.320
θ range (deg)	1.37< θ <32.57	1.47< θ <32.54
Range of *h,k,l*	±22, ±13, ±44	-21→20, ±26, ±22
Reflections collected/unique	74813/14352	65281/12706
R_{int}	0.0314	0.0193
Refinement Method	Full Matrix Least-Squares on F^2	Full Matrix Least-Squares on F^2
Data/Restraints/Parameters	14352/0/523	12706/0/471
GOF on F^2	1.031	0.957
Final R indices [I>2σ(I)]	R_1=0.0400 wR_2=0.1094	R_1=0.0331 wR_2=0.1111
R indices (all data)	R_1=0.0601 wR_2=0.1222	R_1=0.0395 wR_2=0.1210
Max. Residual Peaks ($e*Å^{-3}$)	1.234 and -1.018	0.594 and -0.360

Table E.1.5. Crystallographic data and experimental data for complexes **10** and **11**.

	$[Cu^{II}(TPMA)Br][ClO_4]$ (10)	**$[Cu^{II}(TPMA)Br][BPh_4]*CH_3CN$ (11)**
Formula	$C_{18}H_{18}BrClCuN_4O_4$	$C_{44}H_{41}BBrCuN_5$
Color/shape	green/rhomboids	green/rhomboids
Formula Weight	533.26	794.08
Crystal System	monoclinic	monoclinic
Space Group	P 21/c	P 21/c
Temp (K)	150	150
Cell Constants		
***a* (Å)**	14.2907(6)	14.1435(4)
***b* (Å)**	9.5062(4)	17.8829(5)
***c* (Å)**	29.7578(13)	15.0883(4)
α (deg)	90	90
β (deg)	92.3810(10)	100.33
γ (deg)	90	90
V ($Å^3$)	3754.33(18)	3754.33(18)
Formula units/unit cell	8	4
Density calc'd (gcm^{-3})	1.754	1.405
μ (mm^{-1})	3.225	1.685
F(000)	2136	1636
Diffractometer	Bruker Smart ApexII	Bruker Smart ApexII
Radiation, graphite-monochromated	Mo Kα (λ=0.71073 Å)	Mo Kα (λ=0.71073 Å)
Crystal size (mm)	0.570 x 0.330 x 0.300	0.460 x 0.390 x 0.300
θ range (deg)	1.43< θ <32.49	1.78< θ <32.57
Range of *h,k,l*	±21, ±14, -45→43	±20, -26→27, ±22
Reflections collected/unique	49735/13788	47251/12871
R_{int}	0.0272	0.0197
Refinement Method	Full Matrix Least-Squares on F^2	Full Matrix Least-Squares on F^2
Data/Restraints/Parameters	13788/0/523	12871/0/470
GOF on F^2	1.082	1.024
Final R indices [I>2σ(I)]	R_1=0.0365 wR_2=0.0771	R_1=0.0321 wR_2=0.0853
R indices (all data)	R_1=0.0511 wR_2=0.0816	R_1=0.0450 wR_2=0.0913
Max. Residual Peaks ($e*Å^{-3}$)	0.894 and -0.463	0.706 and -0.890

E.2. ^{1}H NMR Data of Copper(I) Complexes

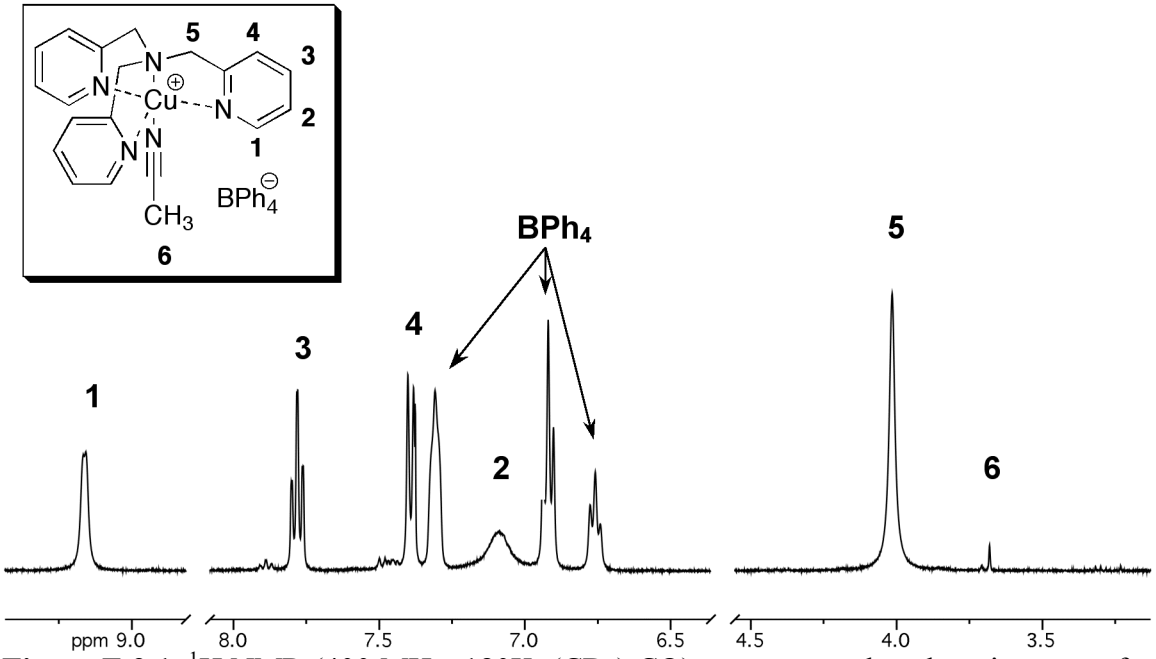

Figure E.2.1. ^{1}H NMR (400 MHz, 180K, $(CD_3)_2CO$) spectrum and peak assignments for $[Cu^I(TPMA)CH_3CN][BPh_4]$ (**1**).

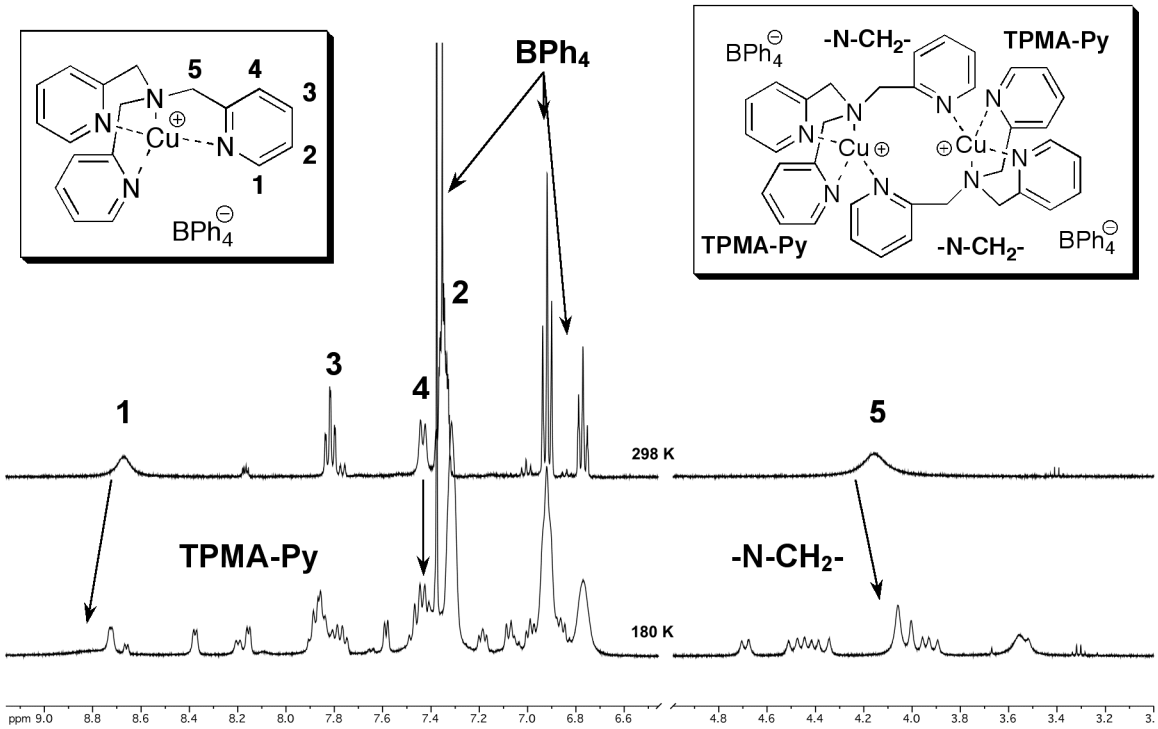

Figure E.2.2. ^{1}H NMR (400 MHz, 298 and 180K, $(CD_3)_2CO$) spectra and peak assignments for $[Cu^I(TPMA)][BPh_4]$ (**2**).

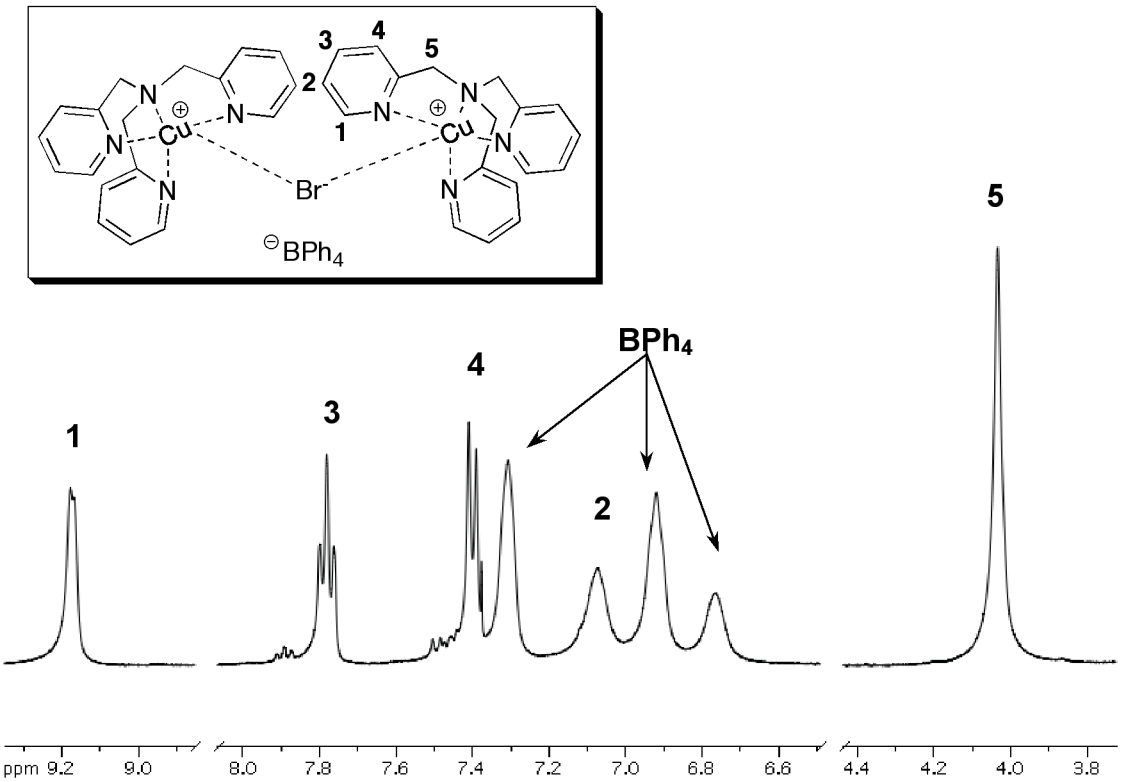

Figure E.2.3. ^{1}H NMR (400 MHz, 180K, $(CD_3)_2CO$) spectrum and peak assignments for $[(Cu^I(TPMA))_2\text{-}\mu Br][BPh_4]$ (**3**).

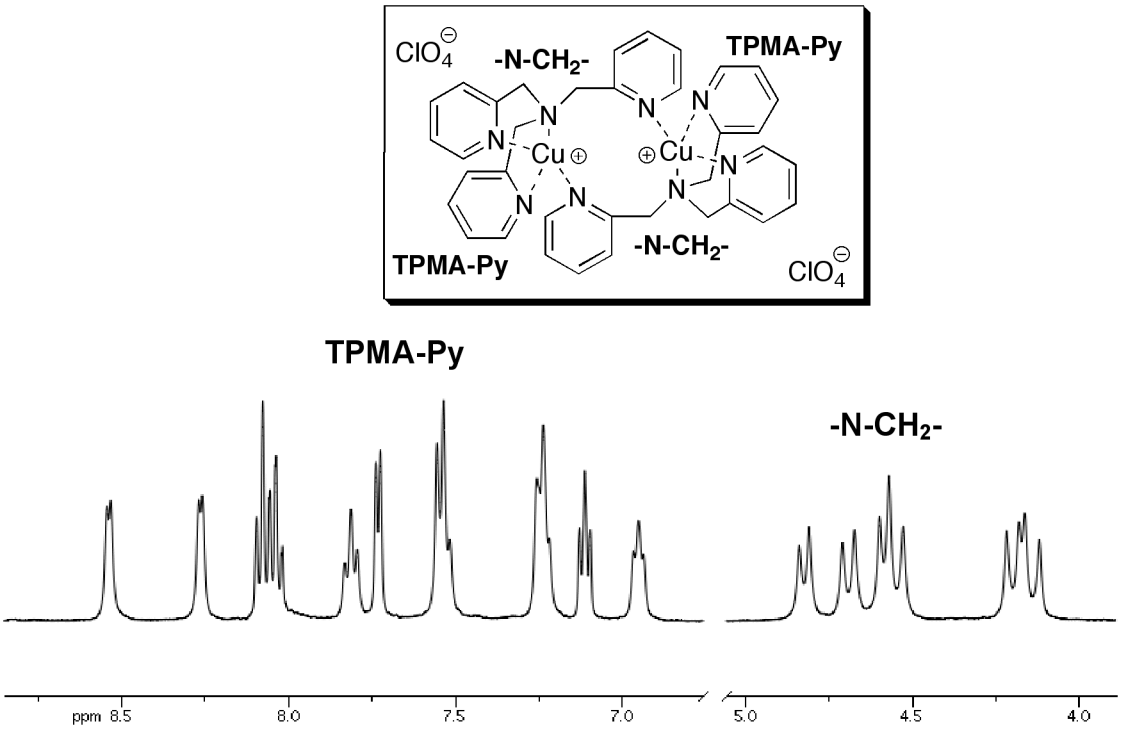

Figure E.2.4. ^{1}H NMR (400 MHz, 185K, $(CD_3)_2CO$) spectrum and peak assignments for $[Cu^I(TPMA)]_2[ClO_4]_2$ (**4**).

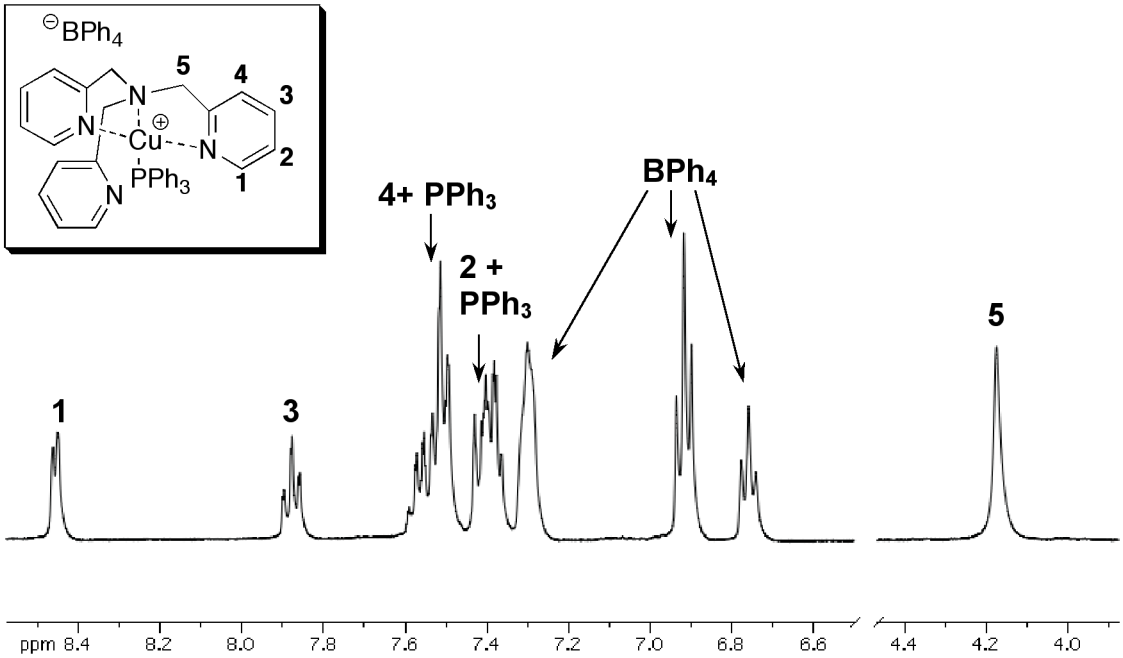

Figure E.2.5. ^{1}H NMR (400 MHz, 180K, $(CD_3)_2CO$) spectrum and peak assignments for $[Cu^I(TPMA)PPh_3][BPh_4]$ (**7**).

E.3. Infrared Spectroscopy of Copper Complexes

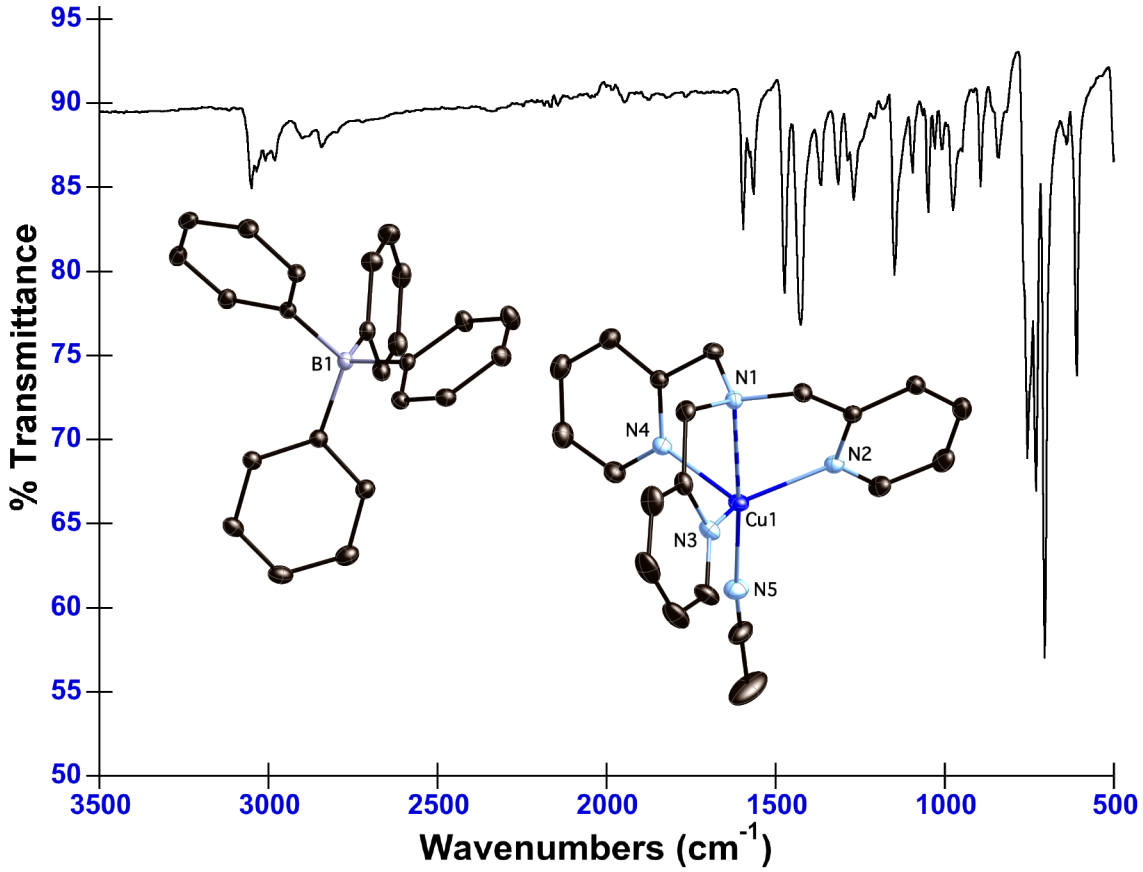

Figure E.3.1. Solid state ATR FT-IR spectrum of $[Cu^{I}(TPMA)CH_3CN][BPh_4]$ (**1**).

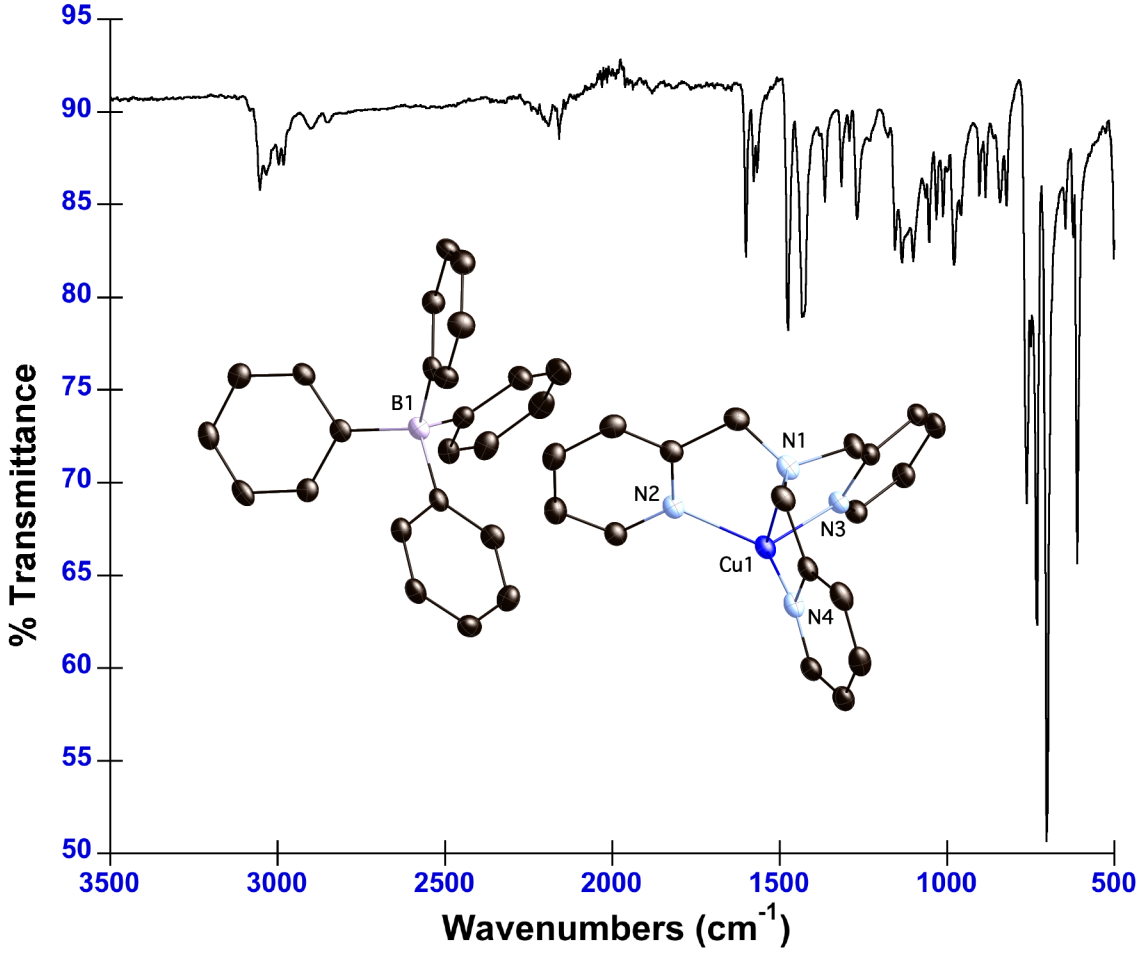

Figure E.3.2. Solid state ATR FT-IR spectrum of $[Cu^{I}(TPMA)][BPh_4]$ (**2**).

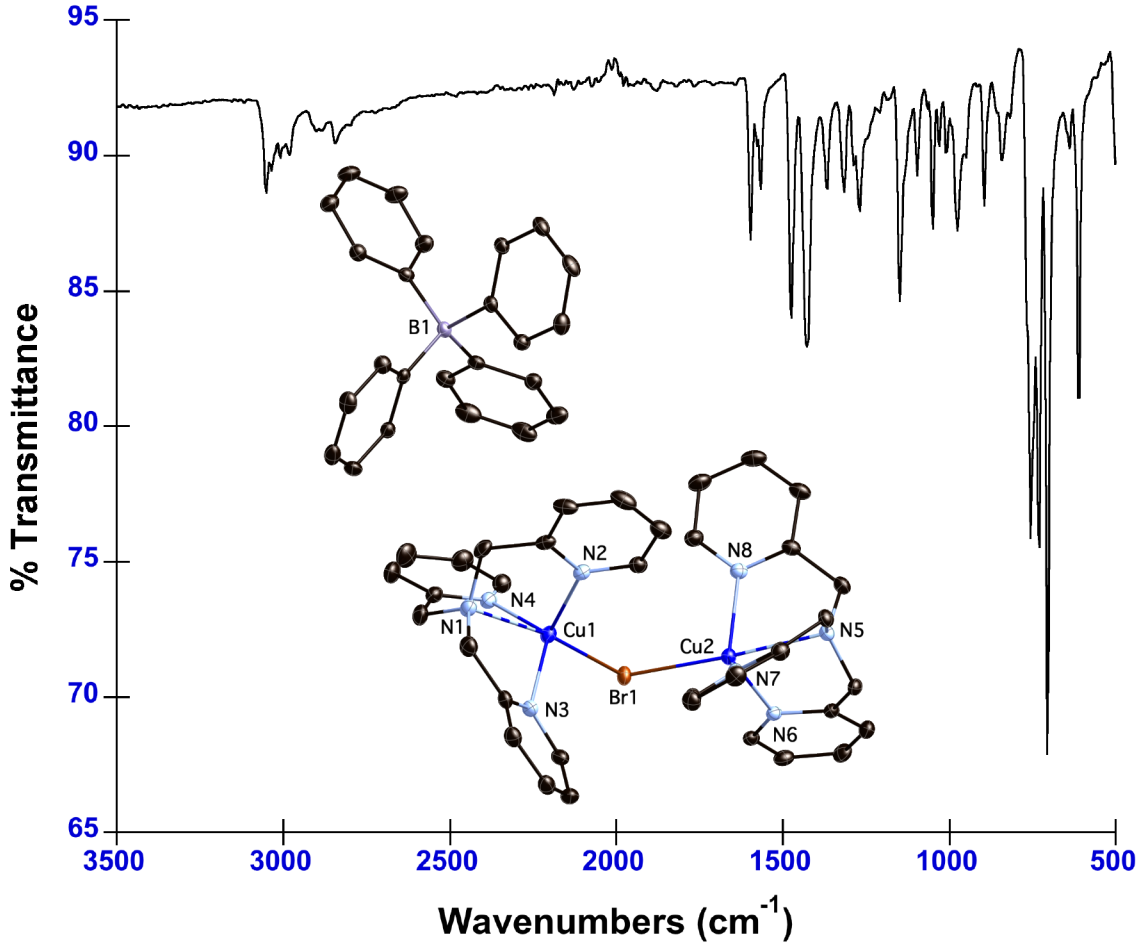

Figure E.3.3. Solid state ATR FT-IR spectrum of $[(Cu^{I}(TPMA))_2\text{-}\mu Br][BPh_4]$ (**3**).

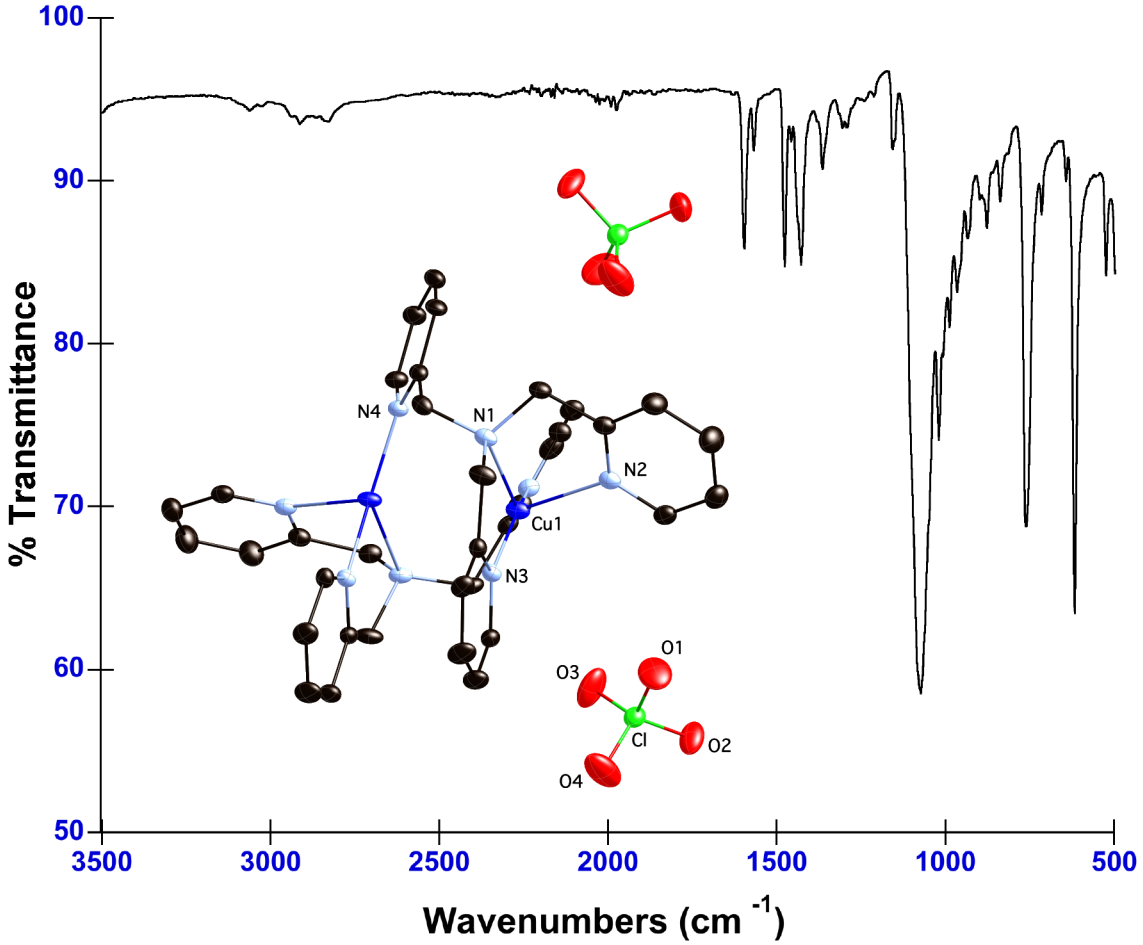

Figure E.3.4. Solid state ATR FT-IR spectrum of $[Cu^{I}(TPMA)]_2[ClO_4]_2$ (**4**).

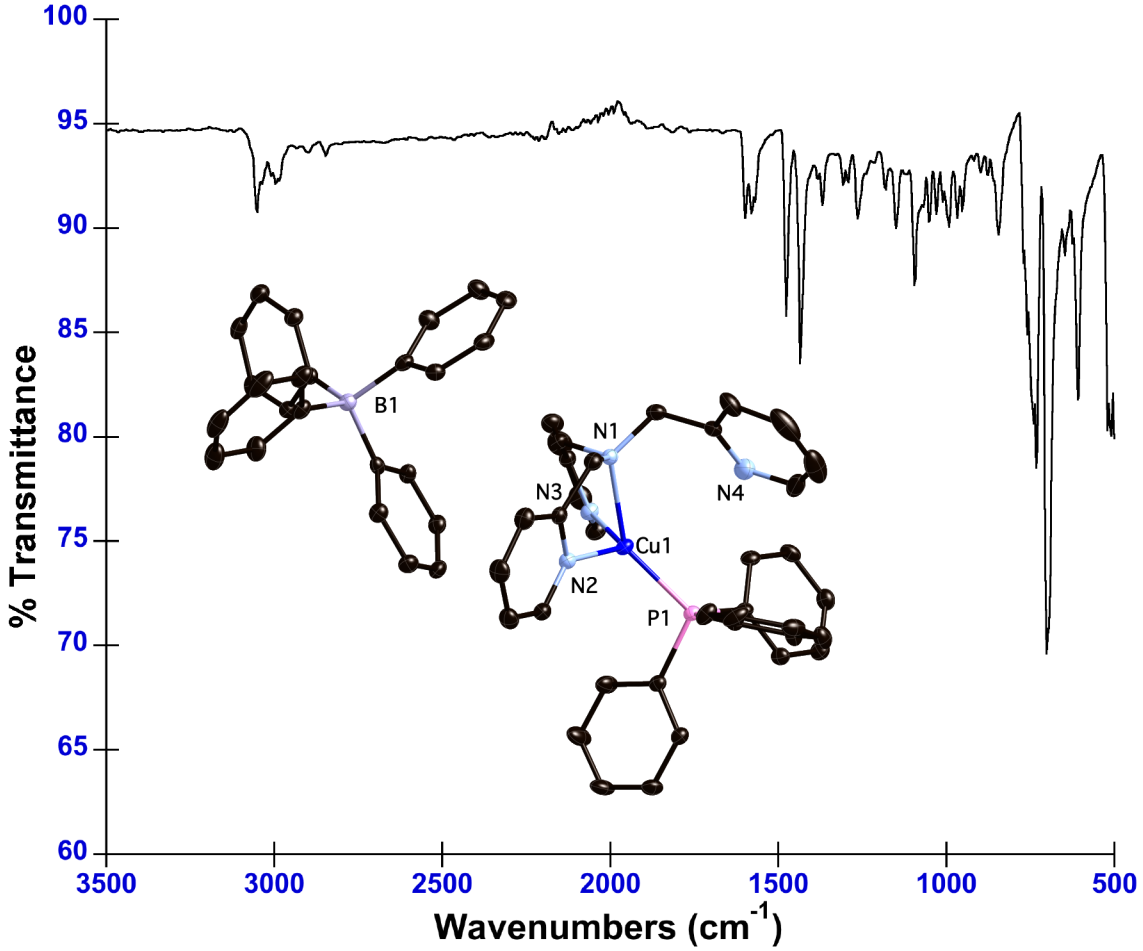

Figure E.3.5. Solid state ATR FT-IR spectrum of $[Cu^{I}(TPMA)PPh_3][BPh_4]$ (**7**).

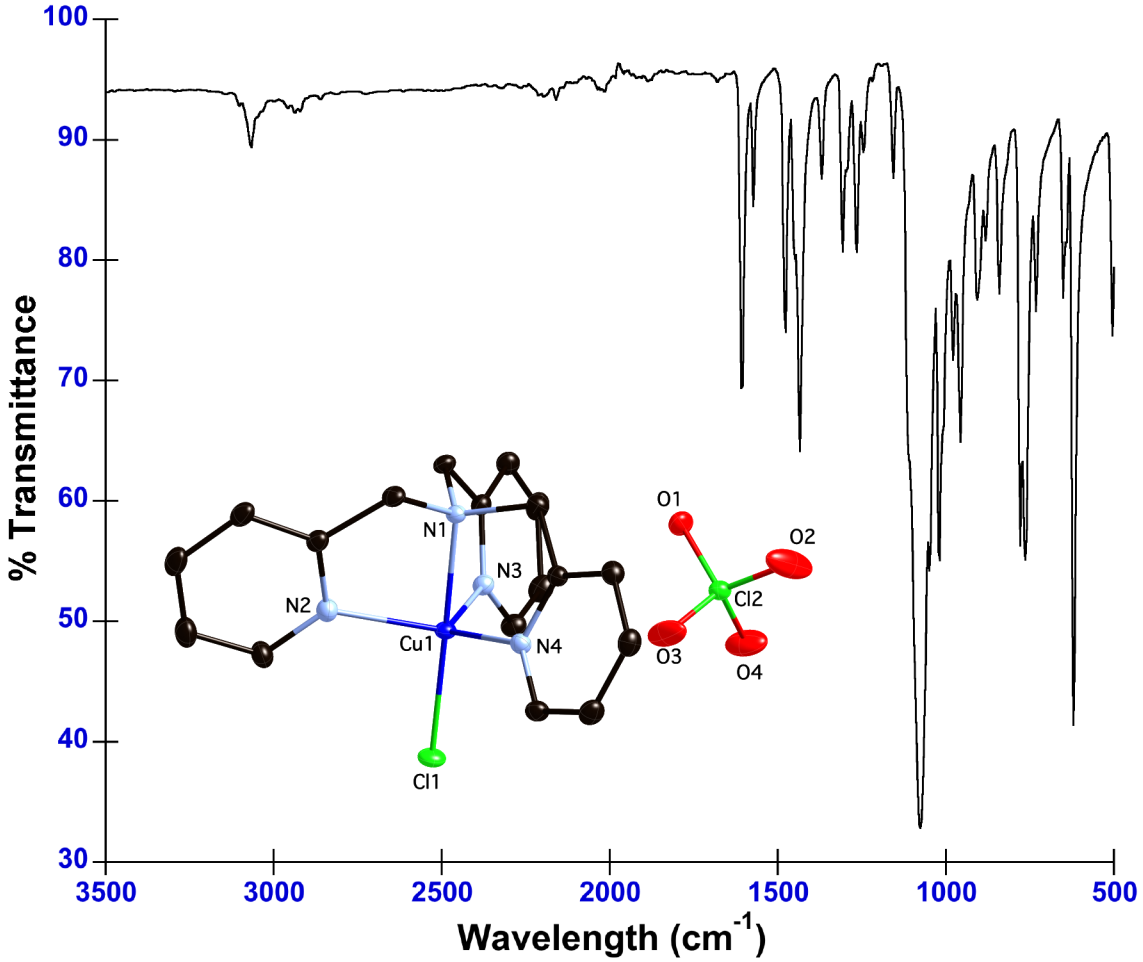

Figure E.3.6. Solid state ATR FT-IR spectrum of $[Cu^{II}(TPMA)Cl][ClO_4]$ (**8**).

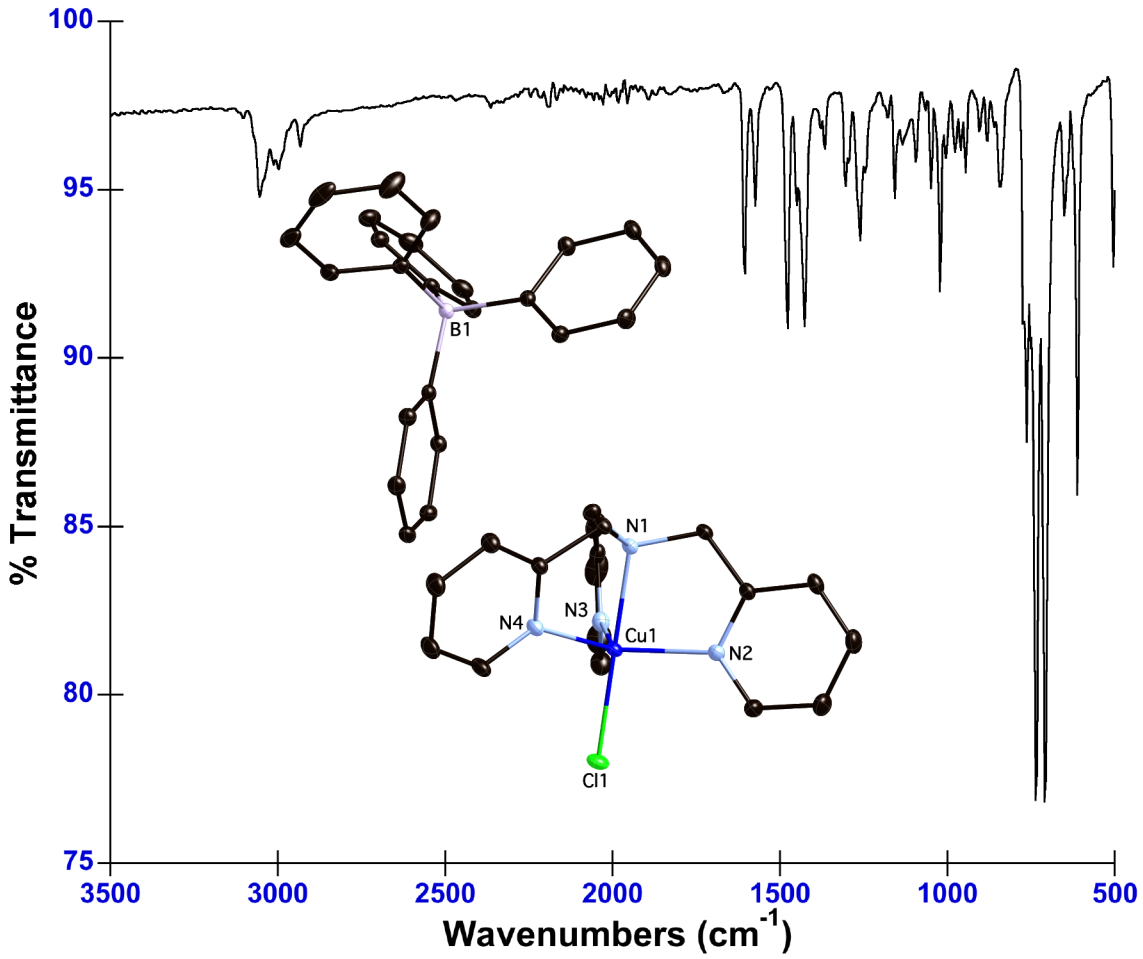

Figure E.3.7. Solid state ATR FT-IR spectrum of $[Cu^{II}(TPMA)Cl][BPh_4]$ (**9**).

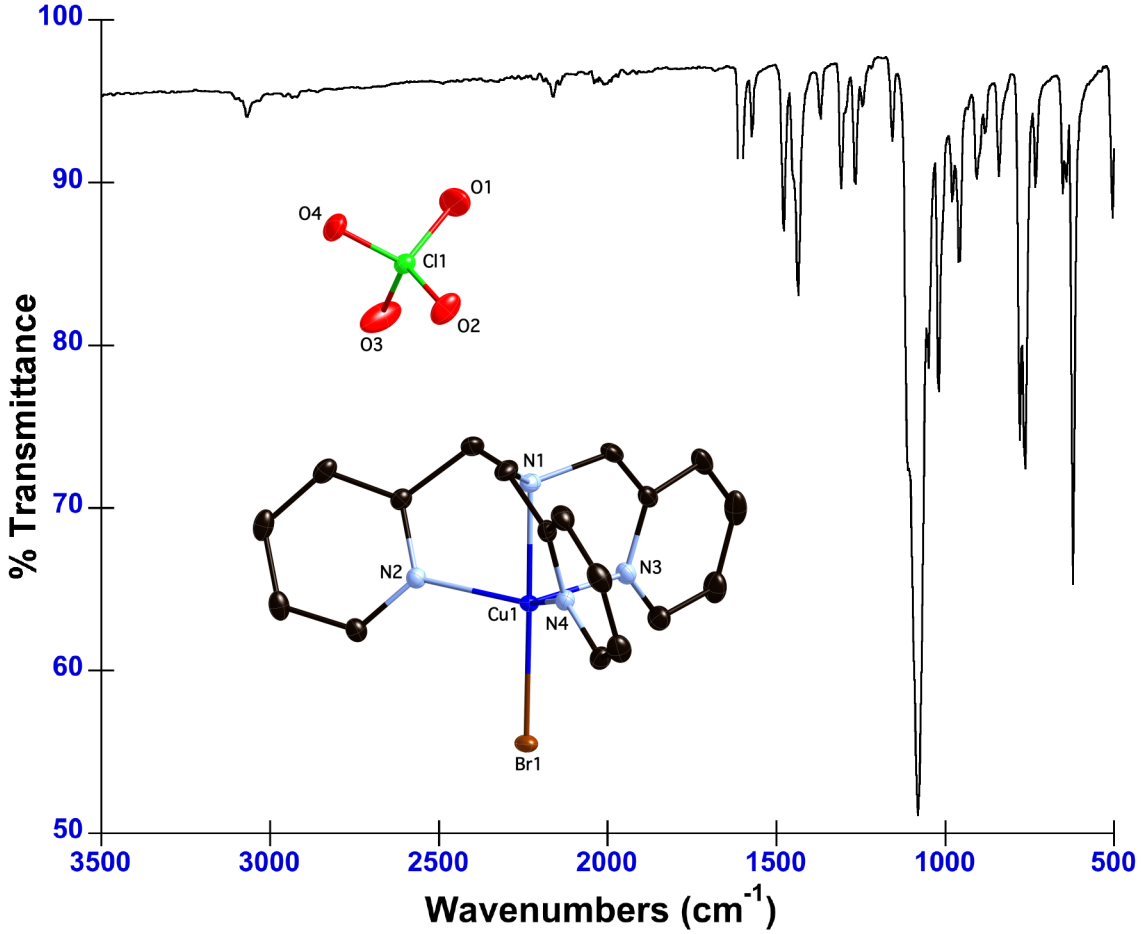

Figure E.3.8. Solid state ATR FT-IR spectrum of $[Cu^{II}(TPMA)Br][ClO_4]$ (**10**).

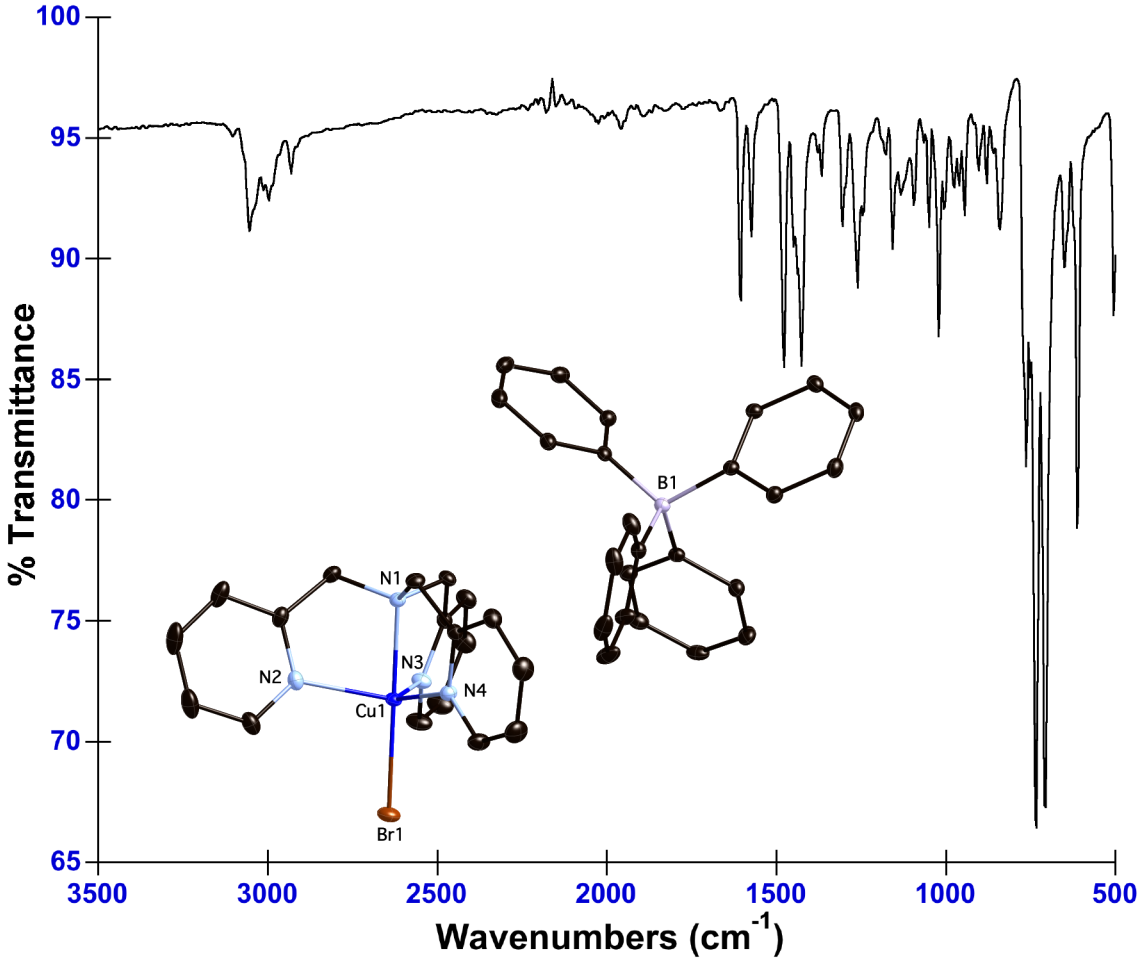

Figure E.3.9. Solid state ATR FT-IR spectrum of $[Cu^{II}(TPMA)Br][BPh_4]$ (**11**).

E.4. Unit Cell Packing Diagrams for Copper Complexes

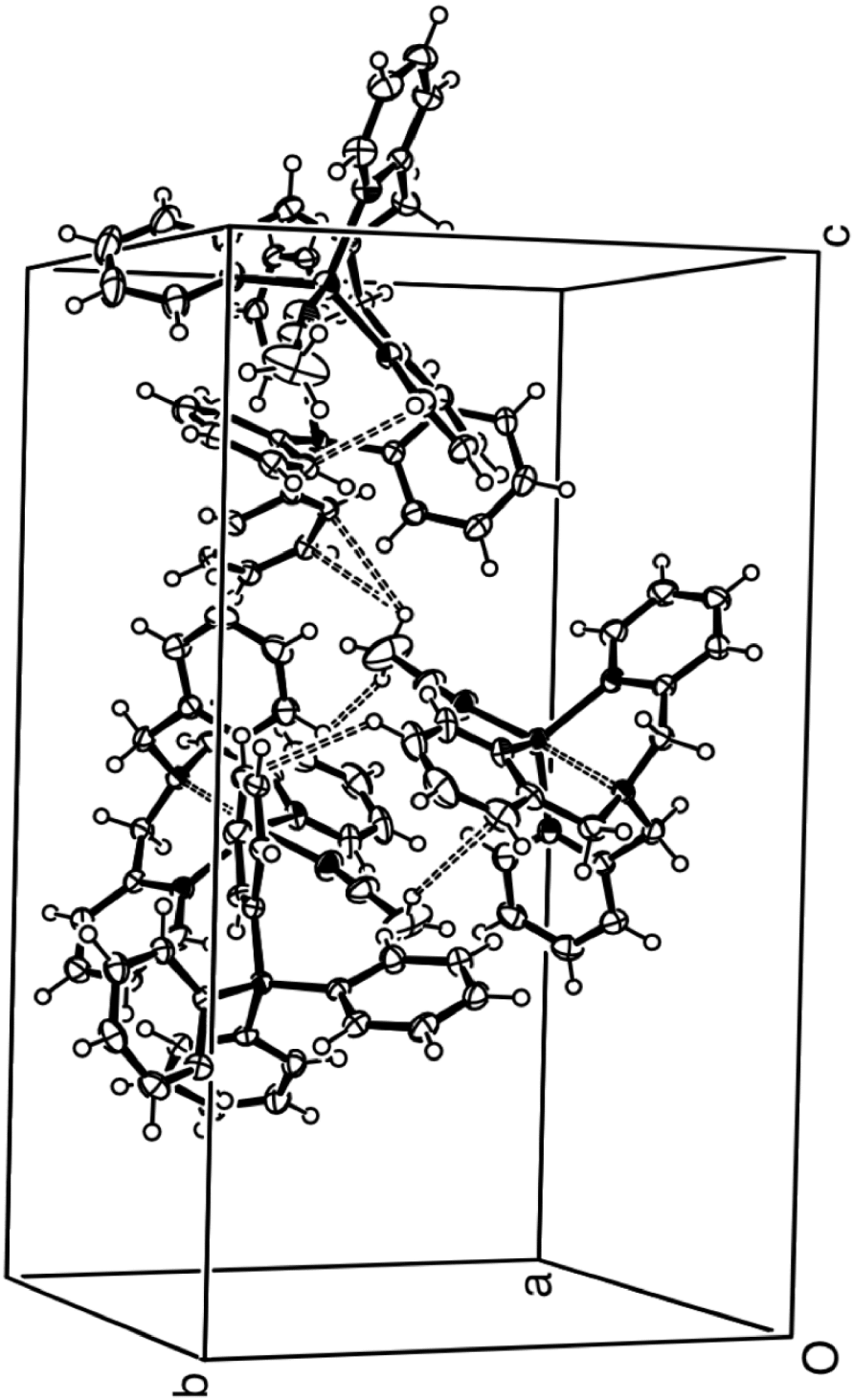

Figure E.4.1. Crystal packing diagram of $[Cu^{I}(TPMA)CH_3CN)][BPh_4]$ (**1**), showing weak C-H---C interactions.

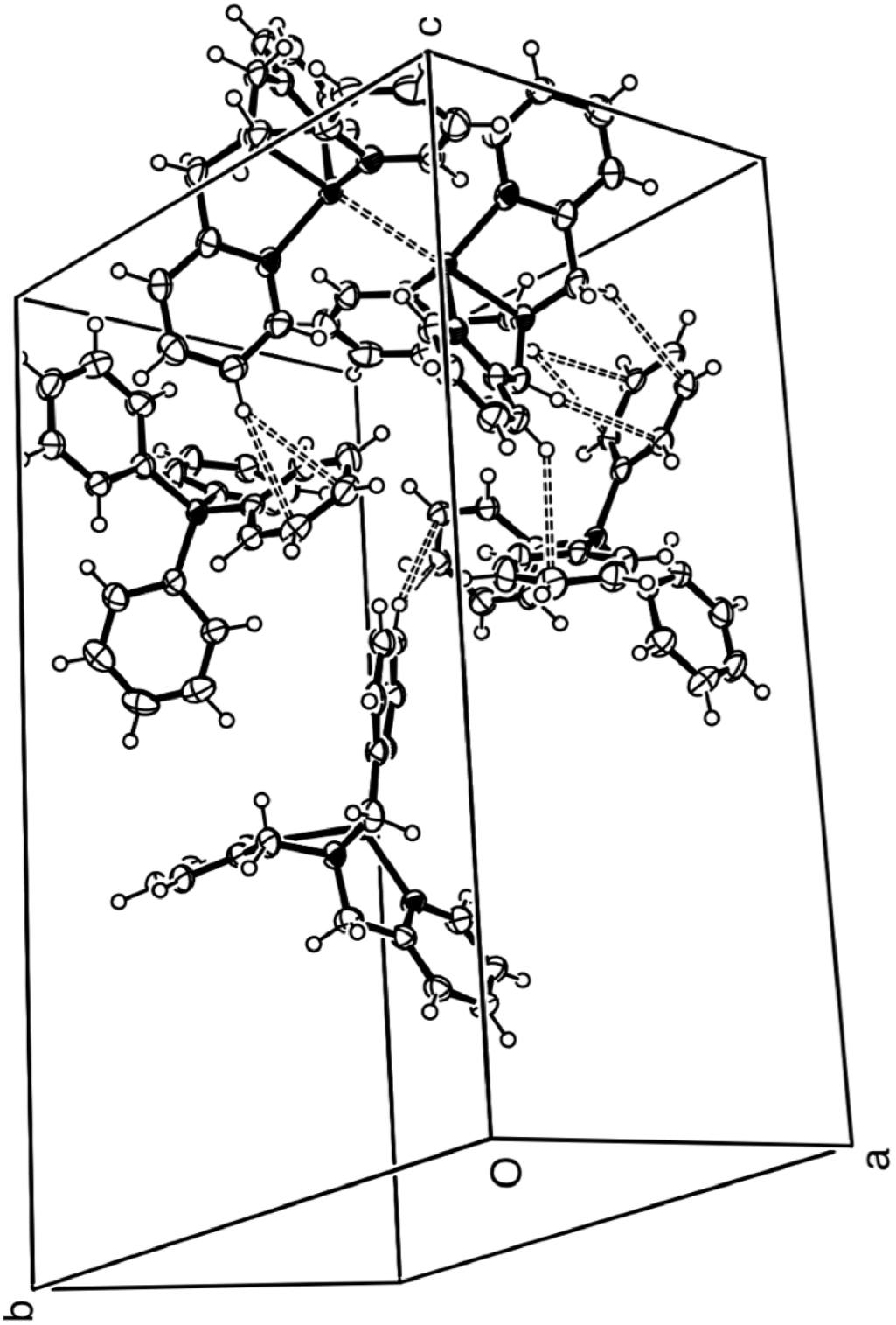

Figure E.4.2. Crystal packing diagram of $[Cu^{I}(TPMA)][BPh_4]$ (**2**), showing a long cuprophilic interactions and weak C-H---C contacts.

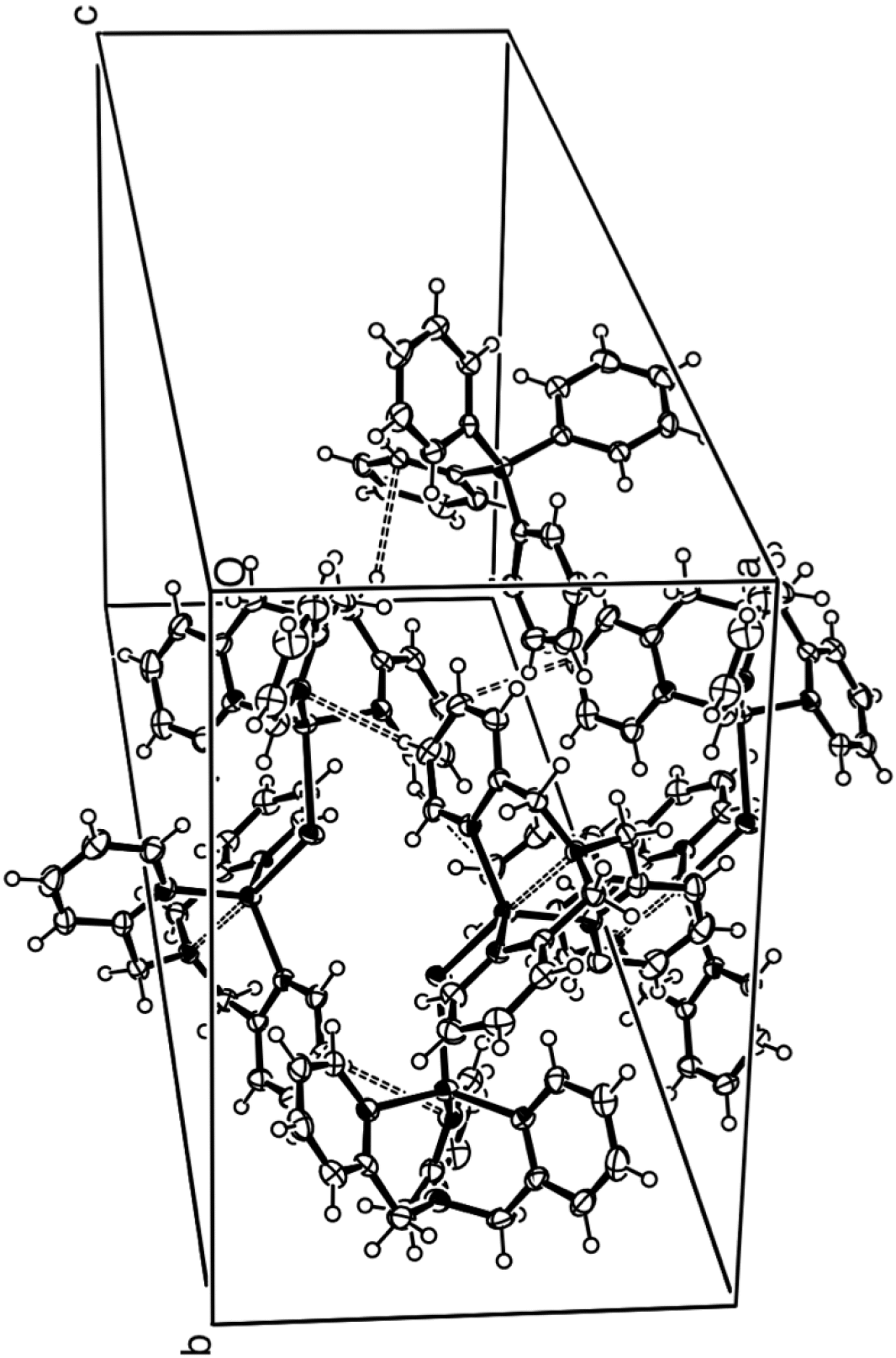

Figure E.4.3. Crystal packing diagram of $[(Cu^{I}(TPMA))_2\text{-}\mu Br][BPh_4]$ (**3**), showing weak C-H---C and dipole N---H-C interactions.

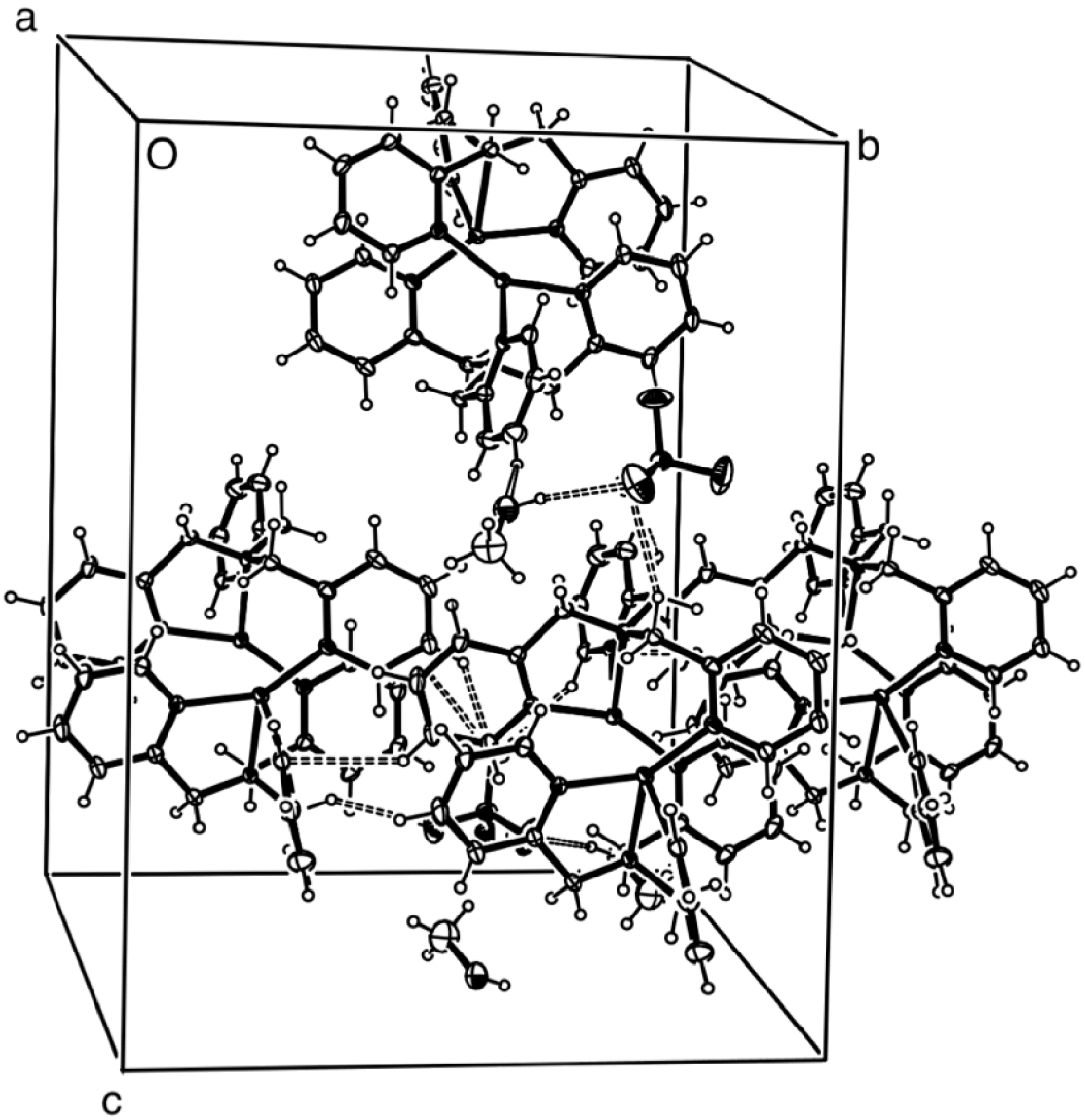

Figure E.4.4. Crystal packing diagram of $[Cu^{I}(TPMA)]_2[ClO_4]_2$ (**4**), showing weak C-H---C interactions, as well as Cl-O---H-C and Cl-O---H-O short contacts involving the solvent molecule (CH_3OH) and counter-ion (ClO_4^-).

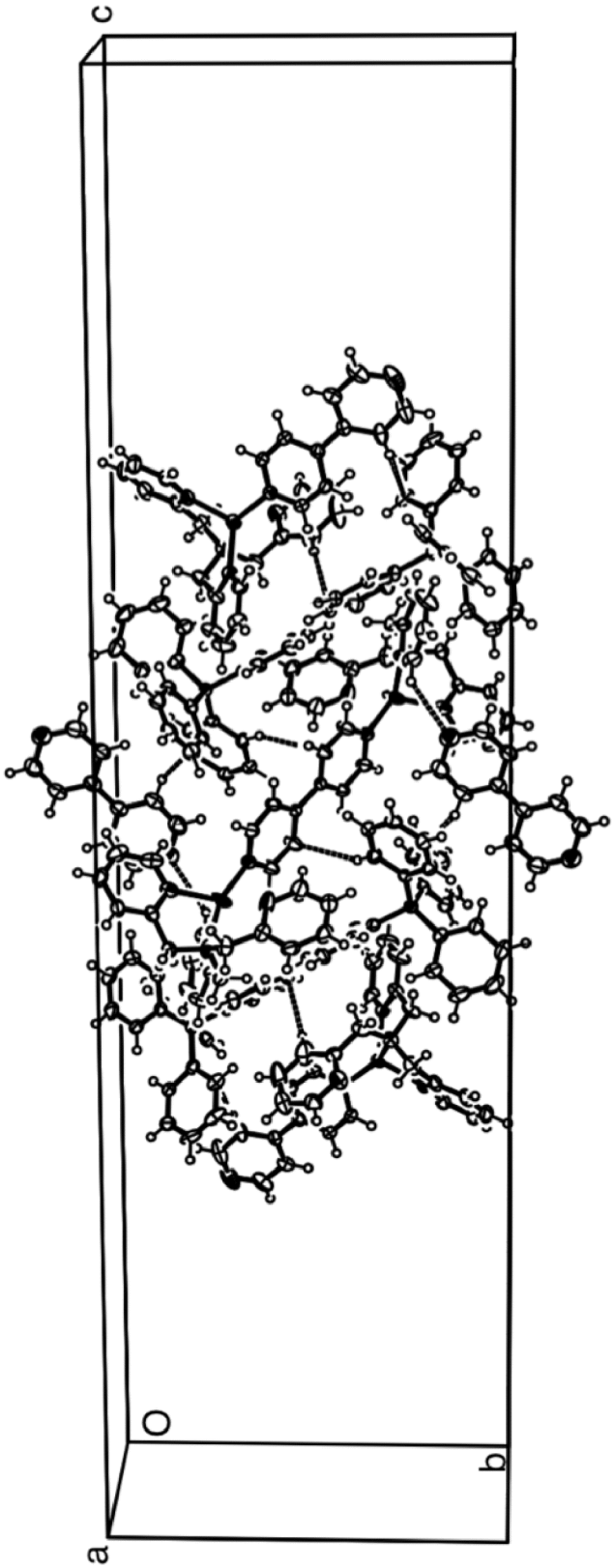

Figure E.4.5. Crystal packing diagram of $[Cu^{I}(TPMA)dipy][BPh_4]$ (**5** and **6**), showing weak C---H-C and N---H-C intermolecular interactions.

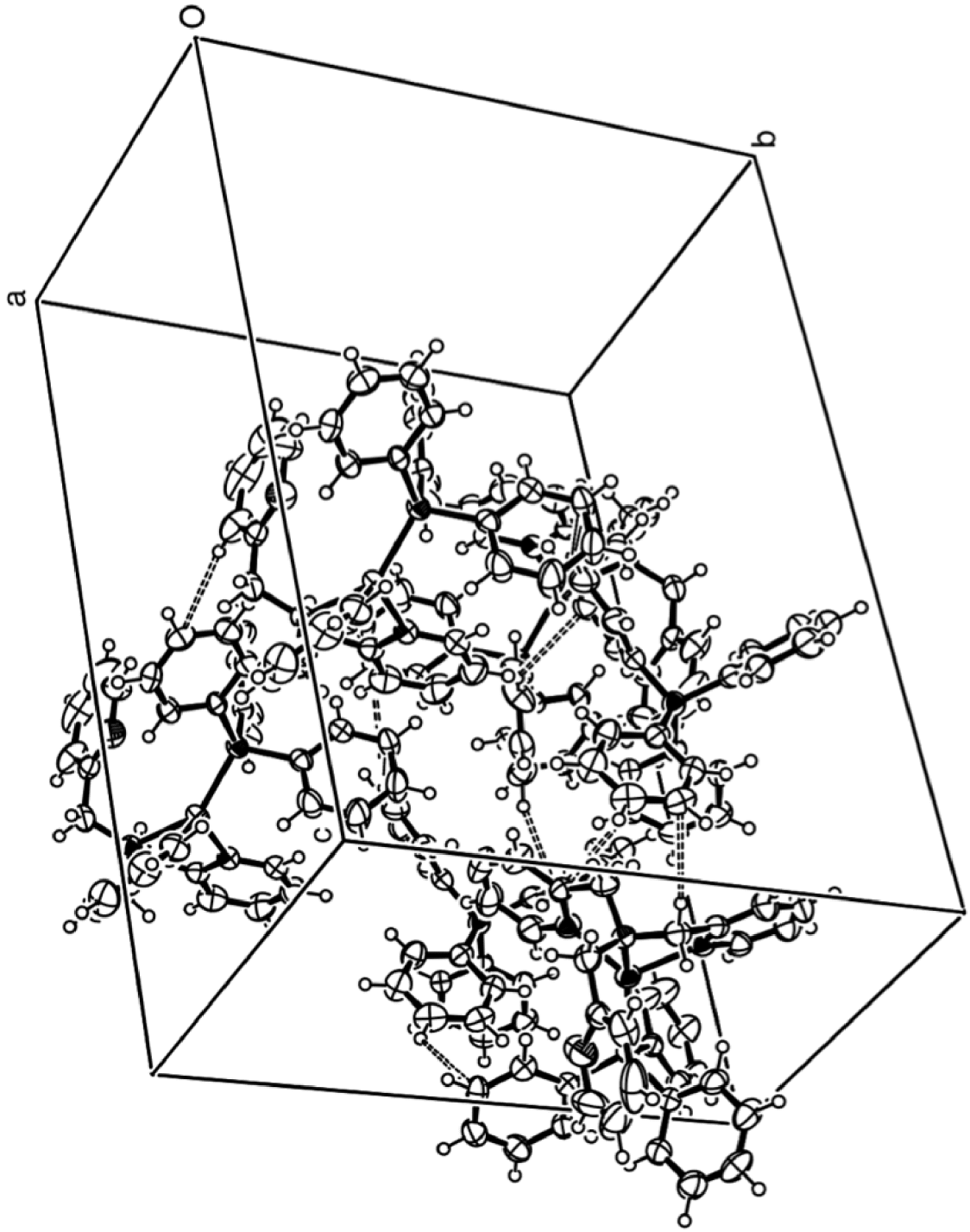

Figure E.4.6. Crystal packing diagram of $[Cu^{I}(TPMA)PPh_3][BPh_4]$ (**7**), showing weak C-H---C interactions.

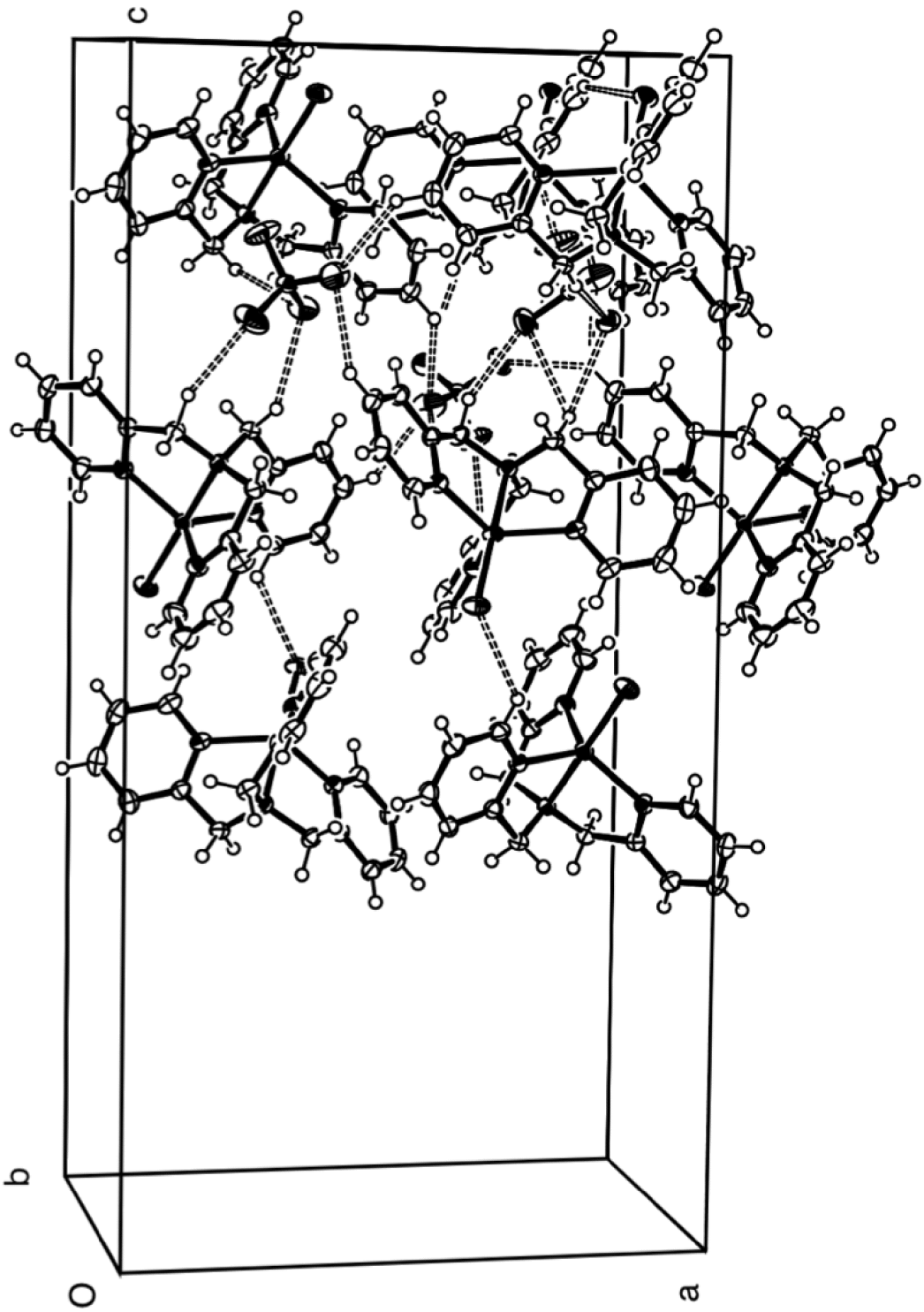

Figure E.4.7. Crystal packing diagram of $[Cu^{II}(TPMA)Cl][ClO_4]$ (**8**), showing weak C-H---O and C-H---Cl interactions.

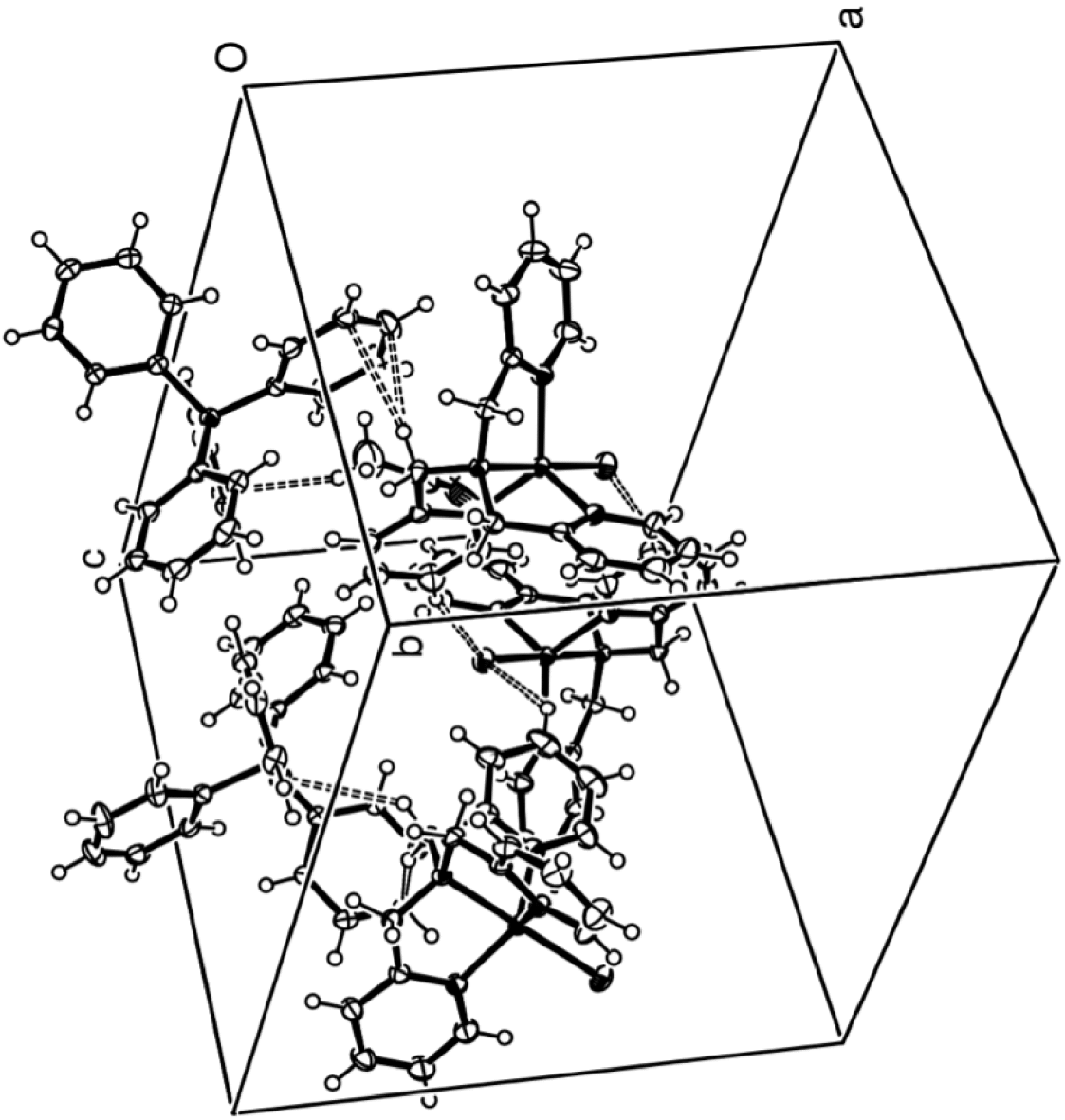

Figure E.4.8. Crystal packing diagram of $[Cu^{II}(TPMA)Cl][BPh_4]$ (**9**), showing weak C-H---C and C-H---Cl interactions.

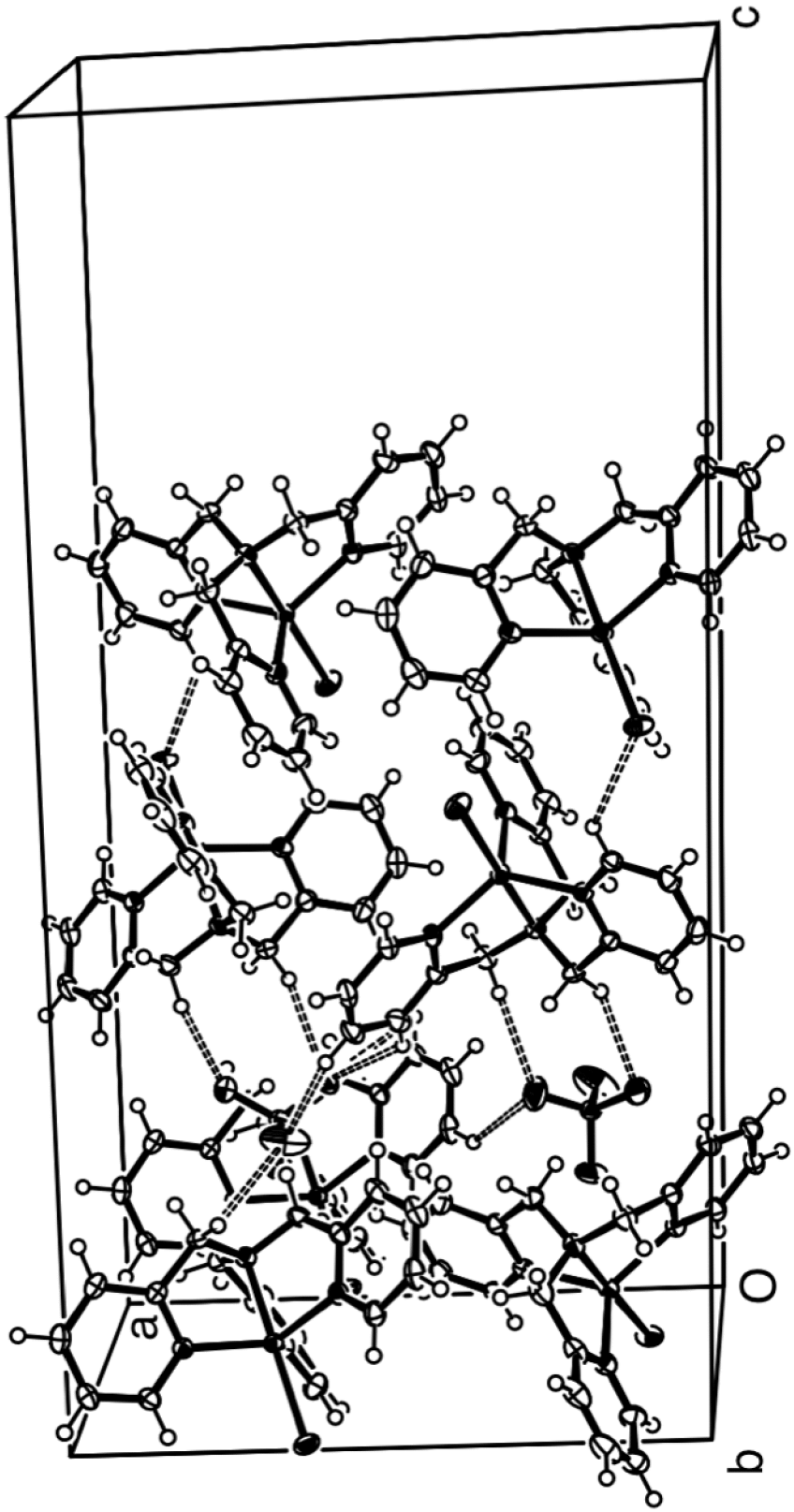

Figure E.4.9. Crystal packing diagram of $[Cu^{II}(TPMA)Br][ClO_4]$ (**10**), showing weak C-H---C, C-H---Br, and C-H---O interactions.

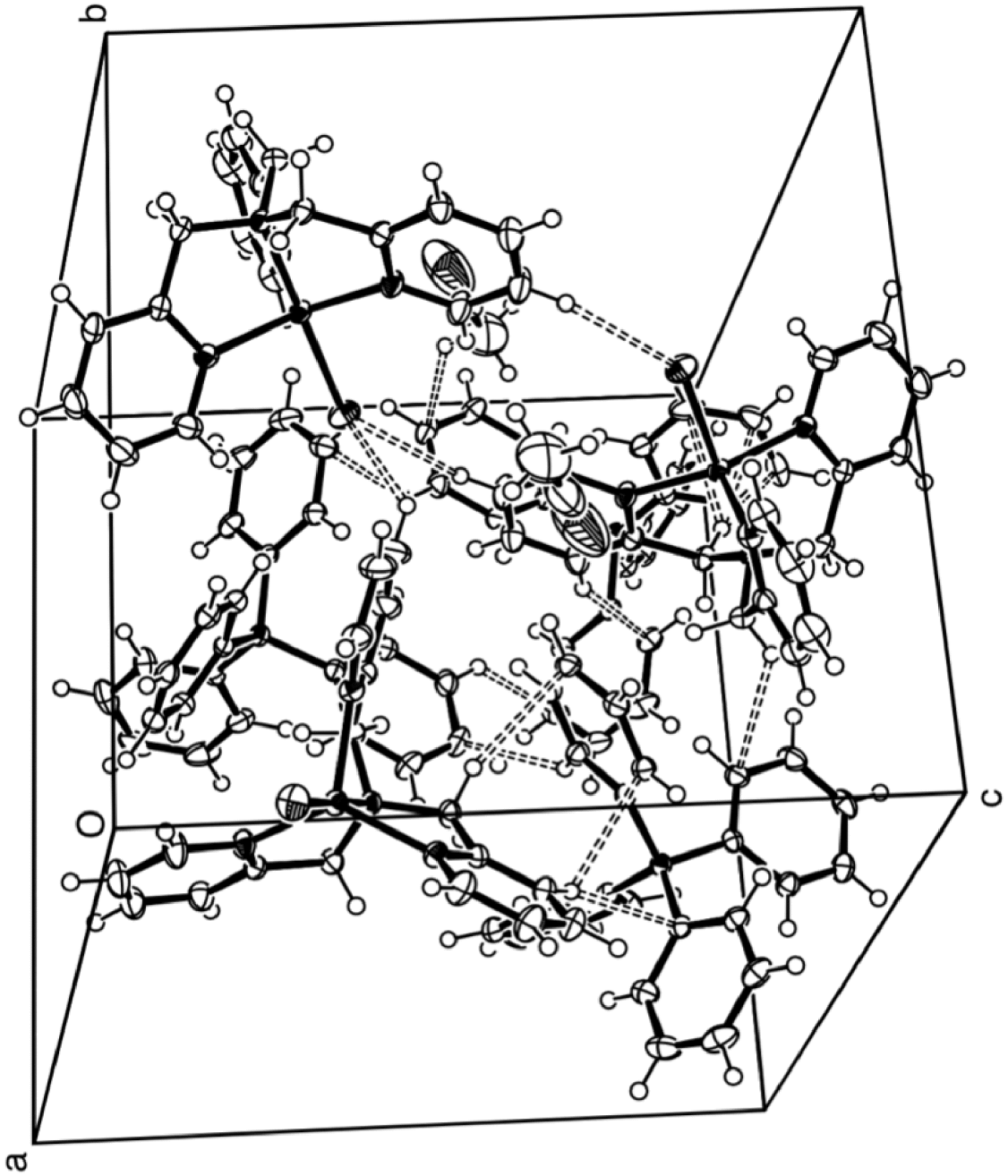

E.4.10. Crystal packing diagram of $[Cu^{II}(TPMA)Br][BPh_4]$ (**11**), showing weak C-H---Br and C-H---C interactions

Appendix F.

F.1. Equilibrium Constants for [Cu^I(TPMA)Y] (Y=Cl, ClO_4, BPh_4)

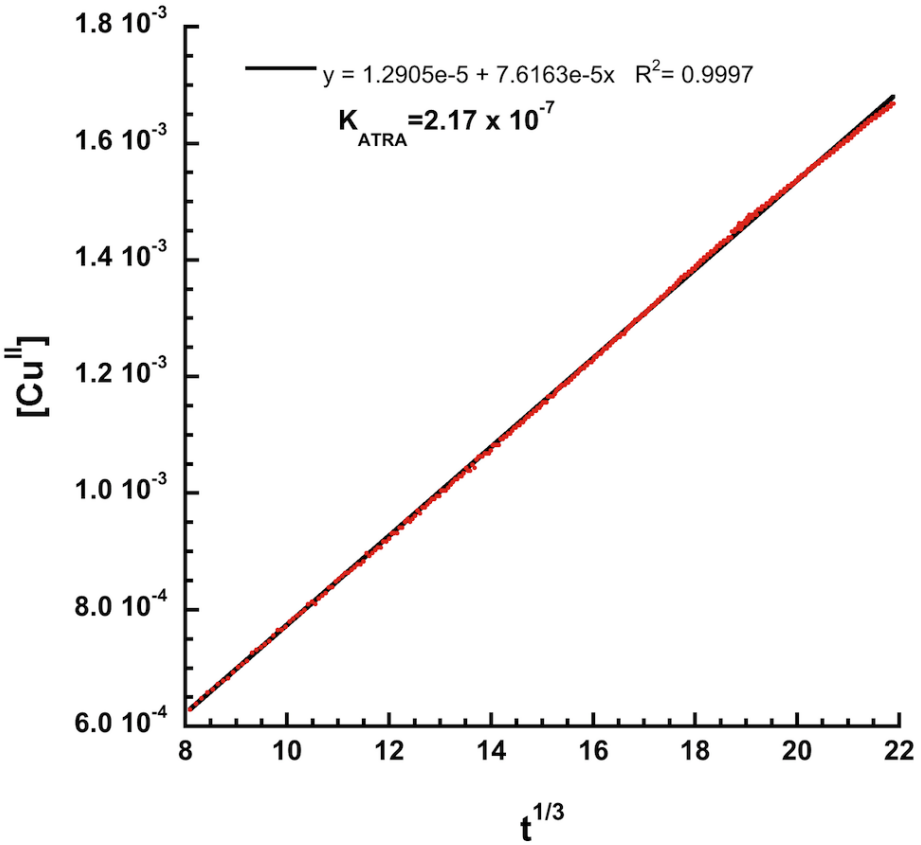

Figure F.1.1. Calculation of equilibrium constant using 1:1 ratio of [Cu^I(TPMA)Cl] to BzCl in CH_3CN. $[Cu^I]_0$=5 mM.

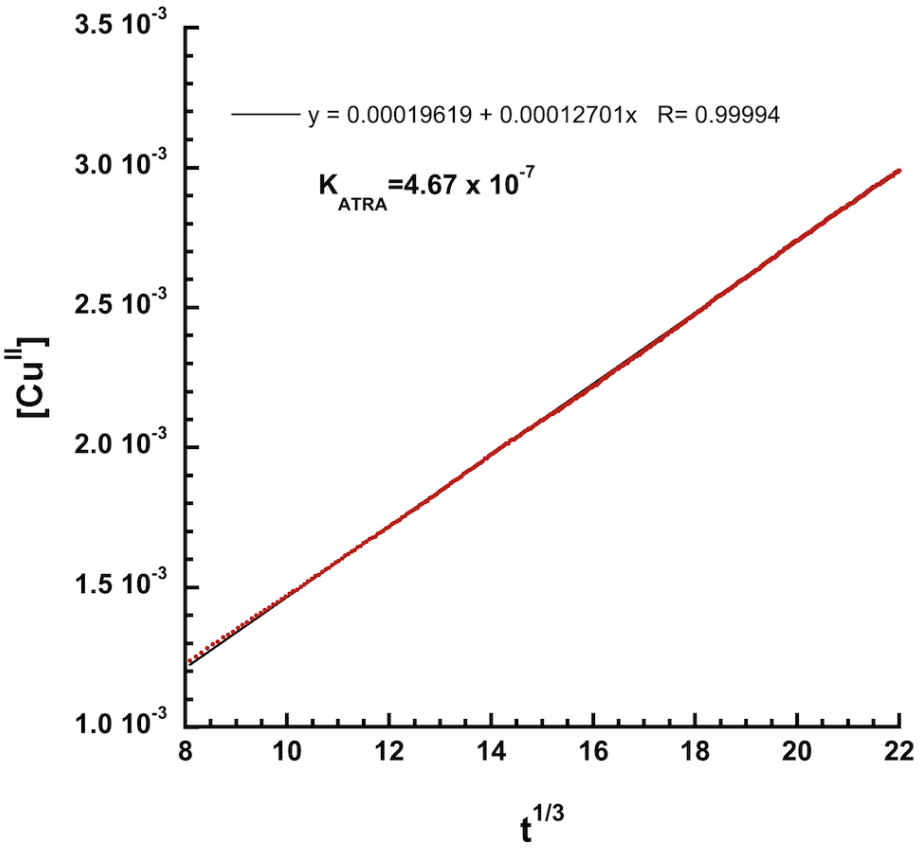

Figure F.1.2. Calculation of equilibrium constant using 1:1 ratio of $[Cu^{I}(TPMA)ClO_4]$ to BzCl in CH_3CN. $[Cu^{I}]_0$=5 mM.

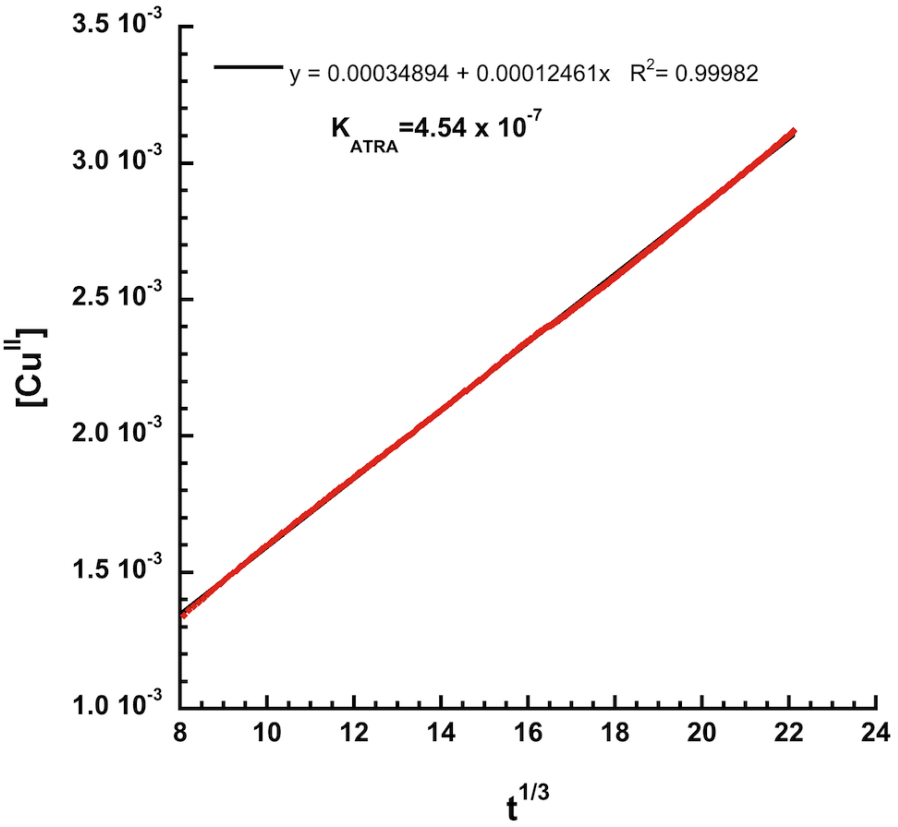

Figure F.1.3. Calculation of equilibrium constant using 1:1 ratio of $[Cu^{I}(TPMA)BPh_4]$ to BzCl in CH_3CN. $[Cu^{I}]_0$=5 mM.

F.2. Formation of $[Cu^{I}Cl_2][TBA]$ by Addition of TBA-Cl to $[Cu^{I}(TPMA)Cl]$

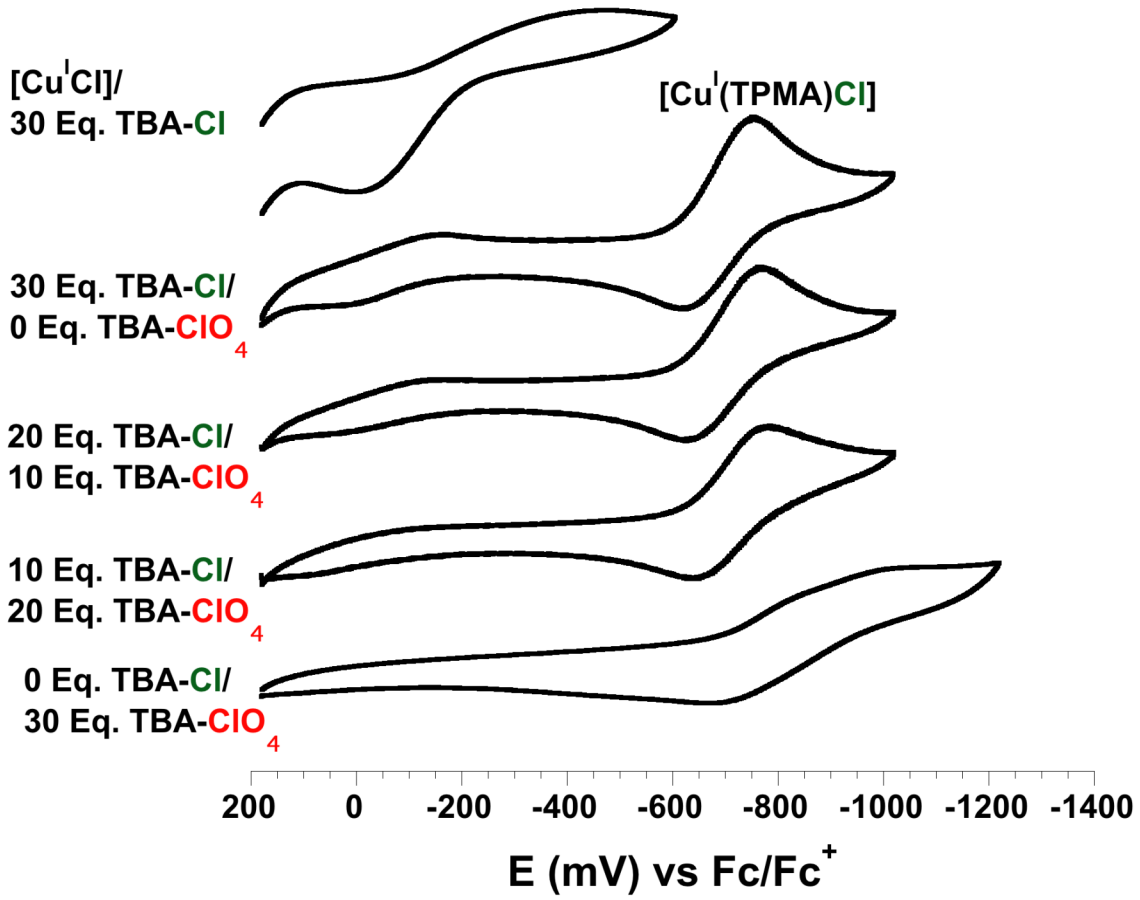

Figure F.2.1. Effect of TBA-Cl on redox potential of $[Cu^{I}(TPMA)Cl]$ with TBA-ClO_4 as supporting electrolyte. Scan rate = 100 mV/s, waves reported with respect to Fc/Fc^{+} couple.

F.3. Crystallographic Information for $[Cu^{I}(TDAPA)CH_3CN][ClO_4]$.

Table F.3.1. Crystal Parameters for $[Cu^{I}(TDAPA)CH_3CN][ClO_4]$

	$[Cu^{I}(TDAPA)CH_3CN][ClO_4]$
Formula	C_{26} H_{33} Cl Cu N_5 O_4
Color	colorless
Shape	rhomboid
Formula Weight	578.56
Crystal System	orthorhombic
Space Group	P b c a
Temp (K)	150K
Cell Constants	
***a*, Å**	14.2806(3)
***b*, Å**	17.6277(3)
***c*, Å**	23.2185(4)
α, deg	90
β, deg	90
γ, deg	90
V, $Å^3$	5844.89(19)
Formula units/unit cell	8
Dcal'd, gcm^{-3}	1.315
μ, mm^{-1}	4.791
F(000)	2416
Diffractometer	Bruker Smart ApexII
Radiation, graphite monochr.	Mo Kα (λ=0.71073 Å)
Crystal size, mm	0.49 x 0.31 x 0.22
θ range, deg	$2.26 < \theta < 32.50$
Range of *h,k,l*	-21-20, ±25, ±34
Reflections collected/unique	101504/10290
R_{int}	0.0299
Refinement Method	Full Matrix Least-Squares on F^2
Data/Restraints/Parameters	10290/0/341
GOF on F^2	1.031
Final R indices [I>2σ(I)]	R1=0.0695 wR2=0.2361
R indices (all data)	R1=0.0875 wR2=0.2596
Max. Resid. Peaks ($e*Å^{-3}$)	4.121 and -0.892

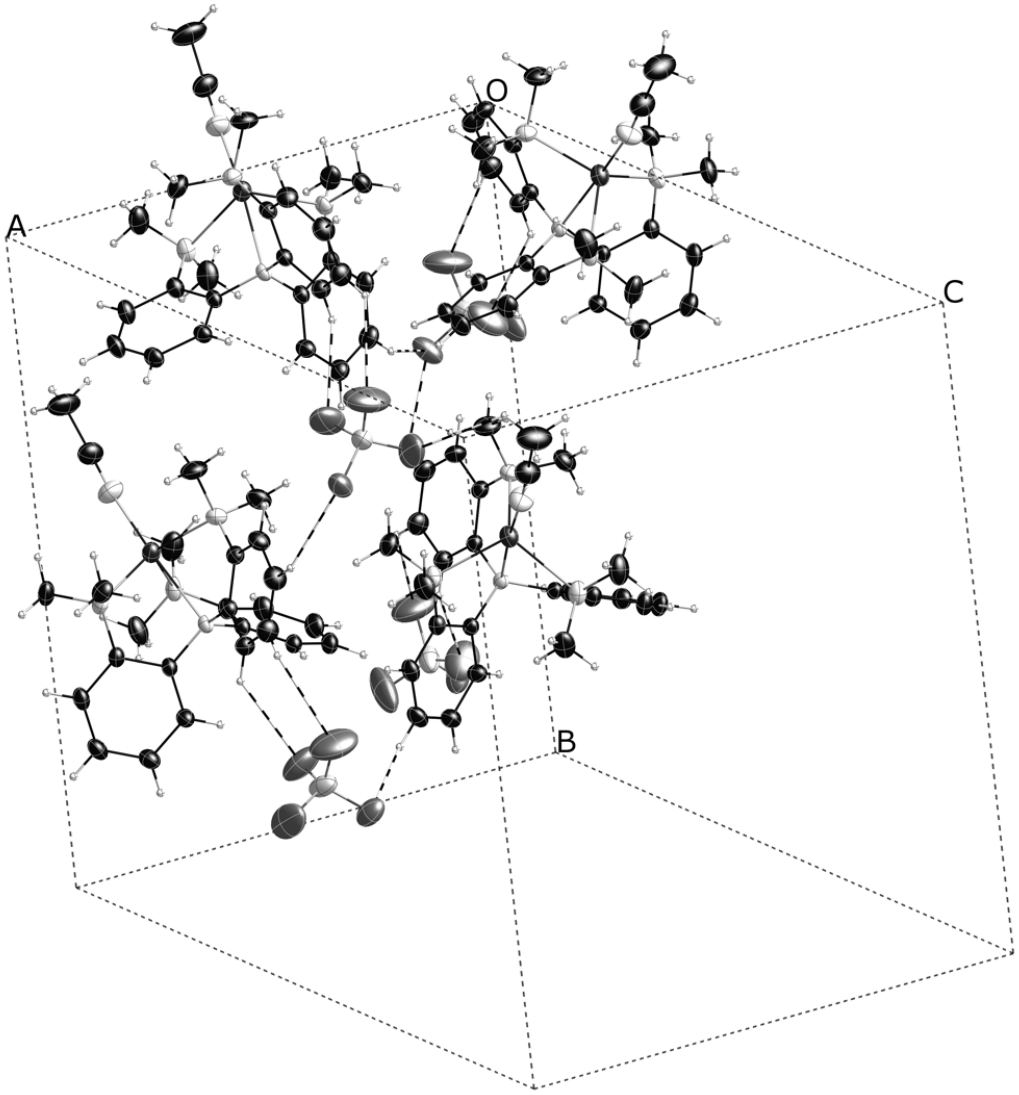

Figure F.3.1. Unit cell packing diagram of $[Cu^{I}(TDAPA)CH_3CN][ClO_4]$ at 50% probability ellipsoids, with weak C-H---C and Cl-O---H interactions drawn.

F.4. Synthesis of Copper(I) Phosphine Complexes

[$Cu^I(PPh_3)_3$][BPh_4] – In a glovebox, [$Cu^I(CH_3CN)$][ClO_4] (0.250 g, 0.76 mmol), was dissolved in 10 mL acetone followed by addition of PPh_3 (0.601 g, 2.29 mmol). To the resulting solution, $NaBPh_4$ (0.261 g, 0.76 mmol) was added. 3 mL methanol was added and the solution was left to sit over night at RT. Large colorless crystals precipitated and 0.40 g were collected (45% yield). ^{1}H-NMR (400 MHz, acetone-*d*6, 298K): δ 7.46 (t, *J* = 7.4 Hz, 9H), 7.36-7.32 (m, 8H), 7.29 (t, *J* = 7.0 Hz, 18H), 7.19 (t, *J* = 8.8 Hz, 18H), 6.92 (t, *J* = 7.4 Hz, 8H), 6.77 (t, *J* = 7.2 Hz, 4H).). FT-IR (solid) ν (cm^{-1}) = 3054(w), 1580(w), 1477(m), 1434(m), 1093(m), 742(s), 690(s), 612(m), 499(s). Anal. Calcd for $C_{78}H_{65}BCuP_3$ (1169.63): C, 80.10; H, 5.60; N, 0.00. Found: C, 80.23; H, 5.54; N, 0.00.

[$Cu^I(PPh_3)_4$][BPh_4]($CH_3)_2CO$* – In a glovebox, [$Cu^I(CH_3CN)$][ClO_4] (0.250 g, 0.76 mmol), was dissolved in 10 mL acetone followed by addition of PPh_3 (1.0 g, 3.81 mmol). To the resulting solution, $NaBPh_4$ (0.261 g, 0.76 mmol) was added. 1 mL methanol was added and left to sit over night at -35°C. Colorless crystals precipitated and 0.48 g collected (42% yield). ^{1}H-NMR (400 MHz, acetone-*d*6, 298K): δ 7.44 (td, *J* = 7.4, 1.3 Hz, 12H), 7.36-7.34 (m, 8H), 7.29 (td, *J* = 7.8, 1.8 Hz, 24H), 7.19 (ddd, *J* = 9.7, 8.3, 1.3 Hz, 24H), 6.92 (t, *J* = 7.4 Hz, 8H), 6.77 (t, *J* = 7.2 Hz, 4H). FT-IR (solid) ν (cm^{-1}) = 3053(w), 1716(w), 1580(w), 1477(m), 1434(w), 1091(m), 741(s), 692(s), 612(m) ,498(s).

*$[Cu^{I}(PPh_3)_3CH_3CN][ClO_4]$ *$(CH_3)_2CO$* – In a glovebox, $[Cu^{I}(CH_3CN)][ClO_4]$ (0.250 g, 0.76 mmol), was dissolved in 10 mL acetone followed by addition of PPh_3 (0.601 g, 2.29 mmol). The solution was left to sit over night at -35°C. Colorless crystals precipitated and 0.603 g was collected (75% yield). ^{1}H-NMR (400 MHz, acetone-*d*6, 298K): δ 7.46 (td, *J* = 7.4, 1.3 Hz, 9H), 7.27 (td, *J* = 7.8, 1.6 Hz, 18H), 7.16 (ddd, *J* = 10.4, 8.3, 1.2 Hz, 18H), 2.07 (s, 3H). FT-IR (solid) ν (cm^{-1}) = 3057(w), 1710(w), 1480(w), 1434(m), 1087(s), 740(m), 691(s), 622(m), 519(s). Anal. Calcd for $C_{59}H_{54}ClCuNO_5P_3$ (1048.98): C, 67.55; H, 5.19; N, 1.34. Found: C, 67.69; H, 5.11; N, 1.29.

F.5. Crystallographic Information for Copper(I) Phosphine Complexes.

Table F.5.1. Crystal Parameters for $[Cu^{I}(PPh_3)_4][BPh_4]$ and $[Cu^{I}(PPh_3)_3CH_3CN][BPh_4]$

	$[Cu^{I}(PPh_3)_4][BPh_4]*(CH_3)_2CO$	$[Cu^{I}(PPh_3)_3CH_3CN][ClO_4]*(CH_3)_2CO$
Formula	$C_{99}H_{86}BCuOP_4$	$C_{59}H_{54}ClCuNO_5P_3$
Color	colorless	colorless
Shape	rhomboid	rhomboid
Formula Weight	1489.91	1048.93
Crystal System	triclinic	triclinic
Space Group	P -1	P -1
Temp (K)	150K	150K
Cell Constants		
***a*, Å**	14.8859(8)	10.5153(8)
***b*, Å**	15.7298(8)	13.4234(10)
***c*, Å**	16.8083(9)	19.3711(14)
α, deg	91.416(3)	102.7740(10)
β, deg	91.544(3)	104.3170(10)
γ, deg	90.928(3)	95.2620(10)
V, Å^3	3932.5(4)	2552.6(3)
Formula units/unit cell	2	2
Dcal'd, gcm^{-3}	1.258	1.365
μ, mm^{-1}	0.409	0.625
F(000)	1564	1092
Diffractometer	Bruker Smart ApexII	Bruker Smart ApexII
Radiation, graphite monochr.	Mo Kα (λ=0.71073 Å)	Mo Kα (λ=0.71073 Å)
Crystal size, mm	0.50 x 0.39 x 0.27	0.31 x 0.30 x 0.15
θ range, deg	1.21 < θ < 32.40	1.12 < θ < 32.65
Range of *h,k,l*	±22, -22→23, -24→25	±15, -20→19, ±29
Reflections collected/unique	68304/26054	33197/17031
R_{int}	0.0393	0.0197
Refinement Method	Full Matrix Least-Squares on F2	Full Matrix Least-Squares on F2
Data/Restraints/Parameters	26054/0/957	17031/0/634
GOF on F^2	1.121	1.063
Final R indices [I>2σ(I)]	R1=0.1227 wR2=0.3690	R1=0.0467 wR2=0.1430
R indices (all data)	R1=0.1374 wR2=0.3764	R1=0.0617 wR2=0.1592
Max. Resid. Peaks (e*Å^{-3})	4.063 and -1.037	2.510 and -1.221

Table F.5.2. Crystal Parameters for $[Cu^{I}(PPh_3)_3][BPh_4]$

	$[Cu^{I}(PPh_3)_3][BPh_4]$
Formula	$C_{78}H_{65}BCuP_3$
Color	colorless
Shape	rhomboid
Formula Weight	1169.56
Crystal System	monoclinic
Space Group	P 21/c
Temp (K)	150K
Cell Constants	
***a*, Å**	16.741(2)
***b*, Å**	20.309(3)
***c*, Å**	18.131(2)
α, deg	90
β, deg	94.903(2)
γ, deg	90
V, Å^3	6141.8(14)
Formula units/unit cell	4
Dcal'd, gcm^{-3}	1.265
μ, mm^{-1}	0.479
F(000)	2448
Diffractometer	Bruker Smart ApexII
Radiation, graphite monochr.	Mo Kα (λ=0.71073 Å)
Crystal size, mm	0.52 x 0.32 x 0.16
θ range, deg	1.22 < θ < 32.59
Range of *h,k,l*	±24, ±29, ±26
Reflections collected/unique	77970/21108
R_{int}	0.032
Refinement Method	Full Matrix Least-Squares on F^2
Data/Restraints/Parameters	21108/0/748
GOF on F^2	0.923
Final R indices [I>2σ(I)]	R1=0.0386 wR2=0.1138
R indices (all data)	R1=0.0604 wR2=0.1337
Max. Resid. Peaks (e*Å^{-3})	0.464 and -0.337

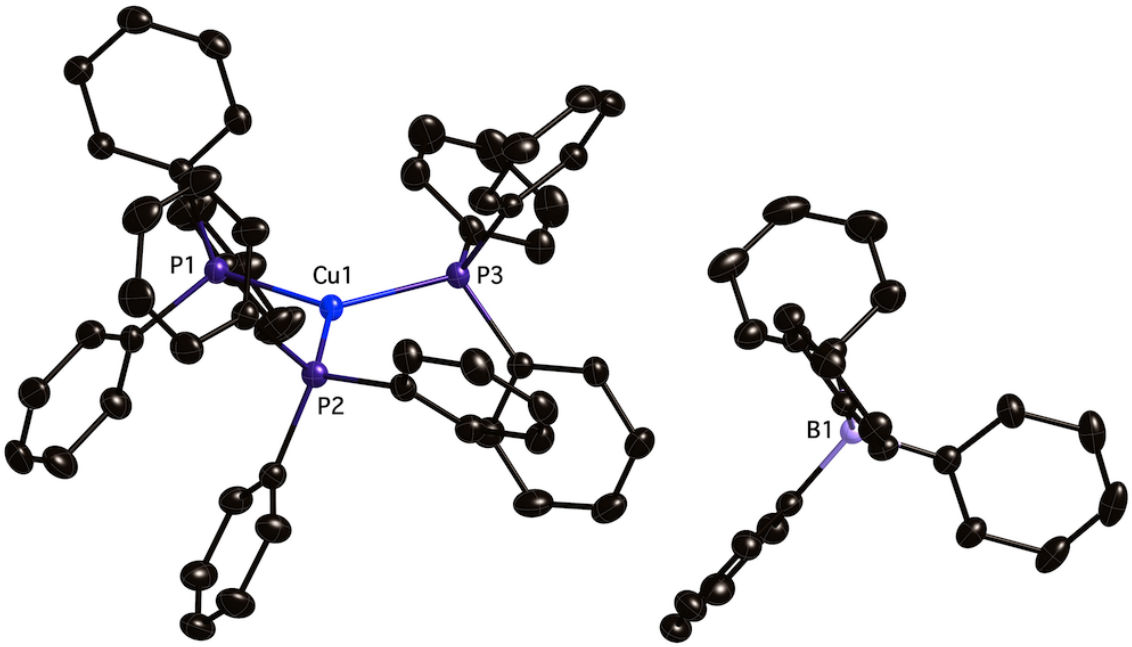

Figure F.5.1. Molecular structure of $[Cu^{I}(PPh_3)_3][BPh_4]$ collected at 150 K, shown at 50% probability ellipsoids with H-atoms omitted for clarity. Selected bond distances [Å] and angles[°]: Cu1-P1 2.2649(5), Cu1-P2 2.2786(5), Cu1-P3 2.2879(4), P1-Cu1-P2 123.984(14), P1-Cu1-P3 119.123(16), P2-Cu1-P3 116.765(16)

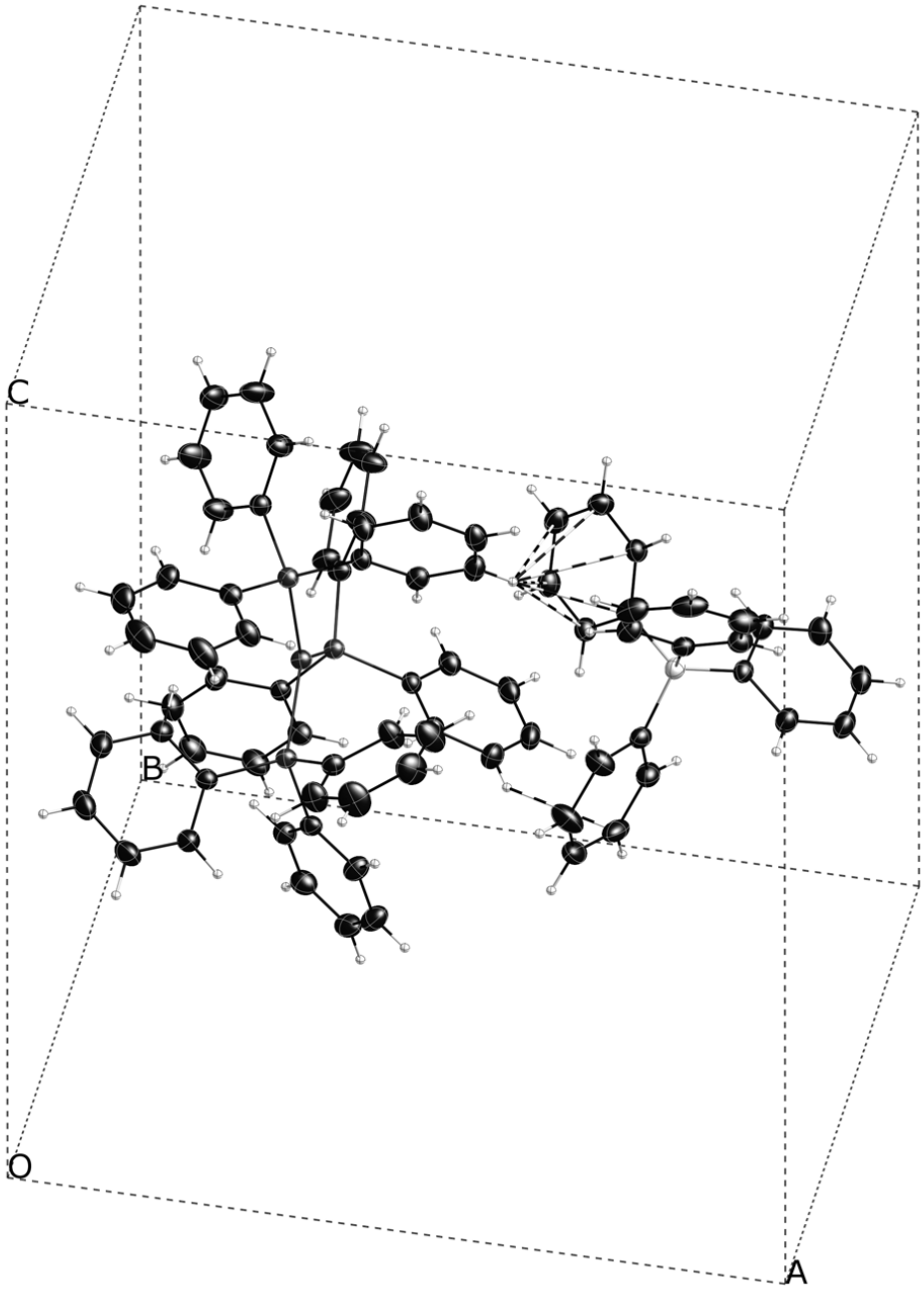

Figure F.5.2. Unit cell packing diagram of $[Cu^{I}(PPh_3)_3][BPh_4]$ at 50% probability ellipsoids, with weak C-H---C interactions drawn.

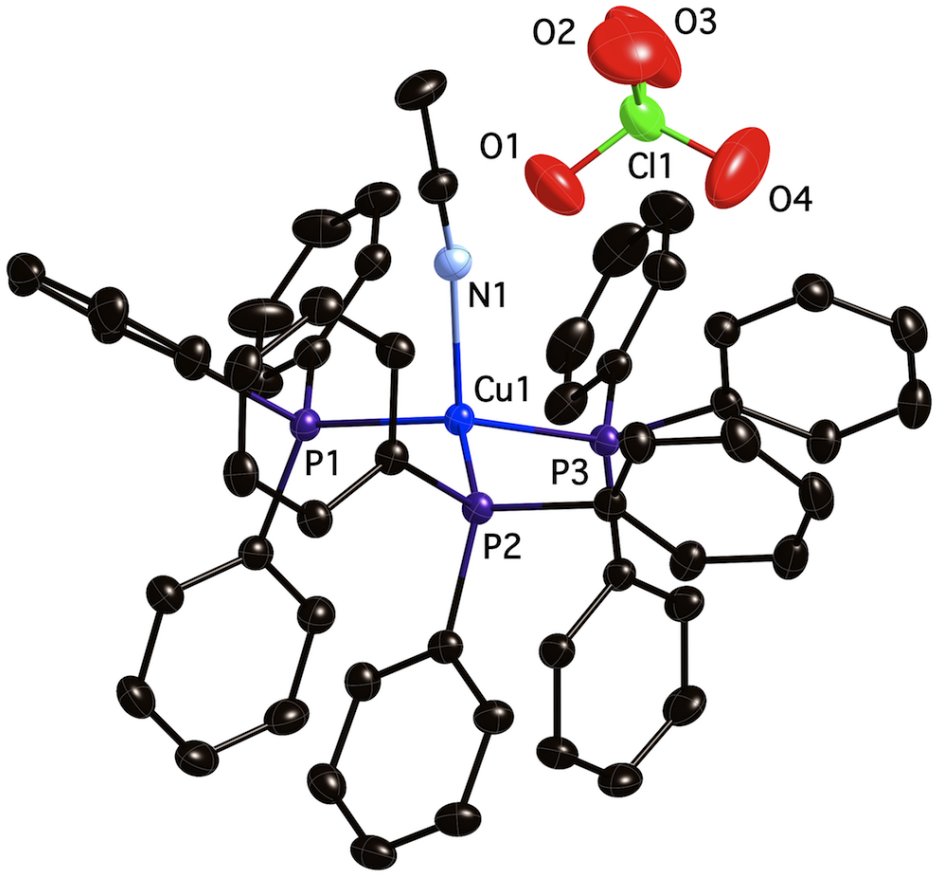

Figure F.5.3. Molecular structure of $[Cu(PPh_3)_3CH_3CN][ClO_4]*(CH_3)_2CO$ collected at 150 K, shown at 50% probability ellipsoids with H-atoms omitted for clarity. Selected bond distances [Å] and angles[°]:Cu1-N1 2.1010(17), Cu1-P1 2.3150(5), Cu1-P2 2.3362(5), Cu1-P3 2.3147(5), N1-Cu1-P3 98.66(5), N1-Cu1-P1 108.46(5), P3-Cu1-P1 112.627(18), N1-Cu1-P2 102.28(5), P3-Cu1-P2 121.443(18), P1-Cu1-P2 111.196(18)

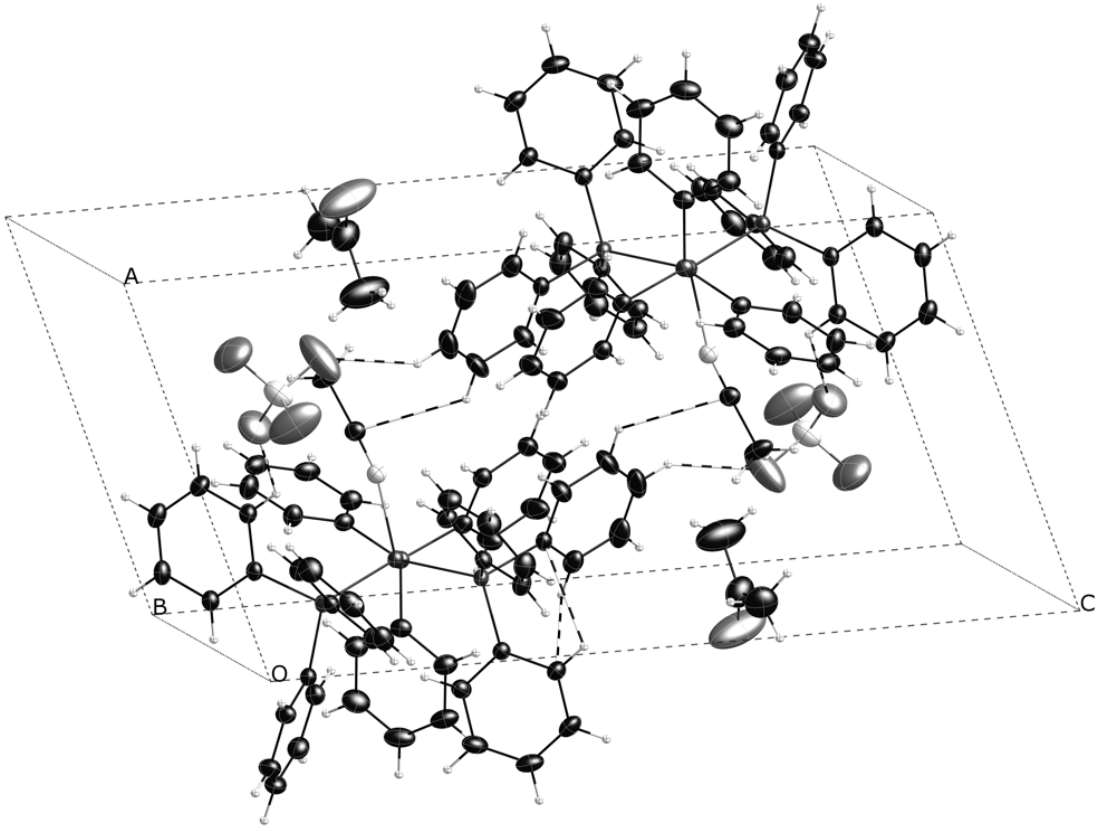

Figure F.5.4. Unit cell packing diagram of $[Cu^{I}(PPh_3)_3CH_3CN][ClO_4]$ at 50% probability ellipsoids, with weak C-H---C and Cl-O---H interactions drawn.

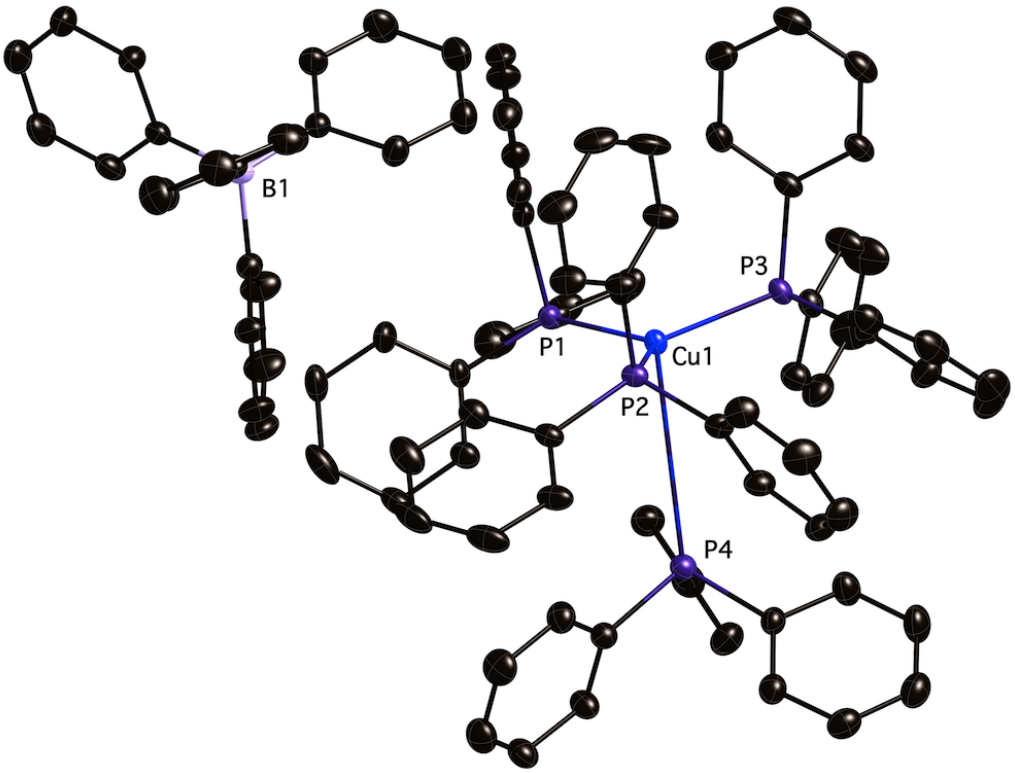

Figure F.5.5. Molecular structure of $[Cu(PPh_3)_3PPh_3][BPh_4]*(CH_3)_2CO$ collected at 150 K, shown at 50% probability ellipsoids with H-atoms omitted for clarity. Selected bond distances [Å] and angles[^{o}]: Cu1-P3 2.3086(15), Cu1-P2 2.3169(15), Cu1-P1 2.3199(15), Cu1-P4 3.9551(17), P3-Cu1-P2 119.95(6), P3-Cu1-P1 120.83(6), P2-Cu1-P1 115.55(6), P3-Cu1-P4 95.83(5), P2-Cu1-P4 100.90(5), P1-Cu1-P4 92.47(5)

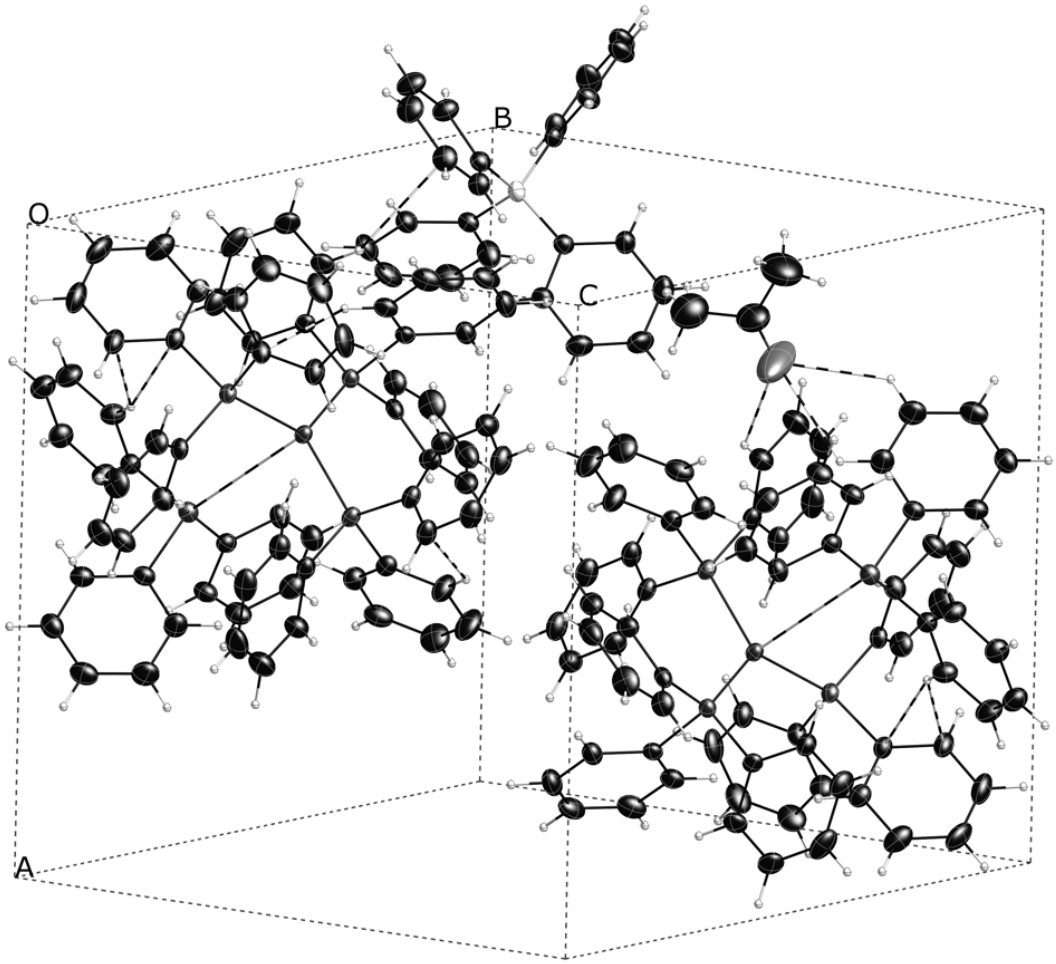

Figure F.5.6. Unit cell packing diagram of $[Cu^{I}(PPh_3)_3PPh_3][BPh_4]*(CH_3)_2CO$ at 50% probability ellipsoids, with weak C-H---C, C-H---P, C-O---H, and Cu---P interactions drawn.

F.6. ^{1}H NMR Spectra of Copper(I) Phosphine Complexes

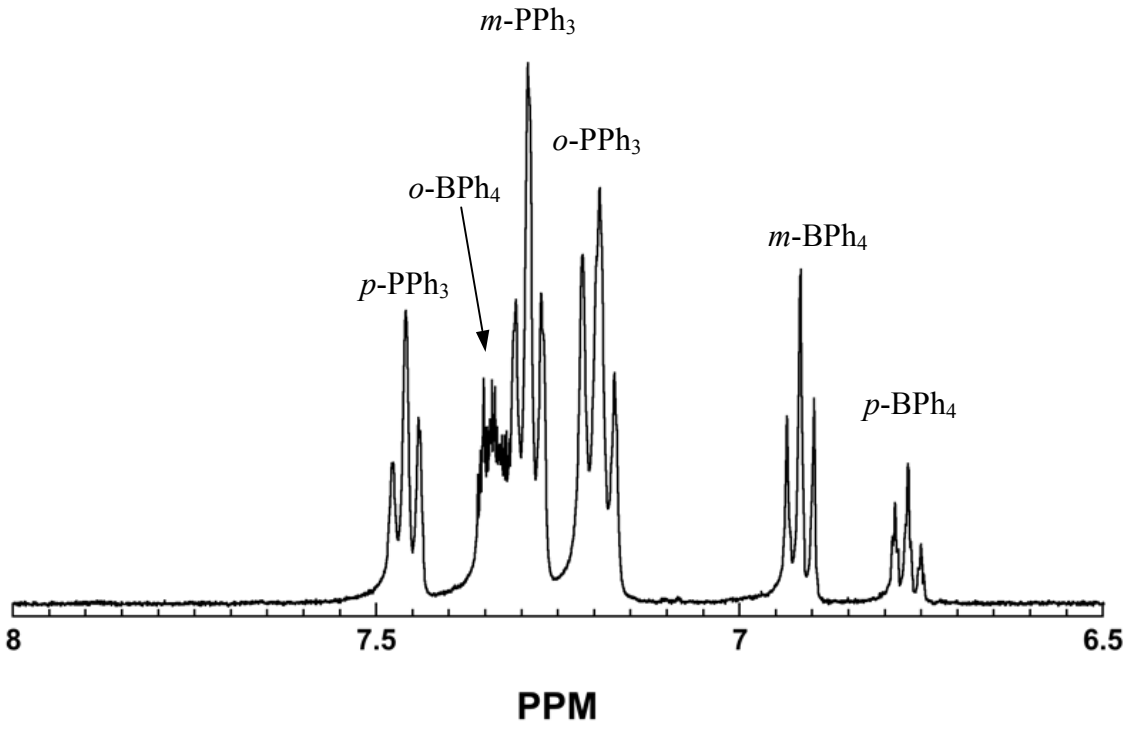

Figure F.6.1. ^{1}H NMR spectrum of $[Cu^{I}(PPh_3)_3][BPh_4]$ in (400 MHz, acetone-*d*6, 298K)

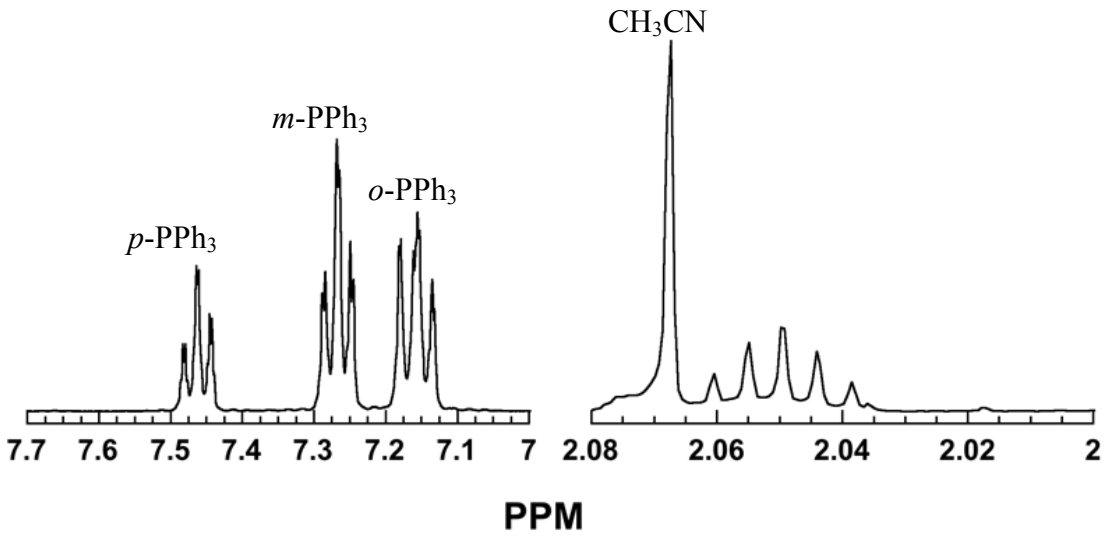

Figure F.6.2. ^{1}H NMR spectrum of $[Cu^{I}(PPh_3)_3CH_3CN][ClO_4]$ in (400 MHz, acetone-*d*6, 298K)

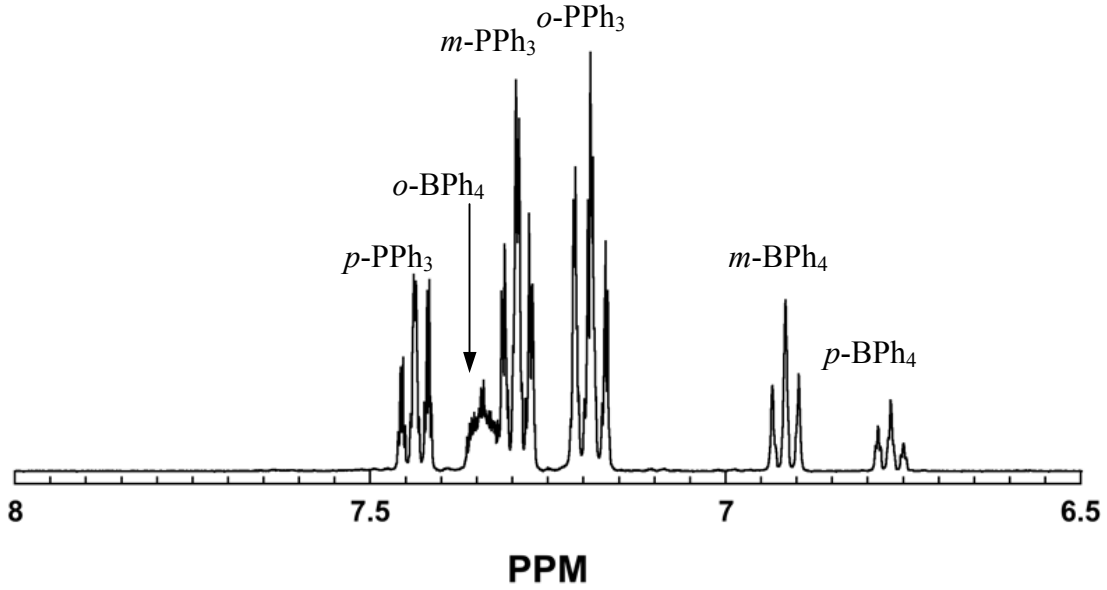

Figure F.6.3. ^{1}H NMR spectrum of $[Cu(PPh_3)_3PPh_3][BPh_4]$ in (400 MHz, acetone-*d*6, 298K)

F.7. Infrared Spectra of Copper(I) Phosphine Complexes

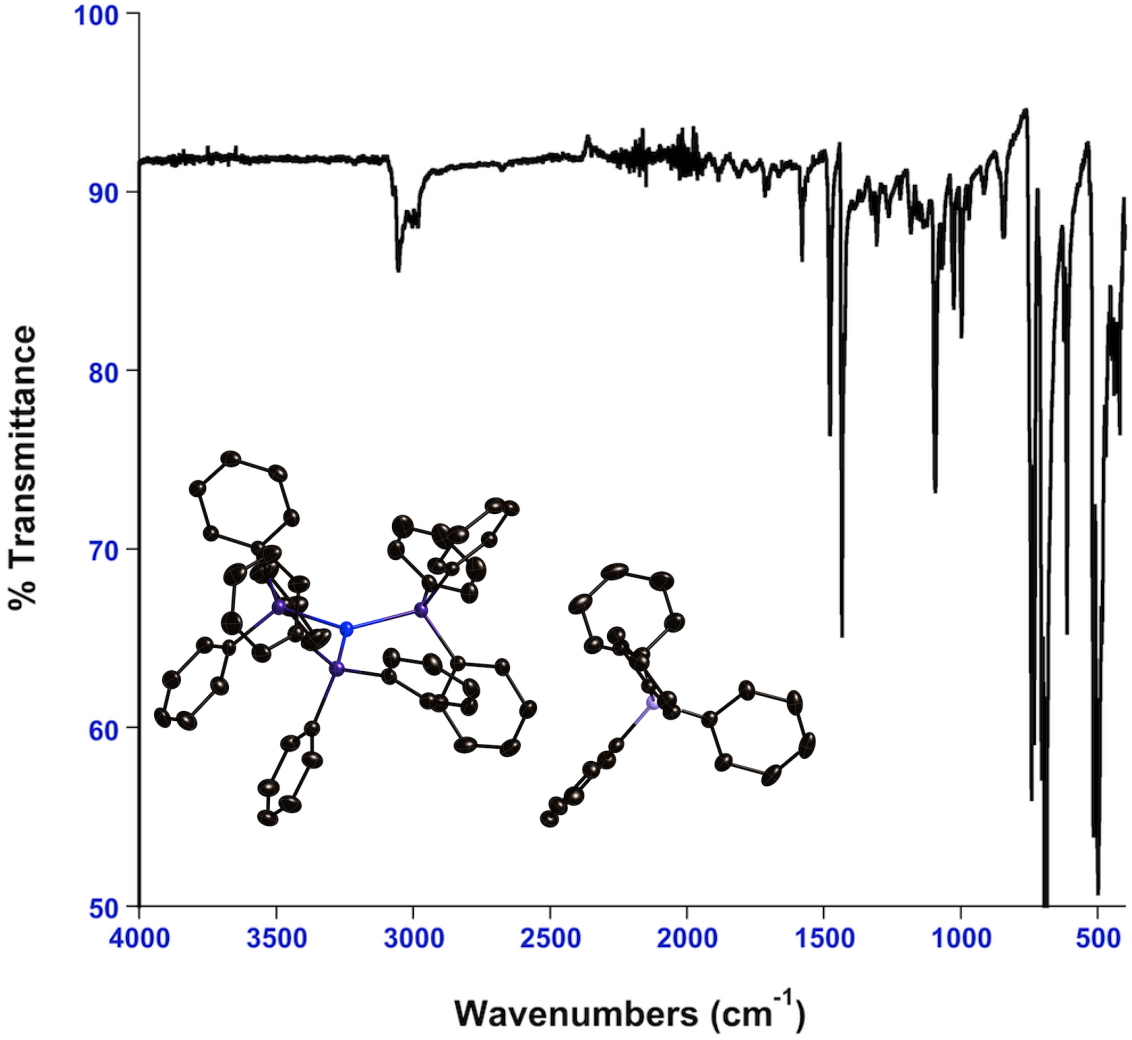

Figure F.7.1. Infrared spectrum of $[Cu^{I}(PPh_3)_3][BPh_4]$ (ATR, FT-IR)

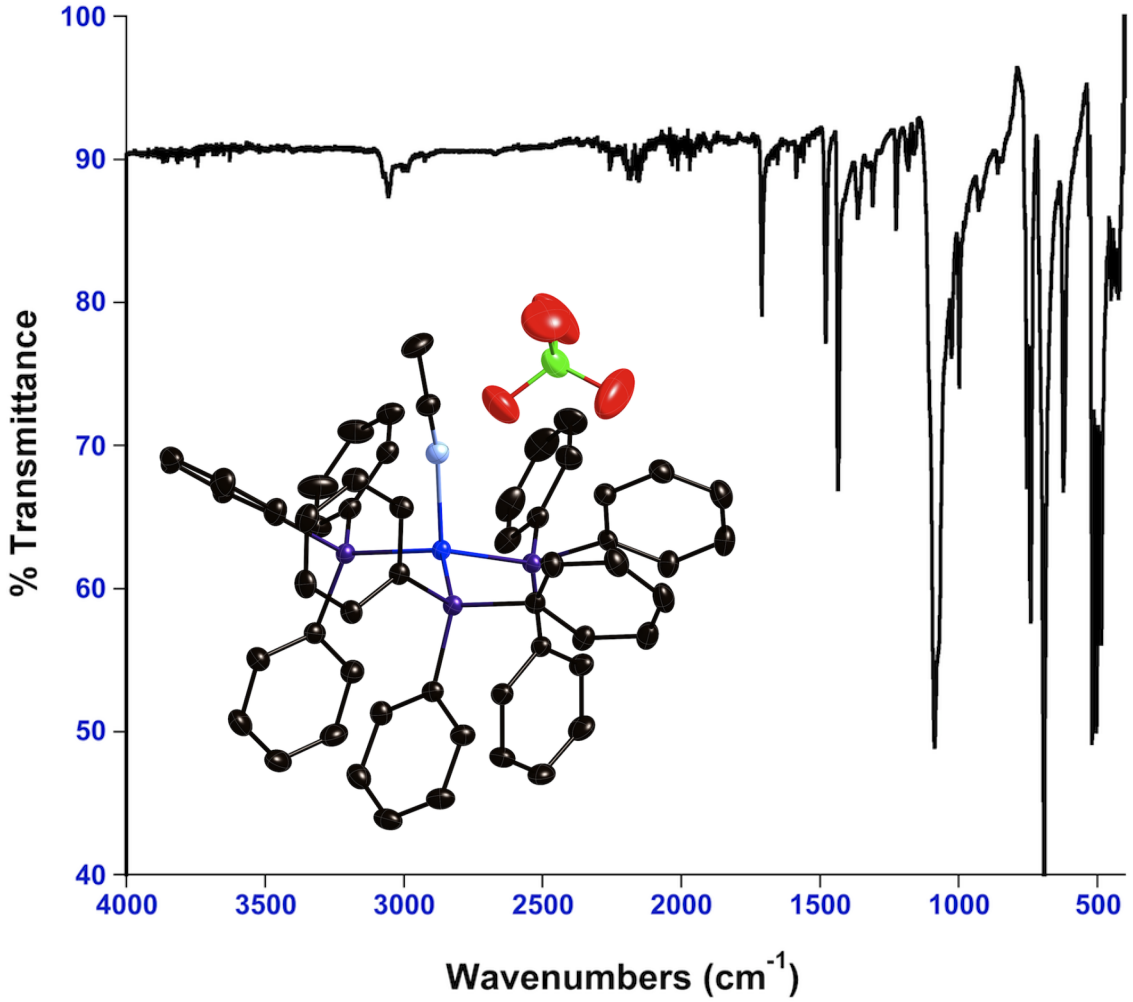

Figure F.7.2. Infrared spectrum of $[Cu^{I}(PPh_3)_3CH_3CN][ClO_4]$ (ATR, FT-IR)

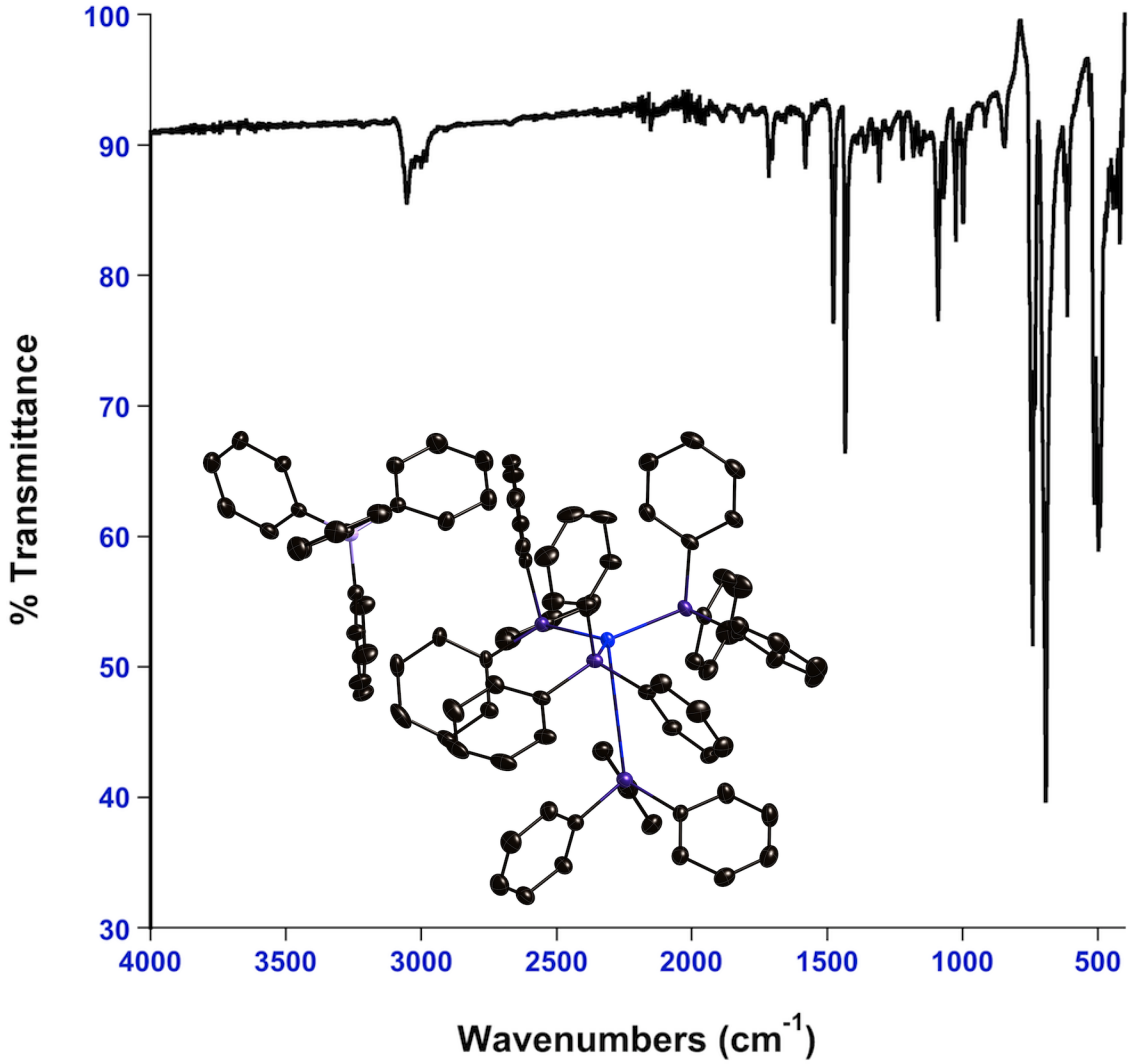

Figure F.7.3. Infrared spectrum of $[Cu^{I}(PPh_3)_3PPh_3][BPh_4]$ (ATR, FT-IR)